

ENVIRONMENTAL AND BIOCHEMICAL
CONTROLS ON THE MOLECULAR
DISTRIBUTION AND STABLE ISOTOPE
COMPOSITION OF LEAF WAX BIOMARKERS

Yvette Eley

Submitted for the Degree of Doctor of Philosophy

School of Environmental Sciences
University of East Anglia

June 2014



© This copy of the thesis has been supplied on condition that anyone who consults it is understood to recognise that its copyright rests with the author and that use of any information derived there from must be in accordance with current UK Copyright Law. In addition, any quotation or extract must include full attribution

Abstract

Leaf wax *n*-alkyl lipids are increasingly used as proxies in palaeoclimate studies. Palaeovegetation assemblages are reconstructed from their molecular distribution patterns, while their $\delta^{13}\text{C}$ and $\delta^2\text{H}$ signals are thought to reflect plant-environment interactions and palaeohydrological shifts, respectively. Such applications depend, however, upon these compounds faithfully recording environmental conditions. To explore the influence of environmental, physical and biochemical controls on *n*-alkane composition, leaf waxes from seven UK saltmarsh plants were analysed over two growing seasons. Linked analysis of sedimentary *n*-alkanes enabled further investigation of leaf wax biomarker integration into saltmarsh sediments.

The molecular distribution and concentration of *n*-alkanes from the saltmarsh plants varied significantly. Bulk and *n*-alkane $\delta^{13}\text{C}$ recorded different seasonal shifts, with a range of up to 13‰ in the offset between bulk and *n*-alkane $^{13}\text{C}/^{12}\text{C}$ values. This indicated that post-photosynthetic $^{13}\text{C}/^{12}\text{C}$ fractionation may be an important additional control on *n*-alkane $\delta^{13}\text{C}$ signals. *n*-Alkane $\delta^2\text{H}$ also varied among the sampled species by >100‰, and could not be explained by physical processes controlling the movement of water inside/outside and within leaves. Comparison with the $^2\text{H}/^1\text{H}$ of chloroplast-synthesised compounds (fatty acids, phytol) suggested these differences instead reflected the varied biochemical mechanisms operating in the chloroplast and cytosol. Sedimentary biomarker analysis further highlighted that small/moderate vegetation change could drive shifts of ~40‰ in sedimentary *n*-alkane $^2\text{H}/^1\text{H}$, while using globally averaged “typical” values to correct for fractionation between source water and *n*-alkane $^2\text{H}/^1\text{H}$ may not be representative of a specific geographical location.

Results demonstrate: (i) the importance of biochemical mechanisms in controlling the molecular and isotopic composition of *n*-alkyl lipids; and (ii) the need to further constrain the influence of vegetation change on the isotope composition of sedimentary *n*-alkanes. Future research should address these areas in other biomes and depositional environments, to ensure accurate interpretation of modern and ancient leaf wax lipid data.

Acknowledgements

Firstly, I would like to thank my supervisors, Dr Nikolai Pedentchouk (UEA), Professor Julian Andrews (UEA), and Professor Lorna Dawson (James Hutton Institute) for their support, advice and guidance over the course of my PhD. They have helped shape my development as an independent researcher, and their combination of good humour, patience and diligence has made the last four years both a steep learning curve and a pleasure at the same time.

I spent a lot of time collecting plants and sediments on the north Norfolk coast as part of my project. I therefore owe a great deal to everyone who helped me with fieldwork, and endured sunny (and not so sunny) days by the sea: Louise Jones, Annette Eley (not forgetting Skeeter), and Joe Dillon. Thanks are also due to Liz Rix, Sarah Wexler, Graham Chilvers, Paul Disdle and Chris Barkway for technical support during my time at UEA. I am indebted to the team at the James Hutton Institute who have hosted me many times during my doctoral studies. Professor Lorna Dawson and Dr Bob Mayes both assisted with analysis of fatty acids, and spent valuable time advising me on lipid biochemistry. Jasmine Ross and Allan Sim provided incredible support with laboratory work, and I could not have achieved everything I have done without their help.

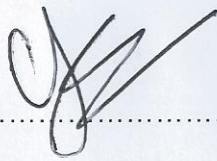
I have been fortunate enough to have discussed my work with a number of people who have an interest in the sedimentology and ecology of the north Norfolk coast. A particular mention goes to Professor John Allen (University of Reading) who provided a wealth of information regarding the sedimentary sequences at Stiffkey, and Professor Tony Davy (UEA) who shared his expert knowledge of the flora of these marshes. I am also grateful to Dr Stuart Black (University of Reading), who put up with multiple questions about isotope mixing models and statistical analysis, and was prepared to read and comment on sections whenever asked. Franz Street (University of Reading) also deserves a special mention for the construction of a fantastic cryogenic extraction line, as does Stuart for letting me use it!

Last, and by no means least, I would like to thank my friends and family for their support, kindness, coffee and willingness to cook me dinner during the last few years. In particular, Hilary Bathgate and Brian Andersen, Louise Jones, Chris Roberts, Alina Mihailova, and Naomi Williams – honestly, I am not sure I could have done it without you all. I also know none of this would have been possible without the enduring support of my mother, who gave me the courage to follow my chosen path, and has never stopped believing in me, even when I was not sure I believed in myself. The final mention here goes to my father, who although no longer here to see me become “*not that kind of doctor*”, always encouraged me to look at the world and ask why.

Declaration

"Declaration

I confirm that this is my own work, and that use of all material from other sources has been properly and fully acknowledged."



A handwritten signature in black ink, consisting of a large, stylized 'Y' followed by several loops and a long horizontal stroke extending to the right. The signature is positioned above a horizontal dotted line.

Yvette Eley

This thesis comprises of 96,934 words.

Contents

Abstract.....	i
Acknowledgements.....	ii
Declaration.....	iii
Contents.....	iv
List of Figures	xi
List of Tables	xvii
List of Abbreviations	xix

Chapter 1: Introduction 1

1.1. THE USE OF LEAF WAX BIOMARKERS AS PALAEOCLIMATE PROXIES.....	3
1.1.1 A proxy for recreating palaeovegetation assemblages.....	3
1.1.2 A proxy for tracing plant-environment interactions	5
1.1.3 A proxy for hydrological change	8
1.1.3.1 <i>Summary of factors influencing precipitation $^2H/^1H$</i>	9
1.1.3.2 <i>Using leaf waxes to reconstruct the δ^2H of precipitation in temperate regions</i>	10
1.1.3.3 <i>Using leaf waxes to reconstruct the δ^2H of precipitation in tropical regions</i>	11
1.1.3.4 <i>Can biochemical mechanisms influence leaf wax $^2H/^1H$</i>	11
1.1.4 The incorporation of leaf waxes into the sedimentary record	13
1.2 SUMMARY OF OUTSTANDING QUESTIONS	14
1.3 AIMS AND OBJECTIVES.....	15
1.3.1 Specific objectives	16
1.4 STRUCTURE OF THESIS	16

Chapter 2: Site description: Stiffkey saltmarsh 20

2.1 INTRODUCTION	20
2.2 RATIONALE FOR SITE SELECTION	20
2.3. STIFFKEY SALTMASH.....	25
2.3.1 Modern site characteristics	25
2.3.2 Modern surface vegetation.....	26
2.4 STIFFKEY SEDIMENTS	28

Chapter 3: Plant leaf waxes: an overview of composition and synthesis..... 32

3.1 INTRODUCTION	32
3.2. SYNTHESIS OF PLANT LEAF WAXES	34

3.2.1 Production of VLCFAs	35
3.2.2 Biosynthetic pathway for <i>n</i> -alkanes	37
3.2.3 Areas for future research	41
3.3 SUMMARY	42

Chapter 4: Variability in the molecular distribution and concentration of leaf wax *n*-alkanes from saltmarsh plants..... 43

4.1. INTRODUCTION	43
4.2 LITERATURE REVIEW	44
4.2.1 Identification of plant inputs to soils and sediments	44
4.2.2 How reliable are molecular distribution ratios for discriminating between plants?	45
4.2.3 Variability in <i>n</i> -alkane concentration among plant species	48
4.2.4 Factors which could drive variability in <i>n</i> -alkane concentration and distribution	49
4.2.4.1 <i>Environmental factors influencing plant leaf wax composition</i>	49
4.2.4.2 <i>The influence of leaf ontogeny on leaf wax composition</i>	51
4.2.5 The importance of understanding <i>n</i> -alkane systematics in saltmarsh plants	52
4.3. AIMS AND OBJECTIVES.....	52
4.4. SAMPLE COLLECTION	53
4.4.1 Sampling strategy	53
4.4.2 Weather station data	55
4.5. ANALYTICAL METHODS.....	58
4.5.1 <i>n</i> -alkane extraction, identification and quantification	58
4.5.2 Quantifying the percentage recovery of <i>n</i> -alkanes	59
4.6. RESULTS	60
4.6.1 Percentage recovery of <i>n</i> -alkanes	60
4.6.2 Molecular distribution profiles for plants sampled at Stiffkey	60
4.6.3 Molecular distribution patterns among different marsh sub-environments	65
4.6.4 <i>n</i> -Alkane ratios	67
4.6.5 Variation in <i>n</i> -alkane concentration among sampled species.....	68
4.6.6 <i>n</i> -Alkane concentrations across different marsh sub-environments.....	74
4.7. DISCUSSION	75
4.7.1 The magnitude of interspecies variation in <i>n</i> -alkane distribution patterns	75
4.7.2 The influence of seasonality on <i>n</i> -alkane distribution patterns	80

4.7.3 The influence of spatial variation in marsh characteristics on <i>n</i> -alkane distribution patterns	81
4.7.4 Discrimination between species using molecular distribution ratios	82
4.7.5 The magnitude of interspecies variability in <i>n</i> -alkane concentrations	83
4.7.6 The influence of seasonality on <i>n</i> -alkane concentrations	87
4.7.7 The influence of spatial variation in marsh characteristics on <i>n</i> -alkane concentrations	88
4.8. CONCLUSION.....	90
4.9. SUMMARY	91

**Chapter 5: Interspecies variation in the carbon isotope composition
of bulk plant tissue and *n*-alkanes from saltmarsh plants 92**

5.1 INTRODUCTION	92
5.2 LITERATURE REVIEW	93
5.2.1 Bulk carbon isotope profiles of plant biomass	93
5.2.2 Compound-specific isotope analysis of leaf wax biomarkers	100
5.2.3 Using carbon isotopes to consider plant-environment interactions	101
5.2.4 The potential for biochemical mechanisms to influence <i>n</i> -alkane ¹³ C/ ¹² C	105
5.3. AIMS AND OBJECTIVES.....	109
5.4. SITE DESCRIPTION AND SAMPLING STRATEGY.....	110
5.4.1 Site description	110
5.4.2 Sampling strategy.....	110
5.5. ANALYTICAL METHODS.....	110
5.5.1 Bulk carbon and nitrogen isotope analysis.....	110
5.5.2 <i>n</i> -Alkane extraction, quantification and identification	111
5.5.3 <i>n</i> -Alkane δ ¹³ C analysis	111
5.5.4 Calculation of carbon isotope discrimination.....	112
5.5.5 Analysis of the percentage carbon and nitrogen content.....	113
5.6. RESULTS	113
5.6.1 Bulk δ ¹³ C.....	113
5.6.2 <i>n</i> -Alkane δ ¹³ C	118
5.6.3 Correlation between seasonal trends in bulk and <i>n</i> -alkane δ ¹³ C.....	119
5.6.4 Seasonal shifts in the offset between bulk and <i>n</i> -alkane δ ¹³ C	120
5.6.5 Calculating Δ ¹³ C values from bulk and <i>n</i> -alkane δ ¹³ C	122
5.6.6 Percentage carbon composition of bulk leaf tissue.....	124
5.6.7 Percentage nitrogen composition of bulk leaf tissue.....	128
5.6.8 Bulk nitrogen isotopes	131
5.6.9 The relationship between seasonal shifts in abundance and	

concentration of <i>n</i> -alkanes and their carbon isotope composition.....	133
5.6.10 Spatial variation in bulk and <i>n</i> -alkane $\delta^{13}\text{C}$ across marsh	
sub-environments	135
5.7. DISCUSSION	137
5.7.1 Interspecies variation in bulk and <i>n</i> -alkane $\delta^{13}\text{C}$	137
5.7.2 Seasonal trends in plant bulk and <i>n</i> -alkane $\delta^{13}\text{C}$	138
5.7.2.1 <i>Water availability</i>	139
5.7.2.2 <i>Salinity/osmotic stress</i>	142
5.7.3 Spatial variation in carbon isotope composition across marsh	
sub-environments	144
5.7.4 Calculating carbon isotope discrimination from bulk and	
<i>n</i> -alkane carbon isotope ratios	146
5.7.5 The relationship between carbon content and carbon isotope	
composition	147
5.7.6 Are species-specific adaptations to salinity significant?	149
5.7.7 Are seasonal shifts in the relative abundance of leaf wax	
<i>n</i> -alkane homologues significant?	154
5.8. CONCLUSION.....	155
5.9 SUMMARY	156
Chapter 6: Understanding $^2\text{H}/^1\text{H}$ systematics of leaf wax <i>n</i>-alkanes in	
coastal plants	157
6.1. INTRODUCTION	157
6.1.1 Previous focus on physical mechanisms	158
6.1.2 An overview of leaf water models.....	159
6.1.3 Studies considering biochemical influences on leaf wax $^2\text{H}/^1\text{H}$	162
6.2. AIMS AND OBJECTIVES.....	163
6.3. SITE DESCRIPTION AND SAMPLING STRATEGY	163
6.3.1 Site description	163
6.3.2 Sampling strategy	164
6.4. ANALYTICAL METHODS.....	165
6.4.1 Leaf, xylem and soil water extraction	165
6.4.2 Water isotopic analysis.....	166
6.4.3 <i>n</i> -Alkane extraction and identification	166
6.4.4 <i>n</i> -Alkane hydrogen isotope analysis	167
6.5. RESULTS	167
6.5.1 Soil water $^2\text{H}/^1\text{H}$ composition.....	167
6.5.2 Xylem water $^2\text{H}/^1\text{H}$ composition.....	171
6.5.3 Leaf water $^2\text{H}/^1\text{H}$ composition.....	172

6.5.4 <i>n</i> -Alkane ² H/ ¹ H composition	175
6.5.5 ² H/ ¹ H fractionation between soil, xylem and leaf water and <i>n</i> -C ₂₉ alkane	179
6.5.6 Relationship between carbon and hydrogen isotope composition of <i>n</i> -alkanes	182
6.6. DISCUSSION	182
6.6.1 The significance of spatial differences in soil water	183
6.6.2 The significance of temporal differences in soil water	184
6.6.3 The significance of soil water uptake by halophytes and non-halophytes	185
6.6.4 The significance of leaf water	188
6.6.5 Comparison of ² H/ ¹ H fractionation among C ₃ and C ₄ plants at Stiffkey with previously published research	192
6.7 CONCLUSION	194
6.8. SUMMARY	195
Chapter 7: The role of biochemical and metabolic processes in controlling interspecies variation leaf wax <i>n</i>-alkane ²H/¹H	196
7.1 INTRODUCTION	196
7.2 REVIEW	197
7.2.1 Sources of hydrogen for terrestrial plants	197
7.2.2 The potential for interspecies differences in phytochemistry to influence <i>n</i> -alkane ² H/ ¹ H	201
7.2.3 The potential for variation in NADPH sources and pools to influence <i>n</i> -alkane ² H/ ¹ H	203
7.2.4 The potential for plant biochemical responses to environmental stress to influence <i>n</i> -alkane ² H/ ¹ H	204
7.3 AIMS AND OBJECTIVES	205
7.4 SAMPLING STRATEGY	206
7.4.1 Site description	206
7.4.2 Fatty acids and phytol	206
7.4.3 Bulk leaf tissue	207
7.4.4 Samples for starch extraction	207
7.5 ANALYTICAL METHODOLOGY	207
7.5.1 Extraction and analysis of phytol for ² H/ ¹ H analysis	207
7.5.2 Extraction and analysis of fatty acids for ² H/ ¹ H analysis	211
7.5.3 Preparation and analysis of bulk plant tissue for analysis of ² H/ ¹ H, percentage nitrogen, percentage carbon content, and δ ¹⁵ N	212
7.5.4 Extraction, preparation, and analysis of starch for ² H/ ¹ H analysis	213
7.5.4.1 <i>Presumptive starch test</i>	213

7.5.4.2 Starch extraction.....	214
7.5.4.3 Hydrogen isotope analysis	216
7.6 RESULTS	217
7.6.1 $^2\text{H}/^1\text{H}$ of phytol	217
7.6.2 $^2\text{H}/^1\text{H}$ values of fatty acids.....	220
7.6.3 $^2\text{H}/^1\text{H}$ of starch	223
7.6.3.1 Presumptive starch test	223
7.6.3.2 Quantification and correction for exchangeable hydrogen in starch.....	225
7.6.3.3 Corrected $^2\text{H}/^1\text{H}$ of starch.....	227
7.6.4 $^2\text{H}/^1\text{H}$ of bulk plant tissue.....	228
7.6.5 Percentage nitrogen composition and C:N ratio of bulk leaf tissue	231
7.6.6 Relationship between <i>n</i> -alkane $^2\text{H}/^1\text{H}$ and foliar $\delta^{15}\text{N}$	234
7.7. DISCUSSION	235
7.7.1 The hydrogen isotope composition of phytol	236
7.7.1.1 Differences in phytol $^2\text{H}/^1\text{H}$ between C_3 and C_4 plants.....	238
7.7.1.2 Differences in phytol $^2\text{H}/^1\text{H}$ among C_3 plants	239
7.7.1.3 Comparison of phytol and <i>n</i> -alkane $^2\text{H}/^1\text{H}$ values.....	243
7.7.2 The hydrogen isotope composition of fatty acids.....	244
7.7.2.1 Differences in $^2\text{H}/^1\text{H}$ of FA chain lengths	244
7.7.2.2 Interspecies differences in the $^2\text{H}/^1\text{H}$ values of FAs.....	247
7.7.3 The hydrogen isotope composition of starch	250
7.7.4 Interspecies differences in the response to environmental stress	252
7.7.5. Directions for future research	257
7.8. SUMMARY	258
Chapter 8: Distinguishing shifts in palaeohydrology from shifts in vegetation: a challenge for interpreting sedimentary leaf wax <i>n</i>-alkanes	261
8.1. INTRODUCTION	261
8.1.1 Sedimentary samples collected at Stiffkey.....	264
8.2 HOW VALID ARE THE ASSUMPTIONS USED IN PALAEOHYDROLOGICAL STUDIES?	265
8.2.1 Hydrogen isotope fractionation between source water and <i>n</i> -alkanes is relatively consistent among angiosperms.....	265
8.2.2 Sedimentary biomarker signal averages plant inputs across varying spatial scales	266
8.2.3 Modern spatial studies can be used to interpret temporal changes in $\delta^2\text{H}$ signal	267
8.3 SENSITIVITY OF THE SEDIMENTARY BIOMARKER RECORD TO VEGETATION CHANGE.....	271

8.3.1 Scenario 1.....	275
8.3.2 Scenario 2.....	276
8.4 THE SUCCESS OF METHODS TO QUANTIFY VEGETATION CHANGE	278
8.4.1 Carbon isotope composition of <i>n</i> -alkanes.....	278
8.4.2 Using molecular distributions to identify vegetation change.....	282
8.4.3 Alternative approaches to identifying and quantifying vegetation change	284
8.5 USING MIXING MODELS TO QUANTIFYING SOURCE INPUTS: A ROBUST APPROACH FOR THE FUTURE?.....	286
8.5.1 Source apportionment models	286
8.5.2 Application of the Collins model to the Stiffkey core data.....	289
8.5.3 Application of the IsoSource model to the Stiffkey core	295
8.5.4 Application of the IsoConc model to the Stiffkey core	298
8.5.5 Summary: use of source apportionment models to track vegetation inputs	300
8.6 A CASE STUDY FROM THE STIFFKEY CORE	304
8.7 CONCLUSION.....	311
8.8 SUMMARY	314
Chapter 9: Summary and conclusion.....	315
9.1. MOLECULAR DISTRIBUTION AND CONCENTRATION	315
9.2 THE RELATIVE INFLUENCE OF ENVIRONMENTAL AND BIOCHEMICAL MECHANISMS ON <i>n</i> -ALKANE $\delta^{13}\text{C}$	317
9.3 THE RELATIVE INFLUENCE OF ENVIRONMENTAL AND BIOCHEMICAL MECHANISMS ON <i>n</i> -ALKANE $^2\text{H}/^1\text{H}$	320
9.4 CAN METABOLIC AND BIOCHEMICAL PROCESSES INFLUENCE <i>n</i> -ALKANE $^2\text{H}/^1\text{H}$	321
9.5 DISTINGUISHING SHIFTS IN PALAEOHYDROLOGY FROM CHANGES IN VEGETATION IN SEDIMENTARY SEQUENCES	323
9.6 FINAL COMMENT	324
References.....	325
Appendices.....	352
Appendix 1: Conference abstracts from the thesis	352
Appendix 2: Papers published from the thesis	359
Appendix 3: Additional data pertaining to Chapter 4	376
Appendix 4: Additional data pertaining to Chapter 5	391
Appendix 5: Additional data pertaining to Chapter 6	402
Appendix 6: Additional data pertaining to Chapter 7	410
Appendix 7: Additional data pertaining to Chapter 8	414

List of Figures

Figure 1.1	Illustration of a transverse view of wax secreting epidermal cells.	2
Figure 1.2	Box and whisker plots of global leaf $\Delta^{13}\text{C}$ values by biome.	7
Figure 1.3	Schematic illustration of the fractionation of water in a cloud as a function of Rayleigh distillation.	9
Figure 1.4	Overview of the processes affecting hydrogen isotopic-composition of lipid biomarkers from phototrophic organisms.	12
Figure 1.5	Diagram showing the thesis structure – coloured arrows indicate how the findings of one chapter feed into the following chapters	19
Figure 2.1	A) Average (\pm SE) carbon burial rates in different coastal ecosystems; and B) Frequency distribution of organic carbon content in salt marsh, mangrove and seagrass sediments.	22
Figure 2.2	Aerial photo of Stiffkey saltmarsh.	23
Figure 2.3	Two examples of drainage ditches at Stiffkey.	24
Figure 2.4	White-ish deposit, thought to be salt, observed on the soil surfaces of the upper marsh in August 2012, Stiffkey	26
Figure 2.5	Examples of the different morphology of species sampled from Stiffkey for this project.	27
Figure 2.6	Sediment core ^{137}Cs profiles plotted against depth (A) and excess ^{210}Pb profiles plotted against cumulative sediment density (B) at Stiffkey..	29
Figure 2.7	Map showing the location of Stiffkey marsh relative to Blakeney spit	31
Figure 3.1	Examples of SEM images of <i>Arabidopsis thaliana</i> stems, showing the crystalloid structures common to epicuticular waxes.	33
Figure 3.2	Relative percentages of wax constituents found in <i>Arabidopsis</i> (data from Kunst, 2003)	35
Figure 3.3	Simplified pathways for wax biosynthesis in <i>Arabidopsis</i> stems. (Samuels et al., 2008)	36
Figure 3.4	Schematic showing the activity of FAEs in generating FAs with >20 carbons.	38
Figure 3.5	Reactions and products of the decarbonylation and reductive pathway, derived from the study of <i>Arabidopsis</i> .	40
Figure 3.6	Main lipid classes and biochemical pathways involved in the production secondary plant lipids.	41
Figure 4.1	Maximum and minimum daily temperatures, averaged by month, from Cromer weather station during 2011 and 2012 (MIDAS).	56
Figure 4.2	Mean relative humidity recorded at Cromer weather station during 2011 and 2012.	56
Figure 4.3	Total amounts of rainfall recorded at Cromer weather station for each calendar month during 2011 and 2012 (MIDAS).	57
Figure 4.4	Total hours of sunshine recorded for each calendar month at Lowestoft weather station during 2011 and 2012	57
Figure 4.5	Molecular distributions of odd-chain n-alkanes from species sampled at Stiffkey saltmarsh over 15 months from June 2011 to September 2012.	63

Figure 4.6	Seasonal variation in the percentage composition of long-chain n-alkanes from the species sampled at Stiffkey, normalised to the total peak area of odd-chain alkanes.	64
Figure 4.7	The influence of marsh sub-environment on CPI values in samples collected during 2011 from species growing at multiple locations across Stiffkey marsh.	66
Figure 4.8	Box and whisker plot showing calculated n-C ₃₁ /n-C ₂₇ ratios for woody and non-woody plant species at Stiffkey saltmarsh.	68
Figure 4.9	Total concentration of odd-chain (n-C ₂₁ to n-C ₃₅) alkanes for all sampled species across the 2011 and 2012 growing seasons.	71
Figure 4.10	Seasonal variation in n-alkane concentrations for a) <i>Atriplex portulacoides</i> , b) <i>Elytrigia atherica</i> , and c) <i>Limonium vulgare</i> , sampled across the 2011 and 2012 growing seasons.	72
Figure 4.11	Seasonal variation in n-alkane concentrations for a) <i>Phragmites australis</i> , b) <i>Salicornia europaea</i> , and c) <i>Spartina anglica</i> , sampled across the 2011 and 2012 growing seasons.	73
Figure 4.12	Seasonal variation in n-alkane concentrations for <i>Suaeda vera</i> sampled across the 2011 and 2012 growing seasons.	74
Figure 4.13	n-Alkane distribution patterns from a) <i>Spartina anglica</i> (Stiffkey, North Norfolk, UK; this study), b) <i>Spartina patens</i> (Maine, USA; Tanner et al., 2007), and c) <i>Spartina alterniflora</i> (Maine, USA; Tanner et al., 2007).	76
Figure 4.14	Comparison of n-alkane concentrations of species from the same genus growing at different geographical locations.	84
Figure 5.1	Histogram showing the normal distribution of C ₃ and C ₄ carbon isotope values.	93
Figure 5.2	Schematic of C ₃ plant physiology and biosynthetic pathways of carbon fixation.	94
Figure 5.3	Schematic representation of the Calvin-Benson-Bassham cycle.	95
Figure 5.4	Schematic of C ₄ plant physiology and biosynthetic pathways of carbon fixation.	68
Figure 5.5	Summary of the influence of changes in <i>C_i/C_a</i> on the carbon isotope composition of plant tissue.	101
Figure 5.6	A schematic network of chemical reactions.	107
Figure 5.7	Seasonal trends in bulk plant leaf, n-C ₂₇ , n-C ₂₉ and WA n-alkane carbon isotope ratios from all species sampled at Stiffkey.	116
Figure 5.8	Correlation between bulk plant leaf carbon isotope signatures and WA n-alkane isotope signatures	119
Figure 5.9	Calculated Seasonal variation in the apparent fractionation (ϵ) between bulk leaf and WA alkane $\delta^{13}\text{C}$ values from species sampled at Stiffkey during 2011 and 2012.	121
Figure 5.10	Correlation between carbon isotope discrimination values calculated from bulk plant leaf tissue, and n-C ₂₉ alkane data	122
Figure 5.11	Seasonal trends in carbon isotope discrimination values calculated A) from bulk plant leaf $\delta^{13}\text{C}$ values, and B) from n-C ₂₉ $\delta^{13}\text{C}$ values.	123
Figure 5.12	Carbon content of species sampled at Stiffkey, grouped by plant life form.	125
Figure 5.13	Carbon content of plant species sampled at Stiffkey grouped by their choice of compatible solute to maintain osmotic potential.	125

Figure 5.14	Correlation between carbon content and bulk plant tissue carbon isotope composition for <i>Elytrigia atherica</i> and <i>Phragmites australis</i> (C ₃ monocots)	126
Figure 5.15	Correlation between carbon content and bulk plant tissue carbon isotope composition for <i>Limonium vulgare</i> and <i>Salicornia europaea</i> (C ₃ Perennials/Annuals)	127
Figure 5.16	Correlation between carbon content and bulk plant tissue carbon isotope composition for <i>Atriplex portulacoides</i> and <i>Suaeda vera</i> (C ₃ Woody shrubs)	127
Figure 5.17	Percentage nitrogen composition (A) and percentage carbon composition (B) of plant biomass.	130
Figure 5.18	Nitrogen isotope composition of bulk leaf tissue from samples collected during 2011 and 2012.	131
Figure 5.19	Seasonal shifts in nitrogen isotope composition of bulk plant tissue across 2011 and 2012. A) C ₃ and C ₄ monocots, B) Dicots and succulents.	132
Figure 5.20	Correlation between the percentage abundance of n-C ₂₇ and n-C ₂₉ δ ¹³ C values. A) including data from <i>Suaeda vera</i> ; B) excluding data from <i>Suaeda vera</i>	134
Figure 5.21	Correlation between: A) the percentage abundance of n-C ₂₉ and n-C ₂₇ δ ¹³ C values including <i>Suaeda vera</i> (left), and excluding <i>Suaeda vera</i> (right); B) the percentage abundance of n-C ₂₉ and n-C ₂₇ δ ¹³ C values including <i>Suaeda vera</i> (left), and excluding <i>Suaeda vera</i> (right)	134
Figure 5.22	Bulk (a) and n-alkane (b) carbon isotope composition from species growing at multiple marsh sampling sites.	136
Figure 5.23	Data from Briens and Lahrer (1982) showing the difference in soluble carbohydrate, methylated onium (nitrogenous) compounds, and free proline between dicots and monocots (highlighted in red)	150
Figure 6.1	Cryogenic extraction line at the University of Reading.	165
Figure 6.2	Comparison of soil water hydrogen isotope composition from AM (0:7:30 to 8:00) and PM (12:00 to 14:00).	170
Figure 6.3	Comparison of xylem water hydrogen isotope composition from AM (0:7:30 to 8:00) and PM (12:00 to 14:00).	170
Figure 6.4	Measured soil water δ ² H, xylem water δ ² H, leaf water δ ² H, and n-alkane δ ² H values from all species sampled in September 2012.	171
Figure 6.5	Measured n-C ₂₉ alkane δ ² H (yellow circles) and leaf water δ ² H (blue circles) values for all plants sampled across the Stiffkey marsh in June 2011.	173
Figure 6.6	Leaf water ² H/ ¹ H from all species sampled across 2012.	174
Figure 6.7	Measured leaf water ² H/ ¹ H for three species sampled at the ridge site between 7:30 and 8:00 and again between 12:00 and 14:00 on 7 th September 2012.	174
Figure 6.8	Bivariate plot of n-C ₂₇ and n-C ₂₉ alkane δ ² H values for all species sampled across the 2012 growth season.	176
Figure 6.9	Seasonal variation in n-C ₂₉ alkane δ ² H and leaf water δ ² H values for all plants sampled during the 2012 growth season.	177
Figure 6.10	Bivariate plot of ACL and n-C ₂₉ alkane δ ² H (September 2012) showing no correlation between the two parameters.	178

Figure 6.11	Calculated fractionation ($\epsilon_{wax/lw}$ ‰) between n-C ₂₉ alkane δ^2H and leaf water δ^2H from samples collected in June 2011 at Stiffkey saltmarsh.	180
Figure 6.12	Calculated fractionation ($\epsilon_{wax/lw}$ ‰) between n-C ₂₉ alkane δ^2H and leaf water δ^2H from samples collected across the 2012 growth season.	181
Figure 7.1	Conceptual overview of the processes affecting the hydrogen isotope composition of lipid biomarkers from phototrophic organisms.	197
Figure 7.2	NADPH is the primary immediate biosynthetic precursor of hydrogen for lipids and is generated by diverse mechanisms associated with different central metabolic pathways as indicated.	199
Figure 7.3	Simplified schematic of the compartmentalisation of production of lipids analysed in this study.	206
Figure 7.4	Flow diagram illustrating the method used for extracting phytol.	208
Figure 7.5	Schematic illustrating the acetylation of the phytol molecule.	210
Figure 7.6	The structure of phthalic acid.	211
Figure 7.7	Preparation of samples for presumptive starch test	214
Figure 7.8	A sample from <i>Atriplex portulacoides</i> undergoing starch extraction.	216
Figure 7.9	Schematic of the set-up used for quantifying exchangeable hydrogen in starch.	217
Figure 7.10	Interspecies variation in the $^2H/^1H$ of phytol from samples collected in August 2012.	219
Figure 7.11	Calculated fractionation between the $^2H/^1H$ of phytol and weighted average alkane isotope composition (red) bulk biomass isotope composition (yellow) and leaf water isotope composition (blue).	219
Figure 7.12	Comparison of the isotope composition of palmitic, linoleic and linolenic fatty acid $^2H/^1H$.	220
Figure 7.13	Comparison of $^2H/^1H$ of leaf water, phytol, fatty acids and n-alkanes for the seven Stiffkey species.	222
Figure 7.14	Comparison of the magnitude of interspecies variation in $^2H/^1H$ for leaf water (blue), phytol (green), fatty acids (yellow) and n-alkanes (red).	223
Figure 7.15	<i>Limonium vulgare</i> leaves stained with Lugol's solution.	224
Figure 7.16	Cross-plot of the hydrogen isotope composition of the equilibration water and the starch grains from the equilibration experiment.	227
Figure 7.17	Seasonal variation in bulk hydrogen isotope composition.	228
Figure 7.18	Correlation between bulk and weighted average n-alkane $^2H/^1H$ values. Blue = dicot/succulent functional types, green = C ₃ and C ₄ monocot functional types.	230
Figure 7.19	Comparison of fractionation between (A) bulk leaf tissue $^2H/^1H$ and WA alkane isotopic composition, and (B) fractionation between bulk leaf tissue $^2H/^1H$ and leaf water isotopic composition.	232
Figure 7.20	Relationship between: A: %N composition of plant biomass and n-C ₂₉ $^2H/^1H$; B: %C composition of plant biomass and n-C ₂₉ $^2H/^1H$; and C: C:N ratio of biomass and n-C ₂₉ $^2H/^1H$	233

Figure 7.21	Bi-plot of foliar nitrogen isotope values with n-C ₂₉ hydrogen isotope values, showing the positive relationship between these two measurements for monocots (A) and the negative relationship for dicots and succulents (B).	234
Figure 7.22	Schematic of the biosynthesis pathway of phytol, showing the hydrogenation step of the immediate precursor GGPP.	237
Figure 7.23	Schematic showing the light reactions of the thylakoid membrane.	241
Figure 7.24	Difference in the pattern of relative enrichment and depletion of deuterium in phytol and n-C ₂₉ from the Stiffkey species.	243
Figure 7.25	Major pathway of polyunsaturated FAs in microalgae.	246
Figure 7.26	Relative enrichment and depletion in deuterium for isoprenoid and acetogenic lipids analysed from the Stiffkey species.	249
Figure 7.27	Seasonal comparison of carbon and nitrogen percentage composition from species sampled across 2012 at Stiffkey.	253
Figure 7.28	Simplified biochemical network for central metabolism.	254
Figure 7.29	Schematic summarising potential biochemical mechanisms which could influence isoprenoid and acetogenic lipid hydrogen isotope compositions.	260
Figure 8.1	An overview of the processes affecting the hydrogen-isotopic composition of lipid biomarkers from phototrophic organisms.	261
Figure 8.2	Julian Andrews with the 1m core sampled from the UM	264
Figure 8.3	Schematic illustrating the complexities inherent in using a calibration carried out at the spatial scale to validate the interpretation of data from a chronosequence at one geographical location.	268
Figure 8.4	Comparison of the isotopic fractionation between source water and n-alkanes ($\epsilon_{w/a}$)	270
Figure 8.5	Variation in the concentrations of n-C ₂₇ and n-C ₂₉ among the seven saltmarsh plants sampled at Stiffkey in September 2012	272
Figure 8.6	Pie chart illustrating the relative contribution of n-C ₂₉ from each of the seven studied saltmarsh plants	274
Figure 8.7	Comparison of WA sedimentary n-C ₂₉ ² H/ ¹ H values using the original percentage inputs from September 2012 (green), and the modelled percentage inputs using Scenario 1 (yellow).	276
Figure 8.8	Comparison of WA sedimentary n-C ₂₉ ² H/ ¹ H values using the original percentage inputs from September 2012 (green), and the modelled percentage inputs using Scenario 2 (yellow).	277
Figure 8.9	Evaluating the suitability of using the carbon isotope composition of n-C ₂₉ to constrain the extent of vegetation change in sedimentary sequences	279
Figure 8.10	Pie chart illustrating the relative contribution of n-C ₂₉ from each of the seven studied saltmarsh plants, with the n-C ₂₉ $\delta^{13}\text{C}$ values	280
Figure 8.11	Comparison of WA sedimentary n-C ₂₉ $\delta^{13}\text{C}$ values using the original percentage inputs from September 2012 (green), and the modelled percentage inputs using Scenario 2 (yellow).	281

Figure 8.12	Comparison of WA sedimentary n-C ₂₉ δ ¹³ C values using the original percentage inputs from September 2012 (green), and the modelled percentage inputs using Scenario 2 (yellow).	281
Figure 8.13	Evaluating the suitability of using molecular distribution parameters and indices from the Stiffkey species to constrain the extent of vegetation change	283
Figure 8.14	Percentage contribution estimates of vegetation generated using the Collins model.	291
Figure 8.15	Measured (yellow) and modelled (grey) ACL values for the Stiffkey core samples.	293
Figure 8.16	Measured (blue) and modelled (grey) carbon isotope composition of the n-C ₂₉ alkane from the Stiffkey core samples.	293
Figure 8.17	Measured (red) and modelled (grey) carbon isotope composition of the n-C ₃₁ alkane from the Stiffkey core samples.	294
Figure 8.18	Measured (blue) and modelled (grey) hydrogen isotope composition of the n-C ₂₉ alkane from the Stiffkey core samples.	294
Figure 8.19	Measured (red) and modelled (grey) hydrogen isotope composition of the n-C ₂₉ alkane from the Stiffkey core samples.	295
Figure 8.20	Comparison of the output from IsoSource (yellow) with output from the Collins (1997) model (blue).	296
Figure 8.21	Modelled versus measured carbon isotope composition (A) and hydrogen isotope composition of n-C ₂₉ (B).	297
Figure 8.22	Ternary plot, IsoConc output	301
Figure 8.23	Modelled versus measured carbon isotope composition (A) and hydrogen isotope composition (B) of n-C ₂₉ .	302
Figure 8.24	Record of the isotopic and molecular composition of n- alkanes from the 1 m core collected in the UM at Stiffkey	305
Figure 8.25	Reconstruction of the hydrogen isotope composition of palaeoprecipitation from a 1 m sediment core from Stiffkey saltmarsh	307
Figure 8.26	Calculated hydrogen isotope composition of precipitation from surface sediments	312

List of Tables

Table 4.1	Plant species sampling strategy in June 2011, August 2011 and October 2011, Stiffkey saltmarsh	54
Table 4.2	Plant species sampling strategy followed between March 2012 and September 2012, Stiffkey saltmarsh	54
Table 4.3	Preparation of standards to quantify percentage recovery during extraction	59
Table 4.4	<i>n</i> -Alkane molecular data for species sampled at Stiffkey marsh, June, August and October 2011	61
Table 4.5	<i>n</i> -Alkane molecular data for species sampled at Stiffkey marsh, March-September 2012	62
Table 4.6	<i>n</i> -alkane concentrations (in µg per g of dry plant material) for species sampled in 2011	69
Table 4.7	<i>n</i> -alkane concentrations (in µg per g of dry plant material) for species sampled in 2012	70
Table 5.1	Carbon isotope fractionations associated with photosynthesis (sourced from O'Leary, 1988)	96
Table 5.2	Environmental factors influencing the carbon isotope composition of C ₃ plants (reproduced from Arens <i>et al</i> , 2000, plus data from Guy and Wample, 1982). Factors thought potentially significant at Stiffkey marsh are highlighted in red	102
Table 5.3	Carbon isotope composition of <i>n</i> -alkanes (<i>n</i> -C ₂₇ , <i>n</i> -C ₂₉ , <i>n</i> -C ₃₁ , weighted average) and bulk plant tissue, sampled during the 2011 growing season	114
Table 5.4	Carbon isotope composition of <i>n</i> -alkanes (<i>n</i> -C ₂₇ , <i>n</i> -C ₂₉ , <i>n</i> -C ₃₁ , weighted average) and bulk plant tissue, sampled during the 2012 growing season	115
Table 5.5	Carbon and nitrogen percentage composition of plant biomass; C:N ratio and δ ¹⁵ N ratios of bulk leaf tissue	129
Table 5.6	Bulk and <i>n</i> -alkane carbon isotope composition from plants growing in multiple sub-habitats at Stiffkey (October 2011)	135
Table 6.1	δ ² H for <i>n</i> -alkanes and leaf water, and calculated hydrogen isotope fractionation; June 2011	168
Table 6.2	δ ² H for <i>n</i> -alkanes, leaf water, soil water and xylem water, with calculated hydrogen isotope fractionation between soil water (sw), xylem water (xw) and leaf water (lw)	169
Table 7.1	² H/ ¹ H of phytol	218
Table 7.2	² H/ ¹ H of FAMES from the Stiffkey species, September 2012	221

Table 7.3	Results from starch accumulation tests	224
Table 7.4	Starch hydrogen isotope data	227
Table 7.5	Bulk plant tissue $^2\text{H}/^1\text{H}$	229
Table 8.1	Concentration in $\mu\text{g g}^{-1}$ dry mass of <i>n</i> -alkane homologues produced by Stiffkey species, September 2012	272
Table 8.2	Original percentage inputs of the 7 saltmarsh species from September 2012, compared with modelled percentage inputs used to test the impact of Scenario 1	275
Table 8.3	Original percentage inputs of the 7 saltmarsh species from September 2012, compared with modelled percentage inputs used to test the impact of Scenario 2	277
Table 8.4	Input criteria used with the Collins model	290
Table 8.5	Seasonally averaged carbon and hydrogen isotope values (data from 2011) used for modelling source apportionment using IsoConc	299
Table 8.6	Calculation of the concentration of hydrogen and carbon in the <i>n</i> -C ₂₉ contributed from each of the plant functional groups defined in this study	299
Table 8.7	Percentage inputs of each of the defined plant groups, defined by the IsoConc model	301
Table 8.8	Percentage contribution, epsilon values (relative to OIPC) sediment data and calculated $\delta^2\text{H}_{\text{PPT}}$ from October 2011	310

List of Abbreviations

A	Photosynthetic rate
ACL	Average chain length
C_a	CO ₂ partial pressure of atmosphere
CAM	Crassalucean acid metabolism
C_c	CO ₂ partial pressure in the chloroplast
C_i	CO ₂ partial pressure in the intercellular space
CPI	Carbon preference index
DOXP	1-deoxy-d-xylulose-5-phosphate
E	Transpiration
ε	Net apparent fractionation
FA	Fatty acid
FAE	Fatty acid elongase
FAME	Fatty acid methyl ester
FAS	Fatty acid synthase
g_m	Mesophyll conductance
g_s	Stomatal conductance
L	Effective path length
NADPH	Nicotinamide adenine dinucleotide phosphate
OD	Ordinance datum
OEP	Odd-over-even predominance
OM	Organic matter
PETM	Palaeocene/Eocene Thermal Maximum
PFT	Plant functional type/group
PSI	Photosystem I
PSII	Photosystem II
RuBP	Ribulose-1, 5-biphosphate
rH	Relative humidity
SOM	Soil organic matter
VLCFA	Very long chain fatty acid
WA	Weighted average <i>n</i> -alkane composition
WUE	Water use efficiency

Chapter 1

Introduction

As Earth's climate changes, there is a growing requirement to produce high-resolution records of past climatic shifts, to constrain models predicting the future impacts of rising CO₂ levels (Jones *et al.*, 2001; Beerling *et al.*, 2007; Diefendorf *et al.*, 2010; Schmittner *et al.*, 2011; Brannacot *et al.*, 2012). Anthropogenic influences on the carbon cycle are, however, potentially on a larger scale than those observed during Earth's recent past. This has required studies to focus instead on records from earlier geological epochs, where the climate was hotter and CO₂ levels higher, than conditions reported by modern observations and near instrumental records (e.g. Pagani *et al.*, 2006; Slujis *et al.*, 2006; Beerling *et al.*, 2007; Diefendorf *et al.*, 2010). Much remains to be discovered about how Earth and its ecosystems respond to environmental change, however. Key questions requiring further research include the way in which hydrological cycles (Schmidt, 2010; Brannacot *et al.*, 2012) and terrestrial ecosystems, respond to rapid changes in climate (Smith *et al.*, 2007; Diefendorf *et al.*, 2010). Furthering understanding of how ecosystems responded to changing environmental conditions through geological time is therefore crucial in order to accurately predict the effects of future climate shifts.

Traditional archives recording past climatic fluxes can have temporal and/or spatial limitations. Many lacustrine records, for example, date primarily from the Holocene or Pleistocene (Pancost and Boot, 2004). Ice cores, which record changes in the hydrological cycle, are generally limited to high altitude (e.g. Thompson *et al.*, 2003; Vimieux *et al.*, 2009) or high latitude (e.g. Andersen *et al.*, 2004) environments. Carbonate materials such as speleothems (e.g. Bar-Matthews *et al.*, 1997; McDermott, 2004; Matthey *et al.*, 2008; Van Rangelbergh *et al.*, 2013), soil carbonates (e.g. Cerling *et al.*, 1989; Cerling and Quade, 1993; Tipple and Pagani, 2007) or fossil bones/teeth (e.g. Quade *et al.*, 1992; Cerling and Sharp, 1996; Cerling *et al.*, 1997; Tipple and Pagani, 2007) can also be limited in their geographical range and temporal resolution (Freeman and Colorusso, 2001).

In recent decades, the search for a palaeoclimate proxy suitable for contexts where traditional archives are not available has been focused on lipid biomarkers. In particular, compounds originating from the epicuticular waxes coating leaves of terrestrial and aquatic higher plants (Fig. 1.1) have received considerable attention (e.g. Huang *et al.*, 2000; Schefuß *et al.*, 2005; Pagani *et al.*, 2006; Sachse *et al.*, 2012 and references contained therein). Compounds within the leaf wax matrix make a direct contribution to the organic fraction of soils and sediments via leaf fall and incorporation into the soil organic matter (SOM) profile (Lichtfouse *et al.*, 1994; Dawson *et al.*, 2004). These compounds are also present in the marine environment, as a result of river and wind transport (Schefuß *et al.*, 2003; Pancost and Boot, 2004). Once incorporated into the sedimentary record, leaf wax biomarkers show a high degree of resilience to degradation (Lightfouse *et al.*, 1994; Pancost and Boot, 2004; Buggle *et al.*, 2010), and have some, albeit limited, chemotaxonomic specificity (Rommerskirchen *et al.*, 2006). The molecular composition of leaf wax lipids therefore has the potential to provide valuable information for palaeoclimatic and palaeoecological studies.

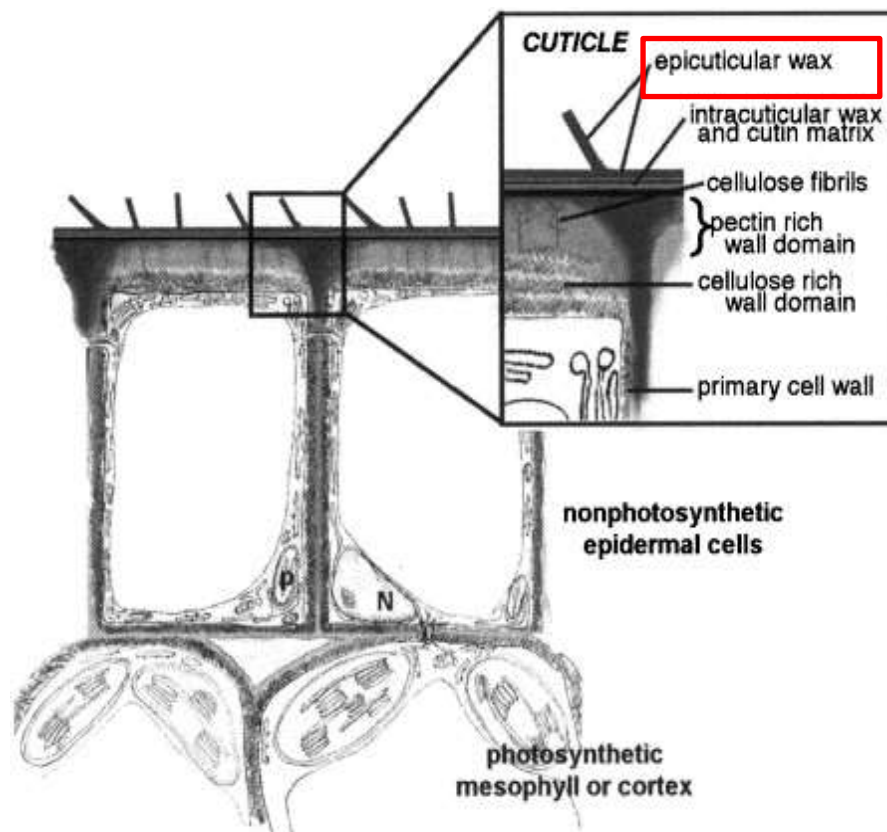


Figure 1.1: Illustration of a transverse view of wax secreting epidermal cells showing the components of the cuticle, cell wall domains, and the non-photosynthetic epidermal cell, highlighting the epicuticular wax layer in red (adapted from Kunst & Samuels, 2003).

With the advances in stable isotope methodologies since the 1990's (e.g. Hayes *et al.*, 1990; Sessions *et al.*, 1999; Meier-Augenstein, 1999), it is now also possible to perform routine analysis of the carbon and hydrogen isotopic composition of lipid biomarkers using gas-chromatography isotope ratio mass spectrometry (GC/IRMS). This methodological advancement has resulted in many studies utilising the carbon and hydrogen isotope composition of lipids from a range of photosynthetic organisms to recreate palaeohydrological and palaeoclimatic regimes (e.g. Huang *et al.*, 1999; Freeman and Colarusso., 2001; Pancost and Boot, 2004; Schefuß *et al.*, 2005; Pagani *et al.*, 2006; Tierney *et al.*, 2008, 2011). Leaf wax *n*-alkyl lipids have emerged as a key proxy in both marine (e.g. Freeman and Colarusso, 2001) and terrestrial (e.g. Tierney *et al.*, 2010) sedimentary sequences, and have been used to investigate palaeoclimate conditions dating back as far as the Cenomanian/Turonian boundary in the Cretaceous period (Kuypers *et al.*, 1999).

Outstanding questions remain to be explored, however, regarding the relative importance of environmental and biochemical mechanisms in controlling the molecular and isotopic information recorded by leaf wax *n*-alkanes. This has resulted in complications when seeking to distinguish plant physiological and/or biochemical effects from climate shifts in the sedimentary biomarker record. At present, this has effectively meant that biomarker-based palaeoclimate reconstructions tend to be qualitative in nature, rather than quantitative (Sachse *et al.*, 2012). To establish the rationale for the research areas to be addressed in this thesis, this chapter first provides an overview of the main palaeoclimate uses of leaf wax biomarkers and their associated limitations. A series of outstanding issues are then summarised, which lead directly into the main aims and objectives of the thesis. Finally, a summary of the thesis structure is provided.

1.1. THE USE OF LEAF WAX BIOMARKERS AS PALAEOCLIMATE PROXIES

1.1.1 A proxy for recreating palaeovegetation assemblages

The relative abundance of particular *n*-alkane homologues common to higher plants (e.g. *n*-C₂₁ to *n*-C₃₅; Eglinton *et al.*, 1962), and a range of calculated indices such as the average chain length (ACL), carbon preference index (CPI) and odd-over-even predominance (OEP) have been used to reconstruct patterns of surface vegetation from lipids extracted from sedimentary sequences (Liu *et al.*, 2005; Zhang *et al.*, 2006; Liu *et al.*, 2008; Bai *et al.*, 2009).

Ratios of the $n\text{-C}_{31}$, $n\text{-C}_{29}$ and $n\text{-C}_{27}$ alkanes to each other have also been frequently used in a palaeoclimate context to discriminate between woody and non-woody plant species, on the basis that woody plants have higher proportions of $n\text{-C}_{27}$ and $n\text{-C}_{29}$, while non-woody species are dominated by $n\text{-C}_{31}$ (Cranwell, 1973; Zech *et al.*, 2010; Yamamoto *et al.*, 2010; Schatz *et al.*, 2011; Bush and McInerney, 2013). Previous research into the vegetative history of the Carpathian basin, for example, used n -alkane data to distinguish time intervals (between 26 and 12 ka BP) where steppe vegetation was dominant over trees (Schatz *et al.*, 2011). A similar methodological approach was used by Zech *et al.* (2010) when examining a 240 kyr permafrost palaeosol sequence from Siberia. In this study, a suite of different n -alkane ratios, including $n\text{-C}_{29}/n\text{-C}_{27}$, $n\text{-C}_{31}/n\text{-C}_{27}$, and $n\text{-C}_{31}/n\text{-C}_{29}$ were used, in conjunction with pollen data, to detect shifts in surface vegetation. Zech *et al.* (2010) identified shifts from larch forests to steppe tundra during the Weichselian glaciations, with reforestation occurring during the Late Glacial/early Holocene.

Zhang *et al.* (2006) also used n -alkane distribution ratios to produce palaeovegetational profiles for the Loess Plateau of China. This study considered the concentration, distribution, carbon preference index (CPI), average chain length (ACL) and the ratios of specific alkanes ($n\text{-C}_{31}/(n\text{-C}_{29}+n\text{-C}_{31})$) to examine interglacial and glacial vegetation dynamics recorded in Loess sequences. Working on the premise that leaf waxes from woody plants are dominated by $n\text{-C}_{27}$ and/or $n\text{-C}_{29}$ whereas grasses have $n\text{-C}_{31}$ as their most abundant chain length, Zhang *et al.* (2006) concluded from the molecular distribution of n -alkanes in Loess Plateau sequences that the vegetation history of the study site had remained constant over 170 kyr, with grasses remaining dominant. Some increases in tree numbers were also inferred from increased $n\text{-C}_{27}$ and $n\text{-C}_{29}$ contributions, particularly during cold stages (Zhang *et al.*, 2006).

Recent studies have injected a note of caution however, suggesting that reliance on leaf wax molecular distribution patterns and indices to identify vegetation shifts from sedimentary n -alkanes may not be valid. Bush and McInerney (2013), for example, highlighted that n -alkane distribution patterns can vary to such an extent across plant species that considerable care is required when seeking to identify different chemotaxonomic groups. This study confirmed the earlier findings of Bush *et al.* (2012), who showed that ratios of $n\text{-C}_{27}$, $n\text{-C}_{29}$ and $n\text{-C}_{31}$ were ineffective in discriminating between graminoids and other woody plants. In addition, molecular distribution indices such as ACL and CPI have been shown to display such random

variation that Bush and McInerney (2013) concluded they should not be used to describe palaeovegetation sequences.

1.1.2 A proxy for tracing plant-environment interactions

Analysis of the carbon isotope composition of leaf wax biomarkers has become widespread in studies seeking to recreate palaeoecological and palaeoclimatic conditions (e.g. Pancost and Boot, 2004; Eglinton and Eglinton, 2008). Leaf wax *n*-alkane $\delta^{13}\text{C}$, for example, can be used in a similar fashion to measurements of bulk plant material to reconstruct relative percentages of C_3 and C_4 vegetation. Bull *et al.* (1999) demonstrated this, producing a mixing model to describe the relative inputs of C_3 and C_4 grasses (*Spartina anglica* and *Puccinella maritima*) to modern saltmarsh sediments. Schefuß *et al.* (2003) used a similar approach, here applying binary mixing models based on *n*-alkane $\delta^{13}\text{C}$ to determine the vegetative source of organic compounds in central east African dusts, and thus defining atmospheric circulation patterns. They found that C_4 plants growing in the Sahara, the Sahel and Gabon supplied most of the C_4 -derived organic matter (OM) in these aerosols (Schefuß *et al.*, 2003). The use of this method to trace the rise and spread of C_4 species from ancient leaf wax lipids preserved in the geological record is also well established, and illustrated by studies such as Huang *et al.* (2000), Freeman and Colorusso (2001), and Tipple and Pagani (2007).

Changes in palaeovegetation sequences, including shifts from C_3 to C_4 vegetation and vice versa, can in turn be related to climatic factors such as aridity, rainfall, and $p\text{CO}_2$ (Ratnayake *et al.*, 2006). Sinninghe Damsté *et al.* (2011) used the carbon isotope composition of *n*- C_{27+} alkanes from fossil plant leaf waxes to reconstruct vegetation profiles from Lake Challa, in equatorial Africa during the last glacial cycle. Records indicate that C_4 species dominated during the glacial period, with a shift towards a mixed C_3/C_4 assemblage occurring during the Holocene. A C_4 -dominant trend was also observed during the Younger Dryas period (13.0 – 11.7 cal kyr BP). Sinninghe Damsté *et al.* (2011) linked these data to shifts in $p\text{CO}_2$, suggesting C_4 plants dominated during glacial periods (lower CO_2 concentrations), with C_3 plants resurgent during the Holocene (higher CO_2 concentrations). Castaneda *et al.* (2009) used a similar approach to identify periods during the last 192,000 years where the plume of dust transported to the oceans from the Sahara contained significant contributions from C_3 species. These increases in C_3 input coincided with the wetter climates of the African Humid Period (Castaneda *et al.*, 2010).

A suite of studies of the Paleocene-Eocene Thermal Maximum (PETM) further demonstrate the appeal (and potential complexity) of using the carbon isotope composition of leaf wax *n*-alkyl lipids to investigate changes in climate through deep geological time. Many studies utilising other proxies such as soil carbonates and marine carbonates have identified a negative carbon isotope excursion (CIE) occurring during the PETM, thought to be (at least in part) due to a substantial release of ¹³C-depleted carbon and associated global warming (Dickens *et al.*, 1995; Zachos *et al.*, 2005; Pagani *et al.*, 2006a). To investigate hydrological and climatic conditions during this event, Pagani *et al.* (2006b) analysed *n*-alkanes from terrestrial plants and aquatic organisms extracted from an Arctic Ocean marine core. They observed a CIE in terrestrial plant *n*-alkanes of -4.5 to -6‰, well in excess of shifts in the marine carbonate signal (~ 2.5 to 3‰). The modelled environmental conditions prevalent at the Arctic sampling location precludes previous explanations of this offset which are based on the physiological response of plants to higher levels of humidity (Pagani *et al.*, 2006b). Instead, Pagani *et al.* (2006b) suggest their plant leaf wax $\delta^{13}\text{C}$ data indicate the release of almost double the previously estimated amount of carbon into the atmosphere. Smith *et al.* (2007) also analysed PETM sedimentary lipids from Bighorn Basin in Wyoming. This study, however, offers an alternative explanation for the relative magnitude of the CIE observed in leaf wax lipids. Here, the authors suggest that changes in plant communities, in particular a shift from mixed angiosperm/conifer assemblages to purely angiosperm assemblages, could result in amplification of the CIE contained within these biomarkers (Smith *et al.*, 2007).

The study of Handley *et al.* (2008) provides a valuable additional illustration of some of the complexities encountered when interpreting *n*-alkane $\delta^{13}\text{C}$. Data presented in this study suggests that climatic conditions in East Africa during the PETM veered toward higher temperatures and increased evaporation, rather than elevated humidity. Interestingly in light of the discussion in 1.1.1, attempts by Handley *et al.* (2008) to utilise ACL values to identify any vegetation change were somewhat confounded by the fact that ACL can shift in response to both changes in plant community structure and temperature/aridity. Interpretation of *n*-alkane $\delta^{13}\text{C}$ was further complicated by the fact that different alkane chain lengths recorded different magnitudes of CIE, with highest found in the *n*-C₂₉ record, and the lowest in that reported for *n*-C₃₁. Handley *et al.* (2008) could not fully account for this phenomenon, but speculated that it could result from these alkanes being derived from different sources.

The need to further constrain mechanisms controlling *n*-alkane carbon isotope composition is emphasised by those studies assuming the same processes control $\delta^{13}\text{C}$ at the bulk and specific compound level. While previous work on C_3 plants has shown a clear link between climatically influenced plant physiology and bulk $\delta^{13}\text{C}$ values (e.g. Farquhar *et al.*, 1989; Ehleringer *et al.*, 1992; Dawson *et al.*, 2002), further research is needed to establish whether the same link can be seen in leaf wax biomarkers. Despite this limitation, some recent studies have used bulk and *n*-alkane $\delta^{13}\text{C}$ interchangeably to explore plant-environment interactions. Diefendorf *et al.* (2010), for example, set out to consider global trends in carbon isotope discrimination ($\Delta^{13}\text{C}$) across a range of biomes. This study compiled a large $\delta^{13}\text{C}$ dataset from previous publications, and used these to derive typical $\Delta^{13}\text{C}$ ranges for key biome types (Fig. 1.2).

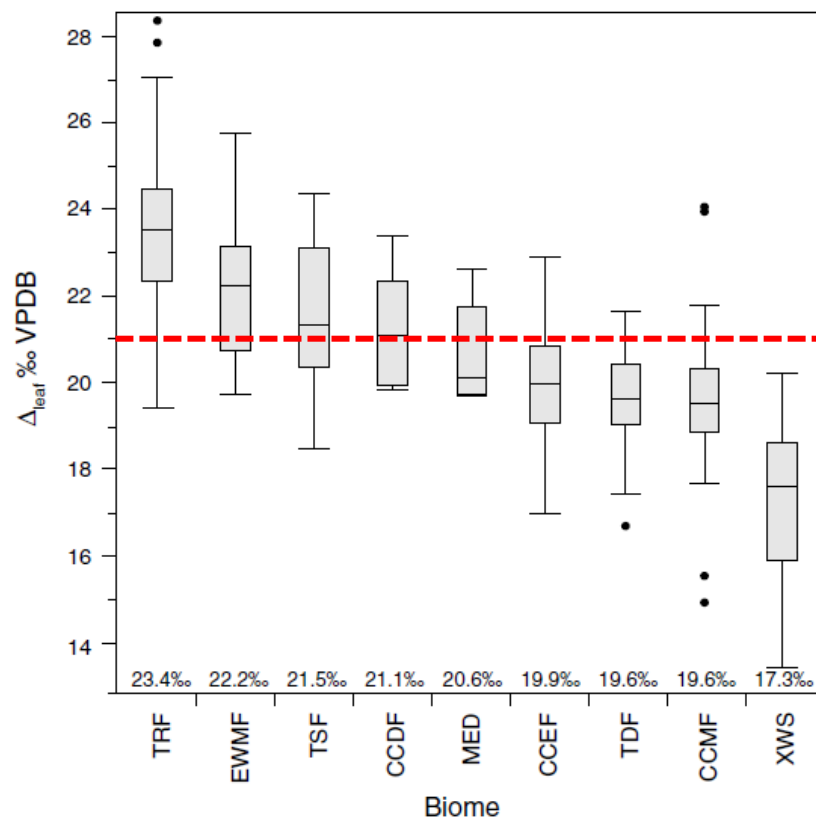


Figure 1.2: Box and whisker plots of leaf values by biome. Biome accounts for 66% ($p < 0.0001$) of the variability in $\Delta^{13}\text{C}$ leaf in an ANOVA model. Abbreviations: tropical rain forest (TRF), evergreen warm mixed forest (EWMF), tropical seasonal forest (TSF), cool-cold deciduous forest (CCDF), cool-cold evergreen forest (CCEF), cool-cold mixed forest (CCMF), tropical deciduous forest (TDF), xeric woodland scrubland (XWS) (Diefendorf *et al.*, 2010). The red dashed line illustrates the extent of the variability in this study, with $\Delta^{13}\text{C}$ value of 21‰ falling within the EWMF, TSF, CCDF and MED biomes.

This study used both *n*-alkane and bulk $\delta^{13}\text{C}$ for this purpose, applying a fixed correction factor to adjust for the fact that *n*-alkanes are ^{13}C -depleted versus bulk tissue. Fig. 1.2 shows, however, that there is considerable variability in the $\Delta^{13}\text{C}$ values proposed for each defined biome type. Without further study to understand environmental and biochemical controls on *n*-alkane $\delta^{13}\text{C}$, it is difficult to establish whether using these values interchangeably with bulk tissue contributed to this variability.

1.1.3 A proxy for hydrological change

Reconstructing past hydrological change is an important consideration for future climate models, and hence the interest in leaf wax biomarkers as palaeohydrological proxies is growing. A particular focus of recent research is on tropical areas where a paucity of data (e.g. the limited geographical range of ice cores; Thompson *et al.*, 2003; Andersen *et al.*, 2004; Vimieux *et al.*, 2009) limits understanding of hydrological regimes (Tierney *et al.*, 2008, 2011). Leaf wax biomarkers have been considered to be “direct recorders” of hydrological conditions at the continental scale (Schefuß *et al.*, 2005), and are thought to integrate influences ranging from source water $\delta^2\text{H}$, evaporation, precipitation amount and vapour sources (Leider *et al.*, 2013). All of these factors can vary in importance, however, depending upon the particular depositional environment (e.g. lacustrine, marine) under consideration (Leider *et al.*, 2013).

The hydrogen isotope composition of sedimentary leaf wax biomarkers has been used both to reconstruct the hydrogen isotope composition of palaeoprecipitation (e.g. Pagani *et al.*, 2006b; Niedermeyer *et al.*, 2010; Schefuß *et al.*, 2011; Feakins *et al.*, 2012; McGill *et al.*, 2013), and to investigate the availability of moisture (e.g. Schefuß *et al.*, 2005; Tierney *et al.*, 2008; McGill *et al.*, 2013; Terwilliger *et al.*, 2013). Leaf wax lipid $^2\text{H}/^1\text{H}$ ($\delta^2\text{H}_{\text{wax}}$) has been used to recreate hydrological regimes over many different temporal scales, ranging from the Holocene (e.g. Liu and Huang, 2005), Quaternary (e.g. Huang *et al.*, 2002; Tierney *et al.*, 2011), Miocene (e.g. Yang and Huang, 2003), Eocene (e.g. Hren *et al.*, 2010; Tipple and Pagani, 2010), and the Palaeocene-Eocene Thermal Maximum (PETM) ~55 million years ago (Pagani *et al.*, 2006b; Tipple *et al.*, 2011). This section will first summarise the factors influencing global patterns of precipitation $\delta^2\text{H}$ values, before detailing how leaf wax lipids are currently being applied in temperate and tropical zones.

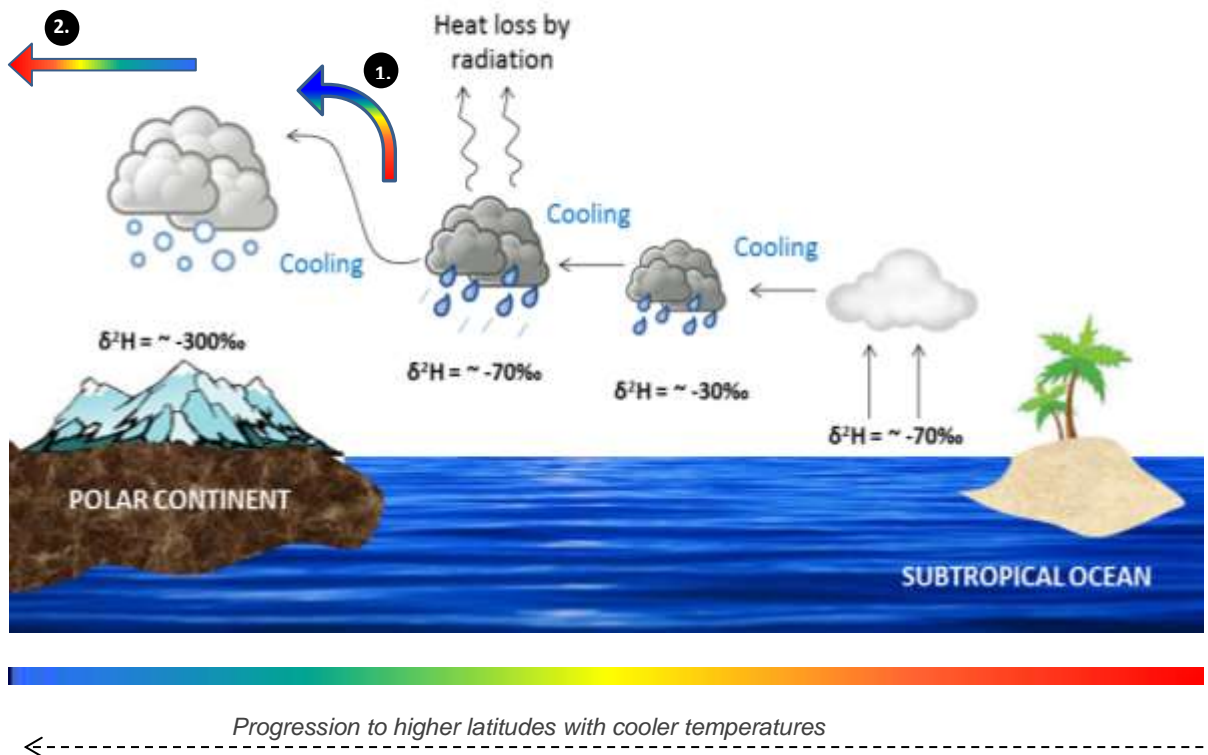


Figure 1.3: Schematic illustration of the fractionation of water in a cloud as a function of Rayleigh distillation. The cloud forms at the equator (where the evaporated water will be depleted in ^2H relative to sea water) and moves to higher latitudes losing water, which is enriched in ^2H , resulting in the $^2\text{H}/^1\text{H}$ value of the cloud becoming lower. As the cloud moves pole-ward, its isotope composition becomes more ^2H -depleted and as the temperature falls, the fractionation factor increases so that precipitation over the poles will have extremely low $^2\text{H}/^1\text{H}$. Additional factors that influence the $^2\text{H}/^1\text{H}$ of precipitation include orographic uplift (1) and the continental effect (2), expanded upon further in the text below (adapted from Allègre, 2008).

1.1.3.1 Summary of factors influencing precipitation $^2\text{H}/^1\text{H}$

In high latitude regions, the $\delta^2\text{H}$ of rainwater is driven by a progressive deuterium depletion that is coeval with a reduction in temperature (Dansgaard, 1964; Pagani *et al.*, 2006b; Allègre, 2008; Niedermeyer *et al.*, 2010). Figure 1.3 presents a schematic depiction of the fractionation associated with: (i) the evaporation of water; (ii) the formation of clouds; and (iii) the movement of clouds to high latitudes which incorporates processes such as distillation (following Rayleigh's law) within the clouds (Allègre, 2008). As the clouds move toward the poles, temperature decreases (and therefore fractionation increases), whilst distillation becomes more effective, resulting in the highly depleted isotope values identified at the pole itself (Allègre, 2008) (Fig. 1.3). Additional influences on the isotopic composition of

precipitation include orographic effects (Fig. 1.3), where the upward transport of clouds over a mountain range results in increased condensation and enhanced rainout of the heavier isotopes, prior to clouds moving inland (Allègre, 2008). Continental effects have also been observed, where the centre of a large land mass or continent typically receives precipitation that is depleted in ^{18}O and ^2H . This is a result of the fact that isotopically enriched rain forms and falls from a diminishing vapor mass as clouds move across a continent, driving increasing depletion in the residual vapour and ^2H -depleted rainfall as the cloud moves inland (Allègre, 2008) (Fig. 1.3).

In the tropics, the isotopic composition of rainwater is not purely a function of temperature gradients as in high latitudes (Allègre, 2008). Rather, it is a factor of precipitation amount, such that rainout events control the extent of re-evaporation and ^2H -enrichment of precipitation (Dansgaard, 1964; Tierney *et al.*, 2008; Niedermeyer *et al.*, 2010; Terwilliger *et al.*, 2013). Where high rainfall events occur, the extent of re-evaporation is limited, and hence precipitation $\delta^2\text{H}$ is relatively low, while the reverse is true of areas with lower rainfall amounts (Niedmeyer *et al.*, 2010; Douglas *et al.*, 2012).

1.1.3.2 Using leaf waxes to reconstruct the $\delta^2\text{H}$ of precipitation in temperate regions

In high latitude regions, the $^2\text{H}/^1\text{H}$ signal of leaf wax compounds has been used to reconstruct the isotopic composition of rainfall from important climatic events such as the PETM (Pagani *et al.*, 2006b). This study relied on the assumption of a consistent net apparent fractionation (ϵ_{net}) between source water and leaf wax *n*-alkanes of -130 to -100‰ for higher plants, and used these values to calculate rainfall $^2\text{H}/^1\text{H}$ values ranging from -125 to -95‰ prior to the PETM, shifting to -65 to -30‰ during the early stages of the event. Feakins *et al.* (2012) also used leaf wax *n*-alkyl lipid $^2\text{H}/^1\text{H}$ values to reconstruct the isotopic composition of precipitation falling over the margins of Antarctica during the mid-Miocene. Average *n*-C₂₈ fatty acid $\delta^2\text{H}$ (ranging from -165 to -121‰) was used to determine precipitation hydrogen isotope composition using a fixed $\epsilon_{\text{lipid/water}}$ value of $-121 \pm 2\%$ originally derived for the *n*-C₂₉ alkane, adjusted further to account for $\epsilon_{\text{acid/alkane}}$ of 25‰ (Feakins *et al.*, 2012). Using these values for ϵ , Feakins *et al.* (2012) proposed that precipitation over the Antarctic margin had a hydrogen isotope composition of $\sim -50\%$, indicative of temperatures some 11 °C warmer than present.

1.1.3.3 Using leaf waxes to reconstruct the $\delta^2\text{H}$ of precipitation in tropical regions

In tropical environments, the sedimentary leaf wax biomarker $^2\text{H}/^1\text{H}$ signal has been interpreted as reflecting the shifts in moisture availability driven by changes in precipitation amount (e.g. Schefuß *et al.*, 2011), as factors such as aridity are thought to exert an important second-order effects over the relationship between the hydrogen isotope composition of precipitation and the $^2\text{H}/^1\text{H}$ signal recorded by leaf waxes (e.g. Tierney *et al.*, 2010, 2011). Such reconstructions are based on the assumption that lower relative humidity has the potential to increase evaporation of soil and/or leaf water, resulting in ^2H -enriched water available for lipid biosynthesis (Niedermeyer *et al.* 2010; Schefuß *et al.*, 2011). Schefuß *et al.* (2005), for example, concluded that $\delta^2\text{H}_{\text{wax}}$ recorded a balance between precipitation and evaporation, with higher rainfall resulting in relatively low leaf wax $\delta^2\text{H}$ values, while increasing aridity was paralleled by relatively high leaf wax $\delta^2\text{H}$ values.

Leaf water $^2\text{H}/^1\text{H}$ is typically ^2H -enriched relative to meteoric water (e.g. Flanagan *et al.*, 1991; Flanagan and Ehleringer, 1991; Smith and Freeman, 2006). In tropical climates, this deuterium enrichment is enhanced by the influence of soil evaporation, and transpiration from leaves occurring in dry and arid conditions (Smith and Freeman, 2006; Douglas *et al.*, 2012). However, debate remains as to the extent that leaf wax *n*-alkanes record this transpiration signal, and hence the value of $\delta^2\text{H}_{\text{wax}}$ as a palaeoaridity proxy remains to be fully established. Grasses grown in controlled greenhouse conditions, for example, indicate that transpiration is not a major control on $\delta^2\text{H}_{\text{wax}}$ (McInerney *et al.*, 2011). In contrast, other studies of trees and grasses have found that transpiration can be an important factor influencing $\delta^2\text{H}_{\text{wax}}$ (e.g. Feakins and Sessions, 2010; Kahmen *et al.*, 2012). From the perspective of palaeoclimate reconstruction, many studies continue to assume that leaf waxes in arid environments generally record this evaporative signal despite the conflicting findings from modern plants (e.g. Leider *et al.*, 2013).

1.1.3.4 Can biochemical mechanisms influence leaf wax $^2\text{H}/^1\text{H}$?

In 2012, Sachse *et al.* (2012) reviewed factors controlling isotopic fractionation between environmental water and lipids from phototrophic organisms (Fig. 1.4). They found that net apparent fractionation of $^2\text{H}/^1\text{H}$ between source water and lipid can be influenced by biochemical, physical and environmental factors. Relatively

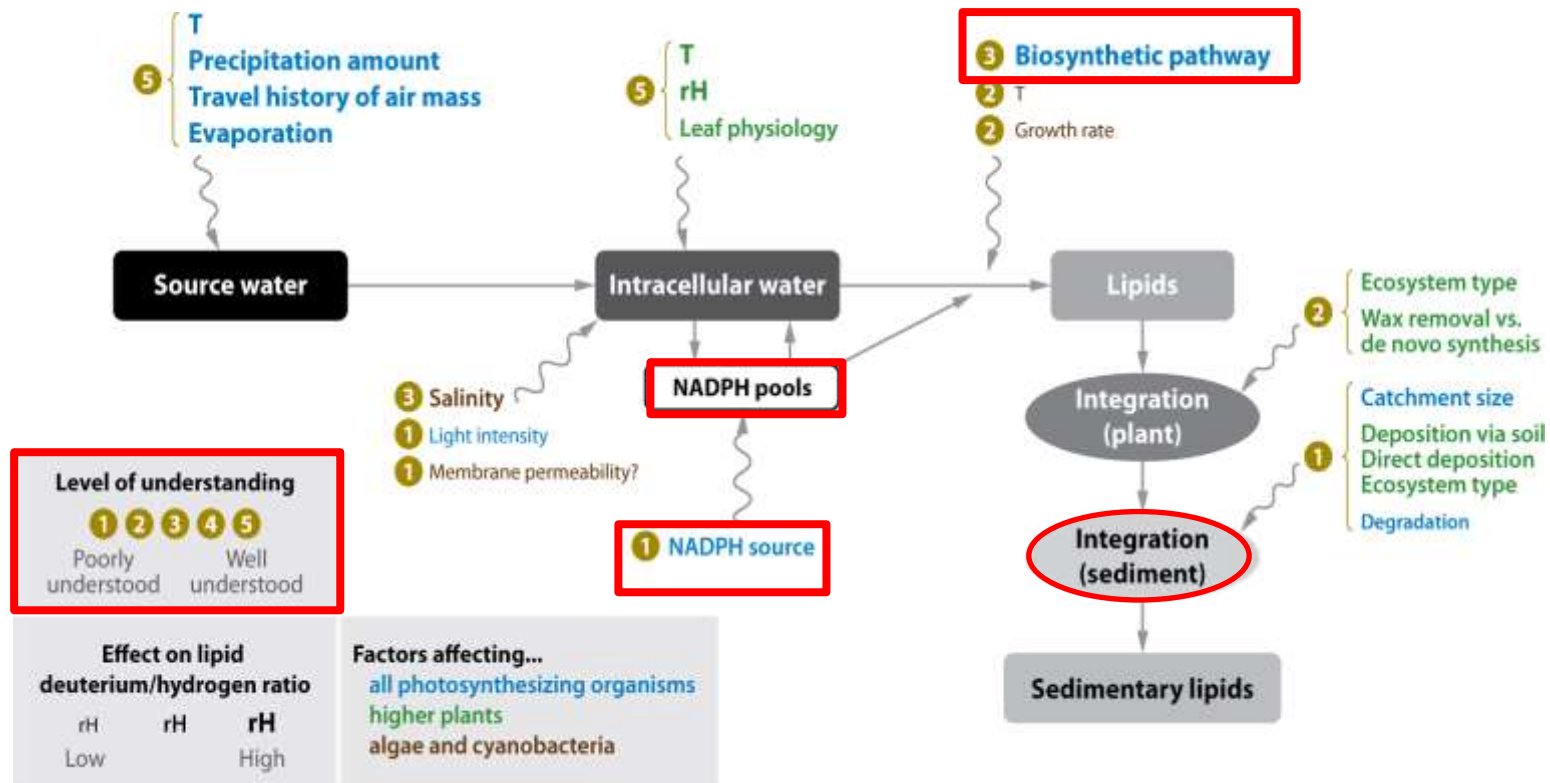


Figure 1.4: Overview of the processes affecting hydrogen isotopic-composition of lipid biomarkers from phototrophic organisms. Abbreviations: H, Hydrogen; NADPH, nicotinamide adenine dinucleotide phosphate (reduced); rH, relative humidity; T, Temperature (Sachse et al., 2012). Note the “level of understanding” ascribed to each of the various processes (highlighted in red) and the fact that the importance of NADPH sources and pools, and biochemical pathways, remain poorly understood. This figure also highlights that the factors influencing the integration of leaf wax biomarkers into sediments also require further investigation.

few studies have given detailed consideration to the influence of biochemistry on leaf *n*-alkane $^2\text{H}/^1\text{H}$. Typically, it forms a speculative hypothesis to explain a lack of correlation between measured and/or modelled leaf water and leaf wax hydrogen isotope compositions (e.g. Feakins and Sessions, 2010; Kahmen *et al.*, 2013). Sachse *et al.* (2012) acknowledge that the importance of biochemical processes remains very poorly constrained (Fig. 1.4), limiting the accuracy of palaeohydrological reconstruction from lipid biomarkers.

1.1.4 The incorporation of leaf wax lipids into the sedimentary record

Fig. 1.4 highlights that in addition to constraining the relative importance of environmental and biochemical mechanisms in controlling the carbon and hydrogen isotope composition of leaf wax lipids, practical considerations relating to the incorporation of biomarkers into the sediment record also require further investigation (Sachse *et al.*, 2012).

Analysis of sedimentary lipids requires consideration of the dynamics of spatial and temporal integration of OM, including leaf wax biomarkers, into the geological record (Jacob *et al.*, 2007). This is an area where a large number of outstanding questions remain, such as the size of the catchment, the significance of direct deposition from atmospheric dusts, and the importance of ecosystem type (Jacob *et al.*, 2007; Sachse *et al.*, 2012) (Fig.1.4). At present, with the exception of peat deposits (e.g. Seki *et al.*, 2009; Nichols *et al.*, 2010; Brader *et al.*, 2010), leaf wax biomarkers extracted from sediments generally cannot be attributed to individual species. Instead, it is accepted that they are likely to originate from a mixture of plants across varied spatial scales, ranging from small catchments to large river basins (Sachse *et al.*, 2012) (Fig. 1.4). This inability to define detailed source inputs from particular species, or indeed plant functional groups, can potentially cause complications when seeking to recreate past climate regimes from sedimentary biomarkers. In particular, it renders the influence of vegetation change difficult to decouple from the influence of changing climates (e.g. Nelson *et al.*, 2013).

To date, methods for identifying, quantifying and correcting for vegetation change when reconstructing past environments are generally limited to examination of *n*-alkane carbon isotope composition (Schefuß *et al.*, 2005; Tierney *et al.*, 2011), or other proxies such as pollen (Feakins, 2013). However, it is possible that carbon isotope values will not capture shifts in the relative assemblage of C_3 plant species, while pollen distribution and preservation bias may add uncertainty to palaeoclimate reconstructions if it is used to correct leaf wax biomarker signals (Feakins, 2013).

New approaches are therefore required to ensure that vegetation change can be decoupled from climate shifts when interpreting sedimentary leaf wax biomarker data.

1.2 SUMMARY OF OUTSTANDING QUESTIONS

The previous discussion illustrates that a range of issues remain to be explored regarding the use of leaf wax *n*-alkanes in palaeoclimate reconstructions. For example, the chemotaxonomic potential of molecular distribution indices (e.g. ACL, CPI, Section 1.1.1) has been called into question by recent studies that show that variability can be too high to allow for successful recreation of palaeovegetation sequences (Bush and McInerney, 2013). The carbon isotope composition of *n*-alkanes also requires further investigation to look in detail at the extent to which the *n*-alkane $\delta^{13}\text{C}$ signal faithfully replicates bulk tissue carbon isotope composition (Section 1.1.2). At present, it is assumed that environmental factors such as water availability are recorded in shifts in *n*-alkane $\delta^{13}\text{C}$ in a manner analogous to that of bulk tissue (e.g. Tipple and Pagani, 2007; Diefendorf *et al.*, 2010). The limited studies that have considered linked bulk and compound-specific carbon isotope analysis of the same plant, however, suggest that this may not be valid given the array of interlinked cellular metabolic processes (van Dongen *et al.*, 2011) which could influence the flow of carbon through biosynthetic pathways (e.g. Dungait *et al.*, 2008, 2010, 2011; Tcherkez *et al.*, 2011; Cernusak *et al.*, 2013).

Another key area where additional research is required relates to the use of *n*-alkane $^2\text{H}/^1\text{H}$ as a palaeohydrological proxy. Interpretation of the sedimentary biomarker $\delta^2\text{H}$ signal requires detailed understanding of the mechanisms controlling hydrogen isotope fractionation between source water and *n*-alkyl lipids ($\epsilon_{l/w}$). The existence of large ranges in published *n*-alkyl $\delta^2\text{H}$ and $\epsilon_{l/w}$ among modern plant species growing at a single location (e.g. Pedentchouk *et al.*, 2008) complicates interpretation of lipid hydrogen isotope data from the geological record, as the mechanisms responsible for these interspecies differences are poorly constrained. Previous research has had limited success explaining *n*-alkyl $\delta^2\text{H}$ by reference to physical processes controlling the movement of water inside/outside and within the leaf, while the relative importance of biochemical processes remains largely unexplored (Section 1.1.3; Fig. 1.4). Finally, the previous discussion illustrates that it is also necessary to evaluate the influence that the magnitude of interspecies variation in *n*-alkane $^2\text{H}/^1\text{H}$, coupled with variability in *n*-alkane production among different plant species, can have on the fidelity of the sedimentary record (Section

1.1.4). Significant differences in alkane production and hydrogen isotope fractionation suggest that the lipid signal incorporated into the sedimentary record could be sensitive to relatively small-scale changes in vegetation assemblages, and new methods are required to identify and address this issue.

1.3 AIMS AND OBJECTIVES OF THESIS

To advance this field and address the outstanding issues identified in Section 1.2, the *overarching aim* of this thesis is to **evaluate the relative importance of environmental and biochemical mechanisms in controlling the information recorded in the molecular distribution and stable isotope composition of leaf wax *n*-alkanes** of seven saltmarsh plants growing in a temperate coastal ecosystem. These plants have a global distribution in coastal ecosystems, and have physical and biochemical adaptations to their environment that are common across a range of diverse biomes where plants experience environmental stresses (Bohnert and Jensen, 1996). The findings of this study therefore have broad implications for palaeoclimatic reconstruction, not only for plants growing in diverse coastal habitats, but for any location where plants display biochemical adaptive responses to external stress.

In addition to this, a *secondary aim* is to **evaluate how sensitive the sedimentary *n*-alkane $^2\text{H}/^1\text{H}$ record is to changes in the overlying plant communities at the saltmarsh site**. The selection of Stiffkey saltmarsh as the study location for this project offers a complex setting to test the key assumptions relating to the incorporation of leaf wax biomarkers into sediments. There is the potential that sediment accretion will contain both local biomarkers (from the surface vegetation studied as part of this project) and imported organic material which is likely to originate from sedimentary sinks to the east of the study site (discussed further in Chapter 2 and Chapter 8). Local-scale sedimentary transport, including the continued removal and redistribution of material with tidal influxes (especially during storms and spring tides, Chapter 2) also has the potential to influence the leaf wax biomarker content of sediments across the marsh.

Despite this complexity, the in-depth organic geochemical characterisation of *n*-alkanes from plants at Stiffkey, coupled with analysis of sedimentary leaf wax lipids, offers a valuable opportunity for: (i) understanding the incorporation of plant *n*-alkanes into local sediments; and (ii) demonstrating the complexity of linking overlying vegetation to sedimentary biomarker signals. As saltmarshes store more

organic matter than any other terrestrial or coastal biome (Duarte *et al.*, 2005), understanding leaf wax biomarker dynamics in such locations is also crucial for studies of other marine depositional environments.

1.3.1 Specific objectives

In order to achieve the aim of this thesis, a series of specific objectives have been developed. These include:

1. Evaluate the extent of variability in leaf wax *n*-alkane concentration and composition among seven saltmarsh plants, both spatially across the marsh sub-environments, and temporally across a growing season.
2. Quantify the extent of variability in bulk and leaf wax *n*-alkane $\delta^{13}\text{C}$ signatures across a range of C_3 and C_4 species growing at a temperate coastal saltmarsh, and to identify whether they are being influenced by the same biochemical and environmental factors.
3. Investigate whether differences in the $^2\text{H}/^1\text{H}$ of leaf water (driven by mechanisms that control the movement of water molecules inside, outside and within the leaf) can account for interspecies variation in *n*-alkane $^2\text{H}/^1\text{H}$ among seven saltmarsh plants.
4. Identification of potential biochemical mechanisms which may account for interspecies variation in *n*-alkane $^2\text{H}/^1\text{H}$ among the saltmarsh plants.
5. Investigate the sensitivity of the Stiffkey sedimentary record to changes in surface plant cover, and evaluate approaches to identifying and quantifying vegetation change.

1.4 STRUCTURE OF THESIS

This thesis comprises of nine chapters. **Chapter 2** presents a detailed description of the study site, Stiffkey Marsh, where all plant and sediment samples analysed for this study have been collected. **Chapter 3** provides an overview of the nature, composition and synthesis of leaf wax *n*-alkanes, highlighting areas where further research is required to map the precise biochemical pathways generating these compounds. In **Chapter 4**, *n*-alkane distribution and concentration data from seven saltmarsh plants (including succulents, monocots, and dicots) spanning two growing seasons is presented. This chapter examines whether molecular distribution patterns show sufficient chemotaxonomic specificity for use as palaeovegetation

proxies, evaluating the effectiveness of distribution indices such as ACL and CPI. Chapter 4 then quantifies the amount of *n*-alkanes produced by the sampled species, and identifies differences of an order of magnitude in the concentration of key homologues produced. These findings add to recent studies that have reported variability in *n*-alkane concentrations among angiosperms and gymnosperms (Diefendorf *et al.*, 2011), by demonstrating that variability in *n*-alkane production is also an issue among angiosperms growing in a single geographical location.

Chapter 5 investigates interspecies variation in the carbon isotope composition of bulk tissue and leaf wax *n*-alkanes from the Stiffkey plants, and discusses whether the *n*-alkane $\delta^{13}\text{C}$ signal faithfully tracks the signal contained in bulk tissue. Results show that bulk and *n*-alkane $\delta^{13}\text{C}$ does not follow the same seasonal patterns in all species. This chapter discusses whether post-photosynthetic fractionation, potentially arising from the allocation of the precursor pyruvate to other metabolic pathways in response to seasonal changes in environmental conditions, may be being recorded in *n*-alkane carbon isotope ratios. **Chapter 6** presents linked analysis of soil water, xylem water, leaf water, and *n*-alkane hydrogen isotope composition from the saltmarsh plants to evaluate the extent to which environmental and physical mechanisms that control the flow of water into and out of a leaf can account for interspecies variation in *n*-alkane $^2\text{H}/^1\text{H}$. This chapter makes a novel contribution to knowledge, establishing that for these species, biochemical mechanisms have a greater influence over *n*-alkane $^2\text{H}/^1\text{H}$ than environmental processes. **Chapter 7** builds on the findings of Chapter 6 and makes the first exploratory study of biochemical mechanisms that have the potential to influence *n*-alkane $^2\text{H}/^1\text{H}$. By analysing the $^2\text{H}/^1\text{H}$ of a range of compounds (e.g. phytol, fatty acids, starch) synthesised in different plant compartments, this chapter opens new avenues for future research to fully constrain the precise nature of biochemically-moderated hydrogen isotope fractionation in leaf wax biomarkers. In particular, this chapter identifies that the production and catalysis of osmoregulatory compounds may have an important influence on *n*-alkane $\delta^2\text{H}$, and may also be an underlying driver of the more negative *n*-alkane $\delta^2\text{H}$ values typically found in monocots relative to dicots. These findings are wide-reaching and indicate that a holistic approach to the study of hydrogen cycling within secondary metabolic processes is essential to understand the $\delta^2\text{H}$ signal recorded in *n*-alkanes from modern plants and ancient sediments.

Chapter 8 represents a shift in focus, turning attention from analysis of modern surface vegetation to *n*-alkanes from surface sediments and a 1 m core dating back to the 1500's. This chapter makes the first evaluation of the sensitivity of the sedimentary leaf wax lipid $^2\text{H}/^1\text{H}$ record to changes in surface vegetation cover, drawing together results from Chapters 4, 5, 6 and 7. Findings show that small-to-moderate changes in surface vegetation have the potential to drive shifts of up to $\sim 40\text{‰}$ in sedimentary *n*-alkane $\delta^2\text{H}$. Methods for identifying vegetation change commonly applied to the geological record may not record these modest changes – results show that molecular distribution and carbon isotope composition are not able to successfully discriminate among species at Stiffkey. Chapter 8 then applies a series of mixing models to plant and sediment data from Stiffkey to constrain vegetation change, before evaluating three different approaches for reconstructing the $^2\text{H}/^1\text{H}$ of palaeoprecipitation from sedimentary *n*-alkanes. Finally, **Chapter 9** reflects upon the results of this study, and discusses the wider relevance of this thesis for biomarker-based palaeoclimate reconstruction. Figure 1.5 provides an overview of the thesis structure, illustrating how the findings of each chapter are integrated.

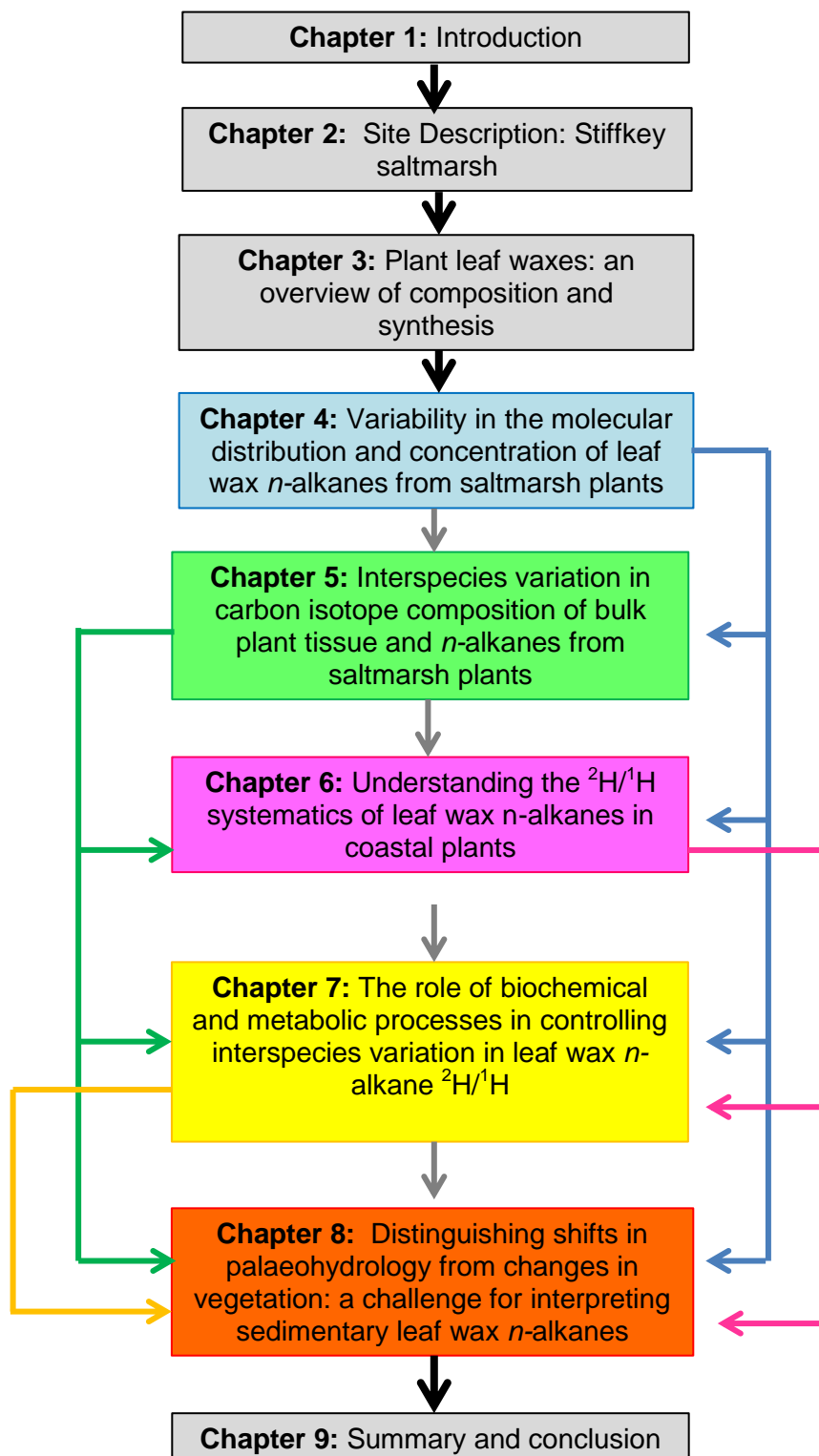


Figure 1.5: Diagram showing the thesis structure – coloured arrows indicate how the findings of one chapter are integrated into subsequent chapters.

Chapter 2

Site Description: Stiffkey saltmarsh

2.1 INTRODUCTION

All data presented in this thesis come from samples collected at Stiffkey saltmarsh, on the north Norfolk coast. Saltmarshes typically contain a wide variety of micro-environmental habitats (Davy, 2009), and are populated by plant species with very diverse physiological and biological adaptations to local conditions. This makes them ideal sites for research into the mechanisms controlling the molecular distribution and stable isotopic composition of leaf wax biomarkers. This chapter will first review the rationale for the selection of a saltmarsh study site, before detailing the modern conditions and vegetation encountered at Stiffkey. Finally, an overview of the modern sediments at Stiffkey, combined with studies considering the recent evolution of this part of the north Norfolk coastline, will be provided.

2.2 RATIONALE FOR SITE SELECTION

Salt marshes are defined as areas of land regularly flooded by sea water that are covered with halophytic vegetation, and are of great importance in lowland coastal regions (Allen, 2000). From the perspective of fulfilling the overarching aims of this project (Section 1.3, Chapter 1), salt marshes represent an interesting environment in which to investigate the complex interplay between the influence of environmental and biochemical mechanisms on the composition of leaf wax biomarkers from terrestrial plants.

Coastal biomes typically contain diverse plant communities exposed to a range of environmental stresses during the course of a growing season. Species-specific physiological and biochemical adaptations employed by saltmarsh plants to ameliorate harsh environmental conditions, such as salinity and root anoxia, have

been extensively studied previously (e.g. Parida and Das, 2005; Davy *et al.*, 2011). This enables a thorough evaluation of the role of these survival strategies on leaf lipid biomarker compositions. Saltmarshes are also the point where terrestrial and marine ecosystems meet (Davy, 2009), making them valuable locations for recording environmental change. In particular, they are uniquely influenced by sea level rise (Gehrels *et al.*, 1996), changes in salinity (Malamud-Roam and Ingram, 2004) and changes in climatic regimes (Tanner *et al.*, 2010; Duarte *et al.*, 2005, 2013, 2014). This makes them useful analogs for modelling how plant communities react to changes in sea level and climate, with application to both studies of the geological past, and attempts to model future ecological change (Bertness and Ewanchuk, 2002; Duarte *et al.*, 2014).

Coastal saltmarshes are critical components of the global carbon cycle (Duarte *et al.*, 2005). Global saltmarsh cover has been estimated to range from 22,000 to 400,000 km² (Duarte *et al.*, 2013). Typical salt marsh primary productivity, 700 to 1000 gC/m² per year (Little, 2000), is significantly higher than that in the pelagic environment, 50 to 600 gC/m² per year (Lalli and Parsons, 1997). The biomass generated in this type of setting therefore contributes significant amounts of organic material (OM) to the marine environment (Mitsch and Gosselink, 2000). Globally saltmarshes are known to have higher levels of primary production than other coastal biomes such as mangroves (Fig. 2.1), and greatly exceed the productivity of grasslands, cultivated plant communities and forest ecosystems (Mitsch and Gosselink, 2000; Richardson, 2000). In total, approximately ~50% of organic carbon stored in ocean sediments is found in vegetated sedimentary environments such as saltmarshes (Duarte *et al.*, 2005; 2013). Indeed, the carbon content in vegetated marine sediments is far higher than that found in shelf and deltaic environments, with between 1126 to 3534 Tg C y⁻¹ of organic carbon available for export to the open ocean (Duarte *et al.*, 2005). Saltmarshes are therefore “hot spots” of carbon storage in ocean biogeochemical cycles (Duarte *et al.*, 2005, 2013).

As attempts to understand the vegetation record contained in sediments are extended through the use of leaf wax biomarkers, a detailed understanding of the information recorded in the leaf wax compounds from saltmarsh species will be of considerable importance for reconstructing coastal habitats. Findings from this study will therefore have important implications for tracing terrestrial vegetation inputs to coastal and near-shore marine sediments. Many of the plant species found in saltmarshes around the UK coast are also distributed around the coastlines of

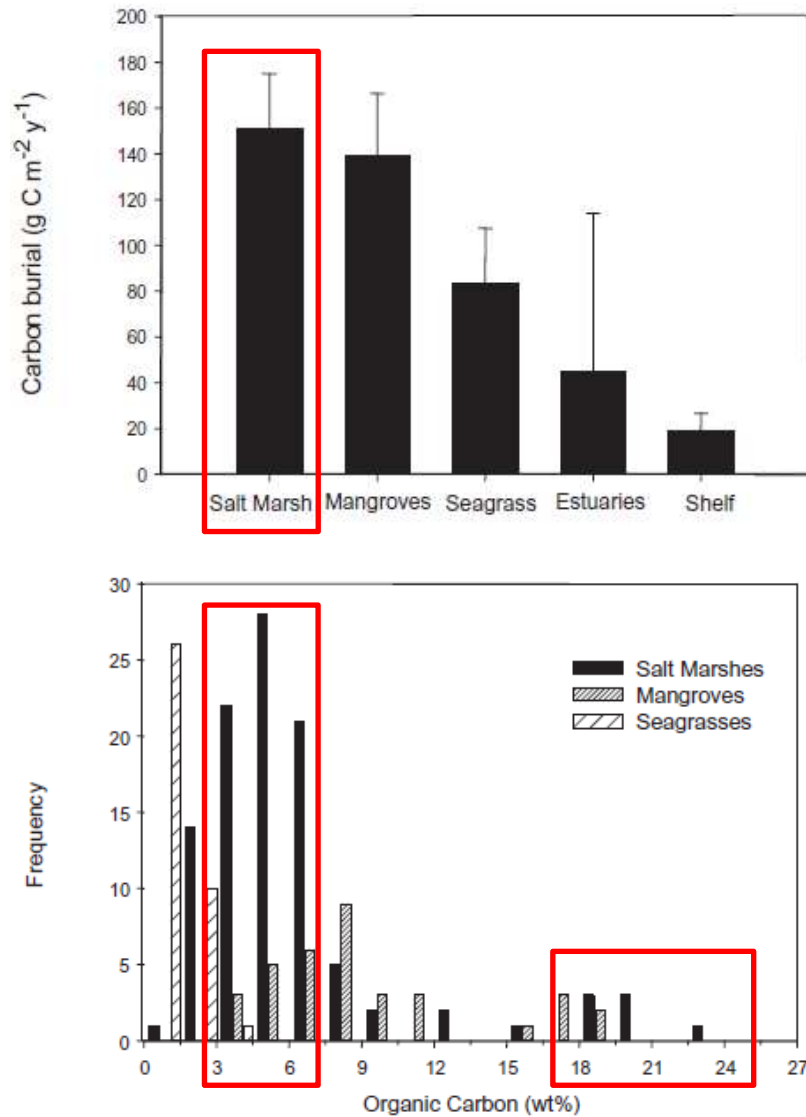


Figure 2.1: A) Average (\pm SE) carbon burial rates in different coastal ecosystems; and B) Frequency distribution of organic carbon content in salt marsh, mangrove and seagrass sediments (Duarte *et al.*, 2005). Saltmarsh habitats are highlighted in each figure (red).

continental Europe, and even those of Africa, Australia and China (Akhani *et al.*, 1997; Krikwon and Hedge, 2000; Ainouche *et al.*, 2004), rendering analysis of their leaf wax biomarker molecular and stable isotopic properties valuable on a national and international scale.

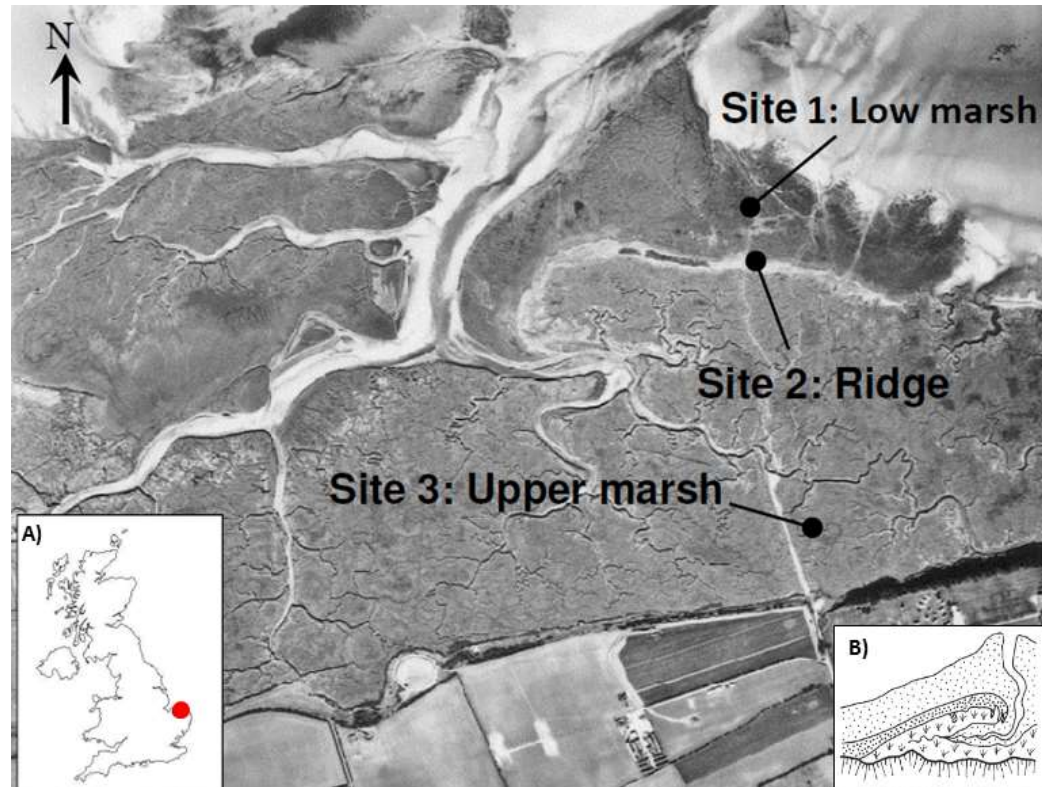


Figure 2.2: Aerial photo of Stiffkey saltmarsh, showing the location of the three sampling locations used for this study, and the dendritic pattern of drainage ditches transporting salt water onto the marsh (Allen, 2000). Insert A shows the location of the site on the north east coast of the UK (red spot), while insert B is a schematic of a typical open coast back-barrier saltmarsh (Allen, 2000).



Figure 2.3: Two examples of drainage ditches at Stiffkey. A) Small drainage ditch photographed in August 2011 during sampling of the upper marsh, B) the largest tidal inlet channel found at Stiffkey, which transports sea water to the higher levels of the marsh.

2.3. STIFFKEY SALTMASH

2.3.1 Modern site characteristics

Stiffkey, situated on the north Norfolk coast, is typical of an open coast back-barrier saltmarsh, and dates from the Holocene (Moeller *et al.*, 1996; Allen, 2000) (Fig. 2.2). This saltmarsh is typical of those found along the north Norfolk coastline with sand prograding in a westerly direction and gravel barriers fronting vegetated marshes that contain fine-grained, silty sediments (Boomer and Horton, 2006).

The site can be divided into ecologically distinct zones. The low marsh (LM) and upper marsh (UM), defined by Jeffries (1977), are separated by a well-drained gravel and sand ridge (Ridge; Fig. 2.2) formed by onshore emplacement of offshore barrier sediments (Boomer and Woodcock 1999). Seawater inundation onto the upper marsh is by tidal flow through a dendritic channel network across the marsh (Fig. 2.2 and 2.3) and also by spring tidal inundation. Neap tides range from 2 to 3 m, although they can be as low as 0.2 m (Pye, 1992; Callaway *et al.*, 1996). Spring tides can be in excess of 5 m and storm surges from the North Sea can occur (Callaway *et al.*, 1998; Andrews *et al.*, 2000). Sea levels in the locality are rising annually by approximately 0.6 mm (Boomer and Horton, 2006). There are no rivers or streams draining onto the marsh, therefore rainwater accounts for all near-surface fresh water inputs to the site.

During the summer months, plants growing at Stiffkey are known to experience a range of severe environmental conditions. In particular, as temperatures rise, rainfall decreases and tidal inundation becomes less frequent, hypersalinity can develop in the mid and upper marshes (Jeffries, 1977). Hypersaline conditions were actually observed at Stiffkey in the summer months while carrying out the field sampling conducted as part of this project. When temperatures were high, and soil evaporation levels rose, salt could be clearly seen deposited at the soil surface, giving the ground a whitish appearance (Fig. 2.4). In addition to hypersalinity, plants at Stiffkey are also thought to be nitrogen limited during the summer months (Jeffries, 1977). Past studies have noted that the edaphic conditions at Stiffkey can be severe enough that plants actually modify their growing patterns to ensure sufficient vegetative growth and flowering prior to the onset of summer, with a further growth period taking place as summer gives way to early autumn (Jeffries and Perkins, 1977).



Figure 2.4: White-ish deposit, thought to be salt, observed on the soil surfaces of the upper marsh in August 2012, Stiffkey

2.3.2 Modern surface vegetation

Stiffkey vegetation cover can be zoned according to topography and degree of tidal inundation (Jeffries, 1977; Jeffries and Perkins, 1977; Davy *et al.*, 2011). Plant types present include monocots (*Spartina anglica*, *Elytrigia atherica*, *Phragmites australis*, *Puccinella maritima*), succulents (*Suaeda vera*, *Salicornia europaea*) and dicots (*Limonium vulgare*, *Atriplex portulacoides*). The low marsh at Stiffkey, which receives regular tidal inundation, is colonised by the C₄ grass *Spartina anglica*, the C₃ species *Salicornia europaea* and *Limonium vulgare*, and occasionally the C₃ shrub *Atriplex portulacoides*. The gravel ridge supports a range of C₃ grasses such as *Elytrigia atherica*, with stands of the reed *Phragmites australis* found on the seaward side. *Suaeda vera* and *Atriplex portulacoides* also grow in ≤ 1 m high bushes on the ridge. *Limonium vulgare*, *Atriplex portulacoides* and *Suaeda vera* are particularly abundant in the upper marsh, however, *Spartina anglica* and *Salicornia europaea* proliferate around lower-lying brackish pools and water-logged ground surrounding old drainage channels.



Figure 2.5: Examples of the different morphology of species sampled from Stiffkey for this project: A) The evergreen succulent *Suaeda vera*; B) the C_3 grass *Elytrigia atherica*; C) stands of the C_4 grass *Spartina anglica*; D) the perennial herb *Limonium vulgare*

The distribution of coastal plants at Stiffkey can be explained by considering 'Ellenberg' values for salinity tolerance produced as part of the 1999 'Ecofact' project (Hill *et al.*, 1999). An Ellenberg rating of 0 indicates a species with no salt tolerance, whilst 9 is applied to species known to favour extremely saline conditions where hypersalinity and salt precipitation are common. Under this classification scheme, *Spartina anglica* (7) (Fig. 2.5) is identified as a species of the lower salt marsh; *Salicornia europaea* (9) is a species found in extremely saline and hypersaline conditions; *Atriplex portulacoides* and *Limonium vulgare* (6) (Fig. 2.5) are most common in mid-level salt marshes; *Suaeda vera* (5) (Fig. 2.5) is found typically on the upper edges of marshes where tidal inundation does not often reach; *Elytrigia atherica* (4) is most suited to salt meadows and upper marsh environments; and *Phragmites australis* (2) (Fig. 2.5) is a species that can live in both saline and non-saline habitats but is more predominant in non-saline environments. Species present at the site are adapted for survival in continually damp/wet soils, with the exception of *Elytrigia atherica*, which can tolerate only moderately damp conditions (Hill *et al.*, 1999).

The selected species at Stiffkey vary in terms of their leaf morphology, ranging from *Suaeda vera* which has succulent leaves that are ~2mm long, to the reed *Phragmites australis* which has large broad-blade leaves that can reach ~30cm in length. Life strategies are also different, with evergreen species *Atriplex portulacoides* and *Suaeda vera* living alongside perennials such as *Limonium vulgare*. Finally these plants are also different at the biochemical level – the compatible solutes they use for osmoregulation and amelioration of the harsh saltmarsh conditions, for example, show a degree of species specificity. The main compounds synthesised for these purposes include proteins, amino-acids and sugars/carbohydrates (Bohnert and Jensen, 1996). These biological mechanisms are important since their existence is not limited to saltmarsh plants; indeed they are also widely found in other drought tolerant species (Bohnert and Jensen, 1996), making results from this study of general importance in a range of different biomes where plants experience environmental stresses.

2.4 STIFFKEY SEDIMENTS

The sedimentary sequences at Stiffkey have been studied previously in some detail. The north Norfolk coastline was believed to have been at the edge of the ice cover during the last glaciation, although most research indicates that there was no ice present at the time of the last glacial maximum (Boomer and Horton, 2006).

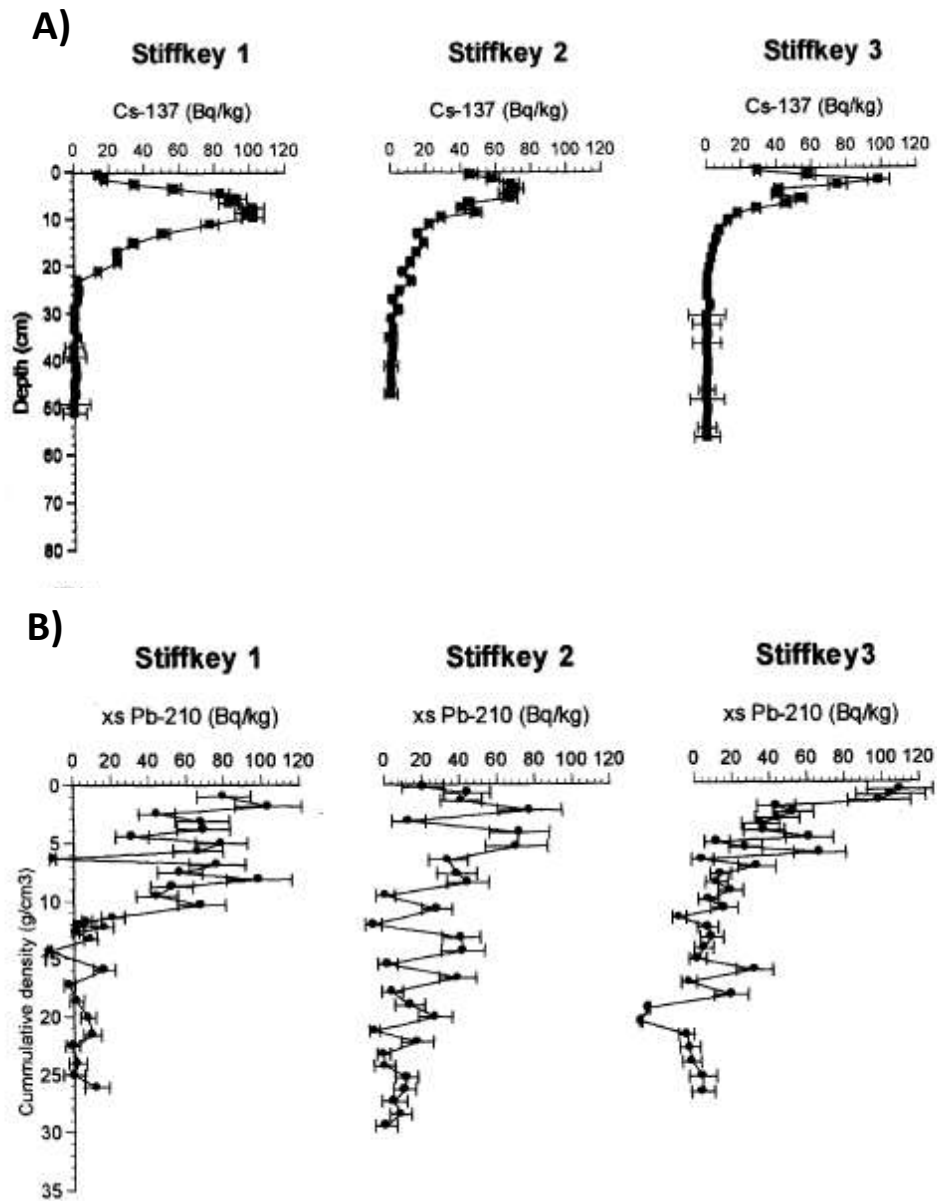


Figure 2.6: ^{137}Cs profiles plotted against depth (A) and excess ^{210}Pb profiles plotted against cumulative sediment density (B) at Stiffkey. Stiffkey 1 = the lower marsh; Stiffkey 2 = 100 m south of Stiffkey Meals (Ridge site, Fig. 2.2); Stiffkey 3 = mature saltmarsh 300 m north of Green Lane car park (Upper marsh, Fig. 2.2) (Andrews et al, 2000).

Sediment cores taken from sites along the north Norfolk coast, from locations including Stiffkey, are generally indicative of rising sea levels during the period, with interspersed fine grained mud, silt and peat alternating with coarser sands (Boomer and Horton, 2006). The base of the Holocene sediments is generally peat, which is thought to have formed as water levels rose prior to the rising sea levels (Andrews *et al.*, 2000). Several studies have published radiocarbon dates from sediment cores taken at Stiffkey, illustrating the age ranges common in sediments on the north Norfolk coast. A calibrated radiocarbon date from the base of a peat layer at Stiffkey, found at approximately 3 m below Ordnance Datum (OD), records an age of 5610 ± 60 years BP, while the surface of the same peat layer has a calibrated ^{14}C age of 5320 ± 50 years BP at a depth of -2.25 mOD (Funnell *et al.*, 2000). ^{137}Cs and excess ^{210}Pb profiles have been used at Stiffkey to derive a sediment accumulation rate (Andrews *et al.*, 2000) (Fig. 2.6). The ^{137}Cs peak in these samples is thought to derive primarily from discharge from Sellafield, which peaked in 1975 (Andrews *et al.*, 2000).

The marsh sub-environments at Stiffkey evolved at different times. The upper marsh sediments are thought to have commenced development at around 4420 years BP (Funnell *et al.*, 2000). In contrast, the lower areas of the marsh remain dynamic, with aerial photographs illustrating that the modern low marsh environment (Fig. 2.2) developed during the 1950s and 1960s, but is currently being eroded (May, 2003).

The coarse gravels, pebbles and sands found at the ridge (also known as Stiffkey "Meals") which divides the upper and lower marsh (Fig. 2.2) extend approximately 1m below the surface of the marsh (Boomer and Woodcock, 1999). These deposits are indicative of a high energy deposition environment, such as a location further towards the sea (Boomer and Woodcock, 1999). The sediments immediately seaward of the ridge include relatively fine-grained silts up to a depth of 5m, with a layer of coarse sand at ~ 1m (Boomer and Woodcock 1999). The presence of this sand layer within otherwise fine-grained sediment is thought to record the event that created the Meals, which occurred approximately 1000 years ago (Boomer and Woodcock, 1999; Funnell *et al.*, 2000). It is unclear precisely what took place at this time, although a sudden change in sea level has been suggested (Boomer and Woodcock, 1999). Whatever the reason, this event is likely to have also influenced the distribution and abundance of plant species growing on the marsh.

Sediment accumulation rates differ between the lower and upper marsh environments (Fig. 2.2). The lower marsh has a rapid accumulation rate of 0.49 g cm^{-2} per year (Andrews *et al.*, 2000). In contrast, the upper marsh has a lower accumulation rate of only $0.12 \text{ g cm}^{-2} \text{ a}^{-1}$ (Andrews *et al.*, 2000). The mid marsh (Fig. 2.2) has an accumulation rate of $0.19 \text{ g cm}^{-2} \text{ a}^{-1}$ (Andrews *et al.*, 2000). These values translate into a linear sedimentation rate of 6.4 mm a^{-1} for the low marsh, 3.6 mm a^{-1} for the mid marsh and 2.1 mm a^{-1} for the upper marsh (Andrews *et al.*, 2000).

Sediments at Stiffkey are reworked across the marsh surface regularly as a result of tidal activity. Sedimentary material containing organic matter (potentially including leaf wax biomarkers) can also be conveyed to the marsh from external sources. Sands and shingles are transported along the north Norfolk coast in a westward direction, and wave-modified ebb tidal deltas around Blakeney (Fig. 2.7) have been identified as significant sediment sinks in the region (Andrews *et al.*, 2000). At Stiffkey, contributions from external sources could also include wind-blown dust, eroded from the local agricultural fields immediately adjacent to the marsh, which have limited cover during the year.

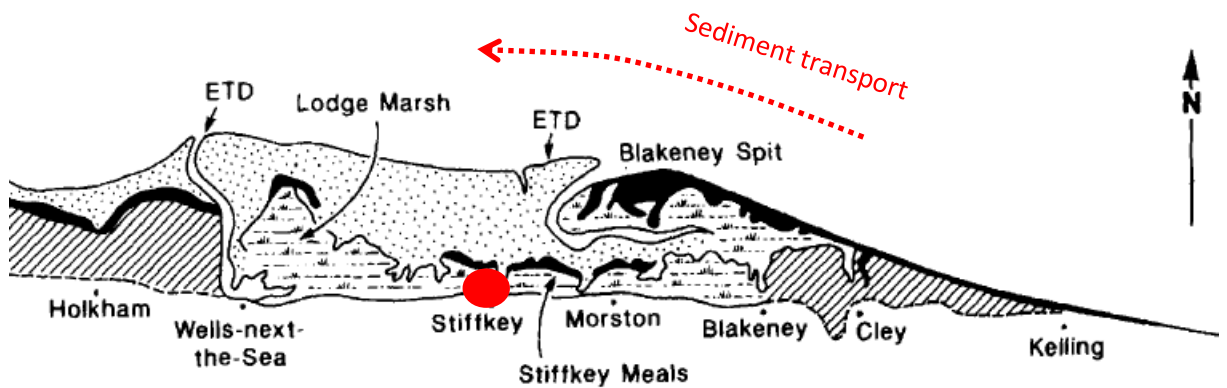


Figure 2.7: Map showing the location of Stiffkey saltmarsh (highlighted in red) relative to Blakeney Spit, where significant sediment sinks are thought to be located. The arrow highlights the westward movement of sands and sediments that has been identified along the north Norfolk coastline, which has the potential to contribute reworked sediment and organic matter to the marshes at Stiffkey (adapted from Andrews *et al.*, 2000).

Chapter 3

Plant leaf waxes: an overview of composition and synthesis

3.1 INTRODUCTION

The term “plant wax” refers to the mixture of lipids found: (i) on the surface of aerial components of higher plants (Baker, 1982) (Figure 1.1, Chapter 1); (ii) within suberin below the soil (Franke & Schreiber, 2007); and (iii) within pollen and seed coatings (Kunst & Samuels, 2003). Epicuticular leaf waxes form a critical barrier between plants and their environment, and this fundamental role has resulted in extensive ongoing study of their chemical and physical properties (e.g. Holloway, 1982; Harwood, 1998; Bernard and Joubes, 2013; Anarat-Cappillino and Sattely, 2014).

The hydrophobic waxy surface of plant leaves proved vital for the terrestrial colonisation and evolution of land plants over 400 million years ago (Bernard and Joubes, 2013). In association with adjustable resistance in the stomata (Riederer and Schneider, 1990; Riederer and Schreiber 2001), this protective wax coating is directly involved in processes such as gaseous exchange (Baker, 1982), water conservation (Harwood, 1998; Riederer, and Schreiber, 2001; Bernard and Joubes, 2013), ultraviolet protection, and the amelioration of abiotic stresses such as pollutants (Harwood, 1998; Kunst & Samuels, 2003; Shepherd *et al.*, 2006; Pollard *et al.*, 2008; Samuels *et al.*, 2008). Interactions between plants and insects also take place at the plant wax interface (Samuels *et al.*, 2008), and complex biochemical mechanisms are thought to coordinate defence responses and cuticle biosynthesis (Riena-Pinto and Yephremov, 2009).

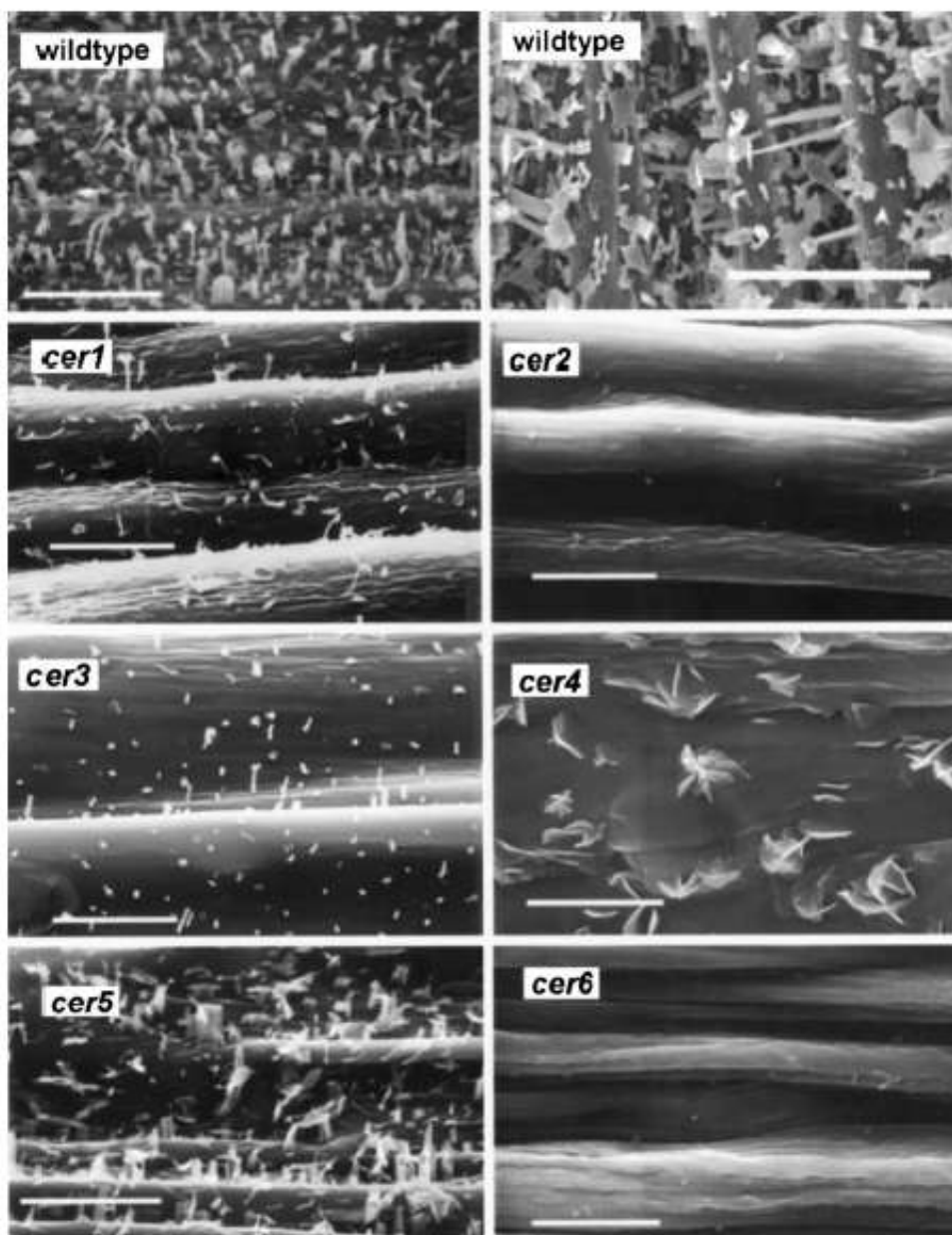


Figure 3.1: Examples of SEM images of Arabidopsis thaliana stems, showing the crystalloid structures common to epicuticular waxes. “Wildtype” individuals display abundant waxes, while mutants (“cer1 – cer6”) have a greatly reduced wax load (sourced from Kunst and Samuels, 2003).

Early physical classifications of leaf waxes identified the existence of diverse structural forms including needles, rods, granular layers and films (Baker, 1982). These classifications were extensions of pioneering work carried out by Amelunxen during the 1960s, who characterised epicuticular waxes using scanning electron microscopy (SEM) (Jeffree, 2006). This early body of work still underpins our understanding of plant leaf waxes today, although it is now widely accepted that the plant cuticle is covered with a wax film, from which crystalline structures can

protrude and be visible under SEM in certain species (Jetter *et al.*, 2000) (e.g. Fig. 3.1). The nature of the crystalline structure can discriminate between plant functional types, as different plant species are associated with different wax morphologies. In cereals, for example, leaf wax structures are generally tubular and range from 2-3 μ m long and 0.22 – 0.26 μ m thick, and are arranged in a complex branched fashion (Baker, 1982), whilst the lobed plates observed in *Quercus robur* species reflect the high predominance of C₂₄ alcohols in their waxes (Post-Beittenmiller, 1996).

The chemical composition of the lipid matrix varies among different plant species, among plant organs, and with maturity (Bull *et al.*, 2013; Bernard and Joubes, 2013). The stems of *Arabidopsis thaliana*, for example, have waxes that contain a significant concentration of alcohols and ketones, despite these compounds being absent in their leaves (Suh *et al.*, 2005). The plant cuticle is generally predominated by long chain aliphatic compounds including primary alcohols, hydrocarbons, secondary alcohols and β -diketones and fatty acids (Baker, 1982; Jetter and Schäffer, 2001). Other secondary compounds identified include triterpenoids, sterols and flavonoids (Kunst & Samuels, 2003). Very long chain fatty acids (VLCFAs), primary alcohols, aldehydes, alkanes and alkyl-esters have been labelled as ubiquitous in almost all plant species (Jetter and Schäffer, 2001). An example of the typical relative abundances of these common leaf wax constituents found in *Arabidopsis* is presented in Fig. 3.2.

3.2. SYNTHESIS OF PLANT LEAF WAXES

Important early investigations into the biosynthetic pathways involved in the synthesis of leaf waxes were carried out by Kolattukudy (see for example: Kolattukudy, 1970; Kolattukudy *et al.*, 1970, 1973). It was during these studies that the biosynthetic relationship between hydrocarbons, secondary alcohols and ketones was identified through observation of the fates of ¹⁴C labelled *n*-nonacosane as it was converted into nonacosanol and nonacosan-15-one (Kolattukudy *et al.*, 1970). More recent studies of the mechanisms facilitating and regulating leaf wax biosynthesis have identified the existence of several key pathways, which are thought to be interchangeable (Von Wettstein-Knowles, 2012). This builds upon much of the earlier work elucidating the biochemical pathways responsible for *n*-alkane production, which had almost exclusively focused on *Arabidopsis* (see for example Shepherd and Griffiths, 2006).

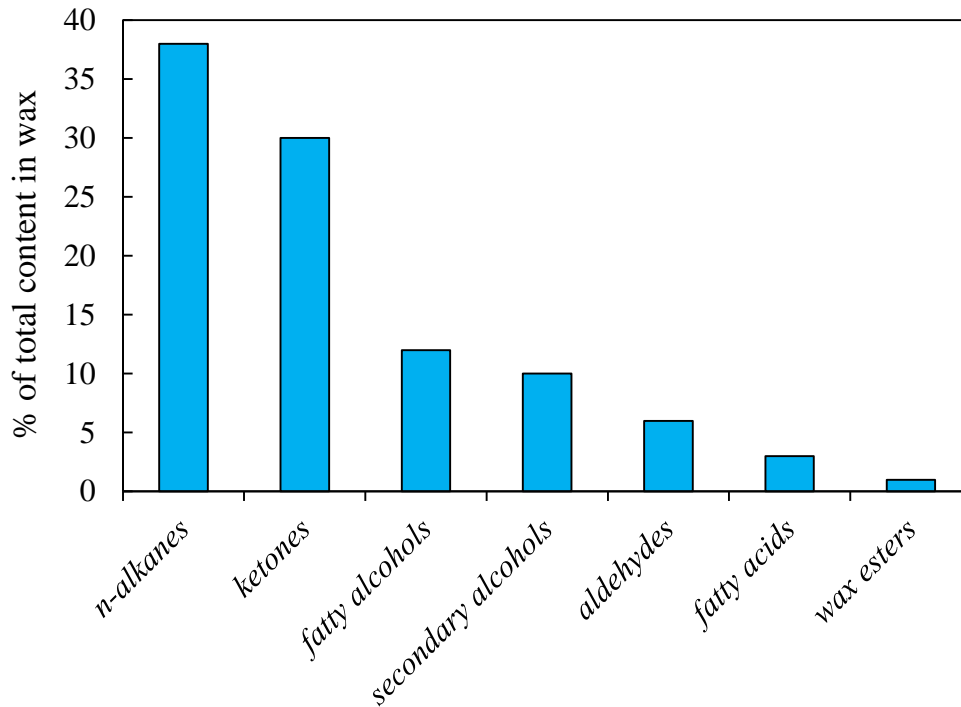


Figure 3.2: Relative percentages of wax constituents found in *Arabidopsis* (data from Kunst, 2003)

The importance of the protective hydrophobic layer to terrestrial plants is highlighted by the fact that the synthesis of cuticular waxes starts very early during the development of *Arabidopsis thaliana*, with a proto-cuticle deposited in the late stage of embryogenesis (Bernard and Joubes, 2013). Development of the cuticle proper is then linked to the developmental stage of the plant, ensuring consistent protection during growth (Bernard and Joubes, 2013).

3.2.1 Production of VLCFAs

The biosynthesis of acetogenic lipids in plant leaves starts with the production of very long chain fatty acids (VLCFAs). The first step in this process is the *de novo* synthesis of C₁₆ and C₁₈ acyl chains (Figure 3.3) in the leucoplasts, (non-photosynthesising plastids found in epidermal cells), by the enzymes of the fatty acid synthase complex (FAS) (Figure 3.3) (Samuels *et al.*, 2008). These fatty acids form the building blocks for all lipid classes, illustrating that these initial intermediates are common to a wide range of biosynthetic pathways (Post-Beittenmiller, 1996; Samuels *et al.*, 2008).

The production of C₁₆ and C₁₈ FAs catalysed by FAS and moves through four repetitive cycles. Synthesis commences with a condensation reaction between

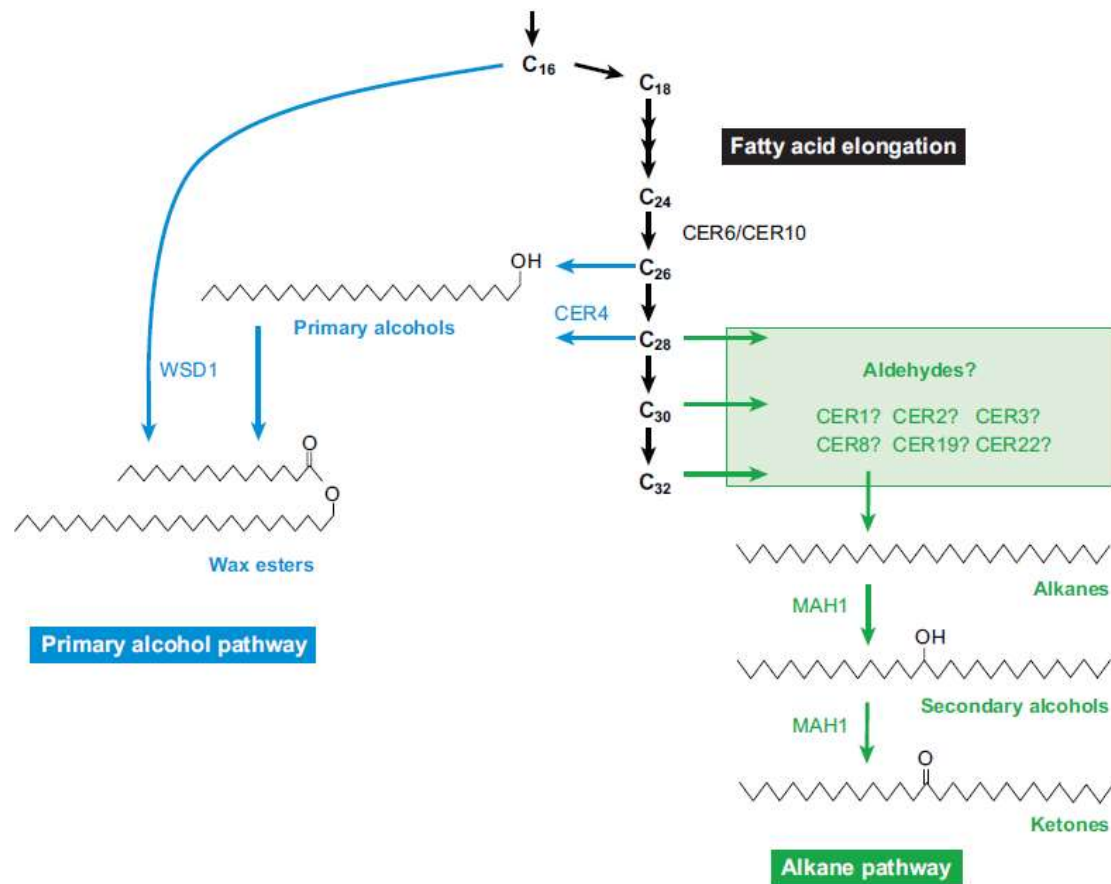


Figure 3.3: Simplified pathways for wax biosynthesis in Arabidopsis stems. (Samuels et al., 2008)

malonyl-acyl carrier protein (ACP) and acetyl-CoA (Post-Beittenmiller, 1996; Shepherd and Griffiths, 2006; Kunst *et al.*, 2007). The next steps in the cycle include the reduction of 3-ketoacyl-ACP, the dehydrogenation of 3-hydroxyacyl-ACP and the reduction of *trans*- Δ^2 -enoyl-ACP (Post-Beittenmiller, 1996). During each of these subsequent cycles, the acyl chain is extended by 2 carbons (Kunst *et al.*, 2007; Fig. 3.4). Reducing power for the relevant stages in the elongation process is provided by NADPH (Post-Beittenmiller, 1996), which has important implications for consideration of the stable isotopic composition of leaf wax biomarkers considered further in Chapters 5, 6 and 7. Once C₁₆ and C₁₈ FA chains have been synthesised, production of VLCFAs shifts from the plastid to the endoplasmic reticulum (Post-Beittenmiller, 1996; Samuels *et al.*, 2008). Here, the C₁₆ and C₁₈ FAs are further elongated to VLCFAs by the activity of fatty acid elongase complexes (FAE) (Figure 3.4 and 3.5; Samuels *et al.*, 2008; Kunst *et al.*, 2009). Enzymes that form these FAE complexes include 3-ketoacyl-CoA synthase, 3-ketoacyl-CoA reductase, 3(R)-hydroxyacyl-CoA dehydrase and (E)-2-3enoyl-CoA reductase (Shepherd and Griffiths, 2006). FAE complexes use acyl-CoA activated substrates to carry out elongation in a manner similar to that recorded for FAS, including condensation, reduction, dehydration and further reduction stages (Shepherd and Griffiths, 2006). It has been suggested that up to 8 different FAE complexes are required to create C₂₀ and C₃₄ FAs (von Wettstein-Knowles, 2012). Elongation commonly results in FAs with a chain length of 20 – 34 carbons (Kunst and Samuels, 2003; Samuels *et al.*, 2008).

During the elongation reaction series, an important partitioning is made between lipid biosynthetic pathways, for example the pathway controlling cuticular lipids and the pathway synthesising membrane glycerolipids, however the precise mechanisms moderating this partitioning remain poorly constrained (Samuels *et al.*, 2008). Studies of genetically modified *Arabidopsis*, however, suggest that the major fraction of C₁₆ acyl chains in an elongating epidermal cell that is engaged in cuticle synthesis will be directed to the pathway for wax formation (Samuels *et al.*, 2008).

3.2.2 Biosynthetic pathway for *n*-alkanes

The synthesis of the long-chain aliphatic components of plant wax initiates in the epidermal cells of the plant, using saturated VLCFAs as precursors (Kunst & Samuels, 2003). Labelling experiments have revealed that entire chains of fatty acids (C₁₀ to C₁₈) are incorporated into long-chain *n*-alkanes in plant leaf

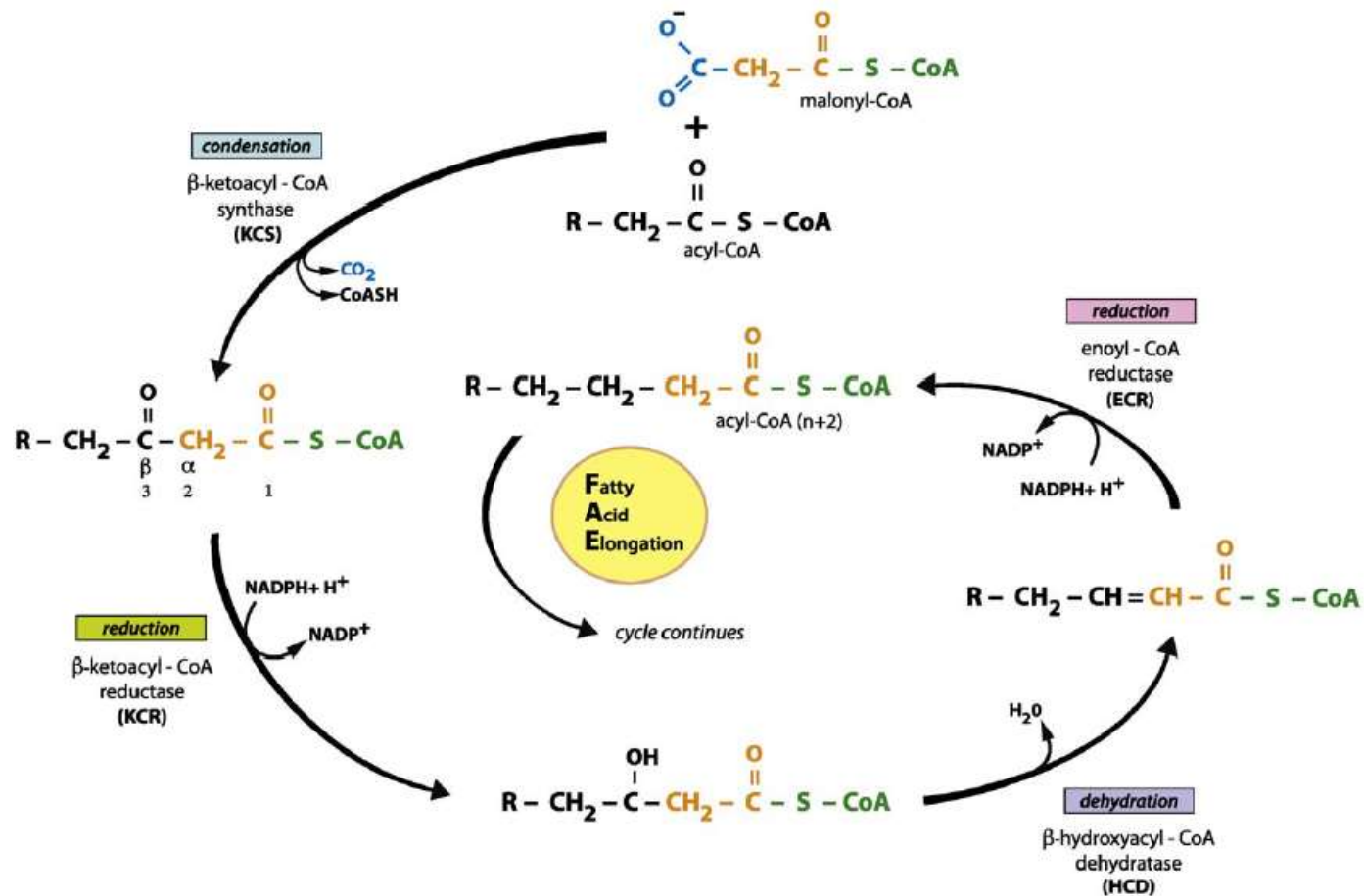


Figure 3.4: Schematic showing the activity of FAEs in generating FAs with >20 carbons. This figure shows the repeated cycles of two-carbon addition. In one cycle, the four enzymes of the FAE complex work sequentially to carry out the condensation of two carbons from malonyl-CoA (carbon donor) to the growing acyl-CoA chain (carbon acceptor), followed by reduction, dehydration, and another reduction reaction, resulting in a fully saturated acyl-CoA (Kunst et al., 2009)

waxes, with preferential incorporation of the longer FAs (Kunst and Samuels, 2008). The biosynthesis of *n*-alkanes is thought to follow an elongation-decarboxylation pathway (Kolattukudy *et al.*, 1970; Shepherd and Griffiths, 2006; Kunst *et al.*, 2009) as illustrated in Fig. 3.5. The precise identification of enzymes catalysing these reactions, however, remains an area of ongoing research, and many of the individual steps ascribed to this pathway remain hypothetical (Kunst and Samuels, 2008). Indeed, as much of the work underpinning the current understanding of leaf wax biosynthesis has been carried out on *Arabidopsis* (e.g. Shepherd and Griffiths, 2006), further complication arises from the fact that other pathways are thought to exist among different plant species for the production of secondary compounds. Post-Beittenmiller (1996) proposed that up to three wax biosynthesis pathways can be present (decarbonylation, acyl-reduction and β -ketoacyl-elongation), with the potential for intermediates such as aldehydes to be shared among pathways as required. The lack of consensus regarding the enzymes driving key stages in the leaf wax biosynthesis pathway is an important factor to consider throughout this thesis, as it makes establishing isotopic fractionation for each point in these reaction networks (e.g. Hayes, 2001) complex.

The immediate precursors of alkanes in the decarbonylation pathway are aldehydes, produced from the reduction of acyl-CoA (Post-Beittenmiller, 1996; Shepherd and Griffiths, 2006; Kunst and Samuels, 2008). The premise that the conversion from aldehydes to alkanes in plants occurs as a result of a decarbonylation reaction (Kunst and Samuels, 2008) was strengthened in 2010, when enzymes capable of such reaction steps were purified and identified for cyanobacteria – one was classified as an acyl-CoA reductase, the other an aldehyde decarbonylase (Schirmer *et al.*, 2010). It was originally proposed that the carbon lost during the decarbonylation reaction was in the form of CO, however experimental evidence now suggests that the co-product is likely to be formate (HCO₂) (von Wettison-Knowles, 2012). Although specific to cyanobacteria, these studies are effectively a proof of concept for the mechanism proposed in higher plants, and therefore the existence of the decarbonylation pathway is generally accepted in the literature (von Wettison-Knowles, 2012).

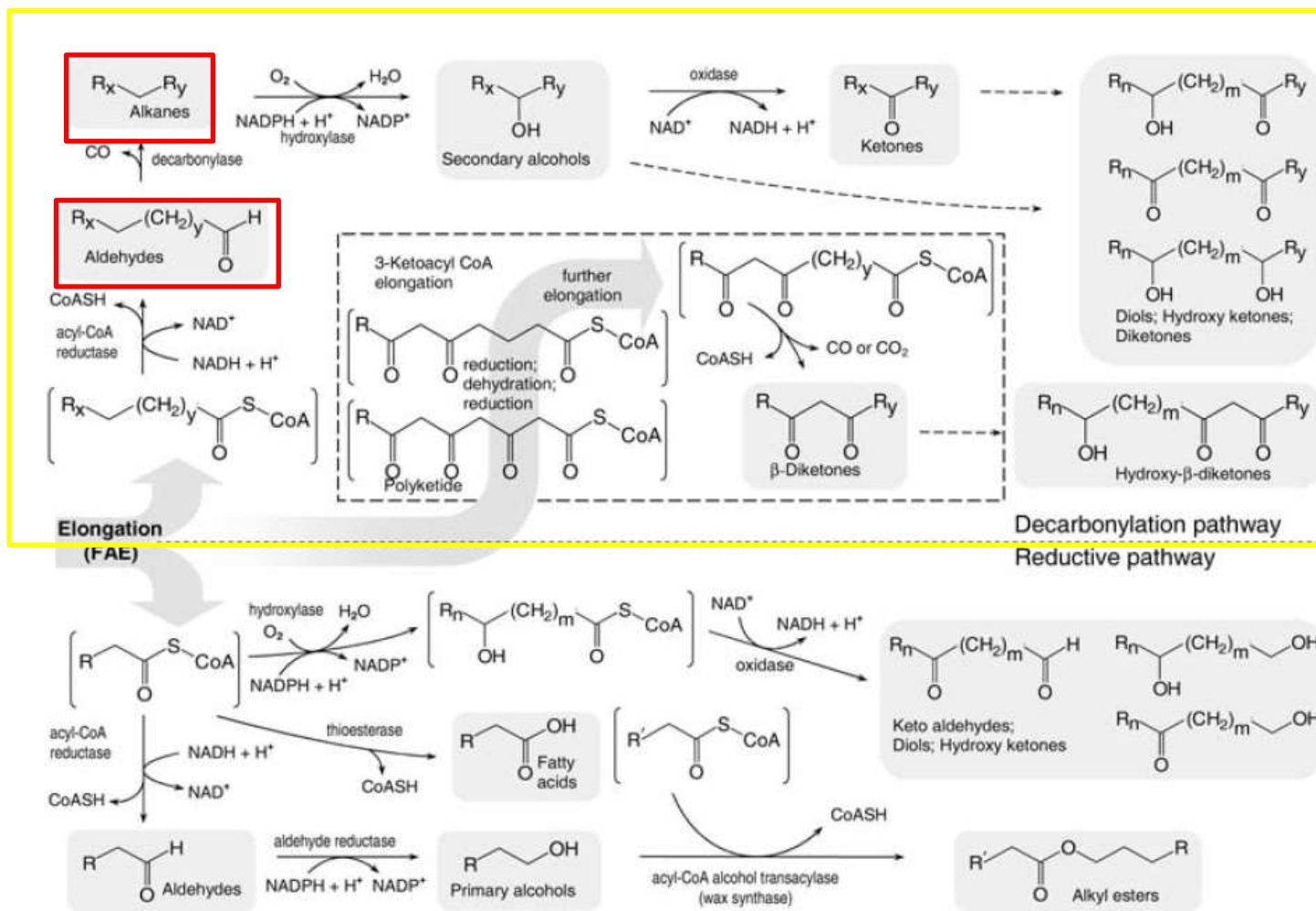


Figure 3.5: Reactions and products of the decarbonylation and reductive pathway, derived from the study of *Arabidopsis* (Shepherd and Griffiths, 2006). The decarbonylation pathway producing *n*-alkanes is highlighted in yellow, with alkanes and their immediate precursors, aldehydes, highlighted in red.

3.2.3 Areas for future research

Despite almost 20 years of concentrated research into the production of plant leaf waxes, often using genetically altered mutants of *Arabidopsis*, which have resulted in the characterisation of enzymes catalysing the major steps in fatty acid elongation (Bernard and Joubes, 2013), there remain questions to be answered about the pathway generating leaf wax *n*-alkyl lipids. These outstanding areas are important from the perspective of this thesis, as they relate to biochemical mechanisms operating within lipid biosynthetic pathways, which could influence the molecular distribution and stable isotope composition of organic compounds found within plant leaf waxes.

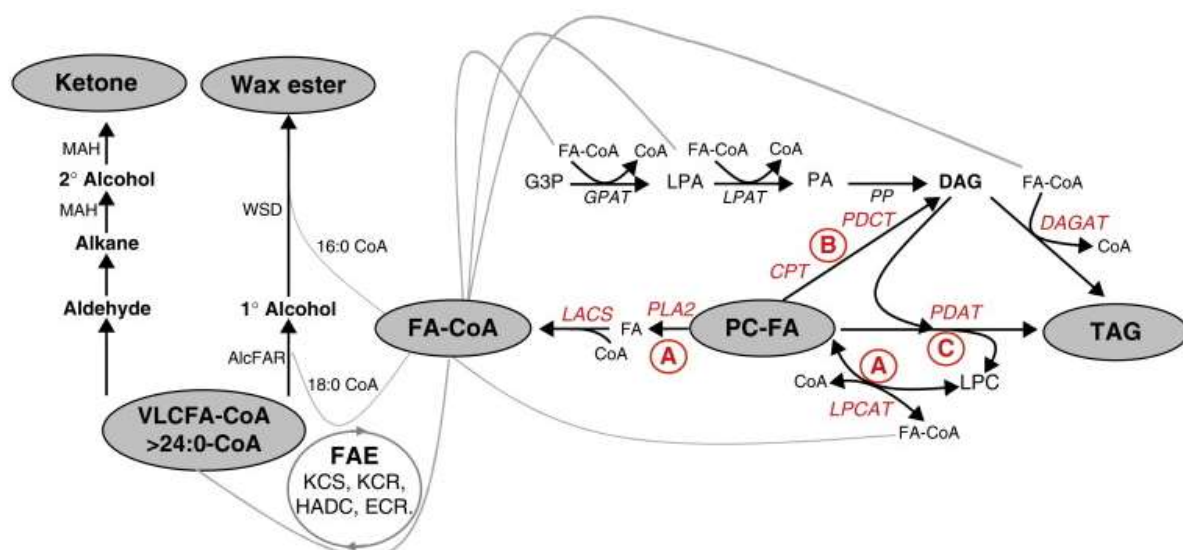


Figure 3.6: Main lipid classes and biochemical pathways involved in the production of secondary plant lipids. Mechanisms A, B and C illustrate how long-chain FAs can be incorporated into triglycerol, and illustrate how the FA-CoA pool can be allocated to a wide range of fates, and that the acyl-CoA pool generated by mechanism A or resulting from direct export from the plastid can be accessed by additional enzymes such as the endogenous FAE elongase system to generate very long chain fatty acids (VLCFAs) and leaf wax biomarkers (Napier *et al.*, 2014).

Of particular significance is the idea that leaf wax biochemical pathways are part of a complex, interrelated network of cellular metabolic processes (Napier *et al.*, 2014; Fig. 3.6), regulated by biotic and abiotic stresses (Bernard and Joubes, 2013). Plants are capable of producing over 200,000 small molecule natural particles and

secondary metabolites (Anarat-Cappillino and Sattely, 2014). This diversity, however, is generated from a relatively limited number of enzymatic transformation steps and branch points in reaction networks (Anarat-Cappillino and Sattely, 2014). It is therefore currently unknown how plants are able to achieve such a startling diversity of secondary compounds from these starting points (Anarat-Cappillino and Sattely, 2014).

Ongoing research into the biosynthetic pathways generating secondary lipids is of great significance for the interpretation of fossil lipid biomarkers in a palaeoclimate context. If plant metabolic networks, and the flux of elements (such as carbon and hydrogen) through them are considered in a holistic fashion (as espoused by van Dongen *et al.*, 2011), there is a fundamental need to investigate what controls the allocation of metabolic precursors to different biosynthesis pathways (Anarat-Cappillino and Sattely, 2014), as this could enhance the information available from the geological record. It is likely that advances in this area will come from integrated genetic and metabolomic studies (Anarat-Cappillino and Sattely, 2014). Without such research, the information recorded in the molecular distribution and stable isotope composition of lipid biomarkers will remain poorly constrained in both modern ecological studies and palaeoclimate reconstructions from leaf wax lipids.

3.3 SUMMARY

- Epicuticular waxes on the aerial components of higher plants are the interface between plants and their environment.
- Very long chain fatty acids (VLCFAs), primary alcohols, aldehydes, alkanes and alkyl-esters have been labelled as ubiquitous in almost all plant species.
- The biosynthesis of *n*-alkanes is thought to follow an elongation-decarboxylation pathway; however some of the individual steps ascribed to this pathway remain hypothetical.
- Pathways generating leaf wax *n*-alkyl lipids are part of a complex cellular metabolic network with multiple demands on acetyl-CoA, which could have important implications for understanding the flow of carbon and hydrogen through reaction networks.

Chapter 4

Variability in the molecular distribution and concentration of leaf wax *n*-alkanes from saltmarsh plants

4.1. INTRODUCTION

As discussed in Chapter 1 and Chapter 3, one of the most abundant compound classes identified in plant leaf waxes are the *n*-alkanes: straight chain saturated hydrocarbons with chain lengths ranging from C₁₇ to C₃₅, displaying a classic predominance of odd-chain to even-chain homologues (odd-over-even predominance, OEP) (Eglinton *et al.*, 1962; Eglinton and Hamilton, 1967; Baker, 1982; Zech *et al.*, 2010; Buggle *et al.*, 2010). Analysis of sedimentary long-chain *n*-alkanes originating from terrestrial vegetation has received considerable attention in the last decade in a variety of fields. Preserved molecular distribution patterns of leaf wax biomarkers recovered from the geological record, for example, have been used to reconstruct patterns of surface vegetation (Liu *et al.*, 2005; Zhang *et al.*, 2006; Bai *et al.*, 2009). These data have in turn been used to evaluate the necessary climatic conditions in which the dominant plant species identified are known to thrive (Zhou *et al.*, 2005). Molecular distribution patterns of leaf waxes have also been used to assist in the provenancing of modern soils as part of forensic investigations (Dawson *et al.*, 2004), and the identification of atmospheric circulation patterns through identifying plant contributions to dust (e.g. Shefuß *et al.*, 2003). This chapter will review these applications and consider limitations in existing knowledge relating to the use of leaf wax biomarkers for recreating surface vegetation assemblages. Key requirements for further research will be highlighted, and the rationale for the aims and objectives of this part of the project will be established.

4.2 LITERATURE REVIEW

4.2.1 Identification of plant inputs to soils and sediments

The molecular distribution pattern of *n*-alkanes in epicuticular wax appears to have a degree of chemotaxonomic potential (Rommerskirchen *et al.*, 2006) and is therefore potentially a useful tool for discriminating between plant species. As a result of this, studies have sought to use these profiles to effect a detailed reconstruction of the composition of vegetation assemblages contributing to soil organic matter (SOM). Such an application would be valuable for modern soil forensic investigations (e.g. Dawson *et al.*, 2004), in addition to palaeoecological studies. Overlapping molecular distribution patterns are, however, common in the higher plant *n*-alkane range C₂₅-C₃₃ (Buggle *et al.*, 2010). Simple usage of *n*-alkane distribution data in modern soils, therefore, appears to lack the species-specific resolution required to relate a soil sample of interest to source vegetation for forensic applications (Eley *et al.*, 2012).

Despite these limitations, *n*-alkane distribution patterns have been commonly utilised in palaeoclimatological studies to reconstruct vegetation histories (see also Chapter 1, Section 1.1.1). Here, broad vegetative distinctions based upon either: (i) average chain length (defined here as a weight-averaged number of carbon atoms of the *n*-alkane homologues in the leaf wax from a particular species, “ACL”) (see for example Zhou *et al.*, 2005); (ii) carbon preference index (the ratio of the proportion of the total alkane fraction with an odd number of carbon atoms to the proportion with an even number of carbon atoms, “CPI”) (Cranwell, 1973; Zhou *et al.*, 2005; Zhang *et al.*, 2006; Buggle *et al.*, 2010); and (iii) ratios of selected *n*-alkane chain lengths to each other (e.g. *n*-C₂₃/*n*-C₂₉ as an indicator of aquatic plants, Zhou *et al.*, 2010) have been used to identify of the relative percentage of different plant functional types (PFTs) contributing to sediments through time. Vogts *et al.* (2009) for example identified broad distinctions between the leaf wax biomarker distribution patterns of rainforest and savannah biomes, suggesting that discrimination between diverse ecosystems may be possible.

Yamada and Ishiwatari (1999) reported molecular distribution patterns and carbon isotope compositions of *n*-alkanes from the Japan Sea. They found that shifts in CPI values correlated with the timing of glacial vs. interglacial periods. This correlation was attributed to plants synthesising longer chain alkanes during glacial periods to contend with the increasing aridity (Yamada and Ishiwatari, 1999). Rao *et al.* (2009) also reported that CPI values of plant-derived *n*-alkanes extracted from surface soils

and sediments show a relationship with climate, rather than varying purely by vegetation type. This study found that CPI values increase with latitude, theorising again that this may be due to plants synthesising greater amounts of long-chain alkanes under cold and dry conditions (Rao *et al.*, 2009).

This link between chain length and climatic regime has also resulted in leaf wax *n*-alkane distributions being used at the continental scale to elucidate dominant atmospheric patterns. Schefuß *et al.* (2003), for example, investigated atmospheric dust samples collected from a West African transect. Plant derived *n*-alkanes extracted from these samples, ablated from terrestrial vegetation, showed a shift in the dominant *n*-alkane, with a C_{max} of *n*-C₃₁ in northern samples compared to *n*-C₂₉ in those collected from rainforested areas of central Africa. Schefuß *et al.* (2003) attributed these shifts in dominant chain-length distribution to moisture availability and aridity, rather than changing vegetation types, with samples from more arid areas having a C_{max} of *n*-C₃₁. Many of these recent interpretations are based on studies in the late 1960s by Eglinton *et al.* (1962), Eglinton and Hamilton (1967) and Del Castillo *et al.* (1967) who identified a trend for longer-chain *n*-alkanes in species adapted to survive in arid areas. Rommerskirchen *et al.* (2006) builds on this approach, by proposing that C₄ input in the geological record can be identified by a predominance of *n*-C₃₁ and *n*-C₃₃, combined with information about the stable carbon isotope composition.

4.2.2 How reliable are molecular distribution ratios for discriminating between plants?

The overall composition of leaf wax varies among different plant species. β -diketones for example are important components of waxes found on cereals, with hentriacontane-14, 16-dione being the most prevalent identified (Baker, 1982). In contrast, leek and *Brassica* leaves contain significant amounts of ketones in addition to *n*-alkanes, although these are not present in barley or maize leaves (Post-Betteinmiller, 1996). The dominant compound in leaf waxes can also vary among species – fatty acids are most abundant in peanut leaves, whereas primary alcohols are highest in alfalfa (Post-Betteinmiller, 1996).

Initial studies by Eglinton *et al.* (1962) showed great promise for the use of leaf wax molecular distributions as tools for identifying different plant species. Cuticular waxes extracted from plants from the Crassulaceae family during this early study showed considerable similarity, suggesting that their composition had a degree of species specificity. As further research on other plant species broadened the

available data, however, it became clear that plants of the same species could display molecular compositions that were diverse, whilst conversely molecular distribution patterns that appeared very similar could derive from different plant species (Eglinton and Hamilton, 1967; Del Castillo *et al.*, 1967). The observed variability in leaf wax composition among plant species of the same family may in part be due to genetic differences, as these have been shown to influence the relative composition of compounds in leaf waxes. Much of this research has been conducted in agricultural science, where crop species have been studied to evaluate the impact of glaucousness (the visible dull white or blue/green coloration on the surface of waxy leaves which is a factor of the β -diketone concentration) on crop yield (see for example Febrero *et al.*, 1998; Merah *et al.*, 2000).

Research has continued to explore whether plant cuticular waxes have any, albeit limited, chemotaxonomic potential. Investigations of *n*-alkane distribution patterns in Solanaceae (Zygadlo *et al.*, 1994; da Silva *et al.*, 2012) have shown some qualitative success. In addition, studies of species in the Lamiaceae (Maffei, 1994), Umbelliferae, Cruciferae and Leguminosae (Maffei, 1996), Cactaceae (Maffei *et al.*, 1997) and Coniferae (Maffei *et al.*, 2004) indicate that a degree of familial and sub-familial taxonomic discrimination is possible through analysis of plant *n*-alkane distribution patterns in certain genera.

Several studies have considered whether *n*-alkanes could be used to discriminate between grass species. The Graminaea are of significant interest for a variety of disciplines as they cover approximately one third of the terrestrial surface of the planet (Maffei, 1994) and are the principle vegetation type associated with grasslands and savannahs (Rommerskirchen *et al.*, 2006). Grasses are difficult to identify at the species level from pollen grains (see for example Holst *et al.*, 2007) or phytoliths (Mulholland, 1989), so biomarker analysis could offer a valuable additional tool for discriminating between different species. Maffei (1996) identified chemotaxonomic differences between leaf waxes from certain C₃ and C₄ species, but based much of his statistical work on C₃ species. In contrast, Rommerskirchen *et al.* (2006) evaluated whether the wax signatures of C₃ and C₄ varied systematically among sub-families of Poaceae. Analysis of *n*-alkane and *n*-alkanol distribution patterns of 35 C₄ and 3 C₃ grasses indicated that at the sub-familial level, some discrimination was possible between the Pooideae (C₃ species) and the combined Chloridoideae and Panicoideae (typically C₄ species), with the C₃ grasses dominated by shorter *n*-alkane chain lengths (C₂₉ and C₃₁, as opposed to C₃₁ and

C₃₃ in the C₄ species analysed). Discrimination beyond the sub-family level was however not possible (Rommerskirchen *et al.*, 2006).

Recent studies have further confirmed that, although still widely used, *n*-alkane distribution patterns (and the ratios commonly calculated from them) may not be as distinctive among PFTs as previously thought. Wang *et al.* (2014) used a range of molecular indices, including ACL, CPI and OEP to investigate shifts in the *n*-alkane distribution from glacial and interglacial periods extracted from a sediment core in Southern China. They found that ACL values displayed remarkably minimal variation throughout their entire 120 m core, however CPI values appeared to allow for the identification of changes in the amount of terrestrial vegetation contributing biomarkers to the lake sediments (Wang *et al.*, 2014). Bush *et al.* (2012) considered intra- and inter-species variability in *n*-alkane distributions among a wide range of plant types. They found significant variability in the *n*-alkane distribution patterns of vascular plants, especially with respect to *n*-C₂₇, *n*-C₂₉ and *n*-C₃₁, the chain lengths often used to discriminate between woody plants and graminoids. Bush *et al.* (2012) also carried out meta-analysis of previously published data to evaluate whether shifts in chain length distribution were driven solely by changes in vegetation, or whether plant responses to environmental and climatic shifts could be contributory factors. They identified a significant correlation between chain length and temperature/latitude, attributed to plants producing longer length alkane chains (with greater hydrophobicity) in warmer and/or more arid climates. These findings are consistent with earlier research identifying a positive link between the production of longer-chain alkanes and ambient temperature (Rommerskirchen *et al.*, 2006; Tipple and Pagani, 2013), and suggest that decoupling sedimentary chain length shifts due to climate from those driven by plant community change is complex.

Bush and McInerney (2013) then analysed 2093 observations of *n*-alkane chain length distributions from both novel experiments and data published in existing literature. They concluded that *n*-alkanes distribution patterns vary to such an extent that considerable caution is required when seeking to identify different chemotaxonomic groups from such data. This study confirmed the findings of Bush *et al.* (2012), in that ratios of *n*-C₂₇, *n*-C₂₉ and *n*-C₃₁ were ineffective in discriminating between graminoids and other woody plants (Bush and McInerney, 2013). In addition, parameters such as ACL and CPI ratios displayed such wide random variation among the data analysed that even qualitative use of these parameters to detect vegetation shifts was not possible.

Such results have significant implications for the use of molecular distribution patterns in palaeoclimate reconstruction. In particular, questions still remain as to whether shifts in *n*-alkane distributions identified in sedimentary lipids may arise from: (i) changes in the make-up of plant communities (Bush and McNerney, 2013), (ii) plant responses to changes in environmental and climatic conditions (Bush *et al.* 2012), or both. Further spatial and temporal studies are therefore needed considering a wide range of plants inhabiting different environmental settings to understand the extent of (i) inter-species variability in *n*-alkane distributions among plants growing at the same geographical location (and hence experiencing the same environmental conditions); (ii) intra-species variability in distribution patterns throughout a growing season; (iii) intra-species and inter-species variability in *n*-alkane distributions throughout climatically different geographical transects.

4.2.3 Variability in *n*-alkane concentration among plant species

In addition to distribution patterns, plants also vary in the concentration of *n*-alkanes they produce. It has been proposed that the total concentration of *n*-alkanes reflect the extent to which the prevailing climate at the time of wax formation is conducive or hostile to plant growth. Low overall concentrations of *n*-alkanes, for example, have been suggested to indicate climates that inhibit vegetation growth, such as low temperatures and/or high aridity (Kawamura *et al.*, 2003; Zhang *et al.*, 2006). An important consideration, however, when seeking to apply such interpretations to sedimentary biomarkers, is the range in concentration of *n*-alkanes produced by different plant species. Significant interspecies variability in the amount of leaf waxes produced by different plants could conceivably result in the over-expression in the geological record of those species with higher concentrations of *n*-alkanes relative to those that produce lower concentrations.

Diefendorf *et al.* (2013) conducted a study of the concentration of leaf wax *n*-alkyl lipids in 46 deciduous and evergreen angiosperm and gymnosperm tree species, representing 24 different families. They found that deciduous angiosperm species produce ~200 times more *n*-alkanes than deciduous gymnosperm species (Diefendorf *et al.*, 2011), an observation also made by Bush and McNerney (2013). Differences also exist between species with long-lived leaves compared to those with a rapid turnover, with long-lived species having higher concentrations of alkanes (Diefendorf *et al.*, 2011). Evergreen angiosperms have also been shown to produce higher concentrations of alkanes than deciduous angiosperms, suggesting that where both species are present, evergreen species will be over-represented in

the sediment record (Diefendorf *et al.*, 2011). Further studies are needed, however, to extend the findings of Diefendorf *et al.* (2011) to a wider range of plant functional types to extend understanding of interspecies variability in *n*-alkane production and constrain this variable in palaeovegetation investigations.

4.2.4 Factors which could drive variability in *n*-alkane concentration and distribution

4.2.4.1 Environmental factors influencing plant leaf wax composition

The total amount, and composition, of plant waxes can be modified by a range of environmental factors (Bianchi and Bianchi, 1990), which can vary considerably across a growing season. These composition changes generally relate to the channelling of acyl precursors into free FAs, and the products of the reductive (producing fatty acids, aldehydes, primary alcohols, and esters) and decarbonylation (producing alkanes, secondary alcohols, and ketones) pathways (Shepherd *et al.*, 2006) (Fig. 3.5, Chapter 3). A prime example is provided by the effect of changes in the amount of radiation reaching the surface of the leaf. Baker (1982) showed that waxes coating the foliage of *Trifolium* species increased in density with increasing radiation fluxes. This is thought to be due to enhanced production of compounds via the decarbonylation pathway in plants growing at higher light intensities (Shepherd *et al.*, 1995; Shepherd *et al.*, 2006). The relationship between light intensity and total wax amount has been shown across a range of species including Brassica (Baker, 1982), kale, and swede (Shepherd *et al.*, 1995) suggesting that it might be a general reaction of plants to environments with higher light intensities.

Variation in diurnal temperatures can also change the composition of different compound classes in leaf waxes. Studies of *Citrus aurantium* leaves concluded that warmer temperatures in the daytime resulted in lower concentrations of *n*-alkanes, 1-alkanols, *n*-alkanoic acids and *n*-alkyl esters, whilst higher night-time temperatures gave rise to higher concentrations of *n*-alkanes, *n*-alkanoic acids and 1-alkanols (Reiderer and Schnieder, 1990). Changes in temperature have also been shown to influence the total wax load - for example in *Brassica oleracea* a greater amount of wax was produced by plant species growing at lower temperatures than higher temperatures (Baker, 1982). Shepherd *et al.* (2006) however notes that the correlation between temperature and wax production is perhaps not as robust as that for irradiation, as it does not apply to all species.

Given that the plants sampled for this study are all adapted for saltmarsh habitats, the response of waxes to salinity and water stress is an important consideration for this chapter. Generally, xerophytic species have thicker surface waxes to minimise water loss from the cuticle (Shepherd *et al.*, 2006), but this is not universal, and differing responses among species have been reported (e.g Tischler and Burson, 1995). Detailed studies of the relationship between the presence and quantity of leaf wax and water loss have generally been carried out on crop plants, with the aim of understanding the link between leaf wax and transpiration. Studies of genetically altered crops have revealed that higher concentrations of wax can reduce the amount of radiation absorbed by a leaf, thus lowering leaf temperature and potentially reducing water loss (Johnson *et al.*, 1983; Richards *et al.*, 1986). Febrero *et al.*, (1998) concluded that the presence of wax gave rise to a 20% increase in the albedo of barley leaves, with the greatest decrease seen in the upper and lower extremes of wavelength measured (485nm – 660nm).

A causal link between leaf wax cover and transpiration has been proposed by several authors, who suggest that the presence of glaucousness could be associated with an increase in transpiration efficiency (Clarke and Richards, 1988). Studies from the early 1980s had raised the possibility that glaucous wheat plants generally produced up to 30% higher yields under water-stressed conditions than non-glaucous individuals,. This was attributed to their enhanced transpiration efficiency, defined as the amount of biomass produced per unit of water transpired, and hence related to intrinsic water use efficiency at the leaf level (Watanabe, 1994; Vadez *et al.*, 2014). More recent studies, however, conclude that the presence of a waxy coating on leaves may not have such a dramatic influence on transpiration. Merah *et al.*, (2000) reported that the imputed positive effect of a wax layer on transpiration was not supported by experimental data, which showed that glaucous and non-glaucous plants differed little in their residual transpiration rates. Instead, field data indicated that glaucous plants could even have lower transpiration efficiency (indicated by higher carbon isotope discrimination) than their non-glaucous counterparts, particularly over longer timescales (Febrero *et al.*, 1998; Merah *et al.*, 2000). Febrero *et al.* (1998) showed that the presence or absence of wax also had no impact upon cuticular conductance. Regardless of the particular relationship with transpiration efficiency, however, the fact remains that plants with a waxy coating have been shown to have a higher yield than those without, especially in drought conditions (Febreo *et al.*, 1998; Merah *et al.*, 2000). This suggests that the full benefits of a wax layer have yet to be constrained.

Detailed studies of the leaf wax composition of halophytes are few; instead research has focused primarily upon the response of salt-sensitive species to saline water, where the introduction of salt typically increased wax production (Mills *et al.*, 2001). Where studies do exist, however, they report that salt-tolerant plants growing in highly saline evaporative conditions display *n*-alkanes with longer carbon chain-lengths than those in growing in less extreme environments (Dodd *et al.*, 1999). Wax composition has been investigated in halophytes of the Chenopodiaceae growing around the Mediterranean, and the presence of longer chains (C₁₉ to C₂₉) 1-chloro-*n*-alkanes has been identified in species such as *Suaeda vera* and *Halimone portulacoides* (the latter a species closely related to *Atriplex portulacoides* found at the study site) (Grossi and Raphel, 2003).

4.2.4.2 *The influence of leaf ontogeny on leaf wax composition*

In addition to environmental influences, plant wax composition is known to vary with the stage of leaf development. These age-related changes were highlighted in an early study by Faboya and Goddard (1980), where the chain-length distribution of *n*-alkanes from the genus *Kyaya* showed a shift from a C_{max} of C₂₉ to C₃₁ as leaves aged. Further analysis of waxes from *Prunus laurocerasus* have shown that changes in: a) the percentage composition of compounds, b) the chain length distribution of compounds, and c) the total amount of waxes can all be observed as the leaf matures from bud-break (Jetter and Schaffer, 2001). This sequential accumulation of different compounds in the epicuticular wax is not thought to arise from differences in the diffusive distribution rates among compound classes. Jetter and Shaffer (2006) note that if this were the case, compounds with similar chain length distributions would diffuse at similar rates, a hypothesis not supported by their experimental data. Instead, ontogenetic regulation of the biosynthesis of accumulated compounds is thought to be likely (Jetter and Shaffer, 2001).

The nature of ontogenetic-driven compositional change in leaf wax varies among different plant species. In juvenile maize leaves, alcohols dominate the epicuticular wax matrix, while more mature leaves are categorised by higher levels of wax esters (Post-Beittenmiller, 1996). In *Prunus laurocerasus*, alcohols also dominate in the first 18 days of leaf development, however in this species *n*-alkanes have been shown to be most abundant as the leaf ages (Jetter and Schaffer, 2001). Recorded changes in the chain length distribution of specific compounds include a shift from a predominance of C₂₂ – C₂₆ fatty acids during the first 30 days after bud-break in *Prunus laurocerasus* to longer chain C₃₀, C₃₂ and C₃₄ fatty acids once the leaf had

been developing for 40+ days (Jetter and Schaffer, 2001). The existence of this apparent sequential accumulation and/or loss of specific compound classes cannot be simply explained by their abrasion through time, or their conversion into other compounds *in-situ* on the leaf surface (Jetter and Schaffer, 2001). Instead, they are thought to be assimilated back into the intracellular compartments of the leaf, and subsequently either metabolised or converted into other compounds (Jetter and Schaffer, 2001).

4.2.5 The importance of understanding *n*-alkane systematics in saltmarsh plants

Limited previous studies exist describing the molecular distribution patterns and absolute concentrations of *n*-alkanes from plants found in saltmarshes, which have been identified as important sites for understanding the cycling of organic matter at the terrestrial / marine divide (Chapter 2). Where such research has been carried out, frequently the focus has been on either one particular species or plant functional group, such as mangroves (Dodd *et al.*, 1999; Ladd and Sachs, 2012, 2013), *Spartina alterniflora* (Bull *et al.*, 1999; Sessions, 2006) or saltmarsh grasses (Wang *et al.*, 2003). Where data pertaining to a range of species are available (see for example Tanner *et al.*, 2007; 2010; Romero and Feakins, 2011) sampling has been carried out at one time interval only during the growing season. Factors such as the time of sampling, local environmental conditions, and the maturity of the plant sampled can influence the concentration and distribution of leaf wax *n*-alkanes, however (Vogts *et al.*, 2009). To date, therefore, very little is known about the extent of seasonal shifts in *n*-alkane distribution patterns and absolute concentrations across a broad range of temperate saltmarsh species found in these important transitional biomes. This gap in knowledge limits the interpretation of leaf wax lipid profiles from sediments (e.g. Bush and McInerney, 2013; Kirkels *et al.*, 2013), in particular those from coastal and near-shore contexts. Without further research, it is difficult to separate shifts in sedimentary *n*-alkane composition driven by changes in vegetation, from differences driven by plant responses to environmental conditions.

4.3. AIMS AND OBJECTIVES

It is clear from the above discussion that a range of questions still exist regarding the molecular distribution patterns of *n*-alkanes in modern plants, which in turn limits the interpretation of leaf wax lipids from the sedimentary record. The overarching aim of this part of the project is to (i) understand the extent of variability in leaf wax

n-alkane composition and concentration among seven saltmarsh species growing in a temperate UK saltmarsh, and (ii) assess the extent to which this variability differs throughout a growing season. This will allow for evaluation of whether interspecies differences in molecular distribution patterns and ratios would be sufficient to allow for detailed identification of vegetation inputs to sediments. In order to fulfil this aim, several research objectives have been produced:

- 1) Quantify the interspecies variation in *n*-alkane distribution for 7 saltmarsh plants across a growing season.
- 2) Investigate the influence of micro-environmental conditions on the molecular distribution of *n*-alkanes, through analysis of species growing in multiple locations across the marsh.
- 3) Evaluate whether molecular distribution ratios and indices can successfully discriminate between the studied species.
- 4) Quantify interspecies variation in *n*-alkane concentration across a growing season.
- 5) Investigate the influence of micro-environmental conditions on *n*-alkane concentrations, through analysis of species growing in multiple locations across the marsh.

4.4. SAMPLE COLLECTION

4.4.1 Sampling strategy

Nine plant species were sampled in June 2011 to determine whether their leaf wax *n*-alkane distributions were sufficiently distinctive to make them worthy of further study (Table 4.1). Seven of these species were selected for further sampling during August and October 2011, with those plants growing across multiple sampling sites (Table 4.2) sampled in each location in June, August and October 2011. Following analysis of results from 2011, sampling throughout the 2012 growing season (defined throughout as the period during which plant growth occurred at the site, generally March – October, Jeffries 1977) focused on the same 7 species but did not consider site micro-habitat (i.e. LM, R, UM, Fig. 2.2 Ch. 2) as the temporal variability exceed spatial variability (Table 4.2) PPE (non-latex gloves) was worn during sample collection to avoid contamination of leaf material. Gloves were changed between sampling each species. Three sample replicates of each species were collected at each sampling interval. Each of these replicates comprised a minimum of five leaves (depending on leaf morphology), sampled from at least three individual plants to ensure a representative signal was obtained from each species.

Care was taken to always select whole, undamaged leaves. Samples were placed in paper envelopes, and dried at 40 °C for ~48 hrs upon returning to the laboratory. They were then stored in a dry, dark environment until required for further analysis.

Table 4.1: Plant species sampling strategy in June 2011, August 2011 and October 2011, Stiffkey saltmarsh

Location	Plant Species	Plant type
Site 1	<i>Spartina anglica</i>	C ₄ grass
Site 1	<i>Triglochin maritima</i>	C ₃ perennial herb
Site 1	<i>Salicornia europaea</i>	C ₃ annual stem succulent
Site 1	<i>Limonium vulgare</i>	C ₃ perennial herb
Site 1	<i>Atriplex portulacoides</i>	C ₃ evergreen shrub
Site 2	<i>Elytrigia atherica</i>	C ₃ grass
Site 2	<i>Phragmites australis</i>	C ₃ reed
Site 2	<i>Puccinella maritima</i> *	C ₃ grass
Site 2	<i>Suaeda vera</i>	C ₃ evergreen leaf succulent
Site 2	<i>Atriplex portulacoides</i>	C ₃ evergreen shrub
Site 3	<i>Triglochin maritima</i> *	C ₃ perennial herb
Site 3	<i>Suaeda vera</i>	C ₃ evergreen leaf succulent
Site 3	<i>Salicornia europaea</i>	C ₃ annual stem succulent
Site 3	<i>Limonium vulgare</i>	C ₃ perennial herb
Site 3	<i>Atriplex portulacoides</i>	C ₃ evergreen shrub

* Plants sampled in June 2011 only

Table 4.2: Plant species sampling strategy followed between March 2012 and September 2012, Stiffkey saltmarsh

Location	Plant Species	Plant type
Site 1	<i>Spartina anglica</i>	C ₄ grass
Site 1	<i>Salicornia europaea</i>	C ₃ annual succulent
Site 2	<i>Elytrigia atherica</i>	C ₃ grass
Site 2	<i>Phragmites australis</i>	C ₃ reed
Site 2	<i>Suaeda vera</i>	C ₃ evergreen succulent
Site 2	<i>Atriplex portulacoides</i>	C ₃ evergreen shrub
Site 3	<i>Limonium vulgare</i>	C ₃ perennial herb

During sampling, the most recent growth was selected from all species. This was straightforward for *Limonium vulgare*, *Salicornia europaea*, the C₄ grass *Spartina anglica* and the C₃ reed *Phragmites australis*, as new leaves were also easy to identify. For the two evergreen species *Atriplex portulacoides* and *Suaeda vera*, sampling focused on the leaves at the tips of stems, to ensure that as far as possible new growth was selected for study throughout. All leaves sampled were, as far as possible, subject to similar levels of exposure to wind, rain and sunlight in order to avoid bias on the basis of canopy position and/or particularly sheltered locations within marsh sub-environments.

4.4.2 Weather station data and seasonal changes in tidal inundation

To evaluate the importance of seasonal changes in local weather conditions on leaf wax composition, weather station data was obtained from the Met Office Integrated Data Archive System (MIDAS) Land and Marine Surface Stations Data. This is an online resource maintained by the National Environmental Research Council (NERC). Data available includes daily and hourly weather measurements of maximum and minimum air temperatures, rainfall amount and relative humidity (rH). Data pertaining to hours of sunshine (not available from MIDAS) were sourced from alternative Met Office data (www.metoffice.co.uk/climate/uk/stationdata). The Lowestoft weather station, some 58 miles south-east of Stiffkey, was the nearest station available for this purpose.

MIDAS data from Cromer shows that seasonal temperatures were similar between the 2011 and 2012 sampling periods. Maximum summer temperatures did not exceed 30 °C, with the highest temperatures occurring in August and September. The lowest temperatures (-2 to -4 °C) occurred each year in February (Fig. 4.1). Mean relative humidity was lower during May – July 2011 than the corresponding period in 2012. Minimum rH values occurred in May 2011 (67%), while the highest values in both years were recorded during the winter months (83 – 88%) (Fig. 4.2). Rainfall patterns showed the greatest variation between the two sampling years, with the amount of precipitation in March, April and May 2011 being the lowest recorded throughout the sampling period (Fig. 4.3). In contrast to 2011, rainfall during 2012 was lowest in February and highest in April. The hours of sunshine occurring at Cromer showed general similarities between 2011 and 2012, however the longest hours of sunshine in 2011 occurred between March and June, whereas in 2012 they were experienced in August and September (Fig. 4.4).

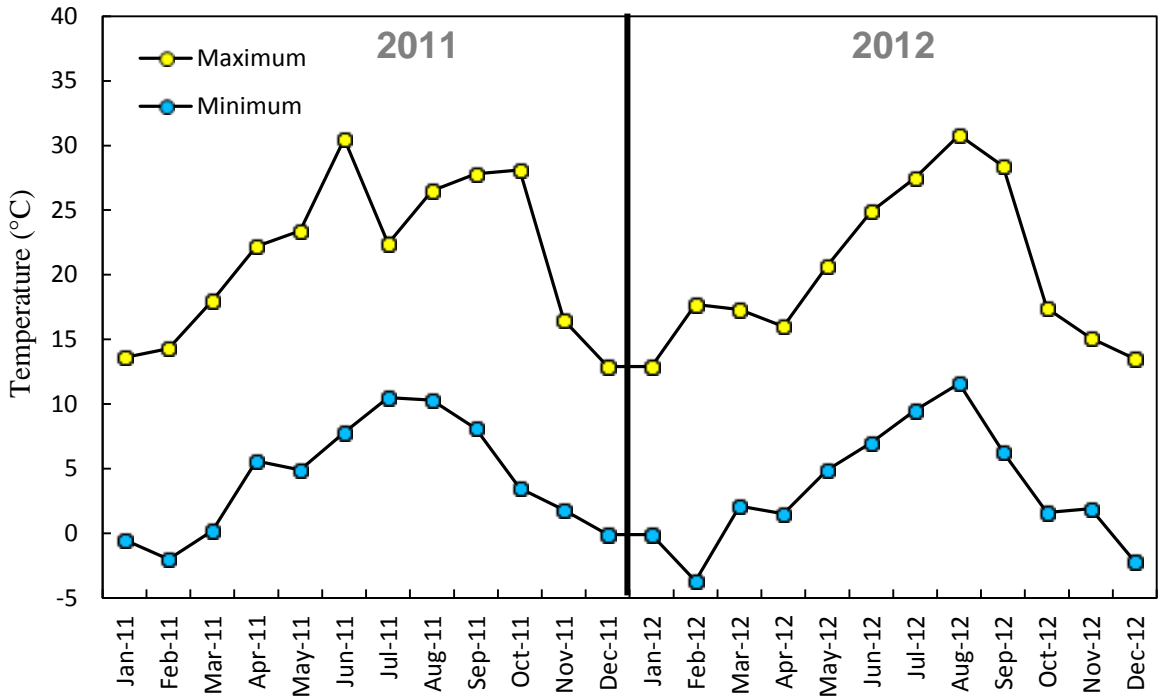


Figure 4.1: Maximum and minimum daily temperatures, averaged by month, from Cromer weather station during 2011 and 2012 (MIDAS). The black line divides data from 2011 and 2012

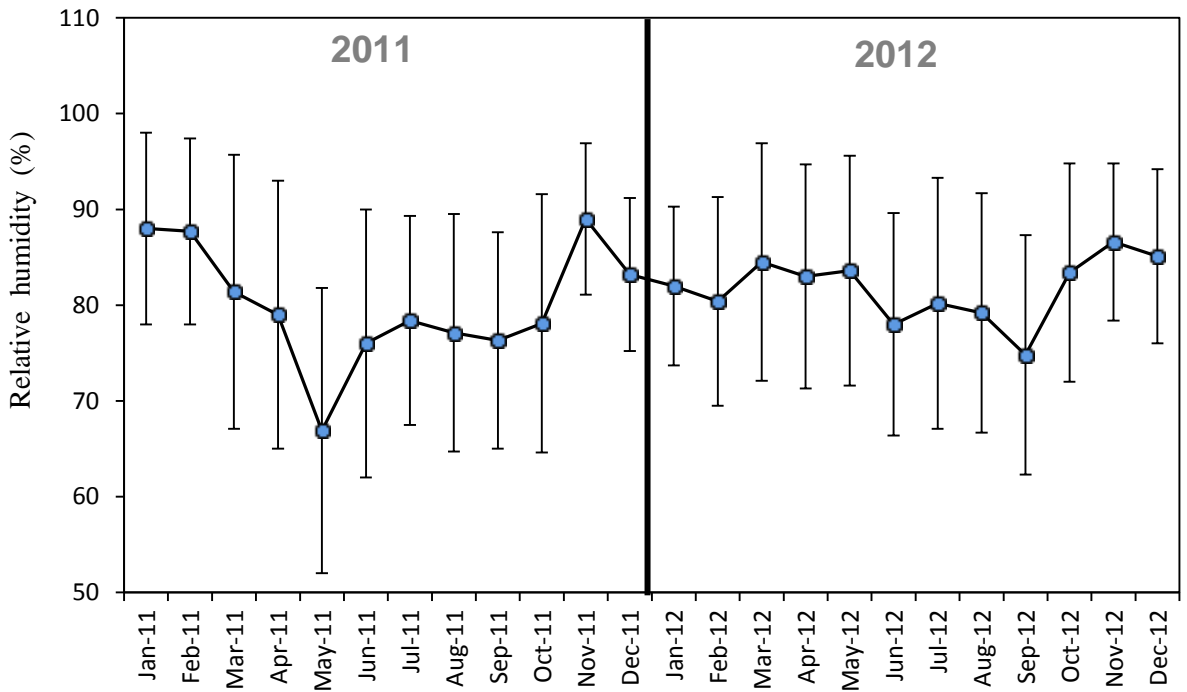


Figure 4.2: Mean relative humidity recorded at Cromer weather station during 2011 and 2012. Error bars show standard deviation of the recorded rH values for each calendar month (MIDAS). The black line divides data from 2011 and 2012

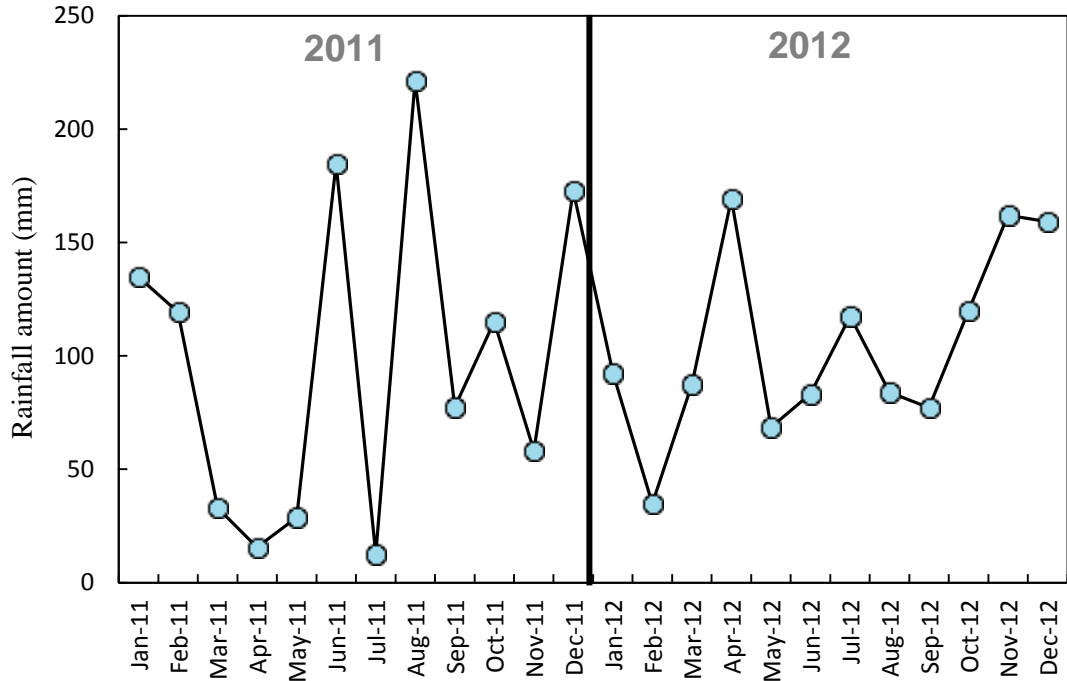


Figure 4.3: Total amounts of rainfall recorded at Cromer weather station for each calendar month during 2011 and 2012 (MIDAS). The black line divides data from 2011 and 2012

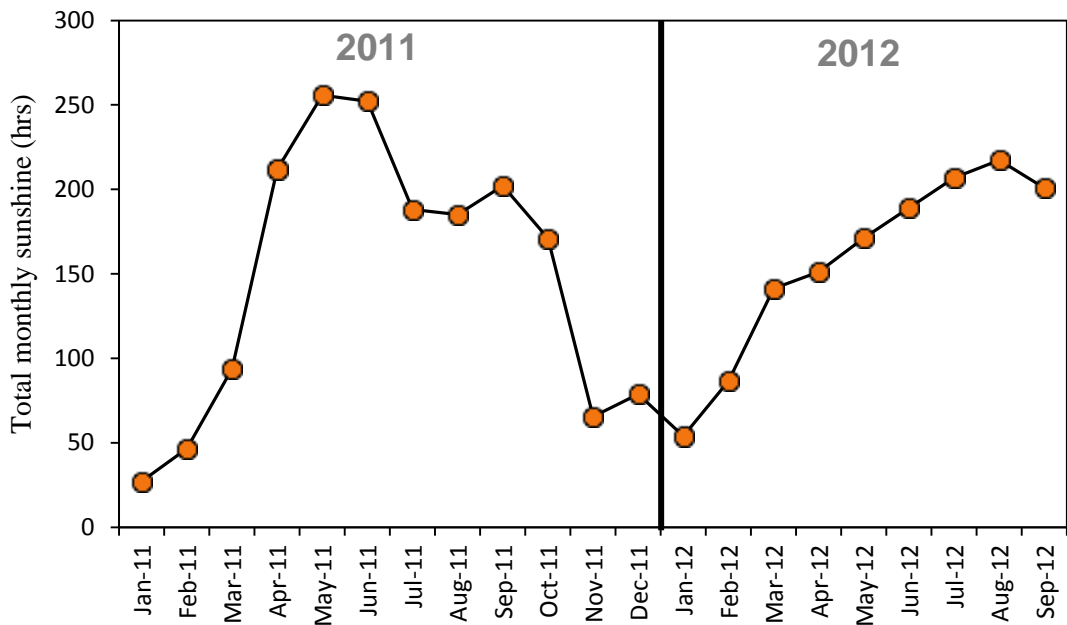


Figure 4.4: Total hours of sunshine recorded for each calendar month at Lowestoft weather station during 2011 and 2012 (www.metoffice.gov.uk). The black line divides data from 2011 and 2012

In addition to seasonal changes in local weather conditions, the plants at Stiffkey experience different degrees of submersion by tides throughout the year. As discussed in Chapter 2, although the low marsh is inundated with each tide, the upper marsh (Fig. 2.2) is only flooded during spring tides and storm surges (Callaway *et al.*, 1998). As water can abrade leaf waxes (Shepherd and Griffiths, 2006), this implies that wax loss from tidal cover in the upper marsh will be highest during spring tides and storm surges, and lowest in the high summer when the upper marsh is mainly dry.

4.5. ANALYTICAL METHODS

4.5.1 *n*-alkane extraction, identification and quantification

Leaf wax *n*-alkanes were extracted from whole leaves by sonication with HPLC grade hexane to obtain the total lipid fraction. The number of leaves used varied among species, from circa three for *Phragmites australis* to over 50 for *Suaeda vera* – i.e. depending upon the overall leaf size. The extract was concentrated to 1 mL under nitrogen gas using a turbovap prior to chromatographic separation. The hydrocarbon fraction was eluted with 4 mL of HPLC grade hexane during column chromatography, using activated silica gel (70-230 mesh, Merck KGaA). Analysis of the molecular distribution and concentration of *n*-alkanes for each species was carried out by injection into an Agilent 7820A gas chromatograph equipped with a flame ionisation detector and a DB-5 capillary column (30 m × 0.32 mm × 0.25 µm) (Agilent Technologies Inc., Santa Clara, USA). The oven temperature was raised from 50 °C to 150 °C at 20 °C min⁻¹, and then at 8 °C min⁻¹ to 320 °C (10 min). *n*-Alkanes were identified by comparison of their elution times with *n*-C₁₆ to *n*-C₃₀ alkane standard (A. Schimmelmann, Indiana University). Average chain length (ACL; Section 4.2.1) and carbon preference index (CPI; Section 4.2.1) values were calculated following the approach of Zhang *et al.*, (2006) (Eq.1 and Eq.2):

$$\text{CPI} = \frac{1}{2} \times \left(\frac{(C_{21}+C_{23}+C_{25}+C_{27}+C_{29}+C_{31}+C_{33}+C_{35})}{(C_{20}+C_{22}+C_{24}+C_{26}+C_{28}+C_{30}+C_{32}+C_{34})} + \frac{(C_{21}+C_{23}+C_{25}+C_{27}+C_{29}+C_{31}+C_{33}+C_{35})}{(C_{20}+C_{22}+C_{24}+C_{26}+C_{28}+C_{30}+C_{32}+C_{34})} \right) \quad (\text{Eq.1})$$

$$\text{ACL} = \frac{(21 * C_{21}) + (23 * C_{23}) + (25 * C_{25}) + (27 * C_{27}) + (29 * C_{29}) + (31 * C_{31}) + (33 * C_{33}) + (35 * C_{35})}{(C_{21} + C_{23} + C_{25} + C_{27} + C_{29} + C_{31} + C_{33} + C_{35})} \quad (\text{Eq.2})$$

Quantification of *n*-alkanes was carried out by the addition of a known concentration of C₁₅ *n*-alkane (Sigma Aldrich) to each sample. As a further precaution, a suite of 6 calibration standards, comprising 5 samples with a known range of C₁₅ concentrations, was also analysed to allow for quantification for any plant samples where the presence of short-chain *n*-alkanes resulted in their co-eluting with the C₁₅ peak.

4.5.2 Quantifying the percentage recovery of *n*-alkanes

A separate study was carried out to evaluate the percentage recovery of *n*-alkanes obtained from these extraction methods. Solid alkane crystals from two *n*-alkane standards (C₂₂ and C₃₄, Sigma Aldrich) were weighed into vials, and 4 mL of hexane was added to prepare a stock solution of known concentration, in accordance with Table 4.3. 50 µL of each of these stock solutions was added to 18 dried leaf samples (collected in June 2011) prior to the addition of solvents for extraction.

Table 4.3: Preparation of standards to quantify percentage recovery during extraction

Recovery standard	Mass of standard (mg)	Concentration of stock solution (mg L ⁻¹)	Concentration in each sample (mg L ⁻¹)
C ₂₂	1.66	415	34
C ₃₄	1.73	433	36

Samples were extracted, purified, identified and quantified in accordance with the method described in Section 4.5.1 above. Water tests of the calibration of the automatic pipettes used for dispensing showed that the 25 µL pipette (used for adding 2 x 25 µL of C₂₂) typically dispensed $24.797 \pm 0.1 \times 10^{-4}$ mg of water, while the 50 µL pipette (used for adding 50 µL of C₃₄) dispensed on average 49.417 ± 0.001 mg of water.

4.6. RESULTS

4.6.1 Percentage recovery of *n*-alkanes

Minimum recovery of C₂₂ in the 18 plant leaf wax extracts was 94%, with maximum values of 125%. Recovery rates for the C₃₄ alkane standard showed a similar range, from 90% to 130%, indicating that there was no significant difference in the recovery of shorter or longer chain *n*-alkanes (student's t-test, $P = >0.05$, Minitab v.16). Those recovery rates in excess of 100% were attributed to the presence of small amounts of *n*-C₂₂ and *n*-C₃₄ in the leaf waxes of the plant samples. As recovery rates were so high in this experiment (in excess of 95% for 17 of the 18 plants) no further correction was made for this in subsequent data sets.

4.6.2 Molecular distribution profiles for plants sampled at Stiffkey

Species sampled at Stiffkey contained long-chain *n*-alkanes in the range *n*-C₂₃ to *n*-C₃₅. *Salicornia europaea* had the highest abundance of *n*-C₂₃ and *n*-C₂₅ alkanes (Fig. 4.5), while *Limonium vulgare* was the only species to consistently contain *n*-C₃₅ (Fig. 4.5) (Appendix 3) above the detection limit. In general, the odd-chain *n*-alkanes accounted for 77 – 95% of the total alkanes extracted from each species, while even-chain alkanes representing only 5 – 23% of the total alkane composition. C_{max} showed some interspecies variability, ranging from *n*-C₂₃ in *Salicornia europaea* and *Triglochin maritima* (Table 4.4 and 4.5) to *n*-C₃₁ for *Limonium vulgare*. The most frequently recorded C_{max} chain length among all species sampled was *n*-C₂₉ (49%, $n = 63$), followed by *n*-C₂₇ (28%, $n = 63$). Species differed in the percentage abundance of the dominant odd-chain alkane in their leaf wax. *Spartina anglica* had the highest percentage contribution from one chain length (*n*-C₂₉, ~60%; Fig. 4.5) while *Salicornia europaea* recorded a far more heterogeneous mix and had all but one chain-length falling within the range 13 – 22% (Fig. 4.5; Tables 4.4 and 4.5).

Species showed different seasonal shifts in percentage *n*-alkane abundance distributions. In *Atriplex portulacoides*, the greatest variability was seen in *n*-C₂₅ and *n*-C₂₉, while shifts of ~10% were observed in the percentage contributions of *n*-C₂₇, *n*-C₂₉ and *n*-C₃₁ in *Limonium vulgare* (Fig. 4.6). In the succulent *Suaeda vera* *n*-C₂₇ and *n*-C₂₉ showed the most variability (Fig. 4.6). Trends in *Salicornia europaea* showed the greatest overall seasonal change in *n*-alkane compositions for any species sampled, with up to 20% changes in the contribution of *n*-C₂₇ and *n*-C₂₃ in both 2011 and 2012 (Fig. 4.6). In some species analysed, the most abundant alkane chain lengths appeared to have an inverse relationship with each other -

Table 4.4: *n*-Alkane molecular data for species sampled at Stiffkey marsh, June, August and October 2011

Month	Site	Plant Species	ACL	CPI	C _{max}	C ₃₁ /C ₂₇	
June	Site 1	<i>Atriplex portulacoides</i>	26	26	25	-	
	Site 2	<i>Atriplex portulacoides</i>	26	26	25	0.1	
	Site 3	<i>Atriplex portulacoides</i>	26	18	25	-	
	Site 2	<i>Elytrigia atherica</i>	28	22	29	4.1	
	Site 1	<i>Limonium vulgare</i>	29	20	29	-	
	Site 3	<i>Limonium vulgare</i>	29	24	29	0.8	
	Site 2	<i>Phragmites</i>	25	6	25	-	
	Site 2	<i>Puccinella maritima</i>	28	14	27	5.8	
	Site 1	<i>Salicornia Europaea</i>	27	6	25	0.8	
	Site 1	<i>Spartina anglica</i>	28	14	29	0.9	
	Site 2	<i>Suaeda vera</i>	27	24	29	0.9	
	Site 3	<i>Suaeda vera</i>	28	20	29	-	
	Site 1	<i>Triglochin maritima</i>	27	3	23	-	
	Site 3	<i>Triglochin maritima</i>	26	6	23	3.0	
	August	Site 1	<i>Atriplex portulacoides</i>	27	17	27	0.2
Site 2		<i>Atriplex portulacoides</i>	27	13	27	0.1	
Site 3		<i>Atriplex portulacoides</i>	27	15	27	0.1	
Site 2		<i>Elytrigia atherica</i>	30	12	29	4.3	
Site 3		<i>Limonium vulgare</i>	30	15	31	4.0	
Site 2		<i>Phragmites</i>	28	7	29	-	
Site 1		<i>Salicornia europaea</i>	26	13	23	0.6	
Site 3		<i>Salicornia europaea</i>	27	7	23	0.9	
Site 1		<i>Spartina anglica</i>	29	15	29	2.0	
Site 3		<i>Spartina anglica</i>	29	15	29	1.1	
Site 2		<i>Suaeda vera</i>	28	18	27	0.3	
Site 3		<i>Suaeda vera</i>	28	34	27	0.5	
October		Site 1	<i>Atriplex portulacoides</i>	26	12	25	0.2
		Site 2	<i>Atriplex portulacoides</i>	28	12	27	-
		Site 3	<i>Atriplex portulacoides</i>	25	7	25	-
	Site 2	<i>Elytrigia atherica</i>	30	10	29	3.5	
	Site 3	<i>Limonium vulgare</i>	30	14	29	1.8	
	Site 2	<i>Phragmites</i>	28	7	29	0.1	
	Site 1	<i>Salicornia europaea</i>	27	18	27	0.2	
	Site 3	<i>Salicornia europaea</i>	24	6	23	-	
	Site 1	<i>Spartina anglica</i>	29	15	29	1.5	
	Site 2	<i>Suaeda vera</i>	28	27	27	0.2	
Site 3	<i>Suaeda vera</i>	27	28	27	0.1		

Table 4.5: *n*-Alkane molecular data for species sampled at Stiffkey marsh, March-September 2012

Month	Location	Plant Species	ACL	CPI	C _{max}	C ₃₁ /C ₂₇
March	Site 2	<i>Atriplex portulacoides</i>	27	17	27	0.2
	Site 2	<i>Elytrigia atherica</i>	29	48	29	3.5
	Site 3	<i>Limonium vulgare</i>	31	13	29	1.9
	Site 1	<i>Spartina anglica</i>	29	18	29	1.2
	Site 2	<i>Suaeda vera</i>	29	33	29	0.7
May	Site 2	<i>Atriplex portulacoides</i>	27	11	27	0.1
	Site 2	<i>Elytrigia atherica</i>	29	44	29	5.5
	Site 3	<i>Limonium vulgare</i>	30	28	29	1.3
	Site 2	<i>Phragmites</i>	27	33	29	-
	Site 1	<i>Salicornia Europaea</i>	25	19	29	1.2
	Site 1	<i>Spartina anglica</i>	28	16	29	0.4
	Site 2	<i>Suaeda vera</i>	28	37	29	0.7
August	Site 2	<i>Atriplex portulacoides</i>	27	15	27	0.1
	Site 2	<i>Elytrigia atherica</i>	30	23	29	3.6
	Site 3	<i>Limonium vulgare</i>	29	20	31	1.6
	Site 2	<i>Phragmites</i>	27	8	29	0.1
	Site 1	<i>Salicornia Europaea</i>	27	18	23	0.8
	Site 1	<i>Spartina anglica</i>	28	15	29	1.0
	Site 2	<i>Suaeda vera</i>	28	29	27	0.3
September	Site 2	<i>Atriplex portulacoides</i>	27	12	27	0.2
	Site 2	<i>Elytrigia atherica</i>	29	9	29	2.8
	Site 3	<i>Limonium vulgare</i>	30	13	29	1.8
	Site 2	<i>Phragmites</i>	27	7	29	0.1
	Site 1	<i>Salicornia Europaea</i>	27	6	27	0.5
	Site 1	<i>Spartina anglica</i>	29	11	29	1.7
	Site 2	<i>Suaeda vera</i>	28	25	27	0.2

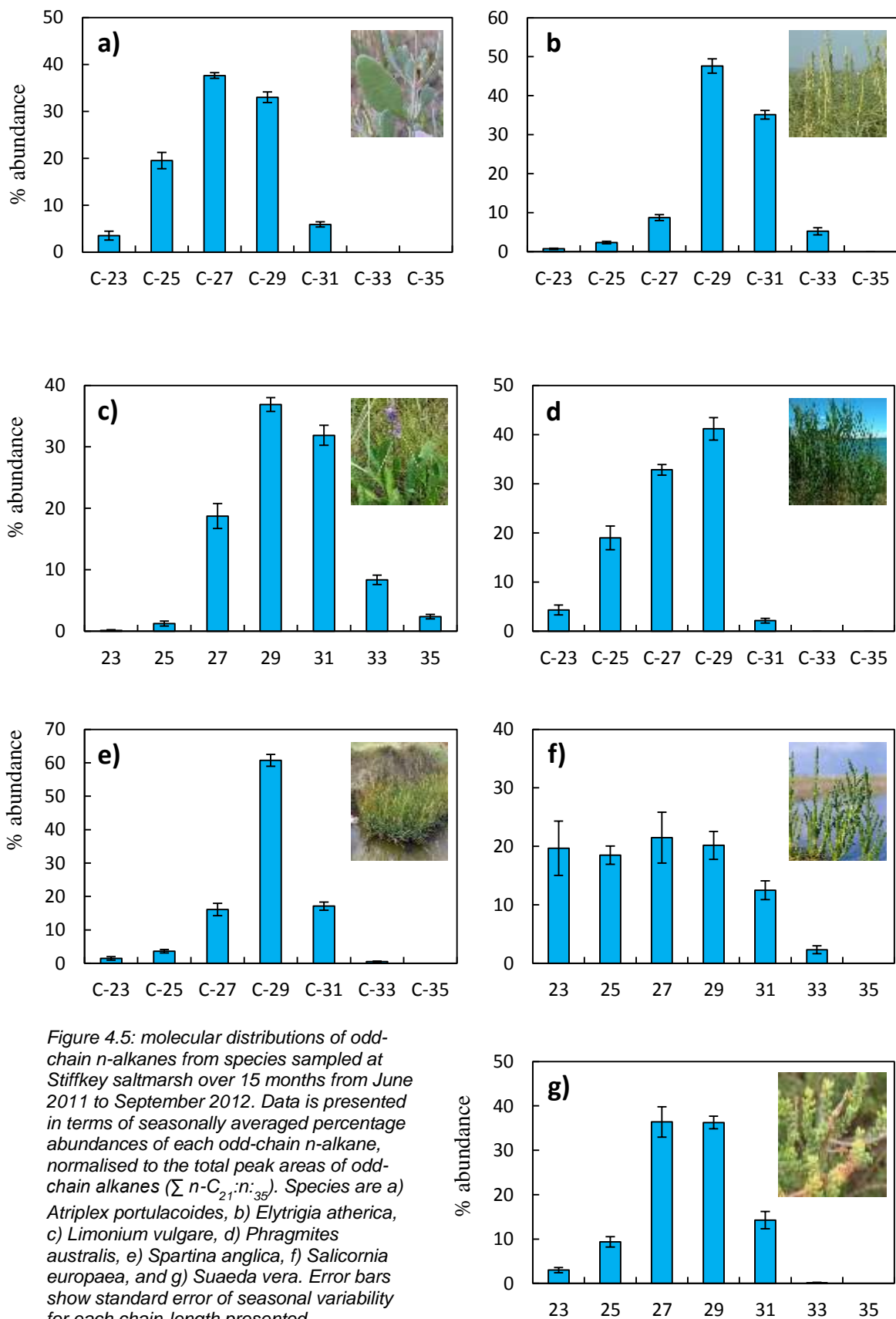


Figure 4.5: molecular distributions of odd-chain *n*-alkanes from species sampled at Stiffkey saltmarsh over 15 months from June 2011 to September 2012. Data is presented in terms of seasonally averaged percentage abundances of each odd-chain *n*-alkane, normalised to the total peak areas of odd-chain alkanes ($\sum n-C_{21};n:_{35}$). Species are a) *Atriplex portulacoides*, b) *Elytrigia atherica*, c) *Limonium vulgare*, d) *Phragmites australis*, e) *Spartina anglica*, f) *Salicornia europaea*, and g) *Suaeda vera*. Error bars show standard error of seasonal variability for each chain-length presented.

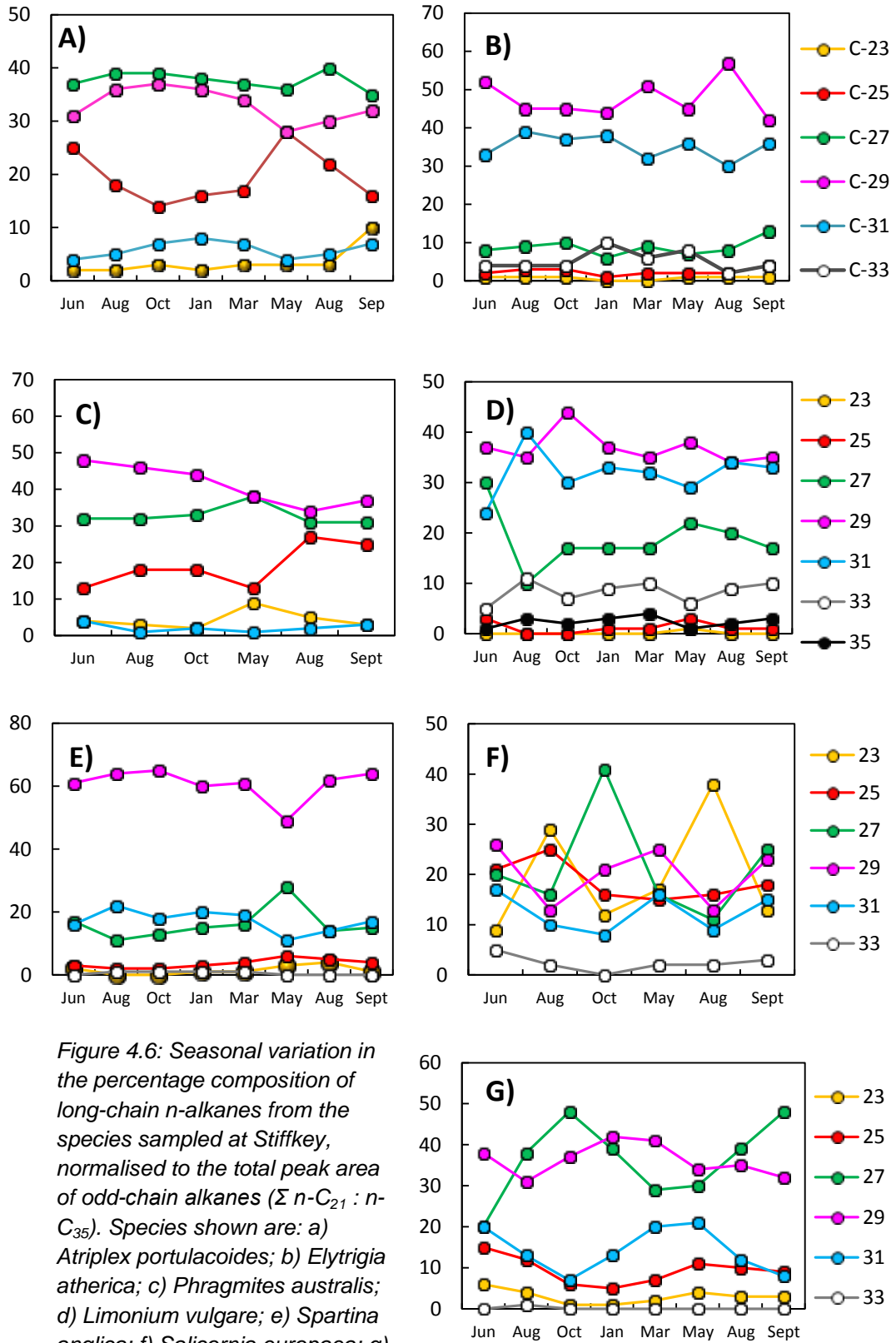


Figure 4.6: Seasonal variation in the percentage composition of long-chain n-alkanes from the species sampled at Stiffkey, normalised to the total peak area of odd-chain alkanes ($\Sigma n-C_{21} : n-C_{35}$). Species shown are: a) *Atriplex portulacoides*; b) *Elytrigia atherica*; c) *Phragmites australis*; d) *Limonium vulgare*; e) *Spartina anglica*; f) *Salicornia europaea*; g) *Suaeda vera*. A colour key for identification of n-alkane chain lengths is shown to the right of each row of graphs.

when one increases, the other decreases, and vice versa. This was particularly noticeable when comparing the percentage abundances of $n\text{-C}_{29}$ and $n\text{-C}_{31}$ in the C_3 grass *Elytrigia atherica* (Fig. 4.6). In the C_4 grass *Spartina anglica* the chain lengths $n\text{-C}_{29}$ and $n\text{-C}_{27}$ also appeared to have this inverse relationship, while in the evergreen succulent *Suaeda vera* this phenomenon was observed with $n\text{-C}_{27}$ and $n\text{-C}_{31}$ (Fig. 4.6). After confirming that these data had a normal distribution (Andersen-Darling test, Minitab v.16, $P > 0.05$), they were analysed statistically to see if there was significant relationship between % abundances of dominant chain lengths for all species sampled. For *Atriplex portulacoides*, $n\text{-C}_{25}$ had a strong negative correlation with both $n\text{-C}_{29}$ (Pearson's product moment correlation, $r = -0.847$, $P < 0.05$), and $n\text{-C}_{31}$ (Pearson's product moment correlation, $r = -0.907$, $P < 0.05$). A strong negative correlation was also found between the % abundance of: (i) $n\text{-C}_{29}$ and $n\text{-C}_{31}$ in *Elytrigia atherica* (Pearson's product moment correlation, $r = -0.894$, $P < 0.05$); (ii) $n\text{-C}_{27}$ and $n\text{-C}_{31}$ in *Limonium vulgare* (Pearson's product moment correlation, $r = -0.915$, $P < 0.05$); and (iii) $n\text{-C}_{27}$ and $n\text{-C}_{31}$ in *Suaeda vera* (Pearson's product moment correlation, $r = -0.938$, $P < 0.05$). The data for *Spartina anglica* did not have a normal distribution, so a Rank Spearman correlation (a non-parametric test for correlation) was carried out in this instance. Again, a strong negative correlation was observed between the % abundances of $n\text{-C}_{27}$ and $n\text{-C}_{29}$ ($r = -0.794$, $P < 0.05$).

4.6.3 Molecular distribution patterns among different marsh sub-environments

During 2011, plant species were sampled across multiple marsh sub-environments where appropriate. Marsh sub-environment did not appear to have any influence over C_{max} during June and August 2011 (Table 4.4). In October 2011, however, *Atriplex portulacoides* had a C_{max} of 27 at the ridge site, compared with a C_{max} of 25 in the LM and UM sites. Similarly, the succulent *Salicornia europaea* had a C_{max} of 27 in the LM in October, compared with a C_{max} of 23 in the UM (Table 4.4). ACL varied by only +/- 1 unit among species growing in multiple habitats during June and August 2011. In October, however, intraspecies variability in ACL across sub-environment increased among some of the sampled species. *Atriplex portulacoides* had ACL values of 26 in the LM, 28 and the ridge, and 25 in the UM in October 2011 (Table 4.4), *Salicornia europaea* presented a similar trend – it had an ACL of 27 in the LM and 24 in the UM (Table 4.4). ACL in *Suaeda vera* appeared relatively insensitive to changes in marsh sub-environment, as it continued to show limited shifts of +/-1 in October (Table 4.4). Of all the ratios calculated from n -alkane distribution data, CPI showed the greatest intra-species variability with marsh micro-

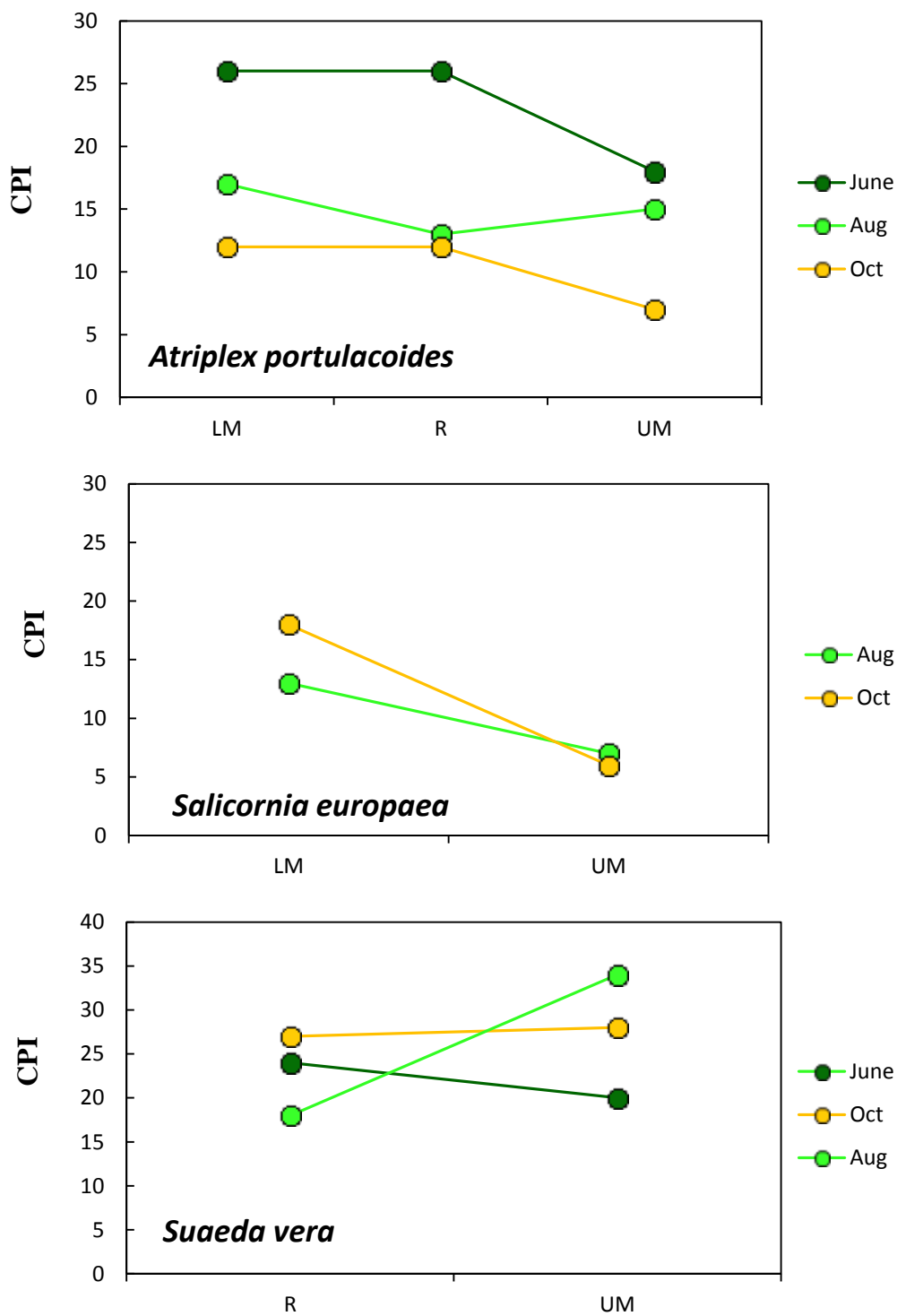


Figure 4.7: The influence of marsh sub-environment on CPI values in samples collected during 2011 from species growing at multiple locations across Stiffkey marsh. Plant species: a) *Atriplex portulacoides*, b) *Salicornia europaea* and c) *Suaeda vera*. LM=low marsh, R=ridge, UM=upper marsh.

habitat throughout the 2011 growing season. CPI in *Atriplex portulacoides* was generally lower in the UM, with a similar trend observed for *Salicornia europaea* (Fig. 4.7). Other species, however, displayed the opposite trend: *Limonium vulgare* had higher CPI values for the UM than the LM in August 2011, while the evergreen succulent *Suaeda vera* had higher CPI values in the UM than the ridge in August and October 2011 (Fig. 4.7; Table 4.4). In June the pattern was reversed, with higher values at the ridge (Table 4.4).

4.6.4 *n*-Alkane ratios

ACL, CPL and $n\text{-C}_{31}/n\text{-C}_{27}$ ratios were calculated for plants sampled from Stiffkey in 2011 (Table 4.4) and 2012 (Table 4.5). ACL values showed limited variability among all species sampled, ranging from 24 to 30 during 2011, and 25 to 31 during 2012. No systematic distinctions were revealed when comparing ACL values from grasses with those from woody shrubs (Table 4.4 and 4.5). CPI values showed greater variability than those calculated for ACL, ranging from 7 to 51 over the entire sampling period. CPI values showed some seasonal periodicity, with values being generally highest for all species early in the growing season (March/April/May) and falling at the end of summer (August/September). Once again, no systematic trends in CPI values between grasses/herbs and woody shrubs could be discerned from these data (Tables 4.4 and 4.5).

The ratio of $n\text{-C}_{31}$ to $n\text{-C}_{27}$ ranged from 0.1 (*Atriplex portulacoides*) to 5.8 (*Puccinellia maritima*) across the 2011 and 2012 growing seasons (Table 4.4 and 4.5). The higher values were typically found in the C_3 grass *Elytrigia atherica* (3.9 ± 0.8) and the C_3 herb *Limonium vulgare* (2.9 ± 1.0). The evergreen woody shrub *Atriplex portulacoides* generally had the lowest $n\text{-C}_{31}/n\text{-C}_{27}$ ratio of ≤ 0.2 (Table 4.4 and 4.5). Low values were not limited solely to woody shrubs at the site, however. The C_3 monocot reed *Phragmites australis*, for example, had an $n\text{-C}_{31}/n\text{-C}_{27}$ ratio of 0.1 in October 2011, August 2012 and September 2012 (Table 4.4 and 4.5). Comparing the $n\text{-C}_{31}/n\text{-C}_{27}$ ratios of woody and non-woody species showed a degree of overlap between these plant functional groups (Fig. 4.8). Although the woody species were categorised by a relatively narrow range of values, the spread of values for the non-woody species was larger, with some individuals having $n\text{-C}_{31}/n\text{-C}_{27}$ ratios that were indistinguishable from woody species.

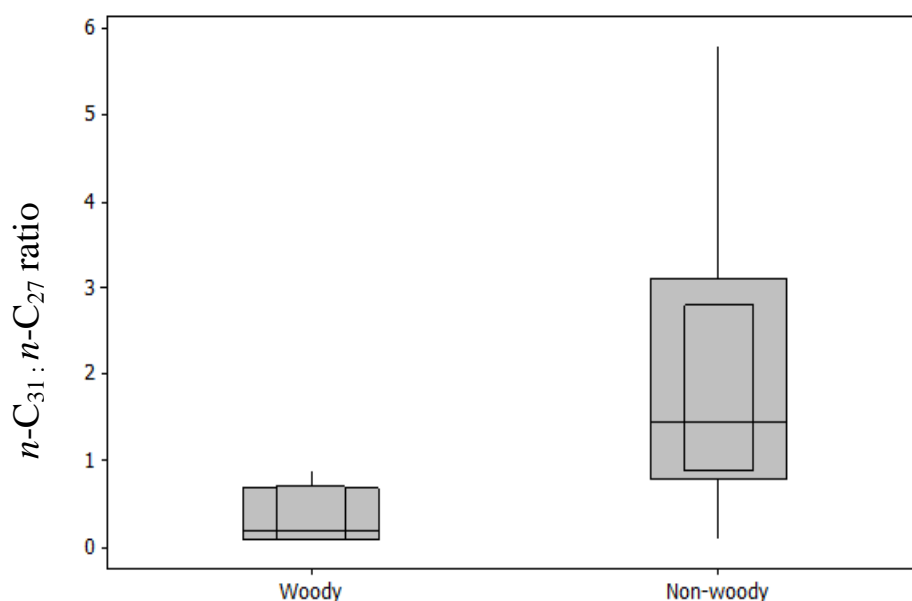


Figure 4.8: Box and whisker plot showing calculated $n\text{-C}_{31}/n\text{-C}_{27}$ ratios for woody and non-woody plant species at Stiffkey saltmarsh. Woody plants: *Atriplex portulacoides*, *Suaeda vera*; Non-woody plants: *Elytrigia atherica*, *Phragmites australis*, *Spartina anglica*, *Salicornia europaea*, *Limonium vulgare*

4.6.5 Variation in n -alkane concentration among sampled species

n -alkane concentrations are reported for $n\text{-C}_{21}$ to $n\text{-C}_{35}$ in Tables 4.5 and 4.6. Total concentrations of odd and even n -alkanes ($n\text{-C}_{21}$: $n\text{-C}_{35}$) varied from 2409 $\mu\text{g g}^{-1}$ dry mass (DM) (*Limonium vulgare*) to as little as 6 $\mu\text{g g}^{-1}$ DM (*Salicornia europaea*) (Fig. 4.9). Total alkane concentration was generally highest in the perennial C_3 herb *Limonium vulgare* (Fig. 4.9), however consideration of individual chain lengths showed that in March 2012 the C_3 grass *Elytrigia atherica* had the highest concentrations of $n\text{-C}_{27}$ and $n\text{-C}_{29}$, but not $n\text{-C}_{31}$ and $n\text{-C}_3$ (Table 4.6). The lowest concentration of n -alkanes in any species sampled was consistently found in *Salicornia europaea*, the C_3 stem succulent (Tables 4.5 and 4.6). *Elytrigia atherica* and *Spartina anglica* reported the highest concentrations of $n\text{-C}_{29}$ among the monocot species sampled, while the reed *Phragmites australis* generally had less than half the concentration of $n\text{-C}_{29}$ found in the other monocots (although it tended to have $\sim 10 \mu\text{g g}^{-1}$ DM more $n\text{-C}_{27}$). The evergreen shrub *Atriplex portulacoides* generally had the highest concentrations of $n\text{-C}_{25}$ of any species sampled (Table 4.5 and 4.6). *Limonium vulgare* was the only species sampled with appreciable concentrations of $n\text{-C}_{35}$, ranging from 8 $\mu\text{g g}^{-1}$ DM to 46 $\mu\text{g g}^{-1}$ DM depending on the sampling interval (Table 4.6 and 4.7).

Table 4.6: *n*-alkane concentrations (in µg per g of dry plant material) for species sampled in 2011

Month	Site	Plant Species	C ₂₁	C ₂₃	C ₂₅	C ₂₇	C ₂₉	C ₃₁	C ₃₃	C ₃₅	
June	Site 2	<i>Atriplex portulacoides</i>	0	3	38	56	46	7	0	0	
	Site 2	<i>Elytrigia atherica</i>	0	3	6	21	138	86	9	0	
	Site 3	<i>Limonium vulgare</i>	0	2	58	676	827	538	120	20	
	Site 2	<i>Phragmites</i>	0	3	11	28	43	3	0	0	
	Site 2	<i>Puccinella maritima</i>	1	3	9	14	99	80	14	0	
	Site 1	<i>Salicornia Europaea</i>	0	2	4	4	6	4	1	0	
	Site 1	<i>Spartina anglica</i>	2	3	6	34	118	31	1	0	
	Site 2	<i>Suaeda vera</i>	0	11	31	49	93	44	1	0	
August	Site 3	<i>Triglochin maritima</i>	1	4	5	14	39	40	6	0	
	Site 1	<i>Atriplex portulacoides</i>	0	4	48	91	65	16	0	0	
	Site 2	<i>Atriplex portulacoides</i>	0	2	19	41	37	6	0	0	
	Site 3	<i>Atriplex portulacoides</i>	0	4	38	77	54	10	1	0	
	Site 2	<i>Elytrigia atherica</i>	0	1	2	5	25	23	2	0	
	Site 3	<i>Limonium vulgare</i>	0	0	2	54	190	219	62	18	
	Site 2	<i>Phragmites</i>	0	2	14	26	37	1	0	0	
	Site 1	<i>Salicornia europaea</i>	0	2	2	1	1	1	0	0	
	Site 3	<i>Salicornia europaea</i>	1	8	8	7	7	7	3	1	
	Site 1	<i>Spartina anglica</i>	1	1	3	19	109	39	1	0	
	Site 3	<i>Spartina anglica</i>	0	1	3	22	108	25	1	0	
	Site 2	<i>Suaeda vera</i>	0	7	21	66	53	22	1	0	
	Site 3	<i>Suaeda vera</i>	0	5	12	26	28	12	0	0	
	October	Site 2	<i>Atriplex portulacoides</i>	2	2	11	29	26	4	0	0
		Site 2	<i>Elytrigia atherica</i>	1	2	7	26	111	91	10	0
Site 3		<i>Limonium vulgare</i>	0	0	1	78	206	137	30	8	
Site 2		<i>Phragmites</i>	0	1	16	30	40	2	0	0	
Site 1		<i>Salicornia europaea</i>	3	3	4	10	5	2	0	0	
Site 1		<i>Spartina anglica</i>	0	1	4	20	105	30	1	0	
Site 2		<i>Suaeda vera</i>	0	2	9	70	54	11	0	0	

Table 4.7: *n*-alkane concentrations (in µg per g of dry plant material) for species sampled in 2012

Month	Site	Plant Species	C ₂₁	C ₂₃	C ₂₅	C ₂₇	C ₂₉	C ₃₁	C ₃₃	C ₃₅
March	Site 2	<i>Atriplex portulacoides</i>	1	7	60	127	118	28	1	0
	Site 2	<i>Elytrigia atherica</i>	1	5	21	107	599	373	71	2
	Site 3	<i>Limonium vulgare</i>	0	0	14	6	190	386	107	46
	Site 1	<i>Spartina anglica</i>	1	1	5	20	76	24	1	0
May	Site 2	<i>Suaeda vera</i>	0	10	36	142	201	103	1	0
	Site 2	<i>Atriplex portulacoides</i>	2	5	51	67	52	8	0	0
	Site 2	<i>Elytrigia atherica</i>	1	2	2	16	97	71	17	1
	Site 3	<i>Limonium vulgare</i>	0	6	28	228	391	295	64	14
	Site 2	<i>Phragmites</i>	0	1	2	6	6	0	0	0
	Site 1	<i>Salicornia Europaea</i>	1	1	1	1	1	1	0	0
	Site 1	<i>Spartina anglica</i>	3	3	5	28	49	10	0	0
	Site 2	<i>Suaeda vera</i>	1	6	15	43	49	31	1	0
August	Site 2	<i>Atriplex portulacoides</i>	1	4	30	56	43	7	0	0
	Site 2	<i>Elytrigia atherica</i>	0	2	3	13	93	49	3	0
	Site 3	<i>Limonium vulgare</i>	0	0	9	134	222	222	58	15
	Site 2	<i>Phragmites</i>	0	3	13	15	17	1	0	0
	Site 1	<i>Salicornia Europaea</i>	1	4	2	1	1	1	0	0
	Site 1	<i>Spartina anglica</i>	1	1	2	5	23	5	0	0
	Site 2	<i>Suaeda vera</i>	0	5	18	68	62	22	1	0
September	Site 2	<i>Atriplex portulacoides</i>	1	19	17	39	37	8	0	0
	Site 2	<i>Elytrigia atherica</i>	0	2	5	17	57	48	5	0
	Site 3	<i>Limonium vulgare</i>	0	1	8	160	311	294	92	26
	Site 2	<i>Phragmites</i>	0	3	20	24	28	2	0	0
	Site 1	<i>Salicornia Europaea</i>	0	2	3	4	4	2	0	0
	Site 1	<i>Spartina anglica</i>	0	1	4	14	71	22	0	0
	Site 2	<i>Suaeda vera</i>	0	4	13	66	44	11	0	0

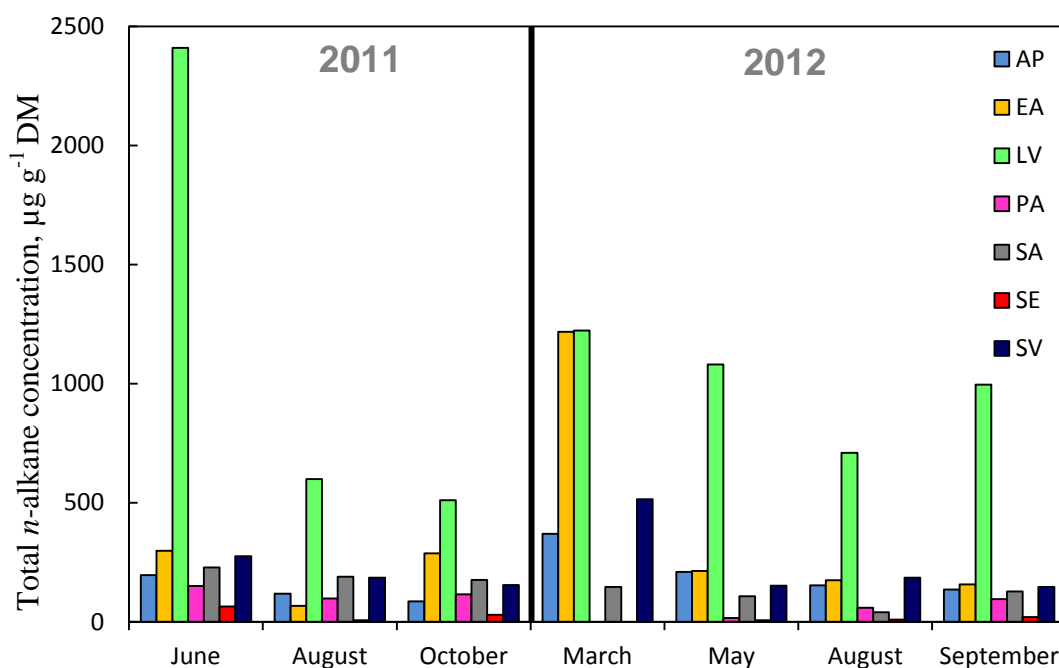


Figure 4.9: Total concentration of odd-chain ($n\text{-C}_{21}$ to $n\text{-C}_{35}$) alkanes for all sampled species across the 2011 and 2012 growing seasons; AP=*Atriplex portulacoides*, EA=*Elytrigia atherica*, LV=*Limonium vulgare*, PA=*Phragmites australis*, SA=*Spartina anglica*, SE=*Salicornia europaea*, SV=*Suaeda vera*. The black line shows the divide between data from 2011 and 2012.

The concentration of n -alkanes was generally highest in all species at the start of the growing season. In *Elytrigia atherica* and *Atriplex portulacoides*, concentrations decreased as the growing season progressed – a trend that was particularly noticeable in 2012 (Fig. 4.10 a and b). However, in other species, wax concentrations appeared to increase at the end of the growing season (October 2011; September 2012). This was particularly noticeable in *Salicornia europaea*, *Spartina anglica* and *Phragmites australis* (Fig. 4.11 a, b and c). In some species, such as *Phragmites australis* and *Spartina anglica*, clear differences were observed when leaf wax concentrations from 2011 were compared with those from 2012 (Fig. 4.11 a and c). *Limonium vulgare* also had considerable annual variation, with very high concentrations of n -alkanes in June 2011, which were not repeated throughout 2012 (Fig. 4.10 c). Other species showed greater consistency across the 2011 and 2012 growing seasons. *Elytrigia atherica*, *Suaeda vera* and *Atriplex portulacoides* in particular recorded similar profiles in both 2011 and 2012, with concentrations peaking in March 2012 (Fig. 4.10 a and b; Fig. 4.12).

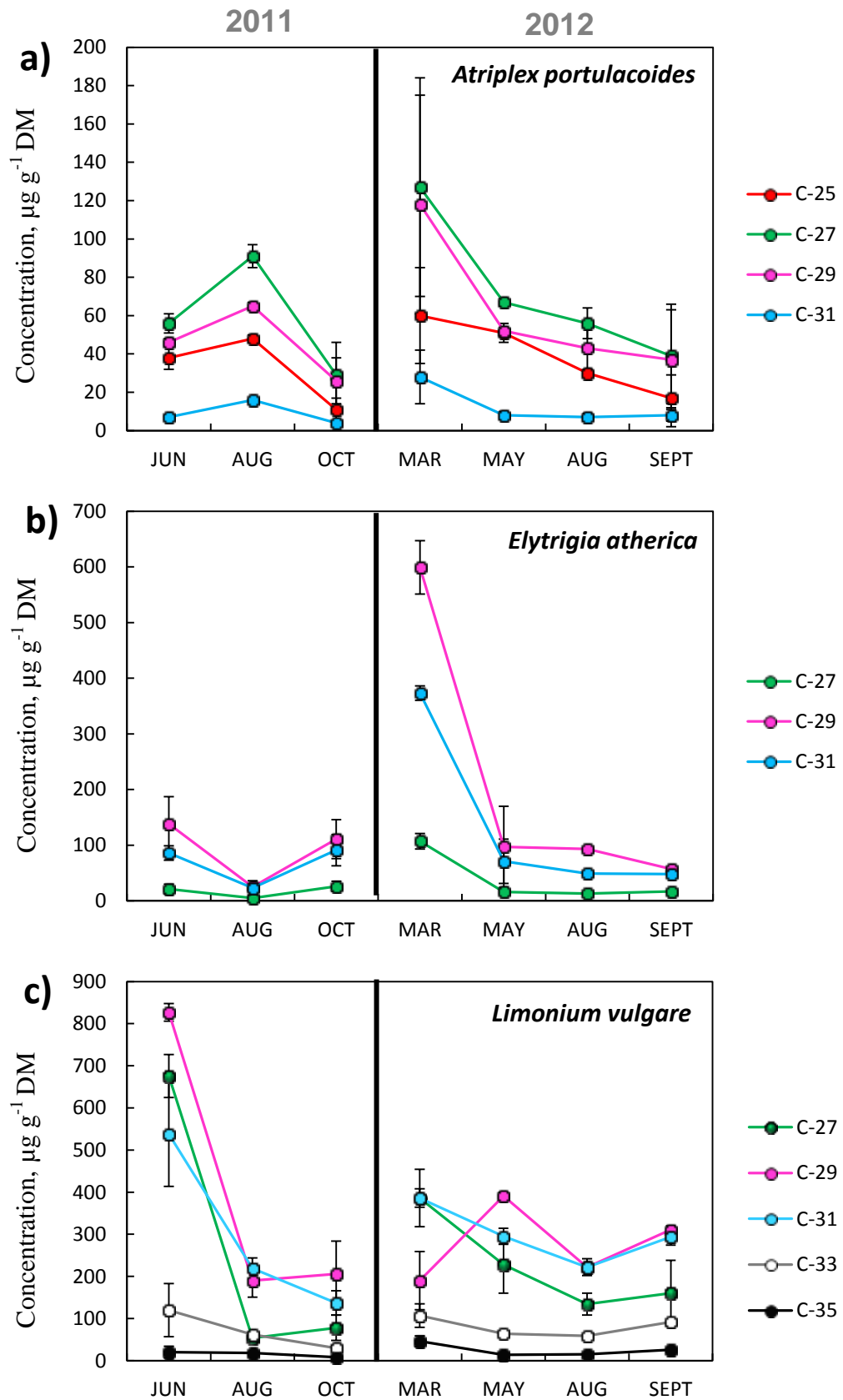


Figure 4.10: Seasonal variation in n-alkane concentrations for a) *Atriplex portulacoides*, b) *Elytrigia atherica*, and c) *Limonium vulgare*, sampled across the 2011 and 2012 growing seasons. Error bars show absolute difference between sample replicates. The black line divides data from 2011 and 2012

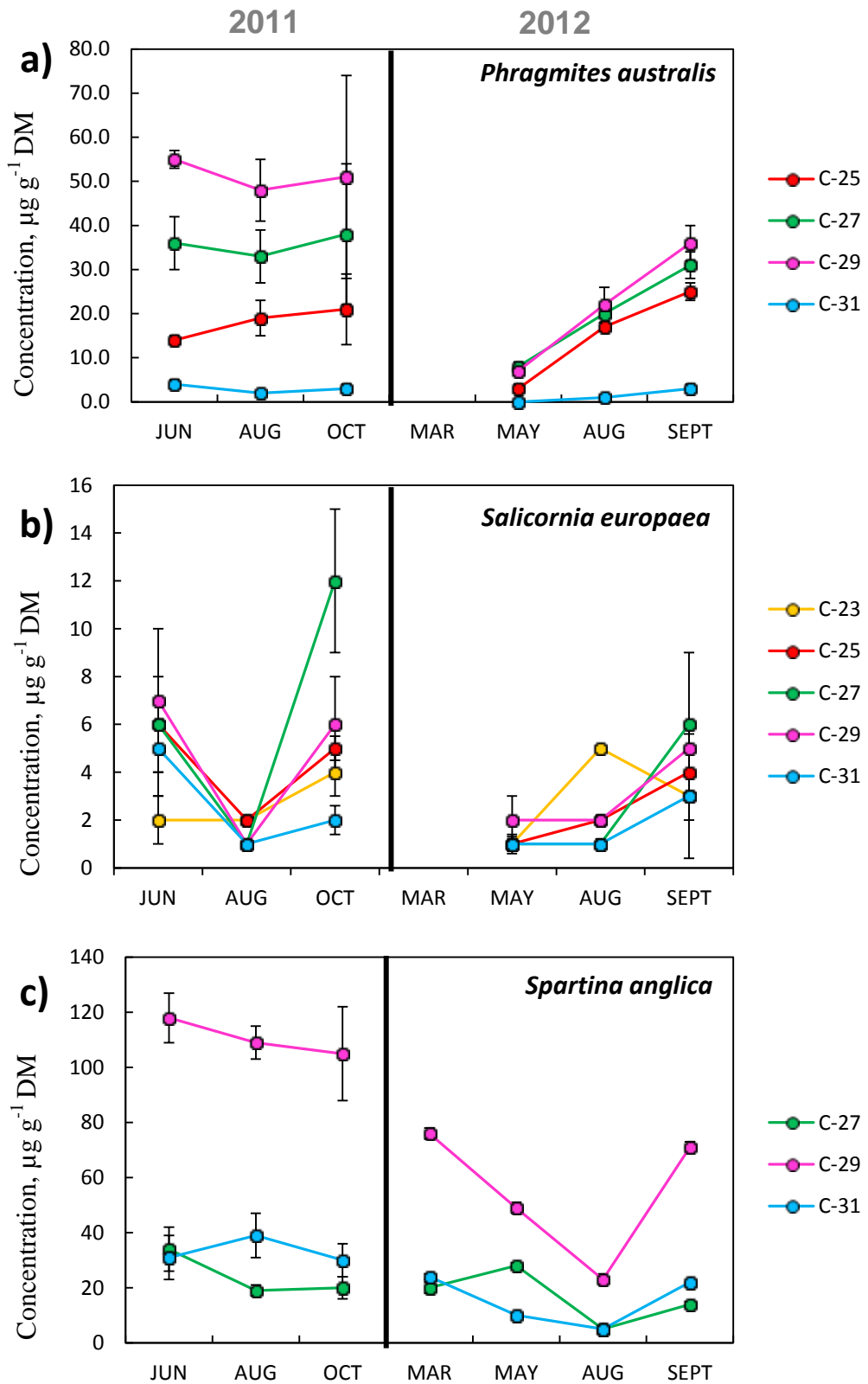


Figure 4.11: Seasonal variation in *n*-alkane concentrations for a) *Phragmites australis*, b) *Salicornia europaea*, and c) *Spartina anglica*, sampled across the 2011 and 2012 growing seasons. Error bars show absolute difference between sample replicates. The central black line divides data from 2011 and 2012

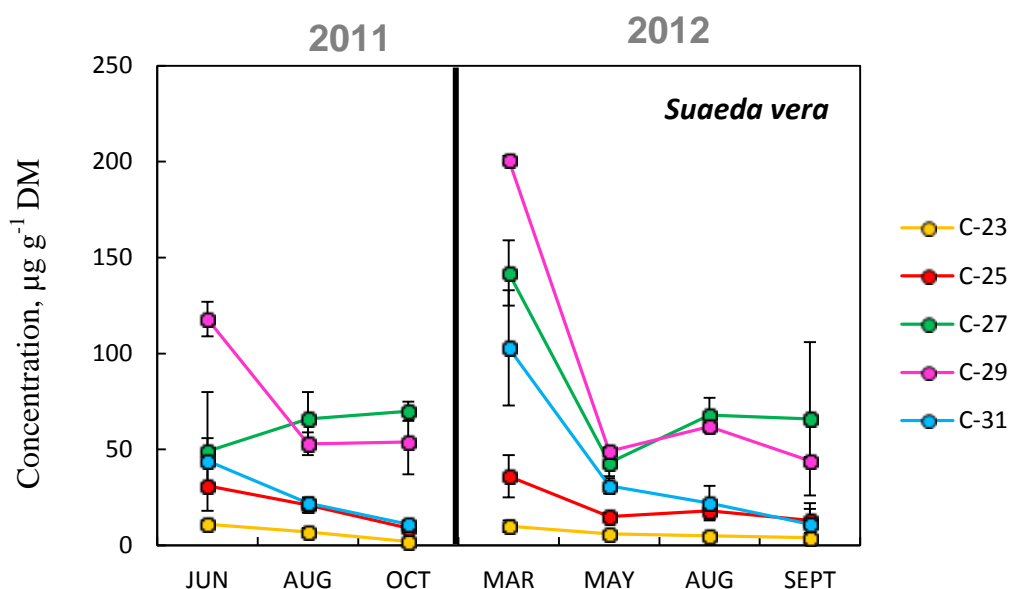


Figure 4.12: Seasonal variation in *n*-alkane concentrations for *Suaeda vera* sampled across the 2011 and 2012 growing seasons. Error bars show absolute difference between sample replicates. The central black line divides data from 2011 and 2012

Examination of any statistically significant correlations between the weather data and the absolute concentrations in those species with the greatest differences between 2011 and 2012 revealed that the concentration of *n*-C₂₇ and *n*-C₂₉ had a negative correlation with rH in *Phragmites australis*. In *Limonium vulgare* however, concentrations of *n*-C₂₉ and *n*-C₃₁ did not correlate with any of the weather parameters for which data was collected.

4.6.6 *n*-Alkane concentrations across different marsh sub-environment

Data from August 2011 allowed for consideration of whether plants growing in different marsh sub-environments produced different concentrations of *n*-alkanes. Variation with micro-habitat appeared to be species specific – *Atriplex portulacoides* had the highest concentration of alkanes at the LM, and the lowest at the ridge, while *Suaeda vera* had higher concentrations at the ridge than the UM. *Salicornia europaea* had higher concentrations in the UM than the LM, while *Spartina anglica* showed no clear trend among dominant chain lengths (Table 4.5).

4.7. DISCUSSION

The leaf wax *n*-alkane data generated in this study showed significant variability in the distribution and concentration among seven coastal species, which does not appear to be systematically linked to their different life form. Variability also exists in the distribution and concentration of *n*-alkanes from a single species (i) across a growing season, and (ii) across different marsh sub-environments. These findings therefore expand existing knowledge about the wax composition and concentration of temperate saltmarsh vegetation, and have important implications for reconstructing vegetation inputs to OM in near-shore coastal sediments.

4.7.1 The magnitude of interspecies variation in *n*-alkane distribution patterns

The seven saltmarsh plants sampled across the 2011 and 2012 growing seasons at Stiffkey show a wide variation in the distribution of *n*-alkanes found in their leaf wax (Fig. 4.5). Many of the plant species, especially the grasses, have *n*-C₂₉ as their most dominant alkane, while the woody evergreens *Atriplex portulacoides* and *Suaeda vera* have both *n*-C₂₇ and *n*-C₂₉ as their most abundant alkane chain lengths. Some species such as *Limonium vulgare*, *Phragmites australis*, and *Atriplex portulacoides* have three prominent chain lengths. Rommerskirchen *et al.* (2006) find that C₄ grasses, particularly of the sub-family NAD-ME (in which the decarboxylase NAD-dependent malic enzyme is predominant in the C₄ biochemical process) and PEP-CK (in which the decarboxylase phosphoenolpyruvate carboxykinase is predominant in the C₄ biochemical process), had greater abundances of *n*-C₃₁ and *n*-C₃₃ compared with both C₃ savanna grasses and C₃ rainforest vegetation. *Spartina anglica* at Stiffkey, however, while also from the PEP-CK sub-family (Voznesenskaya *et al.*, 2006), contains lower levels of *n*-C₃₁ and *n*-C₃₃ than the C₃ grass *Elytrigia atherica*, and the C₃ herb *Limonium vulgare* (Fig. 4.5), suggesting that findings from tropical/arid regimes may not automatically translate into temperate coastal settings.

The *n*-alkane distribution pattern of *Spartina anglica* recorded at Stiffkey is similar to that previously reported for the species *Spartina alterniflora* growing in temperate conditions by Canuel *et al.* (1997), Sessions (2006) and Tanner *et al.* (2007, 2010), with C_{max} of *n*-C₂₉, and the presence of chain lengths ranging from *n*-C₂₃ to *n*-C₃₃. Some variation from previous studies is observed however – Wang *et al.* (2003) reported that while the dominant alkane peak was *n*-C₂₉, *Spartina altherniflora* sampled in a Massachusetts saltmarsh in July of 2001 contained almost equal

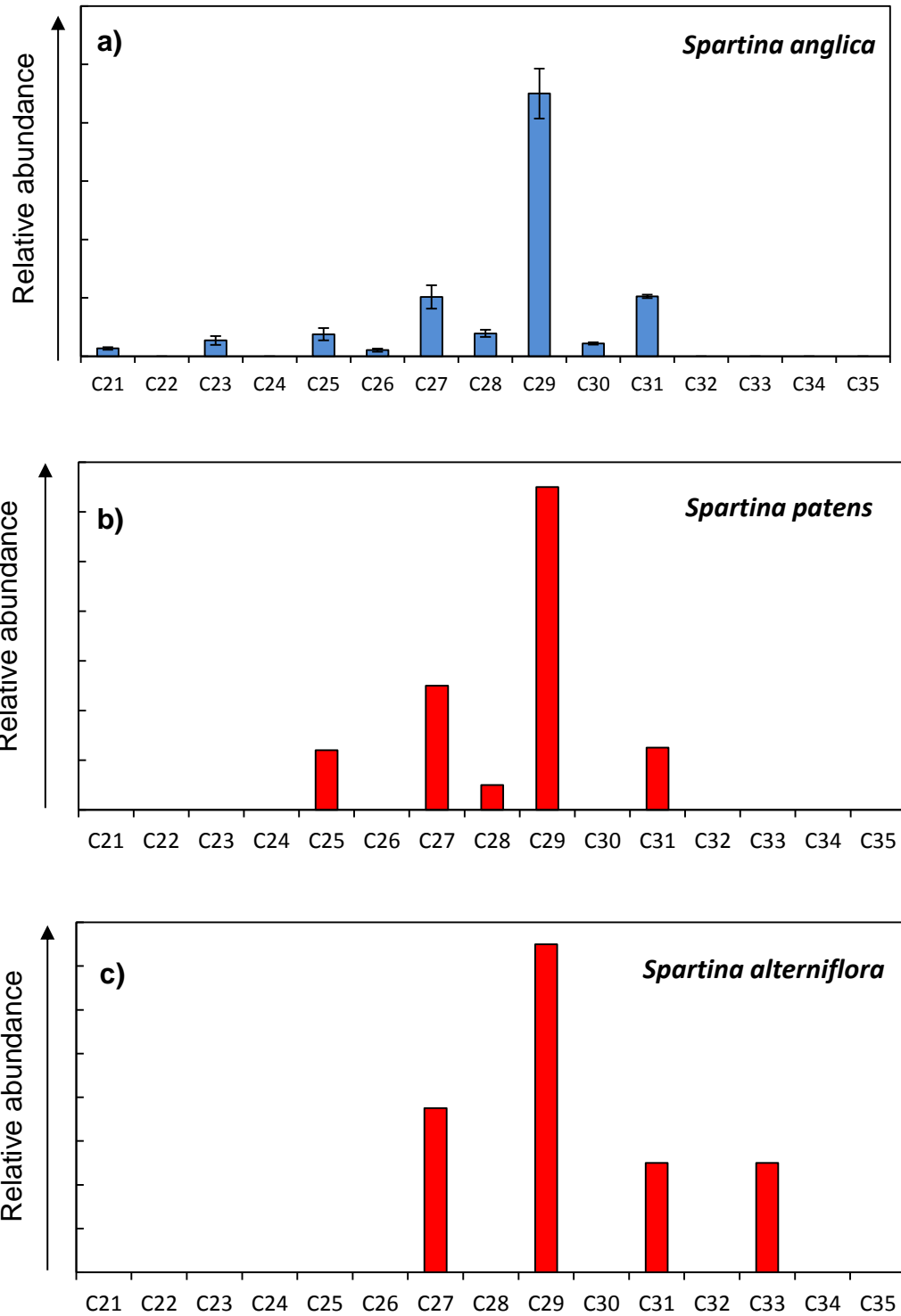


Fig. 4.13: *n*-alkane distribution patterns from a) *Spartina anglica* (Stiffkey, North Norfolk, UK; this study), b) *Spartina patens* (Maine, USA; Tanner et al., 2007), and c) *Spartina alterniflora* (Maine, USA; Tanner et al., 2007).

abundances of $n\text{-C}_{25}$, $n\text{-C}_{27}$ and $n\text{-C}_{31}$. *Spartina anglica* at Stiffkey, in contrast, is almost completely dominated by $n\text{-C}_{29}$ with only minor contributions from other chain lengths.

This variability in distribution patterns among grasses from the same genus is further illustrated by comparison of the Stiffkey *Spartina anglica* data with that presented by Tanner *et al.* (2010), who measured distribution patterns of *Spartina patens* and *Spartina alterniflora* sampled in August 2004 from a Maine saltmarsh (Fig. 4.13). These grass species, also from the genus *Spartina*, show distinct differences in their n -alkane distribution patterns, with *S. patens* appearing similar to *Spartina anglica*. In contrast, *Spartina alterniflora* contains no contribution from chain lengths shorter than $n\text{-C}_{27}$ and is the only species to contain $n\text{-C}_{33}$. Tanner *et al.* (2007) also analysed species from the genera *Limonium*, *Suaeda* and *Atriplex* in the Maine saltmarsh. Species from these genera are also found at Stiffkey, however the distribution patterns of n -alkanes from the Maine species, *Limonium nashii* and *Atriplex petula*, are different from those found in the species *Limonium vulgare* and *Atriplex portulacoides* growing at Stiffkey. As all plants from these different studies were sampled at broadly similar times of year in a temperate climate, it seems unlikely that gross differences in local weather conditions are responsible for the variation in their distribution patterns between the two geographical locations. Bush and McInerney (2013) report wide variation in chain-length distributions among plants of the same functional type, while variation at the genotype level has been observed in studies of genetically manipulated crop species (e.g. Febrero *et al.*, 1998). It is suggested therefore that these different distribution patterns (e.g. Fig. 4.13) arise from genetic variation among the sampled species, and that previous findings reporting significant variability in n -alkane abundances among a single plant genus can be extended to include temperate saltmarsh species.

The most singular distribution pattern observed among the Stiffkey species is found in the stem succulent *Salicornia europaea*. This annual species has a seasonally averaged profile showing almost equal abundances of $n\text{-C}_{23}$, $n\text{-C}_{25}$, $n\text{-C}_{27}$ and $n\text{-C}_{29}$ (Fig. 4.5f). An earlier study seeking to identify organic matter contributing to the Morse River in Maine, USA has also found these relatively short-chain n -alkanes in plants from the genus *Salicornia* (Tanner *et al.*, 2010). In this study, sedimentary n -alkane profiles were often dominated by $n\text{-C}_{25}$, which was identified as a major component of leaf waxes in the species *Salicornia depressa*. The leaf succulent *Suaeda vera* (Stiffkey) also has a similar distribution pattern to the species *Suaeda maritima* growing in Maine (Tanner *et al.*, 2007). The similarity in these distribution

profiles contrasts strongly with the discussion relating to *Spartina anglica*, *Limonium vulgare* and *Atriplex portulacoides* in the previous paragraph. Bush and McInerney (2013) report that some species exert strong genetic control over their *n*-alkane distributions to the extent that plants growing in different locations have very similar *n*-alkane abundance patterns. It would appear from these data that species from the *Salicornia* and *Suaeda* genera may operate in a similar way. Indeed, this may be a feature of some succulent species. Feakins and Sessions (2010) conducted a study of succulent species grown under greenhouse conditions in California. They identified that species from the Aizoaceae and Crassulaceae families had consistent chain length distributions of *n*-alkanes in their leaf wax, although other succulent species sampled as part of their study did not.

Another feature of leaf waxes from *Salicornia europaea* is that *n*-C₂₃ is one of the more abundant alkane chain lengths identified in it (Figs. 4.5 and 4.6). Previously, high levels of *n*-C₂₃ have been thought largely absent in terrestrial higher plants, and therefore this alkane chain length in particular has been proposed as a robust proxy for the presence of *Sphagnum* (Nott *et al.*, 2000; Baas *et al.*, 2000; Pancost *et al.*, 2002; Nichols *et al.*, 2006; Bush and McInerney, 2013), or aquatic/non-emergent plants (Ficken *et al.*, 2002). The high relative abundance of *n*-C₂₃ in *Salicornia europaea* waxes suggests however that the assumption that this homologue is not found in terrestrial higher plants may not be valid for all species, and that the presence of it in sedimentary sequences may not be a definitive diagnostic tool for identifying inputs from *Sphagnum*. Interestingly, shorter chain homologues have been identified in the aquatic marine species *Zostera maritima* ($C_{max} = n-C_{21}$) (Canual *et al.*, 1997), indicating that their presence may be an important feature of some saltmarsh species inhabiting the interface between terrestrial and marine ecological habitats.

Many species at Stiffkey have significant contributions of relatively high molecular weight *n*-alkanes (*n*-C₃₁, *n*-C₃₃, and *n*-C₃₅) (Fig. 4.5 and 4.6). This is particularly noticeable in *Limonium vulgare*, where *n*-C₃₅ makes up between 1 and 4% of the total odd-chain *n*-alkane budget (Fig. 4.6). In *Salicornia europaea*, *n*-C₃₃ makes up between 2 and 5% of the odd-chain alkanes, while in *Spartina anglica*, *Elytrigia atherica* and *Suaeda vera*, *n*-C₃₁ comprises 7 – 39% of the total (Fig. 4.6). The presence of these higher molecular weight alkanes has previously been identified in plants growing in regions of water stress. Typical environments where such phenomena have been report include African savannas (Bush and McInerney, 2013) and the Pyrenees (Dodd and Proveda, 2003). While these ecotomes may

seem drastically different, in both cases plants are exposed to water stress in the form of drought. Dodd and Proveda (2003) hypothesised that if the prevention of cuticular water loss was a dominant driver of wax composition, the existence of winter physiological drought in mountainous regions could be responsible for the predominance of long-chain alkane homologues. However, Dodd and Proveda (2003) theorised that if water loss was the primary mechanism controlling *n*-alkane composition, plants would be more likely to produce waxes with one or two dominant, relatively high weight, alkane homologues. This does not appear to be the case in Pyrenean juniper (Dodd and Proveda, 2003), rainforest species (Vogts *et al.*, 2009), African savannah species (Vogts *et al.*, 2009; Bush and McInerney, 2013) or indeed the species sampled at Stiffkey (Fig. 4.5 and 4.6).

The extent to which leaf wax distribution patterns are affected by environmental stimuli such as water availability remains a matter of ongoing debate in the scientific literature. Studies of plant wax biomarkers found in aerosols, for example, have suggested a link between *n*-alkane chain length distributions and environmental conditions. Simoneit *et al.* (1991) analysed aerosol samples from China, and found that the presence of higher molecular weight alkanes correlated with the transport of aerosols from the hotter south of China. Kawamura *et al.* (2003) carried out a study of ten different plant species growing tropical, sub-tropical and temperate environments, and found that ACL values increased when leaf waxes are produced in warmer climates. Tipple and Pagani (2013) found a correlation between ACL values and latitude, with longer chain lengths being produced in lower latitudes with higher temperatures, while Rommerskirchen *et al.* (2006), report that C₄ grass species adapted to extreme arid tropical and subtropical habitats have higher amounts of longer-chain *n*-alkane homologues. These findings, however, have to be set in the context of the previously discussed caveats regarding ACL (Bush and McInerney, 2013).

Despite the obvious complexity of relating leaf wax composition to cuticle function and environmental conditions arising from the diverse biochemical responses of different plants to abiotic stress (e.g. Dodd and Proveda, 2003), the potential relationship between the presence of higher weight alkane homologues and water stress is interesting to consider in a saltmarsh setting. Saltmarsh species are often water stressed, although in these environments this derives from the salinity of the environmental water rather than simply a shortage of water itself. Many halophytes have physical adaptations to minimise water loss, including thick cuticles (Baker,

1982), and it is therefore plausible that the production of high molecular weight alkanes in epicuticular wax afford the Stiffkey species a further degree of protection.

The overall interspecies plasticity of *n*-alkane distribution patterns at Stiffkey is also potentially related to species-specific adaptations towards their growth environment. Bush and McInerney (2013) argue convincingly that the chemical composition of that wax could conceivably be related to the abiotic conditions encountered by the plant, as the wax layer is the first line of defence between a plant and its environment. At the marsh, each plant is known to have different physical and biochemical adaptations to protect it from the effects of salinity and root anoxia (Davy *et al.*, 2011 and references therein). It is therefore reasonable to conclude that the particular distribution patterns recorded fulfil some biological and/or physical function for each plant sampled, although at present further research is needed to understand precisely why plants growing in the same location display such different patterns of *n*-alkane abundance.

4.7.2 The influence of seasonality on *n*-alkane distribution patterns

Previous studies have presented conflicting results regarding whether *n*-alkane distribution patterns are stable throughout the course of a growing season. Bush and McInerney (2013) found that the *n*-alkane distributions in leaf waxes from a range of temperate trees sampled from the Chicago Botanic Garden do not vary significantly with sampling date. Other research has indicated that major changes in *n*-alkane distributions do occur as leaves are maturing, although once the mature leaf is formed, these patterns do not show any changes (Piasentier *et al.*, 2000; Tipple and Pagani, 2013). Jetter and Schaeffer (2001), however, found that the overall composition of epicuticular wax of *Prunus laurocarpus* changed throughout the growing season, with longer chain *n*-alkane homologues increasing in abundance as the growing season progressed.

All species sampled at Stiffkey show temporal variation in the percentage abundance of the *n*-alkanes in their leaf waxes through 2011 and 2012 (Fig. 4.6). In *Atriplex portulacoides*, for example, the percent contribution of *n*-C₂₅ is highest in June 2011 and May 2012, and then drops by ~10%. The two dominant chain lengths in *Elytrigia atherica*, *n*-C₂₉ and *n*-C₃₁ also vary across the growth season, particularly between March and August 2012. The greatest variability in the distribution of alkanes throughout the sampling interval is found in *Salicornia europaea*, where the amounts of *n*-C₂₃, *n*-C₂₇ and *n*-C₂₉ show shifts of over 20% depending upon the time of collection. The magnitude and direction of the shifts in

homologue distributions varied among species and did not show any predictable trends, suggesting a simple relationship does not exist between distribution patterns and seasonal shifts in environmental conditions.

Given that care was taken to sample new growth throughout this study, an alternative explanation that could account for this apparent lack of coherence in the timing and direction of shifts in distribution patterns is that each of these species has a different life strategy, including differences in the timing of their reproductive cycle. Previous studies, for example, report that when plants enter a reproductive phase, a shift towards shorter chain length *n*-alkanes can occur (Smith *et al.*, 2001; Rommerskirchen *et al.*, 2006). Close examination of the distribution of mid-chain alkanes (*n*-C₂₅ and/or *n*-C₂₇) shows that they do increase during the months of June/August in *Atriplex portulacoides*, and *Limonium vulgare*, while *Suaeda vera* records increasing levels of these homologues from August onwards in both 2011 and 2012. Flowering in the upper parts of the marsh takes place later in the summer, when restrictive conditions such as hypersalinity and nitrogen limitation abate (Davy and Smith, 1985), which would fit with the timing of the increase in relatively short chain *n*-alkanes among some species. Reproductivity may therefore have some influence over the seasonal cycling in chain length distributions, although further research is required to explore this concept further.

4.7.3 The influence of spatial variation in marsh characteristics on *n*-alkane distribution patterns

In addition to temporal variation in *n*-alkane distribution patterns, species growing at multiple locations across the saltmarsh also show some differences in the relative abundance of *n*-alkane homologues in their leaf wax. Data from samples collected in June, August and October 2011 (Table 4.4) demonstrate that indices such as C_{max}, ACL, *n*-C₃₁/*n*-C₂₇ and CPI differed among the species sampled depending upon the particular micro-environmental niche the sampled plant inhabited. The fact that C_{max} is slightly lower in the upper marsh for all species sampled in multiple habitats in October 2011 (despite showing no variation for other sampling intervals) suggests that this may be a more generalised plant response to conditions encountered in this location. One potential explanation for this change occurring in October is that species at the marsh, particularly in the UM – where hypersalinity is a problem in high summer – have a second growing season which occurs around September/October each year (Jeffries, 1977). Previous studies have shown that young leaves tend to have higher abundances of shorter-chain homologues (Jetter

and Schaffer, 2001) and hence this decline in C_{\max} may to some extent be explained by a second growth spurt.

The changes in CPI with marsh sub-environment appear species specific in terms of any trends (Table 4.4; Fig. 4.7). It is currently not clear whether these differences are driven by environmental or biochemical mechanisms (Bush and McInerney, 2011). The fact that CPI, for example, increases in the UM for some species (Fig. 4.7) while decreasing for others (Fig. 4.7) suggests that external factors are not controlling this signal, however. From the perspective of reconstructing plant inputs to sediments, it is noteworthy that spatial variability in the relative abundance of *n*-alkane homologues among species is generally lower than the overall interspecies variability discussed in 4.7.1 and 4.7.2 above.

4.7.4 Discrimination between species using molecular distribution ratios

ACL values calculated for species sampled at Stiffkey are all in the range 25 to 31 (Tables 4.4 and 4.5). Plants with very different life forms, e.g. the evergreen shrub *Atriplex portulacoides* and the annual stem succulent *Salicornia europaea*, regularly record the same ACL value. Equally, monocots using different carbon metabolic pathways, such as *Elytrigia atherica* (C_3) and *Spartina anglica* (C_4) are often indistinguishable based on their ACL. This similarity of ACL values among graminoids with different carbon metabolisms contrasts with the findings of Rommerskirchen *et al.* (2006) who report that C_4 African savannah grasses have higher ACL values than C_3 grasses or C_3 temperate plants. The similarities in ACL reported here indicate that this simplistic molecular distribution ratio will not allow for discrimination among the Stiffkey sampled plants either a) at the species level, or b) at the plant functional type level. Recent research by Bush and McInerney (2013), report similar difficulties in the use of ACL values for distinguishing between plants, and conclude that ACL was not capable of discriminating between even large-scale plant functional groups.

CPI values calculated for all Stiffkey species recorded values ranging from 3 to 48 (Tables 4.4 and 4.5). Again, this ratio shows limited chemotaxonomic potential among the Stiffkey plants, with plant species from different functional groups having either identical or very similar CPI values. For example, in June 2011 *Limonium vulgare* and *Suaeda vera* both have CPI values of 20, while in August 2011 *Limonium vulgare* and *Spartina anglica* have CPI values of 15. There is an overall trend for CPI values to diminish as the growth season progresses, which is

potentially linked to the temporal changes in percentage abundance in the leaf waxes of each species discussed at Section 4.7.2.

In addition to varying among the different plant species sampled, CPI values also shifted considerably in individual species as the growing season progressed (Table 4.4 and 4.5). This may not be a result of changing conditions across the growth season, however, as the precise drivers of these changes in CPI remain unclear. Indeed, variation may be driven by biological as well as climatic factors. Bush and McInerney (2013) carried out a systematic study of the variability in CPI values among a wide range of plant species, and concluded that the variability was so great (CPI values ranged from <1 to >60) that any attempt to use CPI to identifying the nature of vegetative inputs to sediments would be flawed. It is possible therefore that some of the previous studies attributing shifts in CPI values to climate change (e.g. Yamade and Ishiwatari, 1999; Rao *et al.* 2009) could be in error because they do not take into account this species-specific variability. Data from Stiffkey further illustrate that linking CPI ratios to climatic conditions, without further understanding the mechanisms underpinning interspecies variation in *n*-alkane distribution patterns, may potentially be an example of correlation not equalling causation.

Calculation of a range of ratios ($n\text{-C}_{31}/n\text{-C}_{27}$; $n\text{-C}_{31}/n\text{-C}_{29}$; $n\text{-C}_{31}/(n\text{-C}_{29} + n\text{-C}_{31})$; $n\text{-C}_{31}/(n\text{-C}_{27} + n\text{-C}_{31})$) for plant functional groups encountered at Stiffkey (“non-woody” = all monocots, *Limonium vulgare* and *Salicornia europaea*; “woody” = *Atriplex portulacoides* and *Suaeda vera*) showed that the overlap in values compromised successful discrimination among them (Fig. 4.8). Interestingly, the data presented here suggest that it was the within-group variability for the grasses and perennials (i.e. the non-woody category) that was responsible for this overlap (Fig. 4.8). This contrasts with the findings of Bush and McInerney (2013), who report the greatest overlap in the woody species – again highlighting the complexity of the mechanisms controlling interspecies variability in *n*-alkane distributions. Regardless of this disparity, however, these results extend the conclusions of Bush and McInerney (2013), regarding the failure of abundance patterns of *n*-C₂₇, *n*-C₂₉ and *n*-C₃₁ to successfully discriminate between woody and non-woody plants, to saltmarsh species growing in a natural environment.

4.7.5 The magnitude of interspecies variability in *n*-alkane concentrations

Limited studies report the concentration of *n*-alkanes produced by a range of species growing at the same geographical location. This is an important consideration, as the absolute concentration of each compound of interest produced

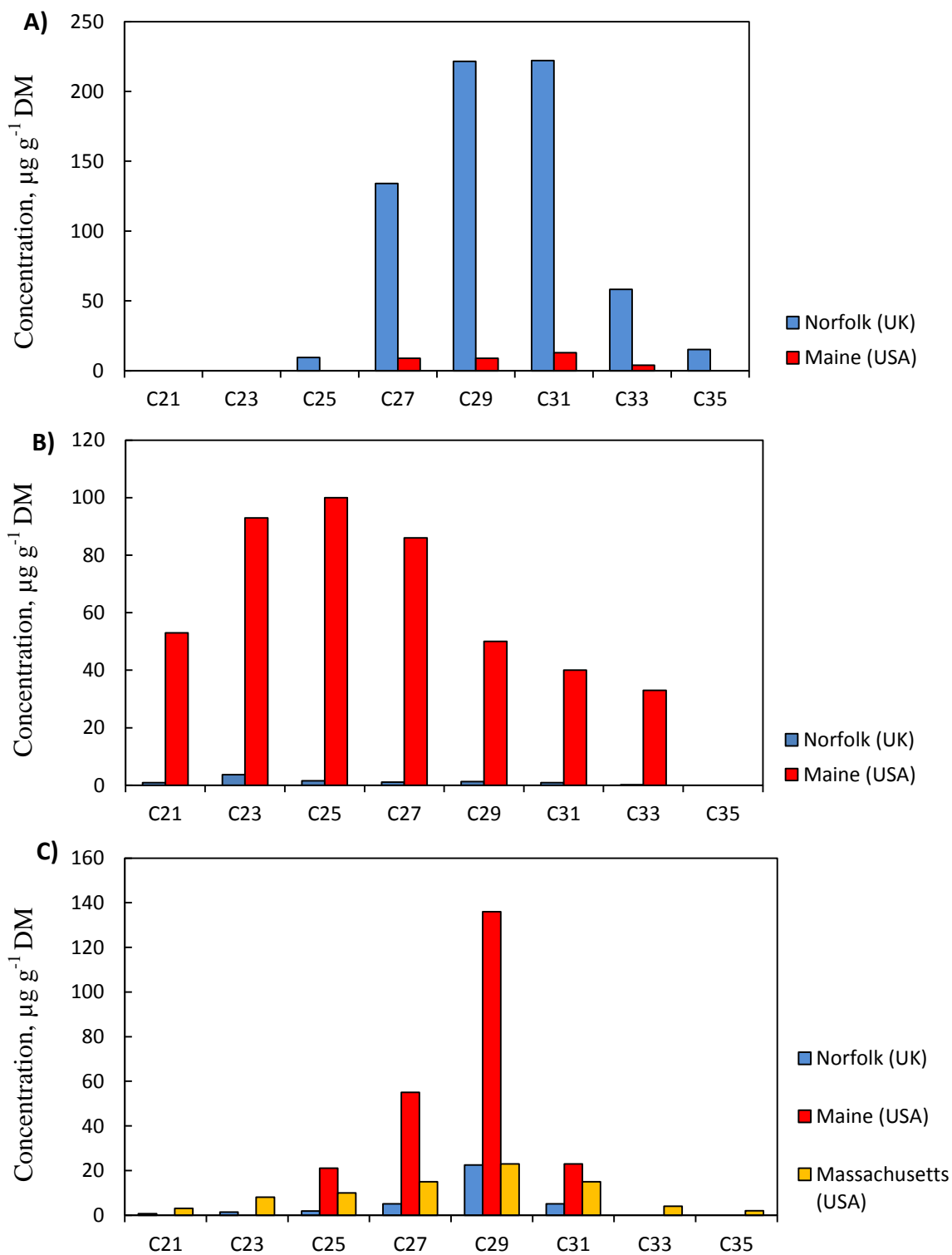


Figure 4.14: Comparison of *n*-alkane concentrations of species from the same genus growing at different geographical locations. A) *Limonium vulgare* (UK) vs *Limonium naashi* (Maine); B) *Salicornia europaea* (UK) vs *Salicornia depressa* (Maine); C) *Spartina anglica* (UK) vs *Spartina patens* (Maine) and *Spartina alterniflora* (Massachusetts). Comparison data sourced from Tanner et al. (2007, 2010) and Wang et al. (2003)

controls the relative preservation of OM from each species (Diefendorf *et al.*, 2011; Kirkels *et al.*, 2013). Studies seeking to either understand vegetation dynamics from leaf wax biomarker distributions, or interpret the stable isotopic composition of these biomarkers to reconstruct past climates, will need to take into account any diversity in the amount of material produced (Diefendorf *et al.*, 2011).

The total concentration ($n\text{-C}_{21}$ to $n\text{-C}_{35}$) of odd and even n -alkanes in the leaf waxes of Stiffkey species varies from 6 $\mu\text{g g}^{-1}$ DM (*Salicornia europaea*, May 2012) to 2409 $\mu\text{g g}^{-1}$ DM (*Limonium vulgare*, June 2011) (Fig 4.9). This exceeds the ranges reported for tropical/arid grasses (Rommerskirchen *et al.*, 2006) but is comparable to the dataset of 46 tree species presented by Diefendorf *et al.* (2011). The amount of $n\text{-C}_{29}$, the most commonly used n -alkane in palaeoclimate research (Sachse *et al.*, 2012), varies by over an order of magnitude between species at each sampling interval, with the highest amounts being produced by *Limonium vulgare* and the lowest amounts by *Salicornia europaea*. A similar pattern emerges when $n\text{-C}_{27}$ and $n\text{-C}_{31}$ are considered (Tables 4.5 and 4.6).

Comparison between total long-chain alkane concentrations ($n\text{-C}_{27}$ to $n\text{-C}_{35}$) from species sampled at Stiffkey and data produced by Rommerskirchen *et al.* (2006) for African savannah grasses show that *Limonium vulgare* at Stiffkey has higher total concentrations of these homologues than the tropical grasses for some sampling intervals. Concentrations of specific n -alkanes from the Stiffkey species are different from those previously published for the same genus in other geographical locations – for example, *Limonium nashii* in Maine (Tanner *et al.*, 2007) had up to 213 $\mu\text{g g}^{-1}$ DM less $n\text{-C}_{29}$ than *Limonium vulgare* (Fig. 4.14) for the same sampling month. In addition, when *Salicornia europaea* data are compared with n -alkane concentrations published for *Salicornia depressa* (Tanner *et al.*, 2007; 2010) (Fig. 4.14), *Salicornia depressa* has over 80 times higher concentrations of $n\text{-C}_{23}$ and $n\text{-C}_{25}$ than *Salicornia europaea*. *Suaeda maritima*, *Atriplex patula* and *Spartina patens* also have higher concentrations of alkanes in the Maine marsh (Tanner *et al.*, 2007, 2010) than species from the same genus at Stiffkey. Data for *Spartina alterniflora* sampled at a Massachusetts saltmarsh (Wang *et al.*, 2003), in contrast, shows similar n -alkane concentrations to those found at Stiffkey (Fig. 4.14).

The variation in n -alkane concentrations observed among the compared species could be due to several mechanisms. Firstly, the degree of wax abrasion due to wind ablation, rainfall and tidal inundation could vary between the sampling sites. Mechanical stresses such as these can ablate wax crystals from leaves (Shepherd

and Griffiths, 2006), and could give rise to lower overall wax concentrations in exposed sites when compared to sheltered ones. Tanner *et al.* (2007, 2010) note that their estuarine site is protected by high cliffs, in contrast to Stiffkey, while Wang *et al.* (2003) does not discuss the extent of exposure of species growing at the Massachusetts site. Although plants can replenish their wax layers, this is not always fast enough to maintain typical wax amounts for a particular species (Shepherd and Griffiths, 2006). It is therefore conceivable that plants growing at sites such as Stiffkey, where they are continually exposed to onshore winds from the North Sea, may display lower concentrations of *n*-alkanes than plants growing in more opportune conditions. This explanation however does not account for the significantly higher concentrations of *n*-alkanes in *Limonium vulgare* (Stiffkey) compared with *Limonium nashii* (Tanner *et al.*, 2007).

An alternative mechanism for these differences is that although the plants under comparison are from the same genus, they differ at the species level. A degree of genetic variation in the biochemical pathways controlling the amount of wax biomarkers they produce is therefore plausible. Plants respond to stresses in their environments through the regulation of stress-related genes (Zhu, 2002). These genetic signals can influence the composition and amount of cuticular wax, primarily through controlling the pathways of wax biosynthesis (Shepherd and Griffiths, 2006). At present, the particular function of many of the genes involved in wax biosynthesis are unknown, although work on mutant species suggests that one source of variation might be found within the fatty acid elongation process (Shepherd and Griffiths, 2006). Some species are even thought to have several different elongation systems, utilising different pools of precursors (Shepherd and Griffiths, 2006; von Wettinson-Knowles, 2012). While further research is needed to fully constrain how these biochemical mechanisms control leaf wax concentration and chemical composition, it is clear that interspecies genetic variation has the potential to fully account for the range in *n*-alkane concentrations observed at Stiffkey.

It is worthy of note here that sample replicates from the same species extracted for *n*-alkane analysis showed considerable variation in concentrations (Appendix 3). Two explanations are proposed for this. Firstly, although care was taken to ensure that new growth was sampled from all species throughout this study, it is possible that occasionally older leaves were selected, especially when sampling evergreen species such as *Suaeda vera* where it is difficult to distinguish growth from previous years. As *n*-alkanes can increase in concentration with age (Jetter and Schaeffer,

2001), the variability in concentration among sample replicates could reflect an occasional bias of older versus younger leaves. Alternatively, this variability could simply reflect differences in the extent of abrasion of waxes from leaves of plants due to micro-scale variation in the exposure of leaves growing on the same plant.

4.7.6 The influence of seasonality on *n*-alkane concentrations

Previous studies have shown that the total concentration of *n*-alkanes in leaf wax can change through the course of a growing season. Studies of *Prunus laurocerasus* showed that the total amount of alkanes increased as the leaf matured (Jetter and Shaeffer, 2001), and this trend has also been reported for other species including *Spartina alterniflora* (Sessions, 2006) and broadleaf forest tree species such as *Acer rubrum*, *Platanus occidentalis*, *Juniperus virginiana*, *Pinus taeda*, and *Pinus strobus* (Tipple and Pagani, 2013). The picture was not so straightforward at Stiffkey, however, where the concentration of waxes appears generally higher in the early growth season (Fig 4.10, 4.11 and 4.12).

Temporal variation in *n*-alkane concentration appears to be species-specific among the Stiffkey species. The highest concentrations of *n*-C₂₇, *n*-C₂₉ and *n*-C₃₁ in *Atriplex portulacoides*, *Elytrigia atherica* and *Suaeda vera* are found in March 2012, i.e. at the very start of the 2012 growing season. *Elytrigia atherica* then shows an overall decline in *n*-alkane concentrations during the rest of the 2012 growth season. In contrast, *Salicornia europaea* had the highest concentration of *n*-C₂₇ in October, while *n*-C₂₅ and *n*-C₂₉ were most concentrated in June 2011, and *n*-C₂₃ was most concentrated in August 2012. No clear systematic variation in *n*-alkane concentration was therefore observed with seasonality, suggesting that these trends were not simply a plant response to local weather conditions. Variation also exists in terms of the *n*-alkane concentrations between the 2011 and 2012 growing seasons among some species. *Elytrigia atherica*, *Salicornia europaea* and *Suaeda vera*, with the exception of the months where they produce significantly greater concentrations of alkanes, have a relatively similar profile for both years. The overall concentration of *n*-alkanes in *Phragmites australis*, however, is lower in 2012 than in 2011. Summer 2012 concentrations in *Limonium vulgare* also fail to reach the levels recorded in June 2011.

The concentration of *n*-alkanes in leaf waxes during the growing season can be: a) increased as a result of plants continuing to produce wax throughout the growth season; b) decreased due to the wax being abraded away by mechanical stress caused by edaphic factors such as wind and rain; or c) influenced by

environmental/climatic factors (Shepherd and Griffiths, 2006). As discussed previously, Stiffkey saltmarsh is situated on the north Norfolk coast, and topographically does not offer plants much in the way of protection from onshore winds and rainfall, unlike other previously published study sites (Tanner *et al.*, 2007). Weather station monitoring data (Figures 4.1 – 4.4) show that relative humidity, maximum/minimum temperatures, and hours of sunlight remain similar for both 2011 and 2012. The greatest variation in weather conditions is observed in terms of the amount of rainfall. In 2011, the total rainfall amount during the months of March, April, May and July was lower than observed in 2012, while June 2011 and August 2011 both had more rainfall than the corresponding months in 2012. Rainfall has been shown to remove wax by weathering (Shepherd and Griffiths, 2006) and it is possible that the high concentrations of wax from leaves sampled in early June reflect the limited weathering taking place in the spring of 2011 – unfortunately data pertaining to wind speed and direction for the two years is not available so a full evaluation of differences in weathering potential from 2011 and 2012 is not possible.

It is interesting to note however that although *Limonium vulgare*, *Phragmites australis* and *Spartin anglica* record their highest concentrations in June 2011, this pattern is not observed for all other species at Stiffkey. This may be due to variability in the susceptibility of different wax crystalline structures to weathering (Shepherd and Griffiths, 2006). The lack of a systematic response to local weather conditions among all species sampled highlights the difficulties in relating changes in the chemical composition of leaf waxes to environmental and climatic stimuli. Such relationships are known to be complex, due to differences in species-specific reactions, ranging in scale from genetic effects through to direct environmental influences (Dodd and Proveda, 2003).

4.7.7 The influence of spatial variation in marsh characteristics on *n*-alkane concentrations

In August 2011, the collection of plants from multiple sampling locations within the marsh permitted consideration of the influence of marsh micro habitat on *n*-alkane concentrations. With the exception of *Salicornia europaea* and *Suaeda vera*, all the species sampled at multiple sites across the marsh (LM, UM and R; Chapter 2) (e.g. *Atriplex portulacoides*, *Spartina anglica*) show similar concentrations across sampling locations (Appendix 3). This suggests that differences in micro-habitat conditions previously identified at Stiffkey, such as hypersalinity and nitrogen availability (Jeffries, 1977), have no systematic influence on *n*-alkane

concentrations. As with many other findings presented here, therefore, the nature of these responses appears to be species specific.

Differences in the extent of the mechanical abrasion of waxes (e.g. by wind and rain, Shepherd and Griffiths, 2006) between the sampling sites could provide an explanation for the intraspecies variation in *n*-alkane concentration observed in *Suaeda vera* and *Salicornia europaea* from different sampling locations. *Salicornia europaea* has higher concentrations of *n*-alkanes in the UM than the LM, which could be due to weathering by tidal inundation in the LM. However, the reason for the higher concentration of *n*-alkanes in *Suaeda vera* growing at the ridge site (which has no shelter from wind and sea-spray), relative to individuals from the same species growing in the upper marsh, remains unclear.

Studies of these two species at Stiffkey have also identified genetic variation at the molecular level among populations growing in different marsh sub-habitats (e.g. Noble, 1990; Davy *et al.*, 1985). Genetic variation has been shown to influence the chemical composition of leaf waxes (Dodd and Afzal-Rafii, 2000; Shepherd and Griffiths, 2006), and hence this could also be a contributory factor in accounting for intraspecies variation in *n*-alkane concentrations observed in these two succulents. This presents a significant problem for reconstructing vegetation assemblages from sedimentary leaf wax data. The genetic composition of a plant species is not static through time; in fact it can show considerable plasticity. The introduction of *Spartina alterniflora* into the UK provides an illustration of this. When it first arrived in the UK in the 19th century, hybridisation with *Spartina maritima* gave rise to a sterile hybrid (*Spartina X townsendii*) (Ainouche *et al.*, 2004). Through time, however, chromosome doubling in this sterile hybrid led to the development of *Spartina anglica* (Ainouche *et al.*, 2004). Other *Spartina* species are also acknowledged to be genetically diverse – *Spartina alterniflora*, for example, is known to display molecular diversity in the chloroplast and nuclear genomes (Ainouche *et al.*, 2004). Therefore even if modern plant species are collected in the vicinity of a sediment core to provide data about the modern vegetation growing at a site, there is no guarantee that these species have not evolved genetically during the geological past.

4.8. CONCLUSION

This aspect of the project aimed to understand the extent of variability in leaf wax *n*-alkane concentration and composition across seven saltmarsh species, and evaluate whether a range of indices traditionally thought to have a degree of chemotaxonomic potential were capable of discriminating between them. Results have demonstrated that there is significant interspecies variation in the molecular distribution patterns of *n*-alkanes from these plants. This variation does not appear to be systematic among plant functional types. ACL values have a limited range at Stiffkey, making this proxy unsuitable for distinguishing between different plant contributions to marsh sediments. Calculated ratios and indices of alkane homologues are also unable to satisfactorily resolve woody vs non-woody species. Large variations in the concentration of individual *n*-alkanes (i) among different species; and (ii) throughout a growing season, also highlight the difficulties in recreating vegetation assemblages of lipids extracted from sediments.

The variation in *n*-alkane distribution patterns and concentration among species from the same genus growing at different locations did not appear to simply derive from local weather conditions or micro-site characteristics. Rather, genetic variation at the species level may be the primary driver of differences in molecular distribution patterns and absolute concentrations of leaf wax *n*-alkanes from these plants. The genetic composition of plant species is not static through time, however, so this has potentially serious consequences for using modern vegetation to evaluate lipids from the sedimentary archive. Even if modern plant species are collected in the vicinity of a sediment core to provide data about the vegetation growing at a site, there is no guarantee that these species have not evolved genetically through time, hence their leaf wax biomarker composition may have also shifted. Further research is required to evaluate the importance of genetic diversity on leaf wax *n*-alkane composition, and to constrain the drivers of interspecies variation in *n*-alkane distribution and concentration, to ensure accurate interpretation of sedimentary lipid biomarkers.

4.9. SUMMARY

- The molecular distribution of *n*-alkane homologues from seven terrestrial saltmarsh species (including grasses, herbs and succulents) from a temperate UK saltmarsh show significant variation, with prominent chain lengths ranging from *n*-C₂₃ (*Salicornia europaea*) to *n*-C₃₅ (*Limonium vulgare*).
- Seasonal changes in the abundance of *n*-alkane homologues show no systematic patterns among the species sampled, suggesting that these shifts are not simply caused by plant responses to local weather conditions and/or environmental stimuli.
- Differences in marsh micro-habitat had no systematic influence on the molecular distribution of *n*-alkanes from the same species sampled across multiple locations, with shifts in molecular distribution observed to be species-specific.
- Interspecies variability in ACL and CPI is so high that these parameters do not offer an effective method of discriminating between plants a) at the species level, and b) at the plant functional type level.
- Ratios of *n*-C₂₇, *n*-C₂₉ and *n*-C₃₁ cannot successfully distinguish between woody and non-woody species due to the high degree of variability among the non-woody category.
- Total concentrations of odd-chain *n*-alkanes vary by up to 2400 µg g⁻¹ DM, with the perennial *Limonium vulgare* producing the highest concentrations and the succulent *Salicornia europaea* producing the lowest concentrations.
- Concentrations of *n*-C₂₇, *n*-C₂₉, *n*-C₃₁ vary by almost an order of magnitude between species at each sampling interval.
- Differences in marsh micro-habitat had no systematic influence on the concentration of *n*-alkanes from the same species sampled across multiple locations.

Chapter 5

Interspecies variation in the carbon isotope composition of bulk plant tissue and *n*-alkanes from saltmarsh plants

5.1. INTRODUCTION

The $^{13}\text{C}/^{12}\text{C}$ ratio of plant tissue can successfully distinguish between C_3 , C_4 and crassalucean acid metabolism (CAM) species, and has been extensively used in the reconstruction of past climates (e.g. Meyers, 1997, 2003; Kohn, 2010; Tipple *et al.*, 2010; Royles *et al.*, 2012). Decades of in-depth investigation focusing on the $^{13}\text{C}/^{12}\text{C}$ profiles of bulk material from C_3 species has confirmed that a relationship exists between plant physiology and environmental conditions. This has been widely attributed to the way in which plant responses to environmental drivers alter the ratio of external and internal concentrations of CO_2 (von Caemerer and Farquhar, 1981; Arens *et al.*, 2000; Dawson *et al.*, 2002; Diefendorf *et al.*, 2010), and has extended the amount of environmental information which can be extrapolated from plant $\delta^{13}\text{C}$ signatures in both modern ecosystem research and palaeoclimate reconstruction.

In general terms, the carbon isotope ratio of leaf wax lipids can be interpreted in a manner similar to that established for bulk plant tissue. For example, leaf wax *n*-alkanes from C_3 plants are depleted in ^{13}C relative to those from C_4 plants (Lockheart *et al.*, 1997; Bi *et al.*, 2004; Chikaraishi and Naraoka, 2007). Recent studies however have sought to extend this application, using bulk and *n*-alkane $\delta^{13}\text{C}$ data from C_3 species interchangeably to derive information about plant-environment relations, both in modern ecosystems and through the geological past (Diefendorf *et al.*, 2010.). While studies of mechanisms controlling the bulk carbon

isotope composition of plants have shown a clear link between climatically influenced plant physiology and bulk $\delta^{13}\text{C}$ values, further research is needed to establish whether the same link can be seen in leaf wax biomarkers. This chapter will therefore commence with a review of the scientific literature relating to factors influencing the bulk carbon isotope composition of plants, before comparing the current state of knowledge of $^{13}\text{C}/^{12}\text{C}$ values at the molecular level. This review will then explore the potential biochemical mechanisms that could influence the carbon isotope composition of leaf wax lipids, identifying key areas for future research. It will also establish the rationale that underpins the aims and objectives of this part of the project.

5.2 LITERATURE REVIEW

5.2.1 Bulk carbon isotope profiles of plant biomass

$\delta^{13}\text{C}$ analysis of bulk plant tissue is an extremely valuable tool for discriminating between the different plant metabolic pathways for the fixation of carbon. C_3 and C_4 plants differ in the extent to which they discriminate against ^{13}C during CO_2 uptake, and therefore $\delta^{13}\text{C}$ values vary among species using these two photosynthetic strategies (Park and Epstein, 1960; O'Leary 1988; Farquhar *et al.*, 1989; Tipple and Pagani, 2007) (Fig. 5.1). Factors controlling the carbon isotope composition of plant leaf material have been studied in considerable detail, with seminal works by Farquhar *et al.* (1982; 1989), Farquhar (1983) and O'Leary (1988) resulting in the development of models describing fractionation between atmospheric CO_2 and plant biomass.

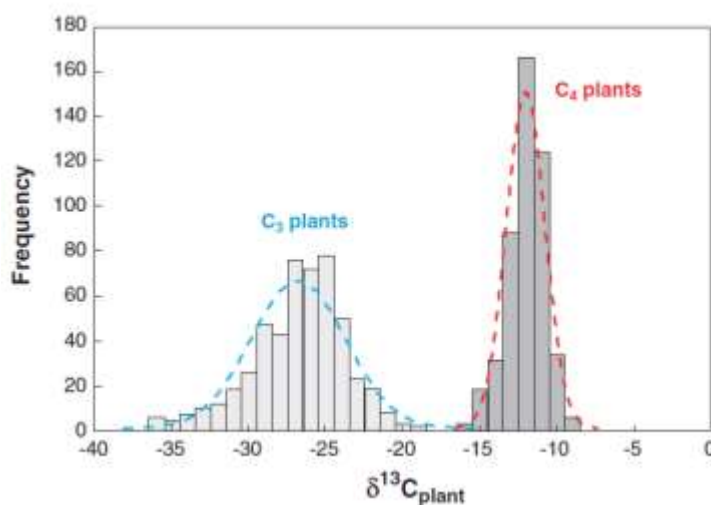


Figure 5.1: Histogram showing the normal distribution of C_3 and C_4 carbon isotope values (Tipple and Pagani, 2007, using data from Cerling and Harris, 1999).

The C₃ pathway (Fig. 5.2), comprising a series of reactions collectively known as the Calvin-Benson-Bassham cycle (Fig. 5.3), is the most ancient pathway fixing carbon identified in terrestrial plants (Tipple and Pagani, 2007; Griffiths *et al.*, 2013). In plants using the C₃ pathway, carbon is fixed through the activity of the enzyme ribulose-1, 5-biphosphate carboxylase/oxygenase (Rubisco) which catalyses a reaction between ribulose-1, 5-biphosphate (RuBP) and CO₂ to produce two 3-carbon phosphoglycerate molecules (Farquhar, 1989; Ehleringer *et al.*, 1991).

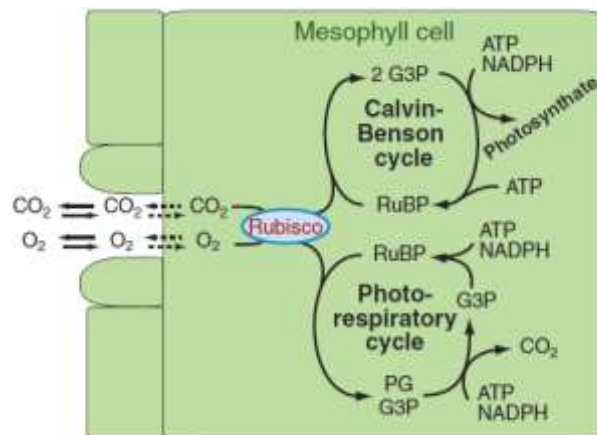


Figure 5.2: Schematic of C₃ plant physiology and biosynthetic pathways of carbon fixation (Tipple and Pagani, 2007)

The C₃ pathway commences when CO₂ diffuses through stomata into the internal space within the leaf (O'Leary, 1988; Fig. 5.2). This CO₂ then dissolves in the cell sap, and diffuses through the chloroplast where an irreversible carboxylation reaction occurs (O'Leary, 1988; Farquhar, 1989). The C₃ pathway fractionates against ¹³C in varying degrees. Whilst the diffusive steps fractionate ¹³C to a lesser extent (4.4‰ in air; 0‰ in water; Roeske and O'Leary, 1984), the carboxylation step provides the most significant kinetic fractionation against ¹³C (~29‰, Roeske and O'Leary, 1984) (Table 5.1; O'Leary 1988) observed during the fixation process. Farquhar (1982, 1989) proposed the following mathematical model for describing the δ¹³C composition of C₃ plants (Eq.1)

$$\delta = \delta_{env} - a - (b - a)C_i/C_a \quad \text{(Eq. 1)}$$

Where δ_{env} is the isotopic composition of atmospheric CO₂ (~ -7.8‰), *a* represents the fractionation caused by diffusion of CO₂ into the leaf, *b* is the fractionation

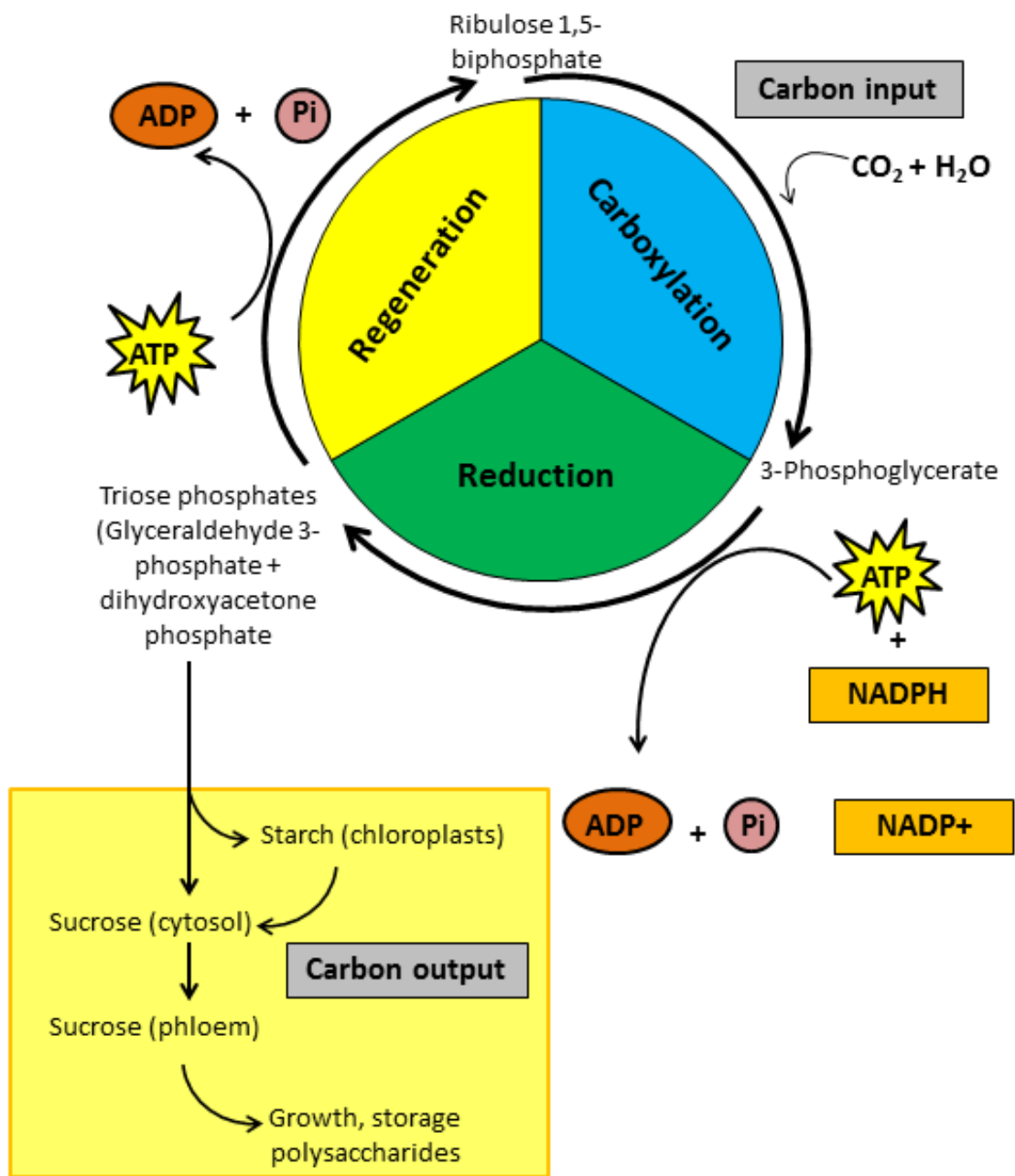


Figure 5.3: Schematic representation of the Calvin-Benson-Bassham cycle, which proceeds in 3 stages: (1) Carboxylation, which covalently links inorganic carbon (CO_2) to a carbon skeleton; (2) Reduction, which forms a carbohydrate (triose phosphate) at the expense of photochemically generated ATP and reducing equivalents in the form of NADPH; and (3) Regeneration, which restores the CO_2 -acceptor ribulose 1,5 biphosphate. At steady state, the input of CO_2 equals the output of triose phosphates. The latter either serve as precursors of starch biosynthesis (chloroplast) or flow into the cytosol for sucrose biosynthesis (adapted from Taiz and Zeigler, 2010)

caused by carboxylation (approximately 27‰ in C₃ plants using Rubisco), and C_i/C_a is the ratio of intercellular and ambient partial pressures of CO₂ (Farquhar *et al.*, 1982, 1989). This model remains widely accepted, and has been extensively used in studies of plant carbon isotope composition. The ratio of intercellular to atmospheric CO₂ concentration, C_i/C_a , is a key component of this mathematical model of C₃ photosynthesis. This parameter relates net assimilation of carbon to stomatal conductance (g_s), reflecting the demand and supply of carbon to the plant (Farquhar *et al.*, 1989; Dawson *et al.*, 2002).

Table 5.1 Carbon isotope fractionations associated with photosynthesis (sourced from O'Leary, 1988)

Process	$\Delta\delta$, ‰*	References
Equilibria		
Solubility of CO ₂ in water	1.1	O'Leary 1984
Hydration of CO ₂	-9.0	Mook <i>et al.</i> 1974
Transport processes		
CO ₂ diffusion in air**	4.4	O'Leary 1981
CO ₂ diffusion in aqueous solution	0.7	O'Leary 1984
Chemical processes		
Spontaneous hydration of CO ₂	6.9	Marlier and O'Leary 1984
Carbonic anhydrase catalized hydration of CO ₂	1.1	Paneth and O'Leary 1985
Phosphoenolpyruvate carboxylase-catalysed reaction of HCO ₃ ⁻ with phosphoenolpyruvate	2.0	O'Leary <i>et al.</i> 1981
Ribulose biphosphate carboxylase-catalysed reaction of CO ₂ with ribulose bisphosphate	29.0	Roeske and O'Leary 1984

*Positive values in this table indicate that the product is depleted in ¹³C compared with the starting state; negative values indicate enrichment; ** Predicted value, this number has not been measured

Recent research has identified that in addition to stomatal conductance, physical barriers to the diffusion of CO₂ across the mesophyll (mesophyll conductance, g_m) into the chloroplast can also limit photosynthesis by 20 to 50% in C₃ plants (Sharkey, 2012; Flexas *et al.*, 2012; Griffiths and Helliker, 2013). The precise mechanism behind the operation of g_m remains poorly constrained, with some studies suggesting that it is mediated by changes in aquaporins or cell walls (Flexas *et al.*, 2006; Tazoe *et al.*, 2011). In addition to g_s , g_m is thought to have a particular influence on the partial pressure of CO₂ in the chloroplast (C_c) (Flexas *et al.*, 2012; Griffiths and Helliker, 2013). There is growing evidence in the literature that g_m is also sensitive to a range of environmental parameters such as drought, salinity and light intensity (e.g. Flexas *et al.*, 2007; Tholen *et al.*, 2012 and references contained therein). Future research into g_m therefore offers significant opportunities to improve understanding of factors influencing the uptake and fixation of carbon during C₃ photosynthesis (Griffiths and Helliker, 2013).

The C₄ photosynthetic pathway (Fig. 5.4) is also built around the Calvin-Benson-Bassham cycle, but contains a number of anatomical and biochemical modifications (Tipple and Pagani, 2007; Griffiths *et al.*, 2013). Phosphoenol pyruvate carboxylase (PEPc), utilised by C₄ plants, has different kinetic isotope effects and utilises a different species of inorganic carbon (HCO₃⁻) than Rubisco in C₃ vegetation (Farquhar *et al.*, 1989). In C₄ plants, CO₂ that has diffused through the stomata is converted into HCO₃⁻ and then fixed by PEPc (Farquhar, 1983; O'Leary, 1988; Tipple and Pagani, 2007; Pyankov *et al.*, 2010) (Fig. 5.4). The resultant malate is transported into the bundle sheath cells, where decarboxylation releases CO₂ to be fixed again via Rubisco (Farquhar, 1983; Pyankov *et al.*, 2010; Griffiths *et al.*, 2013). Ultimately, this CO₂ concentration mechanism allows C₄ plants to maximise upon the compartmentalisation of Rubisco within bundle sheath cells (Griffiths *et al.*, 2013) where CO₂ concentration can be up to ten times greater than found in the atmosphere (Ehleringer *et al.*, 1991; Hatch, 1992; Taylor and Furbank, 1995). As Rubisco can either oxygenate or carboxylate ribulose-1, 5-biphosphate, the presence of high concentrations of oxygen can trigger the conversion of RuBP to phosphoglycoate through photorespiration. Phosphoglycoate has to be converted back into phosphoglycerate in order to be used in the Calvin cycle, which requires energy and gives rise to the loss of previously stored CO₂ (Sharkey *et al.*, 1988; Bauwe, 2011). Photorespiration is therefore a rate limiting step for C₃ photosynthesis, especially in warm environments with low CO₂ concentrations (Ogren, 1984; Ehleringer *et al.*, 1991; Bauwe, 2011). C₄ plants have lower rates of

photorespiration arising from a) lower concentration of photorespiratory enzymes, and b) the release of photorespiratory CO₂ in the bundle sheath cells (Bauwe, 2011). These adaptations therefore give C₄ plants a considerable advantages over their C₃ counterparts in hot, high-light, and arid environments such as tropical savannas (Tipple and Pagani, 2007).

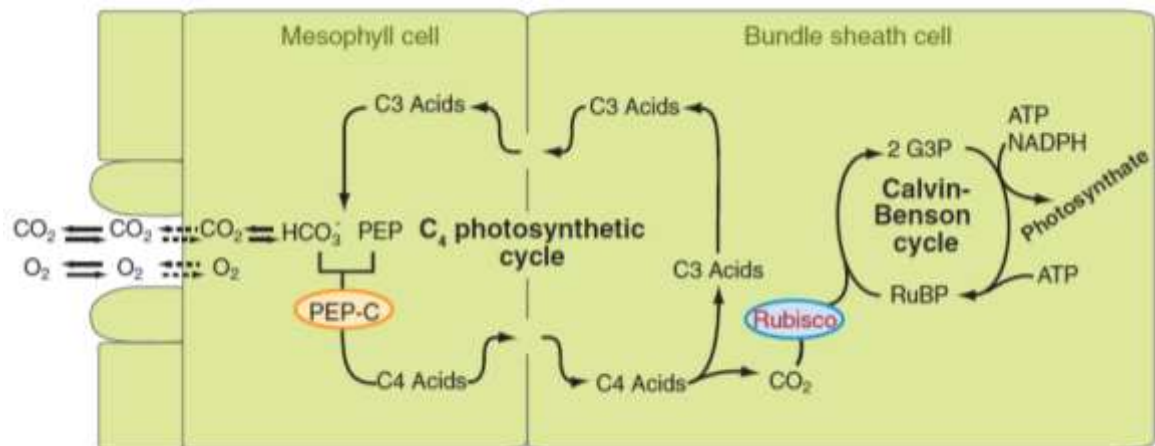


Figure 5.4: Schematic of C₄ plant physiology and biosynthetic pathways of carbon fixation (Tipple and Pagani, 2007)

Rubisco continues to discriminate against ¹³C within the bundle sheath cells of C₄ plants (Farquhar, 1983). Primarily, this is due to the fact that the bundle sheath cells are not leak-tight. Indeed, the degree of ‘leakiness’ (Φ) observed is directly related to C_i/C_a , with Φ being greater with high C_i (Farquhar, 1983). “Leakiness” in this context describes the rate of bundle-sheath CO₂ leakage to the rate of phosphoenolpyruvate carboxylase (Kromdijk *et al.*, 2014). Farquhar *et al.* (1989) derived a mathematical model of fractionation within the C₄ pathway that takes into account levels of Φ (Eq. 2),

$$\delta = \delta_{env} - a - (b_4 + b_3 \Phi - a)C_i/C_a \quad \text{Eq.2}$$

where b_4 represents the fractionation arising from CO₂ fixation ($b_4 = 5.7\%$ at 25 °C), and Φ represents leakiness (Farquhar, 1983). Buchmann *et al.* (1996) found that the three C₄ grass subtypes (NAD-ME, NADP-ME and PEP-CK) displayed different carbon isotope discrimination values thought due to variation in their degree of “leakiness” (Φ), which ranged from 0.22 ± 0.009 to 0.42 ± 0.05 among watered plants growing in sunlit conditions (Buchmann *et al.*, 1996). *Spartina anglica*, the C₄

monocot sampled at Stiffkey, is classified as falling within the phosphoenolpyruvate carboxykinase (PEP-CK) subtype in the Poaceae family (Voznesenskaya *et al.*, 2006). Physiological attributes of the PEP-CK subtype include the presence of a double sheath, with an inner mesophyll sheath and an outer Kranz chlorenchyma sheath and grana-containing bundle sheath chloroplasts (Voznesenskaya *et al.*, 2006). Biochemically, PEP-CK subtypes have the most complex mechanisms and pathways of all three subtypes. A good example of this is their use of both aspartate and malate for supporting the activity of PEP-CK in bundle sheath cells (Voznesenskaya *et al.*, 2006). The PEP-CK subtypes display an intermediate degree of leakiness compared to NAD-ME and NADP-ME subtypes (Buchmann *et al.*, 1996). Recent studies have shown that leakiness can increase under limiting light, and that low-light adapted plants can balance the relationship between C_4 CO_2 concentration and the functioning of the Calvin-Benson-Bassham cycle to reduce leakiness under low-light conditions (Bellasio and Griffiths, 2013; Kromdijk *et al.*, 2014). In addition, some studies suggest that simply looking at leakiness as a function of C_4 sub-type may be overly simplistic, as multiple pathways for decarboxylation can be found within a single species (Kromdijk *et al.*, 2014). It appears therefore that more research will be required further elucidate the species-specific biochemical mechanisms controlling leakiness across a range of C_4 plants (Kromdijk *et al.*, 2014).

While discriminating between C_3 and C_4 species at the bulk level is well established in scientific literature, studies have highlighted how interspecies variability within each of these groups might complicate interpretation. Diefendorf *et al.* (2010), for example, reported ranges of -21 to -35‰ for bulk $\delta^{13}C$ values from a global study pulling together data on a range of C_3 plant functional types. Castenada and Shouten (2011), reviewing the Diefendorf *et al.* (2010) study, consider that this variability in the $\delta^{13}C$ value of the C_3 end member could increase uncertainty when seeking to reconstruct the percentage inputs of C_3 and C_4 species to the geological record. This could be mitigated by further characterisation of the carbon isotope composition of C_3 species growing in particular biomes (Castenada and Shouten, 2011). In addition, the increased interest in constraining the relative influence of g_s and g_m on the uptake and fixation of carbon during photosynthesis should further clarify this issue – g_m responses in particular are thought to be species-specific (Flexas *et al.*, 2012) so could contribute to the variability observed in the ^{13}C values of the C_3 species (Castenada and Shouten, 2011).

5.2.2 Compound-specific isotope analysis of leaf wax biomarkers

The $\delta^{13}\text{C}$ values of *n*-alkanes are typically more ^{13}C -depleted than bulk plant tissue (Conte *et al.*, 2003). This depletion is due to fractionation against ^{13}C that occurs during the oxidation of pyruvate to acetyl-coA by pyruvate dehydrogenase (Lockheart *et al.*, 1997; Hayes, 2001; Dungait *et al.*, 2008, 2010). Further fractionation also occurs at branch points within the fatty acid elongation and desaturation pathways (Chapter 2). Examples include branch points occurring when acyl lipids are diverted to plant membranes to form phospholipids, and the formation of other compound classes from fatty acids by decarboxylation and/or reduction (Dungait *et al.*, 2008). The previously discussed distinctions between photosynthetic pathways are still present at the compound specific level, however, despite this relative depletion. *n*-Alkane values for C_3 plants typically fall in the range -31‰ to -39‰, whilst C_4 plants generally return values of -18‰ to -25‰ (Bi *et al.*, 2005; Tipple and Pagani, 2007). In an analogous manner to bulk isotopic analysis, therefore, $\delta^{13}\text{C}$ values of long-chain *n*-alkanes have been used to investigate the differences in isotopic fractionation occurring in plants using C_3 and C_4 metabolism (Collister *et al.*, 1994).

While data considering interspecies variation in *n*-alkane carbon isotope composition are limited, Castenada and Schouten (2011) theorise that the variability reported for bulk plant tissue is likely to be reflected in leaf wax biomarkers. They call for more studies quantifying interspecies variability in *n*-alkane carbon isotope composition, ideally from a range of different biomes, to assist in assigning values to C_3 end members in models recreating palaeovegetation assemblages. Currently such studies assume that net fractionation (ϵ) between bulk and *n*-alkane $\delta^{13}\text{C}$ is either: (i) constant, with a value of $\sim 4.9\text{‰}$ (Smith *et al.*, 2007; Diefendorf *et al.*, 2010); or (ii) variable with environmental conditions and species, but consistently within the range of -5 to -7‰ for C_3 species, and -8 to -10‰ for C_4 species (Tipple and Pagani, 2007).

It is however also possible that the $^{13}\text{C}/^{12}\text{C}$ ratios of leaf wax compounds are influenced by different mechanisms from those that control the $\delta^{13}\text{C}$ values of bulk tissue. For example, carbon isotope ratios are known to differ among different organic compounds synthesised by a plant (Dungait *et al.*, 2008). This variability reflects factors such as the source of carbon, fractionation occurring during biosynthesis, and the overall cellular carbon budget (Hobbie and Werner, 2004; Dungait *et al.* 2008). Understanding the diversity in *n*-alkane carbon isotope

compositions among a range of species growing at the same geographical location, and comparing this diversity with bulk isotope trends, may therefore provide a method for constraining whether the same mechanisms control the carbon isotope information recorded in bulk tissue and leaf wax *n*-alkanes. This could have important implications for palaeoecological reconstructions, particularly for studies seeking to use *n*-alkane $\delta^{13}\text{C}$ values to consider the relationship between plants and their environment discussed further below.

5.2.3 Using carbon isotopes to consider plant-environment interactions

A considerable body of research has shown that environmental conditions, particularly those exerting influence over C_i/C_a , can give rise to variation in the $\delta^{13}\text{C}$ values recorded in the bulk plant tissue of C_3 species. Plant responses to changes in C_i/C_a are thought to be species-specific, as a result of variation in stomatal opening, and differences in the chloroplast demand for CO_2 (Ehleringer *et al.*, 1992). In addition, interspecies differences in the diffusion of CO_2 through the mesophyll are likely to play an important, but as yet not fully constrained, role in how plants respond to environmental change (Tholen *et al.*, 2012). Broad trends in plant responses to environmental drivers, however, still provide a useful method for linking plant ecophysiology to environmental conditions. Arens *et al.* (2000) reviewed a wide range of literature to compile a summary of abiotic factors driving shifts in plant C_i/C_a , which can be found in Table 5.2, and summarised in Figure 5.5.

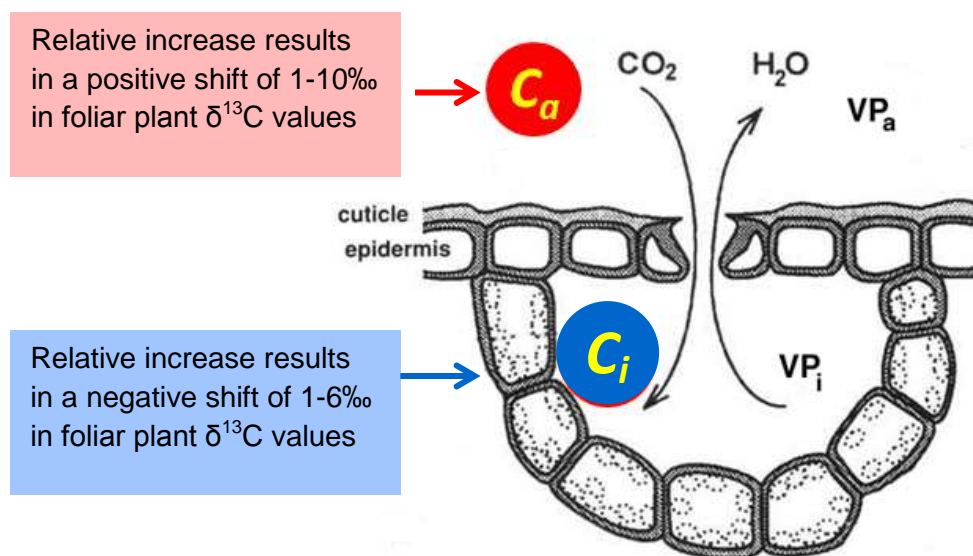


Figure 5.5: Summary of the influence of changes in C_i/C_a on the carbon isotope composition of plant tissue (data pertaining to the magnitude of isotopic shift from Arens *et al.*, 2000)

Table 5.2: Environmental factors influencing the carbon isotope composition of C₃ plants (reproduced from Arens *et al*, 2000, plus data from Guy and Wample, 1982). Factors thought potentially significant at Stiffkey marsh are highlighted in red

Factor	Effect on c_i/c_a	Effect on $\delta^{13}\text{C}$ plant tissue		Ecological conditions
		Range (‰)	Direction	
Recycled CO ₂	little	1 - 5	negative	Within closed canopies or in ecosystems where soil outgassing is high (boreal forest)
low light	increase	5 - 6	negative	forest understory
Water stress / low relative humidity	decrease	3 - 6	positive	arid / semi-arid climates
Osmotic stress	decrease	3 - 10	positive	high-salinity soils, extreme at high $p\text{CO}_2$
Low nutrients	increase	4	negative	nutrient-poor soils
Low temperature	increase	3	negative	polar regions, during ice house times, high altitude
Reduced $p\text{CO}_2$ with altitude	decrease	3 - 7	positive	high mountains
Growth form and deciduousness	increase / decrease	1 - 3	negative / positive	variation between trees, forbs and grasses, and evergreen vs. deciduous species
Age (juvenile vs. adult)	increase in juveniles	2	negative in juveniles	seedlings or saplings vs. reproductive individuals
*Flooding/root anoxia	increase	~1	positive	Species in flooded conditions (Guy and Wample, 1984)
Seasonal variation	increase / decrease	1 - 2	negative / positive	strongest effect in semi-arid and arid climates

The relationship between C_i/C_a and plant carbon isotope values can be broadly explained by the isotope effects arising from the supply and demand of carbon. When C_i is high, stomatal conductance is higher than the rate of photosynthesis, resulting in increased discrimination against ^{13}C and lower $\delta^{13}\text{C}$ values (McCarroll and Loader, 2004). Conversely, where C_i is low relative to C_a , photosynthetic demand for CO_2 is greater than the amount provided, and intercellular CO_2 pressure drops resulting in decreased discrimination against ^{13}C and higher $\delta^{13}\text{C}$ values (McCarroll and Loader, 2004). These environmental factors are thought to be especially significant during periods where the carbon isotope composition of the atmosphere has remained relatively constant (Arens *et al.*, 2000).

At the bulk level, differences in the degree of ^{13}C enrichment among C_3 plants growing at the same location has been qualitatively interpreted as arising from differences in their water use efficiency (WUE) (e.g. Ehleringer *et al.*, 1992). WUE is defined as the ratio of carbon gained from photosynthesis (A) to the rate of water lost through transpiration (E) (Farquhar and Richards, 1984; Siebt *et al.*, 2008; Tan *et al.*, 2009). WUE has been analysed over temporal (Bert *et al.*, 1997; Duquesnay *et al.*, 1998; Feng, 1999; Sauerer *et al.*, 2004) and spatial scales, with a positive shift in $\delta^{13}\text{C}$ interpreted as an increase in WUE.

Carbon isotope values have also been used to consider variation in WUE among plant functional types (Tan *et al.*, 2009). However, such interpretation requires caution, in light of recent studies. Siebt *et al.* (2008) make it clear that interpretation of intrinsic, instantaneous and integrated WUE from carbon isotope data can present some problems – inferring a simple linear relationship between the $\delta^{13}\text{C}$ values of intercellular to ambient CO_2 mole fractions (C_i/C_a) and WUE is very simplistic as photosynthetic ^{13}C discrimination is also sensitive to the ratio of the chloroplast to the ambient CO_2 mole fraction (C_c/C_a) and mesophyll conductance. Mesophyll conductance can vary among species, and also over time, so it cannot be measured with gas exchange equipment (Siebt *et al.*, 2008). The situation is further complicated because WUE in leaves does not always have a direct causal link to photosynthetic ^{13}C discrimination. This is due to the fact that WUE, $\delta^{13}\text{C}$ and $\Delta^{13}\text{C}$, although broadly responsive to similar processes, can also vary independently of each other (Siebt *et al.*, 2008). For example, instantaneous WUE depends upon evaporative demand (the leaf-to-air vapour mole fraction deficit of water vapour) and stomatal conductance, while $\Delta^{13}\text{C}$ depends upon mesophyll conductance and stomatal conductance (Siebt *et al.*, 2008).

Many studies considering plant ecophysiological responses to environmental conditions report carbon isotope discrimination values ($\Delta^{13}\text{C}$) instead of $\delta^{13}\text{C}$ measurements. This is because the basic equation for calculating $\Delta^{13}\text{C}$ (Eq.3, where δ_a is the isotopic composition of air, and δ_p is the isotopic composition of the plant) expresses plant carbon isotopic composition purely in terms of biological processes, rather than combining the influence of source isotope composition and plant discrimination against ^{13}C (Farquhar *et al.*, 1989).

$$\Delta = \frac{\delta_a - \delta_p}{1 - \delta_p} \quad \text{Eq.3}$$

This basic equation has recently been revised by Ubierna and Farquhar (2014) in light of a body of research showing the importance of mesophyll conductance (e.g. Tazoe *et al.*, 2011; Flexas *et al.*, 2012), evaporation and respiration (e.g. Griffiths and Helliker, 2013) on $\Delta^{13}\text{C}$ (Eq.4).

$$\Delta_{\text{com}} = \Delta_b - \Delta_{\text{gs}} - \Delta_{\text{gm}} - \Delta_e - \Delta_f \quad \text{Eq. 4}$$

Where Δ_b is the fractionation associated with Rubisco activity, Δ_{gs} is the stomatal contribution, Δ_{gm} is the mesophyll contribution, Δ_e is the fractionation associated with respiration, and Δ_f is the contribution from photorespiration (Ubierna and Farquhar, 2014). The precise influences of key terms in this new equation require further research (e.g. Tholen *et al.*, 2012; Griffiths and Helliker, 2013). However, many studies continue to rely on Eq.3, especially when considering broad trends in plant tissue under field conditions, and for the interpretation of signals from the geological record.

Considerable work has focused on the relationship between bulk plant tissue $\Delta^{13}\text{C}$ values and environmental parameters (e.g. Farquhar *et al.*, 1989), however it remains unclear whether $\Delta^{13}\text{C}$ calculated from lipid carbon isotope composition records the same information. Despite this, previous research has assumed that the carbon isotope composition of leaf wax *n*-alkanes from C_3 plants records environmental information in a manner analogous to bulk tissue (e.g. Tipple and Pagani, 2007). Diefendorf *et al.* (2010) have proposed, for example, that leaf wax biomarker $\delta^{13}\text{C}$ can be used interchangeably with bulk carbon isotope ratios (after application of a correction factor to account for the relative ^{13}C depletion of leaf wax

lipids relative to bulk tissue) to calculate carbon isotope discrimination ($\Delta^{13}\text{C}$) values. They collected a large amount of $\delta^{13}\text{C}$ data (both bulk and *n*-alkane) from around the world, and found a relatively strong positive correlation ($R^2 = 0.55$, $P < 0.0001$) between $\Delta^{13}\text{C}$ values of leaf tissue and mean annual precipitation. Diefendorf *et al.* (2010) interpreted these results as being indicative of the importance of water-mediated stomatal control on leaf gas-exchange in controlling the $\Delta^{13}\text{C}$ values of C_3 plants on a global scale. In order to further develop an approach for interpreting global plant $\Delta^{13}\text{C}$ trends, Diefendorf *et al.* (2010) defined a range of biome types (e.g. “tropical seasonal forest”, “cool-cold deciduous forest”, Fig. 1.2 Chapter 1) that could be linked to particular $\Delta^{13}\text{C}$ values. The spread of $\Delta^{13}\text{C}$ values defining the biome types proposed by this study however are generally very broad (Diefendorf *et al.*, 2010) (Fig. 1.2 Chapter 1). It is possible the range of $\Delta^{13}\text{C}$ values reported for some of these biome types could potentially be caused by a decoupling of the mechanisms controlling *n*-alkane and foliar carbon isotope composition. Given the current limitation of: (i) surveys detailing *n*-alkane carbon isotope data; and (ii) mechanistic studies of the factors influencing their $^{13}\text{C}/^{12}\text{C}$ values, little is known about other biochemical mechanisms that have the potential to drive *n*-alkane $\delta^{13}\text{C}$ trends (Castenada and Schouten, 2011; Dungait *et al.*, 2008, 2010).

5.2.4 The potential for biochemical mechanisms to influence *n*-alkane $^{13}\text{C}/^{12}\text{C}$

The work of Dungait *et al.* (2008, 2010, 2011) and Castenada *et al.* (2011) highlights the need for further studies characterising the *n*-alkane carbon isotope ratios of a range of different plants, to fully understand the signal that they are recording and quantify the extent of interspecies variation that can be present in a given ecosystem. These limitations in existing knowledge can hamper the interpretation of fossil leaf wax biomarker $\delta^{13}\text{C}$ data. For example, Handley *et al.* (2008) identified shifts of up to 7‰ in lipids from sediments sampled across the Palaeocene-Eocene Thermal Maximum carbon isotope excursion (PETM CIE). Separating $\delta^{13}\text{C}$ shifts in sedimentary lipids arising from climatic influences (such as increasing temperature or humidity) from those due to changes in C_3 plant communities, however, proved complex. In particular, Handley *et al.* (2008) observed that the PETM CIE varied in magnitude across different *n*-alkane homologues. Handley *et al.* (2008) concluded that this variability was due to the different homologues deriving from different sources. It is possible however, given the current lack of knowledge regarding the extent of interspecies variability in *n*-alkane $\delta^{13}\text{C}$ values, that the 7‰ shift could in part be driven by changes in the plant

community and/or variation in the pattern of relative ^{13}C enrichment and depletion carbon isotope composition of *n*-alkane homologues among different species.

The previous sections highlight that a significant volume of research has been carried out in recent decades describing the mechanistic controls on the carbon isotope composition of bulk tissue. This has resulted in a detailed body of literature describing the impact of environmental factors on bulk plant $\delta^{13}\text{C}$, arising from shifts in C_i/C_a (e.g. Farquhar *et al.*, 1982; Farquhar and Richards, 1984; Farquhar *et al.*, 1989; Evans and von Caemmerer, 2013; Griffiths and Helliker, 2013). However, limited research has considered whether compound-specific $\delta^{13}\text{C}$ records the same trends as bulk tissue. If they do display similar trends, this would support the proposition that they are influenced by the same mechanisms, whereas if they do not, the implication is that other (as yet unconstrained) factors are important for understanding *n*-alkane $\delta^{13}\text{C}$ signals.

Studies of stable isotope fractionation in biological systems have shown that the composition of specific compounds can be strongly influenced by the flux of material through reaction networks (Hayes, 2001; Hobbie and Werner, 2004; Farquhar *et al.*, 2003; Dungait *et al.*, 2008) (Fig. 5.6). In particular, branch points in the network can exert considerable influence on mass balance as they control the relative flux of material into products and reactants (Farquhar *et al.*, 2003). Tcherkez *et al.* (2011) proposed that the fluxes of carbon through plant metabolic processes can give rise to considerable redistribution of ^{12}C and ^{13}C that occurs after carbon is fixed during photosynthesis. Taken together, these studies suggest that a detailed understanding of the carbon isotope composition of organic compounds such as leaf wax biomarkers might require a more holistic consideration of plant metabolic networks as a whole (Tcherkez *et al.*, 2011; van Dongen *et al.*, 2011), to assess factors which might influence the isotopic composition of carbon incorporated into *n*-alkanes.

In addition to changes in seasonal environmental conditions at Stiffkey (discussed in Chapter 4), several biochemical factors could influence the flux of carbon through plant metabolic networks in species sampled as part of this study. These biochemical mechanisms could therefore be important for understanding interspecies variation in *n*-alkane $^{13}\text{C}/^{12}\text{C}$. The carbon taken up by the leaf can have a variety of fates within plants. It can be incorporated into structural compounds, stored in non-structural organic compounds, or respired back into the atmosphere

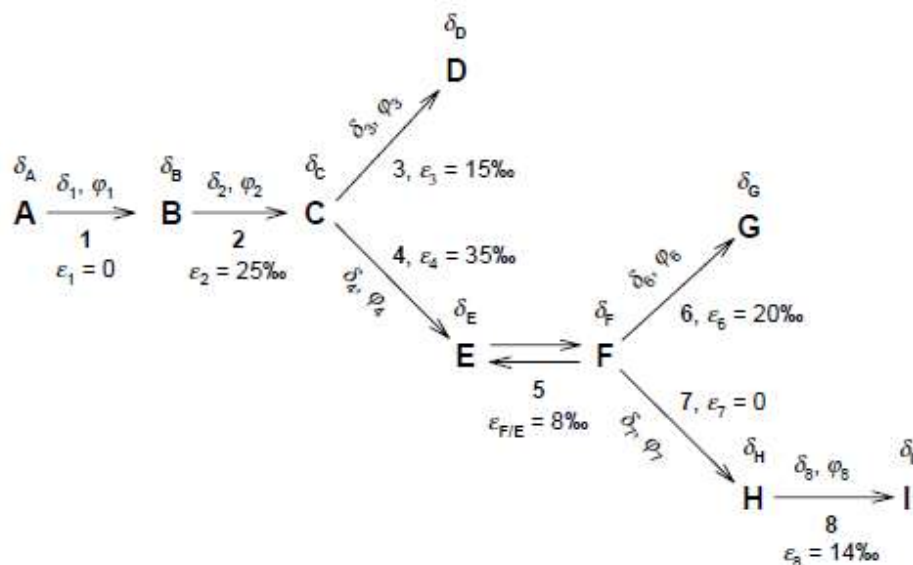


Figure 5.6: A schematic network of chemical reactions. Letters indicate carbon positions within reactants and products. Isotopic compositions of these positions are indicated by δ s with alphabetical subscripts. Reactions are designated by numbers and the δ s, ϕ s, and ϵ s with numerical subscripts indicate respectively: Isotopic compositions of the carbon being transmitted by a reaction, the flux of carbon being transmitted (moles/time), and the isotope effect associated with the reaction. (from Hayes, 2001)

(Cernusak *et al.*, 2013). Post-photosynthetic metabolic processes allow for further fractionation, and can result in dissimilar n -alkane $\delta^{13}\text{C}$ values occurring in different plant organs and compartments (Cernusak *et al.*, 2013). Diefendorf *et al.* (2011) theorise that changes in the flux of pyruvate within a plant cell, including the partitioning of it to fates other than acetyl-CoA, can shift the isotopic composition of acetogenic lipids such as n -alkanes, giving rise to ^{13}C -depleted lipids when their production decreases. But what could drive such changes in acetyl-CoA allocation across a growing season?

One answer could be the nature of compounds synthesised by the plants at Stiffkey to protect themselves from salinity. Typical compounds include carbohydrates, and nitrogenous compounds such as proline (Briens and Lahrer, 1982) produced by the glutamate pathway (Ashraf and Foodad, 2007), sorbitol and mannitol produced in the cytosol (Sharkey, 2012), and quaternary ammonium compounds such as glycine betaine (Ashraf and Foodad, 2007). The production of carbohydrates in response to environmental stresses could alter the total concentration of pyruvate within the plant leaves (Rhodes *et al.*, 1986; Good and Zaplachinski, 1994), while enhanced amino-acid synthesis could result in shifts in the allocation of pyruvate to different metabolic pathways (Diefendorf *et al.*, 2011). Results presented in Chapter 4 also

demonstrate that the relative abundance of *n*-alkane homologues (*n*-C₂₅, *n*-C₂₇, *n*-C₂₉, *n*-C₃₁, *n*-C₃₅) produced by the Stiffkey species vary considerably. Changes in the flux of carbon through the *n*-alkane biosynthetic pathway (Shepherd and Griffiths, 2006) could therefore also influence the carbon isotope composition of the *n*-alkanes both: (i) among different species; and (ii) within one species across the annual growing season.

Consideration of the schematic reaction network provided by Hayes (2001) (Figure 5.6) illustrates how these mechanisms may operate in practice. Synthesis of different compounds, each involving a particular array of enzymes, will be associated with different isotope effects, which will in turn lead to variation in the carbon isotope composition of the remaining carbon pool available for subsequent synthesis of other compounds (Hayes, 2001; Tcherkez *et al.*, 2011). For the species sampled at Stiffkey, the relative flux of carbon at each break point (such as “C”, Fig. 5.6) in the reaction network will therefore be a factor of the range and concentration of compounds synthesised by the plant in order to survive in the saltmarsh habitat. Inter-species differences in the amount of carbon diverted to each pathway following the break point (i.e. “D” and “E”, Fig. 5.6) will in turn result in a different isotopic composition of the reaction products (Hayes, 2001; Diefendorf *et al.*, 2011).

Detailed analyses of the nature and concentration of osmoregulatory compounds produced by the Stiffkey plants are outside of the scope of this thesis. It is proposed, however, that analysis of the percentage composition of carbon and nitrogen, coupled with previous studies of osmolytes in the species found at Stiffkey (e.g. Briens and Lahrer, 1982), can be used to qualitatively evaluate the relative proportions of the dominant compound classes (nitrogenous compounds vs. carbohydrates) synthesised by these saltmarsh plants. This information could be used to evaluate whether any relationship exists between these parameters and the $\delta^{13}\text{C}$ values of bulk tissue and *n*-alkanes. Analysis of the nitrogen isotope ratios of bulk plant tissue could also provide valuable details regarding differences in nitrogen resource use, and cycling within these plants (e.g. Pardo and Nadelhoffer, 2010, and references contained therein), which could be informative when considering plant responses to nutrient stress. The isotopic composition of amino acids is known to be ¹⁵N-enriched relative to total organic biomass in cyanobacteria, green algae, and seagrass species (Macko *et al.*, 1986, 1987), suggesting that foliar $\delta^{15}\text{N}$ values could also represent a qualitative proxy for distinguishing between those species accumulating nitrogenous compounds from those accumulating carbohydrates for osmoregulation.

As discussed above, consideration of the trends in bulk and *n*-alkane $\delta^{13}\text{C}$ across a growing season are important when exploring the mechanisms that control isotopic composition. The flux of carbon into different metabolic pathways within a plant cell is likely to change throughout the growing season. This could arise in response to biological demands on the plant, which can change during reproduction (Donovan and Ehleringer, 2003), or as a result of shifts in environmental conditions such as water, nutrient availability and salinity (i.e. the enhanced production of osmoregulatory compounds in high summer). Comparison of bulk and *n*-alkane $\delta^{13}\text{C}$ shifts across the 2011 and 2012 growing seasons at Stiffkey will therefore allow for evaluation of whether calculated carbon isotope discrimination values record the same trends at the bulk and molecular level, as proposed by Diefendorf *et al.* (2010). Further consideration of spatial variation in bulk and *n*-alkane $\delta^{13}\text{C}$ across the marsh sub-environments, carried out in October 2011, will also provide further information about how the variation in environmental conditions experienced in these microhabitats is recorded in $^{13}\text{C}/^{12}\text{C}$ values of foliar tissue and individual organic compounds.

5.3. AIMS AND OBJECTIVES

Given the requirement for further research to address the issues raised in the above review, the aim of this part of the project is to quantify the extent of variability in bulk and leaf wax *n*-alkane $\delta^{13}\text{C}$ signatures across a range of C_3 and C_4 species growing at a temperate coastal saltmarsh, and to identify whether they are being influenced by the same biochemical and environmental factors. In order to fulfil this aim, a series of research objectives have been established:

- 1) Measure interspecies variability in bulk and *n*-alkane $\delta^{13}\text{C}$ values across two growing seasons.
- 2) Identify whether compound-specific $\delta^{13}\text{C}$ values record the same seasonal patterns in carbon isotope composition as bulk plant tissue.
- 3) Compare seasonal patterns in $\Delta^{13}\text{C}$ calculated for bulk plant tissue with those calculated from *n*-alkane $\delta^{13}\text{C}$ for the studied C_3 species.
- 4) Measure interspecies variation in $\delta^{15}\text{N}$, percentage C, and percentage N for the saltmarsh plants across two growing seasons.
- 5) Identify whether any relationship exists between seasonal shifts in (i) $\delta^{15}\text{N}$; (ii) percentage C; and (iii) percentage N content, and the $\delta^{13}\text{C}$ ratios of bulk plant tissue and *n*-alkanes for the sampled plants.

- 6) Compare carbon isotope values with data pertaining to leaf wax concentration and molecular distribution (data presented in Chapter 4) to examine whether seasonal shifts in the production and composition of leaf wax secondary compounds influence their $\delta^{13}\text{C}$ values.
- 7) Compare the bulk and *n*-alkane carbon isotope composition of bulk leaf tissue and *n*-alkanes from species growing across multiple marsh sub-environments at a single sampling interval, to investigate the extent to which shifts in environmental conditions across the marsh are recorded in bulk and *n*-alkane $^{13}\text{C}/^{12}\text{C}$ values.

5.4. SITE DESCRIPTION AND SAMPLING STRATEGY

5.4.1 Site description

The sampling site discussed in this chapter, Stiffkey marsh, has been previously described in Chapter 2.

5.4.2 Sampling strategy

Plants sampled in 2011 and 2012 for this chapter were collected in accordance with the sampling description provided in Chapter 4. Note that every effort was made to sample new growth from all plant species throughout the course of this study, to ensure that as far as possible leaves reflected seasonal shifts in environmental conditions.

5.5. ANALYTICAL METHODS

5.5.1 Bulk carbon and nitrogen isotope analysis

Samples of plant leaf tissue were milled in a Spex CertiPrep cryogenic mill, to avoid overheating and fractionation during grinding. Milled samples were weighed into tin capsules, crimped, and then analysed for $\delta^{13}\text{C}$ and $\delta^{15}\text{N}$ using a Delta XP ThermoFisher isotope-ratio mass spectrometer interfaced with a CosTech elemental analyser. To ensure sufficient powdered sample, leaves from both replicates collected for each plant were homogenised to give a representative signal. Each batch of samples included replicate analyses of the in-house standard, casein ($\delta^{15}\text{N} = +6.15\text{‰}$, $\delta^{13}\text{C} = -23.37\text{‰}$, previously calibrated against the International Atomic Energy Agency (IAEA) reference materials during an inter-laboratory comparison exercise as part of EU Project SMT4-CT98-2236), which was used for the drift

correction of raw analytical measurement data. The long-term performance of the mass spectrometer was monitored by analysis of a secondary reference material, collagen ($\delta^{15}\text{N} = +6.12\text{‰}$, $\delta^{13}\text{C} = -17.98\text{‰}$), which was included with every batch of samples (Appendix 4). Casein standards of different masses were also used to check instrument linearity before each analysis. All carbon isotope measurements are expressed relative to Vienna Pee Dee Belemnite (VPDB), while nitrogen isotope values are expressed relative to atmospheric nitrogen. All values are reported in 'per mil' notation (‰). Samples and standards were both prepared and analysed using the same methods, to ensure compliance with the principle of identical treatment (PIT, Chesson *et al.*, 2009). Care was taken to accurately weigh samples and standards to ensure that their peak intensities were within the linear range of the Delta XP, and commensurate with one another. During all sample and standard measurements, 3 reference gas pulses were passed through the mass spectrometer. Reproducibility of CO_2 reference gas $\delta^{13}\text{C}$ was typically $\pm 0.03\text{‰}$; for the N_2 reference gas reproducibility of $\delta^{15}\text{N}$ was also typically $\pm 0.03\text{‰}$. Reproducibility of $\delta^{13}\text{C}$ measurements of the in-house collagen standard was $\pm 0.3\text{‰}$ ($n = 28$), while for $\delta^{15}\text{N}$ measurements reproducibility was $\pm 0.1\text{‰}$ ($n = 28$) (Appendix 4). All samples were analysed in duplicate; absolute differences between analytical replicates of the same sample for $\delta^{13}\text{C}$ did not exceed 0.6‰ , and for $\delta^{15}\text{N}$ did not exceed 0.7‰ .

5.5.2 *n*-Alkane extraction, quantification and identification

Plant leaf waxes were extracted, quantified and identified as described in Chapter 4.

5.5.3 *n*-Alkane $\delta^{13}\text{C}$ analysis

Carbon isotope signatures of *n*-alkanes were measured using a Delta V Advantage ThermoFisher isotope-ratio mass spectrometer interfaced with GC-Isolink Trace GC Combustion and High temperature conversion systems, using an Agilent DB-5 capillary column (30 m \times 0.32 mm \times 0.25 μm) (Agilent Technologies Inc., Santa Clara, USA). The combustion system was maintained at 1020 °C for $\delta^{13}\text{C}$ analysis. The GC oven temperature was programmed from 50 °C, which was then raised at a rate of 30° C min⁻¹ until the temperature reached 220 °C, and then to 320 °C at a rate of 6 °C min⁻¹. The final temperature was held for 5 minutes. Carbon isotope compositions of *n*-alkanes are reported based on duplicate analyses of well-resolved peaks. $\delta^{13}\text{C}$ values are expressed relative to Vienna Pee Dee Belemnite (VPDB), based on in-house reference gases (CO_2 , BOC) adjusted daily using a

standard mixture of $n\text{-C}_{16}$ to $n\text{-C}_{30}$ alkanes (the isotope ratios of which were measured offline by A. Schimmelmann, Biogeochemical Laboratories, Indiana University). During all sample and standard measurements, 6 reference gas pulses were passed through the mass spectrometer. Reproducibility of CO_2 $\delta^{13}\text{C}$ values was typically $\pm 0.02\text{‰}$. Isotope data are presented using “per mil” notation (‰). Absolute differences between duplicate sample analyses did not exceed 2‰, with typical variation ranging from 0.1 to 1‰. Repeat measurements of the same sample were typically not more than 0.5‰ (Appendix 4). Relative mean square (RMS) errors for standard measurements ($n\text{-C}_{16}$ to $n\text{-C}_{30}$ alkanes, A. Schimmelmann, Biogeochemical Laboratories, Indiana University) did not exceed 0.5‰ ($n = 144$) throughout sample analysis. In addition to individual n -alkane $\delta^{13}\text{C}$ values, the molecular distribution data presented in Chapter 4 was used to calculate a weighted average (WA) carbon isotope composition for each species. The equation used for this calculation is as shown below (Eq. 5), where RA represents relative abundance, expressed as a percentage of the total odd-chain alkanes, produced by each species.

$$\delta^{13}\text{C}_{\text{WA}} = ((RA_{23} * \delta^{13}\text{C}_{\text{C23}}) + (RA_{25} * \delta^{13}\text{C}_{\text{C25}}) + (RA_{27} * \delta^{13}\text{C}_{\text{C27}}) + (RA_{29} * \delta^{13}\text{C}_{\text{C29}}) + (RA_{31} * \delta^{13}\text{C}_{\text{C31}}) + (RA_{33} * \delta^{13}\text{C}_{\text{C33}}) + (RA_{35} * \delta^{13}\text{C}_{\text{C35}})) / (RA_{23} + RA_{25} + RA_{27} + RA_{29} + RA_{31} + RA_{33} + RA_{35}) \quad (\text{Eq. 5})$$

5.5.4 Calculation of carbon isotope discrimination

Carbon isotope discrimination (Δ) was calculated from bulk leaf $\delta^{13}\text{C}$, and weighted average n -alkane $\delta^{13}\text{C}$, using Equation 3 (above) to ensure results from this study were comparable with previous research (e.g. Diefendorf *et al.*, 2010). A range of previous studies (Conte and Weber, 2002; Smith *et al.*, 2007; Diefendorf *et al.*, 2010) chose to apply correction factor to n -alkanol and n -alkanoic acid data prior to calculating $\Delta^{13}\text{C}$, to make values comparable with bulk leaf carbon isotope discrimination values. The correction applied is shown in Eq. 6,

$$\bar{\delta}_x = \bar{\delta}_{\text{wax}} + \varepsilon_f \quad (\text{Eq. 6})$$

where $\bar{\delta}_{\text{wax}}$ is the averaged carbon isotope composition of the measured biomarker, and ε_f is the mean biosynthetic isotopic fractionation between leaf wax compound class and bulk leaf carbon (Conte and Weber, 2002). Typical values for ε_f are -4.9‰ (Smith *et al.*, 2007; Diefendorf *et al.*, 2010). However, the accuracy of the ε_f term is open to question, as studies describing the fractionation between bulk and n -alkane carbon isotope composition are limited (Conte and Weber, 2002). Because of this

uncertainty, no such correction factor has been applied to this data. Whilst this will not change the relative trends in Δ among the plants sampled at Stiffkey saltmarsh, qualitative comparison with other (corrected) $\Delta^{13}\text{C}$ values will require careful consideration.

5.5.5 Analysis of the percentage carbon and nitrogen content

The percentage of total C and N in the leaves of each species was quantified using a Carlo Erba EA 1108 Elemental Analyser. Plant leaf tissue was ground to a fine powder under liquid nitrogen using a cryogenic mill and weighed into tin capsules for analysis. The dried ground samples were placed inside the autosampler which was purged with helium. During analysis, the combustion reactor was kept at a temperature of 904 °C. When a sample was dropped, a pulse of O₂ was injected to ensure that the sample underwent flash combustion. Helium was used as the carrier gas to transport the gas products of flash combustion through the combustion reactor, where oxidation with copper (II) oxide and platinised alumina converts sample carbon to CO₂, and all the nitrogen-containing compounds to nitrogen oxides (NO_x). The CO₂ and NO_x gases were then passed through a quartz reduction column containing copper wire which acted as a reduction catalyst, reducing the nitrogen oxides to N₂ gas. The resulting gases were separated on a chromatographic column and detected by a thermal conductivity detector (TCD). Acetanilidide and sulphanilamide standards were analysed at the start of each run, and used to calibrate the instrument. These standards were also analysed every ~10 samples, to monitor instrument performance (Appendix 4). All data were blank corrected using empty tin capsules.

5.6. RESULTS

5.6.1 Bulk $\delta^{13}\text{C}$

Bulk tissue from the seven saltmarsh species sampled across the 2011 and 2012 growing seasons showed maximum variability (assumed due to seasonal shifts) in the C₃ monocot grass *Elytrigia atherica* (~ 5‰; Table 5.3 and 5.4; Fig. 5.7B). In contrast, the species with the most consistent bulk ¹³C/¹²C composition throughout the entire sampling period was the C₃ reed *Phragmites australis* (0.9‰) (Table 5.3 and 5.4; Fig. 5.7D). The seasonal variability in $\delta^{13}\text{C}$ values was greater in the two evergreen *Atriplex portulacoides* and *Suaeda vera* (3‰) than in the perennial *Limonium vulgare* and the annual succulent *Salicornia europaea* (2‰)

Table 5.3: Carbon isotope composition of *n*-alkanes (*n*-C₂₇, *n*-C₂₉, *n*-C₃₁, weighted average) and bulk plant tissue, sampled during the 2011 growing season

Month	Location	Plant species	$\delta^{13}\text{C } n\text{-C}_{27}$	AD _{n-C27}	$\delta^{13}\text{C } n\text{-C}_{29}$	AD _{n-C29}	$\delta^{13}\text{C } n\text{-C}_{31}$	AD _{n-C31}	WA	$\delta^{13}\text{C bulk}$	AD _{13C bulk}
June	Site 2	<i>Atriplex portulacoides</i>	-30.5	1.1	-31.3	1.4	-32.6	1.4	-31.0	-25.7	0.0
	Site 2	<i>Elytrigia atherica</i>	-36.6	0.6	-37.1	0.4	-36.2	0.6	-36.7	-28.6	0.1
	Site 3	<i>Limonium vulgare</i>	-33.5	0.3	-32.7	0.3	-32.3	0.4	-32.9	-25.8	0.1
	Site 2	<i>Phragmites australis</i>	-32.9	0.2	-32.9	0.4	-	-	-32.9	-25.5	0.0
	Site 1	<i>Salicornia Europaea</i>	-31.9	1.3	-31.0	2.3	-31.8	1.9	-31.8	-28.1	0.0
	Site 1	<i>Spartina anglica</i>	-25.1	0.3	-25.6	0.2	-24.9	0.1	-25.3	-13.9	0.2
	Site 2	<i>Suaeda vera</i>	-36.7	0.2	-35.3	0.1	-35.4	-	-35.6	-29.8	0.0
August	Site 2	<i>Atriplex portulacoides</i>	-29.8	0.2	-31.2	0.1	-32.5	0.7	-30.5	-25.3	0.0
	Site 2	<i>Elytrigia atherica</i>	-34.3	0.1	-35.2	0.1	-33.4	0.5	-34.5	-25.6	0.1
	Site 3	<i>Limonium vulgare</i>	-34.3	0.2	-35.0	0.2	-34.6	0.3	-34.6	-26.8	0.2
	Site 2	<i>Phragmites australis</i>	-33.3	0.1	-33.3	0.1	-	-	-33.2	-26.0	0.0
	Site 1	<i>Salicornia Europaea</i>	-32.7	0.3	-32.9	0.2	-33.2	-	-32.7	-25.8	0.1
	Site 1	<i>Spartina anglica</i>	-24.0	0.2	-24.7	0.1	-24.8	0.2	-24.6	-14.3	0.0
	Site 2	<i>Suaeda vera</i>	-36.6	0.6	-35.5	0.4	-34.0	0.5	-35.9	-29.4	0.0
October	Site 2	<i>Atriplex portulacoides</i>	-30.4	0.1	-31.1	0.1	-32.2	-	-30.9	-24.9	0.1
	Site 2	<i>Elytrigia atherica</i>	-35.2	0.3	-35.3	0.3	-34.2	0.3	-34.8	-25.9	0.2
	Site 3	<i>Limonium vulgare</i>	-34.3	0.1	-34.2	0.3	-33.1	0.3	-32.6	-25.3	0.1
	Site 2	<i>Phragmites australis</i>	-33.3	0.1	-33.3	0.1	-	-	-33.9	-25.8	0.1
	Site 1	<i>Salicornia Europaea</i>	-32.1	0.5	-32.4	1.0	-32.6	0.4	-32.2	-25.8	0.6
	Site 1	<i>Spartina anglica</i>	-24.3	0.1	-25.3	0.2	-26.5	1.4	-25.4	-14.2	0.4
	Site 2	<i>Suaeda vera</i>	-38.2	0.0	-37.3	0.1	-	-	-37.6	-28.3	0.2

*WA = weighted average *n*-alkane carbon isotope composition; AD = absolute difference between sample duplicates. Where no AD value is given, only one replicate had sufficient concentrations of that homologue for $\delta^{13}\text{C}$ analysis, so the isotope value represents data from that sample only. All values given to one d.p.

Table 5.4: Carbon isotope composition of *n*-alkanes (*n*-C₂₇, *n*-C₂₉, *n*-C₃₁, weighted average) and bulk plant tissue, sampled during the 2012 growing season

Month	Location	Plant species	$\delta^{13}\text{C } n\text{-C}_{27}$	AD _{n-C27}	$\delta^{13}\text{C } n\text{-C}_{29}$	AD _{n-C29}	$\delta^{13}\text{C } n\text{-C}_{31}$	AD _{n-C31}	WA	$\delta^{13}\text{C } \text{bulk}$	AD _{13C bulk}
March	Site 2	<i>Atriplex portulacoides</i>	-31.9	0.4	-31.9	0.2	-	-	-31.9	-27.9	0.5
	Site 2	<i>Elytrigia atherica</i>	-37.5	0.1	-36.5	0.1	-36.6	0.1	-36.6	-28.6	0.0
	Site 3	<i>Limonium vulgare</i>	-36.2	-	-36.4	0.2	-35.0	0.3	-35.8	-27.1	0.5
	Site 1	<i>Spartina anglica</i>	-24.2	0.3	-25.0	0.4	-25.0	0.2	-24.7	-13.6	0.0
	Site 2	<i>Suaeda vera</i>	-39.5	0.2	-38.5	0.3	-37.9	0.5	-38.6	-31.4	0.2
May	Site 2	<i>Atriplex portulacoides</i>	-29.9	1.2	-31.3	0.5	-31.0	0.8	-31.4	-27.4	0.1
	Site 2	<i>Elytrigia atherica</i>	-38.7	0.5	-39.6	0.2	-39.3	0.2	-39.0	-30.7	0.0
	Site 3	<i>Limonium vulgare</i>	-31.4	0.6	-31.1	0.7	-30.9	0.6	-31.1	-25.0	0.1
	Site 2	<i>Phragmites</i>	-32.8	0.1	-34.0	0.2	-	-	-33.1	-26.0	0.0
	Site 1	<i>Salicornia Europaea</i>	-32.5	0.7	-31.0	0.3	-32.3	0.5	-32.2	-27.6	0.0
	Site 1	<i>Spartina anglica</i>	-25.9	0.2	-26.4	0.1	-	-	-26.1	-13.5	0.0
	Site 2	<i>Suaeda vera</i>	-40.0	0.2	-37.7	0.3	-36.2	0.2	-37.9	-30.4	0.1
August	Site 2	<i>Atriplex portulacoides</i>	-31.8	0.4	-32.4	0.6	-	-	-32.0	-26.0	0.0
	Site 2	<i>Elytrigia atherica</i>	-36.7	0.1	-37.8	0.0	-36.6	0.2	-37.3	-27.7	0.0
	Site 3	<i>Limonium vulgare</i>	-32.4	0.0	-32.4	0.3	-32.1	0.1	-32.2	-25.2	0.0
	Site 2	<i>Phragmites</i>	-32.6	0.3	-32.9	0.2	-	-	-32.6	-25.2	0.0
	Site 1	<i>Salicornia Europaea</i>	-32.8	0.2	-33.4	0.1	-33.5	0.1	-32.9	-27.5	0.0
	Site 1	<i>Spartina anglica</i>	-24.0	0.1	-24.7	0.0	-	-	-24.6	-13.0	0.0
	Site 2	<i>Suaeda vera</i>	-37.0	0.6	-35.9	0.6	-34.4	0.6	-36.1	-29.2	0.0
	Site 2	<i>Atriplex portulacoides</i>	-31.7	0.2	-32.0	0.4	-32.2	0.2	-31.8	-26.6	0.1
September	Site 2	<i>Elytrigia atherica</i>	-36.7	0.1	-37.0	0.0	-35.3	0.0	-36.2	-27.6	0.0
	Site 3	<i>Limonium vulgare</i>	-32.8	0.4	-32.9	0.4	-32.3	0.4	-32.5	-25.5	0.1
	Site 2	<i>Phragmites</i>	-32.6	0.3	-32.7	0.1	-	-	-32.6	-25.1	0.0
	Site 1	<i>Salicornia Europaea</i>	-32.7	0.5	-31.6	0.3	-32.1	0.5	-32.2	-26.5	0.0
	Site 1	<i>Spartina anglica</i>	-24.5	1.2	-25.6	0.5	-25.3	0.1	-25.2	-13.4	0.0
	Site 2	<i>Suaeda vera</i>	-37.7	0.3	-36.4	0.2	-	-	-36.8	-29.0	0.1

*WA = weighted average *n*-alkane carbon isotope composition; AD = absolute difference between sample duplicates. Where no AD value is given, only one replicate had sufficient concentrations of that homologue for $\delta^{13}\text{C}$ analysis, so the isotope value represents data from that sample only. All values given to one d.p.

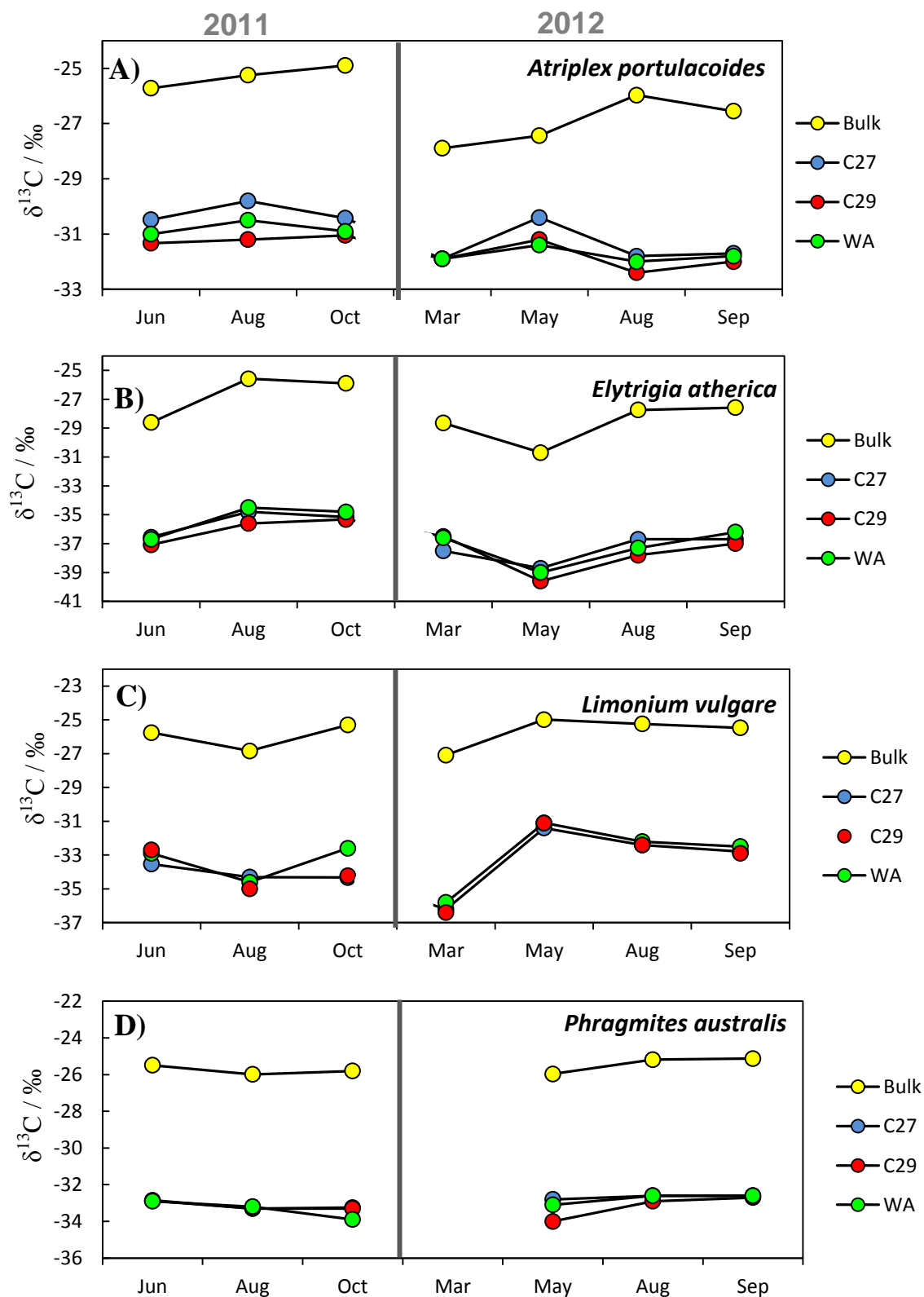


Figure 5.7: Seasonal trends in bulk plant leaf, $n\text{-C}_{27}$, $n\text{-C}_{29}$ and WA $n\text{-alkane}$ carbon isotope ratios from all species sampled at Stiffkey. A) *Atriplex portulacoides*, B) *Elytrigia atherica*, C) *Limonium vulgare*, D) *Phragmites australis*. Sample replicates at the bulk level did not vary by more than 0.6‰, while $n\text{-alkane}$ sample replicates varied by no more than 2‰.

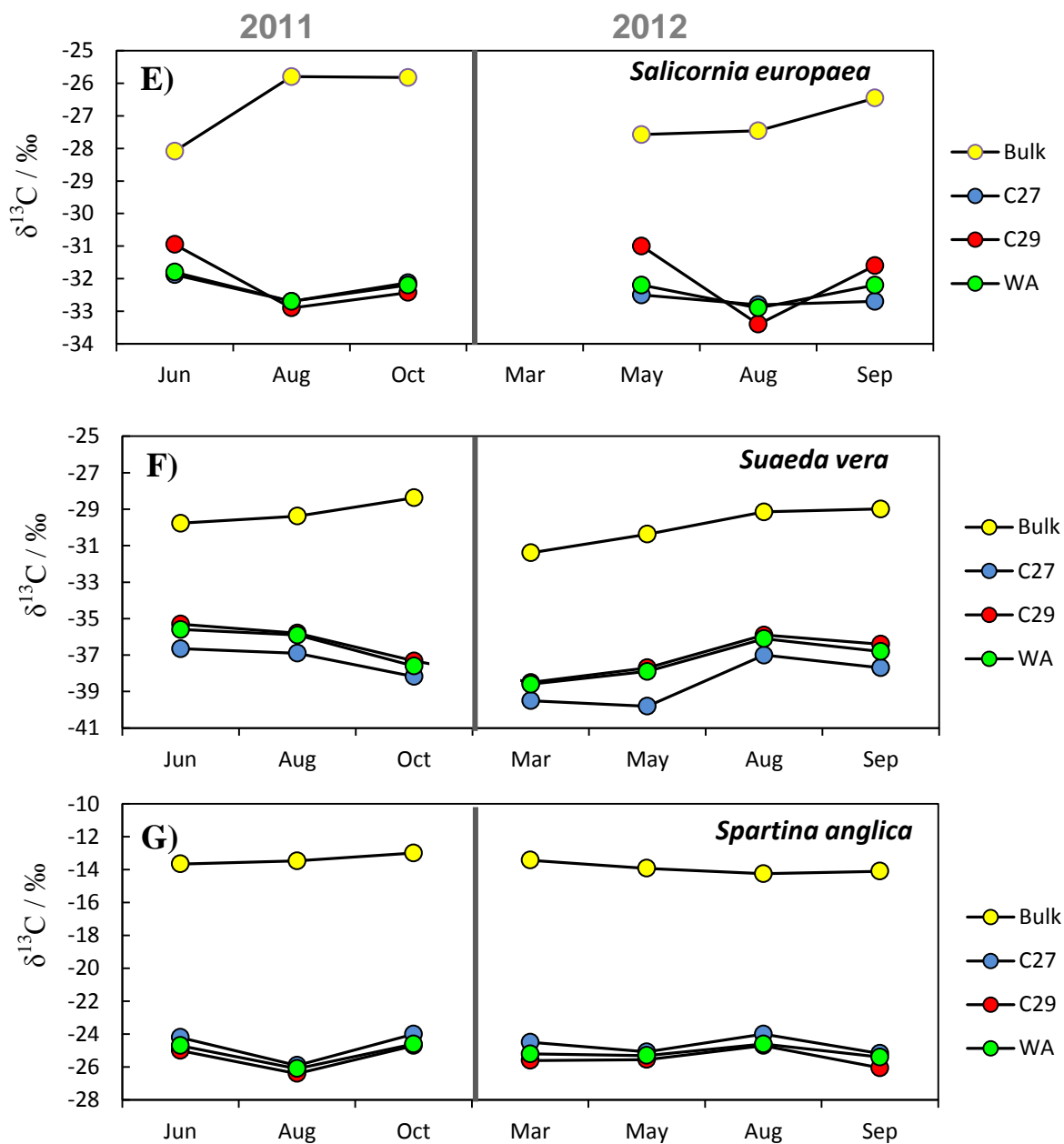


Figure 5.7 Cont.: Seasonal trends in bulk plant leaf, $n\text{-C}_{27}$, $n\text{-C}_{29}$ and WA $n\text{-alkane}$ carbon isotope ratios from all species sampled at Stiffkey. E) *Salicornia europaea*, F) *Suaeda vera*, G) *Spartina anglica*. Sample replicates at the bulk level did not vary by more than 0.6‰, while $n\text{-alkane}$ sample replicates varied by no more than 2‰.

(Tables 5.3 and 5.4; Fig. 5.7). No systematic pattern of ^{13}C -enrichment or depletion was observed with plant life form. The most ^{13}C -enriched bulk tissue among the C_3 species was found in the evergreen shrub *Atriplex portulacoides*, while the most ^{13}C -depleted was found in the evergreen succulent *Suaeda vera*. Among the C_3 species, ^{13}C -enrichment in bulk tissue isotope tissue was generally greater in the summer months (Tables 5.3 and 5.4), and relatively lower in the early growth season, e.g. March and May 2012 (Table 5.4). Total interspecies variation in bulk carbon isotope composition among C_3 species was 6.4‰, ranging from -31.4‰ to -24.9‰ (Table 5.3 and 5.4). The C_4 monocot, *Spartina anglica* had a bulk $\delta^{13}\text{C}$ signal that varied by <1‰ in 2011 and 2012 (Table 5.3 and 5.4).

5.6.2 *n*-Alkane $\delta^{13}\text{C}$

Carbon isotope measurements of $n\text{-C}_{27}$, $n\text{-C}_{29}$ and $n\text{-C}_{31}$ are presented in Tables 5.3 and 5.4. In addition to these homologues, weighted average (WA) *n*-alkane carbon isotope compositions were also calculated using Equation 5 (Tables 5.3 and 5.4). Maximum seasonal variation in weighed average *n*-alkane $^{13}\text{C}/^{12}\text{C}$ composition for the six C_3 species sampled (9‰) exceeded that observed in bulk tissue by 3‰ (Table 5.3 and 5.4). Intraspecies seasonal variability was also different from that observed at the bulk tissue level, with the greatest variability in lipid $\delta^{13}\text{C}$ values during the sampling period observed in *Limonium vulgare* (5‰). *Phragmites australis* had one of the most consistent *n*-alkane $\delta^{13}\text{C}$ profile throughout 2011 and 2012, but at the compound-specific level the lowest overall variation occurred in the stem succulent *Salicornia europaea*. The most positive *n*-alkane $\delta^{13}\text{C}$ ratios were consistently found in *Atriplex portulacoides* (as opposed to *Phragmites australis* at the bulk level), while the most negative values were recorded for *Elytrigia atherica* and *Suaeda vera* (Tables 5.3 and 5.4).

Comparison of the seasonal trends in *n*-alkane and bulk $\delta^{13}\text{C}$ values for each species during the sampling period are shown in Figure 5.7. These trends showed different patterns from those observed for bulk plant tissue for some C_3 species. The seasonal trends observed in *Suaeda vera* differed, for example, between bulk and *n*-alkane data, with a trend towards more positive values observed between June 2011 and October 2011 in the bulk tissue compared to a consistent shift to more negative values for the same period in the *n*-alkane values (Fig 5.7 F). *n*-Alkane data for *Salicornia europaea* showed a similar trend across both 2011 and 2012 becoming ~0.5‰ lower in August, while the bulk isotope data instead had more

negative $\delta^{13}\text{C}$ during the early growth season becoming progressively more positive as the season progressed (Fig. 5.7 E).

Overall, seasonal variation in the carbon isotope composition of $n\text{-C}_{27}$, $n\text{-C}_{29}$ and WA alkanes among the C_3 species was higher than that observed at the bulk level, typically ranging from 5 - 9‰. In contrast, the maximum variability of carbon isotope composition of $n\text{-C}_{29}$ from the C_4 grass *Spartina anglica* was no greater than 2‰ throughout the entire sampling period. The greatest range in n -alkane carbon isotope composition among all species was observed in May 2012, however interspecies variability in n -alkane $\delta^{13}\text{C}$ did not appear to be as strongly linked to the summer months as that observed in the bulk data (Fig. 5.7).

5.6.3 Correlation between seasonal trends in bulk and n -alkane $\delta^{13}\text{C}$

When carbon isotope data from bulk tissue and weighted average n -alkanes were compared from all C_3 species sampled across the 2011 and 2012 growing seasons, a positive correlation ($r = 0.67$, $P = <0.05$, $n = 40$, Rank Spearman correlation, Minitab v.16) was observed (Fig. 5.8). Bulk isotope data were then compared with weighted average n -alkane data for individual plant species to look into the relationship between bulk tissue and secondary compound $\delta^{13}\text{C}$ in more detail.

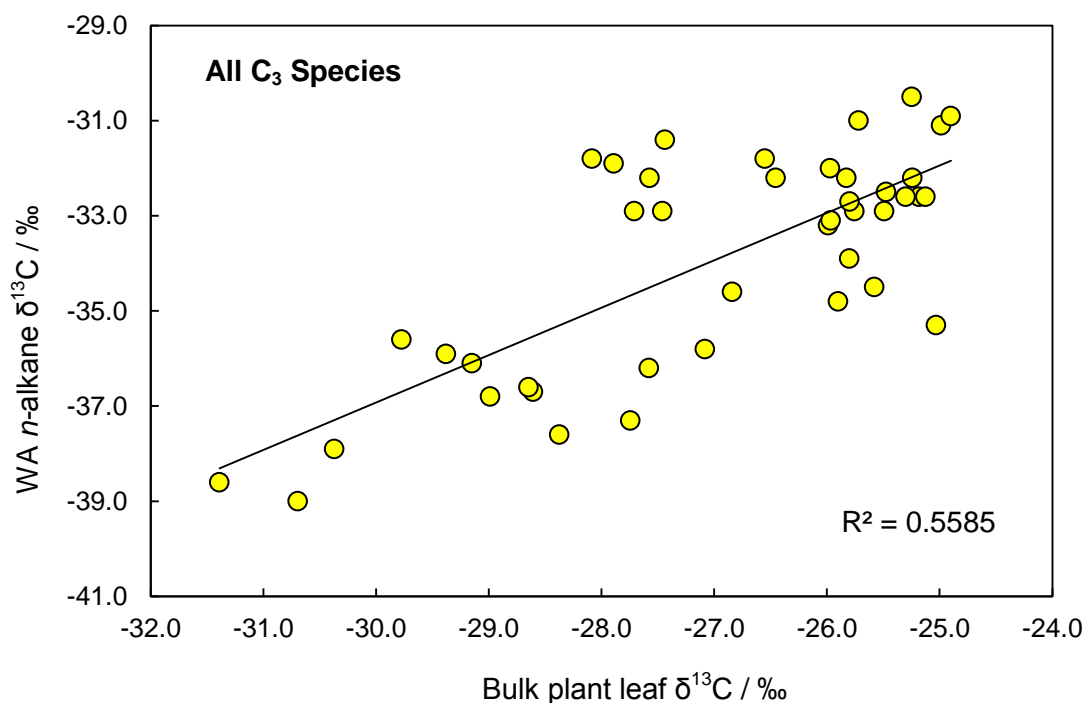


Figure 5.8: Correlation between bulk plant leaf carbon isotope signatures and WA n -alkane isotope signatures from all C_3 species sampled at Stiffkey in 2011 and 2012

Results showed that for the C₃ monocot *Elytrigia atherica* the seasonal trends in bulk and WA δ¹³C were closely related to each other, which is supported by a strong positive correlation ($r = 0.95$, $P = <0.05$, $n = 7$, Pearson's product moment correlation, Minitab v.16) in their δ¹³C values. For the other C₃ monocot *Phragmites australis*, the relationship was strongly positive, but significant only at the 90% confidence interval ($r = 0.7$, $P = 0.1$, $n = 6$, Pearson's product moment correlation, Minitab v.16). The C₃ dicot *Limonium vulgare* also had a significant positive correlation between WA alkane and bulk δ¹³C ($r = 0.95$, $P = <0.05$, $n = 7$, Pearson's product moment correlation, Minitab v.16). However, for other species sampled, including the C₄ monocot *Spartina anglica*, the C₃ succulents *Salicornia europaea* and *Suaeda vera* and the C₃ dicot *Atriplex portulacoides*, no statistically significant relationship was observed between their individual bulk and *n*-alkane carbon isotope values (Rank Spearman/Pearson's product moment correlation, $P = >0.05$, Minitab v.16). This may be due to differences in the timing of ¹³C-enrichment and ¹³C-depletion at the bulk and molecular level in these species across the growing seasons. *Salicornia europaea*, for example, recorded an almost inverse relationship between bulk and WA δ¹³C during June, August and October 2011 (Fig. 5.7E), while *Atriplex portulacoides* had subtle discrepancies in the 2012 sampling period where bulk δ¹³C was most positive in August – the same period where WA *n*-alkane δ¹³C was conversely most negative (Fig. 5.7A). The C₄ species *Spartina anglica* had only a 1-2‰ seasonal variability in both the bulk and WA δ¹³C signals, however, the WA profile showed regular month-on-month shifts of 1‰ that were not replicated in the bulk profile (Fig. 5.7G).

5.6.4 Seasonal shifts in the offset between bulk and *n*-alkane δ¹³C

Carbon isotope values of *n*-alkanes from C₃ species at Stiffkey were on average 7 ± 2 ‰ lower than those of the bulk tissue. However, the variability in the seasonal trends observed for the six Stiffkey species (above) formed the rationale for further consideration of whether the offset between bulk and lipid δ¹³C shifted with the seasons. Offset values were calculated using Equation 7.

$$\epsilon_{WA\ alkane / bulk} = \frac{\left(\frac{^{13}C}{^{12}C} \right)_{WA\ alkane}}{\left(\frac{^{13}C}{^{12}C} \right)_{bulk}} - 1 = \frac{(\delta^{13}C)_{WA\ alkane} + 1}{(\delta^{13}C)_{bulk} + 1} - 1$$

(Eq 7)

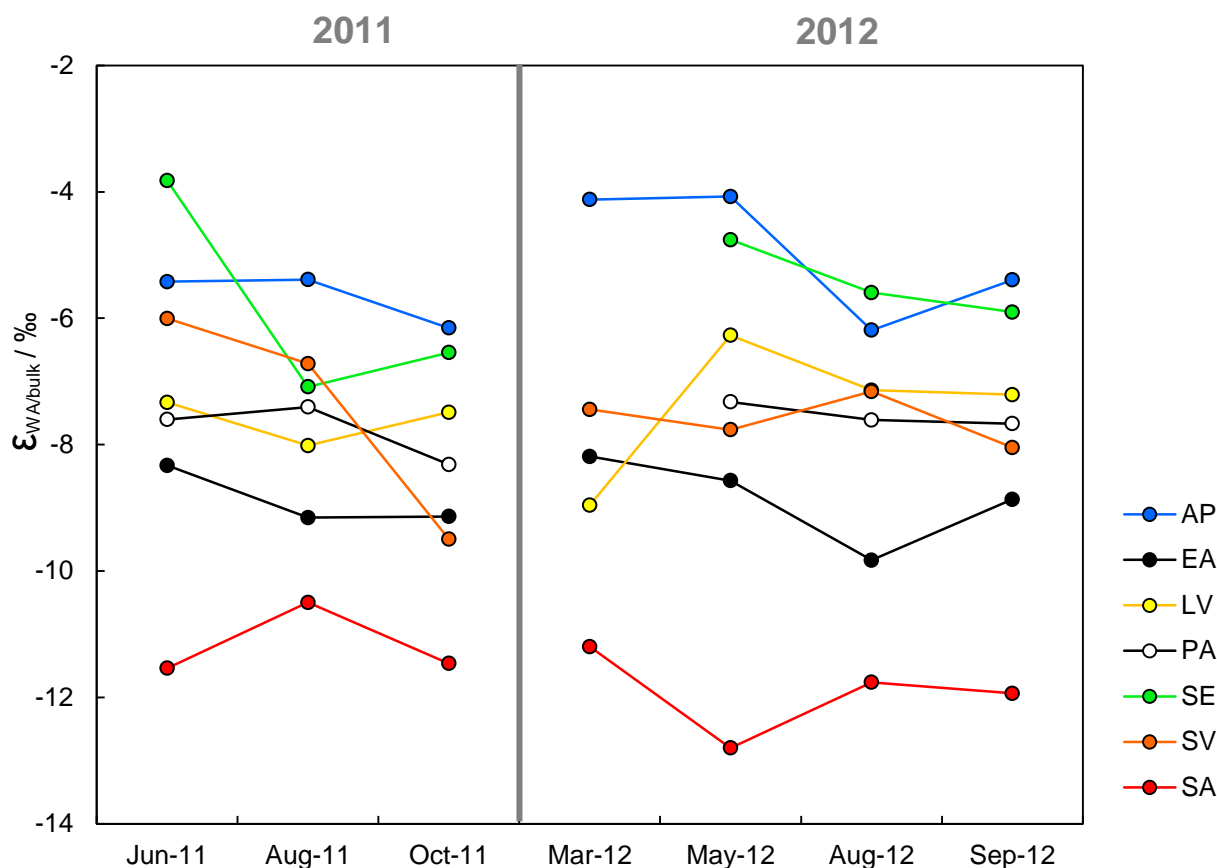


Figure 5.9: Calculated Seasonal variation in the apparent fractionation (ϵ) between bulk leaf and WA alkane $\delta^{13}\text{C}$ values from species sampled at Stiffkey during 2011 and 2012. Abbreviations; AP, *Atriplex portulacoides*; EA, *Elytrigia atherica*; LV, *Limonium vulgare*; PA, *Phragmites australis*; SE, *Salicornia europaea*; SV, *Suaeda vera*; SA, *Spartina anglica*. The grey line separates data from the 2011 and 2012 growing seasons.

These data showed that there was considerable intra- and inter-species variability in the relationship between bulk and weighted average n -alkane carbon isotope ratios (Fig. 5.9), with n -alkane carbon isotope values in C_3 plants ranging from 4 to 13‰ lower than bulk values across the 2011 and 2012 growth seasons (Fig. 5.9), and 11 to 13‰ for the C_4 monocot *Spartina anglica*. Among the C_3 species, WA $\delta^{13}\text{C}$ values from *Elytrigia atherica* were generally the most ^{13}C -depleted relative to bulk tissue resulting in the greatest fractionation ($\epsilon_{\text{wa/bulk}}$), while WA values from *Salicornia europaea* and *Atriplex portulacoides* were consistently the most ^{13}C -enriched resulting in these species having lower values of $\epsilon_{\text{wa/bulk}}$ between n -alkane and bulk $\delta^{13}\text{C}$ (Fig. 5.9). *Suaeda vera*, *Limonium vulgare* and *Salicornia europaea* recorded the maximum seasonal variability (4‰) in the relationship between their WA and bulk tissue $\delta^{13}\text{C}$ values, while *Phragmites australis* (1‰), *Elytrigia atherica* (2‰) and *Atriplex portulacoides* (2‰) were the most consistent. Seasonally, the greatest ^{13}C -

depletion in WA values versus bulk tissue generally occurs in C₃ species later in the growth season (e.g October 2011, August and September 2012), while the least depletion is observed earlier, particularly during June 2011, and March/May 2012 (Fig. 5.9). A notable exception to this rule is the sample from *Limonium vulgare* from March 2012 – this was when newly emergent leaves were sampled. Carbon isotope signatures of *n*-alkanes from the C₄ grass *Spartina anglica* were 10 to 13‰ lower than bulk depending on the sampling period (Fig. 5.9). Comparison of $\epsilon_{wa/bulk}$ values between *n*-C₂₇ and bulk, and *n*-C₂₉ and bulk, showed that *n*-C₂₉ was typically ~1‰ lower than *n*-C₂₇ relative to bulk tissue.

5.6.5 Calculating $\Delta^{13}\text{C}$ values from bulk and *n*-alkane $\delta^{13}\text{C}$

Carbon isotope discrimination values for the C₃ species at Stiffkey showed different trends depending upon whether bulk or *n*-C₂₉ $\delta^{13}\text{C}$ values are used in the calculation (*n*-C₂₉ was selected for this calculation as this remains one of the most common terrestrial plant *n*-alkanes reported in sedimentary studies). This resulted in a correlation between $\Delta^{13}\text{C}$ values calculated with bulk versus *n*-C₂₉ data with a coefficient of 0.6 (Fig. 5.10). Seasonal shifts in $\Delta^{13}\text{C}$ values calculated using bulk carbon isotope profiles (Fig. 5.11A) showed an overall tendency to be highest in June during 2011 and March/May during 2012. In both years, the $\Delta^{13}\text{C}$ values then decreased towards the end of the sampling period (October 2011; September 2012). *Suaeda vera* consistently had the highest $\Delta^{13}\text{C}$ values, while *Limonium vulgare*, *Atriplex portulacoides* and *Phragmites australis* had the lowest $\Delta^{13}\text{C}$ values.

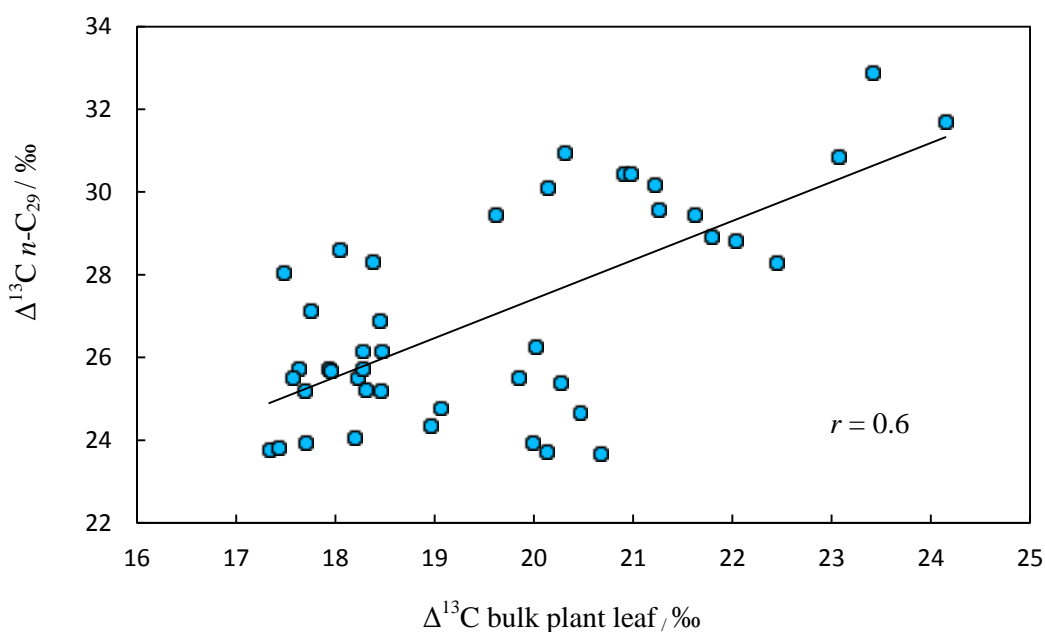


Figure 5.10: Correlation between carbon isotope discrimination values calculated from bulk plant leaf tissue, and *n*-C₂₉ alkane data

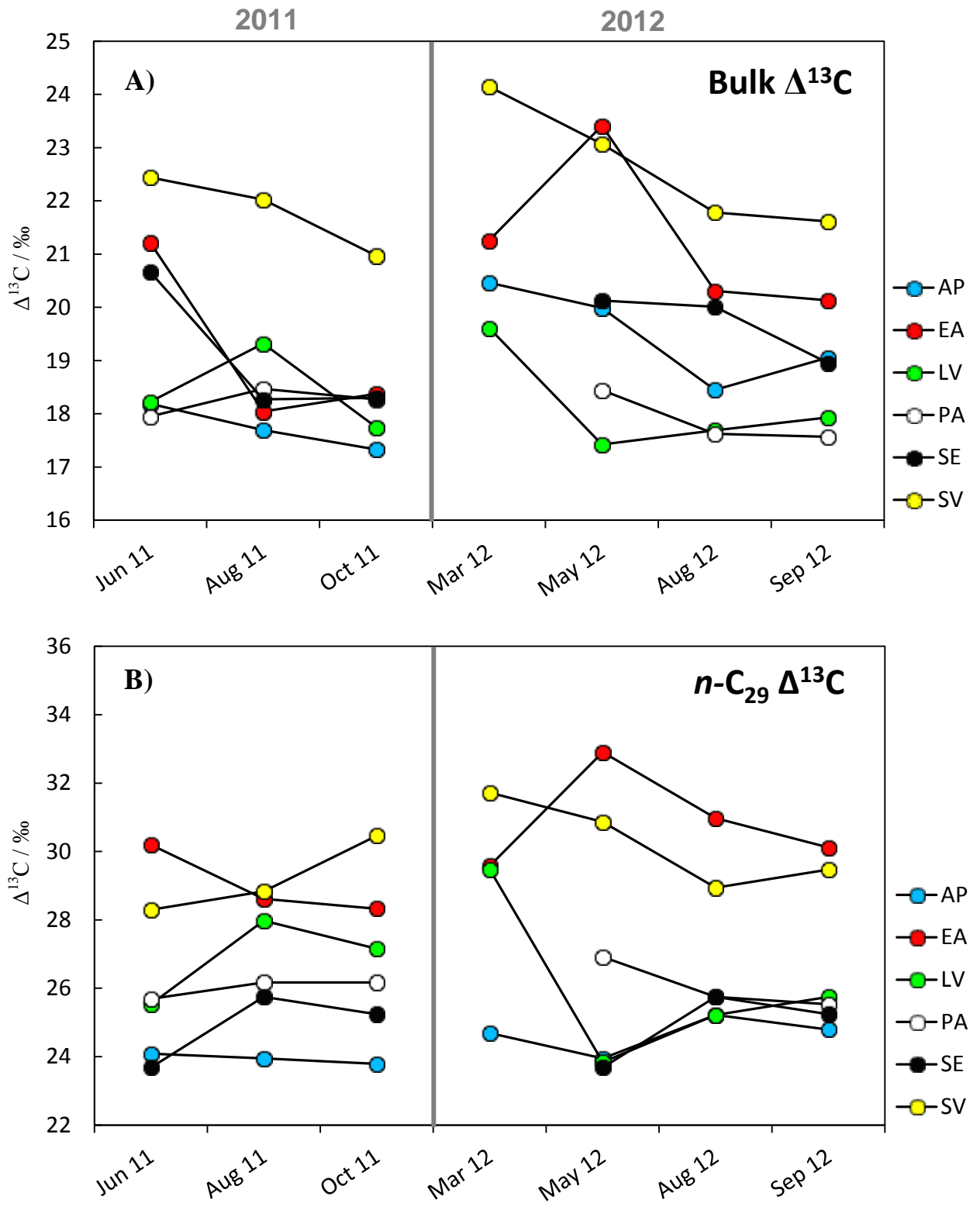


Figure 5.11: Seasonal trends in carbon isotope discrimination values calculated A) from bulk plant leaf $\delta^{13}\text{C}$ values, and B) from $n\text{-C}_{29} \delta^{13}\text{C}$ values. The black line separates data from the 2011 and 2012 growing seasons.

$\Delta^{13}\text{C}$ trends based on $n\text{-C}_{29}$ carbon isotope data, however, showed that the seasonal shifts differ among the species (Fig. 5.11B). *Elytrigia atherica*, for example had higher $\Delta^{13}\text{C}$ values than *Suaeda vera* in June – August 2011 and May – September 2012, in contrast to the data generated using the bulk isotope values. In addition, the compound-specific $\Delta^{13}\text{C}$ data for *Suaeda vera* showed a steady increase during the 2011 sampling period, with the highest value occurring in March 2012. *Suaeda vera* values then recorded a steady decline until August 2012, with a slight rise again in September 2012. In contrast, the bulk discrimination data show a sharp rise between April and June 2011, with a steady decline until October 2011. Similar discrepancies can be seen when comparing trends for the evergreen succulent *Atriplex portulacoides*. Here, $n\text{-C}_{29}$ -calculated discrimination values recorded limited variability across 2011 and 2012, with maximum values observed in August 2012. A 3‰ decline between April 2011 and October 2011 was observed, however, when bulk discrimination data were examined, with a sharp 3‰ increase occurring again in March 2012. Bulk discrimination values for *Atriplex* then declined until August 2012, where the lowest $\Delta^{13}\text{C}$ value for this species observed in 2012 was recorded. The annual succulent *Salicornia europaea* also displayed greater variability in the $\Delta^{13}\text{C}$ bulk-calculated values compared with the $\Delta^{13}\text{C}$ compound-specific-calculated values (Fig. 5.11).

5.6.6 Percentage carbon composition of bulk leaf tissue

The percentage carbon composition of bulk leaf tissue from the C_3 species at Stiffkey ranged from $21.59 \pm 0.01\%$ (*Salicornia europaea*, May 2012) to $45.12 \pm 0.32\%$ (*Phragmites australis*, August 2011). *Phragmites australis* and *Elytrigia atherica* typically had the highest carbon content of all C_3 plants sampled in 2011 and 2012 (Table 5.5; full details of all sample replicates can be found in Appendix 4). In contrast, the lowest %C content recorded during the 2011 and 2012 growth seasons was consistently found in the annual succulent *Salicornia europaea* (Table 5.5). %C in the leaves of the C_4 grass *Spartina anglica* across 2011 and 2012 ranged from $35.79 \pm 1.04\%$ to $41.34 \pm 0.32\%$ (Table 5.5). The amount of carbon varied with plant life form across the 2011 and 2012 growth seasons, with grasses/reeds (C_3 and C_4 monocots) generally containing the highest amounts of carbon, and other dicots and woody shrubs containing lower amounts (Fig. 5.12). Fig. 5.12 also shows that the greatest variability in carbon content across the 2011 and 2012 sampling periods is found in the perennials and annuals (*Limonium vulgare* and *Salicornia europaea*).

Similar differences were also observed when plant species were grouped into those that produced carbohydrates preferentially as compatible solutes for osmoregulation (grasses and reeds), versus those that produced nitrogenous compounds such as amino acids (woody shrubs, perennials) (Fig. 5.13; Briens and Lahrer, 1982).

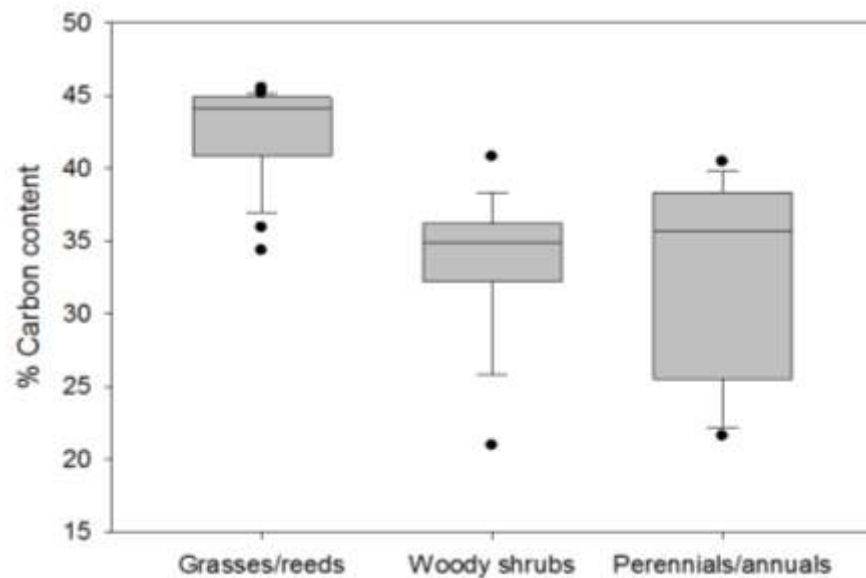


Figure 5.12: Carbon content of species sampled at Stiffkey, grouped by plant life form. "Grasses/reeds" includes *Spartina anglica*, *Elytrigia atherica*, *Phragmites australis*; "Woody shrubs" includes *Suaeda vera* and *Atriplex portulacoides*; "Perennials/annuals" includes *Limonium vulgare* and *Salicornia europaea*.

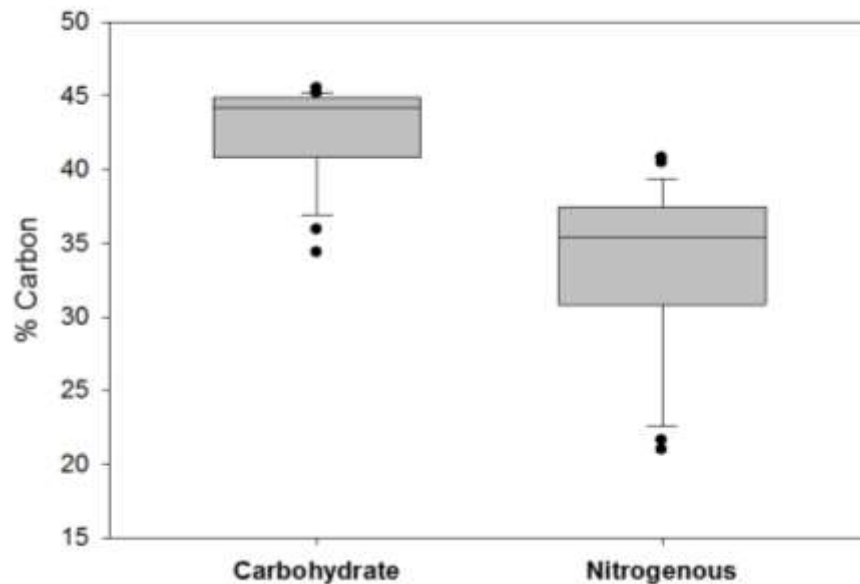


Figure 5.13: Carbon content of plant species sampled at Stiffkey grouped by their choice of compatible solute to maintain osmotic potential. "Carbohydrate" group includes *Spartina anglica*, *Elytrigia atherica*, *Phragmites australis*; "Nitrogenous" group includes *Atriplex portulacoides*, *Suaeda vera*, *Limonium vulgare* and *Salicornia europaea* (classification based on Briens and Lahrer, 1982)

The percent carbon composition of the C₃ grasses and reeds had a positive relationship with their bulk carbon isotope composition, with a correlation coefficient of 0.6, and a *P* value of 0.06 (*n* = 14, Rank Spearman correlation, Minitab v.16) (Fig. 5.14). A significant relationship between WA alkane δ¹³C and %C was also observed for these C₃ monocots (*r* = 0.6, *P* = <0.05, *n* = 14).

For the dicots and succulents, the relationship appeared to vary among plants with different growth strategies. The perennial and annuals (*Limonium vulgare* and *Salicornia europaea*) had a positive relationship between the percentage carbon content in their leaves and their bulk δ¹³C ratios (*r* = 0.7, *P* = <0.05, *n* = 11, Rank Spearman correlation, Minitab v.16) (Fig. 5.15), but not their WA alkane ¹³C/¹²C. In contrast, a negative relationship (*r* = -0.6, *P* = <0.05, *n* = 16, Rank Spearman correlation, Minitab v.16) is observed between the carbon content of the leaves from the woody evergreen shrubs *Atriplex portulacoides* and *Suaeda vera* and their bulk carbon isotope composition (Fig. 5.16), although again here no significant relationship exists between %C and the *n*-alkane data. Uniquely for this dataset, % C and WA alkane ¹³C/¹²C are correlated in *Spartina anglica* (*r* = 0.8, *P* < 0.05, *n* = 7, Rank Spearman correlation, Minitab v.16), but this time no relationship exists between %C and bulk tissue ¹³C/¹²C.

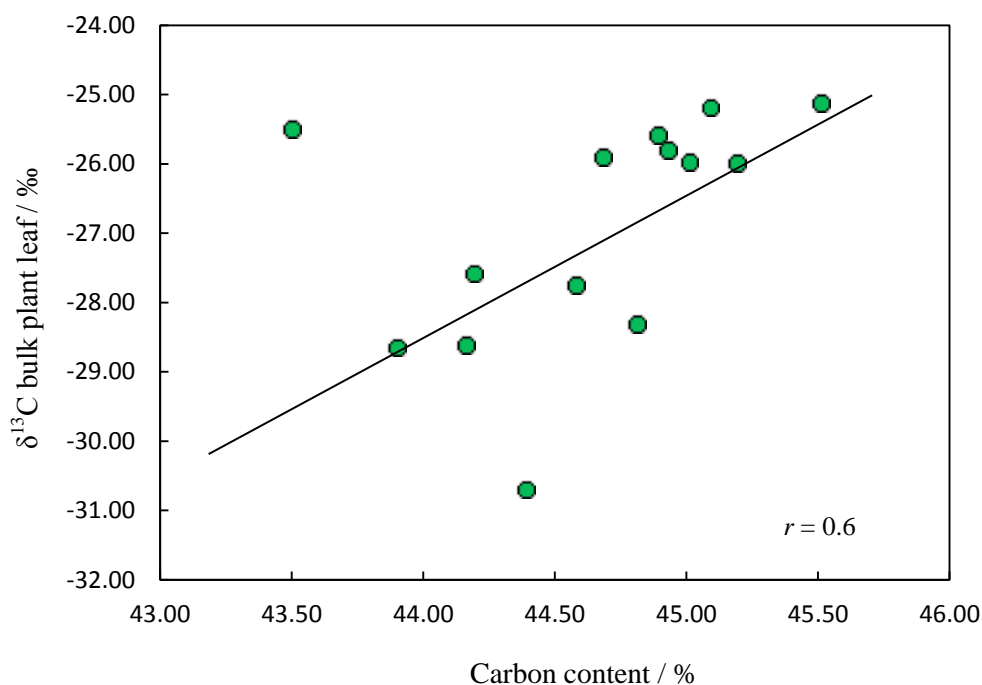


Figure 5.14: Correlation between carbon content and bulk plant tissue carbon isotope composition for *Elytriga atherica* and *Phragmites australis* (C₃ monocots)

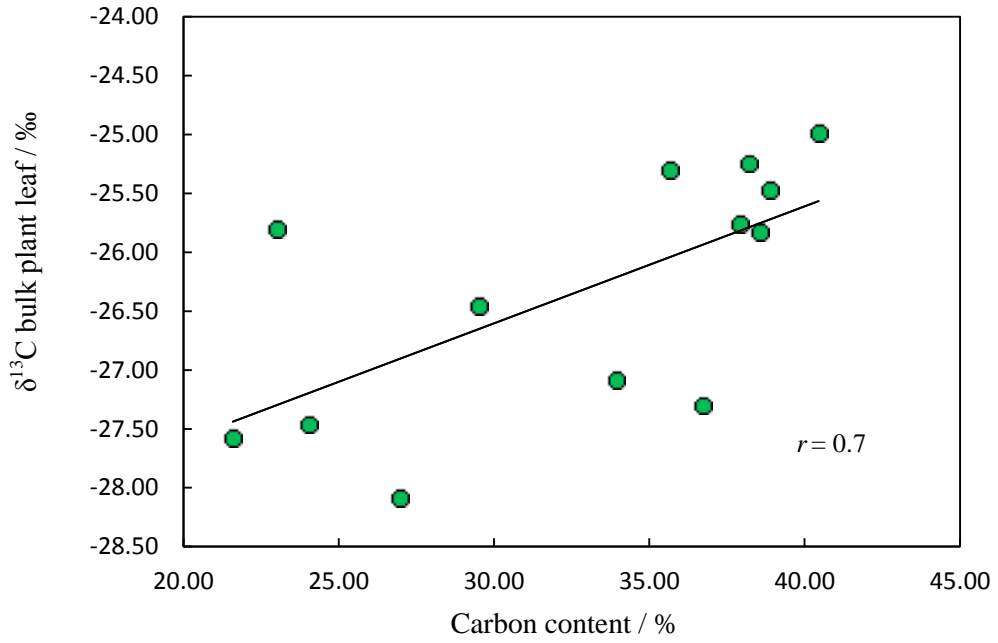


Figure 5.15: Correlation between carbon content and and bulk plant tissue carbon isotope composition for *Limonium vulgare* and *Salicornia europaea* (C_3 Perennials/Annuals)

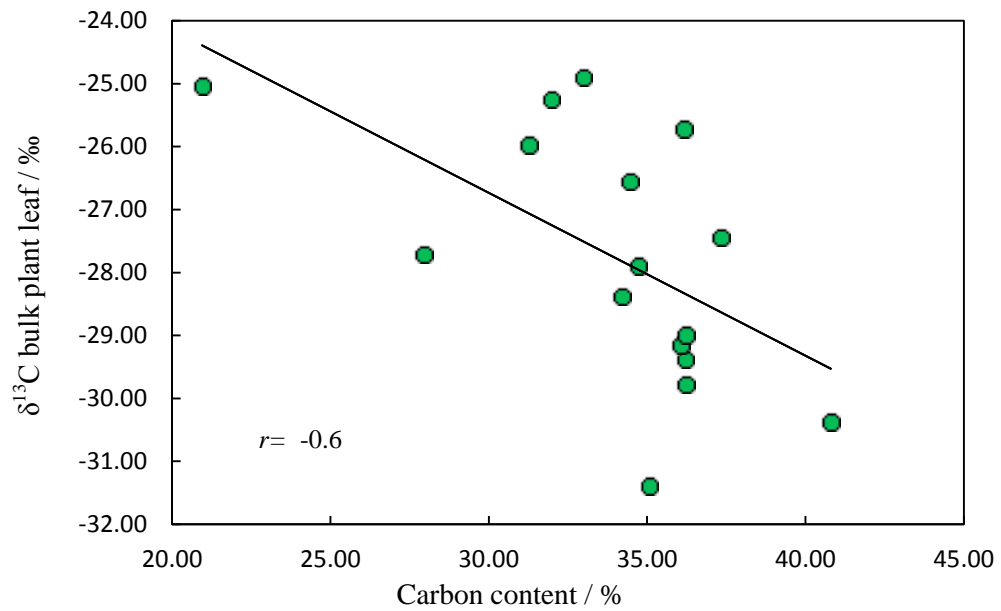


Figure 5.16: Correlation between carbon content and and bulk plant tissue carbon isotope composition for *Atriplex portulacoides* and *Suaeda vera* (C_3 Woody shrubs)

5.6.7 Percentage nitrogen composition of bulk leaf tissue

The % N contained within the Stiffkey plants varied from ~0.5% to 4% depending upon the particular species and the sampling period (Table 5.5). Among the grasses, *Elytrigia atherica* (C₃) consistently had the lowest nitrogen content (ranging from 0.51 ± 0.03 to $1.84 \pm 0.07\%$), while *Phragmites australis* (C₃) and *Spartina anglica* (C₄) both had levels generally ranging from 1 to 3% (Figure 5.19). Among the dicots and succulents, *Limonium vulgare* generally reported a higher percentage nitrogen composition (ranging from $0.98 - 3.9 \pm 0.03\%$) than the stem succulent *Salicornia europaea* which contained 0.51 ± 0.03 to $2.10 \pm 0.17\%$ nitrogen (Table 5.5; Fig. 5.17).

For *Limonium vulgare*, nitrogen content was highest in late spring (e.g. May 2012) and lowest in March 2012 when sampling of very young leaves was undertaken. *Salicornia europaea* in contrast had the highest nitrogen content in June and October 2011, and reported much lower values during the 2012 sampling period (Figure 5.17). The two evergreen species, *Atriplex portulacoides* and *Suaeda vera*, show very different seasonal trends in nitrogen composition. *Atriplex portulacoides* generally has higher percentage nitrogen content at the beginning of the growth season, with lower values during high summer (August 2011; August 2012), while the leaf succulent *Suaeda vera* reported the highest percentage nitrogen levels in June 2011 and May 2012 (Fig. 5.17). Full details of all sample replicate measurements for %N can be found in Appendix 4

For the C₃ monocots, %N and WA *n*-alkane $\delta^{13}\text{C}$ had a positive correlation ($r = 0.7$, $P < 0.05$, $n = 13$, Rank Spearman correlation, Minitab v.16) although %N and bulk $\delta^{13}\text{C}$ did not. In contrast the C₄ monocot *Spartina anglica* had a strong negative correlation ($r = -0.78$, $P < 0.05$, $n = 7$, Pearson's product moment correlation, Minitab v.16) between leaf %N and WA *n*-alkane $\delta^{13}\text{C}$. For the dicots and succulents, a positive correlation (significant at a 90% confidence interval) existed between %N and WA *n*-alkane $\delta^{13}\text{C}$ in *Limonium vulgare* ($r = 0.7$, $P = 0.06$, $n = 7$, Pearson's product moment correlation) and *Salicornia europaea* ($r = 0.7$, $P = 0.07$, $n = 6$, Pearson's product moment correlation). However, *Atriplex portulacoides* and *Suaeda vera* displayed a negative relationship between leaf %N and $\delta^{13}\text{C}$ at both bulk and WA alkane level ($r = -0.6$, $P < 0.05$, $n = 7$ for each species, Rank Spearman correlation, Minitab v.16).

Table 5.5: Carbon and nitrogen percentage composition of plant biomass; C:N ratio and $\delta^{15}\text{N}$ ratios of bulk leaf tissue

Month	Plant species	%N	A.D $\%N$	%C	A.D $\%C$	C:N	$\delta^{15}\text{N}$ (‰)	$AD_{\delta^{15}\text{N}}$
Jun-11	<i>Atriplex portulacoides</i>	2.05	0.01	36.16	0.00	17.6	6.66	0.02
	<i>Elytrigia atherica</i>	1.23	0.00	44.16	0.00	35.8	4.97	0.11
	<i>Limonium vulgare</i>	2.51	0.00	37.92	0.08	15.1	4.84	0.00
	<i>Phragmites australis</i>	2.42	0.08	43.50	0.98	18.0	6.52	0.15
	<i>Salicornia Europaea</i>	2.00	0.00	26.96	0.04	13.5	8.83	0.08
	<i>Spartina anglica</i>	1.95	0.00	39.40	0.02	20.2	7.43	0.06
	<i>Suaeda vera</i>	3.08	0.00	36.21	0.08	11.8	7.12	0.08
Aug-11	<i>Atriplex portulacoides</i>	1.27	0.03	31.97	0.13	25.1	8.06	0.28
	<i>Elytrigia atherica</i>	0.72	0.02	44.89	0.03	62.4	3.01	0.04
	<i>Limonium vulgare</i>	2.24	0.01	37.19	0.13	16.6	5.39	0.07
	<i>Phragmites australis</i>	1.87	0.03	45.19	0.32	24.1	7.69	0.09
	<i>Salicornia Europaea</i>	1.14	0.01	23.00	0.94	20.1	10.07	0.04
	<i>Spartina anglica</i>	2.08	0.00	41.34	0.02	19.9	8.43	0.01
	<i>Suaeda vera</i>	1.23	0.06	36.20	0.36	29.4	9.37	0.26
Oct-11	<i>Atriplex portulacoides</i>	1.95	0.04	32.92	0.13	16.9	9.04	0.63
	<i>Elytrigia atherica</i>	1.84	0.07	44.79	0.22	24.3	3.45	0.69
	<i>Limonium vulgare</i>	1.90	0.11	35.71	0.55	18.8	3.28	0.17
	<i>Phragmites australis</i>	2.46	0.06	44.93	0.18	18.3	5.44	0.65
	<i>Salicornia Europaea</i>	2.10	0.17	28.55	0.64	13.6	7.73	0.26
	<i>Spartina anglica</i>	2.59	0.21	40.24	0.31	15.6	7.50	0.06
	<i>Suaeda vera</i>	2.59	0.00	34.63	0.26	13.4	10.55	1.44
Mar-12	<i>Atriplex portulacoides</i>	1.61	0.05	34.72	0.29	21.6	9.49	0.47
	<i>Elytrigia atherica</i>	1.28	0.04	43.90	0.65	34.2	3.79	0.04
	<i>Limonium vulgare</i>	0.98	0.00	33.93	0.04	34.6	3.25	0.53
	<i>Spartina anglica</i>	1.03	0.03	35.79	1.04	34.7	6.59	0.49
	<i>Suaeda vera</i>	3.33	0.04	35.07	0.25	10.5	9.46	0.10
May-12	<i>Atriplex portulacoides</i>	1.47	0.01	37.33	0.03	25.4	9.13	0.07
	<i>Elytrigia atherica</i>	1.37	0.00	44.39	0.18	32.3	2.69	0.04
	<i>Limonium vulgare</i>	3.90	0.03	40.45	0.26	10.4	4.63	0.15
	<i>Phragmites australis</i>	3.04	0.04	45.01	0.04	14.8	5.05	0.03
	<i>Salicornia Europaea</i>	1.22	0.01	21.59	0.01	17.7	8.91	0.02
	<i>Spartina anglica</i>	2.92	0.01	39.34	0.05	13.5	7.35	0.02
	<i>Suaeda vera</i>	3.73	0.01	40.80	0.01	11.0	7.96	0.23
Aug-12	<i>Atriplex portulacoides</i>	1.06	0.03	31.30	0.04	29.5	7.30	0.01
	<i>Elytrigia atherica</i>	0.51	0.03	44.69	0.29	88.4	3.23	0.11
	<i>Limonium vulgare</i>	1.75	0.02	38.19	0.06	21.8	4.72	0.00
	<i>Phragmites australis</i>	2.28	0.03	45.07	0.08	19.7	6.44	0.19
	<i>Salicornia Europaea</i>	0.51	0.03	24.05	0.60	47.5	6.92	0.20
	<i>Spartina anglica</i>	1.24	0.00	41.05	0.37	33.2	8.62	0.28
	<i>Suaeda vera</i>	2.41	0.04	36.07	0.14	15.0	6.00	0.09
Sep-12	<i>Atriplex portulacoides</i>	1.02	0.06	34.46	0.17	33.8	9.43	0.04
	<i>Elytrigia atherica</i>	0.61	0.01	44.19	0.02	72.0	2.47	0.15
	<i>Limonium vulgare</i>	3.03	0.01	40.61	0.01	13.4	6.55	0.10
	<i>Phragmites australis</i>	2.21	0.01	45.51	0.04	20.6	7.04	0.02
	<i>Salicornia Europaea</i>	1.05	0.03	29.51	0.04	28.1	6.35	0.01
	<i>Spartina anglica</i>	1.36	0.02	41.04	0.00	30.3	8.96	0.22
	<i>Suaeda vera</i>	3.03	0.04	36.15	0.37	11.9	9.98	0.23

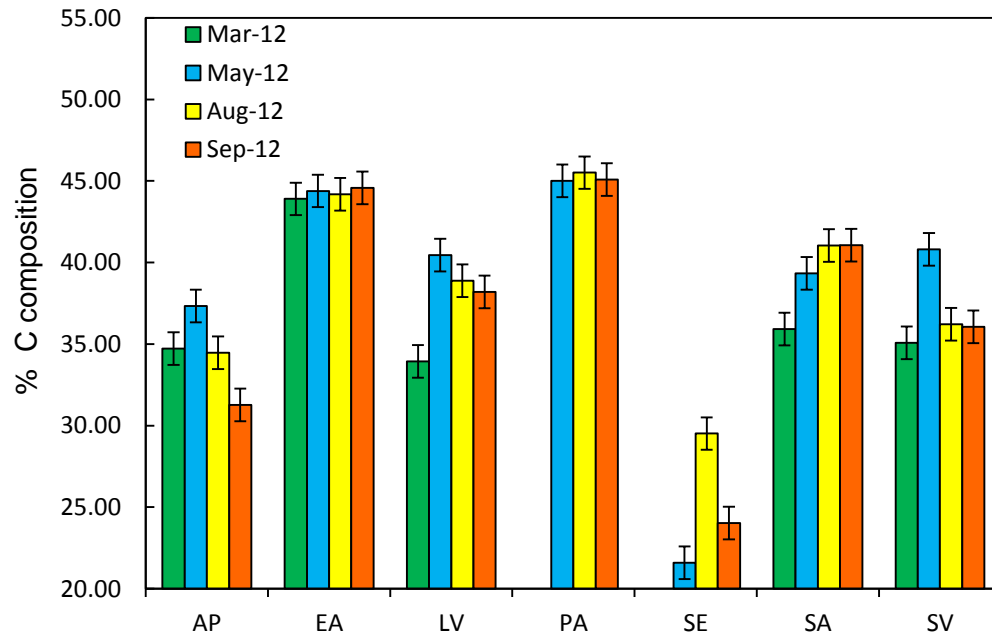
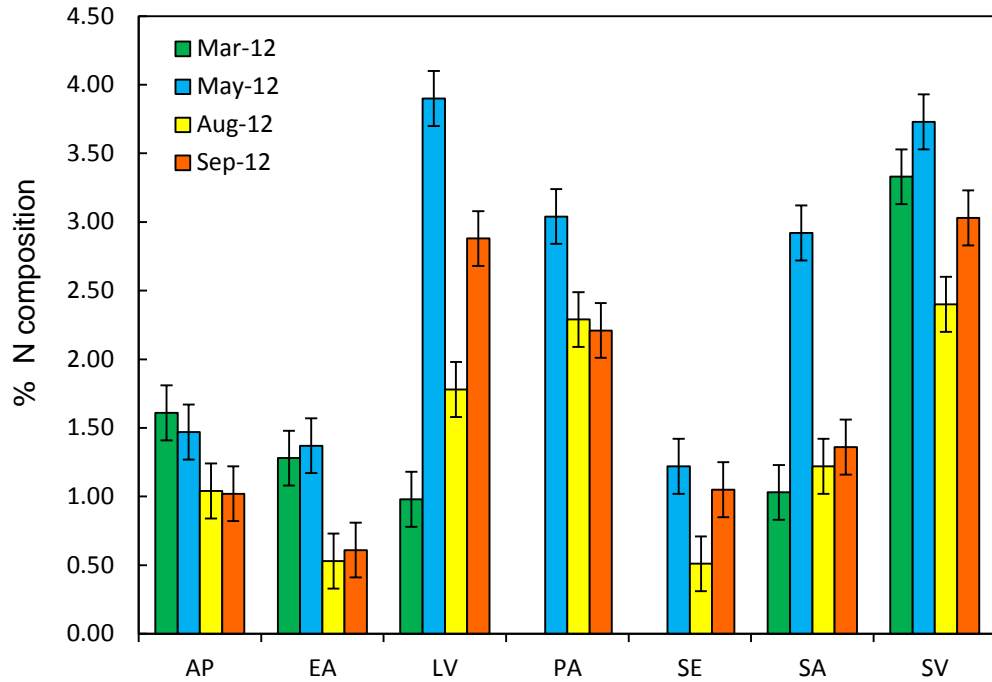


Figure 5.17: Percentage nitrogen composition (A) and percentage carbon composition (B) of plant biomass; Abbreviations: AP, *Atriplex portulacoides*; EA, *Elytrigia atherica*; LV, *Limonium vulgare*; PA, *Phragmites australis*; SE, *Salicornia europaea*; SA, *Spartina anglica*; SV, *Suaeda vera*. Error bars show absolute difference between sample replicates, which did not exceed 0.2% for %N measurements, and 1% for %C measurements.

5.6.8 Bulk nitrogen isotopes

The nitrogen isotope composition of bulk leaf tissue varied between the C₃ and C₄ monocots (*Elytrigia atherica*, *Phragmites australis*, *Spartina Anglica*) and dicots/succulents (*Limonium vulgare*, *Atriplex portulacoides*, *Salicornia europaea*, *Suaeda vera*), with dicots and succulents generally having ¹⁵N-enriched biomass relative to the monocots (Fig. 5.18) (Table 5.5) (all data for sample replicates is given in Appendix 4).

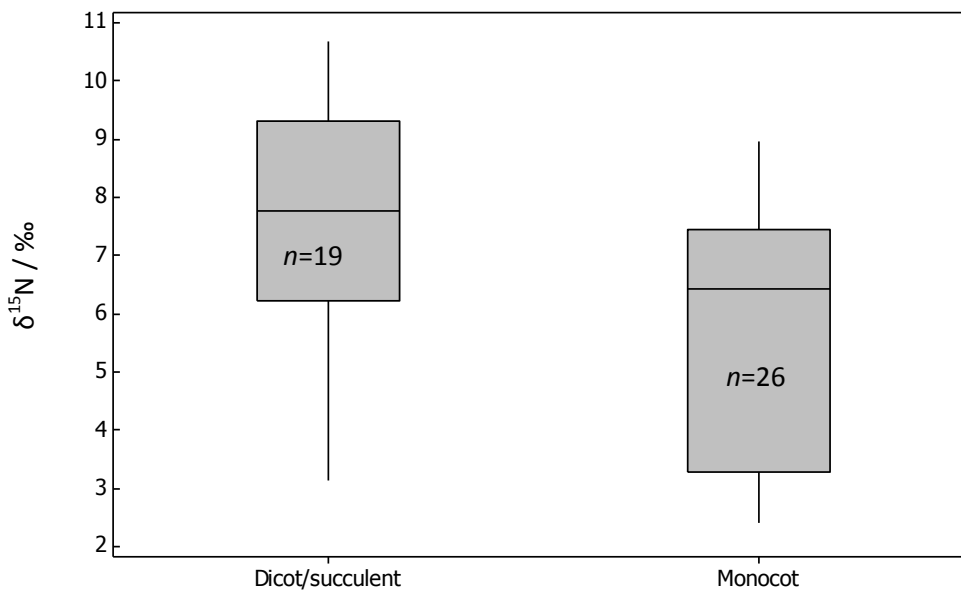


Figure 5.18: Nitrogen isotope composition of bulk leaf tissue from samples collected during 2011 and 2012. “Dicots/succulents” include *Limonium vulgare*, *Atriplex portulacoides*, *Suaeda vera* and *Salicornia europaea*. “Monocots” include *Elytrigia atherica*, *Phragmites australis* and *Spartina anglica* (C₄).

Bulk leaf tissue from *Atriplex portulacoides*, *Suaeda vera* and *Salicornia europaea* were generally the most ¹⁵N-enriched (Table 5.5; Fig. 5.19). In contrast, *Elytrigia atherica* and *Limonium vulgare* had the most ¹⁵N-depleted leaf tissue (Table 5.5; Fig. 5.19). Among the monocots, the C₄ grass *Spartina anglica* had the most ¹⁵N-enriched leaf tissue, and *Elytrigia atherica* had the most ¹⁵N-depleted (Fig. 5.19). Species also varied in the magnitude of seasonal shifts in leaf δ¹⁵N values. The greatest seasonal variability in a single species was found in *Suaeda vera* (4‰ between June and October 2011 and August and September 2012). In contrast the most consistent leaf δ¹⁵N values were observed in the C₃ monocot *Elytrigia atherica*

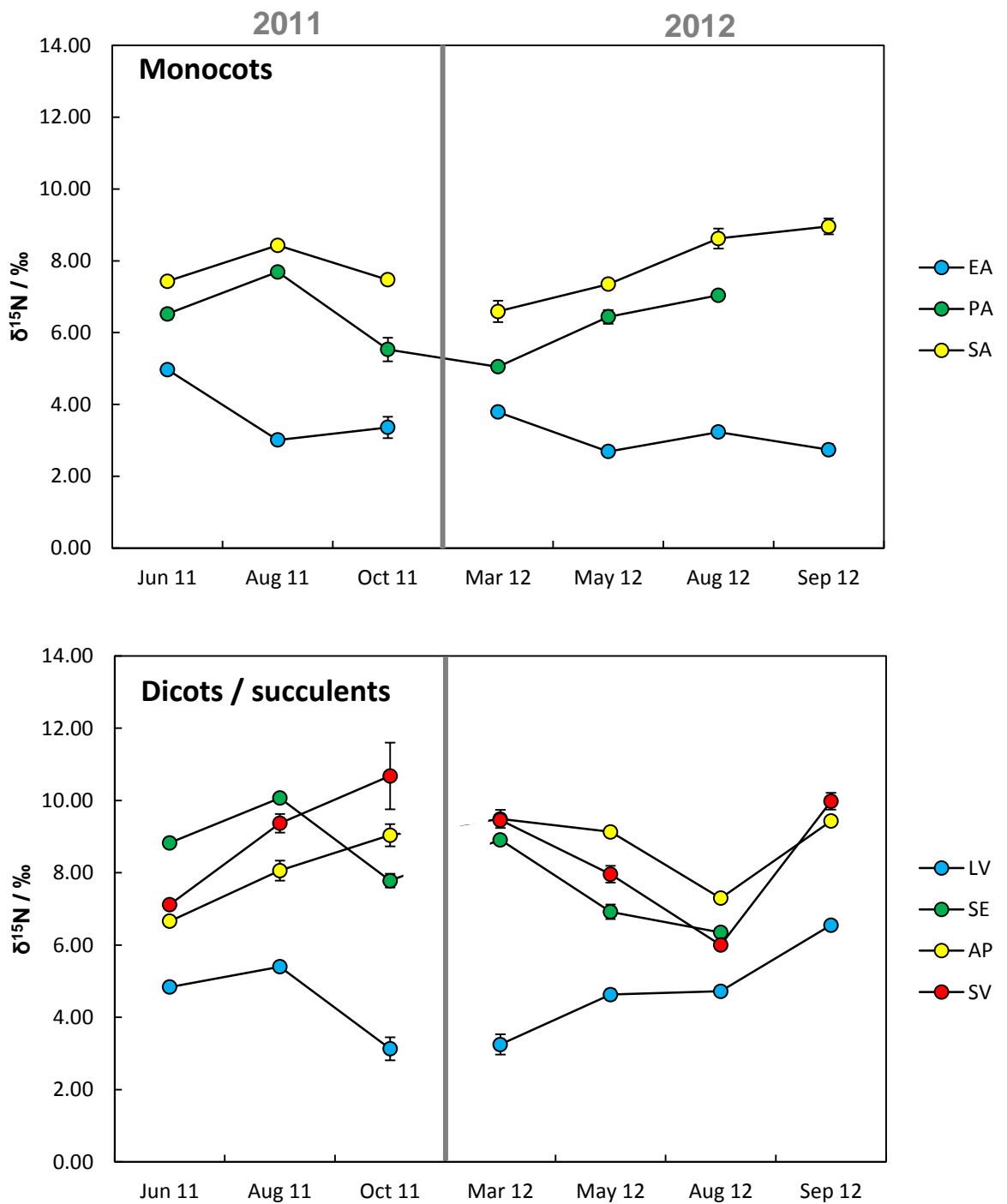


Figure 5.19: Seasonal shifts in nitrogen isotope composition of bulk plant tissue across 2011 and 2012. A) C_3 and C_4 monocots, EA = *Elytrigia atherica*, PA = *Phragmites australis*, SA = *Spartina anglica*; B) Dicots and succulents, LV = *Limonium vulgare*, SE = *Salicornia europaea*, AP = *Atriplex portulacoides*, SV = *Suaeda vera*. Error bars show absolute differences between sample duplicates. The black line distinguishes samples collected in 2011 and 2012.

and the C₄ monocot *Spartina anglica* (Table 5.6; Fig. 5.19) with shifts no greater than 2‰. With the exception of the evergreen *Atriplex portulacoides* and the succulents *Salicornia europaea* and *Suaeda vera* (which all show an increasing negative trend between March 2012 and August 2012), seasonal traits in leaf δ¹⁵N appear to be mainly species-specific, with no uniform trends across the different plant life forms (Fig. 5.19). Comparison of percentage N content with leaf δ¹⁵N showed no significant relationship.

Statistical comparison between the nitrogen isotope composition of bulk leaf tissue and the WA alkane carbon isotope composition show that there is a strong positive correlation ($r = 0.77$, $P < 0.05$, Pearson's product moment correlation, $n = 13$, Minitab v.16) for the C₃ monocots *Elytrigia atherica* and *Phragmites australis*. A weaker, but still significant, correlation ($r = 0.58$, $P < 0.05$, Rank Spearman correlation, $n = 13$, Minitab v.16) also existed between bulk leaf δ¹³C and leaf δ¹⁵N for the C₃ monocots. No correlation existed between leaf δ¹⁵N and WA alkane δ¹³C, or bulk leaf δ¹³C, for the C₄ monocot *Spartina anglica*. For the dicots and succulents, a negative trend is generally observed between leaf δ¹⁵N and WA alkane δ¹³C as well as between leaf δ¹⁵N and bulk tissue δ¹³C although this is not statistically significant for any of the species sampled.

5.6.9 The relationship between seasonal shifts in abundance and concentration of *n*-alkanes and their carbon isotope composition

Seasonal shifts in the δ¹³C of the most prevalent *n*-alkanes in all species studied, *n*-C₂₇ and *n*-C₂₉, were compared to changes in their concentration and percentage distribution presented previously in Chapter 4. No statistically significant relationship was found when seasonal shifts in *n*-alkane concentrations of *n*-C₂₉ and *n*-C₂₇ were compared with: a) their respective carbon isotope composition; b) the influence of [*n*-C₂₉] on δ¹³C_{*n*-C₂₇}; and c) the influence of [*n*-C₂₇] on δ¹³C_{*n*-C₂₉} (in all cases, $P > 0.05$, $n = 39$, Rank Spearman correlation, Minitab v.16). When seasonal shifts in the percentage abundance of key alkane chain lengths were compared to seasonal changes in δ¹³C values, the percent abundance of *n*-C₂₇ had a weak positive correlation with δ¹³C values of *n*-C₂₇ and *n*-C₂₉ ($r = 0.3$, $P < 0.05$, $n = 39$).

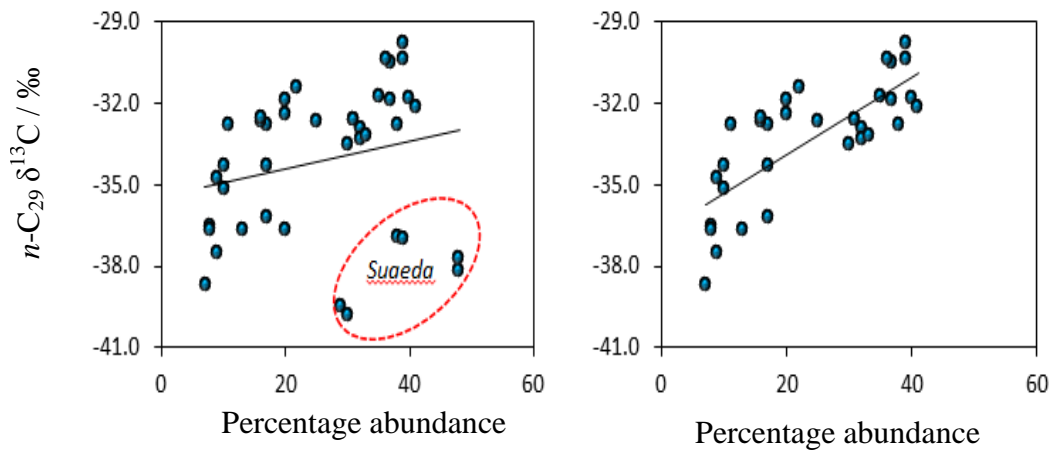


Figure 5.20: Correlation between the percentage abundance of $n\text{-C}_{27}$ and $n\text{-C}_{29}$ $\delta^{13}\text{C}$ values. (left) including data from *Suaeda vera*; (right) excluding data from *Suaeda vera*

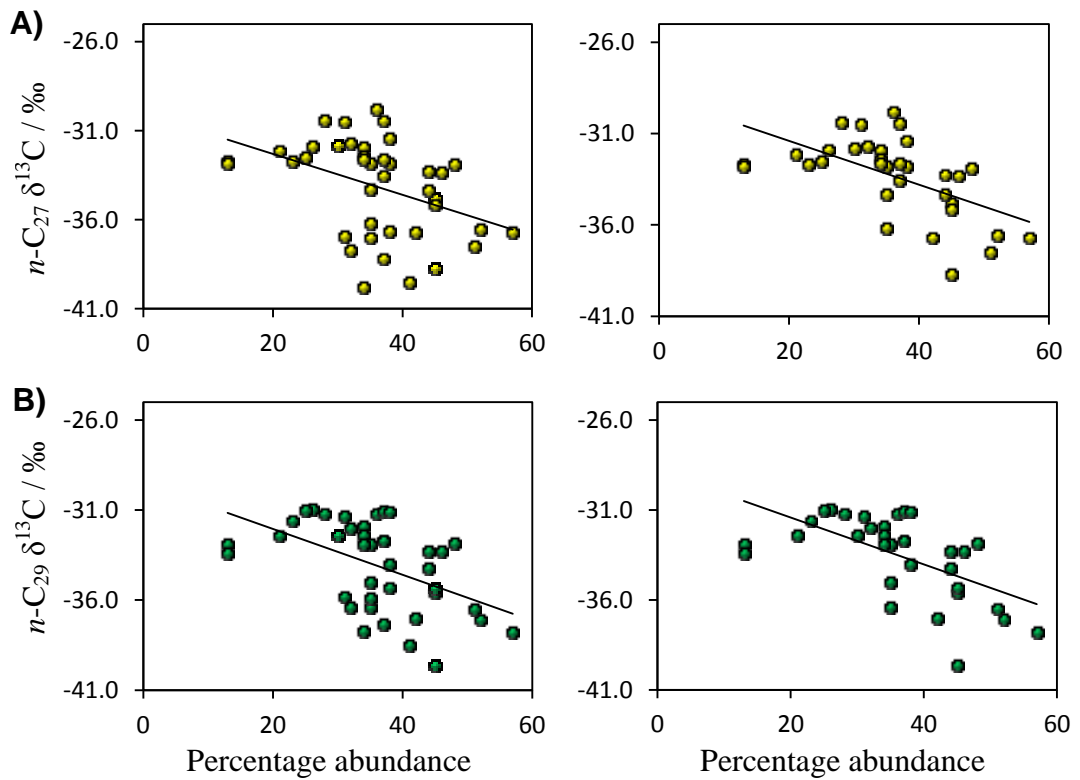


Figure 5.21: Correlation between: A) the percentage abundance of $n\text{-C}_{29}$ and $n\text{-C}_{27}$ $\delta^{13}\text{C}$ values including *Suaeda vera* (left), and excluding *Suaeda vera* (right); B) the percentage abundance of $n\text{-C}_{29}$ and $n\text{-C}_{29}$ $\delta^{13}\text{C}$ values including *Suaeda vera* (left), and excluding *Suaeda vera* (right)

Examination of the bivariate data plot for $n\text{-C}_{27}$ abundance and $\delta^{13}\text{C}$ $n\text{-C}_{27}$ and $n\text{-C}_{29}$ (Fig.5.20) suggested that data from the succulent *Suaeda vera* may be responsible for this relatively weak correlation. Removal of *Suaeda vera* data from consideration resulted in a much stronger correlation with a coefficient of 0.8. The percentage abundance of $n\text{-C}_{25}$ had a stronger positive correlation with $n\text{-C}_{27}$ and $n\text{-C}_{29}$ $\delta^{13}\text{C}$ values (in both cases, $r = 0.5$, $P < 0.05$, $n = 39$). Removal of *Suaeda vera* made no difference to this correlation. In a striking contrast, a strong negative correlation was observed between the percentage abundance of $n\text{-C}_{29}$ and the carbon isotope composition of $n\text{-C}_{27}$ ($r = -0.5$, $P < 0.05$, $n = 39$) and $n\text{-C}_{29}$ ($r = -0.5$, $P < 0.05$, $n = 39$) (Fig. 5.21). Removal of *Suaeda vera* resulted in an increase in the strength of this correlation to -0.7 in respect of $n\text{-C}_{27}$ carbon isotopes, and -0.6 in respect of $n\text{-C}_{29}$ carbon isotopes.

5.6.10 Spatial variation in bulk and n -alkane $\delta^{13}\text{C}$ across marsh sub-environments

The carbon isotope composition of bulk leaf tissue and the $n\text{-C}_{29}$ alkane from species growing at multiple sub-habitats across Stiffkey sampled in October 2011 are shown in Table 5.6 and Figure 5.22. The carbon isotope composition of bulk leaf tissue for the two evergreen shrubs, *Atriplex portulacoides* and *Suaeda vera*, was $\sim 1\text{‰}$ more positive in the UM sub-environment than the R and LM sample sites (Fig. 5.22 A), with the most negative values recorded in the R site. In the two perennial species *Limonium vulgare* and *Salicornia europaea*, (which only grow at the LM and UM sites), this variation was small enough to be within analytical error (i.e. $\leq 0.3\text{‰}$) (Fig. 5.22 A).

In contrast, the variation in the carbon isotope composition of the n -alkanes (Fig. 5.22 B) is far greater in an individual species across the marsh sub-environments, although individual plants growing at the UM still consistently had more positive $\delta^{13}\text{C}$ values than those found in the LM and R sites (Fig. 5.22 B). For *Atriplex portulacoides* n -alkane carbon isotope composition varied $\sim 2\text{‰}$ between the UM and LM sites, while for *Suaeda vera* there was a positive shift of 3‰ between individuals growing at the R and UM sites (i.e. greater than the difference between sample replicates). For *Limonium vulgare* and *Salicornia europaea*, the magnitude of spatial variability remained lower at the compound-specific level than that observed for the woody evergreens. n -Alkane shifts were still in the order of 1‰ for these two species - higher than observed in bulk foliar tissue (Fig. 5.22 B), but within the difference observed between sample replicates.

Table 5.6: Bulk and *n*-alkane carbon isotope composition from plants growing in multiple sub-habitats at Stiffkey (October 2011)

Sampling site	Species	<i>n</i> -C ₂₉	AD _{<i>n</i>-C₂₉}	Bulk	AD _{bulk}
LM	<i>Atriplex portulacoides</i>	-31.9	0.6	-25.3	0.9
R	<i>Atriplex portulacoides</i>	-31.1	0.1	-24.9	0.1
UM	<i>Atriplex portulacoides</i>	-30.6	0.6	-24.1	0.1
LM	<i>Salicornia Europaea</i>	-32.4	0.9	-25.8	0.6
UM	<i>Salicornia Europaea</i>	-31.6	0.0	-26.0	0.7
LM	<i>Limonium vulgare</i>	-34.1	0.6	-25.5	0.6
UM	<i>Limonium vulgare</i>	-34.2	0.3	-25.3	0.1
R	<i>Suaeda vera</i>	-37.3	0.1	-28.4	0.2
UM	<i>Suaeda vera</i>	-35.1	0.2	-27.1	0.3

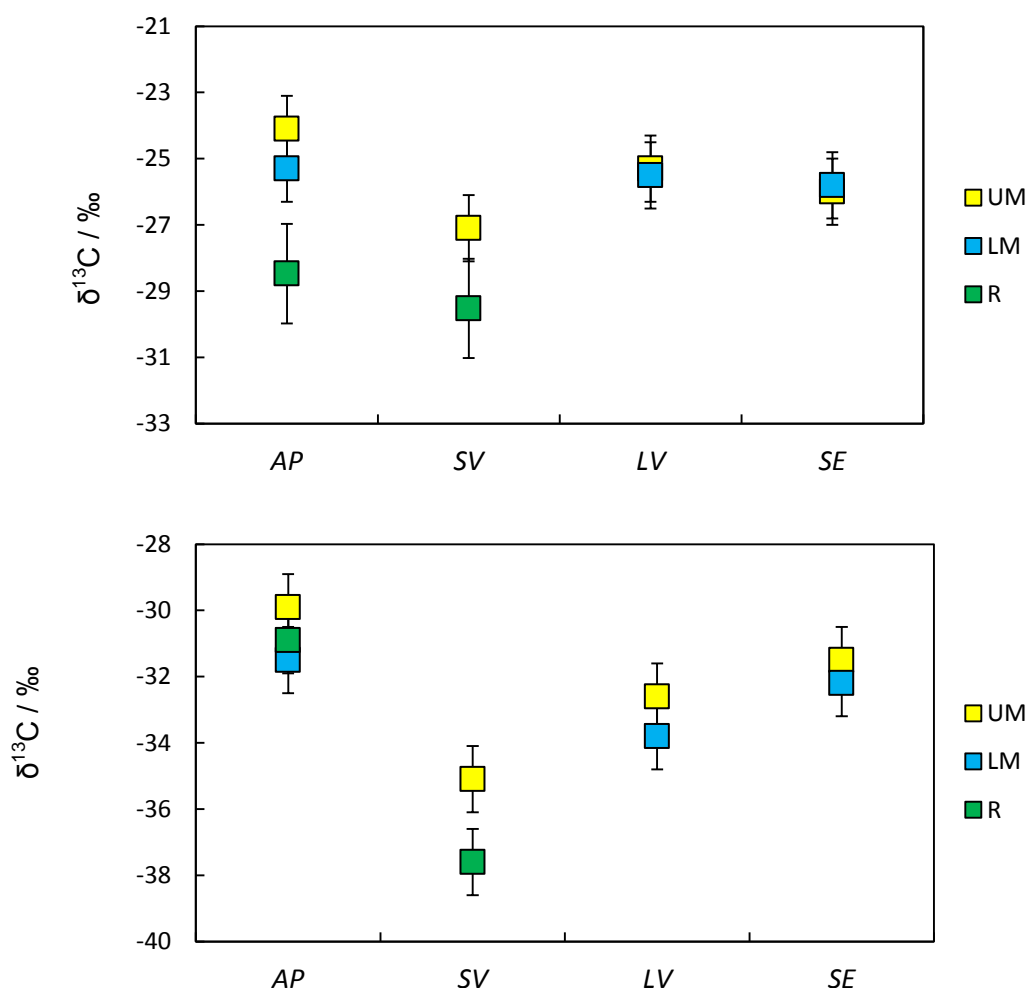


Figure 5.22: Bulk (a) and *n*-alkane (b) carbon isotope composition from species growing at multiple marsh sampling sites. AP = *Atriplex portulacoides*, SV = *Suaeda vera*, LV = *Limonium vulgare*, SE = *Salicornia europaea*. UM = Upper marsh, LM = Lower marsh, R = Ridge. Error bars show absolute difference between sample replicates of leaves from the same species which varied by no more than 1‰ at the bulk level and *n*-alkane level

5.7. DISCUSSION

5.7.1 Interspecies variation in bulk and *n*-alkane $\delta^{13}\text{C}$

Interspecies variation in bulk tissue from the saltmarsh plants sampled at Stiffkey across the entire study period show a total range of 6‰ among the C_3 species (-25.2 ± 0.03 to 31.4 ± 0.2 ‰; Table 5.3 and 5.4) and fall within the typical range for C_3 species predicted by Diefendorf *et al.* (2010). The C_4 *Spartina anglica* had bulk leaf $\delta^{13}\text{C}$ values ranging from -13.0 ± 0.01 ‰ to -14.3 ± 0.01 ‰, typical of C_4 plants (Collister *et al.*, 1994; Tipple and Pagani, 2007; Castenada and Schouten, 2011). For each individual sampling period, bulk carbon isotope ratios varied by no more than 4‰ (Tables 5.3 and 5.4), with the evergreen succulent *Suaeda vera* generally having the most ^{13}C -depleted composition (note care was taken to sample new leaves at each interval, to ensure that sampled material was representative of current environmental conditions, Ch. 4). The magnitude of variability in *n*-alkane $\delta^{13}\text{C}$ from the C_3 species at Stiffkey ranged from 5‰ to 9‰ depending upon sampling period, regardless of whether weighted average *n*-alkane, *n*- C_{27} or *n*- C_{29} $\delta^{13}\text{C}$ is being considered (Tables 5.3 and 5.4). This variability among plants growing at the same geographical location is commensurate with that previously reported for *n*-alkanes (Diefendorf *et al.*, 2011) and other compound classes such as fatty acids (11‰, Dungait *et al.*, 2008).

Previous studies have found that the $\delta^{13}\text{C}$ values of leaf wax lipids sampled from a prairie ecosystem can be quantitatively related to the carbon isotopic composition of total plant carbon (i.e. bulk plant material), with a consistent offset that appeared insensitive to environmental stresses that alter carbon isotope discrimination (Conte *et al.*, 2003). Conte *et al.* (2003) only considered plants sampled at one time interval, however. The seasonal data from Stiffkey suggest that the relationship between bulk and leaf wax $\delta^{13}\text{C}$ may not be so straightforward for these saltmarsh species. Here, seasonal variation in the offset (ϵ) between the bulk and *n*-alkane $\delta^{13}\text{C}$ ranges both: (a) among the different species sampled, and (b) throughout the course of the growing season (Fig. 5.9). This is not surprising given the interspecies range in the pattern of seasonal carbon isotope shifts at the bulk and molecular levels (Fig 5.7), particularly in the stem succulent *Salicornia europaea*. Data from the C_3 and C_4 monocot species have a far more consistent pattern in the offset between bulk and *n*-alkane $\delta^{13}\text{C}$, however (Fig. 5.9), suggesting that the

mechanisms controlling bulk and *n*-alkane $\delta^{13}\text{C}$ in monocots may be distinctive to those in the dicots and succulents.

Studies of bulk tissue carbon isotopes suggest that seasonal shifts in $^{13}\text{C}/^{12}\text{C}$ is strongly influenced by environmental parameters that change the ratio of C_i/C_a ratio, (Arens *et al.*, 2000; Fig. 5.5). Bulk plant tissue, however, is a composite signal, comprised of a range of different compounds, all of which potentially having a different carbon isotope composition (Hayes, 2001; Dungait *et al.*, 2008). The current lack of knowledge of the extent of variability in the $\delta^{13}\text{C}$ values of different compounds comprising the bulk tissue means that, at present, it is difficult to evaluate whether biochemical variation is also an important factor influencing bulk tissue isotopic composition (Dungait *et al.*, 2010). The bulk and *n*-alkane seasonal data from Stiffkey provide an ideal opportunity to evaluate whether they respond in the same way to environmental changes known to occur at the site over the course of a growing season (e.g. salinity, nutrient stress; Jeffries, 1977, discussed in detail in Chapter 2), and explore whether changes in the *n*-alkane signal can influence the bulk isotopic composition of these plant leaves.

5.7.2 Seasonal trends in plant bulk and *n*-alkane $\delta^{13}\text{C}$

The seasonal trends in Stiffkey plant $\delta^{13}\text{C}$ do not follow the same pattern for all species at the bulk and molecular level (Fig. 5.7). While the C_3 and C_4 monocot species (*Elytrigia atherica*, *Phragmites australis* and *Spartina anglica*) show relatively consistent trends across bulk and *n*-alkane $\delta^{13}\text{C}$ shifts (Fig. 5.7B, D and G), others such as *Salicornia europaea* (Fig. 5.7E) have an almost inverse relationship. In order to explain this variability in seasonal trends at the bulk and compound specific level, it is first necessary to consider the environmental conditions to which these species regularly exposed.

It is well established that plants growing in saltmarshes are subject to a range of adverse conditions, including (but not limited to) salinity, nitrogen limitation, root anoxia, waterlogging, redox potential and high concentrations of toxic sulphur-containing compounds (Drake, 1989; Parida and Das, 2005; Maricle *et al.*, 2007; Song *et al.*, 2009; Davy *et al.*, 2011). It is the consistent presence of these stress factors that drive adaptive responses in species commonly found in saltmarshes, which encompass changes in leaf physiology/morphology and shifts in biochemical mechanisms (Drake, 1989; Parida and Das, 2005; Maricle *et al.*, 2007). These adaptations in turn may influence the carbon isotope composition of bulk leaf tissue

and specific compound classes of plants growing at Stiffkey, as a result of shifting the allocation of carbon through cellular metabolic networks (Section 5.2.4).

Although *in-situ* measuring of environmental parameters (such as salinity, soil pH, soil water potential) were not carried out as part of this study, environmental conditions at Stiffkey marsh are well documented. The site was the subject of a series of studies in the 1970s, and seasonal shifts in water availability, nutrient stress and salinity were well constrained (Jeffries, 1977; Jeffries and Perkins, 1977). These specific edaphic parameters have all been shown to influence the bulk $\delta^{13}\text{C}$ composition of plant material via their impact on C_i/C_a (Arens *et al.*, 2000; Table 5.2; Fig. 5.5). The interspecies variation observed among C_3 species at the bulk level is therefore thought to reflect the physiological responses of these plants to site-specific environmental parameters (Dungait *et al.*, 2008; Cernusak *et al.*, 2013).

The bulk signal is strongly influenced by the carbohydrate content of leaves, which is approximately 75% (Dungait *et al.*, 2008). The carbohydrate carbon isotope composition has been shown to be sensitive to changes in C_i/C_a (Brugnoli *et al.*, 1988), further supporting the view that interspecies variation at the bulk level will reflect environmental parameters effecting changes in these gas exchange rates (Farquhar *et al.*, 1989; Diefendorf *et al.*, 2010). Empirical data from field measurements of photosynthesis from other studies of saltmarsh plants strengthen this assertion. Previous studies of a range of Mediterranean saltmarsh species including *Atriplex portulacoides*, for example, have illustrated that the net photosynthetic rate decreases in summer due to stomatal limitation of gas exchange, occurring principally as a result of limited water availability (das Neves *et al.*, 2008).

5.7.2.1 Water availability

Lower marsh environments such as the sandflat at Stiffkey are subject to tidal inundation throughout the course of the year (Jeffries, 1977; Maricle *et al.*, 2007), and hence plants here receive a regular water supply all year round. Low-lying levels that receive these regular tidal inputs suffer from complications such as waterlogging, root anoxia and regular fluxes in salinity, which can negatively influence plant productivity (Maricle *et al.*, 2007; Davy *et al.*, 2011). To counter this, some species have specific physical adaptations. *Spartina anglica*, for example, is classified as helomorphic due to the fact it has developed aerenchyma (a network of intercellular spaces extending from the root to the upper parts of the plant) ensuring an oxygen supply to the roots during water logging (Minden *et al.*, 2012).

The topography of Stiffkey, however, means that during early summer, tides do not always cover the upper marsh (Jeffries, 1977), as the modern upper marsh surface is +2.7 mean ordnance datum (mOD), the Ridge +3.9 mOD (Funnell *et al.*, 2005) and the lower marsh is ~0 to - 0.5 mOD (Andrews *et al.*, 2000). As a result of evapotranspiration and relatively low rainfall in summer months (Fig. 4.3, Chapter 4), the upper marsh and other elevated environments at Stiffkey have been shown to have drier soils and lower water availability than those of the lower marsh (Jeffries, 1977). It is worthy of note that field studies have reported that precipitation has limited impact upon in-situ soil water potential in saltmarshes (ψ_W^{Soil}) on a daily basis, with prolonged changes in weather conditions required to alter ψ_W^{Soil} (Guy *et al.*, 1986). The slight variation in overall precipitation amounts recorded for 2011 and 2012 (Fig. 4.3, Chapter 4) should not, therefore, confound interpretation of the relevance of water availability across the 2011 and 2012 growing seasons.

It has long been known that a decrease in soil water availability gives rise to concurrent reductions in photosynthesis, transpiration and stomatal conductance (Wong *et al.*, 1985; Farquhar *et al.*, 1989). The reduction in stomatal conductance can give rise to diminishing C_i values, and hence decreases in Δ and corresponding increases in $\delta^{13}C$ of bulk plant material (Farquhar *et al.*, 1989). When considering plant-water relations, positive shifts in bulk $\delta^{13}C$ during a growing season have been previously interpreted as plants adapting their water use strategies to enhance WUE (Farquhar and Richards, 1984; Siebt *et al.*, 2008; Tan *et al.*, 2009). At Stiffkey, bulk $\delta^{13}C$ data for the C_3 monocot *Elytrigia atherica* (Ridge site) show a shift of 2 to 3‰ towards ^{13}C -enriched values as the summer progresses in both 2011 and 2012 (Fig. 5.7). Similar shifts are seen in *Atriplex portulacoides* and *Suaeda vera* at the Ridge (Table 5.3 and 5.4), suggesting that this sub-habitat might experience a degree of water stress in late summer, when rainfall decreases and soil evaporation rises with the warm temperatures. Unfortunately, *in-situ* measurements of photosynthesis rates, gas exchange rates and soil water potential were not possible as part of this project. However, field monitoring of leaf water potential (Ψ) from *Atriplex portulacoides* growing in a Spanish saltmarsh shows that Ψ is greatest in spring and winter, and lowest in summer (das Neves *et al.* 2008). In addition, intrinsic WUE also differs among the Spanish halophytes, with maximum rates found in summer (das Neves *et al.* 2008). While local weather conditions are not as extreme at Stiffkey as those found in Spain, the summer months remain the hottest (Chapter 4), so it is plausible that similar (if less pronounced) changes in Ψ and WUE occur in the Stiffkey plants. Based on these assumptions, the data from the Ridge site

suggest that moisture availability (and responses to changes in it) might control some of the temporal variability observed in the bulk carbon isotope composition of the species at Stiffkey at this sampling location.

Not all plants at the Ridge respond in the same way across the 2011 and 2012 growing seasons. The C₃ reed *Phragmites australis* in particular shows very little seasonal variation in bulk $\delta^{13}\text{C}$ composition across both sampling years (Fig. 5.7D). *Phragmites australis* has been shown to have extensive root networks, however, reaching depths of up to 1.5 m, and an extensive perennial rhizome, which allows it to make use of water from areas around the stand (Lissner and Schierup, 1997), which may potentially also have lower salinity levels (see the discussion below). Differences in rooting depth and patterns are known to influence the carbon isotope composition of plant leaf tissue (Diefendorf *et al*, 2011), and therefore the remarkably consistent $\delta^{13}\text{C}$ signature of *Phragmites australis* (Fig. 5.7D) may simply reflect the ability of this species to utilise different water resources than other plants at the Ridge. Interestingly, plants growing on the low marsh site, such as *Salicornia europaea*, have bulk tissue that also becomes ¹³C-enriched during the summer months (Fig. 5.7E; Tables 5.3 and 5.4). As the low marsh receives regular tidal inundation throughout the year, it is unlikely that water stress alone is responsible for these shifts in *Salicornia europaea*.

At the compound specific level, it is interesting to note that the trends observed at the bulk level are not faithfully recorded by all species sampled. While *Elytrigia atherica* records near identical seasonal trends in bulk tissue and *n*-C₂₉ (Fig. 5.7B), *Atriplex portulacoides* and *Salicornia europaea* have almost inverse profiles for bulk and *n*-C₂₉ $\delta^{13}\text{C}$ values across the sampling periods (Fig. 5.7 A and E). For example, bulk $\delta^{13}\text{C}$ values from *Atriplex* show progressive ¹³C-enrichment between June - October 2011 and March - August 2012. In contrast, *n*-C₂₇, *n*-C₂₉ and weighted *n*-alkane $\delta^{13}\text{C}$ values all record a consistent ¹³C-depletion between August - October 2011 and May - September 2012 (Fig. 5.7A). A similar divergence of trends occurs between bulk and *n*-alkane $\delta^{13}\text{C}$ data from the stem succulent *Salicornia*, (particularly between June 2011 and May 2012, Fig. 5.7E), and the evergreen succulent *Suaeda* (June - October 2011; March to September 2012, Fig. 5.7). These data suggest that different information is being recorded at the bulk and molecular level in these saltmarsh species.

5.7.2.2 Salinity/osmotic stress

In addition to water stress, the seasonal patterns in the data discussed in Section 5.7.2.1 could also be due to osmotic stress. Salinity has a close inter-relationship with water availability: some models of crop plants predict that in water-stressed conditions salinity can actually confer a degree of protection from drought (Shani *et al.*, 2001; Glenn *et al.*, 2012). Similar results have been reported for halophytes, with *Spartina* showing enhanced growth in the presence of NaCl even when under drought conditions (Brown *et al.*, 2006).

Osmotic stress has been shown to result in a positive shift in plant $\delta^{13}\text{C}$ values of between 3 and 10‰ (Arens *et al.*, 2000; Table 5.2; Fig. 5.5). This is due to the effect of salinity on C_i/C_a (Guy *et al.*, 1986). In non-halophyte species, metabolic effects of increasing salinity include stomatal closure which gives rise to a decrease in Δ (and a concurrent positive shift in $\delta^{13}\text{C}$) as a result of a decrease in C_i (Farquhar *et al.*, 1989; Arens *et al.*, 2000). Studies of halophytes also show a positive shift in bulk tissue $\delta^{13}\text{C}$ when grown in saline soils with low Ψ_W^{Soil} (Guy *et al.*, 1986). These studies illustrate that an increase in salinity, which lowers Ψ_W^{Soil} , generally requires plants to enhance their WUE, resulting in ^{13}C -enriched biomass (Guy *et al.*, 1986), thus linking this abiotic factor to the discussion regarding water availability in section 5.7.2.1 above.

At Stiffkey, whilst all species show some degree of salt tolerance, Ellenberg indices (used as indicator values for plant tolerance to a range of environmental conditions, and discussed in detail in Chapter 2) suggest that *Elytrigia atherica* from the Ridge site displays the most sensitivity to salt stress (Hill *et al.*, 2000). Although not regularly inundated by tides, increasing salinity at the ridge may result in an upwards movement of brackish water ascending through soil capillaries (Rowell, 1994). Water moves upwards in soils as a result of uptake by plants and also from areas of low partial pressure (wet soil) to areas of dry partial pressure (dry soil) (Rowell, 1994). During the warmer months, increased evaporation of water from the surface layers of soil could serve to draw more of this saline water to the surface (Rowell, 1994), where it would be available for root uptake. The maximum upward flux of water would be dependent upon the hydraulic properties of the soil, which has a greater percentage of sand on the ridge (Miyazaki, 2006). This type of water movement in soils is termed 'capillary rise', and has been shown to lead to surface salinisation of soils in saline environments (Sarkar and Halder, 2005). As discussed above (5.7.2.1) *Elytrigia atherica* shows a positive trend in $\delta^{13}\text{C}$ values (at

both the bulk and the *n*-alkane level), as summer progresses in both 2011 and 2012 (Fig. 5.7B). Given that salinity impacts upon C_i/C_a in a similar fashion to water stress, it is possible that the trends observed in bulk $\delta^{13}\text{C}$ values of *Elytrigia atherica*, (and indeed of *Atriplex portulacoides* and *Suaeda vera*) arise from a change in gas exchange rates driven by a combination of water stress and salinity stress.

Changes in salinity do not, however, appear a sensible mechanism to explain the seasonal shifts in bulk $\delta^{13}\text{C}$ values from the low marsh *Salicornia europaea* (Fig. 5.7). As the low marsh is consistently inundated by tides, the conditions for hypersalinity, (a common occurrence on the upper marsh, e.g. Jeffries, 1977; Passioura *et al.*, 1992), do not occur. Root anoxia, another environmental mechanism driving positive shifts in plant $\delta^{13}\text{C}$ (Arens *et al.*, 2000) is also likely to be constant across the year for *Salicornia* in the tidal low marsh. This suggests that a temporal factor such as maturation (Arens *et al.*, 2000) may be responsible for the positive shifts in the carbon isotope composition of bulk tissue observed in this species as the growing season progresses.

As mentioned in 5.7.2.1, the seasonal trends observed in bulk and *n*-alkane $\delta^{13}\text{C}$ values do not necessarily follow each other (Fig. 5.7), again highlighting that changes in C_i/C_a as a result of salinity do not necessarily imprint in the same way upon all compound classes in a plant. This has important implications, particularly for those studies where the carbon isotope composition of leaf wax biomarkers has been proposed as a proxy for salinity changes. In their study of mangroves, for example, Ladd and Sachs (2013) identified a positive trend between water salinity and $\delta^{13}\text{C}$ of *n*-C₃₁, *n*-C₃₃ and bulk leaf tissue along a river estuary transect. They interpreted this as a shift in the WUE of mangrove leaves in the face of increasing salinity depending upon their position within the estuary. Findings from the research undertaken at Stiffkey, however, suggest that this response might be species specific, because at the *n*-alkane level, there is no obvious trend for *n*-C₂₇, *n*-C₂₉ or weighted alkane $\delta^{13}\text{C}$ values to become more ^{13}C -enriched in the summer months when hypersalinity is highest. Indeed, across a range of species, including *Limonium vulgare* (which grows in the UM where hypersalinity would be most expected, Passouria *et al.*, 1992), *Salicornia europaea*, *Suaeda vera* and *Atriplex portulacoides*, *n*-alkane isotope ratios become ^{13}C -depleted in the months where hypersalinity is most common (Fig. 5.7). Prior to a general movement to interpret shifts in the *n*-alkane $\delta^{13}\text{C}$ composition of C₃ halophyte and saltmarsh species as a palaeosalinity proxy, therefore, further studies of a wide range of modern saltmarsh

species will be required to test whether they behave in the same way as the mangrove trees studied by Ladd and Sachs (2013). In order to fully investigate the importance of environmental factors, such monitoring should include seasonal measurements of factors such as soil water content, salinity, pH, and nitrogen content. *In-situ* measurements of gas exchange rates and photosynthetic rates should also be carried out as part of such projects. In addition, as leaf morphology differs so greatly among the sampled plant species (e.g. Fig. 2.5, Ch. 2), future studies should also consider factors such as leaf mass per area (LMA) (Roderick and Cochrane, 2002). LMA has been shown to have a significant relationship with the carbon isotope composition (and indeed carbon isotope discrimination), suggesting a relationship between water availability/stress, leaf structure and carbon isotope systematics (e.g. Lamont *et al.*, 2002) that would be worthy of further exploration in saltmarsh plants.

5.7.3 Spatial variation in carbon isotope composition across marsh sub-environments

In October 2011, species were sampled from multiple locations across the marsh, to consider the importance of spatial variation in micro-habitats across all marsh sub-environments. $\delta^{13}\text{C}$ values for bulk tissue were highest for the two evergreen species *Atriplex portulacoides* and *Suaeda vera* at the UM site, with a negative shift of $\sim 1\text{‰}$ observed in bulk in the LM or R sites respectively, depending upon species distribution (Fig. 5.22). Bulk tissue from the two perennial species, *Limonium vulgare* and *Salicornia europaea* showed far lower variation across the UM and LM sites (Fig. 5.22). At the compound-specific level, patterns of relative ^{13}C enrichment and depletion were generally very similar, with the UM site having the highest $\delta^{13}\text{C}$ values, and the R and LM sites the lowest. The magnitude of the intraspecies shifts between the sites was higher at the *n*-alkane level, however (Fig. 5.22), with variation more than twice that seen in bulk tissue. As changes in water availability can drive a positive shift of between 3 and 6‰ in the $\delta^{13}\text{C}$ of bulk tissue (Arens *et al.*, 2001; Table 5.2), these bulk data suggest that the UM site is likely to experience higher levels of water stress than the R and LM sites. This seems somewhat implausible, however, as parts of the UM are known to remain waterlogged, while the R site is more free-draining (Jeffries, 1977). It is perhaps more likely that salinity and osmotic stress (discussed further below) has a stronger influence on these values.

Salinity, as shown in Section 5.7.1.2, can also drive a positive shift in the carbon isotope composition of bulk plant tissue (Arens *et al.*, 2001). Salt is likely to be a greater problem in the UM than other marsh sub-environments, as the lack of regular tidal flushing means that ions can concentrate around plant roots (Passioura *et al.*, 1992). This could explain why the $\delta^{13}\text{C}$ of bulk tissue and *n*-alkanes from the UM site are consistently the highest from all sub-habitats (Fig. 5.22). *Atriplex portulacoides* is a particularly interesting species when looking at marsh sub-environments, as it grows across all the sampling sites. There appears to be a systematic negative shift in $\delta^{13}\text{C}$ at both the bulk and *n*-alkane levels moving from the UM to the LM, which suggests that the concentrations of salt around roots diminishes seaward (Fig. 5.22). This seems logical, given the flushing of the LM with tides (Passioura *et al.*, 1992), but would require further experimental work and sample collection to investigate fully.

The fact that the magnitude of shift in a single species across the marsh sub-habitats differs subtly however, depending upon whether bulk or *n*-alkane $\delta^{13}\text{C}$ values are considered is also qualitative support for the previous argument that other mechanisms in addition to changes in C_i/C_a are influencing the carbon isotope composition of *n*-alkanes. Caution needs to be applied, given the seasonal trends in bulk and *n*-alkane $\delta^{13}\text{C}$ values, before automatically assuming that similar patterns in $\delta^{13}\text{C}$ values mean that similar mechanisms are controlling the signal recorded in bulk tissue and individual organic compounds.

In addition, these data have only been interpreted here in light of environmental factors. It is worthy of note that genetic variation is also known to have a significant impact upon bulk tissue carbon isotope values among varieties of plants from the same species (Dungait *et al.*, 2008). Such genetic variation, for example, has been shown to lead to differences among cultivars in terms of the kinetic properties of enzymes such as Rubisco, which in turn can alter the isotopic fractionation associated with carbon fixation (Tcherkez and Farquhar, 2005). It is known that populations of some species at Stiffkey, such as *Salicornia europaea* and *Suaeda vera* (Davy and Smith, 1985; Noble, 1990) can vary genetically with marsh sub-environment, and therefore possible that some of the differences observed with marsh sampling location arise from genetic differences. Future studies considering the response of species to environmental conditions should ideally include analysis of the genetic profile of the plants under investigation, to evaluate the importance of this biological component across a wide range of habitats, in addition to the environmental and physiological measurements discussed in Section 5.7.2.

5.7.4 Calculating carbon isotope discrimination from bulk and *n*-alkane carbon isotope ratios

The range in offset between bulk and *n*-alkane $\delta^{13}\text{C}$ values observed among the Stiffkey C_3 species (arising from the variation in seasonal trends in carbon isotope composition observed at the bulk and molecular level among) results in somewhat different patterns in carbon isotope discrimination depending upon whether bulk or compound-specific data is used for calculating $\Delta^{13}\text{C}$ (Fig. 5.11). $\Delta^{13}\text{C}$ trends are often used to draw qualitative conclusions about interspecies differences in water use efficiency (WUE) among C_3 species growing at the same geographical location (e.g. Ehleringer *et al.*, 1992; Donovan and Ehleringer, 1994). $\Delta^{13}\text{C}$ values have also been used to investigate global-scale patterns in leaf carbon isotopes. Diefendorf *et al.* (2010) calculated carbon isotope discrimination values from published $\delta^{13}\text{C}$ ratios from a range of plant species to understand the relationship between $\Delta^{13}\text{C}$ and environmental conditions, in an attempt to enhance interpretation of variability in $\delta^{13}\text{C}$ signals from ancient terrestrial organic material. Their study was based on the premise that carbon isotope discrimination in C_3 species is moderated by stomatal control of gas exchange at the leaf level, which in turn is responsive to changes in water availability.

This mechanism is well described for bulk plant material (see for example Farquhar *et al.*, 1989; Donovan and Ehleringer, 1994; Cernusak *et al.*, 2013). However the Stiffkey data show that the relative WUE ranking of species is dependent upon whether bulk leaf tissue or *n*-alkane $\delta^{13}\text{C}$ ratios are used for calculating $\Delta^{13}\text{C}$ (Fig. 5.11). This illustrates the fact that comparing bulk and *n*-alkane $\Delta^{13}\text{C}$ values, and even in some instances comparing $\Delta^{13}\text{C}$ values calculated from different alkane chain lengths, may not be valid. The implicit assumption made by Diefendorf *et al.* (2010) that the influence of moisture availability on stomatally moderated gas exchange is the dominant mechanism recorded in leaf wax biomarkers (and hence in the geological lipid record) may also be invalid, because the results of this study suggest that there is another mechanism – such as the metabolically-driven post photosynthetic fractionation of carbon discussed further at Section 5.7.6 below (e.g. Tcherkez *et al.*, 2011; Werner *et al.*, 2011) – that is potentially the most important control on leaf wax *n*-alkane $\delta^{13}\text{C}$ ratios.

5.7.5 The relationship between carbon content and carbon isotope composition

Species sampled at Stiffkey differ in their percentage carbon composition. The grasses in particular have relatively high amounts of carbon ($\geq 39\%$) (Fig. 5.12; 5.17) compared to the shrubs, perennials and annuals. This is potentially due to their containing higher amounts of cellulose and/or hemicellulose than these other plant life forms (Vogel, 2008). Previous studies considering the amount of cellulose in the C_4 monocot *Spartina alterniflora* report, for example, that it could contain up to 44% ash-free dry weight hemicellulose in leaf tissue (Benner *et al.* 1987)

In the C_3 and C_4 monocots, perennials and annuals (i.e. *Limonium vulgare* and *Salicornia europaea*), the carbon content has a positive relationship with the carbon isotope composition, such that increasing amounts of carbon correlate with ^{13}C -enriched bulk tissues (Fig. 5.14 and 5.15). In contrast, the evergreen woody shrubs *Atriplex portulacoides* and *Suaeda vera*, have a negative relationship between %C and $\delta^{13}C$ values. (Fig. 5.16) As carbohydrates including cellulose, hemicellulose, starches and sugars make up approximately 70% of the tissues in green plant cells, variation in their $\delta^{13}C$ composition can exert a significant influence over the bulk carbon isotope composition (Dungait *et al.*, 2008). Variation in the composition of bulk tissue among the grasses/reeds, perennials/annuals and woody evergreens may therefore explain the different trends in correlations observed between %C and bulk $\delta^{13}C$ observed in this dataset.

Studies of the carbon isotope composition of cellulose and hemicellulose have shown that cellulose and hemicellulose is enriched in ^{13}C by 1-2‰ when compared to bulk plant tissue (Benner *et al.*, 1987). It therefore follows that Stiffkey grasses, where cellulose and hemicellulose comprises a higher proportion of cell tissue (Vogts, 2008), there will be a positive relationship between %C and bulk $\delta^{13}C$ values (Fig. 5.14). The positive relationship identified for *Limonium vulgare* and *Salicornia europaea* (Fig. 5.15) is somewhat puzzling, as plants from this functional type are not noted for having significantly high amounts of cellulose or hemicellulose (Vogel, 2008), and are thought to preferentially accumulate nitrogenous compounds (as opposed to carbohydrates) to maintain their osmotic potential (Briens and Lahrer, 1982). The accumulation of nitrogenous compounds does not in itself, however, preclude the coeval accumulation of carbohydrates and sugars (Briens and Lahrer, 1982), and the positive correlation between bulk $\delta^{13}C$ and carbon content suggests that these two species are potentially accumulating carbohydrates that are relatively

^{13}C -enriched, leading to a bulk signal that is more positive the higher the carbon content becomes. Fig. 5.17 supports this assertion for *Limonium vulgare*, which has a high percentage composition of both nitrogen and carbon. *Salicornia europaea*, however, has the lowest concentration of both carbon and nitrogen in bulk tissue (Fig. 5.17). These somewhat contradictory trends suggest that further seasonal analysis of the sugar and amino acid content of these species by high-performance liquid chromatography (a technique suitable for the quantification of carbohydrates and amino acids, Briens and Lahrer, 1982) would be required to confirm these theories.

The negative relationship between carbon content and bulk carbon isotope composition observed for *Atriplex portulacoides* and *Suaeda vera* (Fig. 5.16) also requires some further consideration. A simple interpretation would be to assume that in these species, the increasing carbon content is contained within a compound class that is ^{13}C -depleted relative to bulk tissue. The woody shrubs are known to accumulate predominantly nitrogenous compounds to maintain osmotic potential (Briens and Lahrer, 1982). Nitrogenous compounds such as amino-acids have been reported to be ^{13}C -depleted relative to carbohydrates (Schmidt, 2003) and hence the accumulation of this compound class by some species more than others might explain the negative trend. *Suaeda vera* in particular has a relatively high percentage nitrogen content (Fig. 5.17) which offers qualitative support for this theory. Again, HPLC analysis of seasonal shifts in the concentration of amino-acids would add weight to this hypothesis.

A statistically significant relationship between the carbon content and *n*-alkane $\delta^{13}\text{C}$ values was only identified in the C_3 and C_4 monocots at Stiffkey (although no relationship was observed between bulk $^{13}\text{C}/^{12}\text{C}$ and %C in *Spartina anglica*). The existence of a relationship between %C and bulk tissue $\delta^{13}\text{C}$, and the corresponding lack of one between %C and *n*-alkane $\delta^{13}\text{C}$, in the remaining dicots and succulents is important from the perspective of the mechanisms that control the stable isotope composition of different compound classes, as it further supports the assertion that *n*-alkane carbon isotope composition may be decoupled from bulk leaf tissue $\delta^{13}\text{C}$ in some species. It is interesting that the presence or lack of a relationship between %C and WA alkane $\delta^{13}\text{C}$ appears to follow the broad distinction between monocots and dicots, noted above, in terms of the predominant osmoregulatory compounds they produce to protect themselves from salinity (Briens and Lahrer, 1982; Fig. 5.23 below).

5.7.6 Are species-specific adaptations to salinity significant?

Studies of CAM species have previously theorised that shifts in carbon allocation among species to mitigate water availability had the potential to explain variability of 0.5 to 12.8‰ in the depletion of lipids relative to bulk tissue (Boom *et al.*, 2014). It is therefore interesting to consider whether changes in carbon allocation among the Stiffkey C₃ and C₄ plants represent a viable mechanism to account for interspecies differences in *n*-alkane δ¹³C. Tcherkez *et al.* (2011) proposed that the isotopic composition of plant compound classes is a function of the nature, direction and magnitude of metabolic fluxes. Applying this hypothesis to Stiffkey, it is therefore possible that gross differences in the biochemistry among the studied species is (at least partially) responsible for the variation in offset observed between bulk and secondary compound δ¹³C values, both (a) among different species, and (b) in one species across a growing season.

One area of well-studied variation among the biochemistry of these species relates to their adaptations to salinity. Such adaptations have been divided into low-complexity and high-complexity mechanisms (Parida and Das, 2005). Major processes such as photosynthesis are protected by high-complexity mechanisms such as WUE, whilst low-complexity adaptations are thought to involve alteration of biochemical pathways (Parida and Das, 2005). Ideal plant protective solutes are those which are non-toxic and compatible with cytoplasm enzymes across a range of concentrations (Rhodes *et al.*, 2002). Such favourable compounds include quaternary ammonium compounds, amino-acids and carbohydrates (Briens and Lahrer, 1982; Hare and Cress, 1997; Rhodes *et al.*, 2002; Ashraf and Foodad, 2007). It has been proposed that species can be divided into: a) species that only synthesise high levels of carbohydrates; b) species that synthesise carbohydrates and nitrogenous compounds; and c) species that accumulate higher concentrations of nitrogenous compounds than carbohydrate compounds (Briens and Larher, 1982) (Fig. 5.23).

It is widely recognised that significant inter-species variation exists in terms of the amino-acid responses of plants exposed to salinity (Ullrich, 2002). Of the species identified at Stiffkey, plants in the Chenopodiaceae (*Suaeda vera*, *Atriplex portulacoides*, *Salicornia europaea*) and the Poaceae are all known to accumulate glycine betaine to a high degree during periods of salt and drought (Rhodes *et al.*, 2002; Martěnez *et al.*, 2004). Glycine betaine is highly significant for plants as it has been shown to protect photosynthetic mechanisms (Rubisco and Photosystem II) in

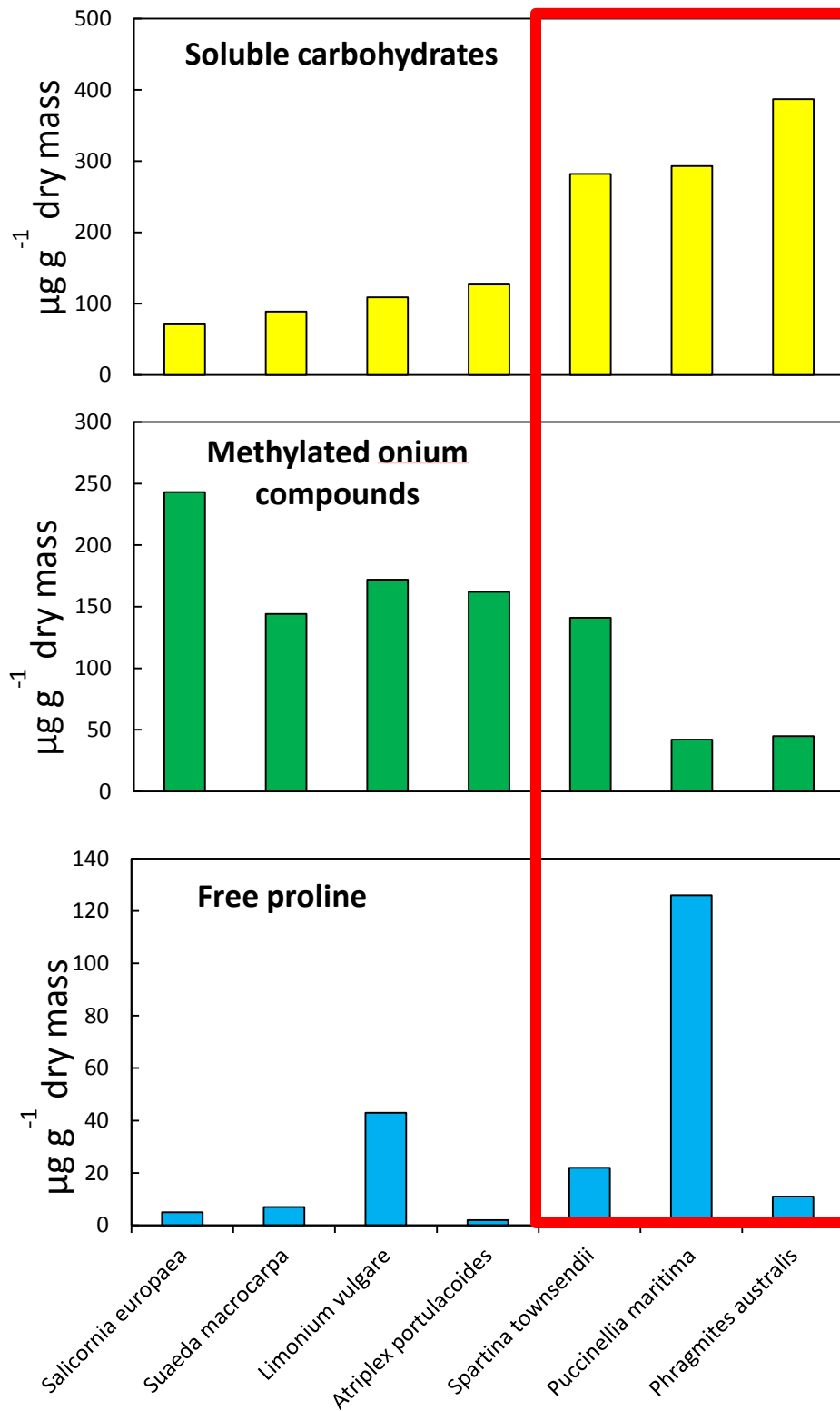


Figure 5.23: Data from Briens and Lahrer (1982) showing the difference in soluble carbohydrate, methylated onion (nitrogenous) compounds, and free proline between dicots and monocots (highlighted in red)

plants under osmotic stress (Martěnez *et al.*, 2004). Proline is also a very common osmolyte, synthesised by a wide variety of plants (Briens and Lahrer, 1982). Some species at Stiffkey contain compatible solutes that are less common. *Limonium vulgare*, for example, is a member of the Plumbaginaceae. Species in this family have been shown to synthesise β -alanine-betaine by direct N-methylation of the amino-acid β -alanine (Rhodes *et al.*, 2002). It is interesting to note that experimental data suggest that plants do not simply vary all of these osmolytes upon being exposed to environmental stress – *Atriplex portulacoides* species have been shown, for example, to maintain proline levels whilst raising glycine betaine levels in response to drought (Martěnez *et al.*, 2004).

In addition to nitrogenous compounds, carbohydrates (e.g. soluble sugars) can also be synthesised as compatible solutes for osmoregulation (Briens and Lahrer, 1982). *Atriplex portulacoides*, for example, has been shown to generate enhanced concentrations of malate when under osmotic stress, whilst *Phragmites australis* and *Limonium vulgare* synthesise raffinose (Briens and Lahrer, 1982). From the perspective of carbon partitioning within plants (and the potential such carbon flow has upon stable isotope compositions), the percentage of soluble carbohydrate in leaf (and root) dry material has been shown to vary considerably among species. The roots of *Limonium vulgare* and *Spartina anglica* can contain in excess of 15%, while the leaves of *Spartina anglica* and *Phragmites australis* can contain 7 to 10% (Briens and Lahrer, 1982). Briens and Lahrer (1982) conclude that *Spartina anglica* and *Phragmites australis* preferentially synthesise soluble carbohydrates, whilst *Atriplex portulacoides*, *Limonium vulgare*, *Salicornia europaea* and *Suaeda vera* all accumulate nitrogenous compounds. Additionally, plants that are tolerant to salinity can produce a range of additional proteins to aid in detoxification and protection against reactive oxygen species (Zhu, 2001).

Carbohydrates and amino-acids/nitrogenous compounds typically have different carbon isotope ratios, with amino-acids depleted in ^{13}C relative to carbohydrates (Schmidt *et al.*, 2003). Analysis of carbon and nitrogen composition of bulk plant tissue shows that the monocots (preferentially accumulating carbohydrates), do have higher %C than other plant life forms at Stiffkey (Fig. 5.12 and 5.13). However, the picture is not as clear when %N is considered (Fig. 5.17), with different plant life forms having very similar %N. This suggests that these species are likely to be producing a mixture of carbohydrate and nitrogenous compounds (Briens and Lahrer, 1982), the precise composition of which may vary as the growing season progresses (Fig. 5.17). Indeed it is possible that each of these species produce their

own specific mix of osmoregulatory compounds (e.g. Ullrich, 2002). This could lead to different carbon flow patterns – and thus carbon isotope fractionation – through the acetogenic lipid biosynthesis pathway (Hayes, 2001; Diefendorf *et al.*, 2011) among these plants.

Furthermore, the existence of a statistically significant relationship between the nitrogen content of bulk leaf tissue and the WA *n*-alkane $^{13}\text{C}/^{12}\text{C}$, but (with the exception of the evergreens) not between %N and bulk $^{13}\text{C}/^{12}\text{C}$, again suggests a degree of decoupling between the mechanisms influencing bulk and leaf wax *n*-alkane carbon isotope composition. The nature of this relationship is highly variable, however. For example, the C_3 monocots (*Elytrigia atherica* and *Phragmites australis*), have a positive relationship between %N and WA *n*-alkane $^{13}\text{C}/^{12}\text{C}$, while the C_4 monocot *Spartina anglica*, has a negative relationship. In addition among the dicots/succulents, the perennials/annuals (*Salicornia europaea* and *Limonium vulgare*) have a positive relationship between %N and WA *n*-alkane $^{13}\text{C}/^{12}\text{C}$, while the evergreens (*Atriplex portulacoides* and *Suaeda vera*,) have a negative relationship which also persists at the bulk level. It is possible these differing relationships reflect the balance between the relative proportions of different osmolytes produced by these species – both *Atriplex portulacoides* and *Suaeda vera*, for example are known to accumulate glycine betaine under times of stress (Rhodes *et al.*, 2002; Martinez *et al.*, 2004). Without further characterisation of the specific suite of compounds accumulated by each species, however, no firm conclusions can be drawn on this point.

Interestingly, the relationship between $\delta^{15}\text{N}$ and carbon isotope composition also appears to broadly differ among those species that typically produce carbohydrate osmoregulatory compounds (monocots) and those that produce nitrogenous compounds (dicots and succulents). The C_3 monocots have a positive correlation between foliar $\delta^{15}\text{N}$ and both *n*-alkane and bulk $^{13}\text{C}/^{12}\text{C}$, while in contrast the dicots and succulents have a negative (but not statistically significant) relationship. In order to account for these diverse relationships, it is first necessary to consider factors which control the $^{15}\text{N}/^{14}\text{N}$ of plants. The nitrogen isotope composition of plant leaf material is known to be a function of a range of complex processes (Pardo and Nadelhoffer, 2010). These include the source of N taken up, the depth of roots, any micorrhizal associations, N loss and N cycling within the plant, and the fractionation processes involved in nitrogen fixation (Handley and Raven, 1992; Handley *et al.*, 1999; Pardo and Nadelhoffer, 2010). All plant species at Stiffkey have positive foliar $\delta^{15}\text{N}$ values (Table 5.6; Fig. 5.19). A range of factors, including drought, N limitation

and association with arbuscular mycorrhizas can all produce leaf tissue which is relatively ^{15}N -enriched (Handley *et al.*, 1999). Studies of mycorrhizal associations in saltmarsh plants are limited, however, vesicular-arbuscular mycorrhizas have been linked to *Atriplex portulacoides*, *Salicornia europaea*, *Suaeda vera*, and *Phragmites australis* (Harley and Harley, 1987 and references contained therein). It is likely that the positive foliar $\delta^{15}\text{N}$ values from the Stiffkey species can therefore be attributed, at least in part, to the mycorrhizal associations of these saltmarsh plants. Variation in mycorrhizal association, drought and nutrient stress are thought to account for up to $\sim 4\%$ interspecies variation in $^{15}\text{N}/^{14}\text{N}$ (Handley *et al.*, 1999).

Variability in plant $\delta^{15}\text{N}$ at Stiffkey is, however, up to 6% among the C_3 species (Fig. 5.19). As these plants also vary in the nature of their preferred compatible solutes synthesised to protect them from the high salinities encountered at the marsh, (with monocots generally producing more carbohydrate compounds and dicots/succulents producing more nitrogenous based compounds; Briens and Lahrer, 1982) it is possible that these broad differences in biochemical adaptations could also influence nitrogen isotope composition. Such differences could potentially account for: (i) variation in foliar $^{15}\text{N}/^{14}\text{N}$, and: (ii) the difference in relationship between $^{15}\text{N}/^{14}\text{N}$ and n -alkane $\delta^{13}\text{C}$ between carbohydrate-producing (monocots) and amino-acid producing (dicots/succulents) species. The isotopic composition of amino acids is known to be ^{15}N -enriched relative to total organic biomass in cyanobacteria, green algae, and seagrass species (Macko *et al.*, 1986, 1987). Where the dicot species are producing more amino-acids, nitrogenous compounds and stress proteins (reflected in increasing ^{15}N -enrichment in their leaf tissue, following Macko *et al.*, 1986, 1987; and also their higher %N composition, Fig. 5.17), pyruvate can be allocated to other metabolic pathways (rather than to acyl-CoA) which has been shown to result in ^{13}C -depleted acetogenic lipids (Diefenorf *et al.*, 2011), hence a negative relationship exists between these two parameters.

In contrast, where species preferentially accumulate carbohydrates, it could simply be the case that the enhanced production of a suite of sugar and carbohydrate osmolytes, alongside some nitrogenous ones, results in a progressive ^{15}N -enrichment, but the coeval ^{13}C -enrichment in the n -alkane signal is controlled by other mechanisms. Further analysis of the nature, concentration and carbon isotope composition of the nitrogenous and carbohydrate osmolytes from each species will therefore be required to fully characterise how the production of these compounds,

and other plant adaptations to salinity, influence the the $\delta^{13}\text{C}$ composition of leaf wax *n*-alkanes.

Such research will be of broad general importance, given that the osmoregulatory strategies displayed by the Stiffkey species are not restricted to saltmarsh plants, but can also be found wherever plants have adapted to water stressed conditions such as arid environments (Bohnert and Jensen, 1996). In addition, the production of osmoregulatory compounds has also been identified in plants growing under other stressed conditions such as high UV light, metal toxicity and extreme cold (Hare and Cress, 1997). Future research should therefore focus on combining analysis of leaf wax lipid $\delta^{13}\text{C}$ with the concentration (and preferably isotopic composition) of osmolytes to test this hypothesis further across a broad range of ecosystems and environments.

Despite the requirement for further analyses evidenced in the previous discussion, some important conclusions can still be drawn from these data. For example, the existence of different relationships between biomass composition, and bulk and biomarker $\delta^{13}\text{C}$, suggests that the carbon isotope composition of leaf waxes is to some extent decoupled from bulk plant tissue. It is possible that this is due to the fact that the reaction networks producing these osmoregulatory compounds, and the respective metabolic fluxes through them, are not necessarily influenced by differences in *C_i/C_a* in the same manner as the dominant components of bulk plant tissue (Dungait *et al.*, 2008). This in turn highlights the fact that great care is required when interpreting shifts in the carbon isotope composition of biomarkers from the geological record in the same way as one would interpret data from bulk plant tissues.

5.7.7 Are seasonal shifts in the relative abundance of leaf wax *n*-alkane homologues significant?

Data from this study (Figs. 5.20 and 5.21) indicate that a relationship exists between seasonal shifts in the relative abundance of the dominant *n*-alkane homologues and the carbon isotope composition of *n*-C₂₇ and *n*-C₂₉, two of the chain lengths most often used in palaeoclimatic reconstructions. This relationship, however, is not straightforward – a positive relationship exists between the percentage abundance of *n*-C₂₅ and *n*-C₂₇ and the $\delta^{13}\text{C}$ ratio of *n*-C₂₉, whereas a negative relationship exists between the percentage abundance of *n*-C₂₉ and the $\delta^{13}\text{C}$ ratio of *n*-C₂₇.

Applying the metabolic fluxes model of Hayes (2001) (Fig. 5.6) and the theory espoused by Tcherkez *et al.* (2011), these relationships can be explained by the fact that in most species at Stiffkey, shorter chain homologues such as n -C₂₅ and n -C₂₇ are ¹³C-depleted relative to n -C₂₉ (Appendix 4). Following the theoretical biosynthetic pathway proposed by Shepherd and Griffiths (2006) (Fig. 3.5, Chapter 3), this depletion should also be present in the immediate precursor compounds, C₂₄ and C₂₆ fatty acids. Unfortunately, fatty acids have not been analysed for these species. Studies where fatty acids have been measured, however, suggest that interspecies variability in FA $\delta^{13}\text{C}$ can be as large as 11‰ (Dungait *et al.*, 2008). Correlations between relative abundance and $\delta^{13}\text{C}$ ratios point to the enhanced production of n -C₂₅ and n -C₂₇ alkanes at certain stages in the growing season (deriving from the decarbonylation of C₂₄ and C₂₆ FAs) incorporating a greater proportion of ¹²C flowing through the reaction network (Fig. 5.6; Hayes, 2001). It is proposed that this results in a ¹³C enriched pool of malonyl-CoA (Shepherd and Griffiths, 2006) available for elongation of C₂₆ FA to C₂₈. This would in turn translate into the production of n -C₂₉ with a relatively ¹³C-enriched isotope ratio. The reverse would be true in circumstances where the abundance of n -C₂₉ increases, as this is accompanied by a coeval reduction in the abundance of other homologues including those with shorter chain lengths. Future studies should combine analysis of molecular distribution, fatty acid $\delta^{13}\text{C}$ and n -alkane $\delta^{13}\text{C}$ in order to fully quantify this apparent 'amount effect' of leaf waxes on their carbon isotope composition.

5.8. CONCLUSION

This chapter aimed to quantify the extent of interspecies variability in bulk and leaf wax n -alkane carbon isotope ratios from a range of saltmarsh species growing in a temperate coastal saltmarsh, and evaluate whether these signals responded in the same way to changes in conditions experienced over a growing season. Temporal trends in bulk and n -alkane $\delta^{13}\text{C}$ did not co-vary for all species across the growing seasons. In general terms, the C₃ grasses and reeds had similar temporal shifts in $\delta^{13}\text{C}$ at the bulk and molecular level, while dicots and shrubs in some cases exhibited an inverse relationship between ¹³C-enrichment and depletion in foliar tissue and n -alkanes. The variation in seasonal shifts in $\delta^{13}\text{C}$ values between bulk and n -alkane data resulted in differences in carbon isotope discrimination patterns depending upon whether bulk or compound-specific data is used for calculating $\Delta^{13}\text{C}$. Comparing bulk and n -alkane $\Delta^{13}\text{C}$ values when reconstructing past climates may not, therefore, be advisable. Results from this study suggest that it is the metabolically-driven post photosynthetic fractionation of carbon, allocating carbon to

different biosynthetic pathways, that is of potentially of greater significance in controlling leaf wax *n*-alkane $\Delta^{13}\text{C}$ (and $\delta^{13}\text{C}$ ratios) than environmental factors.

5.9. SUMMARY

- Seasonal trends in bulk and *n*-alkane $\delta^{13}\text{C}$ values do not record the same trends for all species – monocots have very consistent shifts in $\delta^{13}\text{C}$ at the bulk and molecular level, while dicots and shrubs can have inverse relationships between ^{13}C -enrichment and depletion in bulk and *n*-alkane ratios.
- The offset between bulk and *n*-alkane $\delta^{13}\text{C}$ appears species specific, and can vary by up to $\sim 4\text{‰}$ in a single species across a growing season.
- Calculated $\Delta^{13}\text{C}$ values differ depending upon whether bulk or *n*-alkane data is used – different *n*-alkane homologues from the same species can even produce different $\Delta^{13}\text{C}$ results.
- The relationship between (i) %C content, (ii) %N content, and (iii) $\delta^{15}\text{N}$, and carbon isotope composition at the bulk and molecular level differs among the C_3 monocots, the C_3 perennial/annuals, and the C_3 evergreens, and appears to reflect different metabolic adaptations to salinity between these plant groups.
- There is a complex relationship between the relative abundance of *n*- C_{25} , *n*- C_{27} and *n*- C_{29} with the $\delta^{13}\text{C}$ ratios of *n*- C_{27} and *n*- C_{29} , suggesting that interspecies differences in the flux of material through the biosynthetic pathway generating *n*-alkanes could influence the carbon isotope composition of these biomarkers.

Chapter 6

Understanding $^2\text{H}/^1\text{H}$ systematics of leaf wax *n*-alkanes in coastal plants

*Data from this Chapter has been previously published in: Eley, Y., Dawson, L., Black, S., Pedentchouk, N. (2014) Understanding $^2\text{H}/^1\text{H}$ systematics of leaf wax *n*-alkanes in coastal plants at Stiffkey saltmarsh, Norfolk, UK, *Geochimica et Cosmochimica Acta*, 128, 13 – 28, APPENDIX 2*

6.1. INTRODUCTION

The use of *n*-alkyl lipids to investigate palaeoclimatological and palaeohydrological regimes has received considerable attention in the last decade as a result of analytical advances in compound-specific stable hydrogen isotope methodology (e.g. Hilkert *et al.*, 1999; Meier-Augenstein, 1999). Of particular importance for the utility of these compounds as palaeoclimate proxies is the relationship between their $^2\text{H}/^1\text{H}$ composition and that of environmental water. Previous studies have demonstrated a link between the $\delta^2\text{H}$ values of *n*-alkyl lipids from modern plants and source water across geographically and climatically diverse transects (Huang *et al.*, 2002; Sachse *et al.*, 2004, 2006; Garcin *et al.*, 2012; Tipple and Pagani, 2013; Kahmen *et al.*, 2013b). However, when leaf wax biomarkers from a range of plant species from the same biosynthetic group at individual locations are considered, significant variation in the $\delta^2\text{H}$ values of *n*-alkyl lipids – of up to 80‰ – have been observed (Sachse *et al.*, 2006; Hou *et al.*, 2007; Pedentchouk *et al.*, 2008; Feakins and Sessions, 2010).

Palaeoclimatic reconstructions of source water isotopic composition (Pagani *et al.*, 2006b; Tierney *et al.*, 2008) and moisture availability and aridity (Schefuß *et al.*, 2005; Leider *et al.*, 2013) have often implicitly and/or explicitly relied on the assumption that the biosynthetic $^2\text{H}/^1\text{H}$ fractionation that takes place between the

intracellular water and lipids within the plant is relatively invariant within C₃ and C₄ plant groups. The magnitude of variability in the $\delta^2\text{H}$ values of *n*-alkyl lipids among plant species growing at the same geographical location suggests, however, that this assumption may not necessarily be valid. Interpretation of sedimentary *n*-alkyl $\delta^2\text{H}$ data is further complicated by limited understanding of the reasons for this large interspecies variability. Sachse *et al.* (2012) provided a comprehensive review of the current state of knowledge regarding the factors which control hydrogen isotope composition of lipid biomarkers in photosynthetic organisms. This review highlighted the importance of both physical (e.g. rainfall amount, evaporation, relative humidity, temperature) and biochemical (e.g. NADPH sources, NADPH pools, biochemical pathways) processes (Fig. 1.4, Chapter 1) in controlling $^2\text{H}/^1\text{H}$ composition of photosynthates. However, the relative importance of these separate but interrelated controls remains largely unexplored, particularly when morphologically and biochemically distinct plant species growing in a natural environment are considered.

6.1.1 Previous focus on physical mechanisms

Previous research seeking to explain interspecies variation in *n*-alkane $^2\text{H}/^1\text{H}$ has mainly focused on the use of empirical and modelling studies to investigate various physical processes that control source and intracellular water. Firstly, there are studies (e.g. Hou *et al.*, 2007; Pedentchouk *et al.*, 2008) in which a range of plant species were considered, but coupled leaf water and *n*-alkane $^2\text{H}/^1\text{H}$ measurements were not conducted. Instead, these studies relied on isotopic measurements of environmental water and leaf wax *n*-alkyl compounds, and any differences in $^2\text{H}/^1\text{H}$ fractionation were explained by reference to the physical processes which controlled the movement of water molecules inside, outside and within the leaf according to leaf-water models (e.g. Farquhar and Lloyd, 1993; Barbour *et al.*, 2000; Barbour *et al.*, 2004). The implicit assumption of these models (initially developed for understanding oxygen isotope systematics of plant water) is that they can fully describe hydrogen isotope systematics of leaf water, and thus also account for the differences in the $\delta^2\text{H}$ values of leaf wax lipids among different species (this is discussed further in section 6.1.2 below). The lack of actual measurements of leaf water isotopic composition, however, prevents such studies from evaluating the relative importance of physical and biochemical factors that control leaf water and biosynthate $^2\text{H}/^1\text{H}$ signatures. However, this lack of empirical data did not prevent some researchers from extending their findings further, and considering whether

hydrogen isotope measurements of leaf wax biomarkers could even be used to examine factors such as water use efficiency (WUE) Hou *et al.* (2007) by comparing *n*-alkane $^2\text{H}/^1\text{H}$ and $^{13}\text{C}/^{12}\text{C}$ measurements.

Other studies have included analysis of modelled and/or empirical leaf water hydrogen isotope composition when considering *n*-alkyl lipid $^2\text{H}/^1\text{H}$ to avoid the limitations inherent in the above approach. McInerney *et al.* (2011) examined the impact of relative humidity on leaf wax $\delta^2\text{H}$ by analysing *n*-alkanes from grasses grown both in controlled environmental chambers and across a range of climatically different field sites. Modelled leaf water $\delta^2\text{H}$ values, however, were more positive than would have been expected from empirical *n*-alkane $\delta^2\text{H}$ data. McInerney *et al.* (2011) suggested that ^2H -enriched leaf waters were not the biosynthetic precursor for leaf wax synthesis, as the best correlation between source water and lipid $\delta^2\text{H}$ values was obtained though using 100% xylem water. The potential for biochemical mechanisms being able to explain differences in fractionation between C_3 and C_4 plants was mentioned, but the design of the study did not allow for assessment of its relative importance. Sachse *et al.* (2010) also focused on monocot species, analysing field-grown barley (*Hordeum vulgare*) across one growing season. This study found a correlation between midday leaf water and *n*- C_{31} alkane $\delta^2\text{H}$ values. However, their model, which assumed a 1:1 relationship between leaf water (source) and leaf wax (product), overestimated ^2H -enrichment of the *n*- C_{31} alkane. The authors proposed that this discrepancy could be due to a ^2H -depleted pool of water used during biosynthesis, which may have originated from spatial inhomogeneity in ^2H -enrichment along the length of a leaf. However, this study did not address the question of whether biochemical mechanisms might explain the lack of a 1:1 relationship between source water and *n*-alkane $^2\text{H}/^1\text{H}$.

6.1.2 An overview of leaf water models

As leaf water models are often used to try to account for interspecies variation in *n*-alkane $^2\text{H}/^1\text{H}$, it is important to consider how they have been developed and whether they have any limitations. Many of the leaf water models that have been published focus on oxygen isotope composition, with an implicit assumption that findings will equally apply to hydrogen. Mechanistic models of leaf water oxygen isotopic composition are generally based on the original study of Craig and Gordon (1965), which describes the ^{18}O enrichment of an evaporating water surface. Dongmann *et al.* (1974) provided one of the early modifications of the Craig-Gordon (C-G) model

for use on plant leaves, developing a straightforward box model to describe the enrichment observed as a result of transpiration. Further refinement was proposed by White (1988), who included the effect of leaf water content, Farquhar and Lloyd (1993) who incorporated consideration of the radial Péclet effect (where back-diffusion of ^{18}O enriched water from stomatal pores is countered by the flow of un-enriched water through the leaf veins towards the stomata), and Yakir (1998) who attempted to model two-dimensional leaf water heterogeneity. A significant step in the development of these models occurred when Farquhar and Gan (2003) revised the earlier one-dimensional Péclet model to include both radial and longitudinal Péclet effects. This revised model was designed to accommodate the existence of spatial gradients in leaf water isotopic composition within leaves, developing theories that had been originally applied in earlier research to a model describing isotopic enrichment of water in desert rivers (Farquhar and Gan, 2003).

Unfortunately, the ongoing refinement of the C-G model does not appear to have resulted in a comprehensive understanding of leaf water ^{18}O systematics. Studies still appear to be flexible in their choice of the one-dimensional (1-D) or two-dimensional (2-D) Péclet models when interpreting their data, generally opting for the model that best 'fits' their particular dataset. In addition, there is ongoing debate regarding the extent that leaf waters actually follow the Péclet models, given the lack of consensus in trends observed in empirical studies (Cernusak and Kahmen, 2013). This lack of cohesion indicates that a number of model parameters require further investigation (regardless of whether the focus is on $\delta^{18}\text{O}$ or $\delta^2\text{H}$), and therefore has important implications for studies seeking to apply leaf water models to investigation of *n*-alkane $^2\text{H}/^1\text{H}$ variability. Firstly, the relationship between transpiration (E) and leaf water evaporative enrichment ($\Delta^{18}\text{O}_L$) has been considered in a range of plant species with varying results. Cernusak *et al.* (2008) analysed the leaf water isotopic composition in CAM species. They found that while a negative relationship between E and $\Delta^{18}\text{O}_L$ is predicted for steady-state conditions (where water transpired has the same isotopic composition as water entering the leaf veins), in CAM species daily patterns in stomatal behaviour (open in the morning, closed at midday, and open again in the afternoon) can result in lower rates of E in combination with lower $\Delta^{18}\text{O}_L$ enrichment - i.e. the inverse of the predicted relationship. This is a likely result of lower transpiration in CAM species preventing the system attaining a steady-state (Cernusak *et al.*, 2008). Secondly, the 1-D and 2-D models include the term " L ", which describes the effective path length for water transport from veins to the site of evaporation, into leaf water

models. L cannot be measured directly (Kahmen *et al.*, 2008, 2009; Cernusak and Kahmen, 2013), and therefore its value is normally calculated by performing multiple iterations of the Péclet model with varying values assigned to L until the model returns a result that best fits the trends in the observed leaf water ^{18}O composition (Cernusak and Kahman, 2013). A number of studies have reported the L has a strong inverse correlation with the rate of E within a leaf (e.g. Kahmen *et al.*, 2008) although this finding is not conclusive as other research reports a weak correlation at best (e.g. Ripullone *et al.*, 2008). The recent publication by Song *et al.* (2013) finds that the relationship between E and L is a function of the rate of E , such that the negative relationship is only strongly apparent when rates of E are low ($<2 \text{ mmol m}^{-2} \text{ s}^{-1}$). Song *et al.* (2013) also evaluated the relationship between E and f , the proportional difference of $\Delta^{18}\text{O}_L$ from the isotopic composition of the evaporative site, $\Delta^{18}\text{O}_{\text{es}}$. Interestingly they found the nature of this relationship also depending upon the relative strength of E . Where $E < 1.5 \text{ mmol m}^{-2} \text{ s}^{-1}$, f displayed a negative relationship with E . However, when the rate of E exceeded $1.5 \text{ mmol m}^{-2} \text{ s}^{-1}$, the relationship became positive. The authors concluded that their results highlighted the importance of E in driving variation in L among different plant species, and further that differences in leaf morphology are insignificant (relative to the role of E) in influencing L . Mechanistically, they propose that the existence of the negative relationship between E and L arises from: (i) the movement of water within the leaf; and (ii) environmental and physiological factors that could cause variation in E .

Studies that have considered leaf water $^2\text{H}/^1\text{H}$ have also reported that many of the existing models (particularly the Craig-Gordon model) overestimate the $\delta^2\text{H}$ composition of leaf water (Shu *et al.*, 2008). Such discrepancies are especially significant where high rH lowers E (Da Ines *et al.*, 2010). Application of the 2-D Péclet model can improve the correlation between predicted and observed $^2\text{H}/^1\text{H}$ composition, but even the 2-D models are designed primarily for monocot leaves as they assume a uniform distance between veins which is incompatible with the reticulate venation common among dicots (Šantrůček *et al.*, 2007). Indeed, the inadequacy of relying solely on physical mechanisms to explain leaf water empirical $\delta^2\text{H}$ data was demonstrated in detail by Shu *et al.* (2008), who modelled leaf water oxygen and hydrogen isotope composition along the length of a pine needle. While their model could describe variation along the leaf in empirical $\delta^{18}\text{O}$ data, it could not do the same for $\delta^2\text{H}$ data. The authors proposed that this discrepancy was due to the fact that “certain unknown biological processes may not have been incorporated into our 2D model ... it calls for a re-evaluation of all the other models

for hydrogen isotopic simulations of leaf water since they too lack these processes". The results of this study implied that interpretation of both leaf water and *n*-alkyl lipid $\delta^2\text{H}$ values required a new approach that integrated $^2\text{H}/^1\text{H}$ fractionation during physical processes that control water movement in, out and within the leaf with that which takes place at various stages of photosynthesis.

6.1.3 Studies considering biochemical influences on leaf wax $^2\text{H}/^1\text{H}$

The potential for biochemical processes to influence leaf wax $^2\text{H}/^1\text{H}$ has been considered previously, although in limited circumstances. Kahmen *et al.* (2013) investigated whether evaporative ^2H -enrichment in leaf water was recorded in the leaf waxes of five angiosperm species grown under controlled growth chamber conditions. The results of this study suggested that the influence of evaporative ^2H -enrichment was species-specific; with 18 to 68% of the leaf water ^2H -enrichment reflected in *n*-alkanes. However, interspecies variation of up to 65‰ was observed in $^2\text{H}/^1\text{H}$ fractionation between xylem water and *n*-alkanes. This range in fractionation could not be attributed to differences in measured leaf water evaporative ^2H -enrichment among the studied species. The authors, therefore, theorised that species-specific variation in NADPH sources used for lipid biosynthesis could have been the reason for this variation.

Sessions (2006) studied seasonal shifts in the C_4 saltmarsh grass *Spartina alterniflora*, growing in seawater, which was assumed to have the same isotopic composition throughout the sampling period. The relative ^2H -depletion in lipid $^2\text{H}/^1\text{H}$ observed during the summer months – contrary to the anticipated ^2H -enrichment in summer – was interpreted as a change in the organic substrate used for lipid biosynthesis, i.e. current photosynthate in summer, versus stored carbohydrates during the winter. Feakins and Sessions (2010) also considered whether changes in the source of biosynthates influenced species-specific variation in $^2\text{H}/^1\text{H}$ among CAM plants. Hydrogen isotope fractionation between source water and *n*-alkanes differed by 92‰ among species. However, the authors had not measured xylem or leaf water $\delta^2\text{H}$ as part of this study, but theorised that these differences may have arisen from metabolic moderation of fractionation between leaf water and leaf wax by using a percentage of NADPH generated from heterotrophic pathways for lipid biosynthesis.

6.2. AIMS AND OBJECTIVES

As a result of all the previous research it is possible to hypothesize that if interspecies differences in the $^2\text{H}/^1\text{H}$ composition of leaf wax lipids are driven primarily by differences in the isotopic composition of leaf water, there are several theoretical scenarios that may account for the observed variability among plant species growing at the same site. These include:

1. Differences in the isotopic composition of soil water among site sub-environments;
2. Differences in the isotopic composition of soil water throughout the growing season;
3. Interspecies differences in xylem water, reflecting any fractionation taking place during: (i) root uptake of soil water; and (ii) transport to the site of evaporation in the leaf.
4. Interspecies differences in the isotopic composition of leaf water among plant life forms due to differences in their leaf structure.

The aim of this chapter is to test all of these scenarios and to evaluate whether they provide a comprehensive explanation for differences in the $^2\text{H}/^1\text{H}$ composition of lipids from the C_3 and C_4 plant species sampled at Stiffkey salt marsh. The broad range of plant life forms sampled was ideally suited to the aims of this project due to: (i) their gross variation in leaf morphology; and (ii) their well-studied differences in biochemical adaptations to their environment (discussed in detail in Sections 5.7.5 and 5.7.6, Chapter 5), which provided an ideal platform to test the relative importance of physical and biochemical mechanisms in explaining interspecies variation in the $\delta^2\text{H}$ values of leaf wax *n*-alkanes in terrestrial plant species growing in a geographically restricted natural environment. As the focus of this chapter is on environmental and physical factors, specific biochemical mechanisms and the role of metabolic fractionation will be considered further in Chapter 7.

6.3. SITE DESCRIPTION AND SAMPLING STRATEGY

6.3.1 Site description

The study location and sampling sites are as previously discussed in Chapter 2.

6.3.2 Sampling strategy

Plant samples were collected for a pilot study in June 2011, and then also in March, May August and September during the 2012 growth season. Sampling of all species collected on each occasion took place between 12:00 and 14:00 from 3 sites at Stiffkey (Fig. 3.1 Chapter 3). This two-hour sampling window was unavoidable as a result of high tides. In June 2011, plant species were sampled (i) by plant type (grass, succulent, perennial etc) and (ii) where possible from multiple locations within the marsh (LM, R, UM;), to evaluate the relative importance of marsh sub-environment on leaf lipid $^2\text{H}/^1\text{H}$ (Table 4.1, Chapter 4). The sampling strategy for the period from March to September 2012 was then refined based upon the key findings from the initial results obtained in June 2011. The 2012 sampling focused on gross interspecies differences in hydrogen isotope fractionation between leaf wax, leaf water and environmental water across the growing season. Seven species were selected for study during the 2012 period across the 3 sampling sites (Table 4.2, Chapter 4).

In June 2011 samples were collected for paired leaf wax and leaf water analysis. During 2012, however, sampling also included soil pore water samples for the entire growth season. In September 2012, xylem waters were sampled, as well as leaves from all species between 12:00 and 14:00. In addition soil, leaf and xylem water was also collected from *Elytrigia atherica*, *Suaeda vera*, and *Atriplex portulacoides* at the ridge between 7:30 and 8:00 to allow for investigation of the potential influence of diurnal shifts in xylem and leaf water on *n*-alkane $^2\text{H}/^1\text{H}$ compositions. These three species were chosen because of their close proximity to each other and because they showed the maximum range in *n*-alkane $\delta^2\text{H}$ values among species at one sampling site.

Sampling for *n*-alkane extraction was carried out as described in Chapter 4. Samples for leaf water extraction were collected in triplicate, with each individual analysed sample representing a composite of at least 5 leaves (number dependant on plant leaf morphology) taken from at least 3 different plants at a particular sampling site. The exception to this was the succulent *Salicornia europaea*: this species has no distinct leaves but instead has green photosynthetically active jointed stems (Ellison, 1987). Samples comprising at least 5 green stems were collected during 2012 for leaf water analysis from this succulent species. Samples for soil water extraction were collected in triplicate in March, May and September

2012 from the top ~10 cm of soil in each location. Stem samples were collected in triplicate for each species in September 2012; each sample represents a minimum of 3 stem samples of greater than 5 cm in length. Leaf, stem and soil water samples were placed directly into exetainers, capped, taped with PTFE tape in the field, and then frozen in the laboratory until water extraction. Samples for *n*-alkane analysis were dried at 40 °C for 72 hr, and then stored at room temperature in the dark prior to lipid extraction, as described in Chapter 4.

6.4. ANALYTICAL METHODS

6.4.1 Leaf, xylem and soil water extraction



Figure 6.1: cryogenic extraction line at the University of Reading, showing the pressure gauges attached to each station on the line.

Leaf, xylem and soil water extractions were carried out using cryogenic vacuum distillation based upon the design and operating procedure presented by West *et al.* (2006) (Fig. 6.1). Duplicates of each sample were extracted to enable consideration of a) reproducibility of the extraction method, and b) inherent intraspecies variability in leaf/xylem/soil water isotopic composition. Samples were heated to 80 °C within an evacuated glass line and water was distilled and trapped in an adjacent collection vial submerged in liquid nitrogen. Each station on the extraction line was coupled to a pressure gauge, allowing for accurate determination of completion and monitoring of line stability during sample collection. At the commencement of each

series of extractions, line vacuum pressures at all stations were consistently ≤ 5 mTorr, well within the 60 mTorr recommended by West *et al.* (2006). All leaf, xylem and soil samples were extracted for at least 2 hr to avoid $^2\text{H}/^1\text{H}$ fractionation during distillation.

6.4.2 Water isotopic analysis

Hydrogen isotope signatures of extracted waters were measured using a Delta XP ThermoFisher isotope-ratio mass spectrometer interfaced with a pyrolysis TC/EA equipped with a liquid autosampler. The $\delta^2\text{H}$ values reported here are based on ten analytical replicates of each sample. The first five replicates of each sample were discarded to prevent distortion by memory effects associated with the use of the liquid autosampler. The $\delta^2\text{H}$ values are expressed relative to the VSMOW scale based upon analysis of a suite of international and in-house standards analysed in the same sequence with the water samples. Additional international and in-house standards (e.g. USGS 67400, Norwich tap water) were treated as unknowns and analysed throughout the run to evaluate instrument accuracy. Root mean square (RMS) errors for $^2\text{H}/^1\text{H}$ measurements of international and in-house standards were 1.0‰ ($n = 105$) (standard measurements in Appendix 5).

During all sample and standard measurements, three reference gas pulses were passed through the mass spectrometer. Reproducibility of H_2 reference gas $\delta^2\text{H}$ values after H_3^+ correction was typically $\pm 0.5\%$. Typical standard error among analytical replicates of the same sample was 4‰, while comparison of mean values for leaf and xylem sample duplicates showed that the absolute difference between them was in all cases also less than 4‰. Soil sample duplicates could not be successfully processed for all sampling intervals due to difficulties in extracting sufficient amounts of water from them for reliable stable isotope measurements. However when they were possible, mean values did not vary by more than 4‰ among sample replicates. A conservative approach was therefore adopted, and it was assumed that variability for all singular soil water samples presented here did not exceed 4‰.

6.4.3 *n*-Alkane extraction and identification

Leaf wax lipids were extracted in the manner previously described in Chapter 4.

6.4.4 *n*-Alkane hydrogen isotope analysis

The $^2\text{H}/^1\text{H}$ composition of *n*-alkanes was determined using a Delta V Advantage ThermoFisher isotope-ratio mass spectrometer interfaced with GC-Isolink Trace GC Combustion and High temperature conversion (HTC) system operating at 1420 °C. The initial GC oven temperature was set at 50 °C, which was then raised at a rate of 30 °C min⁻¹ to 220 °C. A second temperature ramp to a final temperature of 320 °C at a rate of 6 °C min⁻¹ followed. The final temperature was held for 5 min. The $\delta^2\text{H}$ values are based on duplicate analyses of well-resolved peaks and reported on the VSMOW scale, based on in-house reference gases (H_2 , >99.995% purity, BOC) adjusted at the beginning and at the end of each sequence using a standard mixture of the *n*-C₁₆ to *n*-C₃₀ alkane standard. Root mean square (RMS) errors for $^2\text{H}/^1\text{H}$ measurements of this standard were 4.0‰ ($n = 780$). During all sample and standard measurements, six reference gas pulses were passed through the mass spectrometer. Reproducibility of H_2 reference gas $\delta^2\text{H}$ values after H_3^+ correction was $\pm 6\%$. Typical absolute differences in *n*-C₂₉ measurements between analytical replicates of the same sample did not exceed 6‰, while absolute differences in mean values among sample replicates of the same species (an indicator of intraspecies variability) was on average 4‰, with a maximum of 10-14‰ for *Atriplex portulacoides* (August 2012), *Phragmites australis* (September 2012) and *Suaeda vera* (September 2012).

6.5. RESULTS

6.5.1 Soil water $^2\text{H}/^1\text{H}$ composition

Soil water from the sandflat was most ^2H -depleted in March (-27‰) and most ^2H -enriched in May (+2‰) (Table 6.2). Between May and September 2012, soil water from the sandflat remained constant within analytical error, varying by only 3‰. Upper marsh soil water samples were not successfully stored for March, however, similar seasonal consistency to that observed in the sandflat was revealed when comparing the May (+2‰) and September (-2‰) soil water samples taken from this location. The greatest seasonal shift in soil water at the site was found at the ridge, where values ranged from -36‰ in March to -5‰ in September (Table 6.2). Soil waters collected before 8:00 in September 2012 had a mean value of -21‰, indicating they were 16‰ ^2H -depleted compared with samples collected between 12:00-14:00 (Fig. 6.2; Appendix 5).

Table 6.1: $\delta^2\text{H}$ for *n*-alkanes and leaf water, and calculated hydrogen isotope fractionation; June 2011

Location	Plant Species	Plant type	$\delta^2\text{H } n\text{-C}_{27}$	AD*	$\delta^2\text{H } n\text{-C}_{29}$	AD*	$\delta^2\text{H } n\text{-C}_{31}$	AD*	$\delta^2\text{H}_{\text{Leaf water}}$	SE _{leaf water}	$\epsilon_{\text{wax/ leaf water}} (\text{‰})$
Site 1	<i>Spartina anglica</i>	C4 grass	-144	3	-157	3	-164	2	27	1	-179
Site 1	<i>Triglochin maritima</i>	C ₃ perennial herb	-124	1	-133	0	-134	1	22	0	-152
Site 1	<i>Salicornia Europaea</i>	C ₃ succulent	-131	6	-132	0	-127	2	29	0	-156
Site 1	<i>Limonium vulgare</i>	C ₃ perennial herb	-116	7	-113	6	-115	6	30	0	-139
Site 1	<i>Atriplex portulacoides</i>	C ₃ evergreen shrub	-131	1	-127	1	-117	0	25	0	-148
Site 2	<i>Elytrigia atherica</i>	C ₃ grass	-197	4	-211	1	-220	2	15	0	-223
Site 2	<i>Phragmites</i>	C ₃ reed	-173	3	-179	1			5	0	-183
Site 2	<i>Puccinella maritima</i>	C ₃ grass	-187	6	-206	1	-210	1	5	0	-210
Site 2	<i>Suaeda vera</i>	C ₃ evergreen succulent	-118	1	-119	1	-115	3	21	0	-137
Site 2	<i>Atriplex portulacoides</i>	C ₃ evergreen shrub	-141	7	-140	9	-135	11	21	1	-158
Site 3	<i>Triglochin maritima</i>	C ₃ perennial herb	-138	9	-135	1	-138	1	32	0	-162
Site 3	<i>Suaeda vera</i>	C ₃ evergreen succulent	-110	0	-116	1	-114	0	27	0	-139
Site 3	<i>Limonium vulgare</i>	C ₃ perennial herb	-117	2	-114	3	-116	4	24	0	-135
Site 3	<i>Atriplex portulacoides</i>	C ₃ evergreen shrub	-134	2	-132	3	-126	1	34	0	-161

* "AD" is the absolute difference between the measured values of the two duplicates

Table 6.2: $\delta^2\text{H}$ for *n*-alkanes, leaf water, soil water and xylem water, with calculated hydrogen isotope fractionation between soil water (sw), xylem water (xw) and leaf water (lw)

Month	Plant species	<i>n</i> -C ₂₇	AD	<i>n</i> -C ₂₉	AD	<i>n</i> -C ₃₁	AD	SW	AD	XW	AD	LW	AD	$\epsilon^2\text{H}_{\text{wax/sw}}$ (‰)	$\epsilon^2\text{H}_{\text{wax/xw}}$ (‰)	$\epsilon^2\text{H}_{\text{wax/lwr}}$ (‰)
March	<i>Atriplex portulacoides</i>	-142	1	-139	2	-128	4	-36	4	-	-	-20	1	-107	-	-121
	<i>Elytrigia atherica</i>	-195	2	-200	2	-197	1	-36	4	-	-	-20	1	-170	-	-184
	<i>Limonium vulgare</i>	-134	1	-124	1	-125	1	-	-	-	-	-26	1	-	-	-100
	<i>Spartina anglica</i>	-130	2	-137	1	-136	2	-26	2	-	-	-25	1	-114	-	-115
	<i>Suaeda vera</i>	-108	2	-97	2	-98	3	-36	4	-	-	-20	1	-63	-	-79
May	<i>Atriplex portulacoides</i>	-151	3	-149	1	-135	3	-33	2	-	-	12	1	-120	-	-159
	<i>Elytrigia atherica</i>	-226	5	-232	2	-232	5	-33	2	-	-	-4	1	-206	-	-229
	<i>Limonium vulgare</i>	-137	3	-121	2	-123	1	2	1	-	-	15	1	-123	-	-134
	<i>Phragmites</i>	-164	1	-178	3	-	-	-33	2	-	-	-8	1	-150	-	-172
	<i>Salicornia Europaea</i>	-141	3	-132	2	-133	1	2	1	-	-	9	1	-133	-	-140
	<i>Spartina anglica</i>	-146	4	-146	2	-141	4	2	1	-	-	10	1	-147	-	-154
	<i>Suaeda vera</i>	-130	1	-127	1	-123	2	-33	2	-	-	4	1	-97	-	-130
August	<i>Atriplex portulacoides</i>	-159	6	-152	6	-135	5	-	-	-	-	-5	1	-	-	-148
	<i>Elytrigia atherica</i>	-229	1	-235	1	-235	1	-	-	-	-	-8	1	-	-	-229
	<i>Limonium vulgare</i>	-132	2	-115	2	-125	2	-	-	-	-	6	1	-	-	-121
	<i>Phragmites</i>	-184	3	-196	3	-	-	-	-	-	-	-15	1	-	-	-184
	<i>Salicornia Europaea</i>	-132	1	-131	1	-136	2	-	-	-	-	5	0	-	-	-136
	<i>Spartina anglica</i>	-158	1	-163	1	-161	3	-	-	-	-	13	1	-	-	-174
	<i>Suaeda vera</i>	-130	2	-129	2	-121	3	-	-	-	-	-4	1	-	-	-126
September	<i>Atriplex portulacoides</i>	-168	4	-166	3	-149	2	-5	1	-31	1	5	1	-162	-139	-170
	<i>Elytrigia atherica</i>	-229	3	-230	1	-232	1	-5	1	-43	2	-6	1	-226	-195	-227
	<i>Limonium vulgare</i>	-135	1	-125	4	-126	3	-2	1	-4	1	15	0	-138	-122	-138
	<i>Phragmites</i>	-201	9	-206	8	-	-	-5	1	-29	1	-2	0	-204	-182	-204
	<i>Salicornia Europaea</i>	-134	3	-127	4	-123	1	-1	0	-	-	20	1	-144	-	-144
	<i>Spartina anglica</i>	-153	4	-163	4	-148	2	-1	0	-9	1	15	1	-162	-155	-176
	<i>Suaeda vera</i>	-139	5	-141	6	-125	2	-5	1	-30	1	4	1	-137	-114	-144

* "AD" is the absolute difference between the measured values of the two duplicates

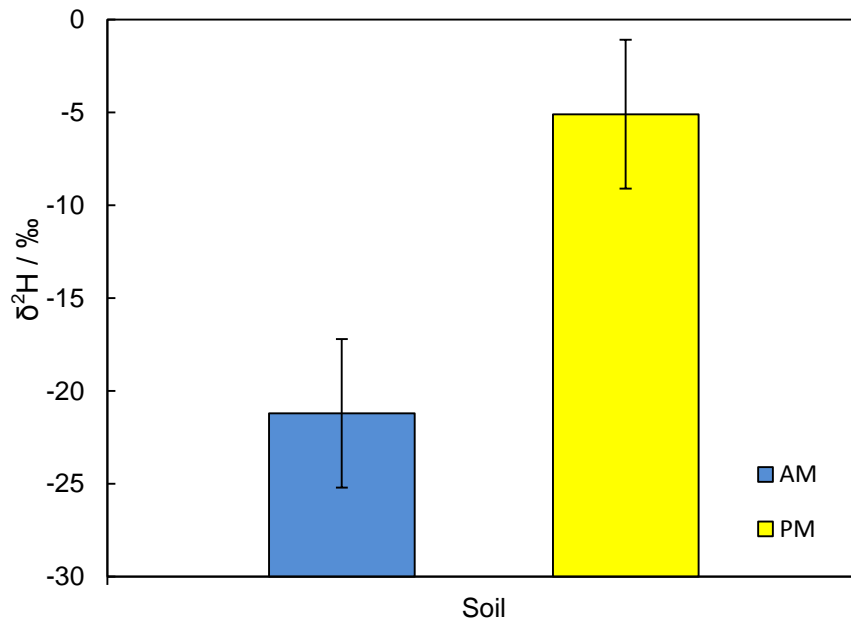


Figure 6.2: Comparison of soil water hydrogen isotope composition from AM (0:7:30 to 8:00) and PM (12:00 to 14:00). Error bars show assumed absolute differences between sample duplicates of 4‰.

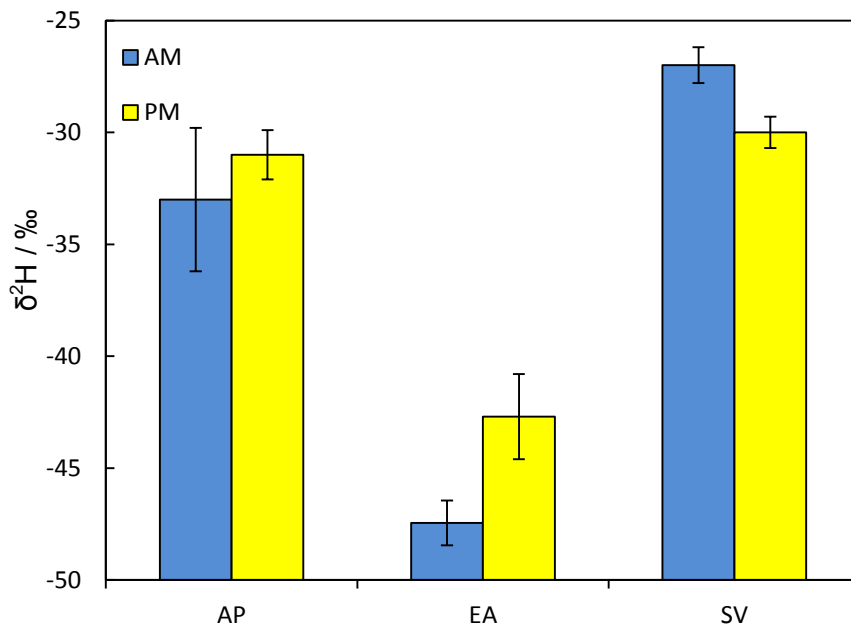


Figure 6.3: Comparison of xylem water hydrogen isotope composition from AM (0:7:30 to 8:00) and PM (12:00 to 14:00). Error bars show absolute differences between sample duplicates. Abbreviations: AP = *Atriplex portulacoides*; EA = *Elytrigia atherica*; SV = *Suaeda vera*.

6.5.2 Xylem water $^2\text{H}/^1\text{H}$ composition

Xylem samples collected from *Elytrigia atherica*, *Atriplex portulacoides* and *Suaeda vera* at the ridge site in September 2012 (a) between 7:30 and 8:00, and (b) between 12:00 and 14:00, varied by no more than 2-3‰. This was lower than both analytical reproducibility (4‰) and intraspecies variability in $^2\text{H}/^1\text{H}$ isotopic composition (4‰). The range of xylem water values among the species sampled in the early morning was 20‰, which was slightly higher than that observed among xylem water samples collected between 12:00 and 14:00 (13‰) (Fig. 6.3; Appendix 5). Xylem waters from the September 2012 sampling interval showed that stem waters were more negative than the soil waters across all sampling sites (Fig. 6.4). *Elytrigia atherica* had the most negative xylem water of all species sampled (-43‰), while *Limonium vulgare* had the most positive (-4‰). Total interspecies variation in xylem water $\delta^2\text{H}$ was 39‰ (Table 6.2).

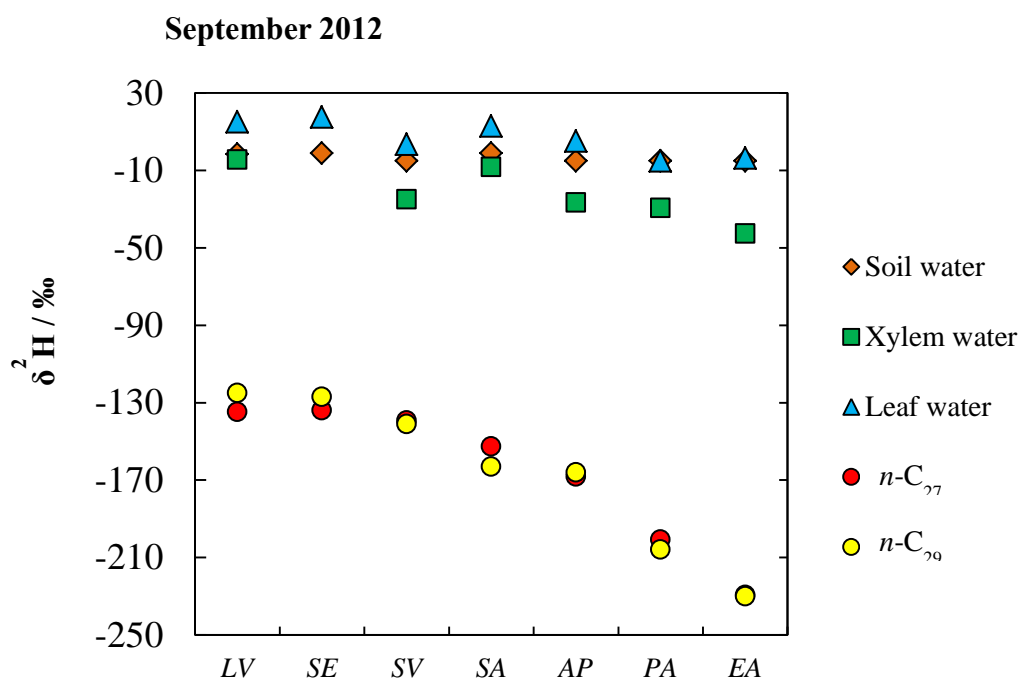


Figure 6.4: Measured soil water $\delta^2\text{H}$, xylem water $\delta^2\text{H}$, leaf water $\delta^2\text{H}$, and n -alkane $\delta^2\text{H}$ values from all species sampled in September 2012. LV = *Limonium vulgare*, SE = *Salicornia europaea*, SV = *Suaeda vera*, SA = *Spartina anglica*, AP = *Atriplex portulacoides*, PA = *Phragmites australis*, EA = *Elytrigia atherica*. The standard error did not exceed 2‰ for soil, xylem, leaf waters and 9‰ for n -alkane measurements.

6.5.3 Leaf water $^2\text{H}/^1\text{H}$ composition

Leaf waters extracted from all species collected at Stiffkey in June 2011 (Table 6.1) varied by no more than 29‰. For those species sampled from multiple locations, upper marsh leaf water samples were generally more ^2H -enriched than those sampled from other locations, but the range of variation was low compared to gross interspecies differences: $\delta^2\text{H}_{\text{LW}}$ from *Atriplex Portulacoides* varied by 13‰ across the marsh, with the most ^2H -depleted leaf water found at the ridge site and the most ^2H -enriched in the upper marsh; $\delta^2\text{H}_{\text{LW}}$ from *Triglochin maritima* varied by 10‰ between the lower and upper marsh. Small shifts of 6‰ were observed in the evergreen succulent *Suaeda vera*, and the perennial herb *Limonium vulgare*, with the most ^2H -enriched value occurring in the upper marsh *Suaeda* and the lower marsh for *Limonium* (Fig. 6.5; Table 6.1).

Leaf water samples collected during 2012 (Table 6.2) showed a total range among all species sampled of 46‰ between the most ^2H -depleted values (-26‰, *Limonium vulgare*, March) and the most ^2H -enriched (+20‰, *Salicornia europaea*, September). Species-specific variation in leaf water $\delta^2\text{H}$ was most limited in March (6‰) and greatest in August (29‰). Leaf waters from all species were generally most ^2H -depleted in March, and ^2H -enriched in September. *Elytrigia atherica* and *Phragmites australis* were generally the most ^2H -depleted in terms of leaf water $\delta^2\text{H}$, whilst *Spartina anglica*, *Limonium vulgare* and *Salicornia europaea* were typically among the most ^2H -enriched. The exception to this overall pattern among species occurred in March, when all species were characterized by $\delta^2\text{H}$ values between -26‰ and -20‰ (Fig. 6.6; Table 6.2). These extremely negative leaf water $\delta^2\text{H}$ profiles were significantly different (Minitab v.16, student's t-test, $P < 0.05$, $n = 10$ individuals per sampling interval comparing those species growing from March to September 2012) to those observed for the same species in all other sampling intervals during 2012.

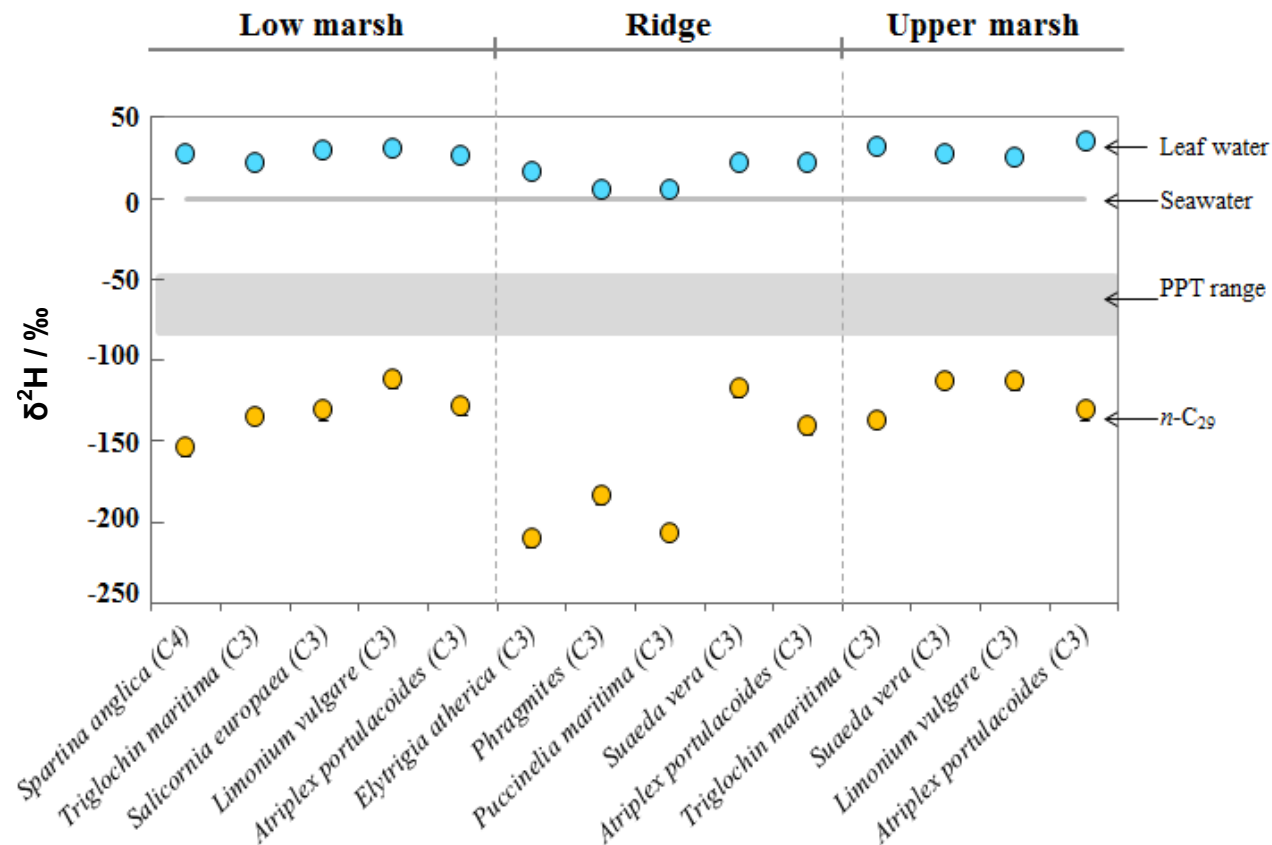


Figure 6.5: Measured $n\text{-C}_{29}$ alkane $\delta^2\text{H}$ (yellow circles) and leaf water $\delta^2\text{H}$ (blue circles) values for all plants sampled across the Stiffkey marsh in June 2011 ("C3" and "C4" refer to plant biochemical pathways). Predicted $\delta^2\text{H}$ values of seawater (grey line) and precipitation (grey shading) are also shown. Plants are grouped by sampling site (Low marsh, Ridge, Upper marsh). Each data point represents a collection of greater than five leaves from a minimum of three separate plants. Maximum standard error associated with these measurements was 5‰ for $n\text{-alkane}$ values and 1‰ for leaf waters. The isotopic composition of sea water (0‰) is highlighted by the straight grey line, whilst the grey shaded area illustrates the maximum seasonal range in precipitation $^2\text{H}/^1\text{H}$ composition estimated using the Online Isotopes in Precipitation Calculator (Bowen et al., 2005).

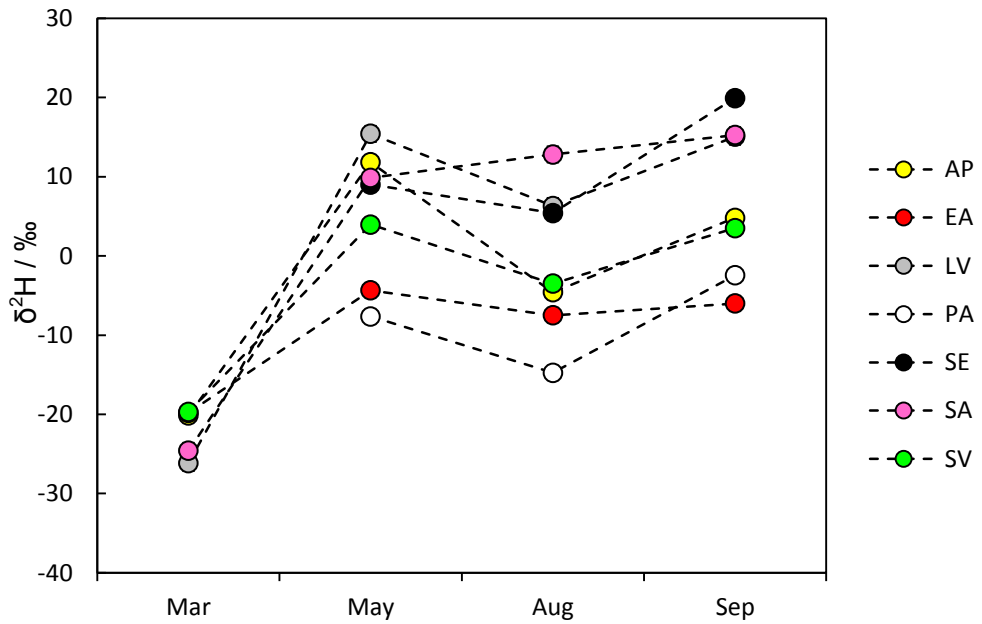


Figure 6.6: Leaf water $^2\text{H}/^1\text{H}$ from all species sampled across 2012. Absolute difference between sample duplicates did not exceed 2‰.

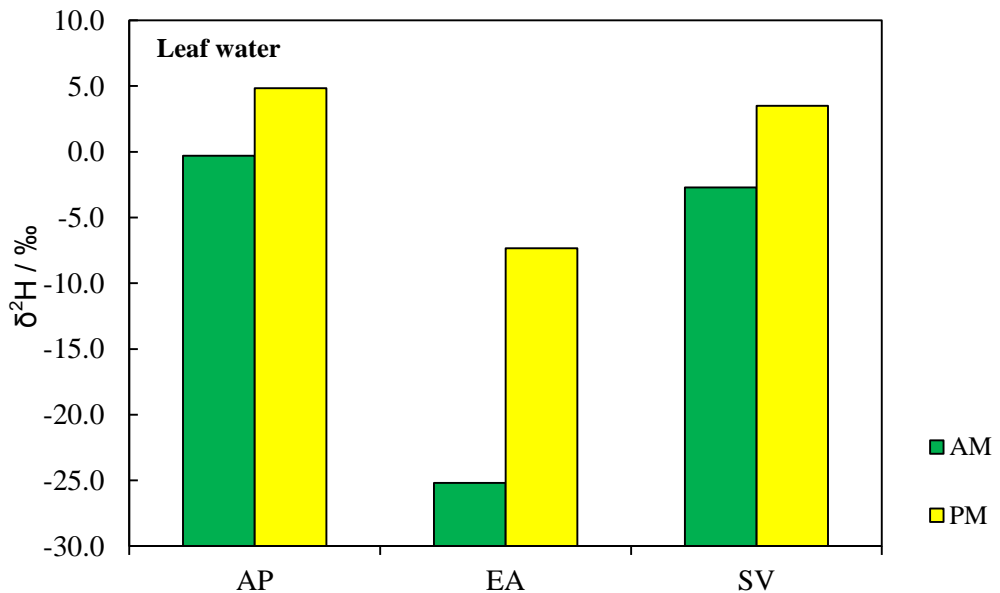


Figure 6.7: Measured leaf water $^2\text{H}/^1\text{H}$ for three species sampled at the ridge site between 7:30 and 8:00 and again between 12:00 and 14:00 on 7th September 2012. The maximum standard error associated with these measurements was 2‰.

Leaf water samples collected at 7:30-8:00 and 12:00-14:00 from *Elytrigia atherica*, *Atriplex portulacoides* and *Suaeda vera* at the ridge site allowed us to investigate diurnal shifts in leaf water isotopic composition. The C₃ grass *Elytrigia atherica* showed the greatest shift in the $\delta^2\text{H}$ of leaf water: it was 19‰ more positive at 12:00-14:00 than at 7:30-8:00. Leaf waters from two other plants showed a ²H-enrichment of only 5-6‰ (Fig. 6.7). Statistical analysis (Minitab v.16, 2013) of interspecies variation in leaf water isotopic composition at each sampling interval indicated that leaf water ²H/¹H was not significantly different (Mann-Whitney U test, P>0.05, n= 7 for comparison of species growing from March to September 2012; n= 5 for comparison of species growing from May to September 2012) among the Stiffkey species. However, *Phragmites australis*, the species that generally had the most ²H-depleted leaf water isotopic signatures, was an exception. Leaf water from *Phragmites* was significantly different from the C₄ grass *Spartina anglica*, and the C₃ species *Salicornia europaea*, *Limonium vulgare*, and *Atriplex portulacoides* (student's t-test, P<0.05, n=6 individuals per species), but could not be distinguished statistically from leaf water from the other C₃ monocot *Elytrigia atherica*.

6.5.4 *n*-Alkane ²H/¹H composition

Analysis of molecular distributions of *n*-alkanes from the sampled species (Chapter 4) showed that *n*-C₂₇ and *n*-C₂₉ alkanes were the most abundant across all species. Because *n*-C₂₇ and *n*-C₂₉ alkane $\delta^2\text{H}$ values were strongly correlated across the growing season (Fig. 6.8), only *n*-C₂₉ $\delta^2\text{H}$ values are focused on in all subsequent data analysis.

The mean *n*-C₂₉ $\delta^2\text{H}$ values from June 2011 showed a total interspecies variation of 98‰, with the C₃ grass *Elytrigia atherica* having the most ²H-depleted *n*-C₂₉ value and *Suaeda vera* the most ²H-enriched. Species collected from multiple sampling sites showed very limited micro-habitat dependent variation ranging from 1‰ (i.e. below the observed maximum intraspecies variability of 6‰ in *n*-C₂₉ ²H/¹H) (*Suaeda vera*) to 9‰ (*Atriplex portulacoides*). The greatest interspecies range in $\delta^2\text{H}_{n\text{-C}_{29}}$ was observed at the ridge site (93‰), while the lowest occurred in the upper marsh (24‰). *n*-C₂₉ from C₃ grasses was on average 45‰ more ²H-depleted than that from the C₄ *Spartina anglica*. Overall, the following pattern was observed for *n*-C₂₉ alkane $\delta^2\text{H}$ values: succulents > perennial herbs > evergreen shrubs > C₄ grass > C₃ monocots (Fig. 6.9, Tables 6.1 and 6.2).

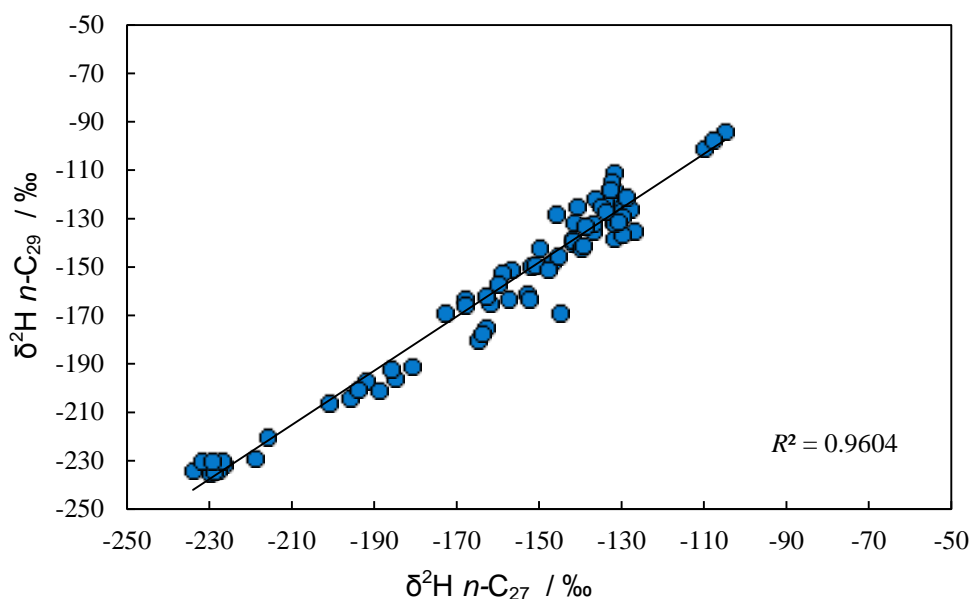


Figure 6.8: Bivariate plot of $n\text{-C}_{27}$ and $n\text{-C}_{29}$ alkane $\delta^2\text{H}$ values for all species sampled across the 2012 growth season showing a strong correlation between the two sets of data.

Mean $\delta^2\text{H}$ values of the $n\text{-C}_{29}$ alkane from the 2012 growing season were remarkably consistent for each individual species across the all sampling intervals (Fig. 6.9; Table 6.2). Seasonal variation from March – September was the highest in the evergreen succulent *Suaeda vera* (44‰), and the lowest in the annual succulent *Salicornia europaea* (5‰). For all other species, seasonal variation in their leaf wax $^2\text{H}/^1\text{H}$ composition fell within the range of 10-35‰. Statistical analysis (Minitab v.16, 2013) confirmed that these differences are not significant (Mann-Whitney U test, $P > 0.05$, $n=10$ for March 2012; $n=14$ for May, August and September 2012).

The greatest interspecies variation in $n\text{-C}_{29}$ occurred in August (120‰), however variability among species exceeded 100‰ for all 2012 study intervals (Fig. 6.9; Table 6.2). *Elytrigia atherica* and *Phragmites australis* consistently recorded the most negative $\delta^2\text{H}$ values. However, unlike the leaf water $^2\text{H}/^1\text{H}$ variation between these C_3 monocots – where *Phragmites australis* was generally more negative than *Elytrigia atherica* – the $n\text{-C}_{29}$ alkane $\delta^2\text{H}$ values of *Elytrigia* were between 23 and

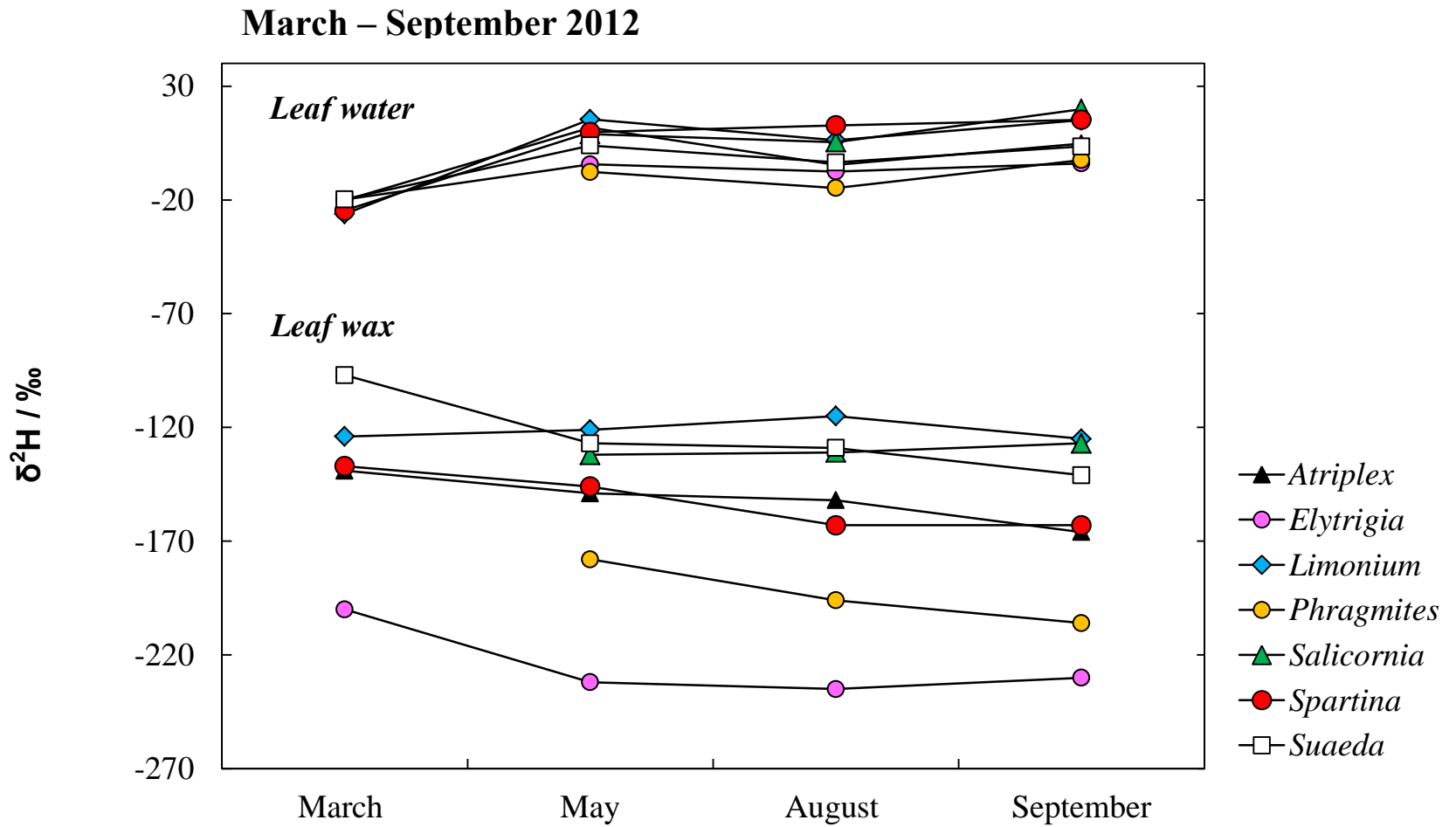


Figure 6.9: Seasonal variation in $n\text{-C}_{29}$ alkane $\delta^2\text{H}$ and leaf water $\delta^2\text{H}$ values for all plants sampled during the 2012 growth season. Each data point represents a collection of greater than five leaves from a minimum of three separate plants. The maximum standard error associated with these measurements was 8‰ for $n\text{-C}_{29}$ alkane and 2‰ for leaf water.

54‰ more negative than those of *Phragmites australis* across the entire growing season. In addition, the most ²H-enriched *n*-C₂₉ values were observed in *Suaeda vera*, *Limonium vulgare* and *Salicornia europaea*, with *Spartina anglica* – a species with one of the more positive leaf water δ²H values – having intermediate *n*-C₂₉ alkane δ²H values across all sampling intervals (Fig. 6.9). Cross-plotting the *n*-C₂₉ alkane δ²H data and ACL values (Fig. 6.10) for September 2012 did not show any correlation between these two parameters. Statistical analysis of interspecies variation in leaf wax hydrogen isotope compositions among all sampled species across the study period (Minitab v.16, 2013) revealed that the ²H/¹H values of waxes were significantly different among most species (Mann-Whitney U test, P<0.05, n=7 for species growing from March to September 2012; n=5 for species growing from May to September 2012). Notable exceptions include a) *Suaeda vera*, and *Limonium vulgare*, and b) the two succulents *Suaeda vera* and *Salicornia europaea*.

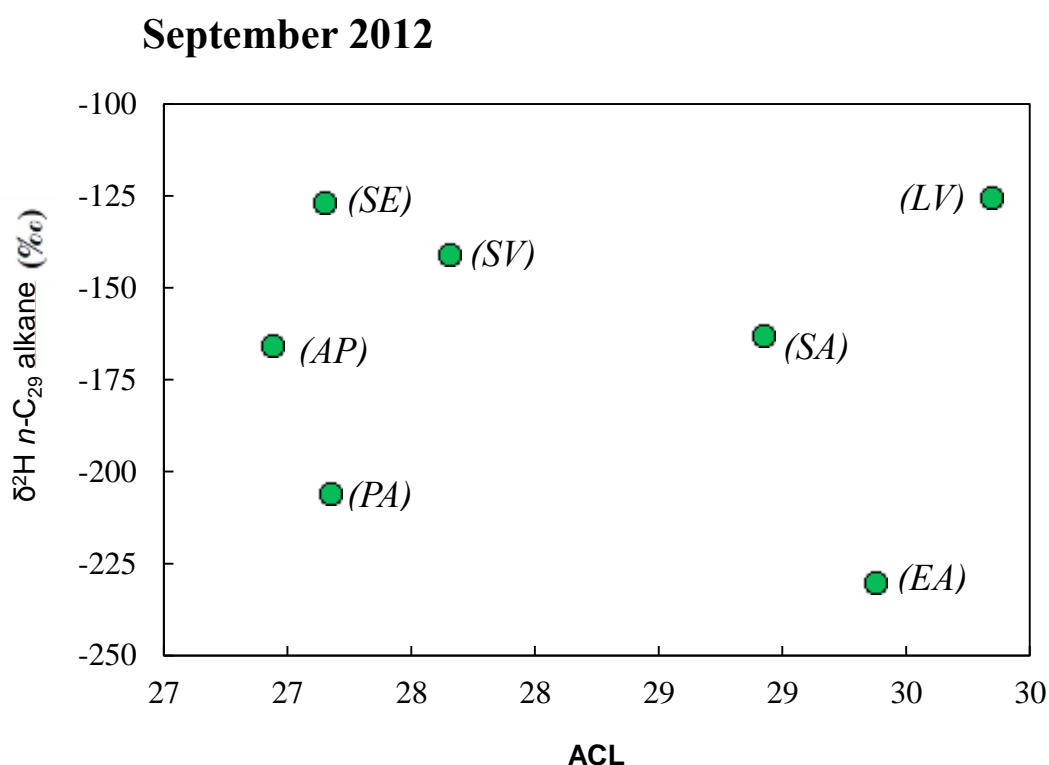


Figure 6.10: Bivariate plot of ACL and *n*-C₂₉ alkane δ²H (September 2012) showing no correlation between the two parameters. Letters in parenthesis denote plant species: AP = *Atriplex portulacoides*, EA = *Elytrigia atherica*, LV = *Limonium vulgare*, PA = *Phragmites australis*, SE = *Salicornia europaea*, SA = *Spartina anglica*, SV = *Suaeda vera*.

6.5.5 $^2\text{H}/^1\text{H}$ fractionation between soil, xylem and leaf water and $n\text{-C}_{29}$ alkane

Halophyte species are exceptions to the rule that plants do not fractionate environmental water during root uptake (Waisel, 1972; Ellsworth and Williams, 2007). ^2H -discrimination occurring during water uptake among the Stiffkey species was calculated using the approach of Ellsworth and Williams (2007) (Eq.1):

$$\Delta^2\text{H} = \delta^2\text{H}_{\text{soil water}} - \delta^2\text{H}_{\text{xylem water}}. \quad (\text{Eq. 1})$$

$\Delta^2\text{H}$ was the highest in the evergreen species *Atriplex portulacoides* and *Suaeda vera* for all halophyte species at Stiffkey (28‰) and the lowest in *Limonium vulgare* (4‰). The C_4 grass *Spartina anglica* had a ΔH value of 13‰. The values reported here exceed those of Ellsworth and Williams (2007), who only reported data from woody xerophytes.

Epsilon values were also calculated to approximate $^2\text{H}/^1\text{H}$ fractionation between mean $n\text{-C}_{29}$ $\delta^2\text{H}$ values and soil water ($\epsilon_{\text{wax/sw}}$), xylem water ($\epsilon_{\text{wax/xw}}$), and leaf water ($\epsilon_{\text{wax/lw}}$) using Equation 2, where $\delta^2\text{H}_{\text{water}}$ represents the hydrogen isotope composition of the leaf water or soil water as appropriate. Epsilon and delta values are reported in per mil (‰), and therefore this equation implies multiplication by 1000 (Cohen *et al.*, 2007).

$$\epsilon_{\text{wax/water}} = \frac{\left(\frac{^2\text{H}}{^1\text{H}}\right)_{\text{wax}}}{\left(\frac{^2\text{H}}{^1\text{H}}\right)_{\text{water}}} - 1 = \frac{(\delta^2\text{H})_{\text{wax}} + 1}{(\delta^2\text{H})_{\text{water}} + 1} - 1 \quad (\text{Eq. 2})$$

In June 2011, the total variation in ϵ between $n\text{-C}_{29}$ and leaf water exceeded 100‰ (Fig. 6.11 a and b). Similar differences were identified throughout the 2012 growing season when the total variation in $\epsilon_{\text{wax/lw}}$ exceeded 86‰ for all sampling intervals (Fig. 6.12). The greatest range in $\epsilon_{\text{wax/lw}}$ during the growing season was observed in August (109‰), and the lowest in September (86‰). The C_3 grass *Elytrigia atherica* consistently had the lowest $\epsilon_{\text{wax/lw}}$ value (-184 to -229‰), whilst *Suaeda vera* and

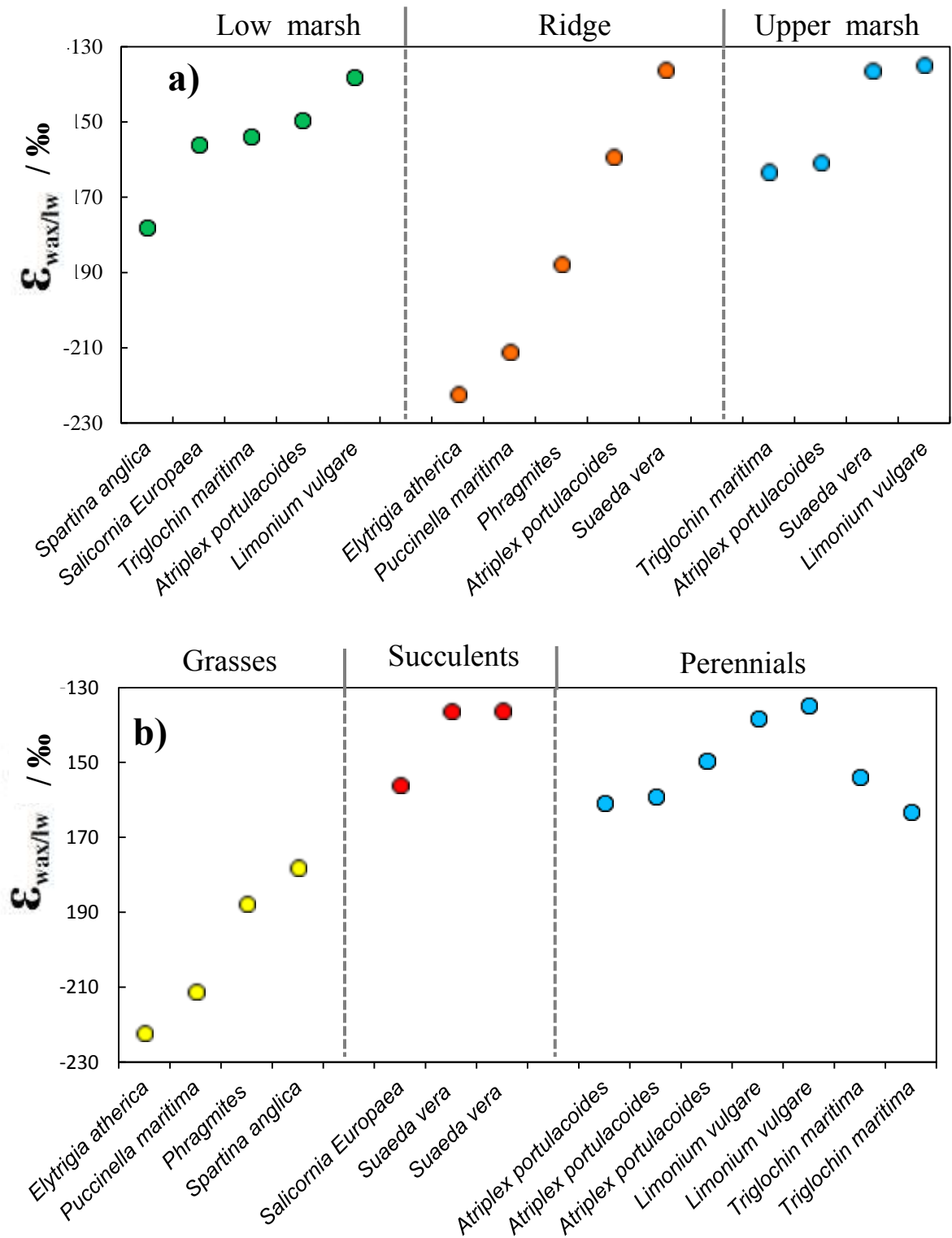


Figure 6.11: Calculated fractionation ($\epsilon_{wax/lw} \text{‰}$) between $n\text{-C}_{29}$ alkane $\delta^2\text{H}$ and leaf water $\delta^2\text{H}$ from samples collected in June 2011 at Stiffkey saltmarsh. Plants are grouped according to a) sampling locations and b) the plant types.

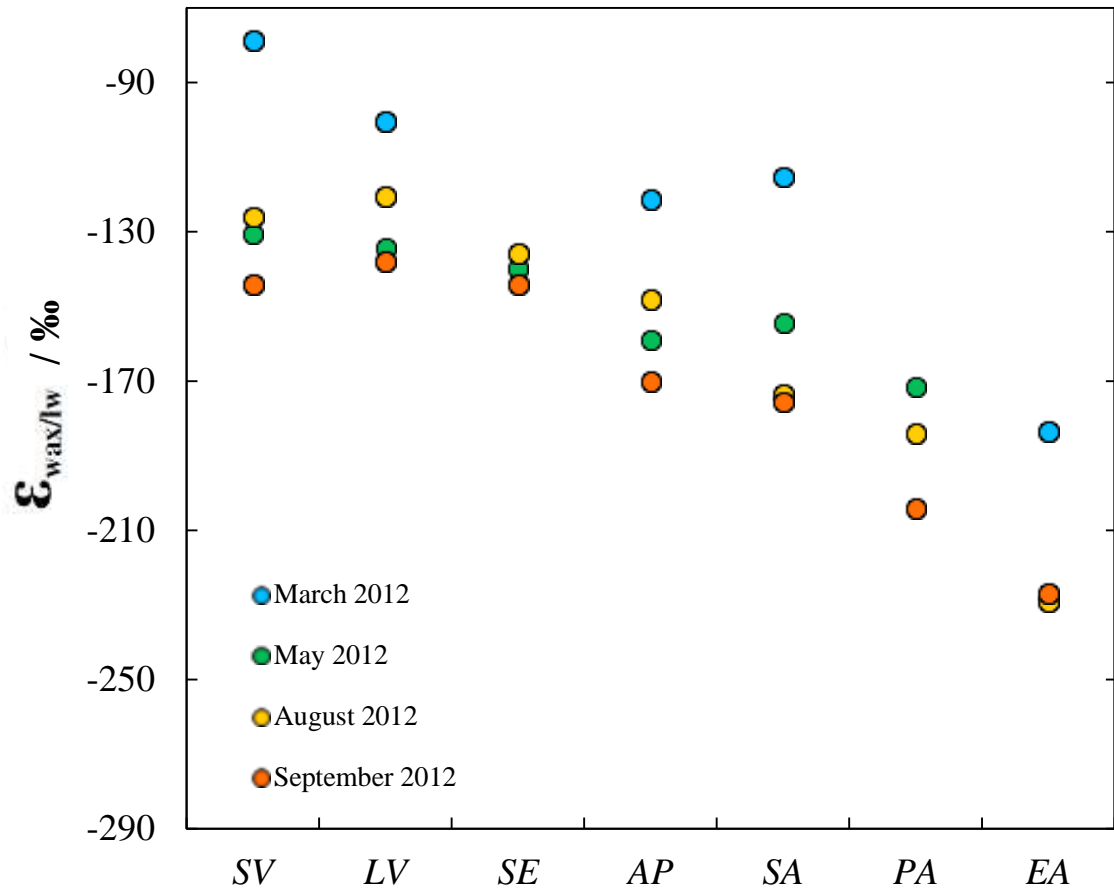


Figure 6.12: Calculated fractionation ($\epsilon_{\text{wax/lw}}$ ‰) between $n\text{-C}_{29}$ alkane $\delta^2\text{H}$ and leaf water $\delta^2\text{H}$ from samples collected across the 2012 growth season at Stiffkey saltmarsh. SV = *Suaeda vera*, LV = *Limonium vulgare*, SE = *Salicornia europaea*, AP = *Atriplex portulacoides*, SA = *Spartina anglica*, PA = *Phragmites australis*, EA = *Elytrigia atherica*.

Limonium vulgare recorded the highest (-79 to -144‰). Across all species, there was a general trend for $\epsilon_{\text{wax/lw}}$ to become lower as the growing season progresses (Fig. 6.12; Table 6.2). The variation in fractionation factors calculated for the plant species at Stiffkey is the largest range in $\epsilon_{\text{wax/lw}}$ reported to date for saltmarsh environments (c.f. Romero and Feakins, 2011). $\epsilon_{\text{wax/sw}}$ values for species growing at the three sites in 2012 ranged from -64‰ for *Salicornia* in March to -228‰ for *Elytrigia atherica* in September. $\epsilon_{\text{wax/sw}}$ variability among the different plant species exceeded 89‰ throughout the growing season.

The C_4 grass, *Spartina anglica*, has $\epsilon_{\text{wax/lw}}$ values that are higher (by up to 74 ‰) than those observed for the C_3 grass *Elytrigia atherica*. When the *Spartina* data are compared with other C_3 species collected in March and May 2012, $\epsilon_{\text{wax/lw}}$ for

Spartina anglica is only 5-6‰ higher than in *Atriplex portulacoides*, although it is 15-36‰ lower than the apparent fractionation observed in *Suaeda vera* and *Limonium vulgare*. As the growth season progresses, the difference in $\epsilon_{\text{wax/lw}}$ among these species increases: in August, where the maximum variation is observed, the $^2\text{H}/^1\text{H}$ fractionation between leaf water and leaf wax $n\text{-C}_{29}$ in *Spartina* is between 25 and 53‰ lower than these other C_3 shrubs and herbs (Fig. 6.12).

6.5.6 Relationship between carbon and hydrogen isotope composition of n -alkanes

Comparison of the carbon (Chapter 5) and hydrogen composition of the $n\text{-C}_{29}$ alkanes from C_3 species sampled during the 2012 growing Stiffkey species revealed no significant correlation (Rank Spearman correlation, $P > 0.05$, Minitab v.16, $n=26$). Neither were any statistically significant correlations observed when weighted averages (calculated for $^2\text{H}/^1\text{H}$ composition as described in Chapter 5) were compared. When the carbon isotope composition of $n\text{-C}_{29}$ was compared with the $^2\text{H}/^1\text{H}$ composition of leaf water for C_3 species sampled over the same period, however, a positive relationship was observed ($r = 0.5$, $P < 0.05$, Rank Spearman correlation, Minitab v. 16, $n = 26$). A statistically significant negative correlation was also observed when $\Delta^{13}\text{C}$ values (previously reported in Chapter 5) were compared with leaf water $\delta^2\text{H}$ signals ($r = -0.5$, $P < 0.05$, Rank Spearman correlation, Minitab v.16).

6.6. DISCUSSION

Many previous studies have sought to explain variation in n -alkane $^2\text{H}/^1\text{H}$ composition among different plant species by reference to the physical processes that control the movement of water molecules inside, outside and within the leaf. If it is assumed that interspecies variation in leaf wax lipid $\delta^2\text{H}$ is primarily driven by differences in the isotopic composition of leaf water, it follows that the $> 100\%$ range in n -alkane $^2\text{H}/^1\text{H}$ compositions observed in this study should be accounted for by a series of scenarios which affect leaf water $\delta^2\text{H}$. These mechanisms include: (i) differences in the isotopic composition of soil water among the three marsh sub-environments; (ii) differences in the isotopic composition of soil water throughout the growing season; (iii) interspecies differences in the isotopic composition of xylem water, reflecting root uptake of soil water and transport to the leaf, and; (iv)

interspecies differences in the isotopic composition of leaf water among plant life forms due to differences in leaf structure, affecting the transpiration of water within the leaf. Each of these scenarios will be considered below, to assess whether they can account for the variation observed in $\delta^2\text{H}_{n\text{-C}_{29}}$ among the Stiffkey plants.

6.6.1 The significance of spatial differences in soil water

Salt marshes are of great significance in lowland coastal regions (Allen, 2000) and represent important depositional environments because they are divisible into discrete micro-environmental zones based on topography and tidal inundation (Vince and Snow, 1984). This characteristic makes salt marshes ideal for studying plant/environment interactions (Vince and Snow, 1984; Romero and Feakins, 2011). Soils and sediments at Stiffkey receive water inputs from two sources: Sea water, which inundates the lower marsh and low-lying areas of the upper marsh daily; and meteoric precipitation, which is especially important on the ridge where no tidal inundation occurs. Previous studies (Romero and Feakins, 2011) have shown that environmental water varies in isotopic composition across salt marsh sites. The data presented here from 2012 demonstrates that this is also true of Stiffkey (Table 6.2) showing that the LM and UM (both sites that regularly receive inputs of saline water) have relatively similar isotopic compositions of source water (-2‰ to +2‰ between May and September 2012). Soil water $^2\text{H}/^1\text{H}$ from the ridge at Stiffkey is up to 35‰ lower than the other two sampling sites.

Despite these spatial changes in the isotopic composition of environmental water, large variations in the $\epsilon_{\text{wax/lw}}$ values observed within each sub-environment at Stiffkey (LM, R, UM) in June 2011 (Fig. 6.11) suggest that source water isotopic composition is not a major factor controlling the hydrogen isotope signals preserved in the $n\text{-C}_{29}$ alkane. This is supported by the limited variation observed in leaf water and n -alkane samples from selected plant species sampled in June 2011. Although no soil waters were collected in June, sampling of species growing in more than one location at Stiffkey allows for evaluation of the impact of marsh sub-environment on the $^2\text{H}/^1\text{H}$ composition of leaf waters and leaf wax lipids. In theory, if spatial variation in environmental water across these sub-environments is significant, one would expect samples of the same individual species from multiple sites to have different $\delta^2\text{H}$ leaf water and n -alkane compositions. Minor discrepancies in leaf water are observed in each species depending upon the particular sub-environment, for example 13‰ between *Atriplex portulacoides* at the R and UM sites and 10‰

between *Triglochin maritima* at the LM and UM sites; Fig. 6.5). However, the magnitude of this spatial variability is insignificant when compared with the range of interspecies $\delta^2\text{H}_{\text{lw}}$ values observed across the marsh as a whole (29‰).

Differences in mean $\delta^2\text{H}_{n\text{-C}_{29}}$ values for these species also show insignificant variation depending on sampling site – *Limonium*, *Triglochin* and *Suaeda* all vary by less than 5‰ between the LM and UM, while *Atriplex* shifts isotopically by 12‰ (Fig. 6.5; Table 6.1). Again, the magnitude of these site-specific isotopic differences in individual species is negligible when compared with the ~100‰ interspecies variation in $\delta^2\text{H}_{n\text{-C}_{29}}$ among all sampled plants. In addition, $\epsilon_{\text{wax/lw}}$ values from *Suaeda*, and *Limonium* show remarkable consistency across multiple sampling sites, with the maximum site-specific variation in one species (10‰ in *Triglochin*; 11‰ in *Atriplex*) an order of magnitude less than the total range in $\epsilon_{\text{wax/lw}}$ observed in the data set as a whole (Fig. 6.11 a and b). Differences in the isotopic composition of soil water among site sub-environments cannot, therefore, explain interspecies variation in leaf water or *n*-alkane $^2\text{H}/^1\text{H}$ composition.

6.6.2 The significance of temporal differences in soil water

In order to examine the influence of environmental water fully, it is important to consider whether differences in plant growth strategy expose them to seasonal variation in the source water $\delta^2\text{H}$ signal. There is conflict in previous research over whether the *n*-alkane $^2\text{H}/^1\text{H}$ is “locked in” at the beginning of the growing season or continually shifts in response to environmental or biological stimuli. Sachse *et al.* (2010) concluded that the *n*-alkane $\delta^2\text{H}$ values for field-grown barley were fixed early during the growing season and did not show seasonal shifts as the plants matured. A similar conclusion was reached by Tipple *et al.* (2013), who analysed the $^2\text{H}/^1\text{H}$ composition of *n*-alkanes, stem water, and leaf water from the riparian angiosperm *Populus angustifolia* throughout a growing season. Leaf water values showed considerable seasonal variation of 55‰, however, *n*-alkane $\delta^2\text{H}$ values remained relatively consistent in the mature leaf. This was interpreted to reflect the fixing of the *n*-alkane $\delta^2\text{H}$ signal during the bud break period, where new waxes are produced from water and stored sugars, suggesting that the *n*-alkane $^2\text{H}/^1\text{H}$ composition reflected these mixed biosynthate sources rather than providing an integrated signal of the growing season as a whole. In contrast, other studies propose that leaf waxes turnover continuously. Jetter and Schäffer (2006) considered that wax production was dynamic, with turnover and recycling of

dominant compound classes during leaf development. Gao *et al.* (2012) sought to quantify regeneration rates of leaf wax compounds by the application of isotopically labelled irrigation water, and concluded that $n\text{-C}_{27} - n\text{-C}_{31}$ n -alkanes are replaced over a timescale of 71-128 days in the grass species *Phleum pratense*.

Plant species growing at the Stiffkey study site are regularly exposed to strong winds from the North Sea, in combination with rain, and tidal inundation. These environmental factors are likely to abrade waxes from the surface of leaves, which means plants have to produce further wax to maintain their protective coating (Shepherd and Griffiths, 2006; Kahmen *et al.*, 2013). Given their exposed coastal location, it is likely that plants growing at Stiffkey were regularly required to replenish their leaf waxes throughout the growing season. On that basis, it was possible to hypothesise that if plants at Stiffkey were synthesising their leaf waxes at different times of year, they may be utilising soil water with different $^2\text{H}/^1\text{H}$ compositions. Temporal variation in soil water isotopic composition (-36‰ in March, $+2\text{‰}$ in May 2012) was therefore examined to evaluate whether these shifts could adequately account for the interspecies variation in leaf wax $\delta^2\text{H}$ observed in this dataset.

Plants at Stiffkey are known to have varied growth strategies. *Suaeda vera*, for example, is an evergreen succulent (Schirmer and Breckle, 1982), *Atriplex portulacoides* is an evergreen shrub (Corerria das Neves *et al.*, 2008), whilst *Limonium vulgare* (Boorman, 1967), *Spartina anglica* and *Phragmites australis* (Burke *et al.*, 2000) are all perennials (the latter two species are grasses, while the former is a flowering perennial). In addition to the soil water data presented here, mean monthly interpolated $\delta^2\text{H}$ profiles of meteoric water at Stiffkey, obtained using the Online Isotopes in Precipitation Calculator (OIPC), version 2.2 (Bowen *et al.*, 2005), were also used for consideration of this temporal parameter (Appendix 5).

In order to evaluate the importance of temporal changes in soil water isotope composition, it is first necessary to consider sources of water inputs at the marsh. At the LM and UM sites, seawater is the main source and is assumed to have an invariant isotopic value throughout the year (see for example Sessions, 2006). At Site 3 seawater ingress is through a dendritic network of tidal channels (Figure 2.1 in Chapter 2), and the proliferation of *Triglochin maritima* and *Salicornia europaea*, species known to require saline water, attest to the importance of sea-water inputs in the upper marsh (Allison, 1992; Davy and Bishop, 1991). However, early in the

growing season, March soil water $\delta^2\text{H}$ from the lower marsh shows a considerably ^2H -depleted relative to other sampling intervals. Examination of local weather station monitoring data (MIDAS, UK Meteorological Office) shows that on the day of sampling rainfall occurred at the site before sampling and after the last high tide. The estimated value for $\delta^2\text{H}$ of precipitation in North Norfolk in March is c. -62‰ (OIPC), and assuming a seawater $\delta^2\text{H}$ value of 0‰ , rainfall is therefore likely to have contributed $\sim 40\%$ of the $^2\text{H}/^1\text{H}$ soil water signal in this sample. It is probable, however, that with the next high tide, the importance of this meteoric water input would be negated. The $\delta^2\text{H}$ data from May and September 2012 support this, as they have a 'near-seawater' isotopic signature, ranging from -2 to $+2\text{‰}$ (Table 6.2). Therefore, regardless of the season during which LM and UM plant species synthesised leaf waxes, temporal isotopic shifts in soil water cannot explain interspecies variation in the $n\text{-C}_{29}$ alkane $\delta^2\text{H}$ values observed in these two locations.

In contrast, the ridge is only rarely inundated by tides and is potentially influenced more strongly by meteoric precipitation. Indeed, this is thought to account for the fact that the most ^2H -depleted soil water is found at this site (Table 6.2). Examination of mean monthly interpolated $\delta^2\text{H}$ values of meteoric water at the Stiffkey site (Appendix 5) for the sampling periods show, however, modelled precipitation $^2\text{H}/^1\text{H}$ ranges from -62‰ (March) to -48‰ (September). Soil waters from the ridge are consistently more ^2H -enriched than these meteoric precipitation $\delta^2\text{H}$ profiles, which is attributed to two likely causes. Firstly, as daytime temperatures rise during the growing season, soil evaporation will increase, particularly from the near-surface depths sampled, resulting in increasing ^2H -enrichment in the remaining pore water. Secondly, as the water table at the site is relatively high, an upwards movement of water through soil capillaries ("capillary rise", Plaster, 2009), particularly during warmer summer months, may carry ^2H -enriched seawater towards the soil surface (Plaster, 2009). When these temporal shifts in environmental water $^2\text{H}/^1\text{H}$ composition are considered in the context of the interspecies variability in leaf wax n -alkane hydrogen isotope compositions observed at this particular sampling site, however, it is clear that temporal variation in the isotopic composition of soil water and precipitation cannot explain the $\delta^2\text{H}_{n\text{-C}_{29}}$ range among the ridge species. In this study, soil water $\delta^2\text{H}$ varied by 31‰ at the ridge across the 2012 growth season, while the average interspecies range in $\delta^2\text{H}_{n\text{-C}_{29}}$ consistently exceeded 100‰ .

In addition to consideration of seasonal shifts in the isotopic composition of environmental water, soil samples collected from the ridge between 7:30 and 8:00 on the 7th of September 2012 (Fig. 6.2) allowed for investigation of diurnal changes in soil water $\delta^2\text{H}$. Sachse *et al.* (2010) suggested that one reason a direct 1:1 relationship was not observed between the $\delta^2\text{H}$ of midday leaf water and $\delta^2\text{H}_{n\text{-C}_{29}}$ in barley was that plants were synthesising these compounds from water that had not been subjected to diurnal ^2H -enrichment. In this study, the hydrogen isotope signature of soil water from the ridge between 7:30 and 8:00 was 16‰ lower compared with soil samples collected between 12.00 and 14.00 (Fig. 6.2), while leaf waxes from species sampled at the ridge in September varied by ~90‰ (Fig.6.9; Table 6.2). Therefore, diurnal variation in environmental water also cannot explain the range in interspecies $\delta^2\text{H}_{n\text{-C}_{29}}$ observed in the coastal plants at Stiffkey.

6.6.3 The significance of soil water uptake by halophytes and non-halophytes

Sachse *et al.* (2010) considered the possibility of a ^2H -depleted pool of water occurring in plants as a source of hydrogen for lipid synthesis, whereas McInerney *et al.* (2011) suggested that xylem water could be used by the plant in preference to leaf waters for lipid biosynthesis. Xerophytes and halophytes are exceptions to the general rule that isotopic fractionation does not occur during water uptake by plants (Ellsworth and Williams, 2007). In these drought and salinity tolerant plants, the mechanism of water uptake by roots is via the symplastic pathway, requiring transport from cell to cell. This transport from cytoplasm of one cell to cytoplasm of the next cell requires energy, and hence leads to diffusional $^2\text{H}/^1\text{H}$ fractionation of water molecules, with xylem waters becoming ^2H -depleted relative to environmental water (Ellsworth and Williams, 2007). For the purposes of this study, it is assumed that the isotopic composition of water in the xylem will reflect the composition of root water, and hence express any fractionation occurring during uptake.

Xylem waters collected between 12:00 and 14:00 at Stiffkey on the 7th of September 2012 allowed for consideration of whether interspecies variation in fractionation occurring during water uptake ($\Delta^2\text{H}$) can explain the variation in $\delta^2\text{H}_{n\text{-C}_{29}}$ in this data set. $\Delta^2\text{H}$ values for the Stiffkey halophytes (those species with an Ellenberg value in excess of 4) show a much greater range than that published by Ellsworth and Williams (2007); however the maximum fractionation observed for *Atriplex portulacoides* is still only 28‰, compared with a minimum fractionation of 4‰ in *Limonium vulgare* (Fig. 6.3). This variation in fractionation during water uptake does

not explain the 41‰ difference between their $\delta^2\text{H}_{n\text{-C}_{29}}$ values. Equally, *Atriplex portulacoides* and *Suaeda vera* growing on the ridge have the same $\Delta^2\text{H}$ values (28‰), but their $\delta^2\text{H}_{n\text{-C}_{29}}$ values differ by 25‰ (Table 6.2; Fig. 6.4).

Some species at Stiffkey are merely salt tolerant and not classified as true halophytes. These include the common reed *Phragmites australis* (Hill *et al.*, 1999; Mauchamp and Mésleard, 2001) and *Elytrigia atherica* (Hill *et al.*, 1999). Interestingly, these species also show xylem water values more negative than the soil water at their sampling location at the ridge site (Table 6.2). Because these plants are not true halophytes, it is unlikely that this is due to their utilisation of the symplastic pathway. Rather, it is suggested that this phenomenon arises from these species having rooting depths below that sampled for soil water, i.e. deeper than c. 10 cm. This would allow them to take up water that has not been subjected to evaporative ^2H -enrichment. *Phragmites australis* in particular has been known to develop roots as deep as 3 m (Thevs *et al.*, 2007), which would allow it to exploit groundwater below the sampling range of this study. Future research should therefore ensure that soil water is sampled across a range of depths, to capture the isotopic composition of water available for uptake at a variety of rooting depths. In addition, the validity of the assumptions made here about xylem water reflecting the isotopic composition of water in the root (i.e. that no further fractionation occurs in the xylem as a result of processes such as evaporation) should be tested by sampling and analysis of root water for these saltmarsh plants.

6.6.4 The significance of leaf water

Physical differences among plants with different life forms, leading to various patterns of utilization of environmental water, have been used to explain variation in $\delta^2\text{H}$ *n*-alkane values observed between both woody plants and grass (Liu *et al.*, 2006). For instance, morphological characteristics have been identified as factors exerting a strong influence upon leaf water isotopic ^{18}O -enrichment (Helliker and Ehleringer, 2002; Barbour *et al.*, 2004). Kahmen *et al.* (2008) suggested that leaf water isotopic ^{18}O -enrichment can differ even among species that are closely related because of differences in the “effective path length” (the distance that water is required to flow from source to evaporation site) in their leaves, which would influence the flow of isotopically enriched water back from the sub-stomatal cavity. Despite the caveats discussed in Section 6.1.2 relating to leaf water model

treatment of $^2\text{H}/^1\text{H}$, it is often assumed that similar factors could potentially influence hydrogen isotopic composition of leaf water as well.

Studies seeking to apply factors relating to leaf water ^2H -enrichment to n -alkane data have attempted to explain observed variation in n -alkane $^2\text{H}/^1\text{H}$ in terms of differences in plant life form on the basis that these physical differences could have influenced evapotranspiration of the source water used by the plant during biosynthesis (Liu *et al.*, 2006). A relationship between the hydrogen isotope composition of leaf wax biomarkers and water use efficiency (WUE) has even been proposed on the basis of this reasoning, with some studies reporting a relatively weak but statistically significant negative correlation (with R^2 values ranging from 0.34 to 0.55) between the $^2\text{H}/^1\text{H}$ and $^{13}\text{C}/^{12}\text{C}$ composition of leaf wax n -alkanes (Hou *et al.*, 2007).

At Stiffkey, plants display very different life forms ranging from succulents, grasses and shrubs. However, leaf waters extracted from morphologically distinct species at the same site in June 2011 (Fig. 6.5) show very little variation in their $\delta^2\text{H}$ values. For example, the ridge contains a range of plant species that differ significantly with respect to their leaf morphology. The reed *Phragmites australis* has large, elongated leaves up to 30 cm long and 2 cm wide, while the leaf succulent *Suaeda vera* has leaves that are only 3 mm in length and approximately 1.5 mm in diameter. However, the $\delta^2\text{H}_{\text{lw}}$ values range from +5‰ to +21‰ whilst $\delta^2\text{H}_{n\text{-C}_{29}}$ values differ by over 65‰ between these species. Similar patterns can be found in the seasonal data from 2012, where statistical analysis (Mann-Whitney U test, $P > 0.05$, $n = 7$ for comparison of species growing from March to September 2012; $n = 5$ for comparison of species growing from May to September 2012) confirms that interspecies variation in leaf water hydrogen isotope composition is generally not significant. Even if species with extreme variation in leaf morphology are compared, such as *Phragmites australis* and *Suaeda vera* – where a statistically significant difference in leaf water does exist – leaf water $^2\text{H}/^1\text{H}$ between these two plants only ranges from 6 to 12‰ between May and September 2012. Leaf wax $n\text{-C}_{29}$ $^2\text{H}/^1\text{H}$ values, however, differ consistently by over 50‰ during the same period (Fig. 6.9).

When all the species sampled at Stiffkey are considered, variability in leaf water $\delta^2\text{H}$ composition is three times lower than that observed in $\delta^2\text{H}_{n\text{-C}_{29}}$ in June 2011, and consistently 4-5 times lower throughout the seasonal time series from 2012. The $^2\text{H}/^1\text{H}$ of n -alkanes ($\delta^2\text{H}_{n\text{-C}_{29}}$) varies across all seasonal sampling periods at Stiffkey

by over 100‰, with the greatest variability observed in August (120‰). In contrast, leaf waters across the same period ($\delta^2\text{H}_{\text{lw}}$) show a total variation of only 29‰ (Fig. 6.9; Table 6.2). This contrast between a large variability of *n*-alkane $\delta^2\text{H}$ and a small range of leaf water $\delta^2\text{H}$ values is particularly striking at the beginning and mid stages of the growth season. In March 2012, the mean values of *n*-C₂₉ show 103‰ variation among sampled species (Fig. 6.6), with only 6‰ shifts in leaf water, whilst in August 2012 the *n*-C₂₉ range exceeds 120‰ and leaf waters vary by only 29‰ (Fig. 6.6 and Fig. 6.9). *Phragmites australis* generally has the most negative leaf water $^2\text{H}/^1\text{H}$ profile, whilst *Limonium vulgare*, *Spartina anglica* and *Salicornia europaea* have leaf waters that are all generally ^2H -enriched compared with other species (Table 6.2). Statistical analysis (student's t-test, $P < 0.05$, $n = 10$ individuals per sampling interval comparing those species growing from March to September 2012) of seasonal shifts in leaf water $^2\text{H}/^1\text{H}$ among each species shows that March 2012 is significantly different from all other months. The range in leaf water $\delta^2\text{H}$ in March 2012 is quite limited compared with all other sampling periods. If the *n*-alkane $^2\text{H}/^1\text{H}$ profiles of the sampled species are in fact fixed at the time of leaf expansion, (e.g. as suggested by Tipple *et al.*, 2013), the range in $\delta^2\text{H}_{n\text{-C}_{29}}$ observed in March 2012 (103‰) has therefore to be attributed to something other than leaf water isotopic composition.

In addition, the data presented here also show that ^2H -depletion and ^2H -enrichment in leaf water and *n*-C₂₉ alkane values do not co-vary, i.e. any similarity in leaf water $^2\text{H}/^1\text{H}$ composition does not necessarily lead to a similarity in *n*-alkane $\delta^2\text{H}$ values. Fig 6.4 presents data from the September 2012 sampling period, and shows that for species with very similar leaf water $^2\text{H}/^1\text{H}$ compositions, *n*-alkane values can vary considerably. For example, whilst *Limonium vulgare* and *Salicornia europaea* have the most ^2H -enriched leaf water and *n*-alkane values, *Atriplex portulacoides*, *Suaeda vera* and *Elytrigia atherica* have leaf water values within 8‰ of each other whereas their *n*-alkane values vary by up to 89‰. In addition, the difference between $\delta^2\text{H}_{\text{lw}}$ of *Limonium vulgare* and *Elytrigia atherica* is 19‰, while the range in *n*-C₂₉ between these species $\delta^2\text{H}$ reaches 105‰.

Similar discrepancies between the magnitude of differences in the hydrogen isotope composition of leaf waters and the hydrogen isotope composition of the *n*-C₂₉ alkane are found throughout all the sampling periods. For example, data collected in June 2011 (Fig. 6.5; Table 6.1) show that *Triglochin maritima* from the low marsh has the most ^2H -depleted leaf water value (+22‰) of plants found in this sub-

environment, but this does not result in *Triglochin maritima* having the most ^2H -depleted $n\text{-C}_{29}$ alkane value. Similarly, the C_4 grass *Spartina anglica* has the most ^2H -depleted $n\text{-C}_{29}$ alkane (-156‰) value in the low marsh, but one of the more ^2H -enriched leaf waters ($+27\text{‰}$). This lack of correlation between leaf water and leaf wax $\delta^2\text{H}$ at the plant species level is also apparent in the June 2011 dataset when species having very similar leaf water values (e.g. *Limonium vulgare* and *Salicornia europaea*, which differ by only 1‰ in the low marsh) synthesized $n\text{-C}_{29}$ alkanes that differ by as much as 20‰ (Fig. 6.5).

At the ridge, where the greatest range in $\epsilon_{\text{wax/lw}}$ values is observed in June 2011, this lack of correlation between leaf water and $n\text{-C}_{29}$ alkane $^2\text{H}/^1\text{H}$ is also present (Fig. 6.5). Here, it is the C_3 reed, *Phragmites australis* that has the most ^2H -depleted leaf water ($+5\text{‰}$), but the $n\text{-C}_{29}$ $\delta^2\text{H}$ value for this species does not follow this trend (Fig. 6.5). The most ^2H -depleted $n\text{-C}_{29}$ alkane value on the ridge is in fact found in another C_3 grass, *Elytrigia atherica*, which has a leaf water $\delta^2\text{H}$ value of $+15\text{‰}$. As observed in the low marsh, similar leaf water $\delta^2\text{H}$ values do not result in similar $n\text{-C}_{29}$ alkane $\delta^2\text{H}$ values: *Atriplex portulacoides*, and *Suaeda vera* and *Elytrigia atherica* all record leaf water $^2\text{H}/^1\text{H}$ values ranging from $+15$ to $+21\text{‰}$, but differ by 93‰ in terms of their $n\text{-C}_{29}$ $\delta^2\text{H}$ values. Even in the upper marsh, where the $\delta^2\text{H}$ values display the smallest overall range among plant species, *Triglochin maritima* and *Atriplex portulacoides* record the highest leaf water $\delta^2\text{H}$ values but in contrast have lowest $n\text{-C}_{29}$ alkane $\delta^2\text{H}$ values (Fig 6.5). Statistical analysis of interspecies variation in $n\text{-C}_{29}$ hydrogen isotope composition supports the principle finding of this study, namely that leaf water $^2\text{H}/^1\text{H}$ is of limited relative importance in controlling leaf wax $\delta^2\text{H}$ values. Variation in midday leaf water $\delta^2\text{H}$ among the sampled species was not found to be statistically significant, while in contrast interspecies variation in $n\text{-C}_{29}$ $\delta^2\text{H}$ was, suggesting some other mechanism was responsible for the $>100\text{‰}$ range in $n\text{-C}_{29}$ reported. This argument is strengthened by the fact that no statistically significant relationship exists between the $\delta^{13}\text{C}$ and $\delta^2\text{H}$ values of the n -alkanes from the 2012 growing season, regardless of whether weighted average or $n\text{-C}_{29}$ alone is compared. In contrast, however, a relationship is observed between the $^2\text{H}/^1\text{H}$ composition of leaf water and the $\Delta^{13}\text{C}$ signal recorded in the n -alkanes of the C_3 species ($r = -0.5$, $P < 0.05$, $n = 22$). These data suggest that while leaf water evaporative enrichment is reflected in the carbon isotope composition of leaf wax n -alkanes (along with other mechanisms discussed in Chapter 5), it is not the dominant signal recorded in their $^2\text{H}/^1\text{H}$ composition.

Previous research has suggested that some plants may utilise pre-dawn leaf water that has not been subject to diurnal evaporative enrichment when synthesising leaf wax *n*-alkanes (Sachse *et al.*, 2010). Leaf water samples collected between 7:30 and 8:00 from three species capturing the full range of *n*-C₂₉ alkane $\delta^2\text{H}$ values at the ridge site (*Elytrigia atherica*, *Atriplex portulacoides* and *Suaeda vera*) show a maximum variation of 25‰ (Fig. 6.7). However, it is insufficient to explain the 89‰ range in the *n*-C₂₉ alkane $\delta^2\text{H}$ values from these species. Taken in consideration with the xylem water discussed above, it becomes apparent that even in the case of the most extreme theoretical scenario whereby *Elytrigia atherica* – the species with the lowest ²H/¹H *n*-C₂₉ value – made use of early morning xylem water (-47‰) for lipid synthesis, while *Suaeda vera* (the species with the highest ²H/¹H *n*-C₂₉ value) instead used evaporatively ²H-enriched midday leaf water (+4‰), the maximum range in the pools of water for lipid synthesis would be 51‰ which still does not satisfactorily explain the 89‰ difference in $\delta^2\text{H}_{n\text{-C}_{29}}$ between them.

6.6.5 Comparison of ²H/¹H fractionation among C₃ and C₄ plants at Stiffkey with previously published research

Earlier work has suggested that C₃ vs. C₄ plants have relatively invariant fractionation factors between *n*-alkanes and leaf/source water. Examples include the generalised apparent fractionation factors between leaf water and *n*-alkyl lipids calculated for C₃ (-117 ± 27‰) and C₄ (-132 ± 12‰) plants (Chikaraishi and Naraoka, 2003; Chikaraishi *et al.*, 2004), which continue to be applied to modern vegetation studies (Tippie *et al.*, 2013) and palaeoclimate reconstructions (van Soelen *et al.*, 2013; Lieder *et al.*, 2013). The data presented here, however, suggest these predicted values may not reflect the true extent of plant lipid ²H/¹H diversity - if, for example, fractionation is calculated between leaf water and the *n*-C₂₉ alkane for September 2012, only half of the C₃ plants sampled have $\epsilon_{\text{wax/lw}}$ values that fall within the range predicted by Chikaraishi and Naraoka (2003; 2004) (Table 6.2). The remaining C₃ species, which include *Elytrigia atherica*, *Phragmites australis* and *Atriplex portulacoides*, have $\epsilon_{\text{wax/water}}$ values that are 26-83‰ lower than the predicted values. This lack of agreement with estimated values is found throughout this dataset – in June 2011, only two C₃ species conform to the predicted values (Fig. 6.11), while between March and August 2012, only *Limonium vulgare*, *Suaeda vera* and *Salicornia europaea* have $\epsilon_{\text{wax/lw}}$ values that regularly fall within the predicted -90 to -144‰ range for C₃ species (Chikaraishi and Naraoka, 2003; 2004). With regards to the C₄-plant group, calculated $\epsilon_{\text{wax/lw}}$ values for the C₄ grass *Spartina*

anglica for both June 2011 (-178‰) and the 2012 growth season (-115 to -176‰ between March and September) exceed the range of -120 to -144‰ for C₄ species published by Chikaraishi and Naraoka (2003, 2004) (Fig. 6.12).

A consistent difference in apparent fractionation among C₃ and C₄ species has also been identified in some studies. For example, Chikaraishi and Naraoka (2003) presented data suggesting that C₄ species had higher apparent fractionation factors compared with C₃ angiosperms and gymnosperms. However, plant functional types were not distinguished in this study, and large standard deviations for the mean $\epsilon_{\text{wax/w}}$ values (C₃ = -116 ± 25‰, C₄ = -133 ± 12‰) give rise to a degree of overlap in the range of these values. Bi *et al.* (2005) published data suggesting that in fact C₄ species are typified by *n*-alkane ²H/¹H compositions of -150.4 ± 42.6‰, while that *n*-alkane $\delta^2\text{H}$ signatures in C₃ species average -175.7 ± 29.5‰. Smith and Freeman (2006) limited their study to C₃ and C₄ grasses, and found that ϵ values were ~20‰ more negative in C₃ grasses relative to C₄ grasses, resulting in more negative *n*-alkane ²H/¹H compositions in C₃ grasses. Their result for C₃ and C₄ monocots cannot be explained by gross anatomical differences in leaves and, therefore, it has been hypothesised that differences in the interveinal distance among C₃ and C₄ grasses – alongside difference in the extent of the backflow of enriched water from around the stomata – are responsible for the variation (Smith and Freeman, 2006; Tierney *et al.*, 2010).

One implication of such studies is that the considerable scatter in *n*-alkane $\delta^2\text{H}$ among plants at a specific site is primarily a function of the very negative apparent fractionation between water and leaf wax lipids inherent in C₃ grasses. The data presented here show that the C₃ grass *Elytrigia atherica* consistently has the largest $\epsilon_{\text{wax/lw}}$ value (up to -227‰), followed by the C₃ monocot reed *Phragmites australis* (up to -204‰), while the average value for the C₄ *Spartina anglica* in 2012 is -154 ± 29‰ (Table 6.2). However, the maximum seasonal variability among Stiffkey species, when excluding both C₃ monocots, is still as high as 97‰, while for each sampling interval this variability ranges from 30 to 50‰ (Table 6.2). Similarly, if the C₃ monocots *Elytrigia atherica*, *Phragmites australis* and *Puccinellia maritima* are excluded from consideration in the June 2011 dataset (Table 6.1), the maximum variability is still 44‰. These data imply, therefore, that interspecies variation in apparent fractionation in the species at this saltmarsh study site is not explained by differences in C₃ versus C₄ photosynthetic pathways, or indeed in plant life form. The magnitude of variability when C₃ monocots are excluded from consideration

also demonstrates that it may not always be accurate to assume that one plant functional type dictates the magnitude of interspecies variation in *n*-alkane $^2\text{H}/^1\text{H}$ at any given location.

6.7 CONCLUSION

Findings from this study suggest that environmental and physical mechanisms driving variation in the $^2\text{H}/^1\text{H}$ composition of soil, xylem and leaf water are not sufficient to explain the range of *n*-alkane $\delta^2\text{H}$ values observed in a range of saltmarsh plants growing in a temperate, coastal ecosystem. In addition, the range of net apparent hydrogen isotope fractionation reported here for these species consistently exceeds 100‰. These findings have considerable implications for the use of leaf wax *n*-alkanes as palaeohydrological proxies (discussed in detail in Chapter 1), as one of the key assumptions underlying such an application is that fractionation between *n*-alkane and source water $^2\text{H}/^1\text{H}$ is relatively constant, with interspecies variability in any given geographical location arising from differences in leaf water evaporative enrichment. As this Chapter has found that the magnitude of *n*-alkane $^2\text{H}/^1\text{H}$ cannot be explained by these environmental and physical mechanisms, further research to identify the key biochemical processes controlling the *n*-alkane hydrogen isotope signal is required to ensure accurate interpretation of lipids from the geological record.

6.8. SUMMARY

- Interpretation of sedimentary *n*-alkyl lipid $\delta^2\text{H}$ data is complicated by a limited understanding of factors controlling interspecies variation in biomarker $^2\text{H}/^1\text{H}$ composition.
- Linked $\delta^2\text{H}$ analyses of soil water, xylem water, leaf water and *n*-alkanes from a range of C_3 and C_4 plants growing at a UK saltmarsh (i) across multiple sampling sites, (ii) throughout the 2012 growing season, and (iii) at different times of the day showed that soil waters varied isotopically by up to 35‰ depending on marsh sub-environment, and exhibited site-specific seasonal shifts in $\delta^2\text{H}$ up to a maximum of 31‰.
- Maximum interspecies variation in xylem water was 38‰, while leaf waters differed seasonally by a maximum of 29‰.
- Leaf wax *n*-alkane $^2\text{H}/^1\text{H}$ consistently varied by over 100‰ throughout the 2012 growth season, resulting in an interspecies range in the $\epsilon_{\text{wax/leaf water}}$ values of -79 to -227‰.
- From the discrepancy in the magnitude of these isotopic differences, it can be concluded that mechanisms driving variation in the $^2\text{H}/^1\text{H}$ composition of leaf water, including (i) spatial changes in soil water $^2\text{H}/^1\text{H}$, (ii) temporal changes in soil water $^2\text{H}/^1\text{H}$, (iii) differences in xylem water $^2\text{H}/^1\text{H}$, and (iv) differences in leaf water evaporative ^2H -enrichment due to varied plant life forms, cannot explain the range of *n*-alkane $\delta^2\text{H}$ values observed throughout the course of this study.

Chapter 7

The role of biochemical and metabolic processes in controlling interspecies variation in leaf wax *n*-alkane $^2\text{H}/^1\text{H}$

7.1 INTRODUCTION

Chapter 6 demonstrated that interspecies variation in the *n*-alkane $\delta^2\text{H}$ signatures of saltmarsh plants growing at Stiffkey during 2012 cannot be fully explained by reference to environmental and physical factors controlling the isotopic composition of water moving into and out of a leaf. Other explanations must therefore be sought to account for the variability in *n*-C₂₉ hydrogen isotope composition observed in this dataset, which consistently exceeds 100‰ for all sampling intervals (Fig. 6.9; Chapter 6). The 2012 review of hydrogen isotopes in lipids biomarkers authored by Sachse *et al.* highlights that lipid $^2\text{H}/^1\text{H}$ values can be influenced by biochemical mechanisms in addition to environmental and physical ones (Fig. 7.1). It follows therefore that investigation of biochemical mechanisms represents the logical next step for explaining the interspecies variation in plant *n*-alkane hydrogen isotope compositions in our data. Sachse *et al.* (2012), however, do not detail particular mechanisms that may contribute towards species-specific biochemical differences, apart from suggesting that variation in: (i) biochemical pathways; and (ii) NADPH sources and/or pools, may explain differences in leaf wax $^2\text{H}/^1\text{H}$ values among plant species.

This chapter seeks to explore possible biochemical mechanisms that could influence *n*-alkane $^2\text{H}/^1\text{H}$ values. The chapter also provides a framework for future research to improve understanding of the cycling of hydrogen among and within plant biochemical compounds. In order to do this, the chapter first reviews the primary source of hydrogen available to plants and lays out the conceptual

approaches to investigating the role of biochemical mechanisms. From this, the chapter moves to define the scope of this part of the project and establish the rationale for the aims and objectives which follow.

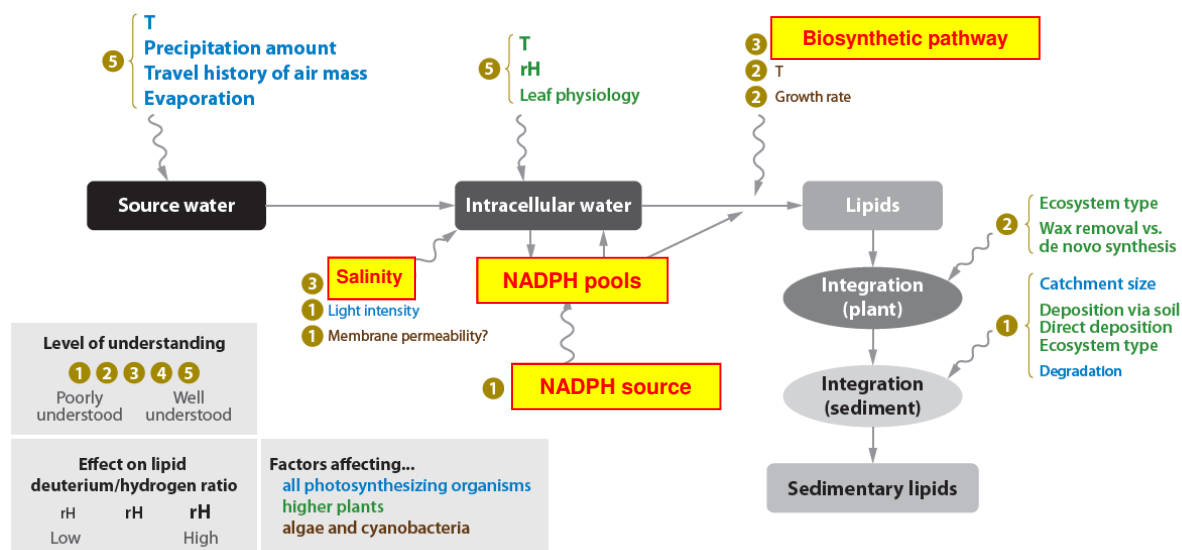


Figure 7.1: Conceptual overview of the processes affecting the hydrogen isotope composition of lipid biomarkers from phototrophic organisms. Abbreviations: H, hydrogen; NADPH, nicotinamide adenine dinucleotide phosphate (reduced); rH, relative humidity; T, temperature. (Sachse *et al.*, 2012). Areas about which very little is currently known are highlighted in red/yellow: NADPH sources/pools, biochemical pathways, and the effects of salinity.

7.2 REVIEW

7.2.1 Sources of hydrogen for terrestrial plants

Water is the *prima facie* source of hydrogen in all organic compounds (Schmidt *et al.*, 2003), and hydrogen ions from water fission are the primary source of hydrogen incorporated into NADPH during photosynthesis (Luo *et al.*, 1991; Schmidt *et al.*, 2003). It is important to consider the role of NADPH in terms of understanding *n*-alkane $^2\text{H}/^1\text{H}$ as this molecule is directly involved in the biosynthetic transfer of hydrogen into secondary compounds through hydrogenation of their carbon skeletons (Sessions, 2006; Sachse *et al.*, 2012). The hydrogen available for NADPH synthesis is significantly ^2H -depleted by up to 600‰ relative to the original source water (Luo *et al.*, 1991). This is due to the dissociation constant (pKa) of

$^1\text{H}_2\text{O}$ being 14.00, while for $^2\text{H}_2\text{O}$ it is 14.9 (Luo *et al.*, 1991). As a result of this, the dissociation of $^2\text{H}_2\text{O}$ is almost 10 times less likely to occur than dissociation of $^1\text{H}_2\text{O}$ (Luo *et al.*, 1991). Water fission during photosynthesis is not the sole source of hydrogen available for NADP^+ reduction in plants, however. A variety of different reactions in metabolic pathways are capable of generating the hydrogen incorporated into NADPH (Valentine, 2009). NADP^+ can be reduced to NADPH by the oxidation of sugars in the pentose-phosphate cycle (OPPP), for example, where the hydrogen derives from C-bound H contained within the sugars (Sessions *et al.*, 1999). Schmidt *et al.* (2003) suggests that these diverse sources give rise to differences in the isotopic composition of NADPH among different plant compartments. The hydride in NADPH produced in the cytosol, for example, where hydrogen can be derived from the OPPP, should theoretically have a very different hydrogen isotope composition than that of the hydride originating from water incorporated during photosynthesis in the chloroplasts (Schmidt *et al.*, 2003).

The need to investigate biochemical processes more fully in phototrophic organisms has been strengthened by recent work investigating factors controlling the $^2\text{H}/^1\text{H}$ values of lipids in microorganisms. These studies have also identified significant variation in the $^2\text{H}/^1\text{H}$ values of lipids among different species. Zhang and Sachs (2007), for example, conducted laboratory studies of hydrogen isotope fractionation associated with palmitic acid production in freshwater green algae (*Eudorina unicocca* and *Volvox aureus*) and three species of *Botryococcus braunii*. Despite growing in water with the same hydrogen isotope composition, they found the $\delta^2\text{H}$ values of palmitic acid varied by $\sim 100\%$ among the different species (Zhang and Sachs, 2007). Studies suggest that this variation in microbial lipid hydrogen isotope composition is due to differences in the metabolic pathways for producing the NADPH used as a reducing agent during secondary compound synthesis (Zhang *et al.*, 2009; Valentine *et al.*, 2009; Fig. 7.2). This has led to the suggestion that biomarker $^2\text{H}/^1\text{H}$ values have the potential to act as a proxy for cellular metabolism in modern cultures, extant organisms and ecosystems (Valentine, 2009; Zhang *et al.*, 2009; Naraoka *et al.*, 2010; Dirghangi and Pagani, 2013a, 2013b). While many of these studies considered chemolithotrophic, phototrophic and heterotrophic organisms, the study of Fisher *et al.* (2013) focused on a hydrotrophic microbial community. Even where microorganisms such as these obtain all of their hydrogen

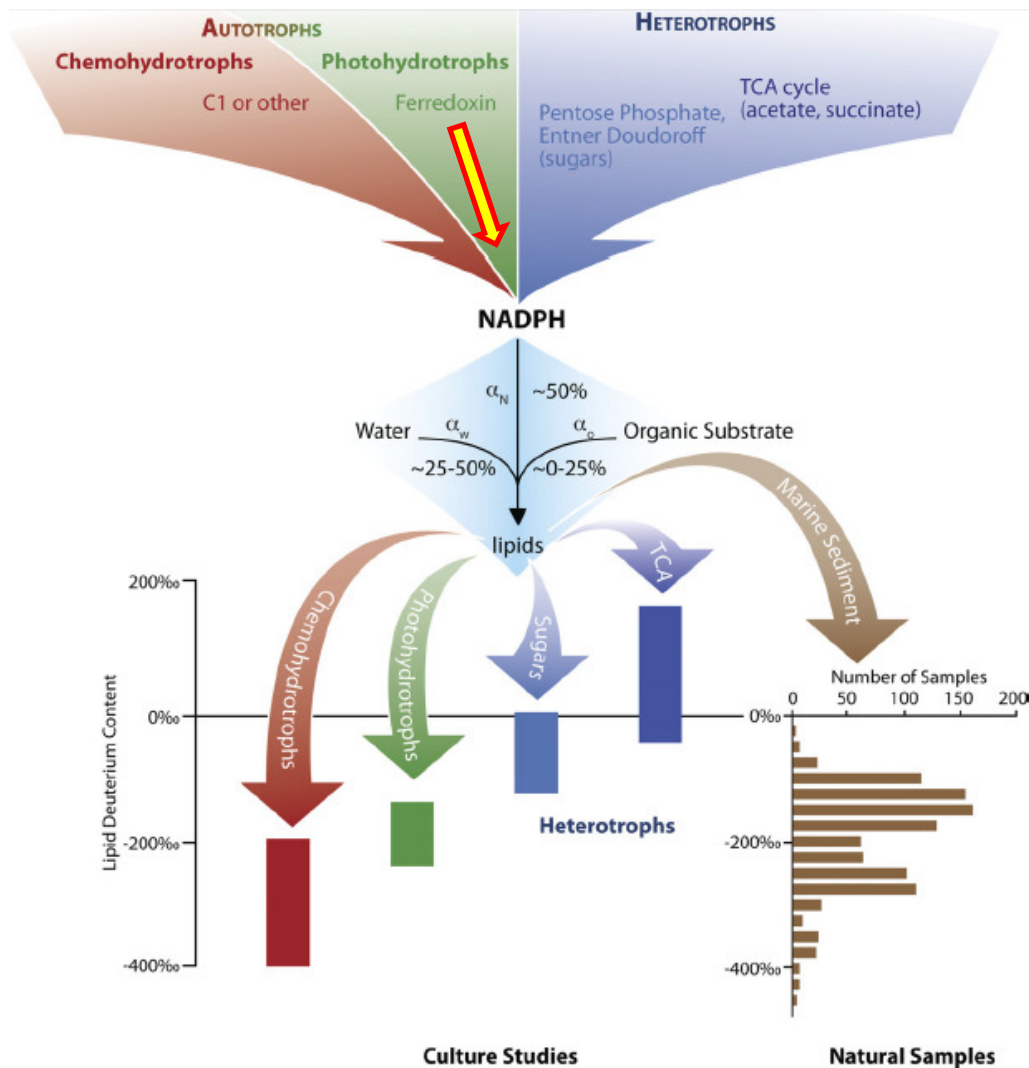


Figure 7.2: At the top: NADPH is the primary immediate biosynthetic precursor of hydrogen for lipids and is generated by diverse mechanisms associated with different central metabolic pathways as indicated. In the middle: The deuterium content of lipids is set by the balance of hydrogen precursors, namely water, NADPH, and organic material. The approximate percentage contribution of each source is indicated. Each reaction is accompanied by a fractionation, designated by α . At the bottom: The deuterium content of lipid biomarkers is displayed, all originating from waters with similar deuterium content. At left are the fatty acids from the cultivation studies of Zhang et al., 2009 distinguished by substrates that feed into the identified metabolic pathways. At right is a histogram summarizing the distribution of deuterium content for ~1,000 analytes extracted from the anoxic marine sediments of the Santa Barbara Basin. Included in the histogram are several classes of compounds, including fatty acids, alcohols, alkanes, and isoprenoids, the latter of which tend to be depleted in deuterium. Fatty acids from this sediment range in deuterium content from -32‰ to -280‰, consistent with distinct contributions from different metabolic pathways (from Valentine, 2009). While this figure relates to microbial lipids, the importance of the hydrogen isotope composition of precursors may also be important for all phototrophic organisms. The yellow arrow highlights the photohydrotrophic organisms, which use many similar biochemical processes for NADPH production as higher plants.

from water, in the same way as plants, Fisher *et al.* (2013) found that biosynthetic steps in addition to NADPH formation contribute to the extent of $^2\text{H}/^1\text{H}$ fractionation in microbial biomolecules. They also found that even though microbial community members were closely related (sharing up to 94% 16S rRNA gene sequence identity) isotopic fractionation was species specific.

Further support for the assertion that biochemical mechanisms may be important for interpreting the hydrogen isotope composition of plant organic compounds comes from research into the $^2\text{H}/^1\text{H}$ composition of cellulose. The isotopic composition of precipitation plays a role in formulating the $\delta^2\text{H}$ signatures of cellulose precursors such as carbohydrates (Yakir, 1992). It has long been accepted, however, that whilst a relationship exists between cellulose and the metabolic water used for its synthesis, metabolic water does not directly correspond isotopically to the ground/environmental water taken up by the plant (Yakir, 1992). Part of this discrepancy has been attributed to post-photosynthetic exchange processes (Yakir, 1992), which have the potential to alter the isotopic composition of carbohydrates originally synthesised during photosynthesis in the presence of water derived from fission in the plastid (Yakir, 1992; Schmidt *et al.*, 2003). Like lipids, some of the hydrogen incorporated into cellulose is synthesised from NADPH generated in the cytosol by the oxidation of these carbohydrates in the pentose-phosphate cycle (OPPP cycle), resulting in cellulose retaining the hydrogen isotope signal of the metabolic water which has exchanged with these sugars (Sessions *et al.*, 1999).

Because differences in NADPH sources and pools are areas identified by Sachse *et al.* (2012) for further research to develop understanding of mechanisms controlling the isotopic composition of leaf lipids, it is appropriate to draw analogies here with the relative importance of physical and biochemical mechanisms in controlling cellulose isotopic composition. If cytosolic processes are also important for controlling leaf wax biomarker $^2\text{H}/^1\text{H}$, similar post-photosynthetic exchange may be at least partially responsible for the lack of correlation observed between leaf water and leaf *n*-alkane $^2\text{H}/^1\text{H}$ from the Stiffkey plants (Chapter 6).

As it is not possible to measure the isotopic composition of NADPH directly, any investigation of biochemical mechanisms which would influence lipid $^2\text{H}/^1\text{H}$ values has to adopt a range of different approaches. In the acetogenic lipid pathway, it is well established that acetyl-CoA is the precursor for fatty acids (Harwood, 1988), which in turn are the precursors for all other acetogenic lipids (Fig. 3.5, Chapter 3) (Harwood, 1988; Quemerais *et al.*, 1995; Schmidt *et al.*, 2003; Zhang *et al.*, 2007).

One method for seeking to identify the biochemical mechanisms which have the potential to influence the $^2\text{H}/^1\text{H}$ of plant leaf wax *n*-alkanes is therefore to investigate compounds metabolised in the biochemical reaction network generating acetogenic lipids (e.g. fatty acids), and compare their isotopic composition with that of compounds produced by other reaction networks, such as the 1-deoxy-d-xylose-5-phosphate (DOXP) pathway generating phytol (e.g. Chikaraishi *et al.*, 2004, 2007), which have different precursors.

In addition, studies of isotope systematics for a variety of elements have highlighted that for any given multi-step metabolic process, such as the generation of acetogenic lipids, the net isotope effect is dependent upon the structure of a reaction network, the relative amounts of material that flow through it, and the isotopic fractionation accompanying branch points within the network (Hayes, 2001; Farquhar *et al.*, 2003; Johnston *et al.*, 2005). Differences in the relative fluxes of material through the biosynthetic pathway generating leaf wax *n*-alkanes, (evidenced by the diverse molecular distribution and concentration patterns of *n*-alkanes in the Stiffkey species, Chapter 4) and variation in the biochemical responses of the sampled species to abiotic perturbations in their environment (e.g. nutrient stress, salinity stress and water stress) could theoretically alter the flow of material through parts of the acetogenic lipid reaction network. Chapter 5 establishes that analysis of percentage carbon and nitrogen content, plus consideration of the nitrogen isotopic composition of foliar leaf material, can assist in identifying different traits among these species in respect of their production of osmoregulatory compounds, and hence these data will also be considered further in this chapter. Chapter 6 also shows that monocot *n*-alkane $\delta^2\text{H}$ values were lower than those from dicots, in accordance with previous studies (e.g. Smith and Freeman, 2006), and this part of the project therefore also considers variation in phytochemical apparatus and processes that have been identified between these two plant functional groups, to explore whether lipid $^2\text{H}/^1\text{H}$ values are reflective of these differences.

7.2.2 The potential for interspecies differences in phytochemistry to influence *n*-alkane $^2\text{H}/^1\text{H}$

Some studies have tried to link differences in the photosynthetic chemistry and apparatus between C_3 and C_4 species with their respective variation in lipid $^2\text{H}/^1\text{H}$ values. Chikaraishi *et al.* (2003) analysed *n*-alkanes from C_3 dicots, and compared them to C_4 monocots. They found that fractionation between water and *n*-alkanes

(ϵ_{i-w}) was $\sim 15\%$ smaller (i.e. $117 \pm 27\%$ versus $132 \pm 12\%$) for C_3 dicots than for C_4 monocots. This approach has been criticised, however (Smith and Freeman, 2006), as it is not a direct comparison of the effects of C_3 and C_4 photosynthetic pathways in plants from the same functional group. Where studies have compared, for example, C_3 and C_4 grasses (Smith and Freeman, 2006) they find that n -alkanes from C_3 grasses are in fact ^2H -depleted compared to C_4 grasses. Smith and Freeman (2006) found that $\epsilon_{\text{lipid-water}}$ values were most negative for C_3 grasses, intermediate for C_4 grasses, and most positive for C_3 dicots, concluding that differences between C_3 and C_4 photosynthetic pathways were not a primary control on the $^2\text{H}/^1\text{H}$ fractionation between water and lipids. This pattern of relative deuterium enrichment and depletion has also been shown to be true for studies of the $^2\text{H}/^1\text{H}$ values of bulk biomass from C_3 and C_4 dicots (Leaney *et al.*, 1985) and cellulose (Sternberg and De Niro, 1983; Sternberg *et al.*, 1984, 1986).

If physiological differences in photosynthetic anatomy and carbon fixation pathways are not viable mechanisms influencing n -alkane $^2\text{H}/^1\text{H}$ variation among these two plant groups, an alternative explanation may be that biochemical differences in the protein content and composition of photosystem I (PSI) and photosystem II (PSII) among the plant species (e.g. Zolla *et al.*, 2003) have a role in establishing interspecies variation in n -alkane $^2\text{H}/^1\text{H}$. This could theoretically be achieved through the influence of PSI and PSII on the composition of chloroplastic NADPH. The very first stage in the biochemical pathway that ultimately results in the production of n -alkanes (and a range of other organic compounds) is the production of photosynthates by the fixation of carbon (Harwood, 1998 (Fig. 5.3, Chapter 5). During this step, where photosynthetic organisms can generate a significant proportion of their NADPH, ^2H -depletion in NADPH can be as high as 600% (Luo *et al.*, 1991; Schmidt *et al.*, 2003; Zhang *et al.*, 2007).

Direct measurement of the protein concentration and composition of PSI and PSII are outside the scope of this chapter, however the percentage composition of biomass nitrogen, and the ratio of nitrogen to carbon, can provide information about the proteins involved in photosynthesis (Evans 1989). In the dark reactions of photosynthesis, nitrogen content has a strong relationship with RuBP carboxylase and other proteins found within the Calvin cycle (Evans, 1989). Secondly, nitrogen is a critical component of the proteins found in the chloroplast thylakoid membranes participating in light reactions of photosynthesis (Evans, 1989). At high intracellular pressures of CO_2 (i.e. high P_i ; $\sim 400\mu$ bar), the rate of CO_2 assimilation depends

upon the ability of a particular plant species to regenerate RuBP (Evans, 1989). The regeneration of RuBP relates to the rate of electron transport, a process controlled by thylakoid proteins (Evans, 1989). This study will, therefore, consider the nitrogen content of bulk plant biomass, to evaluate whether there is any relationship between these values and *n*-alkane $^2\text{H}/^1\text{H}$.

7.2.3 The potential for variation in NADPH sources and pools to influence *n*-alkane $^2\text{H}/^1\text{H}$

The idea that changes in the source or pool of NADPH used for lipid synthesis can influence the hydrogen isotope composition of leaf wax lipids has been briefly explored in other studies. As discussed in Chapter 6, Sessions (2006) observed a gradual ^2H -depletion observed in *n*-alkanes extracted from C_4 grass *Spartina alterniflora*, which ran contrary to the anticipated ^2H -enrichment arising from lipid $^2\text{H}/^1\text{H}$ tracking increased transpiration from leaves in hot weather. Sessions attributed this to the use of stored carbohydrate reserves as precursors for secondary compound synthesis at the start of the growth season, with a switch to relatively ^2H -depleted photosynthate precursors later in the year.

Carbohydrate metabolism is of central importance for plant biochemical processes, as stored carbohydrates are a starting point for biosynthesis of all cellular molecules (Bowsher *et al.*, 2008). Plants contain a wide range of carbohydrates, all of which are polyhydroxy-aldehydes or ketones, with the basic composition $(\text{CH}_2\text{O})_n$. Light and environmental conditions are known to influence the source of carbohydrates available to plants (Bowsher *et al.*, 2008), while species-specific differences have been identified in terms of where plants store excess photoassimilates. For instance, spinach, soybean and tobacco store starch in chloroplasts, while wheat, barley and oat species store sucrose in the vacuole (Bowsher *et al.*, 2008). Therefore, if interspecies variations observed in leaf wax $^2\text{H}/^1\text{H}$ cannot be explained with reference to leaf water hydrogen isotope signals, differences in the utilisation of carbohydrate sources and sinks to generate NADPH may represent a viable alternative explanation for the patterns observed in leaf wax lipids from the saltmarsh plants sampled at Stiffkey (see highlighted areas in Fig. 7.1).

While detailed extraction and analysis of the composition and concentration of carbohydrates, such as soluble sugars, has not been carried out as part of this study, the saltmarsh plants were evaluated to assess whether they store starch to give a qualitative indication of whether differences in carbohydrate accumulation

have any relationship with *n*-alkane $^2\text{H}/^1\text{H}$. Information pertaining to carbon content (Table 5.6, Chapter 5), which could provide qualitative information about the total amount of carbohydrates contained within plant tissues, will also be considered. Where plants do accumulate starch, the hydrogen isotope composition of it will be ascertained, to assess whether the extent of interspecies variation in starch $\delta^2\text{H}$ values can account for the range in *n*-alkane $^2\text{H}/^1\text{H}$ reported in Chapter 6. In addition, examination of a range of organic compounds produced in different plant compartments (e.g. chloroplastic compounds such as C16 and C18 fatty acids, phytol) and incorporating hydrogen from NADPH generated by different biochemical processes, will further constrain the importance of different NADPH pools. The isotopic composition of bulk plant tissue is also likely to be dominated by the carbohydrate signal, as ~75% of bulk plant tissue is carbohydrate (Dungait *et al.*, 2008). These data will also be collected, to examine whether there is a relationship between bulk tissue and starch $^2\text{H}/^1\text{H}$, and bulk tissue and leaf lipid $^2\text{H}/^1\text{H}$.

7.2.4 The potential for plant biochemical responses to environmental stress to influence *n*-alkane $^2\text{H}/^1\text{H}$

An important draw on the reducing power of the cells of many plants facing environmental stresses is the production of a suite of solutes to protect major biochemical processes such as photosynthesis (Parida and Das 2005). The salinity stress experienced by species at Stiffkey, for example, is typically ameliorated by plants producing osmoregulatory solutes to maintain their water balance (Briens and Lahrer, 1982). Osmotic adjustment in saltmarsh plants can include, for example, the collecting of salt from the cytoplasm into the vacuole, which maintains a strong osmotic gradient across the vacuole membrane (Volkmar *et al.*, 1998; Chapter 5). In addition, salt-stressed plants synthesise compatible solute molecules in the cytoplasm, which, although varied, share chemical properties such as a low polarity, high solubility and a large hydration shell (Volkmar *et al.*, 1998). Common compounds of this class include proline ($\text{C}_5\text{H}_9\text{NO}_2$), glycine-betaine ($\text{C}_5\text{H}_{15}\text{NO}_2$), quaternary ammonium compounds, pinitol ($\text{C}_7\text{H}_{14}\text{O}_6$), mannitol ($\text{C}_6\text{H}_{14}\text{O}_8$), and sorbitol ($\text{C}_6\text{H}_{14}\text{O}_6$) (Volkmar *et al.*, 1998; Briens and Lahrer, 1983; Hare and Cress, 1997; Hare *et al.*, 1998).

Studies of the hydrogen isotope composition of typical compounds used for osmoregulation show that they can differ considerably. Schmidt *et al.* (2003) proposed a general range of $^2\text{H}/^1\text{H}$ values for some common organic compounds expressed relative to leaf water with a theoretical value of 0‰. Amino acids and

organic acids were the most ^2H -enriched with an offset of -50‰ (Schmidt *et al.*, 2003). In contrast, both carbohydrates (-110‰) and proteins (-130‰) were relatively ^2H -depleted (Schmidt *et al.*, 2003). It follows, therefore, that changes in the production of these compounds (Ladd and Sachs, 2012), and their potential catalysis and use as respiratory substrates during times of stress (Araujo *et al.*, 2011) could potentially influence the flux of hydrogen transferred through reaction networks. As detailed studies of the proteins, amino acids and carbohydrates produced by each species growing at Stiffkey is outside of the scope of this thesis, %C and %N, and $\delta^{15}\text{N}$ of foliar leaf material will be used to give a first order evaluation of the relative importance of these mitigation strategies on leaf wax biomarker $^2\text{H}/^1\text{H}$.

7.3 AIMS AND OBJECTIVES

The *primary aim* of this chapter is to investigate possible biochemical mechanisms that could lead to interspecies differences in leaf wax *n*-alkane $^2\text{H}/^1\text{H}$ composition. To achieve this aim, a series of research questions have been established. Figure 7.3 provides a simplified schematic of the compartments where different compounds are produced, to accompany these research questions.

- 1) What is the extent of interspecies variation in phytol $^2\text{H}/^1\text{H}$? Is the pattern of deuterium enrichment and depletion among different species the same for phytol and *n*-alkanes?
- 2) What is the extent of interspecies variation in C16 and C18 fatty acid $^2\text{H}/^1\text{H}$? Is the pattern of deuterium enrichment and depletion among different species the same for fatty acids and *n*-alkanes?
- 3) What is the extent of interspecies variation in starch and bulk plant tissue $^2\text{H}/^1\text{H}$? Is the pattern of deuterium enrichment and depletion among different species the same as for *n*-alkanes?
- 4) Does any relationship exist between (i) the carbon and nitrogen content, (ii) C:N ratios, and (iii) $\delta^{15}\text{N}$ values, and the $^2\text{H}/^1\text{H}$ values of *n*-alkanes? Does this relate to the osmoregulatory compound preferred by the sampled species?
- 5) Can interspecies variation in the biochemical response to environmental stress influence the $^2\text{H}/^1\text{H}$ composition of *n*-alkanes?

In addition, a *secondary aim* of this chapter will be to evaluate whether any of these biochemical mechanisms might account for the relative depletion of acetogenic

lipids from monocots compared with dicots, a feature noted in this study (Chapter 6) and also in previous research (e.g. Smith and Freeman, 2006).

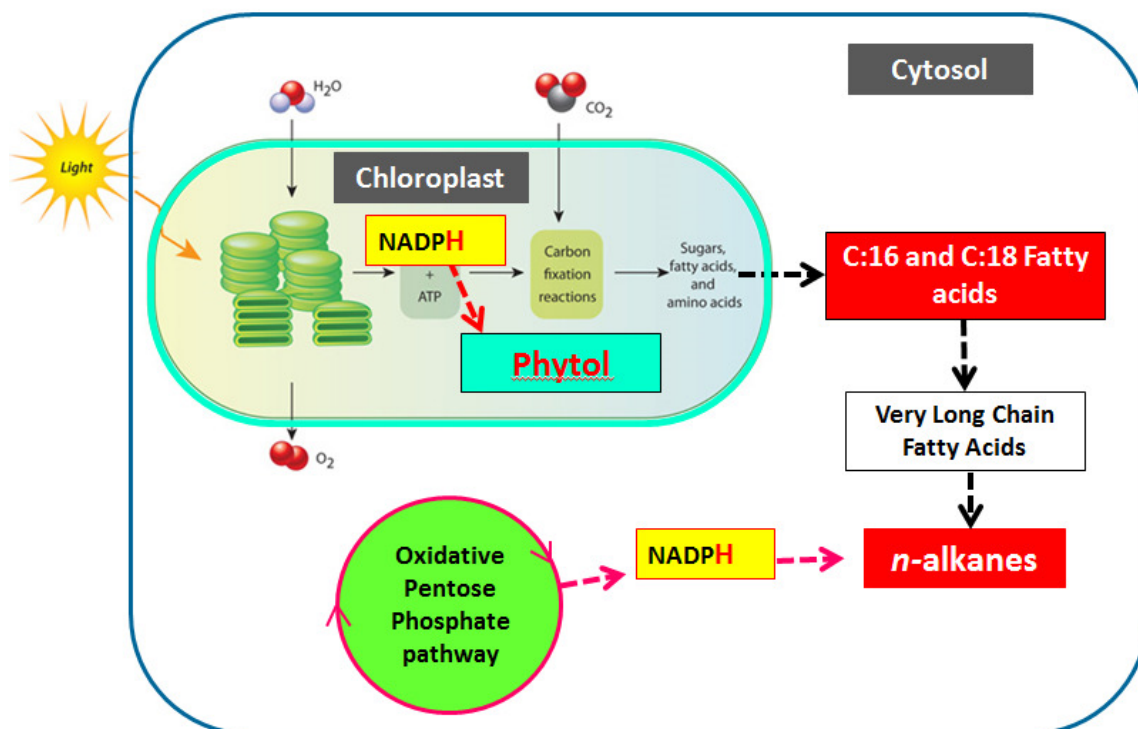


Figure 7.3: Simplified schematic of the compartmentalisation of production of lipids analysed in this study, showing the main stages of the metabolic reaction network to illustrate the conceptual approach to addressing the aims of this chapter.

7.4 SAMPLING STRATEGY

7.4.1 Site description

The sampling site used for this study is Stiffkey saltmarsh, as described in Chapter 2.

7.4.2 Fatty acids and phytol

Samples from September 2012, collected as described in Chapter 4 for analysis of leaf wax biomarkers, were used for fatty acid analysis. Fresh leaf material was required for phytol analysis, however, and so these samples were collected between 13:00 and 15:00 in August 2012 at the same time as samples for analysis

of starch. Phytol samples were placed into sample bags and stored immediately on dry ice in the field for transport back to the laboratory. Samples were then placed in a low temperature freezer at -80°C until required for analysis.

7.4.3 Bulk leaf tissue

Bulk leaf tissue sampled for hydrogen isotope analysis, nitrogen isotope analysis, and percentage carbon and nitrogen analysis were collected as part of the sampling for analysis of leaf wax biomarkers, described in detail in Chapter 4. All samples were dried at 40°C immediately after collecting, and then stored in a dry, dark environment until required for analysis.

7.4.4 Samples for starch extraction

Samples for starch extraction and analysis were collected in August 2012. In order to examine whether plants accumulated starch or used it up on a daily basis, fresh leaves from all plants were collected: (i) between 07:00 and 09:00 in the morning, and (ii) between 16:00 and 17:30 in the late afternoon. Care was taken to select healthy leaves, with no obvious evidence of damage or disease. Plants were placed into sample bags, and immediately stored in dry ice in the field after collection to prevent enzymatic activity. Upon returning samples to the laboratory, they were transferred directly to a low temperature freezer maintained at -80°C, until required for analysis.

7.5 ANALYTICAL METHODOLOGY

7.5.1 Extraction and analysis of phytol for $^2\text{H}/^1\text{H}$ analysis

Phytol extraction was carried out using the method set out by Chikaraishi *et al.* (2004, 2005, 2009). A detailed flow chart describing the method can be found in Figure 7.4. Briefly, fresh frozen plant leaves were ground into a powder using the cryogenic mill. These powdered samples were extracted three times by sonicating with cold acetone for 2 min. Ultra-pure water was added to the acetone solution to give a ratio of 3:1 water to acetone. The extracted pigments were then re-extracted from the acetone/water mix using hexane. To ensure complete extraction of the pigments, the powdered plant material was then placed in acetone again, and stored for 24 h in a freezer until colourless. Any pigments extracted during this step

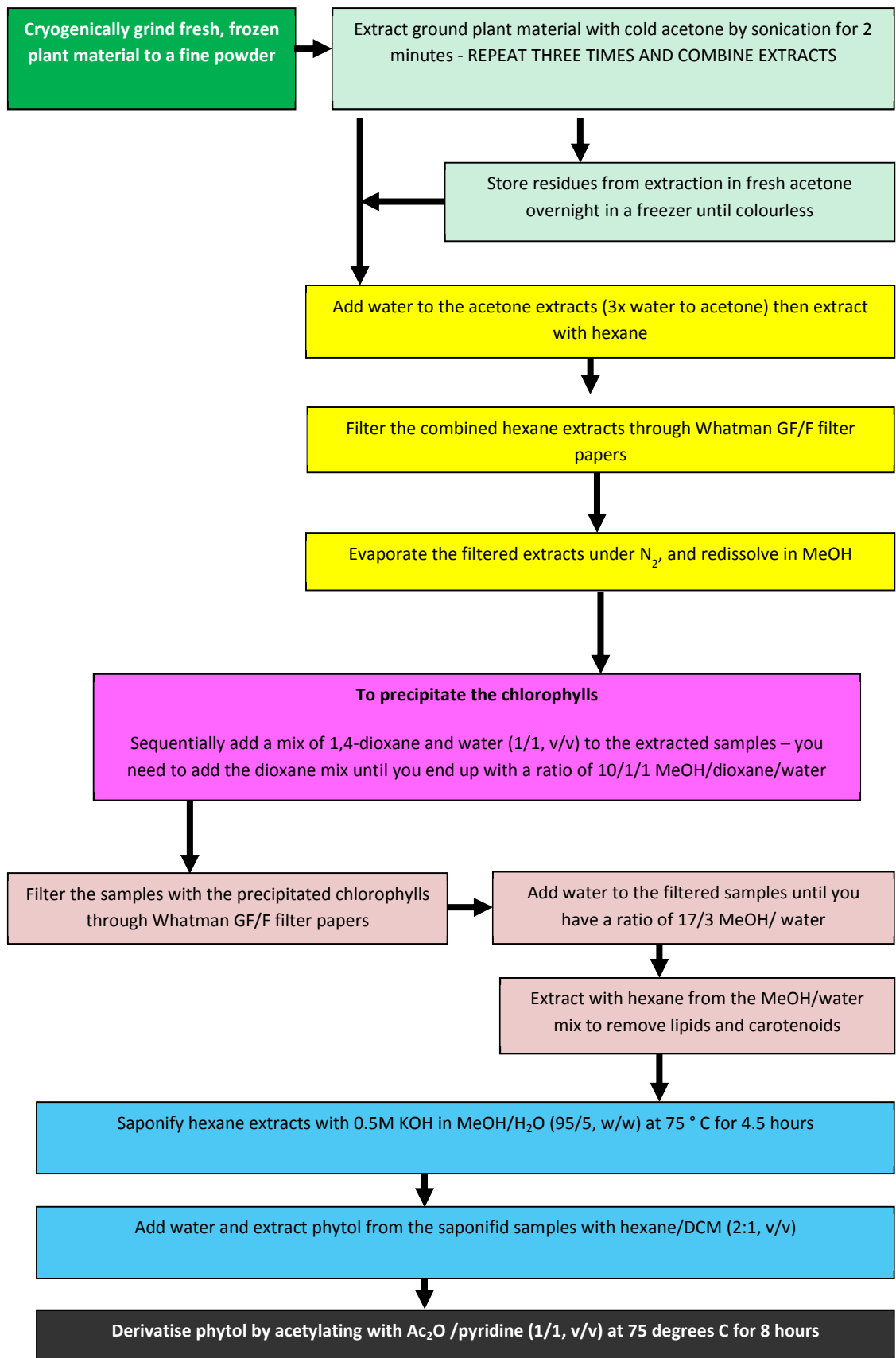


Figure 7.4: Flow diagram illustrating the method used for extracting phytol, (Chikaraishi et al., 2007 and references contained therein)

were re-extracted into hexane in the same way as before. The hexane solutions were filtered with a Whatman GF/F filter (0.7 μ m pore size) and evaporated under N₂. Samples were then re-dissolved in methanol, and chlorophylls were precipitated by the sequential addition of 1,4-dioxane/H₂O (1:1, v/v). After precipitation, solutions were filtered again with a Whatman GF/F filter to remove the chlorophylls. Solutions were then extracted again with hexane from the methanol/H₂O mix, to remove the lipids and carotenoids. Solutions were saponified with 0.5M KOH in MeOH/H₂O (95/5, w/w) at 75°C for 4.5 h. After adding H₂O to the saponified solutions, phytol was extracted using hexane/DCM (2:1, v/v).

Phytol samples were derivatised by acetylating using acetic anhydride and pyridine in the ratio Ac₂O/pyridine (1/1, v/v) at 75°C for 8 h. To correct for the addition of hydrogen during derivatisation, phthalic acid (see detailed discussion below) of known isotopic composition (Schimmelmann, Indiana US) was also derivatised using the same agents (Appendix 6). Phytol samples were analysed on a Perkin Elmer Clarus 500 GC MS, and retention times compared to those obtained for a phytol standard (Sigma Aldrich). During analysis, the GC oven temperature was programmed from 50 °C, and then raised at a rate of 30 °C per min until it reached 120 °C. A second ramp then took the temperature to 310 °C at a rate of 6 °C per min, with this final temperature being held for 15 min. The ²H/¹H of derivatised samples was analysed using a Delta V Advantage ThermoFisher isotope-ratio mass spectrometer interfaced with GC-Isolink Trace GC Combustion and High temperature conversion (HTC) system operating at 1400 °C. The GC oven temperatures used for isotope analysis were as described for the GC/MS. As described in Chapter 6, the $\delta^2\text{H}$ values presented in this chapter are based on duplicate measurements of well-resolved peaks and reported on the VSMOW scale, based on in-house reference gases (H₂, >99.995% purity, BOC) adjusted at the beginning and at the end of each sequence using a standard mixture of an *n*-C₁₆ to *n*-C₃₀ alkane standard (Arndt Schimmelmann, Indiana University). Root mean square (RMS) error for ²H/¹H measurements of this standard was 4.0‰ (*n* = 780). During all sample and standard measurements, 6 reference gas pulses were passed through the mass spectrometer. Reproducibility of H₂ reference gas $\delta^2\text{H}$ values after H₃⁺ correction during phytol analysis was $\pm 6\%$. Due to low concentrations of phytol in the saltmarsh extracts, sample duplicates were combined after GC/MS analysis to ensure sufficient peak intensity for hydrogen isotope analysis. Standard error of analytical replicates of the same sample,

however, did not exceed 4‰, and hence this value is adopted as a conservative error for all phytol data points.

Phytol contains a hydroxyl group, and (as mentioned above) is typically derivatised prior to analysis to replace this with an alternative moiety (Sauer *et al.*, 2001; Fig. 7.5). This derivatisation step both eliminates the hydroxyl (which contains the exchangeable hydrogen) and also improves the suitability of phytol for gas chromatography. Phytol is commonly derivatised using acetic anhydride to form an acetate ester. Acetylation reactions involve the addition of an acetyl moiety to the compound of interest (Fig. 7.5), and therefore the hydrogen added to the compound of interest needs to be accounted for when interpreting $\delta^2\text{H}$ data.

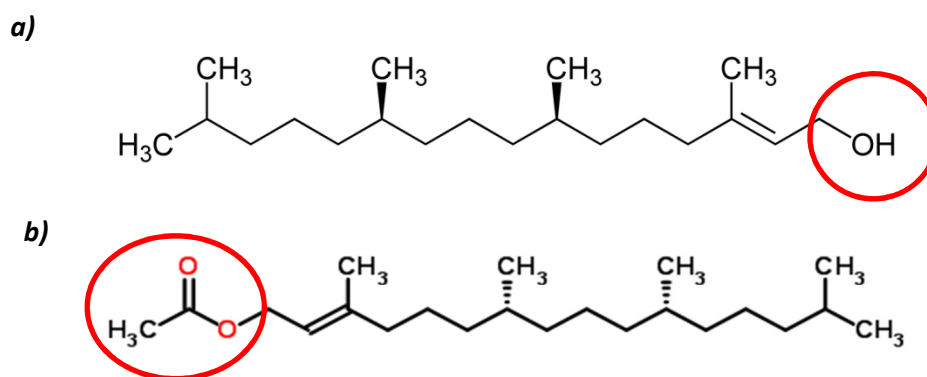


Figure 7.5: Schematic illustrating the acetylation of the phytol molecule – (a) shows the molecular structure of phytol, with the hydroxyl group highlighted in red, (b) shows the acetylated molecule, with the acetyl moiety replacing the hydroxyl group.

There are several approaches for correcting the $^2\text{H}/^1\text{H}$ signatures of phytol to remove the influence of hydrogen added by the acetyl group. One approach involves the use of acetic anhydride that has been measured conventionally for $^2\text{H}/^1\text{H}$ (Sauer *et al.*, 2001). Once the isotopic composition of the derivatising agent is known, a mass balance calculation corrects for any H added (Chikaraishi *et al.*, 2004; Sessions 2006). An alternative method for correcting hydrogen isotope data involves the derivatisation of a standard of known isotopic composition. Phthalic acid is typically used for this approach, in particular when characterising the hydrogen added during methylation of fatty acids to fatty acid methyl esters (Enders *et al.*, 2008; Sessions 2006). The phthalic acid used in this study was produced by Schimmelmann (Indiana State University), and had a hydrogen isotope composition

of -81.9‰. The esterification reaction (as described by Enders *et al.*, 2008) involves the addition of two methyl moieties to the phthalic acid molecule, in substitution for the two hydroxyl groups (Fig 7.6). The acetylation reaction acts in an analogous fashion, however in this instance the two functional groups substituted for –OH at R₁ and R₂ would be acetyl groups. Measured phthalic acid after acetylation was -145 ± 3‰, meaning that the derivatisation agent had a hydrogen isotope value of -187‰ (Appendix 6).

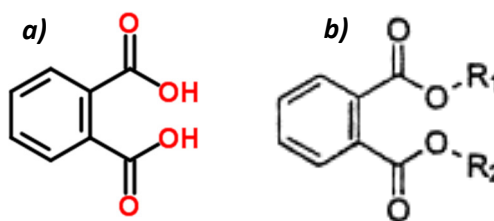


Fig. 7.6: a) the structure of phthalic acid; b) derivatised phthalic acid, R₁ and R₂ here represent acetyl groups.

7.5.2 Extraction and analysis of fatty acids for ²H/¹H analysis

Fatty acid samples were extracted and methylated at the James Hutton Institute in Aberdeen, following the method set out in Garces and Mancha (1993). Dried, chopped plant material was placed in a sample vial, and 3.3mL of a mixture of methanol:toluene:DMSP:H₂SO₄ (in the ratio 39:20:5:2 by volume) was added. The vials were then made up to 5mL total volume with 1.7mL of heptane. Vials were flushed with N₂ gas, sealed, and then placed in a water bath at 80°C for 2 h. After the first few min of heating, vials were agitated vigorously to mix all components into a single phase. After 2 h, the vials were allowed to cool to room temperature, and then were agitated again. Two layers then formed in each vial, with the top layer containing the fatty acid methyl esters (FAMES). Samples were concentrated to ~200µL, and then identified by comparison to retention times of a grain FAME standard (Sigma Aldrich) (Appendix 6) using a Carla Ebra GC/MS complete with a SGE BPX70 column (0.22mm I.D., 0.25µm film thickness, 30mm length). The GC detector was held at 300°C during analysis, while the injector was maintained at 210°C. The oven had an initial temperature of 50°C, which was held for 2 min. The

oven temperature was then raised to a 240°C at a rate of 7°C per min, and then held at this temperature for 18 min.

The $^2\text{H}/^1\text{H}$ values of the FAMES was measured using a Delta V Advantage ThermoFisher isotope-ratio mass spectrometer interfaced with GC-Isolink Trace GC Combustion and High temperature conversion (HTC) system operating at 1400 °C. The GC oven was set with the same temperature programme as described above for GC/MS analysis. All instrument quality control measurements are as stated for phytol analysis above. Analytical reproducibility of triplicate measurements of well-resolved peaks from the same sample did not exceed 6‰, while sample replicates from the same plant species typically did not differ by more than 6‰. Exceptions to this included *Limonium vulgare* where the absolute difference between sample replicates for palmitic acid was 15‰ and *Elytrigia atherica* where the absolute difference between sample replicates for linolenic acid was 17‰.

To correct for hydrogen added during derivatisation, phthalic acid of known isotopic composition (-81.9‰, Arndt Schimmelmann, Indiana University) was also prepared with the methanol:toluene:DMSO:H₂SO₄ mixture, and analysed alongside the FAME samples. The esterification reaction involves the addition of two methyl moieties to the phthalic acid molecule, in substitution for the two hydroxyl groups (Fig 7.6). Measured phthalic acid following derivatisation had a value of $-115 \pm 1\%$, meaning that the derivatising agent had a hydrogen isotope composition of -137‰ (Appendix 6).

7.5.3 Preparation and analysis of bulk plant tissue for analysis of $^2\text{H}/^1\text{H}$, percentage nitrogen, percentage carbon, and $\delta^{15}\text{N}$

Plant tissue for bulk $\delta^2\text{H}$, percentage nitrogen and carbon content, and $\delta^{15}\text{N}$ was sub-sampled from material collected for *n*-alkane analysis, which had been dried at 40 °C for 72 hr, and then stored at room temperature in the dark prior to lipid extraction, as described in Chapter 4. Dried leaf material was cryogenically ground under liquid nitrogen, and then weighed into tin capsules following the approach described for bulk carbon analysis in Chapter 5. The percentage nitrogen and carbon content of plant biomass was quantified using a Carlo Erba EA 1108 Elemental Analyser as described in detail in Chapter 5, while the nitrogen isotope analysis was carried out using a Delta XP coupled to a Costech EA (Chapter 5).

Bulk hydrogen isotopes were measured using a Delta XP ThermoFisher isotope-ratio mass spectrometer interfaced with a CosTech elemental analyser. For analysis of $\delta^2\text{H}$ a sequence of in-house casein and collagen standards were analysed at the start of each sequence, and again after every 20 samples to monitor for any instrument drift. The hydrogen reference gas was calibrated using IAEA 601 (benzoic acid), and an in-house benzoic acid standard supplied by the University of Reading. While IAEA 601 does not have a certified value for hydrogen isotope analysis, its value, and that of the in-house benzoic acid, had been previously calibrated against IAEA CH-7 (polyethelene) by the University of Reading, with reported values of $-83\pm 2\text{‰}$, and $-93\pm 0.5\text{‰}$ respectively. The hydrogen reference gas used for analysis at UEA was calibrated against the in-house benzoic acid standard, and then checked for accuracy against IAEA 601 – the measured value of this international standard using the calibrated reference gas was $82.9\pm 0.9\text{‰}$, commensurate with the values reported by the University of Reading (Appendix 6). During analysis, 3 pulses of the H_2 reference gas were passed through the mass spectrometer, and reproducibility of these reference gas peaks was typically $\pm 0.2\text{‰}$. Samples for bulk $^2\text{H}/^1\text{H}$ analysis were measured in duplicate, with absolute differences between the measured replicates typically lower than 4‰ and not exceeding 7‰ .

7.5.4 Extraction, preparation, and analysis of starch for $^2\text{H}/^1\text{H}$ analysis

7.5.4.1 Presumptive starch test

The presumptive starch test (to establish whether species were storing starch or using it on a diurnal basis) was carried out on plant material that had been frozen at -80°C until required for analysis. A minimum of 3 leaves (depending upon leaf morphology) were sub-sampled into a sample tube, and covered with 80% ethanol (ethanol:de-ionised water, v/v), and placed in a water bath at 80°C to decolourise the leaf (Fig. 7.7). Samples were checked regularly, and the ethanol solution changed at intervals. Once the samples were as close to colourless as possible, they were stained with Lugol's iodine, and left to stand for up to 10 min to test for the presence of starch. Stained samples were photographed, and analysed under a light microscope, to assess whether starch grains could be observed in the morning and/or evening leaf samples. Only those samples containing adequate quantities of starch were selected for further extraction.



Figure 7.7: preparation of samples for presumptive starch test – photo shows the leaf samples in 80% ethanol, prior to immersion in the water bath.

7.5.4.2 Starch extraction

Starch extraction was carried out on leaf material from *Atriplex portulacoides* and *Suaeda vera*, as the presumptive starch test highlighted that these were the only species likely to contain sufficient starch for isotope analysis. The method for starch extraction was adapted from that set out by Hostettler *et al* (2011). Freeze-dried plant material was ground in a cryogenic mill, and then placed in an ice-cold pestle and mortar, placed in ice to maintain a low temperature. Unlike typical starch extraction methodologies, extraction buffers such as 20M HEPES-KOH (pH8), 0.2mM ethylenediaminetetraacetic acid (EDTA), and 0.5% (v/v) Triton X-100, were not used during this process to avoid chemically altering the starch molecule and affecting the $^2\text{H}/^1\text{H}$ of the starch. Instead, the freeze-dried plant material was ground for ~10 min with 0.5% sodium dodecyl sulphate (SDS) solution, which removes proteins bound to the starch. The SDS solution was made with ultra-pure water which had been autoclaved. All solutions were also kept on ice during sample preparation.

After grinding, the homogenate was then filtered through nylon nets of 118 μ M and 48 μ M pore size, using a sample filter unit. The filtrate was then further passed through Miracloth with a pore size of 22 – 25 μ M. During filtration, the filter cloth was changed regularly to make sure it did not become clogged. The filtrate was then overlaid onto a 10 mL cushion of 95% (v/v) Percoll solution in a centrifuge tube. Samples were centrifuged at 2000 \times g for 15 min at a temperature of 20 °C. After centrifuging, the supernatant was removed and any areas containing starch transferred to a microcentrifuge tube. The supernatant and residual green/brown plant material was subsampled, stained with Lugol's solution, and examined under a light microscope to ensure that no starch was still contained in this fraction.

The mixture of plant material (green/brown) and starch (whitish) in the microcentrifuge tube (Fig. 7.8) was resuspended in SDS solution. Simply centrifuging this material did not successfully separate the starch in these saltmarsh plant samples however. Instead, a more successful approach was to spin the resuspended solution at a lower speed (0.8K) for one min. This would result in the starch staying in solution (visible as a white coloured supernatant), while the other green/brown plant tissue formed a pellet at the base of the microcentrifuge tube. The supernatant containing the starch was then pipetted off into a second microcentrifuge tube, spun down to form a pellet, and the (now clear) supernatant discarded. This process was repeated until no further starch was visible in the supernatant after spinning the resuspended sample at a low speed. At this stage, the starch pellet needed to be cleaned, as it still contained some clearly visible impurities. In addition, it also needed to be washed to remove SDS. The starch pellet was therefore resuspended in ultrapure water and then spun back down (hard) into a pellet. This time, any impurities settled on the surface of the starch pellet, and were removed with a pipette. This washing and cleaning step was repeated a minimum of 5 times for each starch sample. Once cleaned, the starch sample was covered and left to dry in a fume hood before storing in the freezer until required for analysis.

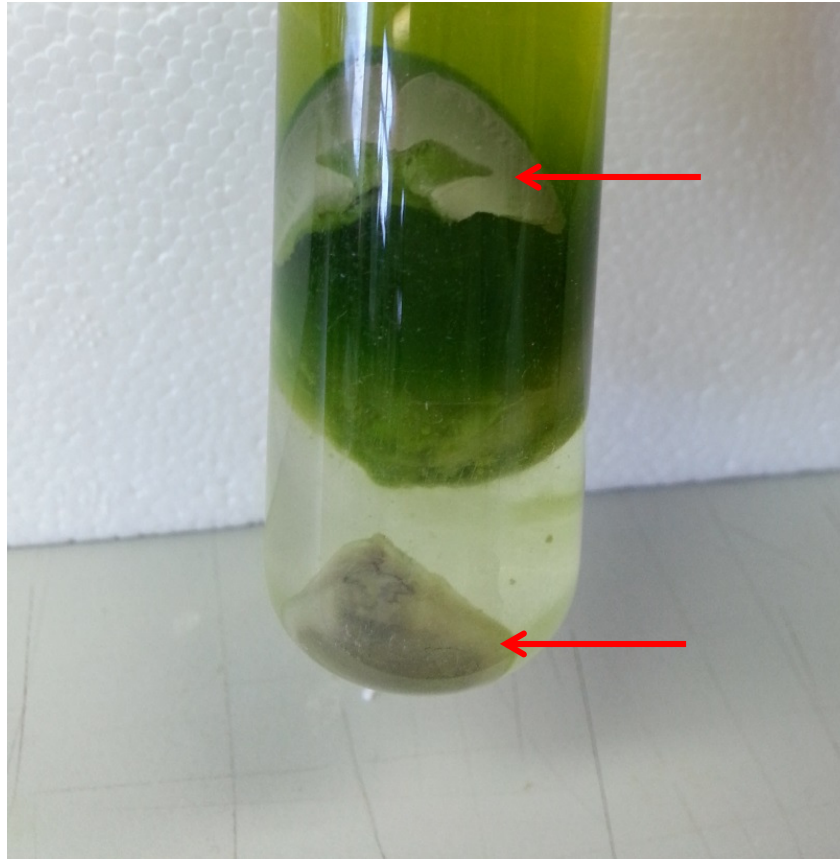


Figure 7.8: A sample from *Atriplex portulacoides* undergoing starch extraction – note the white deposits highlighted in the figure, this is the starch which requires purification.

7.5.4.3 Hydrogen isotope analysis

In order to analyse the hydrogen isotope composition of starch, the amount of exchangeable hydrogen (bound to the hydroxyl groups of the starch molecule) had to be determined. The method of Reynard and Hedges (2008) was followed for this process. Dried samples of starch from *Atriplex portulacoides* and *Suaeda vera* were weighed into tin capsules, crimped and placed in sample trays in three small desiccators. Each of these desiccators contained 150 mL of water of known isotopic composition (laboratory dehumidifier water, laboratory tap-water in-house standard, and Evian bottled water) (Fig. 7.9). In addition to the two Stiffkey species, samples of extracted and purified starch taken from potato, barley and quinoa (obtained from the John Innes Centre) were also subjected to the same approach to evaluate whether the percentage of exchangeable hydrogen differs among a range of plant species. All three desiccators were then sealed, and placed in a drying oven for 7 days at 37 °C to allow the samples to equilibrate with the water vapour in each container. Once the equilibration experiment was completed, samples were

removed from the dessicator and immediately placed in a zero-blank autosampler, coupled to a Delta XP ThermoFisher isotope-ratio mass spectrometer, and analysed as described in Section 7.5.3 above.

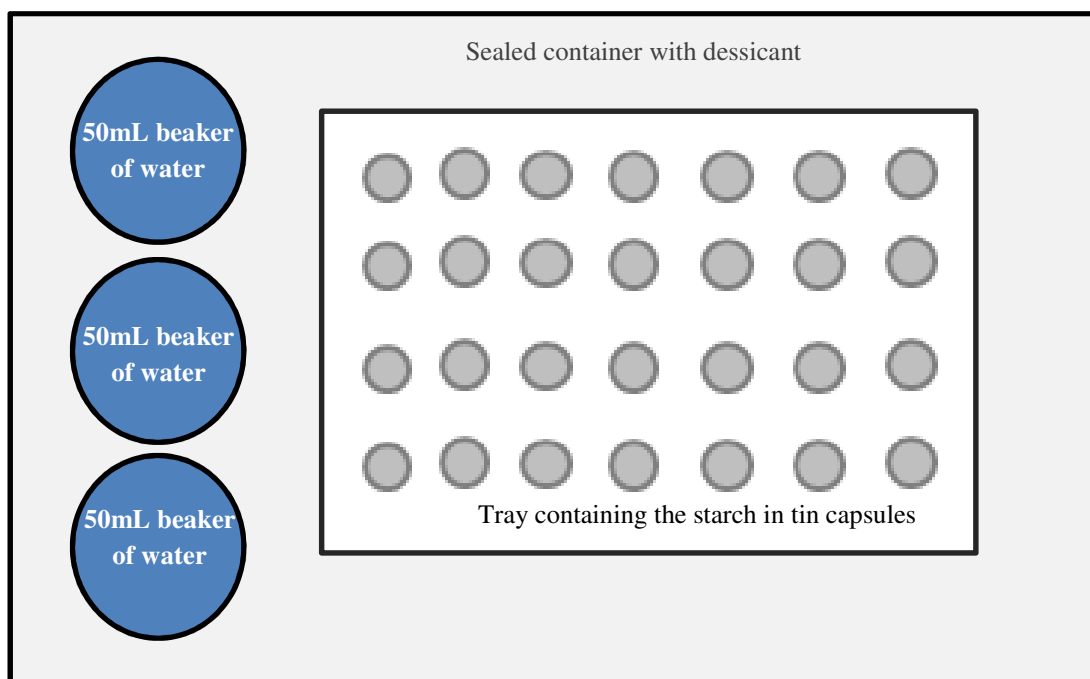


Figure 7.9: Schematic of the set-up used for quantifying exchangeable hydrogen in starch.

7.6 RESULTS

7.6.1 $^2\text{H}/^1\text{H}$ of phytol

Following correction for hydrogen added during acetylation (Section 7.5.1), the $^2\text{H}/^1\text{H}$ values of phytol from species sampled in September 2012 varied by up to 63‰ (Table 7.1; Fig. 7.10). In contrast to data presented for leaf wax *n*-alkanes in Chapter 6, the most ^2H -depleted phytol value was observed for *Atriplex portulacoides* ($-361 \pm 1\text{‰}$) while the most ^2H -enriched was found in the C_4 grass *Spartina anglica* ($-298 \pm 1\text{‰}$). *Limonium vulgare*, a species which typically had one of the more ^2H -enriched *n*- C_{29} profiles, was among the more ^2H -depleted in terms of phytol isotopic composition. The C_3 grass *Elytrigia atherica*, the species with the

most ^2H -depleted $n\text{-C}_{29}$ alkane (Chapter 6), had one of the more intermediate phytol $^2\text{H}/^1\text{H}$ values (Table 7.1, Fig. 7.10).

Statistical comparison of the $^2\text{H}/^1\text{H}$ of phytol and leaf water from August 2012 (Chapter 6) revealed a positive relationship, although this was only significant at an 80% confidence interval ($r = 0.5$, $P = 0.2$, $n=7$, Pearson's moment correlation, Minitab v.16). No relationship was observed between the $^2\text{H}/^1\text{H}$ values of phytol and WA n -alkanes, or phytol $^2\text{H}/^1\text{H}$ and the hydrogen isotope composition of bulk tissue ($P > 0.05$, $n=7$, Rank Spearman correlation, Minitab v.16).

Table 7.1: $^2\text{H}/^1\text{H}$ of phytol

Species	Rep. 1	Rep. 2	Rep. 3	Mean	SE	$\epsilon_{\text{phytol/lw}}$	$\epsilon_{\text{phytol/WA}}$	$\epsilon_{\text{phytol/bulk}}$
<i>Atriplex portulacoides</i> (C_3)	-360	-361	-362	-361	1	-364	-234	-278
<i>Elytrigia atherica</i> (C_3)	-339	-340	-331	-337	3	-332	-138	-235
<i>Limonium vulgare</i> (C_3)	-347	-347	-345	-346	1	-356	-251	-282
<i>Phragmites australis</i> (C_3)	-353	-353	-355	-353	1	-352	-190	-278
<i>Salicornia europaea</i> (C_3)	-302	-316	-315	-311	4	-324	-209	-243
<i>Spartina anglica</i> (C_4)	-299	-298	-295	-298	1	-308	-165	-235
<i>Sueda vera</i> (C_3)	-321	-318	-318	-319	1	-321	-209	-240

*text in parentheses denote C_3 and C_4 plants, "SE" = standard error of analytical measurements of the same sample

Calculated $^2\text{H}/^1\text{H}$ fractionation between phytol and: (i) leaf water; (ii) weighted average n -alkanes (calculated for $^2\text{H}/^1\text{H}$ as for $^{13}\text{C}/^{12}\text{C}$ using Eq. 3 in Chapter 5); and (iii) bulk plant tissue showed that $\epsilon_{\text{phytol/lw}}$ (calculated according to Eq. 2 in Chapter 6) varied by 58‰, while $\epsilon_{\text{phytol/bulk}}$ varied by 47‰. Variation in $\epsilon_{\text{phytol/WA}}$ was almost twice as high as this, reaching 86‰ (Table 7.1; Fig. 7.11).

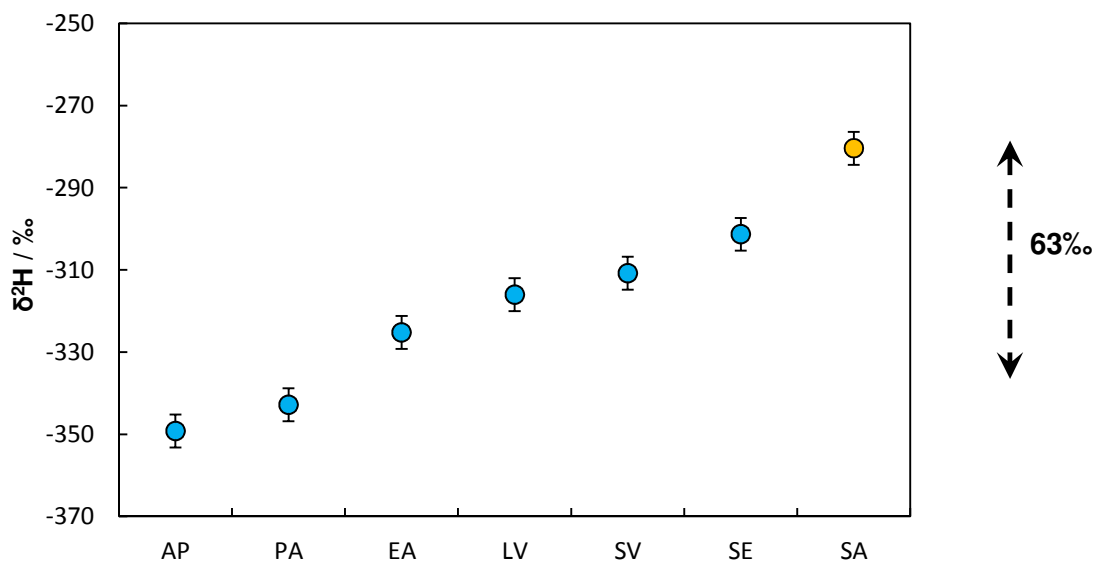


Figure 7.10 Interspecies variation in the $^2\text{H}/^1\text{H}$ of phytol from samples collected in August 2012. AP, *Atriplex portulacoides*; EA, *Elytrigia atherica*; LV, *Limonium vulgare*; PA, *Phragmites australis*; SE, *Salicornia europaea*; SA, *Spartina anglica*; SV, *Suaeda vera*. Analytical error for repeat measurements of the same sample did not exceed 4%.

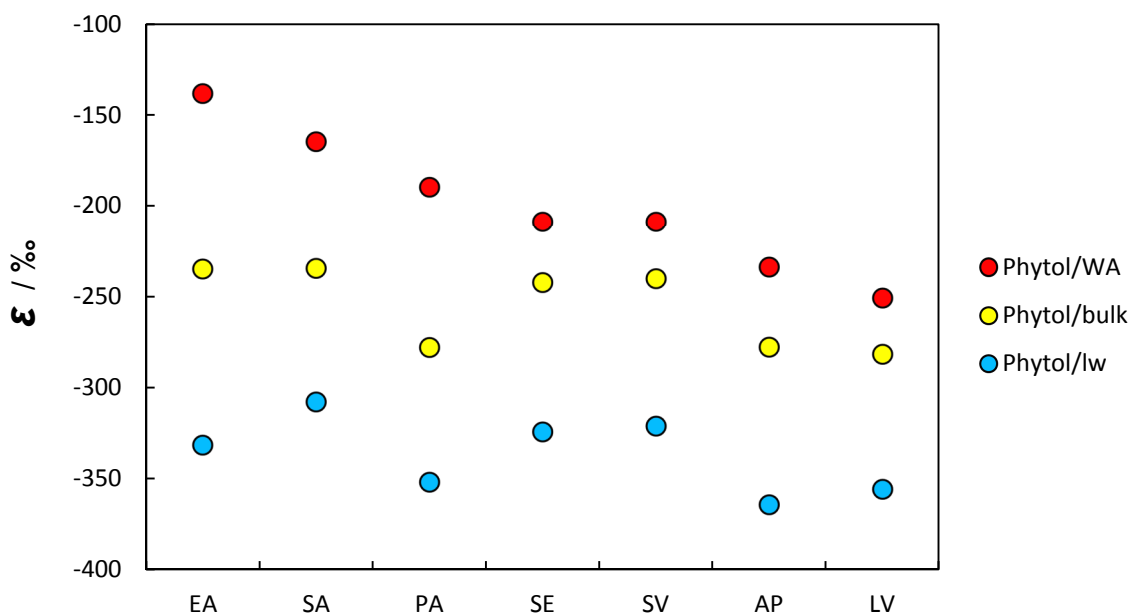


Figure 7.11: Calculated fractionation between the $^2\text{H}/^1\text{H}$ of phytol and weighted average alkane isotope composition (red) bulk biomass isotope composition (yellow) and leaf water isotope composition (blue). AP, *Atriplex portulacoides*; EA, *Elytrigia atherica*; LV, *Limonium vulgare*; PA, *Phragmites australis*; SE, *Salicornia europaea*; SA, *Spartina anglica*; SV, *Suaeda vera*.

7.6.2 $^2\text{H}/^1\text{H}$ values of fatty acids

After correction for hydrogen added during methylation (Section 7.5.2), FAME $^2\text{H}/^1\text{H}$ varied widely both: (i) among plant species; and (ii) between different FA homologues. The most ^2H -enriched FAME measured was linoleic acid, while palmitic acid and linolenic acid both had relatively negative values (Table 7.2, Figs 7.12). Palmitic acid was between 26 and 122‰ ^2H -depleted compared to linoleic acid, with the greatest difference between homologues observed for the C_3 monocot *Phragmites australis* and the least for C_3 the stem succulent *Salicornia europaea*. Linolenic acid was between 39 and 110‰ ^2H -depleted compared to linoleic acid, this time the greatest difference in hydrogen isotope composition between the two homologues was seen in the C_3 monocot *Elytrigia atherica* while the lowest difference was again observed in *Salicornia europaea* (Fig. 7.12). Overall interspecies differences also varied among FA homologues, and went in the order of linoleic < linolenic < palmitic (77‰ < 103‰ < 120‰) (Fig. 7.12). For palmitic and linolenic acid, *Elytrigia atherica* had the most ^2H -depleted FAME value. *Suaeda vera* had the most ^2H -enriched palmitic acid value, while *Limonium vulgare* had the most ^2H -enriched linolenic acid value (Table 7.2, Fig. 7.12).

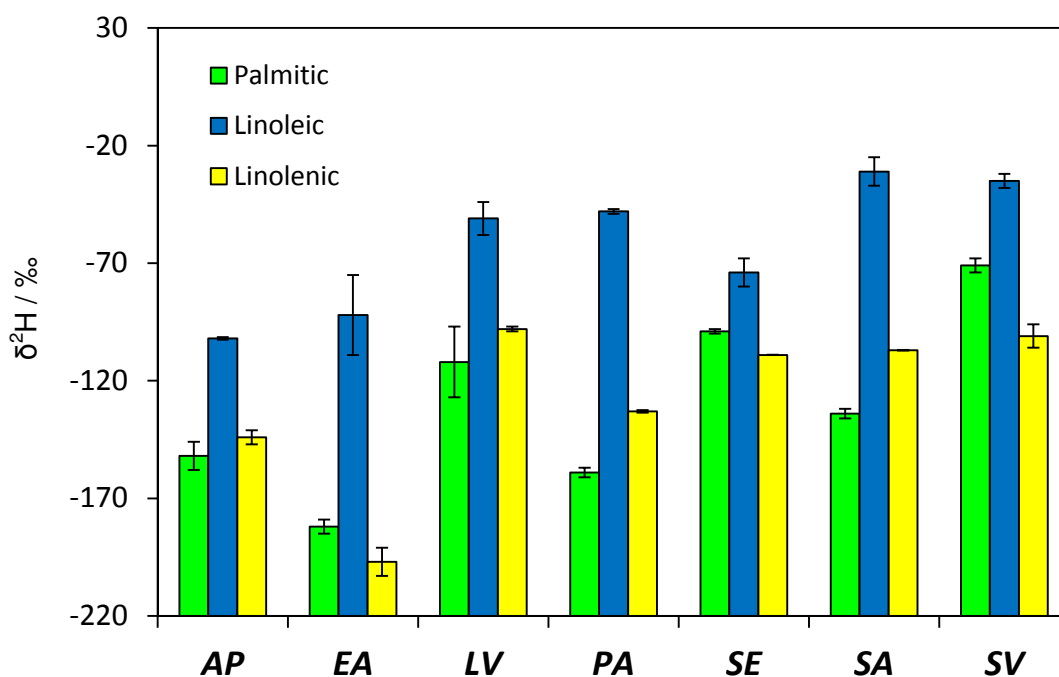


Figure 7.12: Comparison of the isotope composition of palmitic, linoleic and linolenic fatty acid $^2\text{H}/^1\text{H}$. Abbreviations: AP, *Atriplex portulacoides*; EA, *Elytrigia atherica*; LV, *Limonium vulgare*; PA, *Phragmites australis*; SE, *Salicornia europaea*; SA, *Spartina anglica*; SV, *Suaeda vera*. Error bars show absolute differences between sample replicates for each FAME analysed.

Table 7.2: $^2\text{H}^1\text{H}$ of FAMES from the Stiffkey species, September 2012

Species	Palmitic	AD _{palmitic}	Linoleic	AD _{linoleic}	Linolenic	AD _{linolenic}	$\epsilon_{\text{palmitic/wax}}$	$\epsilon_{\text{linoleic/wax}}$	$\epsilon_{\text{linolenic/wax}}$
<i>Atriplex portulacoides</i>	-148		-98		-141				
(C3)	-159		-97		-146				
	-154	6	-98	0	-144	3	16	82	26
<i>Elytrigia atherica</i>	-189		-104		-204				
(C3)	-183		-71		-191				
	-186	3	-87	17	-197	7	57	186	43
<i>Limonium vulgare</i>	-95		-49		-95				
(C3)	-125		-34		-93				
	-110	15	-42	8	-94	1	17	95	35
<i>Phragmites australis</i>	-158		-37		-133				
(C3)	-163		-40		-132				
	-160	2	-38	1	-132	0	58	212	93
<i>Salicornia europaea</i>	-99		-74		-106				
(C3)	-93		-61		-106				
	-93	3	-67	7	-106	0	39	69	24
<i>Spartina anglica</i>	-131		-14		-103				
(C4)	-136		-27		-103				
	-134	2	-21	7	-103	0	35	170	72
<i>Suaeda vera</i>	-65		-24		-103				
(C3)	-66		-30		-92				
	-66	1	-27	3	-98	6	87	133	50

*AD = absolute difference between sample replicates from the same species

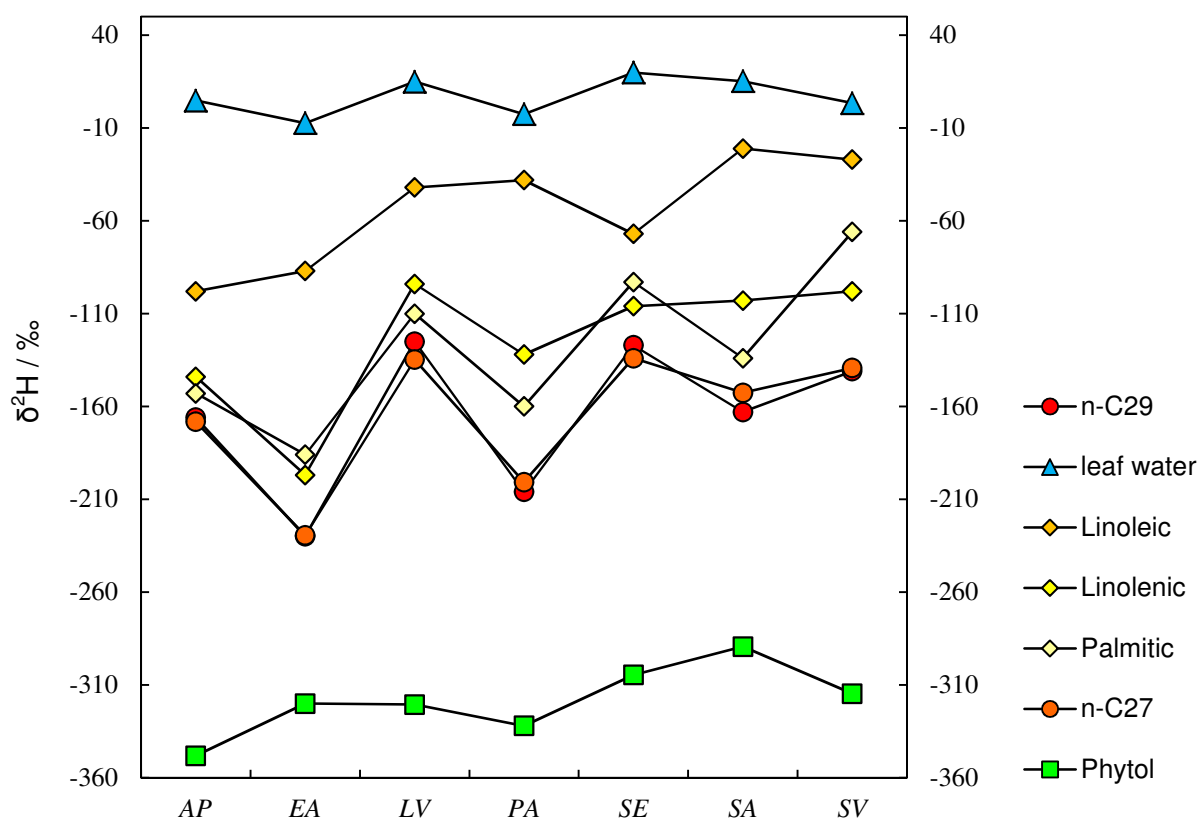


Figure 7.13: Comparison of $^2\text{H}/^1\text{H}$ of leaf water, phytol, fatty acids and n -alkanes for the seven Stiffkey species. Abbreviations: AP, *Atriplex portulacoides*; EA, *Elytrigia atherica*; LV, *Limonium vulgare*; PA, *Phragmites australis*; SE, *Salicornia europaea*; SA, *Spartina anglica*; SV, *Suaeda vera*. Error bars, showing sample replicates, were typically too small to be seen on this plot, however did not exceed 6‰ for $n\text{-C}_{27}$ and $n\text{-C}_{29}$, 4‰ for phytol and 1‰ for leaf water. For FAs, differences between sample duplicates are provided in Table 7.2

Statistical comparison of the FAME $^2\text{H}/^1\text{H}$ with leaf water $^2\text{H}/^1\text{H}$ revealed no relationship between C16 and C18:3 ($P > 0.05$, Pearson's product moment correlation, Minitab v.16). Linoleic acid, however, had a positive relationship with leaf water $^2\text{H}/^1\text{H}$, although that relationship was only significant at a ~90% confidence interval ($r = 0.7$, $P = 0.07$ Pearson's product moment correlation, Minitab v 16). Comparison of the FAMEs with each other revealed that C16 and C18:3 $^2\text{H}/^1\text{H}$ had a strong positive correlation ($r = 0.8$, $P = < 0.05$, Pearson's product moment correlation, Minitab v 16), while C18:2 was not correlated with either C16 or C18:3. Comparison of the FAME $^2\text{H}/^1\text{H}$ values to those of n -alkanes (Chapter 6) showed that the FAME values are generally slightly ^2H -enriched compared to the n -alkanes and phytol, and depleted relative to leaf water (Fig. 7.13). Fractionation calculated between the linoleic and weighted average n -alkane $\delta^2\text{H}$ values revealed

the highest values for $\epsilon_{\text{linoleic/WA}}$ of up to 212‰ (*Phragmites australis*) with *Salicornia europaea* having the lowest (69‰). Fractionation between palmitic and linolenic acid and weighted average *n*-alkane $\delta^2\text{H}$ values was generally far lower, with values as small as 16‰ (Table 7.4). Overall, taking all biomarkers analysed into account, maximum interspecies variability in $^2\text{H}/^1\text{H}$ values increased in the order leaf water < phytol < C18:2 < C18:3 < C16:0 < *n*-alkanes (Fig. 7.14)

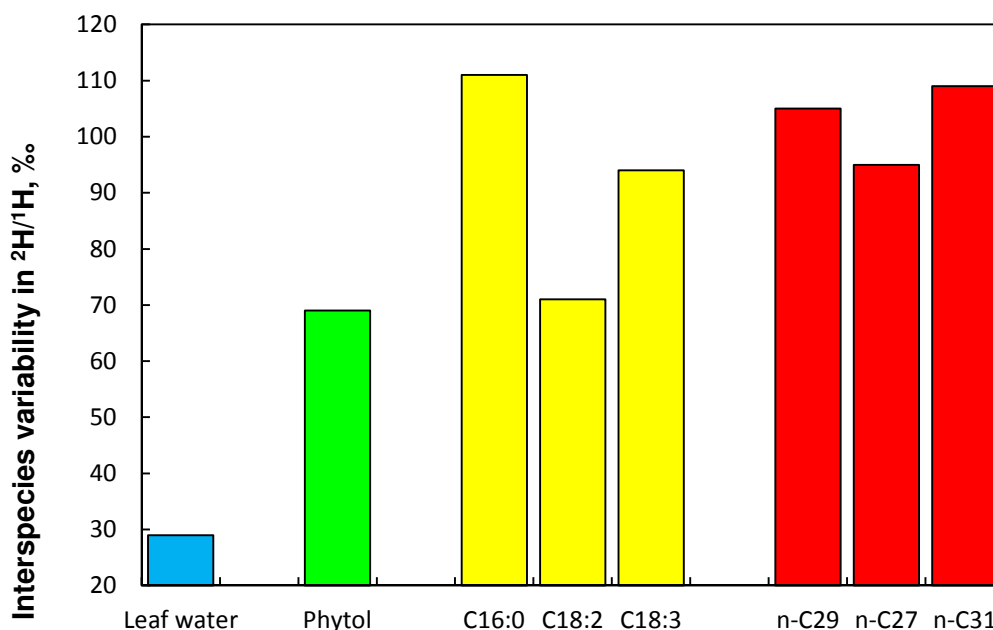


Figure 7.14: Comparison of the magnitude of interspecies variation in $^2\text{H}/^1\text{H}$ for leaf water (blue), phytol (green), fatty acids (yellow) and *n*-alkanes (red)

7.6.3 $^2\text{H}/^1\text{H}$ of starch

7.6.3.1 Presumptive starch test

The presumptive starch test showed that in general, the C_3 and C_4 monocots did not store starch for longer than diurnal cycles (Table 7.3). *Phragmites australis* sampled in the morning was found to contain no starch, whilst the evening sample only showed evidence of a small number of stained starch grains visible under a light microscope. *Elytrigia atherica* had clearly visible starch grains in both the morning and evening samples when viewed under a light microscope, but the percentage starch content did not appear to be very high relative to other dicot species. Similarly, *Spartina anglica*, the C_4 monocot, also had a larger number of starch grains in the evening sample relative to that collected in the morning.

Among the dicot species, results were more variable. Evening samples from the perennial herb *Limonium vulgare* showed much darker staining than those from the morning (Fig. 7.15), illustrating that whilst this species produces a relatively large amount of starch, some of it is utilised during periods of darkness. Leaves from *Atriplex portulacoides*, the evergreen shrub, contained a large amount of starch in both the morning and evening samples, suggestive of long-term carbohydrate storage (Table 7.3). This species also contained two distinctive sizes of starch grain, the larger of which appeared on visual examination under a light microscope to be approximately ten times the size of the smaller grains. The two succulent species sampled at Stiffkey, *Salicornia europaea* and *Suaeda vera*, both tested positive for starch when stained with Lugol's solution. *Salicornia europaea*, however, appeared to turnover some of the starch stored during the day throughout the night, as the evening sample was observed to be darker than the morning sample. This was not the case with *Suaeda vera*, where leaves stained a very dark colour from both morning and evening samples (Table 7.3).

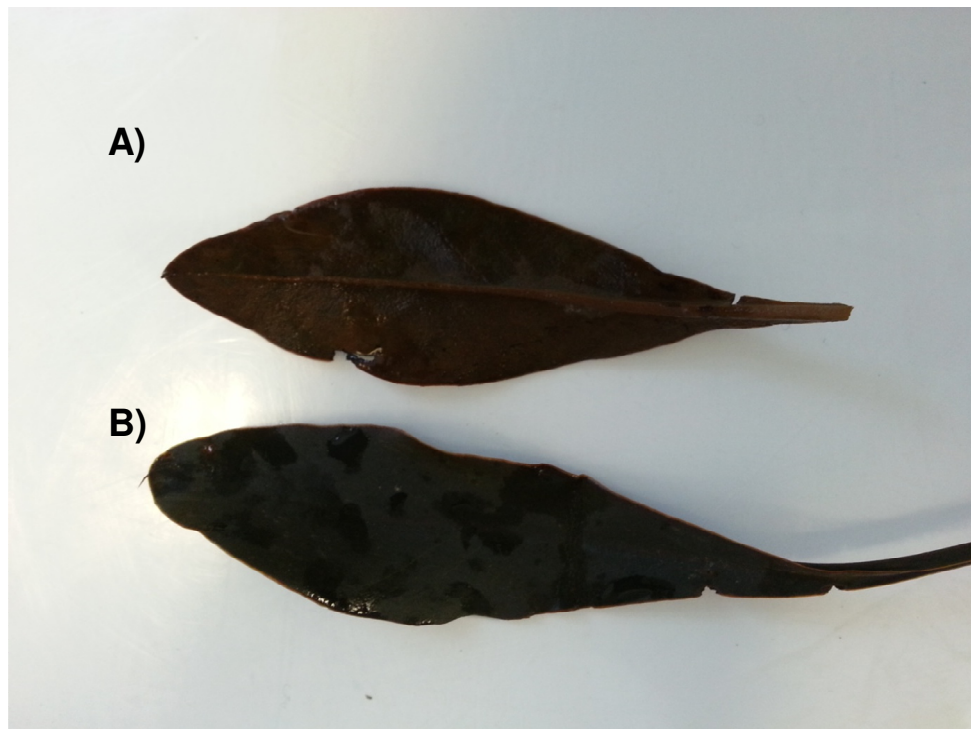


Figure 7.15: *Limonium vulgare* leaves stained with Lugol's solution. A) AM sample, B) PM sample. Note the darker staining to the PM sample.

Table 7.3: Results from starch accumulation tests

Species	Evidence of long-term starch accumulation
<i>Atriplex portulacoides</i>	Yes – species contained a large amount of starch including two different grain sizes
<i>Elytrigia atherica</i>	No - only limited accumulation during diurnal cycles for use in dark respiration
<i>Limonium vulgare</i>	Yes – although a proportion is used during the diurnal cycle
<i>Phragmites australis</i>	No
<i>Salicornia europaea</i>	Yes - although a proportion is used during the diurnal cycle
<i>Spartina anglica</i>	No – only limited accumulation during diurnal cycles for use in dark respiration
<i>Suaeda vera</i>	Yes – species contained a large amount of starch

7.6.3.2 Quantification and correction for exchangeable hydrogen in starch

Exchangeable hydrogen in the starch samples was calculated from the original equation of Reynard and Hedges (2008):

$$\delta^2H_{tot} = (1 - f)\delta^2H_n + f\epsilon + f\left(\frac{\epsilon}{1000} + 1\right)\delta^2H_w \quad (\text{Eq. 1})$$

Where δ^2H_{tot} is a function of the equilibration water (δ^2H_w), the fraction of exchangeable (f) and the non-exchangeable hydrogen (δ^2H_n), and the fractionation factor (ϵ). Eq. 1 was rearranged into Eq. 2 to solve for δ^2H_n

$$\delta^2H_n = \left[\frac{\delta^2H_{tot} - f\left(\frac{\epsilon}{1000} + 1\right)\delta^2H_w}{(1-f)} \right] - f\epsilon \quad (\text{Eq. 2})$$

f , the fraction of exchangeable hydrogen, can also be obtained from Equation 3, where R_{total1} and R_{total2} refers to the isotopic composition of the starch grains exposed to the equilibration waters, and $Rw1$ and $Rw2$ refer to the isotopic composition of the equilibration waters themselves.

$$f_{ex} = \frac{R_{total1} - R_{total2}}{R_{w1} - R_{w2}}$$

(Eq. 3)

f can also be obtained from the equation of the line ($y = mx+c$) obtained from cross plotting the hydrogen isotope composition of the equilibration water with the isotopic composition of the measured starch (Fig. 7.16) (Reynard and Hedges, 2008). In this instance, f is represented by the “ m ” term, while ϵ (Equation 3) is represented by the “ c ” term. Calculations of the exchangeable fraction of hydrogen in starch was carried out for *Atriplex portulacoides* and *Suaeda vera* using both of these approaches, revealing that 27% of the *Atriplex* signal came from exchangeable hydrogen, rising to 41% of the signal recorded by the *Suaeda* starch.

The hydrogen isotope signal (measured values post exchange can be found in Appendix 6) was then corrected for exchangeable hydrogen using Equation 2, which resulted in a value of -174‰ for *Suaeda*, and -159‰ for *Atriplex* (when calculated using the Evian water equilibration experiment). Unfortunately, a very small amount of starch was produced by *Suaeda vera*. This meant that only one replicate per equilibration experiment was possible for this species. When checking the correction for exchangeable hydrogen by performing the calculation again using data from the equilibration experiment that had been carried out with laboratory tap water, a value of -151‰ was obtained for *Atriplex*, but a value of -158‰ was obtained for *Suaeda*. The uncertainty in the measurement of $^2\text{H}/^1\text{H}$ values for *Suaeda vera* (i.e. an absolute difference of 8‰ between the two calculated results) would ideally mean that this result should be repeated to try to reduce this. Taking an average of the values obtained for the calculations gives a final starch hydrogen isotope composition of $-155 \pm 4\text{‰}$ for *Atriplex*, and $-166 \pm 8\text{‰}$ for *Suaeda*. The exchangeable hydrogen fraction in the other starch samples obtained from John Innes Centre, Norwich (where the starch extraction was performed) revealed considerable variation among the different plant species. Because of time constraints, it was not possible to fully ascertain the extraction methods used to purify these comparison starch samples. The amount of exchangeable hydrogen, however, ranged from 3% (Quinoa) to 37% (potato). Starch from two similar monocot species, wild wheat and barley, had 20% exchangeable hydrogen.

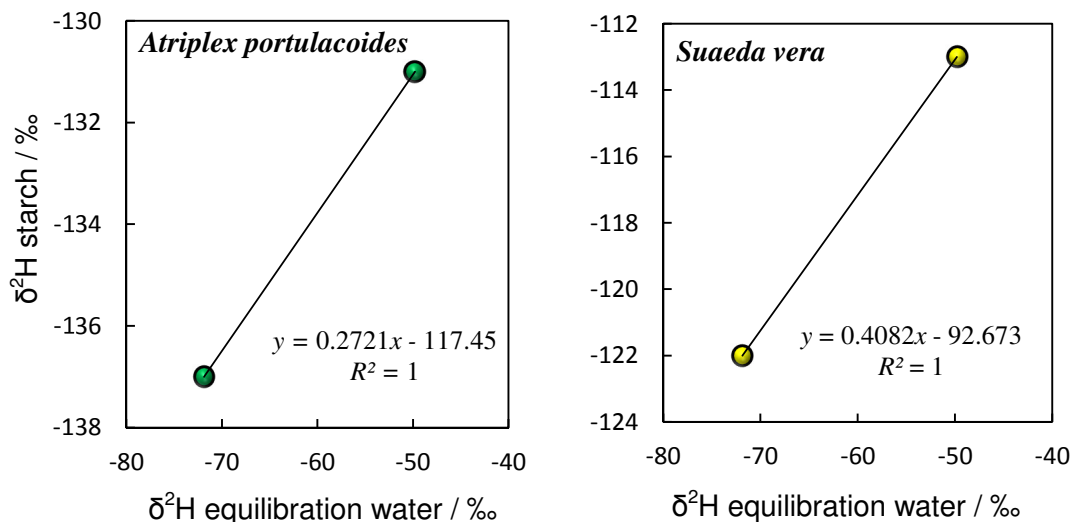


Figure 7.16: Cross-plot of the hydrogen isotope composition of the equilibration water and the starch grains from the equilibration experiment. The equation of the line, used to identify f and ϵ in equation 3

7.6.3.3 Corrected $^2\text{H}/^1\text{H}$ of starch

Comparison of corrected starch $^2\text{H}/^1\text{H}$ from *Atriplex portulacoides* and *Suaeda vera* with those from leaf water, bulk leaf tissue, and WA n -alkanes revealed that starch was between 154 and 171‰ ^2H -depleted relative to leaf water. Starch was also depleted relative to bulk leaf biomass by 57 to 77‰ (Table 7.4). When compared to WA alkane $^2\text{H}/^1\text{H}$ values, starch from *Atriplex* was almost identical to WA alkane values, while starch from *Suaeda* was 40‰ ^2H -depleted (Table 7.4).

Table 7.4: Starch hydrogen isotope data

	Leaf Water	Bulk biomass	Starch	WA alkane	$\epsilon_{\text{starch/lw}}$	$\epsilon_{\text{starch/bulk}}$	$\epsilon_{\text{starch/WA}}$
<i>Atriplex</i>	-1	-104	-155	-155	-154	-57	0
<i>Suaeda</i>	6	-96	-166	-130	-171	-77	-41

7.6.4 $^2\text{H}/^1\text{H}$ of bulk plant tissue

The bulk hydrogen isotope composition of all species sampled over the 2012 growing season (Table 7.5) range from -60‰ (*Spartina anglica*, March) to -133‰ (*Elytrigia atherica*, September). Interspecies variability in bulk $^2\text{H}/^1\text{H}$ values for each sampling interval exceeded 30‰, with the greatest range observed in May (56‰) and September (51‰). *Limonium vulgare* and *Spartina anglica* (the C_4 monocot) generally recorded the most ^2H -enriched bulk tissue values, while *Atriplex portulacoides* and *Elytrigia atherica* were typically the most ^2H -depleted (Fig. 7.17). The greatest range in seasonal shifts in bulk tissue $^2\text{H}/^1\text{H}$ was observed for the C_3 grass *Elytrigia atherica*, and the C_4 grass *Spartina anglica* (Fig. 7.17), which both recorded shifts of 35‰. The stem succulent *Salicornia europaea* had the most consistent bulk $^2\text{H}/^1\text{H}$ values throughout the 2012 growing season, shifting by only 3‰. Comparison of leaf water $^2\text{H}/^1\text{H}$ values with bulk tissue revealed that no statistically significant relationship existed between these two sets of data ($P > 0.05$, Rank Spearman correlation, $n=26$).

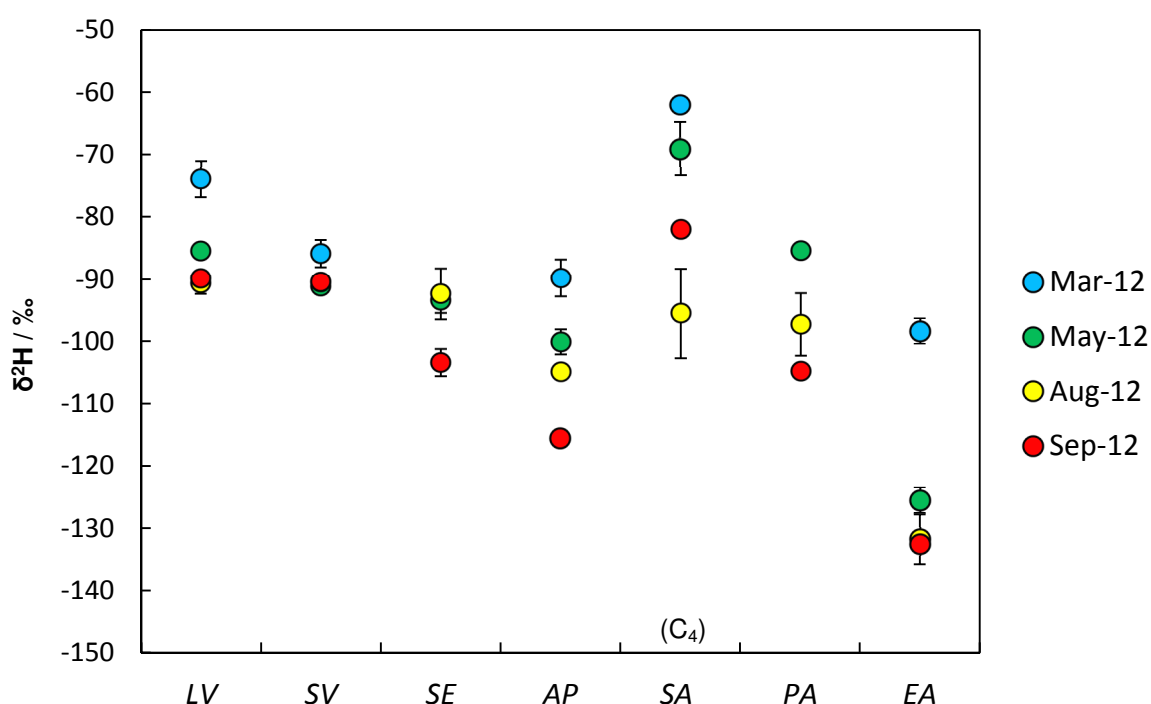


Figure 7.17: Seasonal variation in bulk hydrogen isotope composition; abbreviations: AP, *Atriplex portulacoides*; EA, *Elytrigia atherica*; LV, *Limonium vulgare*; PA, *Phragmites australis*; SE, *Salicornia europaea*; SA, *Spartina anglica*; SV, *Suaeda vera*. Error bars show absolute difference between sample duplicates of the same species.

Table 7.5: Bulk plant tissue $^2\text{H}/^1\text{H}$

Month	Location	Plant species	$\delta^2\text{H}$ bulk	$\text{AD}_{2\text{H}}$ bulk
Mar-12	Site 2	<i>Atriplex portulacoides</i>	-90	3.5
	Site 2	<i>Elytrigia atherica</i>	-98	2.0
	Site 3	<i>Limonium vulgare</i>	-62	0.8
	Site 1	<i>Spartina anglica (C4)</i>	-60	0.5
	Site 2	<i>Suaeda vera</i>	-86	1.6
May-12	Site 2	<i>Atriplex portulacoides</i>	-100	2.6
	Site 2	<i>Elytrigia atherica</i>	-126	2.4
	Site 3	<i>Limonium vulgare</i>	-85	0.1
	Site 2	<i>Phragmites australis</i>	-85	0.8
	Site 1	<i>Salicornia Europaea</i>	-93	2.1
	Site 1	<i>Spartina anglica (C4)</i>	-69	3.7
	Site 2	<i>Suaeda vera</i>	-91	1.0
Aug-12	Site 2	<i>Atriplex portulacoides</i>	-105	0.7
	Site 2	<i>Elytrigia atherica</i>	-132	3.7
	Site 3	<i>Limonium vulgare</i>	-92	0.9
	Site 2	<i>Phragmites australis</i>	-97	4.6
	Site 1	<i>Salicornia Europaea</i>	-92	4.1
	Site 1	<i>Spartina anglica (C4)</i>	-94	6.4
	Site 2	<i>Suaeda vera</i>	-91	0.0
Sep-12	Site 2	<i>Atriplex portulacoides</i>	-116	0.3
	Site 2	<i>Elytrigia atherica</i>	-133	0.2
	Site 3	<i>Limonium vulgare</i>	-90	0.1
	Site 2	<i>Phragmites australis</i>	-105	0.7
	Site 1	<i>Salicornia Europaea</i>	-91	0.8
	Site 1	<i>Spartina anglica (C4)</i>	-82	0.0
	Site 2	<i>Suaeda vera</i>	-103	2.2

Comparison of all bulk $^2\text{H}/^1\text{H}$ data with n -alkane values presented in Chapter 6 shows that there is a statistically significant correlation between bulk and : (i) weighted average n -alkane $^2\text{H}/^1\text{H}$ ($r = 0.6$, $P < 0.05$, Rank Spearman correlation) ; (ii) n - C_{29} alkane $^2\text{H}/^1\text{H}$ ($r = 0.6$, $P < 0.05$, Rank Spearman correlation). Separating plants into C_3 and C_4 monocots, and C_3 dicots and succulents however reveals that the correlation is stronger for the monocots ($r = 1$, $P < 0.05$, Rank Spearman correlation, $n=11$) than the dicots and succulents ($r = 0.8$, $P < 0.05$, Rank Spearman correlation, $n=15$). Regression equations (Minitab v.16) calculated for both datasets were very similar (Fig. 7.18), with the monocots having consistently greater offset between bulk and WA n -alkane $^2\text{H}/^1\text{H}$ values.

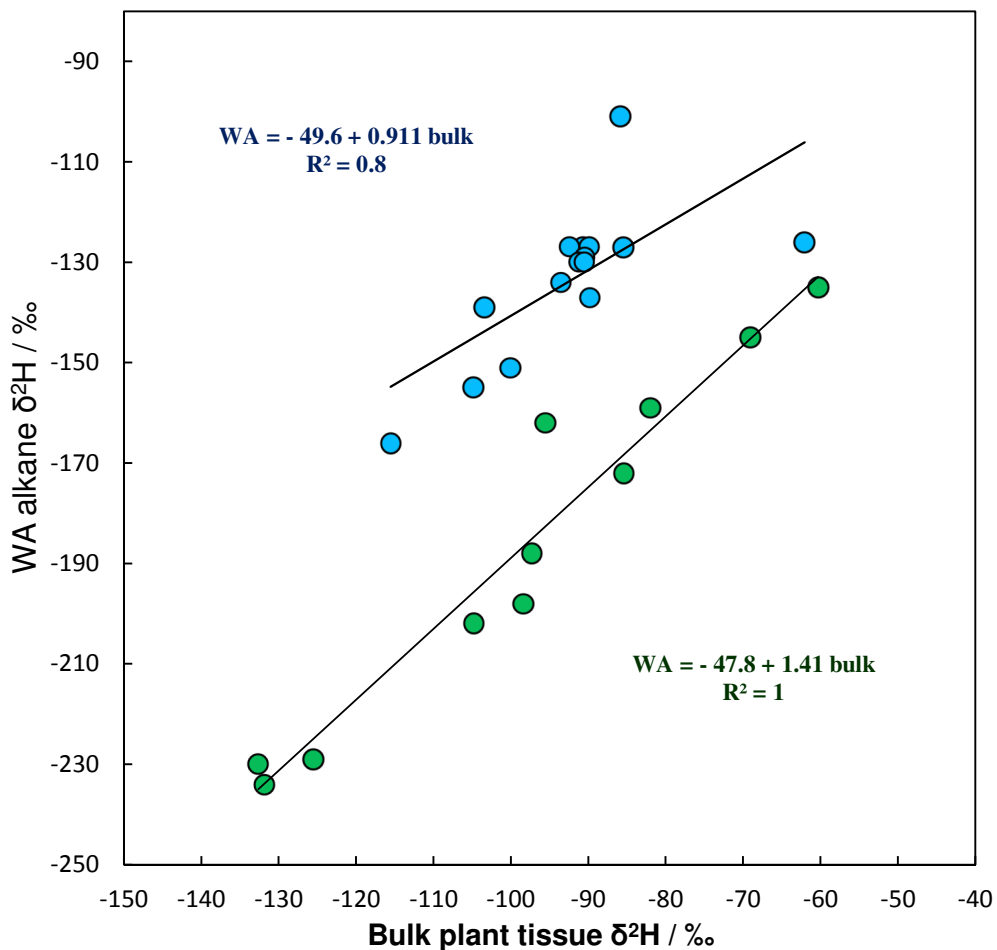


Figure 7.18: Correlation between bulk and weighted average n -alkane $^2\text{H}/^1\text{H}$ values. Blue = dicot/succulent functional types, green = C_3 and C_4 monocot functional types.

Despite the strength of these correlations, close comparison of seasonal patterns in the hydrogen isotope data reveal some interesting differences in the trends observed at the bulk and *n*-alkane level. For example, the C₄ grass *Spartina anglica* has one of the more intermediate *n*-alkane ²H/¹H profiles (Chapter 6), despite having one of the more ²H-enriched leaf water signals across 2012. Bulk ²H/¹H for *Spartina anglica*, however, are among the most ²H-enriched of the sampled species. In addition, *n*-C₂₉ ²H/¹H recorded for the C₃ reed *Phragmites australis* are consistently among the most ²H-depleted (Chapter 6), whereas at the bulk level, tissue from this species is typically more ²H-enriched than the evergreen shrub *Atriplex portulacoides* (Table 7.5, Fig. 7.17).

Calculation of apparent fractionation (using the equation described in Chapters 5 and 6) between: (i) bulk plant tissue and WA alkanes; and (ii) bulk and leaf water, shows that the relationship between bulk plant tissue and *n*-alkane isotopic composition remains very constant for all species throughout 2012 with the exception of the very early growing season (Fig. 7.19A), while the fractionation between leaf water and bulk tissue ranges from ~ -40‰ to -120‰ across the same period and is greatest for *Elytrigia atherica* (Fig. 7.19B). The magnitude of the fractionation between leaf water and bulk plant tissue is, however, almost half of that reported for the *n*-alkane data (Chapter 6).

7.6.5 Percentage carbon and nitrogen composition of bulk leaf tissue

Seasonal changes in the percentage C and N composition of these plants, and their C:N ratios, has been examined in detail in Chapter 5. Investigation of the relationships between %C, %N and C:N ratios and the hydrogen isotope composition of the *n*-C₂₇ and *n*-C₂₉ alkanes for all plant groups, including monocots and dicots, reported a negative correlation for the entire sampling period (June 2011 – September 2012) between *n*-C₂₇, *n*-C₂₉, %C and the C:N ratio ($r = -0.5$, $P < 0.05$, Rank Spearman correlation, $n = 47$, Minitab v.16). The relationship between the ²H/¹H values of *n*-C₂₇ and *n*-C₂₉ alkanes and the %N content for all species appeared relatively weak, although statistically significant ($r = 0.3$, $P < 0.05$, Rank Spearman correlation, $n = 47$, Minitab v.16) (Fig. 7.20 A-C).

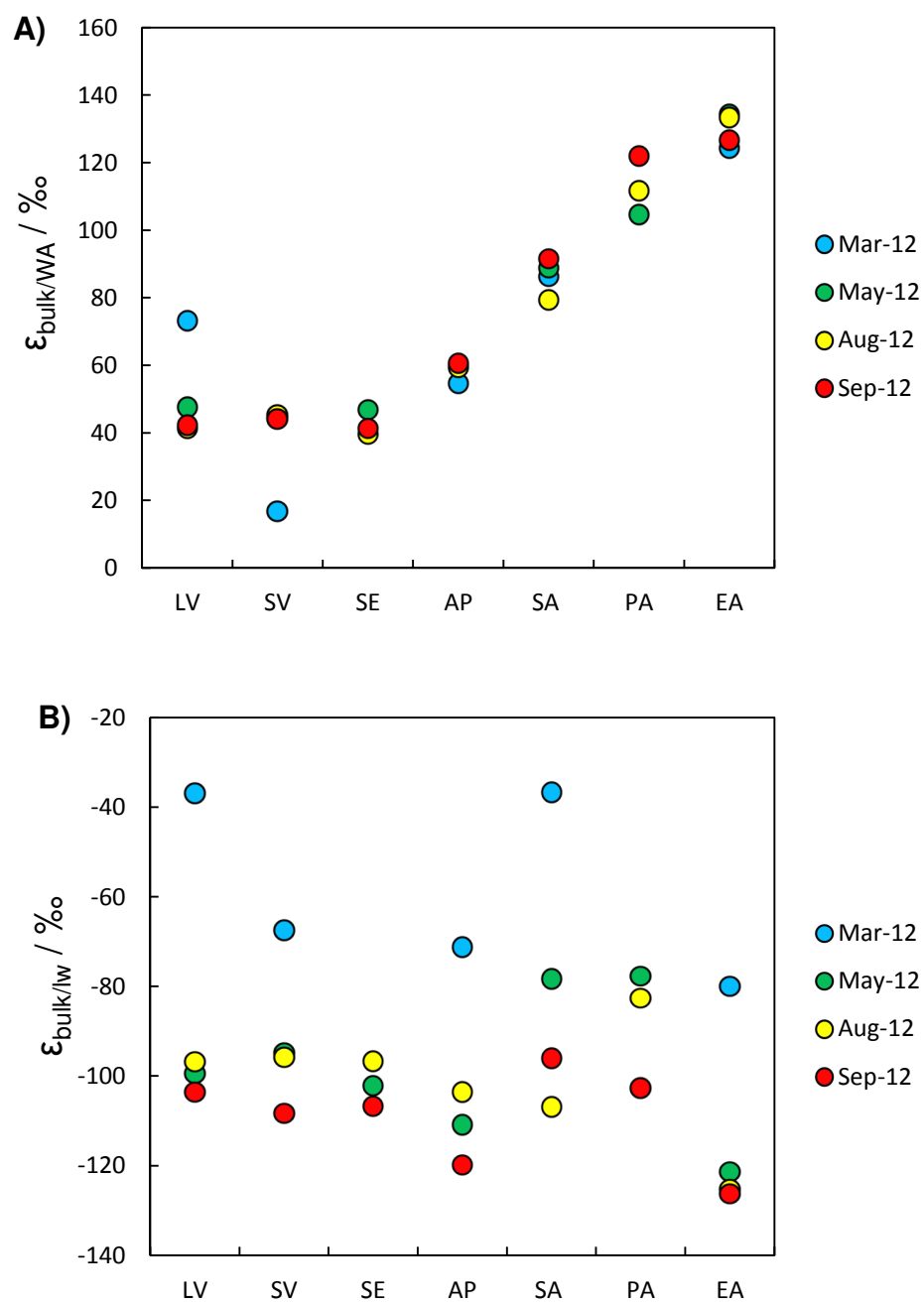


Figure 7.19: Comparison of fractionation between (A) bulk leaf tissue $^2\text{H}/^1\text{H}$ and WA alkane isotopic composition, and (B) fractionation between bulk leaf tissue $^2\text{H}/^1\text{H}$ and leaf water isotopic composition. Abbreviations: LV, *Salicornia europaea*; PA, *Phragmites australis*; SE, *Salicornia europaea*; SA, *Spartina anglica*; SV, *Suaeda vera*.

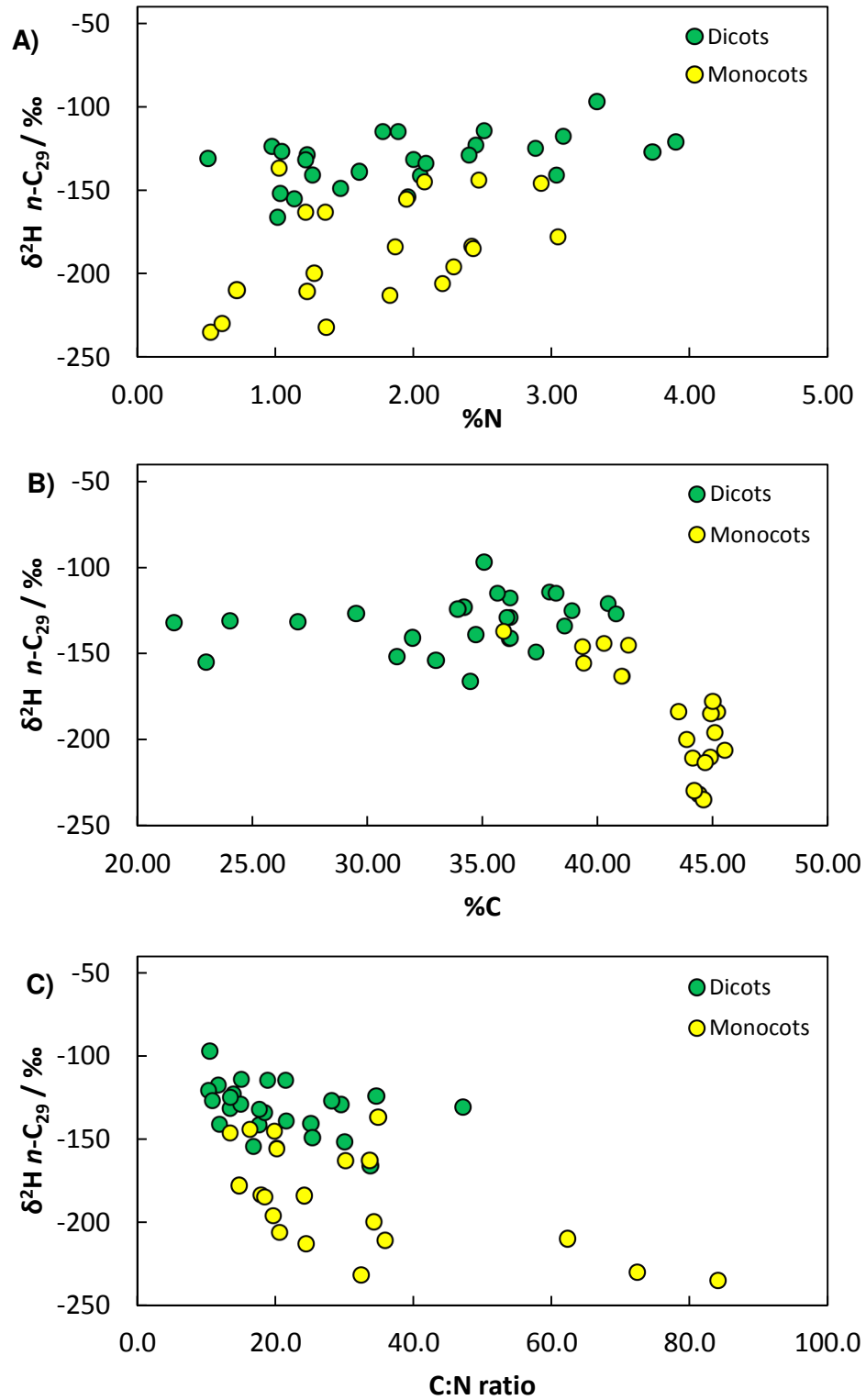


Figure 7.20: Relationship between: A: %N composition of plant biomass and $n\text{-C}_{29} \text{ } ^2\text{H}/^1\text{H}$; B: %C composition of plant biomass and $n\text{-C}_{29} \text{ } ^2\text{H}/^1\text{H}$; and C: C:N ratio of biomass and $n\text{-C}_{29} \text{ } ^2\text{H}/^1\text{H}$

7.6.6 Relationship between n -alkane $^2\text{H}/^1\text{H}$ and foliar $\delta^{15}\text{N}$

Comparison of the nitrogen isotope values presented in Chapter 5 and n -alkane weighted average $^2\text{H}/^1\text{H}$ revealed that there was a statistically significant strong positive relationship between foliar $\delta^{15}\text{N}$ and $n\text{-C}_{29}$ $\delta^2\text{H}$ for the C_3 and C_4 monocots sampled ($r = 0.8$, $P < 0.05$, $n=11$, Pearson moment correlation, Minitab, v.16.1). In contrast, a negative correlation was observed for the dicots and succulents ($r = -0.4$, $n=14$, Pearson moment correlation, Minitab, v.16.1), although this relationship was only significant at an ~80% confidence interval (Fig. 7.21 A and B).

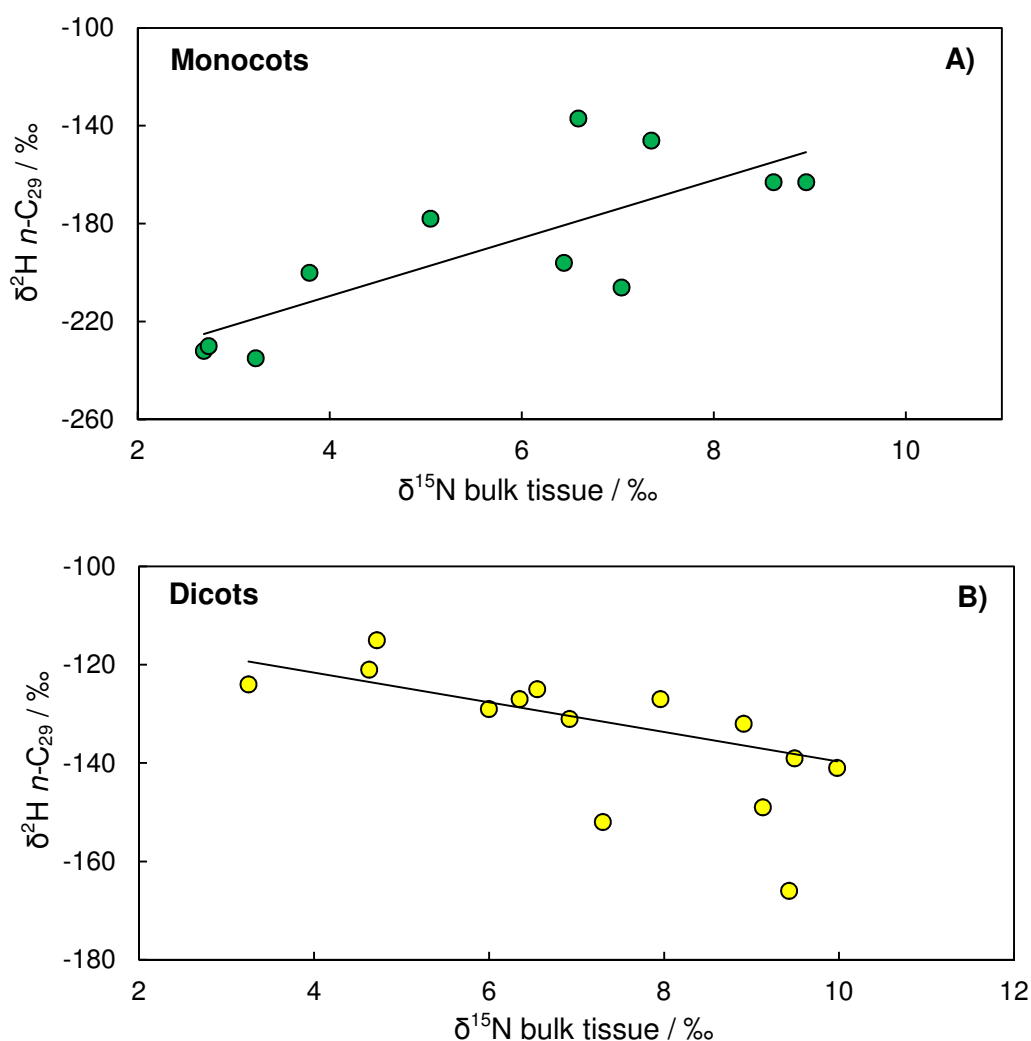


Figure 7.21: Bi-plot of foliar nitrogen isotope values with $n\text{-C}_{29}$ hydrogen isotope values, showing the positive relationship between these two measurements for monocots (A) and the negative relationship for dicots and succulents (B).

7.7. DISCUSSION

The comprehensive review of the use of the $^2\text{H}/^1\text{H}$ composition of lipid biomarkers from phototrophic organism as palaeohydrological proxies, published by Sachse *et al.* (2012) highlighted the potential role of variation in: (i) biochemical pathways; and (ii) the hydrogen contained in NADPH (the dominant reducing power in cells), in driving the large-scale interspecies variability observed in the hydrogen isotope composition of lipids from a range of primary producers. In order to investigate biochemical mechanisms that have the potential to influence leaf wax biomarker $^2\text{H}/^1\text{H}$, a suite of organic compounds generated in different plant compartments (and hence synthesised using NADP(H) that could be derived from different sources) have been analysed as part of this study. These biochemicals include phytol, fatty acids, and starch synthesised in the chloroplast. The hydrogen isotope composition of these compounds has been compared with the $^2\text{H}/^1\text{H}$ data generated for *n*-alkanes, presented in Chapter 6. In addition, the $\delta^{15}\text{N}$ data presented in Chapter 5 have been compared with both the *n*-alkane data from Chapter 6, and the new data presented here, to evaluate any relationships existing between these parameters and the hydrogen isotope composition of leaf wax *n*-alkanes.

These organic compounds were synthesized by different biosynthetic pathways, (DOXP for phytol, acetogenic pathway for FAs and *n*-alkanes) and are known to have varied relationships with source water $^2\text{H}/^1\text{H}$. In C_3 plants for example, the isoprenoid lipid phytol is ^2H -depleted by $\sim 300 - 330\text{‰}$ in comparison to source water (Schmidt *et al.*, 2003; Chikaraishi *et al.*, 2009), while starch and bulk plant tissue are generally ^2H -depleted by 110‰ and 120‰ , respectively (Schmidt *et al.*, 2003). These values are, however, subject to wide variation among plant species and therefore are a guideline only for consideration of typical differences among plant produced compounds. Schmidt *et al.* (2003) proposes that in C_3 species, for example, hydrocarbons are generally 140‰ depleted in deuterium relative to leaf water, but Chapter 6 highlights that variation of over 100‰ among species in their *n*-alkane $^2\text{H}/^1\text{H}$ values is possible. In addition to conducting the first investigation into these metabolic processes influencing leaf wax $^2\text{H}/^1\text{H}$, this study will also highlight where these mechanisms can potentially account for the depletion of *n*-alkane $^2\text{H}/^1\text{H}$ in monocots compared to dicots, as this could provide an important direction for future research.

7.7.1 The hydrogen isotope composition of phytol

Phytol extracted from the C_3 and C_4 species sampled as part of this study ranges in hydrogen isotope composition by 60‰. Two C_3 species, the shrub *Atriplex portulacoides* and the herb *Limonium vulgare* typically have the most ^2H -depleted values, while the C_4 monocot *Spartina anglica* and the C_3 stem succulent *Salicornia* have the most ^2H -enriched (Table 7.1; Fig. 7.10). Calculated fractionation between phytol and leaf water isotopic composition range from -308 to -364‰ (Table 7.1; Fig. 7.11) with the most ^2H -depleted phytol value found in *Atriplex portulacoides* and the most ^2H -enriched in *Spartina anglica*. Fractionation between phytol and WA *n*-alkane $^2\text{H}/^1\text{H}$ ranges from -138 to -234‰ with the greatest depletion again observed in *Atriplex portulacoides* and the least in *Elytrigia atherica* – this is probably due to the extremely ^2H -depleted *n*-alkane values common in *Elytrigia atherica* (Chapter 6).

As phytol and hydrocarbons are synthesised by different biochemical pathways, differences in isotope effects associated with biosynthetic reactions may be expected between these two reaction networks (Sessions *et al.*, 1999). Phytol, like other isoprenoid lipids, is synthesised via the 1-deoxy—d-xylulose-5-phosphate (DOXP) pathway (Lichtenhalter, 1999) (Fig. 7.22) whilst hydrocarbons are synthesised via the acetogenic pathway (Eglington and Hamilton, 1967; Kolattukudy, 1970; Sessions *et al.*, 1999; Chikaraishi *et al.*, 2004, 2009). A study of cucumber cotyledon chlorophyllide-geranygeraniol (GG), chlorophyllide-dihydrogeranygeraniol (DHGG) and chlorophyllide-tetrahydrogeranygeraniol (THGG) found that significantly ^2H -depleted hydrogen is incorporated sequentially during hydrogenation from GG to phytol (Chikaraishi *et al.*, 2009; Fig. 7.22).

Whilst this work was carried out on cotyledons, it is thought that similar enzymes will regulate this biosynthesis pathway in the chloroplasts, so the results of this study should also be applicable to mature green leaves (Chikaraishi *et al.*, 2009). During the final stages of phytol production, hydrogenation of three double-bonds on the immediate precursor occurs. Dehydrogenation and hydrogenation gives rise to significant kinetic isotope effects as a result of enzyme-moderated biochemical reactions, hence the relative depletion in deuterium observed in phytol hydrogen isotope data (Chikaraishi *et al.*, 2005) relative to other organic compounds analysed such as fatty acids and *n*-alkanes (Fig. 7.14). Chikaraishi *et al.* (2004, 2005) estimate that the mean fractionation values for the hydrogen atoms added during

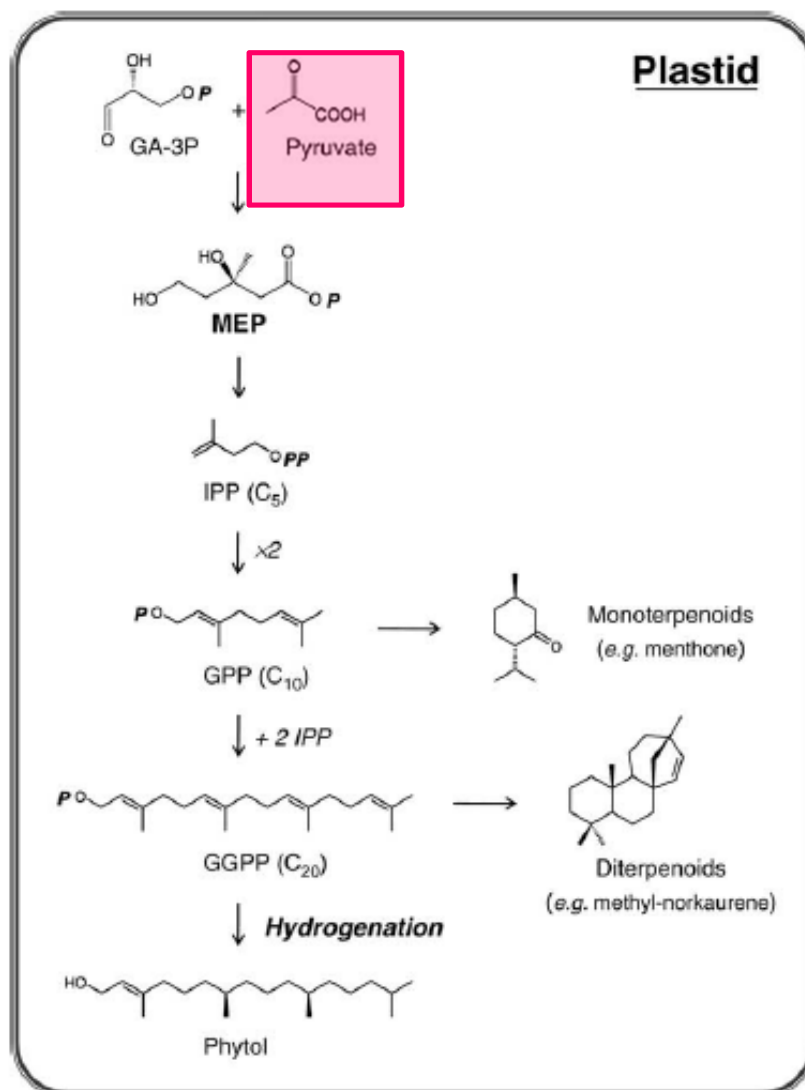


Figure 7.22: Schematic of the biosynthesis pathway of phytol, showing the hydrogenation step of the immediate precursor GGPP. Abbreviations: acetyl-CoA, acetyl coenzyme-A; FPP, farnesyl pyrophosphate; GA-3-P, D-glyceraldehyde-3-phosphate; GGPP, geranylgeranyl pyrophosphate; GPP, geranyl pyrophosphate; IPP, isopentenyl pyrophosphate; MEP, 2-C-methyl-D-erythritol-4-phosphate; MVA, mevalonic acid (from Chikaraishi et al., 2009). Pyruvate is highlighted in red, as this is also an early precursor that is used in the acetogenic lipid biosynthesis pathway.

this step (defined as ${}^2\epsilon_{\text{water}}$) is as much as -600‰ in the C_3 species *Cryptomeria japonica*. The actual ${}^2\text{H}/{}^1\text{H}$ of phytol (and indeed other secondary compounds such as *n*-alkyl lipids) is typically ${}^2\text{H}$ -enriched relative to this, however, due to the fact that the cellular H budget is not simply dependent upon the highly deuterium depleted NADPH produced by photosynthesis (Schmidt *et al.*, 2003). Instead, contributions from NADPH derived from the metabolism of sugars, which are relatively ${}^2\text{H}$ -enriched (Schmidt *et al.*, 2003), are also important for determining the ${}^2\text{H}/{}^1\text{H}$ of these organic compounds.

This study finds a positive relationship between the hydrogen isotope composition of leaf water and phytol, although this is only significant at an 80% confidence interval (Section 7.6.1). This relationship may be due to the relatively rapid turnover of phytol (along with chlorophyll) in the chloroplast. The turnover of chlorophyll in leaves varies with age – in young wheat leaves it can be a matter of hours, while in more mature leaves it can take several days (Stobart *et al.*, 1984). Recent studies have also shown that even in mature leaves, there is a difference in the rate of turnover between chlorophyll *a* and chlorophyll *b*, with chlorophyll *a* incorporating isotopically labelled ${}^{14}\text{C}$ almost instantaneously in mature *Arabidopsis* leaves while no uptake was observed in chlorophyll *b* (Beisel *et al.*, 2010). These rates are well in excess of the 71-128 days previously identified for the turnover of leaf wax *n*-alkanes (Gao *et al.*, 2012). It is therefore possible that this disparity in turnover rates could explain (at least in part) the existence of a relationship between leaf water ${}^2\text{H}/{}^1\text{H}$ and phytol ${}^2\text{H}/{}^1\text{H}$, and the lack of one between leaf water ${}^2\text{H}/{}^1\text{H}$ and *n*-alkane ${}^2\text{H}/{}^1\text{H}$.

7.7.1.1 Differences in phytol ${}^2\text{H}/{}^1\text{H}$ between C_3 and C_4 plants

The ${}^2\text{H}/{}^1\text{H}$ values of phytol from the C_4 grass *Spartina anglica* is ${}^2\text{H}$ -enriched relative to the C_3 species (Table 7.1). This is in accordance with previous studies of phytol hydrogen isotope composition of C_3 , C_4 and CAM plants (Chikaraishi *et al.*, 2004), where C_4 species (all monocots) had phytol isotopic compositions that were ~ 55‰ more positive than C_3 species (a mix of plant functional types including angiosperms and gymnosperms). Although leaf water ${}^2\text{H}/{}^1\text{H}$ was most enriched for *Spartina anglica* during this period (August 2012, data presented in Chapter 6), it was, for example, only 29‰ ${}^2\text{H}$ -enriched relative to the most ${}^2\text{H}$ -depleted leaf water from *Phragmites australis* (Chapter 6). This means that despite the positive relationship

between phytol and leaf water $^2\text{H}/^1\text{H}$, variation in the hydrogen isotope composition of leaf water alone cannot account for the 62‰ difference in phytol $^2\text{H}/^1\text{H}$ between these species.

C_4 plants, however, differ from C_3 species in the way in which they generate NADPH. In C_3 plants, NADPH production generally proceeds by way of the action of ferredoxin-NADP⁺ reductase (Fogel and Cifuentes, 1993). In contrast, some C_4 species also have the ability to generate NADPH from the activity of NADPH-linked malate enzymes when malate is decarboxylated in the bundle sheath cells, while others produce aspartate as a first product of photosynthesis then decarboxylate with an NAD⁺ malate linked enzyme (Fogel and Cifuentes, 1993). These pathways provide an important additional source of NADPH in the bundle sheath cells of C_4 plants (Schmidt *et al.*, 2003).

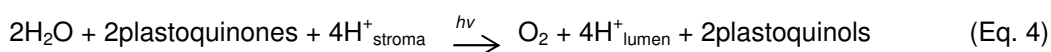
Critically from the perspective of understanding the hydrogen isotope composition of compounds such as phytol in C_4 species, it has been identified that plants capable of generating NADPH from multiple sources tend to produce bulk tissue and cellulose that is ^2H -enriched relative to plants that can only utilise ferredoxin-NADP⁺ (Fogel and Cifuentes, 1993). This is in part due to C_4 plants being able to accumulate a larger pool of reduced coenzyme than C_3 species (Schmidt *et al.*, 2003), which results in less isotope discrimination against deuterium in NADPH from C_4 plants. It would appear that this is a plausible mechanism to account for the relative ^2H -enrichment of phytol from *Spartina anglica*. Further research is required, however, to investigate these biochemical differences between C_3 and C_4 species in more detail.

7.7.1.2 Differences in phytol $^2\text{H}/^1\text{H}$ among C_3 plants

There is also, however, considerable variability of >40‰ in phytol $^2\text{H}/^1\text{H}$ among the C_3 plants studied (Table 7.1, Fig. 7.10). The fact that phytol $^2\text{H}/^1\text{H}$ values have an identifiable positive relationship with the hydrogen isotope composition of leaf water, and no relationship at all with WA *n*-alkane or bulk $\delta^2\text{H}$, suggests that current photosynthate is an important H source for phytol synthesis (Sessions, 2006). Interspecies variation in phytol $^2\text{H}/^1\text{H}$ values among the C_3 plants, however, is greater than that observed for leaf water $^2\text{H}/^1\text{H}$ values (Chapter 6), suggesting that an additional mechanism operating in the chloroplast (which differs among plant

species sampled), must be responsible for the interspecies differences observed. To date, studies have not identified biochemical differences in the DOXP pathway among plant species. This suggests that the biochemical mechanism driving this variation takes effect prior to the allocation of pyruvate to the DOXP pathway. This project has, therefore, hypothesised whether potential variability in the functioning and efficiency of photosynthesis and photolysis may account for the variability of phytol $\delta^2\text{H}$ values among the C_3 species.

Photosynthesis commences in higher plants when the light-harvesting complexes of photosystem II (PSII) absorb light through two types of light-harvesting proteins – the major antenna and the minor antenna (Huber *et al.*, 2001; Nelson and Yocum, 2006; Fig. 7.23). Proteins in the major antenna include Lhcb1, Lhcb2, and Lhcb3, while the minor antenna contains the proteins Lhcb4, Lhcb5 and Lhcb6 (Huber *et al.*, 2001). Oxidative splitting of water during photosynthesis is carried out by PSII, in accordance with Equation 4 (McEvoy and Brudvig, 2006).



Differences in the organisational structure of PSII are thought to alter the efficiency of light-energy transfer from the major light-harvesting complexes to the photochemical reaction centre (Huber *et al.*, 2001). This suggests that if there are systematic variations in the structure and arrangement of PSII and PSI among plant species, interspecies variation in lipid $^2\text{H}/^1\text{H}$ might reflect the differences in the efficiency of the light-harvesting complexes splitting water at the very start of the biophytolysis process.

Previous research has demonstrated that the structure of PSII varies at the plant functional type level. Studies have shown that in dicots, the light-harvesting proteins are generally organised into trimers (Huber *et al.*, 2001), while both monomers and trimers are found in monocots (Huber *et al.*, 2001). Detailed examination of the retention coefficients from reverse-phase HPLC analysis of PSII proteins suggests that there are two distinct groups of isomeric proteins in monocots and dicots, with the differentiation likely arising from variation in hydrophobicity (Huber *et al.*, 2001).

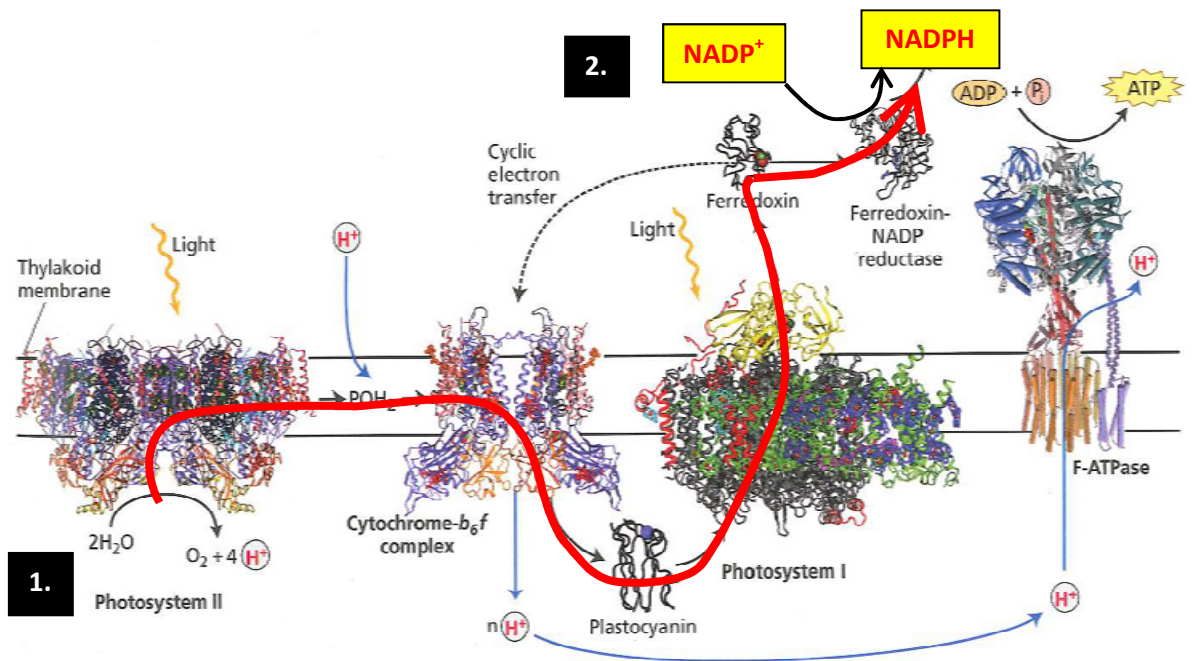


Figure 7.23: Schematic showing the light reactions of the thylakoid membrane. The red arrow marks the approximate flow of electrons from water split during photolysis through into their incorporation into NADPH. At point 1, water is oxidised and protons are released into the lumen by PSII. At point 2, NADP⁺ is reduced to NADPH via the action of ferredoxin and ferredoxin-NADP reductase (adapted from Taiz and Zieger, 2010)

Studies of the proteins of photosystem I (PSI) have revealed that consistent differences are also observed in the masses of PSI proteins between these two plant functional groups. In monocots, analysis of the proteins comprising PSI using reversed-phase HPLC with online detection using electrospray ionisation (ESI) mass spectrometry showed that the mass of light harvesting complex 1 (LHC1) was ~ 400 D greater than for dicots (Zolla *et al.*, 2002). Interestingly, however, the stoichiometry and hydrophobicity of the proteins did not show any significant differences between monocots and dicots, suggesting that the supramolecular organisation of PSI and PSII should be similar across the two phyla (Zolla *et al.*, 2002).

While measurement of the concentration of proteins of PS1 and PSII are outside of the scope of this thesis, evaluation of the %N of plant biomass was undertaken to assess whether gross differences in nitrogen content could be linked to differences in plant species photosynthetic capacity (and hence act as a qualitative proxy for the abundance of photosynthetic proteins) following the approach used by Evans *et al.*

(1989). When data from the 2011 and 2012 growing seasons were binned into monocot and dicot/succulent groups and compared, however, the dicots appeared to contain on average only ~1% more %N than monocots (Table 5.6, Chapter 5). This result is potentially due to the production of nitrogenous solutes for maintaining osmoregulation in dicots (Briens and Lahrer, 1982; discussed further in Section 7.7.4 below) dominating this signal. It would appear that the percent nitrogen content is therefore an imprecise proxy in these saltmarsh plants for investigation of differences in photosynthetic capacity, and that further research would be required to confirm this hypothesis.

Recent work has also identified a significant difference in the way that photosystem proteins respond to environmental stress between monocot and dicot species (Chen *et al.* 2013), and therefore merits further discussion in the context of potential influences on the hydrogen isotope signal transferred to NADPH and secondary compounds. Detailed molecular mechanisms explaining variation in phosphorylation of the minor chlorophyll *a/b*-binding protein of PSII, CP29, remain to be defined (Chen *et al.*, 2013). Studies have shown, however, that CP29 is phosphorylated after exposure to environmental stresses (such as salt stress) in monocots but not in dicots, meaning that stress-damaged PSII proteins may be dephosphorylated and degraded *in-situ* in monocots, without any requirement for their migration into the stroma lamellae for repair as is common in dicots (Chen *et al.*, 2013). The ecophysiological implications of this stronger phosphorylation and desphosphorylation of CP29 in monocots is that it potentially provides enhanced protection from different environmental stresses, particularly with regard to state transition and short term acclimatisation and antenna rearrangements between PSI and PSII. This could potentially influence the water-plastoquinone oxidoreduction occurring during photosynthesis in PSII (Chen *et al.*, 2013). Any changes in the process of water fission could, therefore, have a significant impact on the magnitude of hydrogen isotope fractionation during its incorporation into NADPH during photosynthesis (Luo *et al.*, 1991; Schmidt *et al.*, 2003; Fig. 7.23).

It must be noted that this area of research is in the very early stages, and hence these theories are purely speculative. The data presented here, however, are suggestive of the fact that the differences observed in phytol $^2\text{H}/^1\text{H}$ between C_3 monocots and dicots ($-345 \pm 8\text{‰}$ and $334 \pm 23\text{‰}$ respectively), and indeed between different C_3 plant species, may reflect variation in photosystem structure, composition and function. In order to explore this further, future research should

investigate PSI/PSII organisation and stoichiometry in a range of plants under controlled and natural conditions, to evaluate whether such differences are linked systematically to the hydrogen isotope composition of secondary compounds such as *n*-alkanes.

7.7.1.3 Comparison of phytol and *n*-alkane $^2\text{H}/^1\text{H}$ values

An additional interesting feature of the phytol hydrogen isotope data is that the relative deuterium enrichment and depletion observed for phytol among the sampled species differs from the pattern observed for *n*-alkanes (Figs. 7.13 and 7.24). It is plausible that this phenomenon is directly related to variation in the composition of H available for incorporation into organic compounds synthesised in different plant compartments.

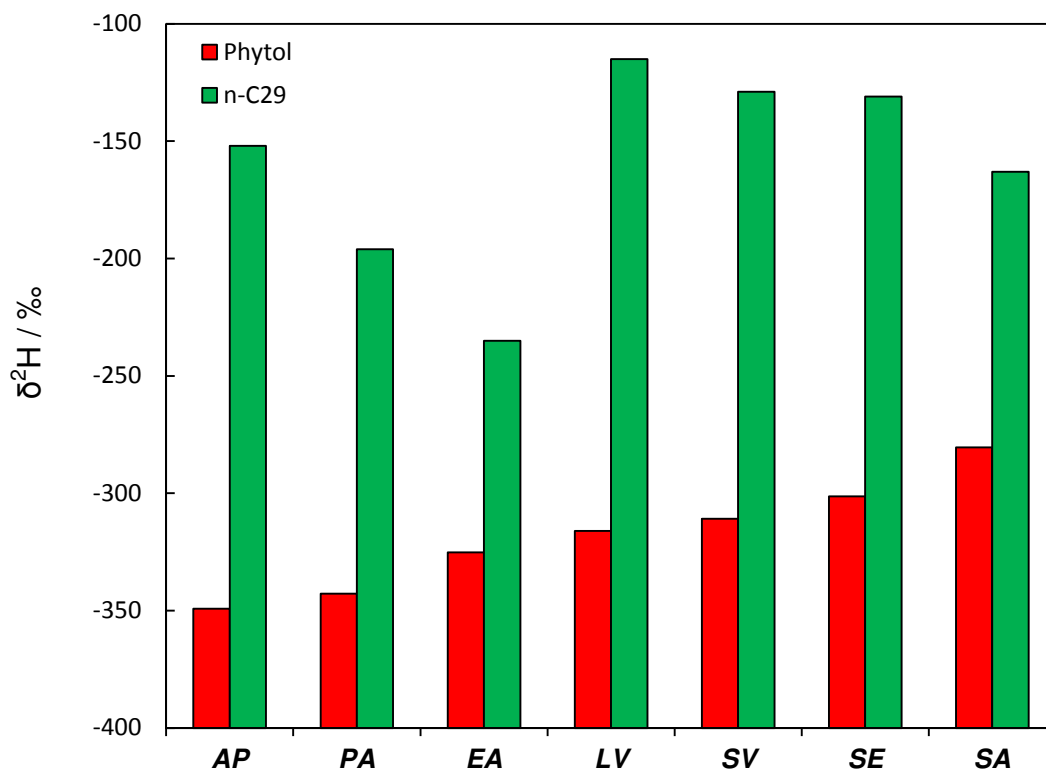


Figure 7.24: Difference in the pattern of relative enrichment and depletion of deuterium in phytol and *n*-C₂₉ from the Stiffkey species (*n*-alkane data from August 2012). Abbreviations: AP, *Atriplex Portulacoides*; PA, *Phragmites australis*; EA, *Elytrigia atherica*; LV, *Limonium vulgare*; SV, *Suaeda vera*; SE, *Salicornia europaea*; SA, *Spartina Anglica*. Absolute differences between sample replicates did not exceed 10‰ for *n*-C₂₉, 15‰ for C₁₆, 17‰ for C_{18:2} and 7‰ for C_{18:3}.

Schmidt *et al.* (2003) proposed that NADP(H) originating from photosynthetic water fission in the plastid and the recycling of sugars occurring in the oxidative pentose phosphate cycle (OPPP) in the cytosol will have very different $^2\text{H}/^1\text{H}$, which can be transmitted to secondary compounds (Schmidt *et al.*, 2003; Sessions *et al.*, 1999; Chikaraishi *et al.*, 2009). The data from the Stiffkey species show differing relationships between isoprenoid and acetogenic lipids and leaf water $^2\text{H}/^1\text{H}$. In particular, phytol synthesised in the chloroplast has a positive relationship with leaf water, while the acetogenic lipids synthesised in the cytosol do not display any relationship at all. This suggests that while the theoretical differences in PSI and PSII structure and organisation discussed above could be important in explaining the interspecies variation of phytol $^2\text{H}/^1\text{H}$, there are likely to be additional biochemical mechanisms influencing the $^2\text{H}/^1\text{H}$ of biomarkers synthesised in other cell compartments.

7.7.2 The hydrogen isotope composition of fatty acids

7.7.2.1 Differences in $^2\text{H}/^1\text{H}$ of FA chain lengths

The $^2\text{H}/^1\text{H}$ of palmitic, linoleic, and linolenic acids varied by over 100‰, although the extent of this variation depended upon the FA homologue (Table 7.2). Linoleic acid, an unsaturated carboxylic acid with an 18 carbon chain and two *cis* bonds, was consistently the most ^2H -enriched of all FAs analysed by 40 - 120‰ (Table 7.2, Fig 7.12), with a total interspecies variation in $\delta^2\text{H}$ of 80‰ (Table 7.2). Linolenic acid is also unsaturated, but this FA has three *cis* double bonds. Linolenic acid from the Stiffkey species varied by 100‰, while the saturated palmitic acid (C16:0) ranged in hydrogen isotope composition by 120‰. The extent of interspecies variation in linolenic and palmitic acids is therefore quite similar to that reported for *n*-alkanes (Chapter 6).

What is interesting in the present study of higher plants growing at Stiffkey, however, is that in addition the interspecies variation in ^2H enrichment and depletion also differ for each FA chain length (Fig. 7.12). This gave rise to some interesting relationships between the FAs and other measured materials. For example, a relationship significant at the 90% confidence interval was found between linoleic acid and leaf water ($r = 0.7$, $P = 0.07$), while none existed between palmitic and linolenic acid and leaf water. Further, the $^2\text{H}/^1\text{H}$ of C16 and C18:3 was positively correlated ($r = 0.8$, $P = 0.02$), while C18:2 had no statistical relationship with either C16 or C18:3.

Previous studies of kinetic hydrogen isotope effects during the biosynthesis of saturated and unsaturated fatty acids in microalgae identified wide variation of up to ~180‰ among FAs from a single species (Chikaraishi *et al.*, 2004). In that study, the saturated palmitic acid (C16:0) had the most ^2H -depleted isotopic value, while the di-unsaturated FA linoleic acid (C18:2) having values that were between 30 and 60‰ more ^2H -enriched. The tri-unsaturated FA linolenic acid (C18:3) had an intermediate $^2\text{H}/^1\text{H}$ that was approximately 20 to 30‰ ^2H -enriched relative to C16:0 (Chikaraishi *et al.*, 2004). Similar patterns in relative ^2H -enrichment and depletion are observed for the FAs extracted from the Stiffkey plants (Fig. 7.12): C16:0 is the most ^2H -depleted, while C18:2 is the most ^2H -enriched (Fig. 7.12; 7.24). Chikaraishi *et al.* (2004) proposed that the variability in $^2\text{H}/^1\text{H}$ values with FA chain length arises from the complex network of desaturation and elongation reactions producing FAs. For each desaturation, 2 H atoms are removed, while elongation adds 4 H atoms. This shows that understanding the fractionation accompanying these steps in the FA reaction network are key to understanding differences in their isotopic signatures.

Palmitic acid is produced in the chloroplast through the activity of fatty acid synthase (FAS) (Billault *et al.*, 2001) and generated from pyruvate, which has been oxidatively decarboxylated in mitochondria to acetyl-CoA and CO_2 (Zhang and Sachs, 2007). There is also a contribution from malonyl-CoA and acetyl-CoA that have been activated by acetyl-CoA carboxylase (Duan *et al.*, 2002). The immediate precursor of palmitic acid is palmitoyl-AcP, which is hydrolysed to C16:0 FA (Zhang and Sachs, 2007). Identification of the sources of H for fatty acid synthesis has been aided by advances in nuclear magnetic resonance (NMR) spectroscopy and isotopic labelling studies (Schwender *et al.*, 2004). The distribution of ^2H along the FA carbon chain has been shown to be non-statistical, with different sources contributing H to specific sites on the molecule. As C16 and C18 FAs are exported from the chloroplast into the cytosol for further elongation and are precursors for *n*-alkane synthesis (Shepherd and Griffiths, 2006; Kunst *et al.*, 2007, 2009), identification of these different hydrogen sources, and evaluation of their relative importance, is significant for the interpretation of the hydrogen isotope signals of leaf wax biomarkers.

Quemerais *et al.* (1995) showed that hydrogen atoms on the methyl group of palmitic acid (C16:0) came from the methyl group of pyruvate, and also from the hydride contained within NADPH. The methyl group of pyruvate, in turn, is linked to

isotopomers 1, 6 and 6' in glucose (e.g. Zhang *et al.*, 1994). Quemerais *et al.* (1995) also found that the protons transferred by NADPH during the reduction of the malonyl-CoA carbonyl group were strongly related to cellular water, as a result of what has been described as “post-malonyl exchange”. However, critically, the deuterium distribution of the lipid component of plants appeared to be more strongly dominated by biochemical mechanisms than the isotopic composition of water absorbed and/or evaporated by plants (Quemerais *et al.*, 1995).

FA chain elongation from C16 to C18 involves the addition of C2 units, with hydrogen at the uneven sites of the FA molecule being supplied by the activity of NADPH –dependent β -ketoacyl-AcP reductase and NADPH-utilising enoyl-AcP reductase (Billault *et al.*, 2001). In contrast, at even chain C sites one hydrogen comes from acetate, while the other derives from NADPH-utilising enoyl-AcP reductase (Billault *et al.*, 2001). Linoleic and linolenic acids, the other dominant FAs identified in this study, are the product of desaturation reactions of C18 in the endoplasmic reticulum (Billault *et al.*, 2001; Chikaraishi *et al.*, 2004; Fig. 7.25). Studies have observed ^2H -depletion at the sites of desaturation (Billault *et al.*, 2001). In addition, Duan *et al.* (2002) noted that the residual oleate pool in peanut

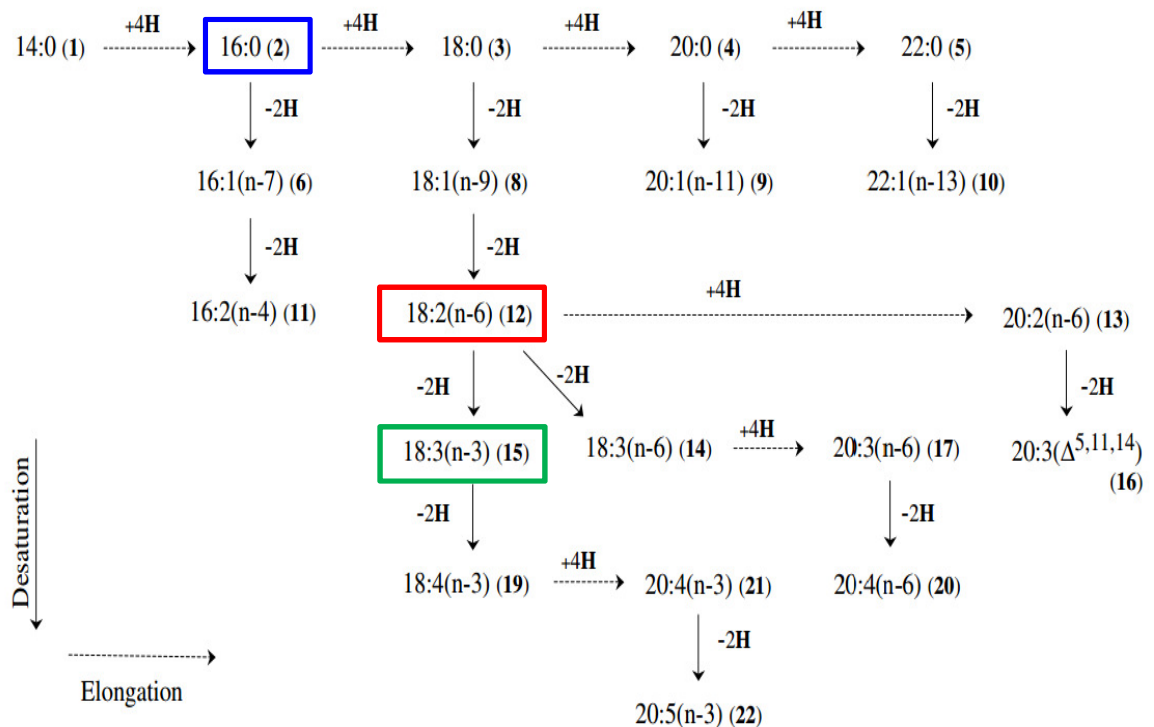


Figure 7.25: Major pathway of polyunsaturated FAs in microalgae (Chikaraishi *et al.* 2004). FAs analysed as part of this study are highlighted as follows: blue, palmitic acid; red, linoleic acid, green, linolenic acid.

seed oil became increasingly ^2H -enriched as desaturation (the removal of two hydrogen atoms from the FA molecule) proceeded. This phenomenon is likely due to desaturation eliminating both *pro-R* hydrogen atoms on the fatty acid molecule, which are relatively ^2H -enriched compared to *pro-S* sites (Bailiff *et al.*, 2009). It is plausible that as linolenic acid is a desaturation product of linoleic acid (Chikaraishi *et al.*, 2004; Bailiff *et al.*, 2009; Fig. 7.25) a similar explanation can account for the relative ^2H -enrichment of C18:2 relative to C18:3 from the Stiffkey plants.

What is more difficult to explain is the apparent relationship between the $^2\text{H}/^1\text{H}$ of leaf water and C18:2. It is plausible that the H atoms in linoleic acid are exchanging with cellular water (Bailiff *et al.*, 2009), and hence picking up a hydrogen signal from leaf water and/or transported photosynthate. Within the constraints of this data set, however, it is difficult to account for why this should affect linoleic acid more than linolenic acid, as no statistical relationship was found between C18:3 and leaf water $^2\text{H}/^1\text{H}$. The situation is further complicated by the existence of a significant relationship between C16 and C18:3, suggesting that the H in their structures may be derived from a similar source. One possible explanation could be that as these plants are under stress, they are also producing linolenic acid from plant membranes (Dombrowski, 2003) to be converted into further protective compounds such as oxylipins (e.g. jasmonates) (Wasternack, 2007). Critically from the perspective of explaining the relationship between linolenic acid and palmitic acid, these membrane-derived C18:3 FAs originate from chloroplast membranes (Wasternack, 2007) suggesting that they contain H from a similar source to that incorporated into C16, which is itself produced in the chloroplast. In the absence of further analysis, however, it is not possible to give a detailed explanation of this phenomenon. Future research could address this issue through the use of site-specific NMR (e.g. Billault *et al.*, 2001), to fully evaluate the source of hydrogen at each position in these three FA molecules, and potentially differentiate between these two distinct sources of C18:3.

7.7.2.2 Interspecies differences in the $^2\text{H}/^1\text{H}$ values of FAs

While these explanations may account for the variation in $^2\text{H}/^1\text{H}$ values among the FAs analysed for each plant species studied, it does not explain the extent of interspecies variation in FA $\delta^2\text{H}$. Such interspecies variation has been previously identified in other photosynthetic organisms. Zhang and Sachs (2007), for example, noted 90 - 100‰ variation in hydrogen isotope fractionation (relative to water)

during synthesis of C16:0 by different families of green algae. What mechanisms could potentially account for the interspecies variation of >100‰ among the FAs from the Stiffkey plants?

The isotope composition of each hydrogen atom in a given FA molecule is a factor of the initial origin of that hydrogen atom, the influence of FAS activity, and any participation in post-elongation modification of the FA chain (e.g. desaturation) (Bailiff *et al.*, 2009). One potential explanation for the observed interspecies variation in FA $^2\text{H}/^1\text{H}$ is that the stereochemistry controlling the introduction of hydrogen atoms for all accessible stereogenic sites (and for each enantiotopic direction of stereogenic sites) varies among organisms. This has been shown previously for studies of fungi, and resulted in the hydrogen isotope composition and distribution of ^2H at the *pro-R* and *pro-S* sites of FAs being highly varied among different organisms (Bailiff *et al.*, 2009). While no studies have confirmed that such differences exist in the *pro-R* and *pro-S* sites of FAs from higher plants, photosynthetic organisms typically have similar biochemical mechanisms producing organic compounds (e.g. Sachse *et al.*, 2012). Indeed the production of FAs appears to follow a common biosynthetic pathway across a range of phototrophic organisms (e.g. Zhang and Sachs, 2007; Billault *et al.*, 2001; Chikaraishi *et al.*, 2004). It is therefore possible that similar differences in stereochemistry may account for some of the species variability in FA $^2\text{H}/^1\text{H}$ observed at Stiffkey.

In addition, the potential for H exchange between acetate and medium water is thought to be responsible for an observed strong transfer coefficient between the hydrogen attached to site 18 of FAs and cellular water, although again this process is very variable (Bailiff *et al.*, 2009). Post-malonyl exchange also has the potential to influence the relative importance of acetate and H_2O to the hydrogen incorporated into FAs (Bailiff *et al.*, 2009). Further study of the FAs from higher plants, utilising site-specific natural isotope fractionation NMR (SNIF-NMR), should help to constrain the relative importance of these biochemical processes.

n-Alkane and fatty acid data from Stiffkey (Fig. 7.13) broadly follow previous studies which have identified that the $^2\text{H}/^1\text{H}$ values of biomarkers from monocot species are generally ^2H -depleted relative to those from dicots, and that C_3 grasses are generally ^2H -depleted relative to C_4 grasses. Smith and Freeman (2006), for example, found that $\epsilon_{\text{lipid-water}}$ values were most negative for C_3 grasses, intermediate for C_4 grasses, and most positive for C_3 dicots. They concluded that differences between C_3 and C_4 photosynthetic pathways were not a primary control on the $^2\text{H}/^1\text{H}$

fractionation between water and lipids. When species are grouped into plant functional types (Dicot/succulent, C₃ monocot, C₄ monocot, Fig. 7.26) palmitic (C16) and linoleic (C18:2) acid have a pattern of ²H enrichment and depletion that appears closer to that of phytol (C₄ monocots > C₃ dicots and succulents > C₃ monocots), rather than linolenic acid (C18:3) and *n*-C₂₉ (C₃ dicots and succulents > C₄ monocots > C₃ monocots) (Fig. 7.26). These data suggest that the ability of C₄ plants to generate NADPH from the activity of NADPH-linked malate enzymes when malate is decarboxylated (as discussed above in relation to phytol, Fogel and Cifuentes, 1993) may exert a stronger influence over phytol, C16 and C18 at the PFT scale. These findings may be limited, however, by the fact that only one C₄ monocot was analysed in this study, and future research should consider other C₄ plants. The pattern observed for the *n*-C₂₉ alkane (Fig. 7.26) is clearly distinctive relative to these other compounds. This highlights that although cellular metabolic processes are interrelated (van Dongen *et al.*, 2011), specific biochemical pathways may be more or less responsive to different factors.

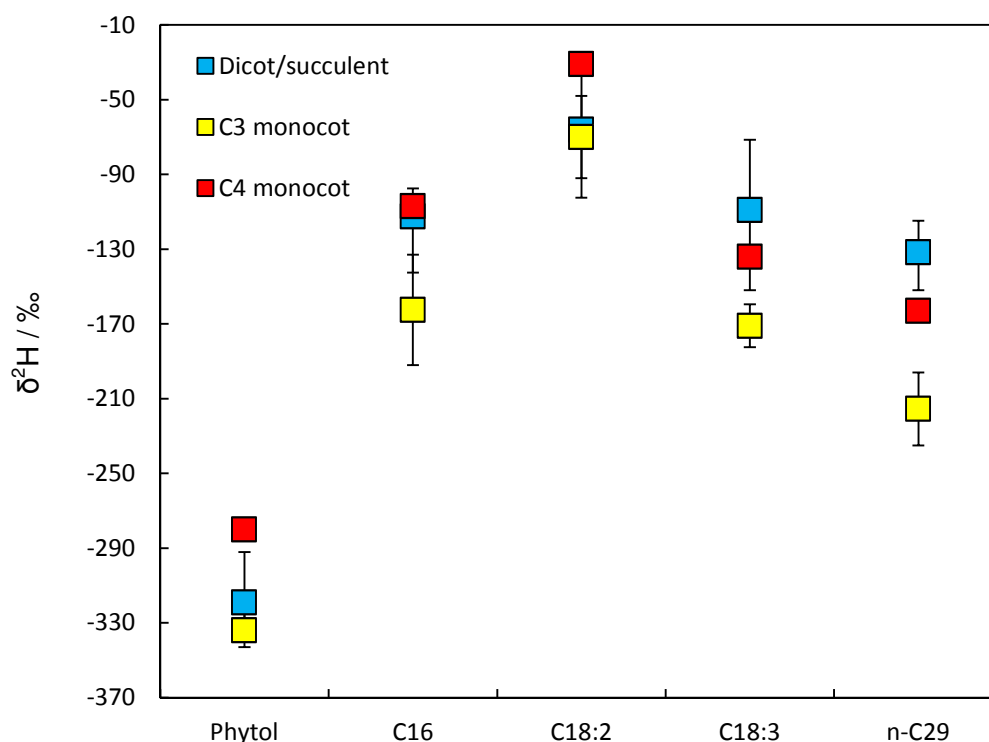


Figure 7.26: Relative enrichment and depletion in deuterium for isoprenoid and acetogenic lipids analysed from the Stiffkey species. Error bars show standard deviation (dicots) or absolute difference between isotopic measurements of compounds for each plant functional type. Groupings are as follows: Dicots/succulents, *Suaeda vera*, *Salicornia europaea*, *Limonium vulgare*, *Atriplex portulacoides*; C₃ monocots, *Elytrigia atherica*, *Phragmites australis*; C₄ monocot is *Spartina anglica*

7.7.3 The hydrogen isotope composition of starch

The fact that the relative pattern of ^2H -enrichment and depletion varies between compounds synthesised in the chloroplast and the cytosol (e.g. phytol vs. *n*-alkanes; Fig. 7.26), suggests that there may be differences in the isotopic composition of NADPH contributing to organic compounds across these plant compartments (e.g. Sessions, 1999; Smith and Freeman, 2006; Feakins and Sessions, 2010; Sachse *et al.*, 2012). Approximately 25% of the hydrogen in leaf lipids is thought to derive from acetate (Sessions, 1999; Zhang *et al.*, 2009), which itself can originate either from photosynthesis products or carbohydrates associated with plant metabolism (Sessions, 2006). Of the remaining 75% of hydrogen in synthesised lipids, 50% is derived from reduced nicotinamide adenine dinucleotide phosphate (NADP(H)) (Zhang *et al.*, 2009), which also has two hydrogen sources: (i) water fission during photosynthesis, and (ii) the recycling of sugars via the oxidative pentose phosphate pathway (OPPPP), where the hydrogen derives from C-bound H contained within the sugars (Schmidt, *et al.*, 2003; Kruger and von Schaewen, 2003; Sessions, 2006).

If the hydrogen incorporated into acetogenic lipids is not being derived solely from leaf water (as argued previously in Chapter 6), then an alternative source must be available. The oxidative pentose phosphate pathway (OPPP) operates in heterotrophic plant tissues and is known to provide a significant series of intermediates and therefore may offer a source of substrates for fatty acid synthesis (Kruger and von Schwanen 2003; Schwender *et al.*, 2004). Significantly, from the perspective of investigating interspecies variation in lipid $^2\text{H}/^1\text{H}$, the OPPP cycle may vary among plant species (Schwender *et al.*, 2004).

Previous studies, for example, have sought to identify the presence or absence of enzymes catalysing OPPP reactions in cytosol and plastids. For example, based on genetic analysis, spinach, maize, tobacco and potato appear to be capable of synthesising the required enzymes in both cytosolic and plastidic tissues (Kruger and von Schwanen, 2003). However, interspecies variation of the non-oxidative section of the pathway is likely, which could introduce species-specific differences in the metabolic activity and carbohydrate oxidation across these cell compartments (Kruger and von Schwanen, 2003). It is currently unknown whether environmental conditions or growth stage may influence the degree of compartmentalisation of the OPPP process (Kruger and von Schwanen, 2003). Even if compartmentalised, however, interaction between plastidic and cytosolic processes in the OPPP

pathway remains possible. Studies of *Arabidopsis thaliana* show that pentose phosphates generated by activity in the cytosol are able to cross into the plastid as a result of action of a membrane protein of the phosphate-transporter family (Kruger and von Schwanen, 2003). Such an interaction allows for generation of NADPH and biosynthetic precursors independently in each compartment (cytosol or plastid) (Kruger and von Schwanen, 2003). All of these issues require further study to evaluate their role in H cycling in plant cellular metabolism and secondary compound synthesis.

Comparison of the exchangeable hydrogen content of the different starches analysed (including those from Stiffkey and those supplied by the John Innes Centre), revealed variation in the amount of hydrogen bound to hydroxyl (OH) groups among the species (Section 7.6.3.2). It would be valuable to explore the extent of this variation in exchangeable H further in future research, both: (i) among different species; and (ii) between different plant organs. It could be that starches vary in respect of the number of OH groups as a result of differences known to exist in structure and morphology (e.g. Hoover, 2001; Tester *et al.*, 2004), altering the extent to which their hydrogen isotope composition will be in equilibrium with cellular water. This in turn could have relevance for tracing the flow of H through the cycling and recycling that accompanies the generation of secondary compounds such as *n*-alkanes (Fig. 7.28 below). In particular, if plants utilise starch with a higher percentage of exchangeable H (i.e. more OH groups), the $^2\text{H}/^1\text{H}$ composition of the starch (and hence the H available for incorporation into secondary compounds) would be likely to reflect cellular water more closely than that of starches with low exchangeable H.

The data from Stiffkey shows that starch from *Atriplex portulacoides* and *Suaeda vera* differed by only 11‰, while overall interspecies shifts in bulk tissue $^2\text{H}/^1\text{H}$ (a signal dominated by the carbohydrate fraction, Dungait *et al.*, 2008) across 2012 were no greater than ~50‰. This falls well short of the variability in hydrogen isotopic composition recorded for the leaf wax *n*-alkanes. In addition, studies of *Brassica* embryos using ^{13}C -labelled glucose suggest that viewed as a whole, the OPPP does not completely metabolise significant amounts of carbohydrates, and therefore the actual contribution of OPPP-derived NADPH for lipid synthesis may not always be high (Kruger and von Schwanen, 2003). Metabolic flux analysis also

supports the view that the OPPP does not always generate a significant percentage of the NADPH required for fatty acid biosynthesis (Schwender *et al.*, 2004).

It is possible that these varied results arise from interspecies differences in the compartmentalisation of the OPPP pathway, as discussed above. The proportion of NADPH derived from the OPPP cycle incorporated in acetogenic lipids could also vary among species. This could potentially be linked to the manner in which different species store carbohydrate reserves. At Stiffkey, there is a general divide between the behaviour of monocots and dicots, such that monocots utilise starch on diurnal cycles, while dicots are more likely to store photosynthates such as starch for longer periods (Table 7.3). This distinction between monocots and dicots represents an important area for further study, given the often-identified depletion in $^2\text{H}/^1\text{H}$ in monocots relative to dicots and trees observed across many different biomes (e.g. Smith and Freeman, 2006). The data presented here suggest that where carbohydrates are used on a rapid, diurnal basis (i.e. in the monocots), the contribution of OPPP derived NADPH is lower than in those species where long-term storage is common, resulting in ^2H -depleted *n*-alkane isotope ratios in those species.

7.7.4 Interspecies differences in the response to environmental stress

In addition to the potential contribution of NADPH derived from the OPPP cycle, there are a range of other metabolic processes which could influence the flow of material into the acetogenic pathway, and potentially influence $^2\text{H}/^1\text{H}$ of secondary compounds. Metabolic processes are controlled at the network level within plants, rather than individual reaction series, and therefore there are multiple possibilities for interaction between different biochemical mechanisms (Schwender *et al.*, 2004; van Dongen *et al.*, 2011). Such mechanisms could include, for example, the synthesis and catabolism of compatible solutes that plants at Stiffkey saltmarsh produce for osmoregulation (discussed fully in Chapter 5). As these osmoregulatory strategies broadly differ between monocots and dicots, in addition to among species, these mechanisms may also help account for the ^2H -depletion of *n*-alkanes in monocots versus dicots (Smith and Freeman, 2006; Fig. 7.26).

Earlier studies showed that the monocot species preferentially accumulate carbohydrates, while the dicots and succulents are more likely to accumulate either nitrogenous compounds, or a mix of nitrogenous and carbohydrate compounds

(Briens and Lahrer, 1982; Fig. 5.23 Ch. 5). Ladd and Sachs (2012) considered whether the production of osmoregulatory solutes could have influenced the $^2\text{H}/^1\text{H}$

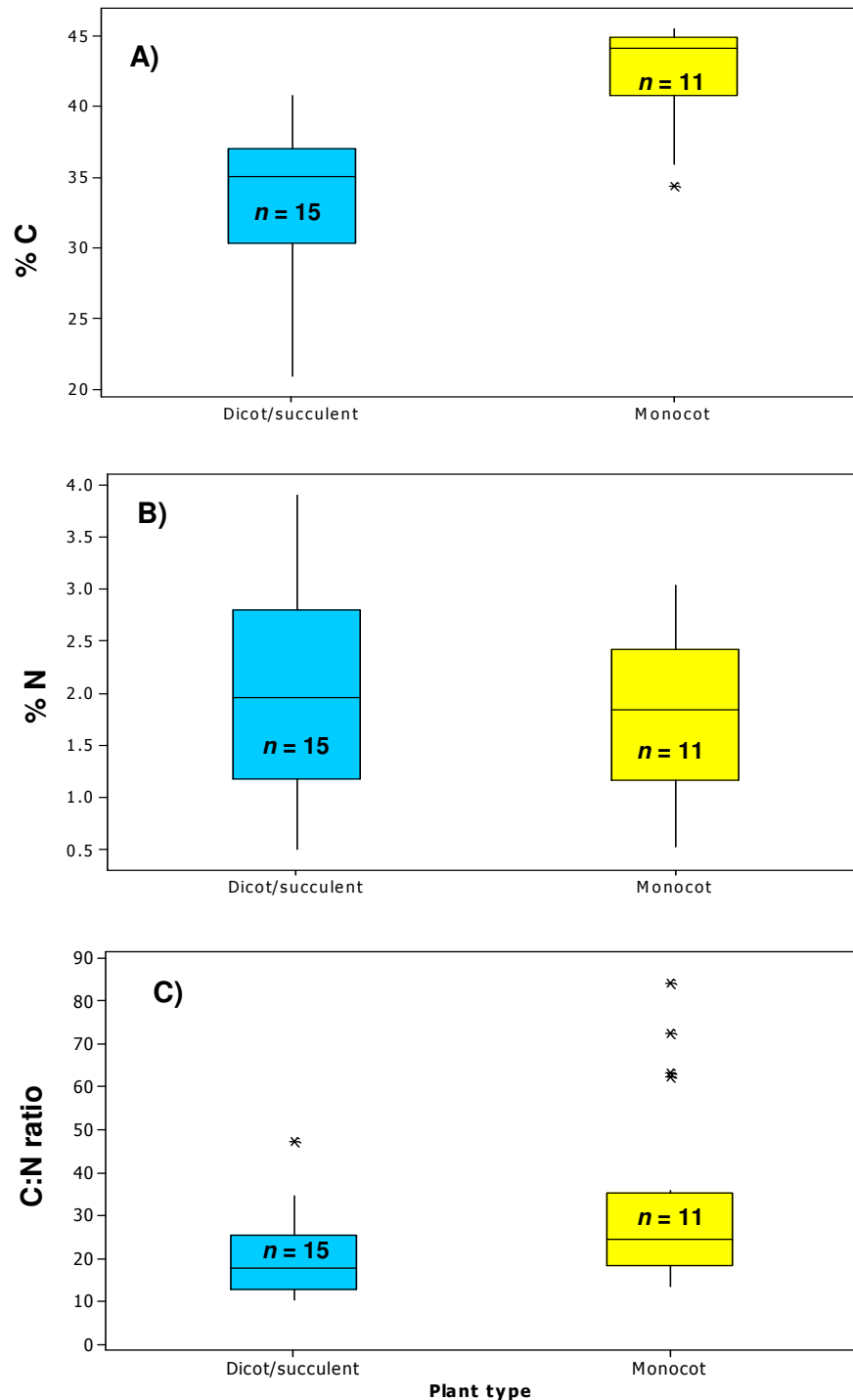


Figure 7.27: Seasonal comparison of carbon and nitrogen percentage composition from species sampled across 2012 at Stiffkey. Monocots: *Elytriga atherica*, *Phragmites australis*, *Spartina anglica*; and dicots/succulents: *Atriplex portulacoides*, *Limonium vulgare*, *Salicornia europaea*, *Suaeda vera*. A: % carbon composition of biomass; B: %N composition of biomass; C: C:N ratio of biomass.

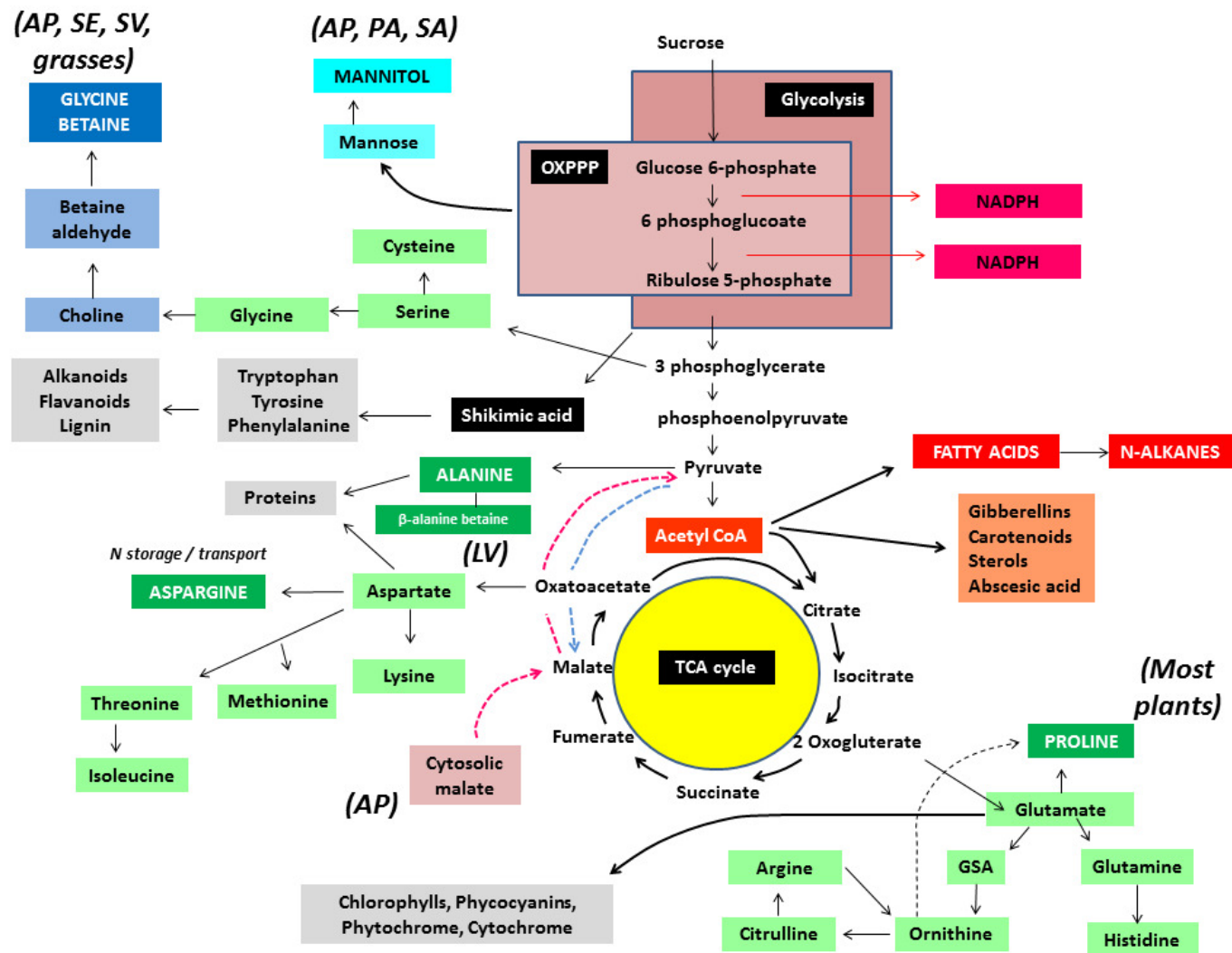


Figure 7.28: Schematic of the key biological processes operating within plants which could potentially influence the hydrogen isotope composition of leaf wax lipids. Abbreviations highlight important compounds for the Stiffkey plants. Data from: Taiz and Zeigler, 2010; Mansour, 2000; Hare et al., 1998; Kishor et al., 2005; Briens and Lahrer, 1982; Loescher, 1987; Wang et al., 2013.

of *n*-alkanes in mangroves through the allocation of pyruvate to the production of compounds such as asparagine, stachyose, glycine betaine (Fig. 7.28), alanine (Fig. 7.28), pinitol and proline (Fig. 7.28). Many of these osmoregulatory solutes are ^2H -enriched relative to pyruvate (Schmidt *et al.* 2003). The hydrogen in pyruvate, the precursor for acetogenic lipids, is derived from water via soluble carbohydrates, and NADPH generated, at least in part, from the OPPP (Ladd and Sachs, 2012, although note Schwender *et al.*, 2004). It is therefore theoretically possible that if plants have a high demand for carbohydrates to protect them from salinity, a greater proportion of hydrogen in pyruvate will come from NADPH, which is up to ~180‰ depleted in deuterium relative to the hydrogen derived from carbohydrates, leading to a ^2H -depletion in *n*-alkanes as pyruvate is a precursor for acetogenic lipid production (Ladd and Sachs, 2012).

These theories suggest that pyruvate in the Stiffkey monocots could be ^2H -depleted relative to dicots due to their enhanced osmoregulatory demand for carbohydrates. This is supported by their increased percentage of carbon content compared to the dicots and succulents (Fig. 7.27 A). Likewise, as the dicot and succulent plant species at Stiffkey predominantly synthesise nitrogenous compounds such as amino acids (e.g. proline) which are produced from glutamate (Szabados and Savouré, 2010) (Fig. 7.28), the ^2H -enrichment of their *n*-alkanes (Fig. 7.26) relative to the monocots could be influenced by the increased input of carbohydrate-derived hydrogen to pyruvate. Variability in the relative proportion of carbohydrates to nitrogenous compounds among the dicots and succulents (Briens and Lahrer, 1982) could also potentially account for some of the interspecies differences in *n*-alkane $^2\text{H}/^1\text{H}$ among this group. The lack of a clear discrimination between the monocots and dicots in terms of their percentage N composition (Fig. 7.27B) and C:N ratios (Fig. 7.27C) may well be illustrative of this species-specificity in terms of production of osmoregulatory solutes (Ullrich, 2002). Further work is required to investigate this, as such findings have potentially wide reaching implications.

Plants use common osmoregulatory compounds such as proline (Fig. 7.28) in response to a range of environmental stresses such as drought, high light/UV intensity, and heavy metals (Szabados and Savouré, 2010). These metabolic protective mechanisms could therefore influence the $^2\text{H}/^1\text{H}$ of species in very diverse environmental and climatic zones. In addition, this mechanism would have an increased impact on the acetogenic pathway compared to the DOXP pathway

(phytol), as the DOXP pathway has both pyruvate and D-glyceraldehyde-3-phosphate as precursors, while acetyl- and manonyl-CoA in the acetogenic pathway derive solely from pyruvate. This could explain some of the difference in the pattern of deuterium enrichment and depletion between phytol and *n*-alkanes observed among the different species sampled in this study (Figs. 7.13 and 7.26).

It is not simply the synthesis of osmoregulatory compounds that could influence the $^2\text{H}/^1\text{H}$ of leaf wax biomarkers. Studies have shown that plants under stress are also capable of catalysing and metabolising materials such as proteins and lipids, especially in conditions where carbohydrates are in short supply (Araujo *et al.*, 2011). Plant species at Stiffkey are regularly exposed to a range of environmental stresses, including salinity, drought and nitrogen limitation (Jeffries, 1977). As there is a broad distinction between monocots and dicots in respect of the osmoregulatory solutes that they accumulate (Fig 5.23, Ch.5), it is theoretically possible that species with an abundance of amino acids versus carbohydrates metabolise these during times of high stress.

The nitrogen isotope composition of proteins is more positive than other organic compounds found in phototrophic cells (Macko *et al.*, 1986, 1987). The ^{15}N -enriched bulk leaf tissue in the Stiffkey dicots and succulents relative to the monocots (Chapter 5) therefore potentially reflects the greater abundance of osmoregulatory proteins in these plant functional types. Proteins also tend to be ^2H -depleted relative to carbohydrates (although amino acids are not) (Schmidt *et al.*, 2003). Therefore the catabolism and subsequent metabolism of proteins in stressed dicots and succulents may give rise to a ^2H -depleted pool of H available for further respiration and metabolism. This in turn could drive the negative relationship between foliar $\delta^{15}\text{N}$ and *n*-alkane $^2\text{H}/^1\text{H}$ (Fig. 7.21) – where protein compounds are highest (high $\delta^{15}\text{N}$) it is theoretically possible that they are degraded and used in times of stress, with a coeval ^2H -depleted hydrogen isotope signal in the *n*-alkanes as more of the ^2H -depleted H pool is used for the synthesis of secondary compounds. Protein catabolism has been shown to support the functionality of the TCA cycle, and also supply electrons to the ubiquinone pool of the mitochondrial electron transport chain (Araujo *et al.*, 2011), so it is clearly an important resource for plants. Despite this, little is known so far about the metabolic fate of substrates produced by protein degradation (Araujo *et al.*, 2011). This therefore remains an area where further

research is required to fully understand whether this is a mechanism capable of influencing leaf wax biomarker $^2\text{H}/^1\text{H}$.

The opposing relationship in the monocots (Fig. 7.21) could in part be simply due to their utilisation of carbohydrates as preferred regulatory solutes, as discussed above. Alternatively, it could reflect the different sources of N used by these saltmarsh plants. N available within the marsh includes nitrate (NO_3^-), ammonium (NH_4^+) and free amino acids (Stewart *et al.*, 1973; Henry and Jeffries, 2003). It is well known that differences exist in the preferences of plants for the form of N that they utilise (Weigelt *et al.*, 2005), which is thought linked to the concentration of different N pools available to them (Warren, 2009). The use of different species of N has an important influence on the NADPH budget of a plant cell. The uptake of NO_3^- requires NADPH to reduce it to NH_4^+ , which can then be taken up by the GS-GOGAT pathway (Evans, 2001), while this is not required for direct uptake of NH_4^+ and free amino acids. In monocots, therefore, the relationship between foliar $\delta^{15}\text{N}$ and n-alkane $^2\text{H}/^1\text{H}$ could conceivably arise from the enhanced use of NADPH to reduce NO_3^- (compared to dicots) resulting again in more H in pyruvate coming from recycled carbohydrates, which would be relatively ^2H -enriched (Schmidt *et al.*, 2003). The coeval positive shift in foliar $\delta^{15}\text{N}$ could be due to the fractionation against ^{15}N accompanying assimilation, which has been shown to result in a ^{15}N -enriched pool of NO_3^- within the plant, especially in the leaves as assimilation occurring in the roots has already enriched the NO_3^- pool (Evans, 2001). However, without further research to investigate the species of N preferentially taken up by these plants (using, for example, labelled N species) it is impossible to make any definitive conclusions from these data.

7.7.5. Directions for future research

The results of research described in this chapter open new directions for empirical study to further probe the precise nature of biochemically moderated fractionation of hydrogen associated with metabolic processes and the synthesis of lipid biomarkers. The potential for different arrangements and concentrations of proteins in PSI and PSII to influence the hydrogen isotope composition of H incorporated into NADPH requires further investigation, using a multiple-method approach combining novel techniques in proteomic research with more traditional CSIA analysis of leaf wax compounds. In addition, SNIF-NMR techniques appear to offer a suitable method for evaluating the relative importance of protein and carbohydrate catabolism in contributing hydrogen for incorporation into secondary compounds.

The potential importance of the production and catalysis of osmoregulatory compounds highlights the need to take a holistic approach to understanding the cycling of hydrogen within plant metabolic processes, and the influence of these mechanisms on the hydrogen isotope composition of biomarkers. Analysis of the $^2\text{H}/^1\text{H}$ values of a range of compatible solutes in plants growing in stressed environments (both under controlled conditions and in natural ecosystems) will allow for further evaluation of the influence of different metabolic demands on the isotopic composition of hydrogen added to pyruvate. In addition to salinity, environmental stresses that should be focused on in future research (where compounds such as proline are known to be an important defence against stress) include drought, high temperature, low temperature, nutrient deficiency, heavy metal toxicity, anaerobiosis, and atmospheric pollution (Hare and Cress, 1997). The fact that this biochemical adaptation is so widespread, and applied in such diverse circumstances, only further illustrates the importance of understanding the influence of this mechanism on the hydrogen isotope composition of secondary metabolites.

The fact that a number of the biochemical processes described here differ between monocots and dicots suggests that the $^2\text{H}/^1\text{H}$ value of acetogenic biomarkers might record important information relating to the biochemical differences between these two plant functional types. Valentine (2009) described the $^2\text{H}/^1\text{H}$ value of bacterial lipids as recording “Isotopic remembrance of metabolism past”, highlighting the potential for microorganism lipid hydrogen isotope signatures to act as a palaeo-metabolic proxies (discussed earlier in Section 7.2.1). The research presented in this chapter gives the first indication that a similar story might remain to be discovered in the hydrogen isotope composition of terrestrial vascular plants.

7.8. SUMMARY

This chapter aimed for the first time to identify a range of biochemical mechanisms that could explain the interspecies variation in *n*-alkane $^2\text{H}/^1\text{H}$ observed in the saltmarsh species studied at Stiffkey, and also the consistent depletion of monocot species relative to dicots. The following bullet points sum up the key findings of this chapter, coloured numbers relate to those found on the accompanying summary figure, 7.29.

- Previous research has shown that PSI and PSII contain different amounts of proteins, and differ in their response to environmental stress. Although speculative as analysis of PSI and PSII proteins was outside the scope of

this thesis, it is theoretically possible that such differences have potential to shift the composition of hydrogen transferred to NADPH, and potentially contribute to interspecies differences in isoprenoid (phytol) and acetogenic (FA and *n*-alkane) lipid $^2\text{H}/^1\text{H}$ 1.

- Variation in the carbon and nitrogen content of bulk biomass of the Stiffkey species appeared related to the nature of osmoregulatory compounds produced to ameliorate the negative impacts of salinity. Monocots and dicots differed in whether they produced carbohydrate- or nitrogenous-based compounds. This difference was reflected in the $^2\text{H}/^1\text{H}$ value of *n*-alkanes, potentially due to shifts in the relative contribution of hydrogen of carbohydrates and NADPH to pyruvate in monocot species with a high demand for carbohydrates 2.
- Variation in the $^2\text{H}/^1\text{H}$ of phytol, synthesised in the chloroplast, differed from the patterns observed for acetogenic lipids, with C_4 species being ^2H -enriched compared to C_3 species. This may be due to the ability of C_4 species to generate NADPH from the degradation of malate 3.
- In addition to their production, the catabolism of osmolytes may also influence the $^2\text{H}/^1\text{H}$ of secondary compounds such as leaf wax lipids as they can be broken down rapidly when stress periods are over. This would mean that hydrogen contained within them could be recycled through the TCA cycle and other related metabolic pathways (c/f Fig. 7.28). As proteins are relatively ^2H -enriched compared to other osmolytes, their catabolism may allow for progressive ^2H -enrichment of the H recycled through the TCA cycle, and hence into the leaf wax *n*-alkanes of dicots vs. monocots 4.

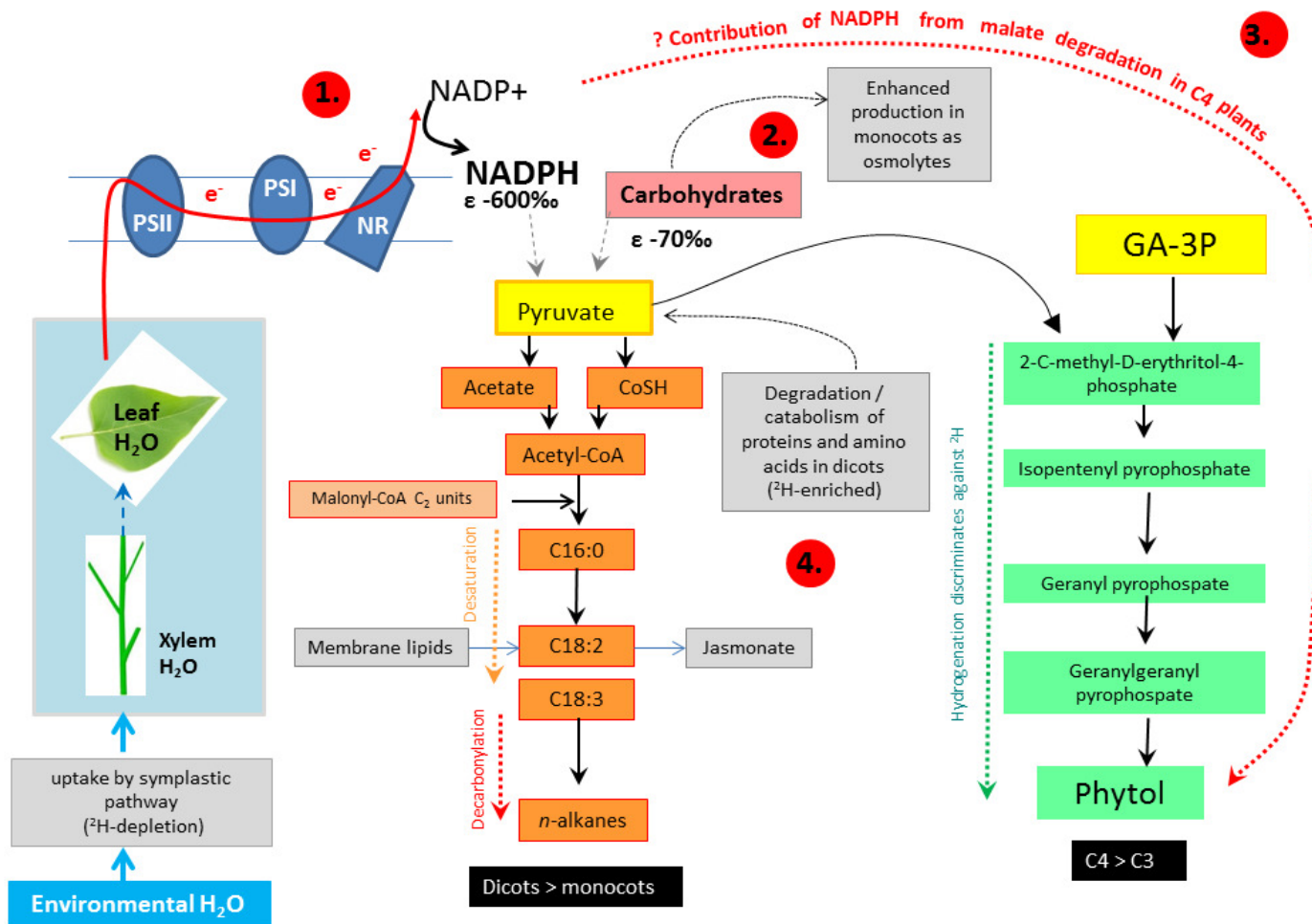


Figure 7.29: Schematic summarising potential biochemical mechanisms which could influence isoprenoid and acetogenic lipid hydrogen isotope compositions. Assumed hydrogen isotope fractionation of $NADPH$ (-600‰) is taken from Liu et al. (1991) and Zhang et al. (2009); the $^2H/^1H$ of carbohydrates is from Ladd and Sachs (2012). The DOXP pathway (phytol synthesis) is summarised from Chikaraishi et al. (2009), while the acetogenic pathway (FAs and alkanes) is summarised from Chikaraishi et al. (2004) and Shepherd and Griffiths (2006). Coloured numbers relate to the bullet points in Section 7.8, Summary.

Chapter 8

Distinguishing shifts in palaeohydrology from changes in vegetation: a challenge for interpreting sedimentary leaf wax *n*-alkanes

8.1. INTRODUCTION

The previous chapters of this thesis explored fundamental scientific questions focused on qualifying the relative importance of biochemical and environmental mechanisms in controlling the molecular distribution (Chapter 4) and stable isotope composition (Chapters 5, 6 and 7) of leaf wax *n*-alkanes. Data presented in them have significant implications for understanding the nature of the biochemical information recorded in leaf wax biomarkers in soils and sediments.

In addition to these issues, however, there are further considerations relating to the integration of leaf wax biomarkers into soils and sediments that are also significant for the accurate interpretation of fossil leaf wax *n*-alkanes (Fig. 8.1). These include: (i) the validity of the assumptions commonly applied to biomarker records in different depositional environments; (ii) the sensitivity of sedimentary lipid $^2\text{H}/^1\text{H}$ to changes in surface vegetation assemblages; and (iii) the selection of appropriate methods for distinguishing fluctuations in the sedimentary biomarker record due to vegetation change from those occurring as a result of climatic shifts. The overarching aim of this chapter is to explore these considerations in detail, through synthesising the information presented in Chapters 4 to 7 with *n*-alkane molecular and isotopic data from Stiffkey saltmarsh sediments.

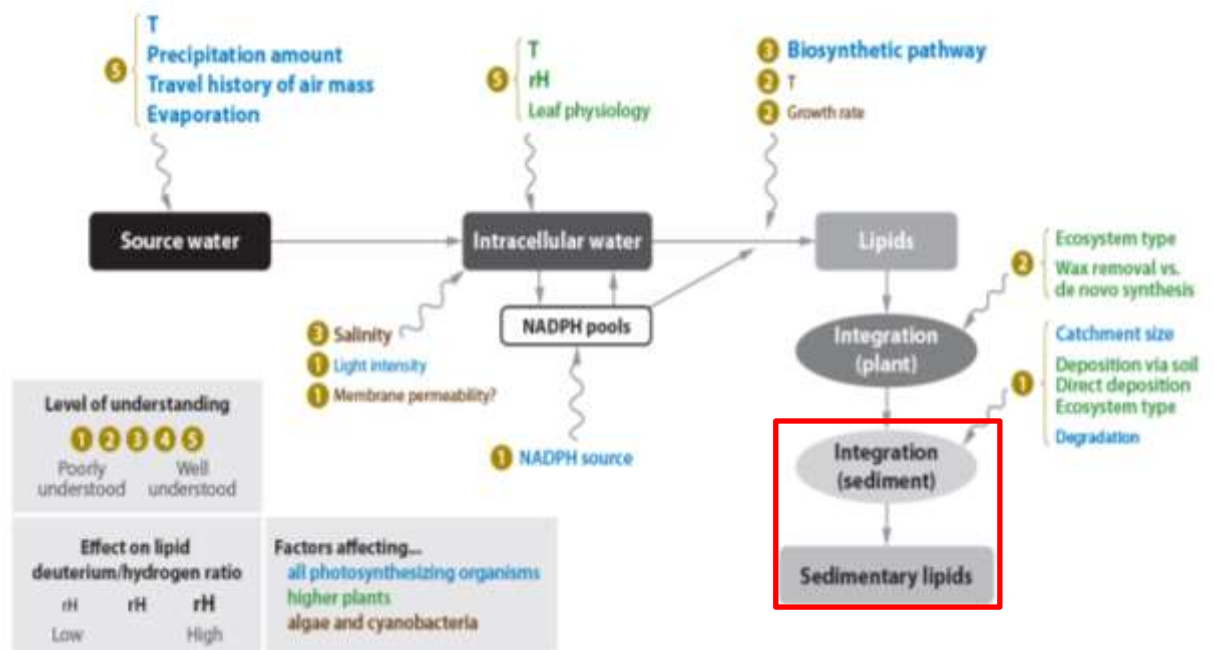


Figure 8.1: An overview of the processes affecting the hydrogen-isotopic composition of lipid biomarkers from phototrophic organisms. Abbreviations: NADPH, nicotinamide adenine dinucleotide phosphate (reduced); rH, relative humidity; T, temperature (Sachse et al., 2012). The red highlighted area shows the focus of this chapter, and the relative lack of current knowledge regarding factors influencing the isotopic composition of sedimentary lipids.

As previously discussed in Chapter 1 (Section 1.2), the selection of a dynamic saltmarsh site for this aspect of the project is challenging, as the potential exists for significant reworking of sediments across the marsh surface daily during tidal inundation. In addition, sediment and organic matter can be transported to Stiffkey by wind and water, adding non-local organic matter (OM) to the site. Despite these complications (which are addressed where relevant throughout this Chapter), the in-depth organic geochemical characterisation of *n*-alkanes from the Stiffkey plants, coupled with analysis of the sedimentary leaf wax lipids, offers a valuable opportunity for: (i) understanding the incorporation of plant *n*-alkanes into local sediments; and (ii) demonstrating the complexity of linking overlying vegetation to sedimentary biomarker signals.

Chapter 6 has made it clear that this is a particular problem for the use of leaf wax *n*-alkane hydrogen isotopes in palaeohydrological studies, given the 100‰ interspecies variation in *n*-C₂₉ δ²H and apparent fractionation between leaf water and *n*-alkanes observed for the saltmarsh plants at Stiffkey. Currently, however, the

basic assumption in palaeohydrological biomarker-based reconstructions is that the relationship between leaf wax $^2\text{H}/^1\text{H}$ and precipitation $^2\text{H}/^1\text{H}$ can be described by an identifiable and (relatively) consistent net apparent fractionation factor, (e.g. Schefuß *et al.*, 2005; Pagani *et al.*, 2006b; Sachse *et al.*, 2012; Tierney and deMenocal, 2013).

A number of studies have shown that there are significant differences in net fractionation between water and *n*-alkane $^2\text{H}/^1\text{H}$ values among different plant life forms growing in the same geographical location (e.g. Chikaraishi *et al.*, 2004; Liu *et al.*, 2008; Hou *et al.*, 2007, 2008; Pedentchouk *et al.*, 2008; Eley *et al.*, 2014). While debate as to the nature of information contained in sedimentary *n*-alkanes continues (e.g. Eley *et al.*, 2014; Chapter 6 and 7) some studies suggest that this variability can effectively be discounted as the sedimentary record averages plant inputs to such an extent that species-specific $^2\text{H}/^1\text{H}$ differences are negated (e.g. Neidermeyer *et al.*, 2010). Alternative approaches seek to correct for it by using other proxies such as *n*-alkane molecular distribution patterns, *n*-alkane carbon isotope composition (e.g. Schefuß *et al.*, 2005) and pollen (Tierney *et al.*, 2008; Feakins, 2013; Nelson *et al.*, 2013) to distinguish between inputs from different plant life forms such as C_3 trees, C_3 grasses and C_4 grasses. Once the contribution from these “end members” has been established, an averaged fractionation factor for each end member (e.g. data produced by Sachse *et al.*, 2012) is typically used to reconstruct the hydrogen isotope composition of past precipitation (Feakins, 2013). When the 100‰ variability in $\delta^2\text{H}$ values (and net apparent fractionation) observed among monocots, dicots and succulents growing at Stiffkey (Eley *et al.*, 2014; Chapter 6) is taken together with the fact that some of these species produce significantly more *n*-alkanes than others (Chapter 4), however, it becomes more difficult to quantify and correct for changes in vegetation assemblages in geological sequences.

This chapter is structured such that the sediment data from Stiffkey will be described first. The assumptions currently applied to palaeohydrological studies will then be reviewed, prior to the sensitivity of the Stiffkey sedimentary record to changes in surface plant cover being evaluated. This chapter will then review and evaluate approaches to identifying and quantifying vegetation change in more detail, using data presented in Chapters 4 – 7 in conjunction with the sedimentary measurements. Finally, this chapter will apply three approaches to reconstructing the $^2\text{H}/^1\text{H}$ value of palaeoprecipitation from sedimentary *n*-alkanes extracted from a 1 m core from Stiffkey to draw together the previous discussion, provide directions

for future research, and to set this study in the wider context of palaeoclimate reconstruction.

8.1.1 Sediment samples collected at Stiffkey

Sedimentary leaf wax *n*-alkanes were extracted from both surface sediments and a 1 m core. The surface sediments were collected in October 2011 from sampling the LM, R and UM sites (Fig. 2.2, Chapter 2). The surface sediments were collected from the top 10 cm of soil after carefully removing visible roots and plant detritus, and stored in aluminium foil containers for transport back to the laboratory. The 1 m core was collected in February 2011 from the UM (Fig. 2.2, Chapter 2), using a gauge auger (Fig. 8.2), and sub-sampled at 5 cm intervals once it had been returned to the laboratory. The outer material from the core edges was removed, and care was taken to ensure that no translocated material was present at each stage of sub-sampling. All sediment samples were thoroughly dried in an oven at 40 °C before being stored in a dark, dry environment prior to further analysis.



Figure 8.2: Julian Andrews with the 1m core sampled from UM (photo courtesy of Nikolai Pedentchouk, 2011)

All methods for the extraction and analysis of the sedimentary *n*-alkane data presented in this chapter are as described in previous chapters: molecular distribution (Chapter 4), carbon isotope composition (Chapter 5), and hydrogen isotope composition (Chapter 6). Analytical reproducibility for $\delta^{13}\text{C}$ measurements of the core sediment samples was better than $\pm 1\text{‰}$ for *n*-C₂₉, and 2‰ for *n*-C₃₁ (Appendix 7). Unfortunately insufficient material remained to perform replicate $^2\text{H}/^1\text{H}$ measurements from the core samples. Reproducibility for surface sediment sample $^2\text{H}/^1\text{H}$ measurements did not exceed 7‰, however (Appendix 7). As this value is in excess of the RMS errors for analysis of the *n*-alkane isotope standard (Chapter 6), a conservative approach is adopted and all core $^2\text{H}/^1\text{H}$ measurements presented in this chapter are assumed to have an uncertainty of at least $\pm 7\text{‰}$. Sediment ages for the 1 m core given throughout this chapter are calculated with reference to the linear sedimentation rates published by Andrews *et al.* (2000) (Chapter 2), with sub-samples dating from the 1980's to the 1520's. Data tables containing the molecular and stable isotope information from the Stiffkey core can be found in Appendix 7.

8.2 HOW VALID ARE THE ASSUMPTIONS USED IN PALAEOHYDROLOGICAL STUDIES?

8.2.1 Hydrogen isotope fractionation between source water and *n*-alkanes is relatively consistent among angiosperms

The palaeohydrological applications of leaf wax lipid $^2\text{H}/^1\text{H}$ reviewed in Chapter 1 (Section 1.1.3) are based on a number of explicit and/or implied assumptions, the validity of which require further consideration. For example, at high relative humidity, where evapotranspiration from leaves is minimal, it is often cited that the net apparent fractionation between source water and *n*-alkane $^2\text{H}/^1\text{H}$ ratios is relatively consistent among angiosperms (Sachse *et al.*, 2004, 2006; Pagani *et al.*, 2006b; Hou *et al.*, 2008; Hren *et al.*, 2010). Recent research, including the findings presented in Chapters 6 and 7, has suggested, however, that this assumption may not be accurate. Studies have found that variation in *n*-alkane $\delta^2\text{H}$ between C₃ and C₄ grasses, for example, could not be explained by reference to evapotranspiration and differences in leaf structure (e.g. Smith and Freeman, 2006; Feakins and Sessions, 2010; Terwilliger *et al.*, 2013) suggesting that biochemical processes might be responsible for such differences.

This assumption has been explored in detail in Chapter 6, where data show that differences in the hydrogen isotope composition of leaf water are not sufficient to fully account for interspecies variation in leaf wax *n*-alkane $\delta^2\text{H}$ (Chapter 6; Eley *et al.* 2014). Findings presented in this thesis therefore suggest that this assumption of a consistent net apparent fractionation factor is simplistic, and does not allow for successful distinction between: (i) shifts in sedimentary lipid $^2\text{H}/^1\text{H}$ driven by climate; and (ii) shifts driven by changes in surface vegetation. In addition, the key findings from Chapter 7 highlight the fact that biochemical variation among plant species and plant functional types may be a more important control on *n*-alkane $^2\text{H}/^1\text{H}$ than leaf physical processes. Future research should explore these areas further, to seek new insights into how the functioning of cellular metabolism influences the isotopic composition of plant secondary compounds.

8.2.2 Sedimentary biomarker signals average plant inputs across varying spatial scales

Another assumption regularly applied in biomarker-based palaeoclimate reconstructions is that sedimentary leaf wax lipids represent an integrated, smoothed regional signal (Polissar and Freeman, 2010). It is further implied that such smoothing negates the influence of species-specific differences in *n*-alkane hydrogen isotope composition (e.g. Niedermeyer *et al.*, 2010; Leider *et al.*, 2013). This has been stated to be especially true of lake sediments, while in contrast leaf wax lipids from soils are thought to potentially record additional variability in microclimate and vegetation (Douglas *et al.*, 2012). The fact that leaf waxes can be transported over considerable distances by aeolian (e.g. Conte and Weber, 2002) and fluvial (Leider *et al.*, 2013) processes has been used to further support the assertion that sedimentary lipids reflect large catchment scales, although Sachse *et al.* (2012) acknowledge that this is an area where more research is required (see highlighted region of Fig. 8.1).

The assumption that the lipid biomarker signal in the geological record represents an averaged input from all terrestrial plant sources is complicated by the fact that plant species do not all produce an equivalent amount of *n*-alkanes. Previous studies have demonstrated that angiosperms produce more *n*-alkanes than gymnosperms, however both species produce the same amount of *n*-alkanoic acids (Diefendorf *et al.*, 2011). To date, however, limited attention has been given to the variability in *n*-alkane production among angiosperm species growing at the same site. Chapter 4 demonstrates that at Stiffkey, plants differ by over an order of

magnitude in terms of the concentrations of *n*-alkanes they produce. This could have important implications for the sensitivity of the sedimentary record to relatively small-scale changes in vegetation assemblages, especially when these shifts involve plants that produce high concentrations of *n*-alkanes with very different $\delta^2\text{H}$ values. These issues are explored further below in Section 8.3.

8.2.3 Modern spatial studies can be used to interpret temporal changes in $\delta^2\text{H}$ signal

One of potentially the most important assumptions made in palaeohydrological reconstructions originates from a series of calibration studies that have been used to generate the “typical” fractionation factors often applied to determine palaeoprecipitation $^2\text{H}/^1\text{H}$ values. These “proof of concept” studies were carried out to determine whether leaf wax lipids recorded the $^2\text{H}/^1\text{H}$ composition of precipitation along large scale geographical transects. Huang *et al.* (2000), for example, published one of the earlier studies showing a statistically significant correlation between the $^2\text{H}/^1\text{H}$ values of palmitic acid (sourced from aquatic organisms) and precipitation from a range of 33 North American lakes. Fig. 8.3 provides a schematic of the type of geographical transect studies being discussed further in the text.

Sachse *et al.* (2004) analysed a range of biomarkers, including those from aquatic and terrestrial plants, from European lake sediments ranging from northern Sweden to southern Italy. The sampling locations varied in mean annual temperature from -2.0°C to 13.7°C, and had precipitation hydrogen isotope compositions ranging from -119.0 to -36.6‰. At these broad geographical and climatic scales, the $^2\text{H}/^1\text{H}$ measured for the *n*-C₂₇, *n*-C₂₉ and *n*-C₃₁ alkanes extracted from the lake sediments correlated with the isotopic composition of mean annual precipitation, lake water and mean annual temperature (Sachse *et al.*, 2004). In a companion study in 2006, Sachse *et al.* investigated the $^2\text{H}/^1\text{H}$ values of individual *n*-alkanes from Birch (*Betula*), Beech (*Fagus*), Oak (*Quercus*), Alder (*Alnus*), Hornbeam (*Carpinus*) and Myrtle (*Myrtus*) as well as non-stomata containing *Sphagnum*, *Cladonia* and moss from 14 sites along the same European transect. The study found that the molecular distribution of *n*-alkanes from dominant vegetation surrounding the lake study sites did not match the distribution of alkanes from the sediments, and attributed this to inputs of aeolian dusts containing alkanes, and/or bioturbation of the lacustrine sediments mixing older material with more recent deposits. This study did not consider the reworking of the sedimentary leaf wax signal by soil microbes,

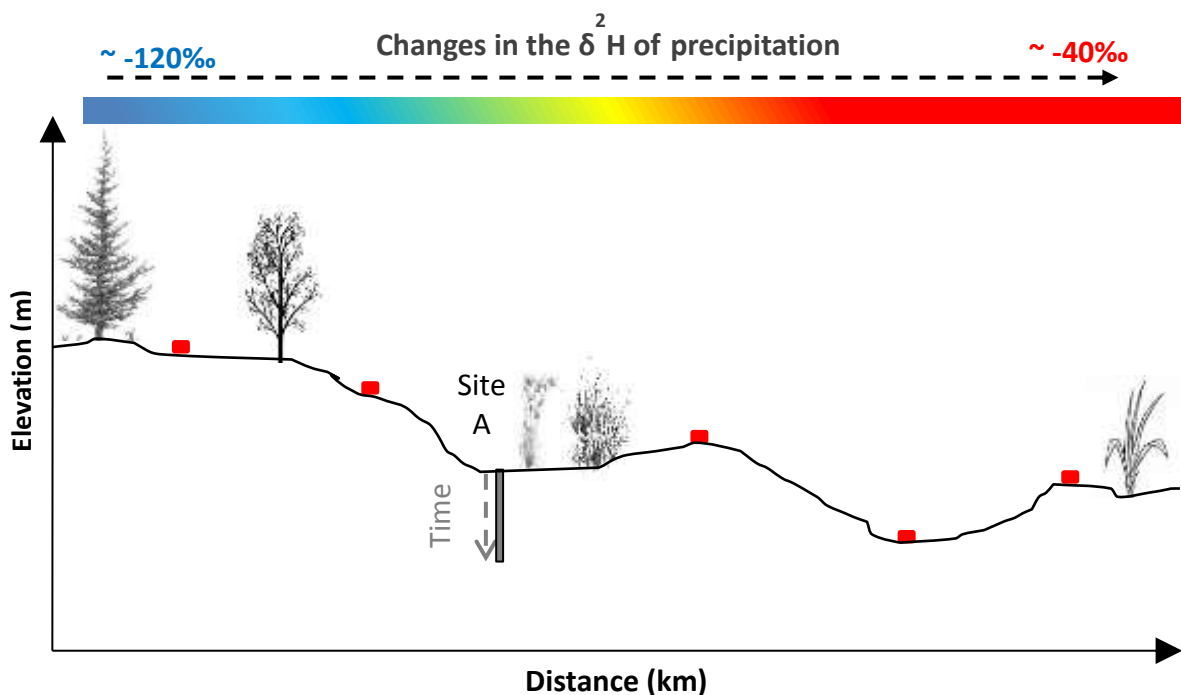


Figure 8.3: Schematic illustrating the complexities inherent in using a calibration carried out at the spatial scale to validate the interpretation of data from a chronosequence at one geographical location. In this figure (not to scale), the red markers represent a surface transect, illustrative of those carried out by Sachse *et al.* (2004) and Garcin *et al.* (2012). “Site A” represents a lacustrine core sequence at a single geographical point. The coloured bar shows the gross variation in precipitation ${}^2\text{H}/{}^1\text{H}$ that can be experienced across broad spatial scales, with the black (top) highlighting $\delta^2\text{H}_{\text{PPT}}$ also shifts as one moves along the transect in a N-S direction. Note the changes in vegetation across the transect – given the widespread interspecies differences in n -alkane ${}^2\text{H}/{}^1\text{H}$ observed across different biomes, it is possible that these shifts in plant cover could also influence surface sediment ${}^2\text{H}/{}^1\text{H}$.

however, which has been shown to influence the molecular distribution (although not ${}^2\text{H}/{}^1\text{H}$) of n -alkanes during leaf litter experiments (Zech *et al.*, 2011).

Results from Sachse *et al.* (2006) also suggested that sedimentary alkanes recorded the n -alkane $\delta^2\text{H}$ values present in autumn around the time of leaf fall. Limited variation in the ${}^2\text{H}/{}^1\text{H}$ values of n -alkanes was identified among the broadleaf species sampled during this study, with only the thick, waxy leaves from *Myrtus* having hydrogen isotope ratios that were $\sim 50\%$ lower than other species growing in close proximity. A statistically significant relationship was observed between $n\text{-C}_{27}$ and $n\text{-C}_{31}$ $\delta^2\text{H}$ and the $\delta^2\text{H}$ of meteoric water, although no relationship was identified between $n\text{-C}_{29}$ and meteoric water. This was attributed to the fact that $n\text{-C}_{29}$ was not produced by species at all sampling sites (Sachse *et al.*,

2006). Fractionation between *n*-alkanes and meteoric water was assumed to be consistent at -160‰ as part of this study (Sachse *et al.*, 2006).

More recent studies have extended these transects into tropical zones, in an attempt to calibrate the use of leaf wax biomarkers as palaeohydrological proxies in equatorial areas. Garcin *et al.* (2012) analysed a North-South transect across Cameroon, sampling 11 lake basins alongside plant xylem water, river water and groundwater samples. In addition, precipitation samples were also collected from rainfall events. The study found that *n*-C₂₉ δ²H extracted from the lake basin sediments was correlated with the hydrogen isotope composition of surface water (which reflects mean annual precipitation across large geographical ranges), linking alkane and water ²H/¹H values on hemispheric spatial scales (Garcin *et al.*, 2012). Data from a transect across Mexico and South America, however, found that variability in the estimated hydrogen isotope composition of precipitation across the transect (25‰) was insufficient to account for the range of δ²H_{wax} observed in modern lake sediments (60‰) (Douglas *et al.*, 2012). This was attributed to changes in aridity across the sampling sites, which accounted for more of the variability in hydrogen isotope fractionation between leaf wax *n*-alkanes and meteoric water, although a large amount of scatter was still observed in the data (Douglas *et al.*, 2012). Changes in the vegetation assemblages, and biochemical differences among individual species, were not explored in these studies as potential mechanisms that could contribute to the scatter observed in data from a single geographical location.

These transect studies have commonly been used to validate the interpretation of data from sedimentary cores. Schuman *et al.* (2006), for example, state that surface sample data from transects provides the framework for a conceptual model to interpret down-core ²H/¹H lipid data, while Niedermeyer *et al.* (2010) consider that the sedimentary biomarker signal represents an integrated, smoothed regional signal that negates the influence of species-specific differences in ²H/¹H. The results presented in this thesis from a temperate saltmarsh, combined with studies of other sedimentary environments, strongly suggest however that these statements oversimplify the picture. Jacobs *et al.* (2007) make it clear that a range of factors, including sources of OM, transport processes, and the residence time of OM in a particular depositional environment, can all influence entrainment and incorporation into the geological record. Indeed, the sedimentary archive therefore potentially records organic biomarker information that includes both spatial and temporal variability (Jacob *et al.*, 2007). Interestingly, many of the transect studies above do

not seek to explain the considerable scatter observed in their data for a single geographical location (e.g Fig. 8.4, data from Sachse *et al.* 2006). This scatter, taken in conjunction with the results presented in Chapter 6 illustrating that leaf water $\delta^2\text{H}$ values do not drive interspecies variation in *n*-alkane $\delta^2\text{H}$ values, suggests that a reliance on geographical transect data (spatial data) to calibrate values for ϵ for use in down-core sedimentary sequences (temporal data) may not be appropriate for all depositional environments. Indeed, the existence of such scatter further illustrates that trends observed across geographical transects (where large-scale shifts in aridity, precipitation $^2\text{H}/^1\text{H}$, and vegetation occur) may not be directly applicable to the temporal changes in conditions recorded down-core in a single geographical location (e.g. Site A, Fig. 8.3).

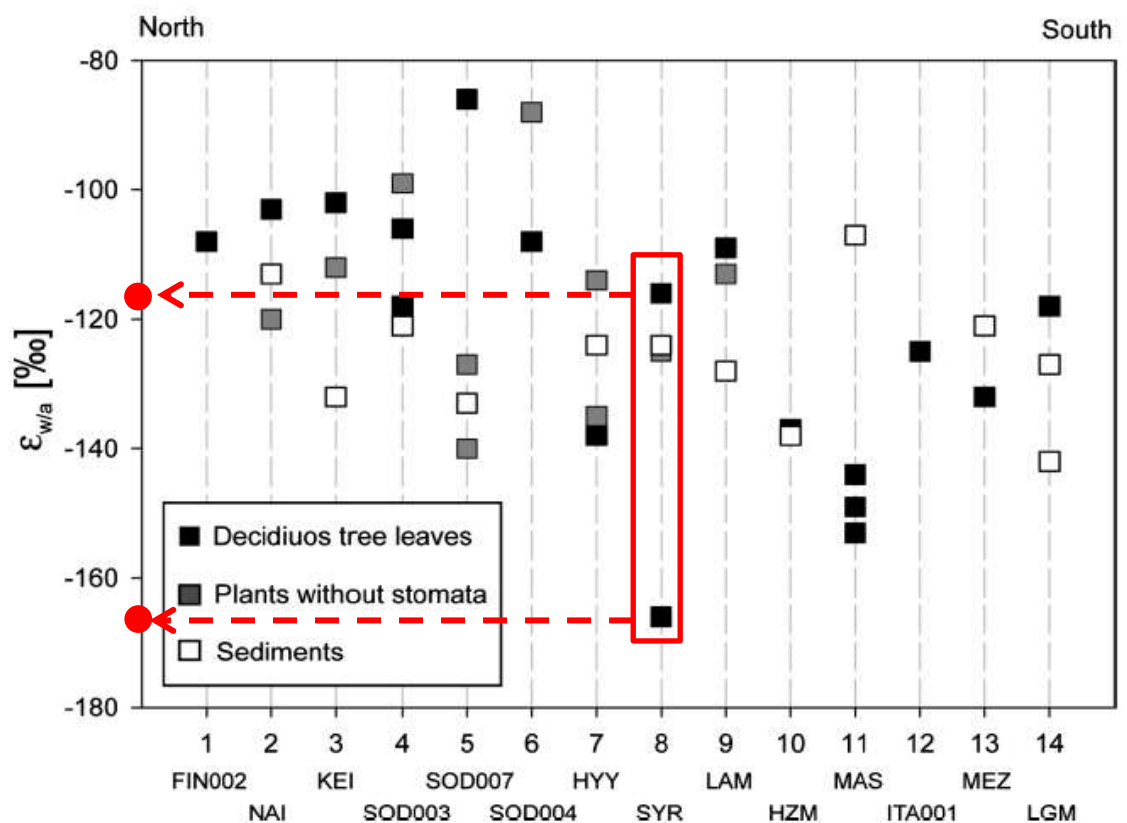


Figure 8.4: Comparison of the isotopic fractionation between source water and *n*-alkanes ($\epsilon_{w/a}$) for the analysed sites, data from Sachse *et al.* (2006). The red highlighted area (and associated arrows) provides an example of the scatter in fractionation factors found in a single geographical location, with two deciduous tree leaves here having values for ϵ that differ by $\sim 50\%$.

8.3 SENSITIVITY OF THE SEDIMENTARY BIOMARKER RECORD TO VEGETATION CHANGE

Despite these potential limitations in common assumptions made when using leaf wax biomarkers for palaeohydrological reconstructions, many studies still consider that vegetation change has to be substantial in order to give rise to interpretative issues within a geological data set. Indeed, minimal changes are assumed to have negligible impact (e.g. Tierney *et al.*, 2010, 2011; Tierney and deMenocal, 2013; Feakins, 2013; Nelson *et al.*, 2013). Typical examples of the magnitude of significant vegetation change envisaged by such studies include shifts from steppe tundra to boreal forest (as Earth moved from glacial to interglacial periods) which influenced the relative proportions of C₃ and C₄ plants (Huang *et al.*, 1999, 2001). No studies have been carried out to date, however, to ascertain the sensitivity of sedimentary lipid ²H/¹H to small or modest scale shifts in vegetation at a particular location. This means that the importance of such changes in surface vegetation could currently be underestimated in palaeoclimate reconstruction based on sedimentary leaf wax biomarkers. Such a paucity of data could be a significant oversight, especially in light of the large variability in *n*-alkane ²H/¹H composition of > 100‰ among species reported in Chapter 6.

Chapter 4 has illustrated the variability in the total concentration of leaf wax compounds produced by the different plant species growing at Stiffkey saltmarsh, which can exceed an order of magnitude. This variability has the potential to influence the relative contribution of each species to the sedimentary record, however to date this issue has received limited attention in studies reconstructing past hydrological conditions from sedimentary leaf wax biomarkers. As discussed in Chapter 4, Diefendorf *et al.* (2011) found that gymnosperms produced significantly lower concentrations of *n*-alkanes than angiosperms. Data from Stiffkey extends these considerations to collections of angiosperms growing at a single geographical location.

Molecular data presented in this thesis also show that the production of a significant concentration of one alkane homologue does not mean that a species produces an equivalent amount of other chain lengths in its leaf wax. For example, while some species at Stiffkey produce an abundance of *n*-C₂₇, they may produce less *n*-C₂₉ and *n*-C₃₁, or vice versa (Table 8.1; Fig. 8.5). *Suaeda vera*, for example, is the second highest producer of *n*-C₂₇ at the marsh, but only the fourth highest producer

of $n\text{-C}_{29}$ (Fig. 8.5). When variability in hydrogen isotope composition is coupled with these significant differences in the concentration of wax produced by some species (Bush *et al*, 2013; Diefendorf *et al.*, 2011), it is clear that further research is required to evaluate the sensitivity of the geological record to small-scale changes in vegetation across a range of depositional environments.

Table 8.1: Concentration in $\mu\text{g g}^{-1}$ dry mass of n -alkane homologues produced by Stiffkey species, September 2012

Species	$n\text{-C}_{25}$	$n\text{-C}_{27}$	$n\text{-C}_{29}$	$n\text{-C}_{31}$	$n\text{-C}_{33}$
<i>Atriplex portulacoides</i>	17	39	37	8	-
<i>Elytrigia atherica</i>	5	17	57	48	5
<i>Limonium vulgare</i>	8	160	311	294	92
<i>Phragmites australis</i>	20	24	28	2	-
<i>Spartina anglica</i>	4	14	71	22	-
<i>Salicornia europaea</i>	3	5	4	2	-
<i>Suaeda vera</i>	13	66	44	11	-

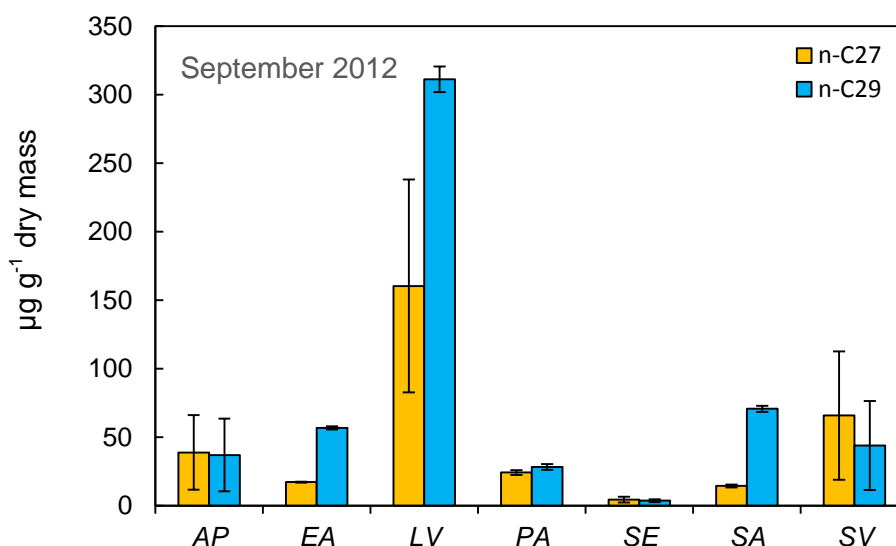


Figure 8.5: Variation in the concentrations of $n\text{-C}_{27}$ and $n\text{-C}_{29}$ among the seven saltmarsh plants sampled at Stiffkey in September 2012. Abbreviations: AP, *Atriplex portulacoides*; EA, *Elytrigia atherica*; LV, *Limonium vulgare*; PA, *Phragmites australis*; SE, *Salicornia europaea*; SA, *Spartina anglica*; SV, *Suaeda vera*. Error bars show absolute differences between sample replicates.

To investigate this issue, plant *n*-alkane concentration data given in Table 8.1 was used to calculate the relative percentage (RA) of *n*-alkane inputs that each of the sampled species could potentially contribute to sediments. From a theoretical perspective, if these seven species contribute different relative amounts of each homologue to sediments, the ²H/¹H composition of sedimentary *n*-C₂₉ should be a weighted average of these different inputs.

This thought experiment makes the fundamental assumptions that: (i) all of the *n*-alkanes from the leaf waxes are incorporated into the sediment, with no loss to wind/water erosion which may differ among different wax crystalline structures; and (ii) there are no significant “external” *n*-alkane inputs deposited at the site from wind and water transport. While such factors will of course be essential for interpreting sedimentary alkanes in a range of natural depositional environments, the purpose of this exercise is simply to evaluate the potential influence of changing the percentage cover of plants to sedimentary *n*-alkane hydrogen isotope composition – a consideration that has received limited attention in previous research.

The weighted average hydrogen isotope composition was calculated here using Eq. 1, where for example δ^2H_{sed} is the ²H/²H of the sedimentary *n*-C₂₉ alkane, $RA_{C_{29}}$ is the relative percentage contribution of *n*-C₂₉ produced by each plant, and $\delta^2H_{C_{29}}$ is the ²H/²H value of *n*-C₂₉ from each plant (δ^2H data used here is from September 2012, originally presented in Chapter 6).

$$\delta^2H_{sed} = ((RA_{C_{29} AP} * \delta^2H_{C_{29} AP}) + (RA_{C_{29} EA} * \delta^2H_{C_{29} EA}) + (RA_{C_{29} LV} * \delta^2H_{C_{29} LV}) + (RA_{C_{29} PA} * \delta^2H_{C_{29} PA}) + (RA_{C_{29} SA} * \delta^2H_{C_{29} SA}) + (RA_{C_{29} SE} * \delta^2H_{C_{29} SE}) + (RA_{C_{29} SV} * \delta^2H_{C_{29} SV})) / (RA_{C_{29} AP} + RA_{C_{29} EA} + RA_{C_{29} LV} + RA_{C_{29} PA} + RA_{C_{29} SA} + RA_{C_{29} SE} + RA_{C_{29} SV})$$

Eq. 1

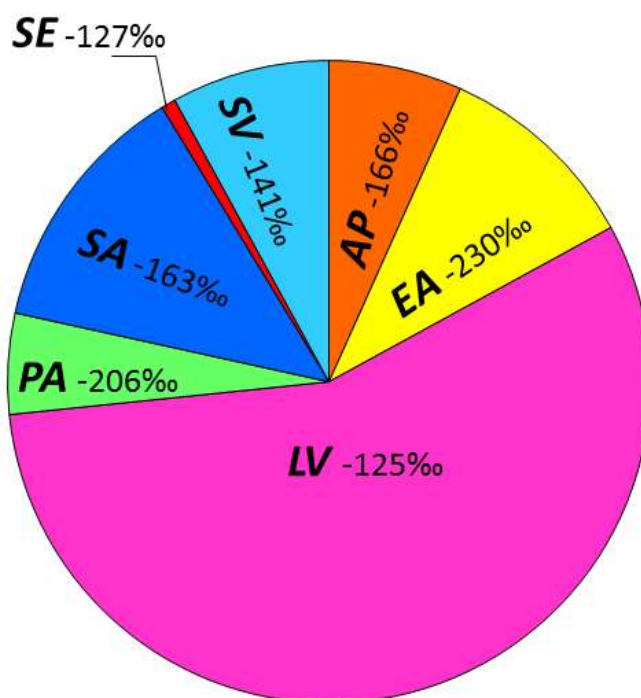


Figure 8.6: Pie chart illustrating the relative contribution of $n\text{-C}_{29}$ from each of the seven studied saltmarsh plants, with their respective $n\text{-C}_{29}$ δ^2H values shown in each segment. Data shown is from September 2012.

Fig. 8.6 illustrates the interspecies variation in relative inputs of $n\text{-C}_{29}$ among the Stiffkey plants, coupled with their $^2H/^1H$ values. As can be seen from Table 8.1 and Fig. 8.6, the perennial *Limonium vulgare* produces the highest percentage input of $n\text{-C}_{29}$ of any species at Stiffkey, while the stem succulent *Salicornia europaea* produces the lowest. Calculating δ^2H_{sed} using Eq. 1 results in a weighted average $^2H/^1H$ $n\text{-C}_{29}$ value of -149‰ . Weighted average net apparent fractionation between $n\text{-C}_{29}$ and source water ($\epsilon_{wax/OIPCw}$) (calculated using the OIPC model output for the $^2H/^1H$ of precipitation, Appendix 5) was -106‰ . This is within the range anticipated for C_3 dicots published by Sachse *et al.* (2012) of $-113 \pm 31\text{‰}$.

To evaluate the effect of changes in vegetation composition on this WA value, two scenarios have been generated, based on plausible anthropogenic and environmental factors that have been previously reported to drive changes in the percentage cover of saltmarsh plants in temperate ecosystems. Once again, these data assume that: (i) all alkanes produced by plant leaves are incorporated into the sediment; and (ii) there are no significant inputs from external sources.

8.3.1 Scenario 1

Saltmarsh vegetation has been significantly altered throughout the Holocene by the practice of grazing livestock. Around the coast of the UK and Europe, archaeological studies have shown that animal husbandry practices dating back to the Bronze Age included the grazing of livestock on saltmarsh sites (e.g. Britton *et al.*, 2008). The grazing of these coastal ecosystems can have a dramatic effect on the distribution of surface vegetation (Adam, 2002). Particular species that are found at Stiffkey saltmarsh, such as *Atriplex portulacoides* and *Phragmites australis* have been shown to be particularly sensitive to grazing (Adam, 2002; Bos *et al.*, 2002). The percentage ground cover of *Limonium vulgare* and *Elytrigia atherica* can also be diminished by these animal husbandry practices (Bakker, 1978; Ungar and Woodell, 1996; Veneklaas *et al.*, 2011). In contrast, *Salicornia europaea* can become a dominant species in a grazed saltmarsh (Jensen, 1985; Kiehl *et al.*, 1996), with surface cover potentially decreasing once grazing ceases (Schroder *et al.*, 2002). The evergreen succulent *Suaeda maritima*, a close relative of *Suaeda vera*, is also known to provide significant ground cover in grazed sites, although it can also flourish in ungrazed environments (Kiehl *et al.*, 1996). Changes to distribution caused by grazing are therefore modelled to decrease the relative contribution of leaf wax *n*-alkanes from *Atriplex portulacoides*, *Limonium vulgare*, *Elytrigia atherica* and *Phragmites australis*, and an increase of those from *Salicornia europaea* and *Suaeda vera* (Table 8.2).

Table 8.2: Original percentage inputs of the 7 saltmarsh species from September 2012, compared with modelled percentage inputs used to test the impact of Scenario 1

Scenario 1	Plant species						
	AP	EA	LV	PA	SA	SE	SV
Sept. 2012	6.7	10.3	56.3	5.1	12.9	0.7	8.0
Scenario 1 assumed values	1	2	25	0	12	35	25

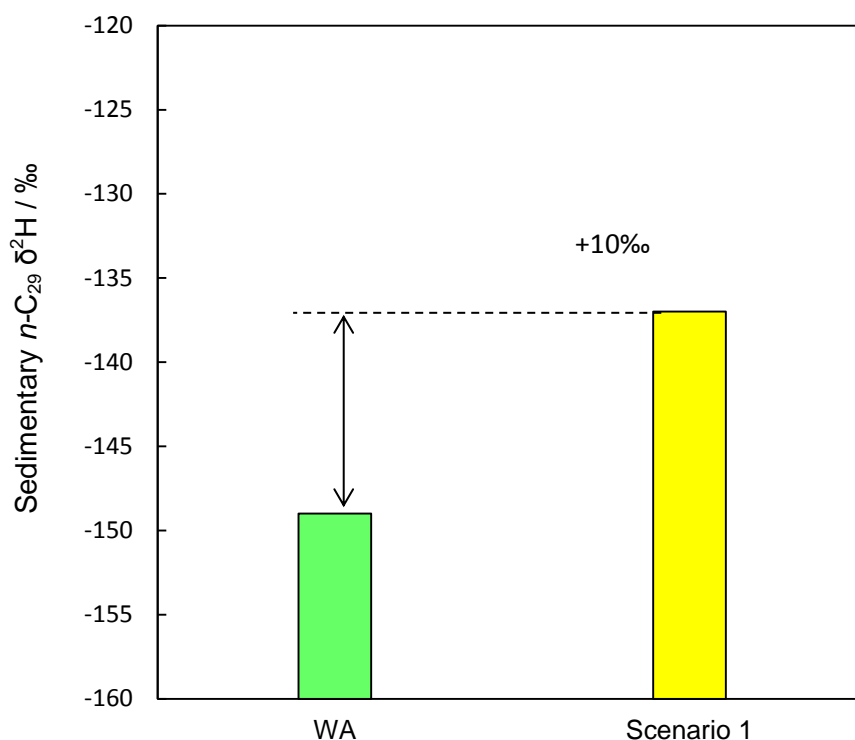


Figure 8.7: Comparison of WA sedimentary $n\text{-C}_{29} \delta^2\text{H} / \text{‰}$ values using the original percentage inputs from September 2012 (green), and the modelled percentage inputs using Scenario 1 (yellow).

Calculation of a revised WA sedimentary $\delta^2\text{H}$ value using these modelled input parameters results in a positive shift of 10‰ (Fig. 8.7). These vegetation shifts also influenced $\epsilon_{\text{wax/OIPCW}}$, changing it to -93‰, which is still just within the range anticipated by Sachse *et al.* (2012) for C_3 dicots.

8.3.2 Scenario 2

Changes in saltmarsh accretion and the extent of waterlogging are known to influence saltmarsh vegetation, and are likely to change as Earth's climate shifts. Changes to accretion rates and waterlogging in particular can alter the patterns of competition and succession among plant species (Veeneklas *et al.*, 2013). A decrease in waterlogging, caused for example by changes in the vertical accretion rate of the marsh, would favour enhanced cover by *Elytrigia atherica* (Davy *et al.*, 2011; Veeneklas *et al.*, 2013), and *Phragmites australis* (Hellings and Gallagher, 1992). However, species such as *Limonium vulgare* (Olf *et al.*, 1988) and *Salicornia europaea* (Davy *et al.*, 2011) have shown positive correlations with tidal inundation, suggesting that where sediments become drier, these species may be out-

competed. Shifts in plant distribution caused by changes in topography are therefore modelled here on an assumed decrease in the proportion of *Limonium vulgare* and *Salicornia europaea*, and an increase in *Elytrigia atherica* and *Phragmites australis* (Table 8.3) as a result of enhanced vertical accretion of the saltmarsh surface. Results showed that increasing the cover of *Elytrigia atherica* so that it contributes 35% of $n\text{-C}_{29}$ to the total signal, and *Phragmites australis* to 15% of the total signal, while reducing the input of *Limonium vulgare* to 22% of the total signal (Table 8.3), results in a 35‰ negative shift in δ^2H_{sed} to -183‰ (Fig. 8.8).

Table 8.3: Original percentage inputs of the 7 saltmarsh species from September 2012, compared with modelled percentage inputs used to test the impact of Scenario 2

Scenario 2	Plant species						
	AP	EA	LV	PA	SA	SE	SV
Sept. 2012	6.7	10.3	56.3	5.1	12.9	0.7	8.0
Scenario 2 assumed values	6.7	35.0	22.0	15.0	12.9	0.7	8.0

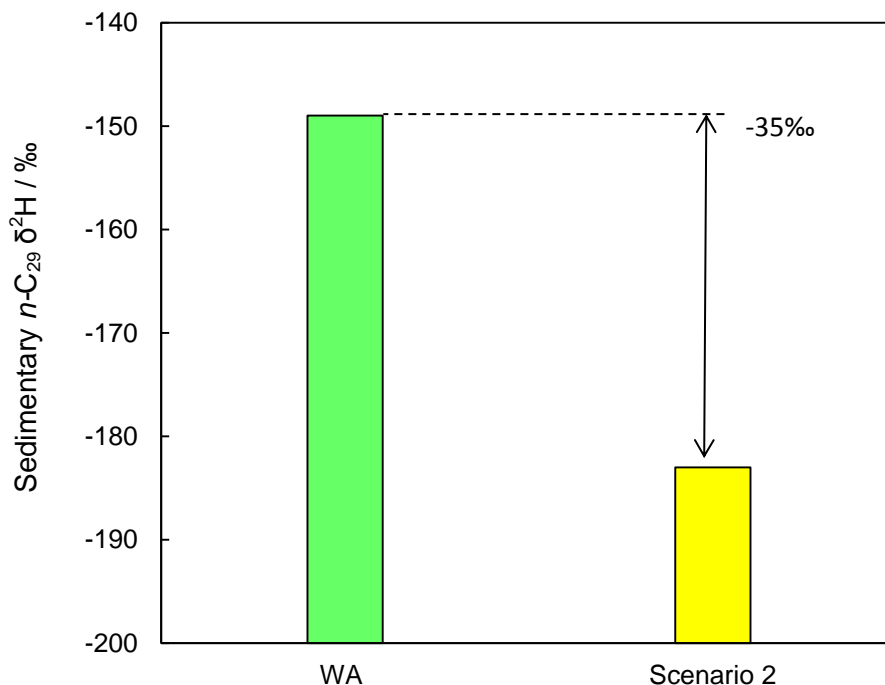


Figure 8.8: Comparison of WA sedimentary $n\text{-C}_{29} \delta^2H/1H$ values using the original percentage inputs from September 2012 (green), and the modelled percentage inputs using Scenario 2 (yellow).

Again, vegetation shifts arising from Scenario 2 also influenced $\epsilon_{\text{wax/OIPCW}}$, changing it this time to -141‰, which just within the lower end of the range anticipated by Sachse *et al.* (2012) for C₃ dicots. The magnitude of the shift in the weighted average ²H/¹H of *n*-C₂₉ available for entrainment into the sediment at Stiffkey, arising from relatively modest changes in the composition of local vegetation, suggests that the hydrogen isotope composition of sedimentary lipids might display a far greater sensitivity to small-scale changes in plant cover than is currently assumed. In particular, it highlights that it is not simply a drastic change in ecosystem or biome type (Schefuß *et al.*, 2005; Tierney *et al.*, 2010, 2011; Tierney and deMenocal, 2013) that represents a challenge when interpreting sedimentary biomarker records. Subtle changes in one ecosystem, which can be driven by a range of climatic, environmental and anthropogenic factors, also need to be successfully identified and quantified, to ensure that the effects of vegetation change and climate can be disentangled when reconstructing past hydrological regimes. Methods of identifying palaeovegetation shifts through time are clearly therefore very important. This chapter will now consider the different approaches commonly utilised, and evaluate their effectiveness against the molecular and isotopic data collected for the Stiffkey plants and sediments.

8.4 THE SUCCESS OF METHODS TO QUANTIFY VEGETATION CHANGE

8.4.1 Carbon isotope composition of *n*-alkanes

Several approaches have been used to identify and quantify vegetation change, in order to ensure robust interpretation of sedimentary biomarker data. One common method uses the carbon isotope composition of leaf wax compounds, which show a typical shift between C₃ and C₄ species (Collister *et al.*, 1994; Chikaraishi and Naraoka, 2004). As discussed in Chapter 5, such distinctions have been used in a palaeoclimate context, for example, to establish the proportion of C₃ and C₄ plants contributing to sediments (Huang *et al.*, 1999, 2001; Bull *et al.*, 1999; Tierney *et al.*, 2010; Niedermeyer *et al.*, 2011), and to explore the expansion of plants capable of using the C₄ photosynthetic pathway during the Late Miocene (Freeman and Colarusso, 2001; Feakins *et al.*, 2005; Tiple and Pagani, 2007).

The Stiffkey *n*-alkane hydrogen isotope data presented in Chapter 6, however, indicate that the greatest variability in leaf wax ²H/¹H is in fact found among C₃ species (e.g. the C₃ monocot *Elytrigia atherica*, vs. the C₃ succulent *Suaeda vera*).

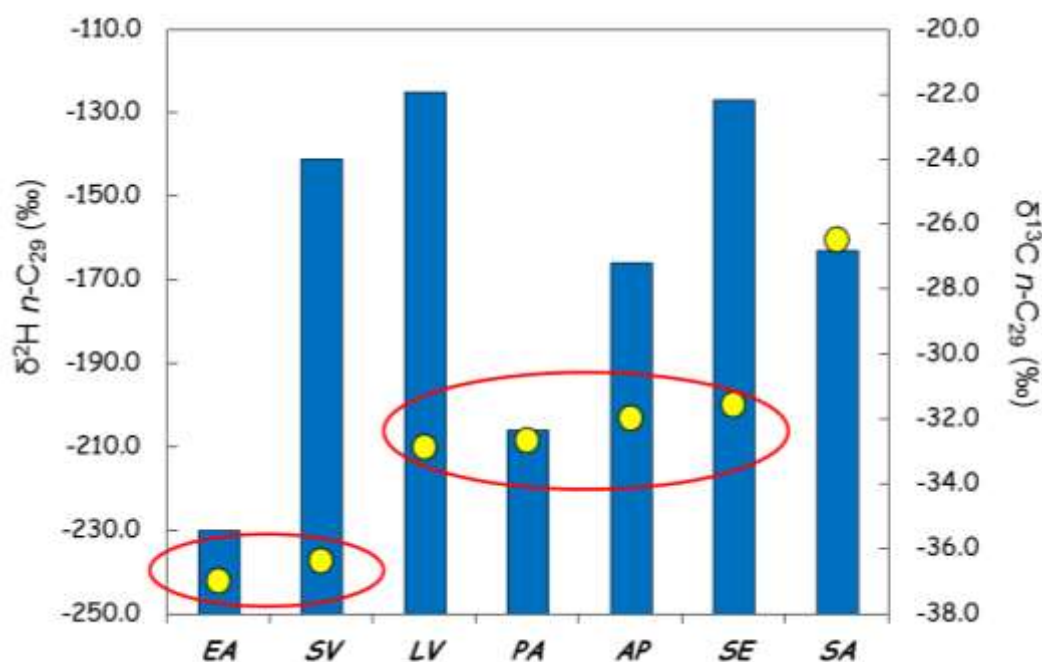


Fig. 8.9: Evaluating the suitability of using the carbon isotope composition (yellow circles) of $n\text{-C}_{29}$ to constrain the extent of vegetation change in sedimentary sequences. EA = *Elytrigia atherica*; SV = *Suaeda vera*; LV = *Limonium vulgare*; PA = *Phragmites australis*; AP = *Atriplex portulacoides*; SE = *Salicornia europaea*; SA = *Spartina anglica*. Note how SA, the C_4 plant, is clearly distinguished from the other species, while: (i) EA and SV; and (ii) LV, PA, AP and SE - samples with very different $^2\text{H}/^1\text{H}$ compositions - are very similar in terms of their $^{13}\text{C}/^{12}\text{C}$ values (data points circled in red). Data shown are from August 2012, similar plots for other sampling intervals can be found in Appendix 7.

While the C_4 monocot *Spartina anglica* can easily be distinguished from the C_3 Stiffkey plants using coupled n -alkane $\delta^{13}\text{C}$ and $\delta^2\text{H}$ measurements, the variability in the carbon isotope composition of leaf waxes from the Stiffkey C_3 species (Chapter 5) may not successfully discriminate between these coastal saltmarsh plants. Reliance on the carbon isotope composition of a compound of interest to identify vegetation change among C_3 species from sedimentary lipids may not, therefore, always provide sufficient resolution. Fig. 8.9 presents carbon and hydrogen measurements from the $n\text{-C}_{29}$ alkane from August 2012 (although similar results are found when plotting other sampling intervals, Appendix 7), illustrating the similarity of carbon isotope values among C_3 species that have widely differing hydrogen isotope compositions. These findings build upon the view expressed by Douglas *et al.* (2012) that the carbon isotope composition of leaf wax n -alkanes might not be a particularly robust indicator of changes in plant communities. Indeed, Castanada and Shouten (2011) estimate that at best, the uncertainty associated with the prediction of vegetation inputs from leaf wax carbon isotope data is in the region of

20%. This lack of precision could in turn lead to further propagation of error when seeking to constrain changes in surface vegetation from sedimentary leaf wax biomarkers.

To further evaluate the value of carbon isotopes in constraining the occurrence of modest vegetation change among a C₃-dominated plant population of the type found at Stiffkey, the vegetation shifts described by Scenario 1 and Scenario 2 (Tables 8.2 and 8.3 above) were also applied to carbon isotope composition of *n*-C₂₉ (previously reported in Chapter 5). Fig. 8.10 shows the carbon isotope composition and relative contribution to sediments from the seven species in September 2012, while Figures 8.11 and 8.12 show the results of applying the vegetation shifts from Scenario 1 and Scenario 2, respectively. Again, this exercise makes the same assumptions as discussed previously with regard to the hydrogen isotope composition of sedimentary *n*-alkanes (Section 8.3), namely that: (i) all plant leaf *n*-alkanes are transferred to the sediment; and (ii) non-local sources of OM are not significant.

It is clear that the negligible shift in the weighted average sedimentary $\delta^{13}\text{C}$ value caused by Scenario 1 (0.06‰; Fig. 8.11) is too small to be identified as arising from changes in vegetation, as it is within: (i) the variation observed among sample replicates (Chapter 5), and (ii) analytical error for *n*-alkane carbon isotope measurements (Chapter 5). More significantly, even though Scenario 2 resulted in a

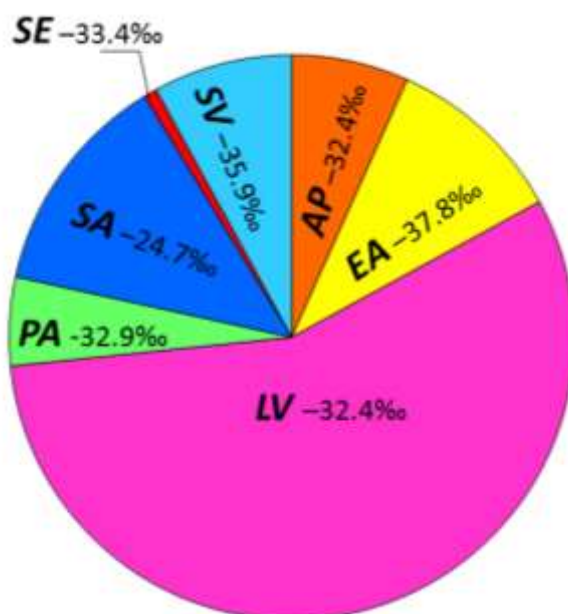


Figure 8.10: Pie chart illustrating the relative contribution of *n*-C₂₉ from each of the seven studied saltmarsh plants, with the *n*-C₂₉ $\delta^{13}\text{C}$ values (September 2012) shown in each segment.

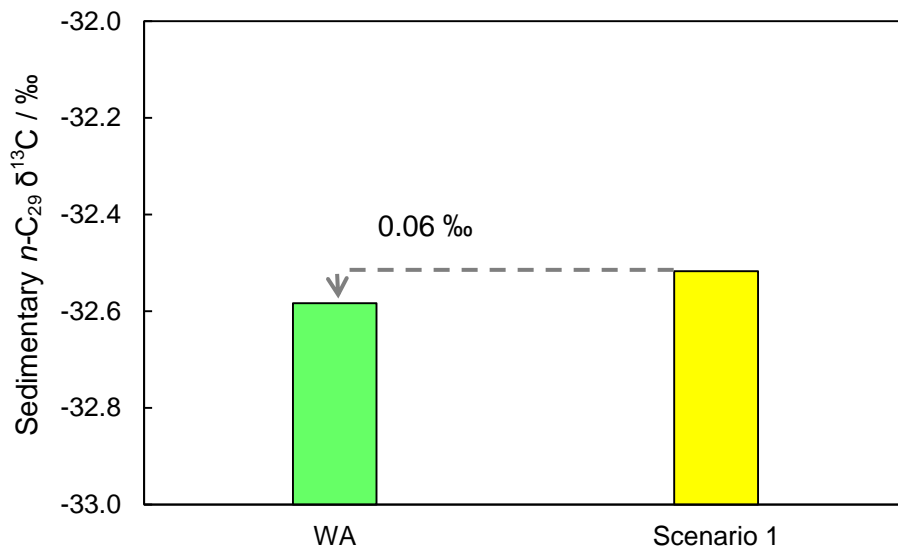


Figure 8.11: Comparison of WA sedimentary $n\text{-C}_{29} \delta^{13}\text{C}$ values using the original percentage inputs from September 2012 (green), and the modelled percentage inputs using Scenario 2 (yellow).

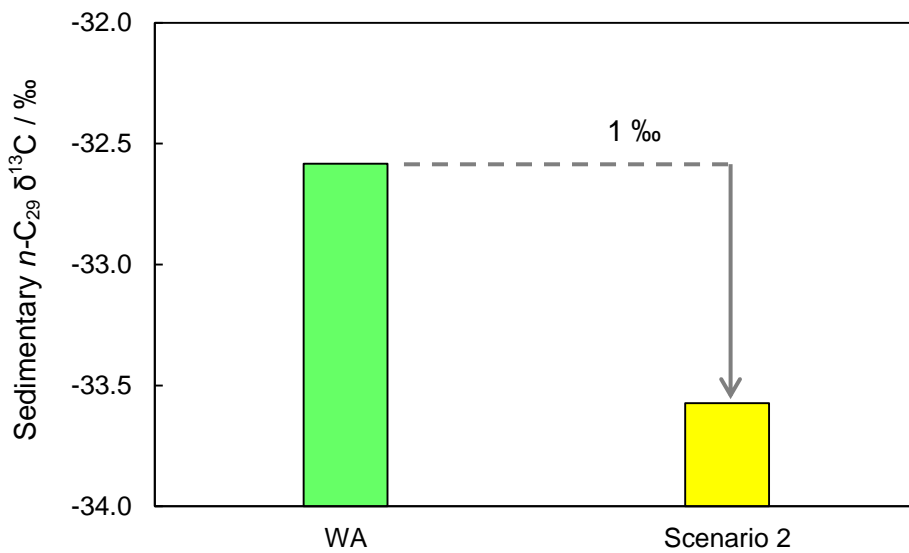


Figure 8.12: Comparison of WA sedimentary $n\text{-C}_{29} \delta^{13}\text{C}$ values using the original percentage inputs from September 2012 (green), and the modelled percentage inputs using Scenario 2 (yellow).

35‰ shift in the $\delta^2\text{H}$ value of the weighted average $n\text{-C}_{29}$ input, it only produced a coeval 1‰ shift in carbon isotope composition (Fig. 8.12). Where studies have previously used linked $\delta^2\text{H}$ and $\delta^{13}\text{C}$ measurements of leaf wax biomarkers to identify down-core vegetation shifts, variation of up to $\sim 3\%$ in the $\delta^{13}\text{C}$ values of sedimentary n -alkanes have discounted as a concern when recreating palaeohydrological conditions (Schefuß *et al.*, 2005). Therefore, it is unlikely that a 1‰ shift in $\delta^{13}\text{C}$ would be viewed as indicating a significant change in plant communities sufficient to give rise to a 35‰ shift in sedimentary alkane $^2\text{H}/^1\text{H}$.

8.4.2 Using molecular distributions to identify vegetation change

An alternative approach to identifying changes in plant communities commonly encountered in palaeoclimatological and palaeohydrological studies is to consider the molecular distribution of the leaf wax biomarkers, as discussed in detail in Chapter 4. To briefly recap, it was traditionally assumed that the distribution of leaf wax compounds, such as n -alkanes, varied in a predictable way among different plant functional types (e.g. Eglinton *et al.*, 1962; Maffei, 1994; Rommerskirchen *et al.*, 2006).

Typically in these studies, vegetation change is quantified by reference to calculated indices used to describe aspects of the n -alkyl lipid distribution patterns. These include parameters such as average chain length (ACL) and carbon preference index (CPI) (e.g. Zhou *et al.*, 2005; Zhang *et al.*, 2006; Zhou *et al.*, 2010; Buggle *et al.*, 2010). In addition, the ratio of specific alkane homologues to each other, such as $n\text{-C}_{31}$ to $n\text{-C}_{27}$ or $n\text{-C}_{29}$, has been used to discriminate between trees and grasses based on the assumption that grasses are the primary source of $n\text{-C}_{31}$ in sediments, while trees produce more $n\text{-C}_{27}$ and $n\text{-C}_{29}$ (Zhang *et al.*, 2006; Zech *et al.*, 2010). Recent studies, however, have suggested that these values are of limited probative value for successfully identifying plant inputs to sediments because they can display either limited variability (ACL), or too much variability (CPI), among plant species (Bush *et al.*, 2012; Bush and McInerney, 2013).

Given the spread of n -alkane $^2\text{H}/^1\text{H}$ values across the Stiffkey species, molecular distribution parameters would need to be sufficiently different to discriminate between plants with relatively positive hydrogen isotope values and those with relatively negative values in order to identify significant vegetation changes in sedimentary sequences. The hydrogen isotope composition of the $n\text{-C}_{29}$ alkane from August 2012 (Fig. 8.13 A) was plotted against: (i) ACL values (Fig. 8.13 B); (ii) CPI values (Fig. 8.13 C); and (iii) the ratio of $n\text{-C}_{27}$ to $n\text{-C}_{31}$ (Fig. 8.13 D). This figure

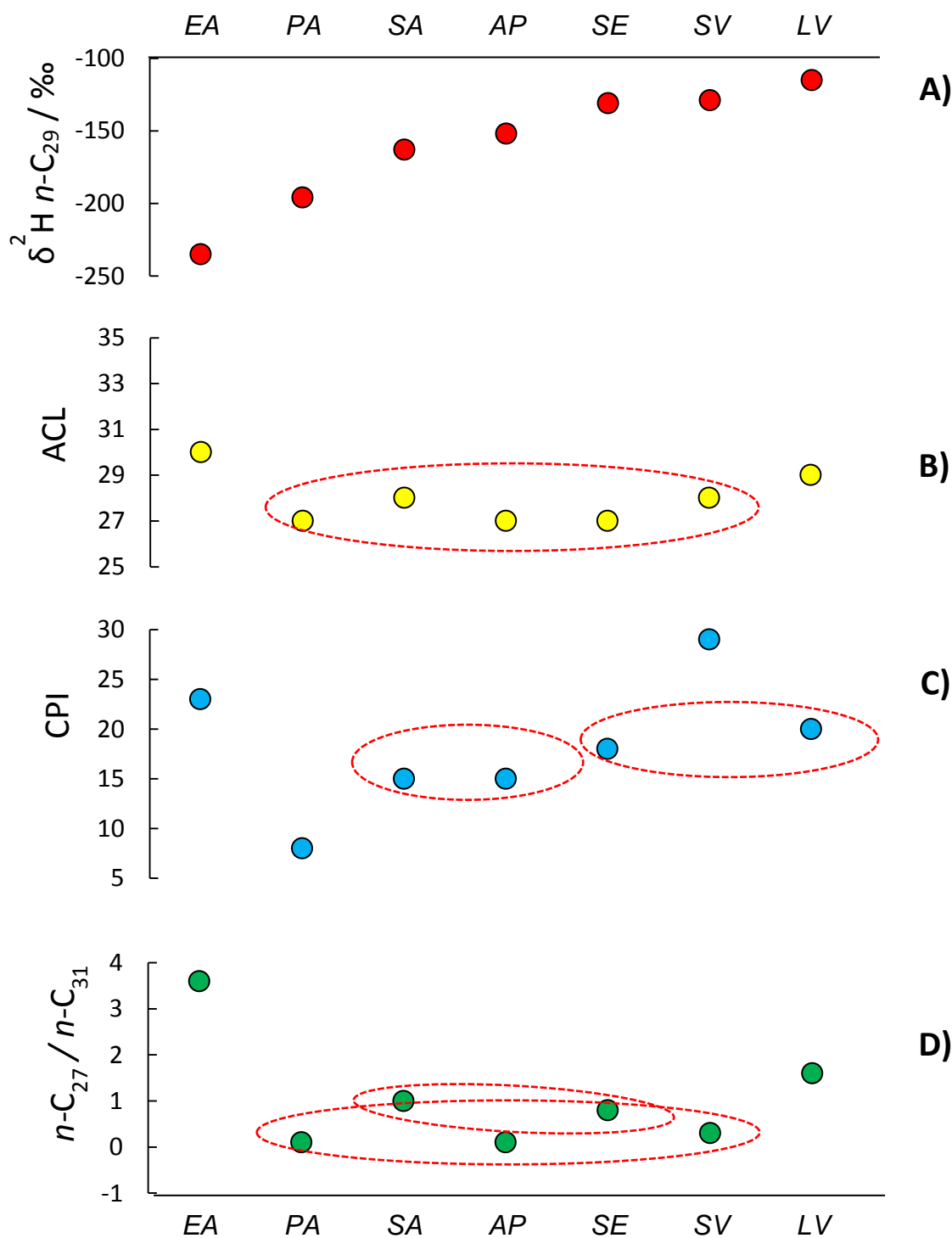


Fig. 8.13: Evaluating the suitability of using molecular distribution parameters and indices from the Stiffkey species to constrain the extent of vegetation change in sedimentary sequences. EA = *Elytrigia atherica*; SV = *Suaeda vera*; LV = *Limonium vulgare*; PA = *Phragmites australis*; AP = *Atriplex portulacoides*; SE = *Salicornia europaea*; SA = *Spartina anglica*. A – $n\text{-C}_{29} \text{ } ^2\text{H}/^1\text{H}$; B – ACL; C – CPI; D – $n\text{-C}_{27} / n\text{-C}_{31}$. In this instance, the similarity in ACL value between EA (C_3) and SA (C_4) could be resolved by looking at their carbon isotope composition, however the C_3 species PA, AP and SE are indistinguishable based on their ACL values. SA, AP, SE and SV have very similar CPI values, and only EA and LV are successfully distinguished based on the ratio of $n\text{-C}_{27}$ to $n\text{-C}_{31}$. Data presented are from August 2012.

reflects the overall conclusions drawn in Chapter 4, demonstrating that none of these indices can successfully discriminate between the sampled species. In particular, none of these indices show predictable variation among those species with very low $^2\text{H}/^1\text{H}$ values and those with very high $^2\text{H}/^1\text{H}$ values.

8.4.3 Alternative approaches to identifying and quantifying vegetation change

Other studies have used proxies such as pollen, in conjunction with leaf wax biomarkers, to identify and quantify vegetation change. Tierney *et al.* (2010), for example, used pollen analysis, in combination with *n*-alkane carbon isotope ratios, to assess the change in dominant plant communities occurring during the Late Quaternary in the environs of Lake Tanganyika. A similar approach was used by Feakins (2013) in a study of the fidelity of the leaf wax biomarker hydrogen isotope record from Miocene-age marine sediments from the Gulf of Aden. Feakins (2013) applied a four end-member mixing model (Eq. 2) to derive a variable fractionation factor that is adjusted for the various inputs from shrubs, C₃ grasses, C₄ grasses and trees, as derived from pollen and leaf wax $\delta^{13}\text{C}$ data. Feakins (2013) then used the averaged fractionation factors for each different plant physiological type (shrubs, grasses, trees) published by Sachse *et al.* (2012) to calculate weighted average $\epsilon_{\text{wax/water}}$ values for the sedimentary sequence.

$$\epsilon_{\text{corr}} = [f_{\text{Amaranth/acaeca}} * \epsilon_{\text{shrub}}] + [f_{\text{grass}} * C3\% * \epsilon_{\text{C3 grass}}] + [f_{\text{grass}} * C4\% * \epsilon_{\text{C4 grass}}] + [f_{\text{tree}} * \epsilon_{\text{tree}}] + \epsilon_{\text{alkane-acid}} \quad (\text{Eq. 2})$$

While the addition of pollen as an independent proxy for vegetation change has the potential to improve the accuracy of palaeohydrological reconstruction from leaf wax $^2\text{H}/^1\text{H}$ values, there are some caveats to this approach. Firstly, as the review of Sachse *et al.* (2012) makes clear, little is known about the catchment scales influencing the integration of leaf wax lipids into the sedimentary record (Fig. 8.1). This is significant, because differences in the catchment scales for pollen and leaf waxes could potentially confound the use of pollen to “correct” the biomarker record (Feakins, 2013). In addition, poor preservation of pollen from some taxa, and the lack of sufficient diagnostic morphology in others, means that not all pollen in a sediment sequence can be successfully identified (Feakins, 2013). Furthermore, there is a difference in the amount of pollen produced by different species (Brostrom

et al., 2004, 2008; Bunting *et al.*, 2005; Soepboer *et al.*, 2007), which results in some taxa being over or under represented in the pollen record (Gosling *et al.*, 2009; Feakins, 2013). It is also established that some plant species produce different overall amounts of wax (Diefendorf *et al.*, 2011) (Chapter 4). To date, no comparison has been made between the production of pollen among different plant species and the amount of wax they produce. If the Feakins (2013) approach is followed, this could, therefore, result in an erroneous determination of a suitable epsilon value. A species that is overexpressed in terms of pollen production but produces relatively small concentrations of leaf wax biomarkers, for example, could conceivably be given a higher weighting using this method than a species that produces far higher concentrations of alkanes (and therefore exerts a stronger influence on the sedimentary biomarker record) but is underexpressed in terms of pollen.

Other approaches to identifying vegetation assemblages also exist, such as analysis of charcoal fragments (Nelson *et al.*, 2013) or plant macrofossils (e.g. Ficken *et al.*, 1998). Alternative techniques include phytolith analysis (e.g. Piperno, 1985, 1991; Piperno *et al.*, 2000), however this method has not been combined with leaf wax biomarkers to date to evaluate their potential to assist in palaeoclimate reconstructions. A potentially exciting development is the analysis of plant DNA extracted from sedimentary sequences (e.g. Parducci *et al.*, 2013; Willerslev *et al.*, 2014). This latter technique appears to complement traditional pollen analysis, as the environmental DNA sequence can provide information about those species that are not well preserved in the pollen record (Parducci *et al.*, 2013; Willerslev *et al.*, 2014). In addition, the use of DNA in this way can allow for more precise taxonomic identification (Sønstebo *et al.*, 2010). Such an approach may be of particular value to studies of depositional environments such as peat bogs and lakes fed by small catchments, where organic matter is entrained and preserved swiftly. In contrast marine sediments (including saltmarshes) are unlikely to be suitable for these methods. This research is still in the early stages, however, and much remains to be understood regarding the extent to which ancient DNA records faithfully reflect surface vegetation assemblages (Parducci *et al.*, 2013). Despite these caveats, the overall implication of these advances is that new and more detailed approaches to correcting for vegetation change in the biomarker record will emerge in the coming years.

It is not simply methods for identifying vegetation change from plant assemblages local to the depositional environment that require further study, however. Additional

complexity comes from the requirement to separate local sediment and OM inputs from those being transported from other sources. At Stiffkey, such sources are likely to include wave-transported matter from the sediment sinks near Blakeney point (located to the east of the marsh, Section 2.4, Chapter 2), and potentially wind-blown dust eroded from the local agricultural fields which have limited cover during the year. Although this project does not seek to quantify local vs. non-local sediment/OM inputs, it is suggested that the addition of other linked analyses may offer a solution to this problem that could be explored in future research. Analysis of the trace element composition of sediments, for example, can provide a geochemical “fingerprint” which has been used successfully in previous studies to identify sediment sources in river catchments (Collins *et al.*, 1997; Haddachi *et al.*, 2014) and drainage basins (Nosrati *et al.*, 2014). A combined inorganic and organic geochemical framework for characterising and distinguishing local and non-local sediment may therefore offer enhanced sensitivity for future studies seeking to: (i) identify, quantify and correct for changes in local vegetation assemblages at a specific geographical location; and (ii) distinguish local and non-local sediment and OM inputs.

8.5 USING MIXING MODELS TO QUANTIFYING SOURCE INPUTS: A ROBUST APPROACH FOR THE FUTURE?

8.5.1 Source apportionment models

Statistical mixing models could provide an alternative approach to the issue of identifying and quantifying vegetation inputs to sediments. Several different mathematical models exist for characterising source apportionment. In stable isotope research, the proportional contribution of several sources to a mixture can be identified by using different isotope systems (Philips and Gregg, 2003). However, where complex mixtures exist, as at Stiffkey, traditional mixing models may not be appropriate as they are only able to fully resolve mixtures where $n+1$ sources exist and n isotope systems are available for analysis (Philips and Gregg, 2001). Clearly, at Stiffkey there are 7 different species that have been sampled throughout the course of this study, and only two isotope systems that can be measured (i.e. $\delta^{13}\text{C}$ and $\delta^2\text{H}$). Any model based on the “ $n+1$ ” criteria would not therefore be suitable for identifying detailed vegetative inputs to the saltmarsh sediments if all 7 plant species are used.

Philips and Gregg (2003) have developed a mathematical model “IsoSource” that was designed to address these problems. This model is based upon the principle of

mass balance conservation and performs multiple iterations based upon comparison of the isotopic composition of the mixed material and the isotopic composition of the potential sources. The model then describes all possible combinations of sources that might give rise to the isotopic composition of the material under examination (Philips and Gregg, 2003).

When developing this model, Philips and Gregg (2003) applied it to a scenario which is very similar to the one found at Stiffkey – two isotope systems, and seven potential sources – although the actual subject matter in their case was identifying dietary inputs. Model output from IsoSource reported similar conclusions about dietary inputs as identified in the original study from which the data had been taken. A slight limitation of this model, however, is that as each of the combinations of sources is restricted to 100%, there are “trade-offs” among the potential sources, especially those contributing relatively small amounts to the mixture (Philips and Gregg, 2003). The IsoSource model has also received some criticism due to the inherent lack of ability of the model to deal with uncertainty and variation, which are commonly encountered in biological systems (Parnell *et al.*, 2012). In practical terms this means that the model output is simply a series of probabilistic feasible solutions to the mixing problem, rather than a detailed quantification of the exact contribution of each source (Layman *et al.*, 2012). Model output may therefore require additional evaluation to assess ecological significance and plausibility (Jackson *et al.*, 2009; Laymen *et al.*, 2012; Fry, 2013).

Other isotope mixing models have been developed based on Bayesian principles. These include the “MixSIR” (Moore and Semmens, 2008) and “SIAR” (Parnell *et al.*, 2009). The MixSIR model, which was based on IsoSource but is designed to incorporate uncertainty and error, has also received some criticism, with a review by Jackson *et al.* (2009) suggesting that it failed to correctly identify source inputs in approximately 50% of the test scenarios analysed. Fundamentally, the performance of MixSIR declined when unquantified error was added to the scenarios (Jackson *et al.*, 2009). MixSIR has been further updated to correct these errors (Parnell *et al.*, 2013).

There are few options that allow for the inclusion of weighting based on concentrations in isotope mixing models. The SIAR model, for example, developed for use with the statistics package R, is based on IsoSource, and includes a component incorporating concentration dependencies of the chemical elements concerned (for example the carbon and nitrogen content of dietary inputs) (Parnell

et al., 2013). Another statistical programme incorporating concentration data is “IsoConc”, which is freely available from the Environmental Protection Agency website (www.epa.gov) as an excel spreadsheet. The IsoConc model was also originally derived to address the issue of the uptake of different concentrations of elements from dietary inputs. In standard isotope mixing models, the proportions of elements (e.g. C and N) are assumed to be equal for each source, which is often not the case for materials such as carbohydrates, lipids and proteins (Philips and Koch, 2002). Interestingly, the proportions of carbon and hydrogen are also not the same in *n*-alkanes (the *n*-C₂₉ alkane, for example, has 29 carbon and 60 hydrogen atoms) suggesting that such a model might also be appropriate for unmixing inputs from these types of organic compounds.

While these isotope mixing models are frequently used (and indeed in many cases have been formulated) for dietary analysis and trophic level characterisation in biological systems (e.g. Parnell *et al.*, 2013), geological and geochemical studies have also developed models to elucidate source inputs to sedimentary materials. Collins *et al.* (1997), for example, developed a statistical model to identify sources of sediments to rivers through analysis of their chemical fingerprint. In a similar way to IsoSource, this multivariate model is designed to satisfy the criteria that all calculated source contributions must be positive, and the sum of all feasible contributions must sum to unity (Eq.3):

$$\sum_{s=1}^n P_s = 1$$

(Eq.3)

Where P_s is the percentage contribution from each source (Collins *et al.*, 1997). Naturally, the Collins model has been revisited by other studies in recent years. Nosrati *et al.* (2014) combined analysis using the Collins multivariate discriminant analysis approach, with assessment of uncertainty using the Bayesian MixSIR model. Other studies have shown that one of the limitations of the Collins model is that it requires a mean value for each source input parameter, rather than, for example, data from individual source samples using the Monte Carlo procedure (Haddadchi *et al.*, 2014). That being said, the basic Collins model is still widely applied to source apportionment, and therefore represents a useful model to attempt to quantify the percentage inputs to the sedimentary *n*-alkane signal from the range of plant species sampled at Stiffkey.

To further evaluate whether source apportionment models and stable isotope mixing models have the potential to elucidate vegetation shifts in sedimentary leaf wax biomarker data, the Collins, IsoSource and IsoConc models were applied to data collected from the 1 m core from Stiffkey. These models were selected because they allowed for: (a) the inclusion of molecular distribution and stable isotope data (Collins *et al.*, 1997) (input criteria detailed in Appendix 7); (b) use of stable isotope data alone (IsoSource); or (c) the inclusion of different weighting to take into account variation in the concentration of C and H in the *n*-alkanes (IsoConc). For this modelling exercise, plant source inputs from 2011 were used as end members. Full details of the molecular and stable isotope data from the Stiffkey 1m core can be found in Appendix 7. As the core is from the upper marsh, however, the C₃ reed *Phragmites australis* was not included in the calculations as its range is limited to the ridge site.

As discussed above, a common limitation with all of these models is their lack of capacity for incorporating uncertainty. For plant data, uncertainty has been previously addressed in earlier chapters where appropriate (concentration, Chapter 4; carbon isotopes, Chapter 5; hydrogen isotopes, Chapter 6). Absolute differences between sediment sample isotope measurement replicates are discussed above in Section 8.1 (~7‰ for ²H/¹H measurements; ~2‰ for ¹³C/¹²C measurements). The molecular distribution values also have errors associated with them. For example, absolute differences in the percentage abundance of *n*-C₂₉ are on average ~10% (*n* = 58) between sample replicates for the whole sampling period (Appendix 3). Given the lack of standardised treatment of uncertainty in Collins, IsoSource and IsoConc, these values have not been applied to the following model outputs. However, conservative estimates of uncertainty on these models from the enclosed data suggest that errors of circa 20-30% would be appropriate. Future development of such source apportionment models for identifying vegetation change will need to incorporate these elements. Despite this, the following exercise is valuable to examine which criteria are most useful when seeking to source vegetation inputs.

8.5.2 Application of the Collins model to the Stiffkey core data

Input criteria for the Collins model is shown in Table 8.4, and included the carbon and hydrogen isotope composition of *n*-C₂₉ and *n*-C₃₁, ACL and the ratio of *n*-C₂₉ to *n*-C₂₇ as that was found to be the most useful for discriminating among plants during early tests of the model. Normalising the data to the maximum value for each of the

Table 8.4: Input criteria used with the Collins and IsoSource models

Plant samples		$\delta^{13}\text{C C}_{29}$	$\delta^2\text{H C}_{29}$	$\delta^{13}\text{C C}_{31}$	$\delta^2\text{H C}_{31}$	ACL	$\text{C}_{29}/\text{C}_{27}$
<i>Atriplex portulacoides</i>		-32.0	-166	-32.2	-149	26.9	0.93
<i>Elytrigia atherica</i>		-37.0	-230	-35.3	-232	29.4	3.29
<i>Limonium vulgare</i>		-32.9	-125	-32.3	-126	29.8	2.04
<i>Spartina anglica</i>		-25.6	-163	-32.1	-147	28.9	0.90
<i>Salicornia europaea</i>		-31.6	-127	-25.3	-123	27.1	4.38
<i>Suaeda vera</i>		-36.4	-141	-35.0	-125	27.7	0.65

Sediment samples	Date	$\delta^{13}\text{C C}_{29}$	$\delta^2\text{H C}_{29}$	$\delta^{13}\text{C C}_{31}$	$\delta^2\text{H C}_{31}$	ACL	$\text{C}_{29}/\text{C}_{27}$
5 cm depth	1988	-32.9	-132	-32.9	-143	30.1	2.52
10 cm depth	1964	-33.0	-150	-34.0	-143	29.8	1.98
15 cm depth	1941	-32.2	-168	-33.3	-162	29.7	1.98
30 cm depth	1869	-32.5	-167	-33.4	-178	29.8	1.64
40 cm depth	1822	-32.3	-111	-34.0	-159	29.6	1.54
60 cm depth	1726	-32.6	-159	-30.6	-166	29.7	1.67
80 cm depth	1631	-32.7	-164	-35.1	-182	29.4	1.65
94 cm depth	1564	-32.1	-133	-34.3	-145	28.9	1.19

input criteria did not influence the model output, so data was not normalised for all subsequent analysis presented here. The Collins model predicts that the plant composition contributing to the upper marsh sediments shifted considerably through the 1 m core, although *Limonium vulgare* is always an important contributor of leaf wax *n*-alkanes (Fig. 8.14). Key periods of change in the vegetation assemblage appear to occur: (i) between 1960s and the 1980s, with *Elytrigia atherica* and *Limonium vulgare* showing as the dominant vegetation in the late 1980s; (ii) between 1869 and 1941, a period where the sandflats of the lower marsh are thought to have been prograding (Allen, 2000; Andrews *et al.*, 2000), and 1671 and 1726, where *Salicornia europaea* is found in the modelled output (Fig. 8.14).

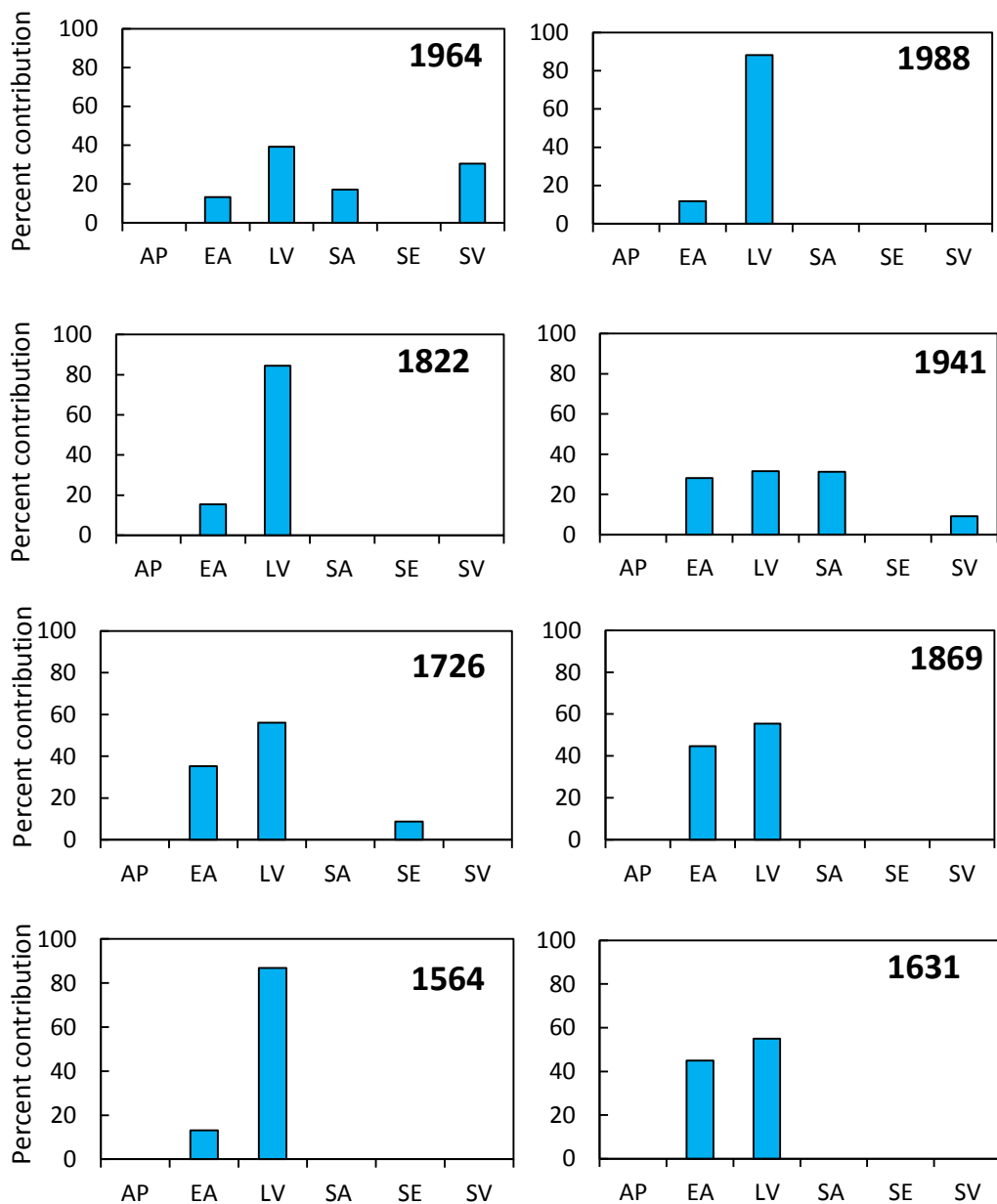


Figure 8.14: Percentage contribution estimates generated using the Collins et al. (1997) source apportionment model. For each time point, the figure shows the relative percentage inputs of each of the six species analysed in this part of the study. bbreviations: AP, *Atriplex portulacoides*; EA, *Elytrigia atherica*; LV, *Limonium vulgare*; SA, *Spartina anglica*; SE, *Salicornia europaea*; SV, *Suaeda vera*.

Looking at these results in detail, it seems that while the findings are *theoretically* possible based on the input criteria (Tables 8.4), they are in some cases *ecologically* unlikely. For example, it is somewhat improbable that *Elytrigia atherica* is found in such high proportions in the UM environment, as it is not acknowledged to be a dominant species in that part of the marsh (Boorman and Ashton, 1997). Interestingly, however, another C₃ monocot, *Puccinellia maritima*, is known to grow in abundance in this marsh sub-habitat, and although not sampled throughout the growing seasons, was collected and analysed in June 2011. The stable isotope and molecular distribution of *Puccinellia maritima* is very similar to *Elytrigia atherica* (Chapter 6) so it is possible that where the Collins model suggests *Elytrigia atherica* as a dominant species, it is in fact identifying *Puccinellia maritima*. The other concern with the output from the Collins model is that in some cases, it only identifies two species as contributing to the sediments (Fig. 8.14). From visual observations during sampling at the site, this is unlikely, as the UM in saltmarshes all along the Norfolk coast is a complex habitat where a number of species such as *Atriplex portulacoides*, and *Salicornia europaea* are also found (Jeffrey and Davy, 1981; Boorman and Ashton, 1997; Davy *et al*, 2011).

To further evaluate the performance of the Collins model, predicted output criteria (i.e. modelled isotope and molecular distribution values) were compared with original values from the sediment. While overall correlations (R^2) between measured and modelled input criteria calculated using the Collins *et al.*(1997) model are all in excess of 0.9 (Appendix 7), detailed comparison of the ACL and isotopic data show that the model performs better for some parameters than others. Modelled and measured ACL values, for example, are shown in Fig. 8.15. The model does not predict this value well, especially for the samples that predate 1800. The modelled carbon isotope compositions for n -C₂₉ and n -C₃₁ also have some discrepancies with the measured data, although this time the model performs better than for ACL. For n -C₂₉, the model consistently predicts lower $\delta^{13}\text{C}$ values relative to the measured material, with large anomalies for those samples from the 1870s and 1620s (Fig. 8.16). For n -C₃₁, the predicted values are typically 3‰ higher than measured values (Fig. 8.17). Interestingly the model performs best when predicting the hydrogen isotope composition of the sedimentary n -alkanes. For n -C₂₉ and n -C₃₁, the modelled $^2\text{H}/^1\text{H}$ values track the measured values more closely (Fig. 8.18 and 8.19), although as observed for carbon, predicted n -C₂₉ values are generally lower than measured values, while n -C₃₁ values are higher.

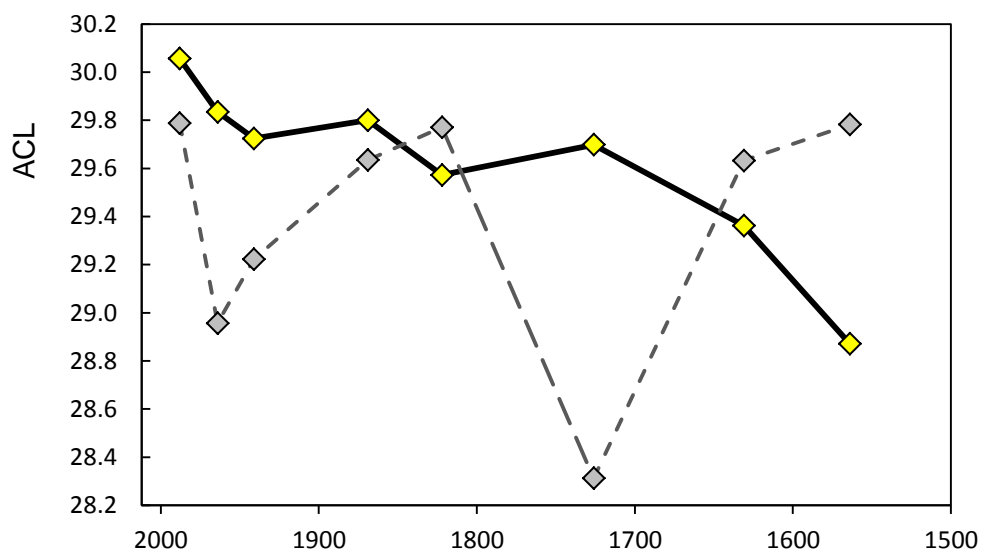


Fig. 8.15: Measured (yellow) and modelled (grey) ACL values for the Stiffkey core samples. Modelled values were computed using the Collins et al.(1997) source apportionment model.

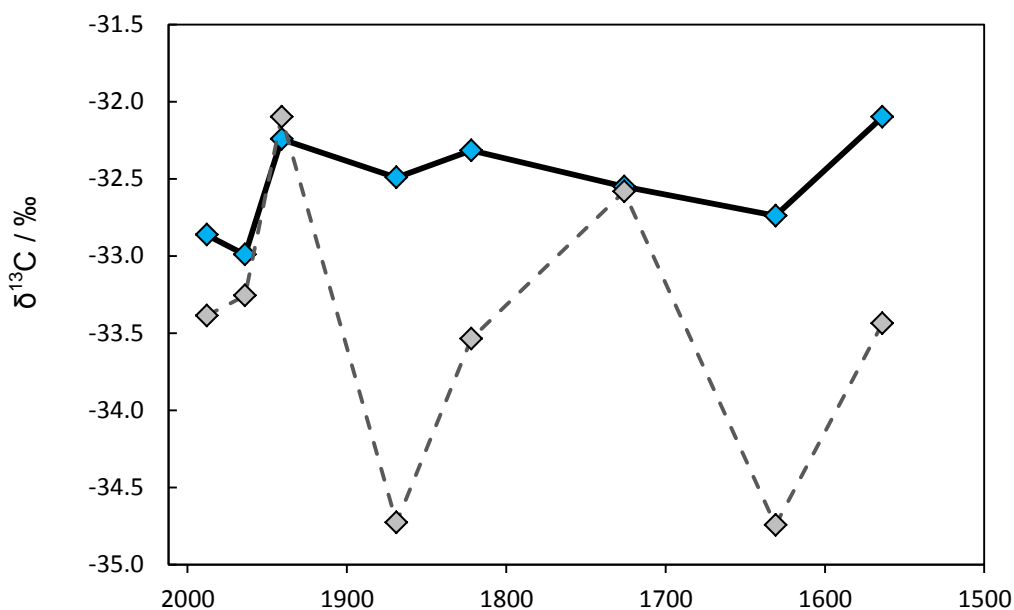


Fig. 8.16: Measured (blue) and modelled (grey) carbon isotope composition of the $n\text{-C}_{29}$ alkane from the Stiffkey core samples. Modelled values were computed using the Collins et al.(1997) source apportionment model. Note the highly varied offset between actual and modelled values, with modelled values depleted in ^{13}C relative to measured values.

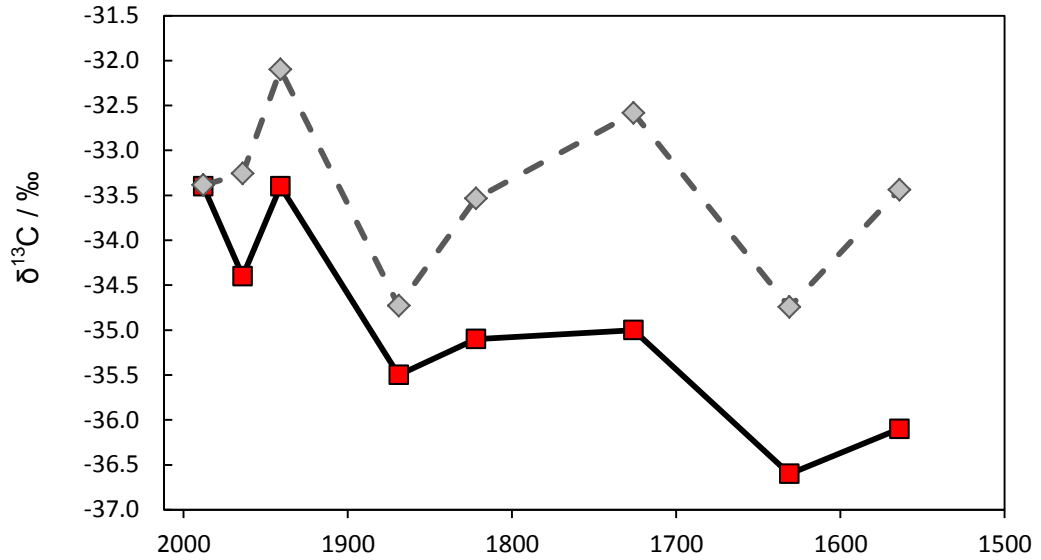


Fig. 8.17: Measured (red) and modelled (grey) carbon isotope composition of the $n\text{-C}_{31}$ alkane from the Stiffkey core samples. Modelled values were computed using the Collins et al.(1997) source apportionment model. Note the varied offset between actual and modelled values, with modelled values enriched in ^{13}C relative to measured values.

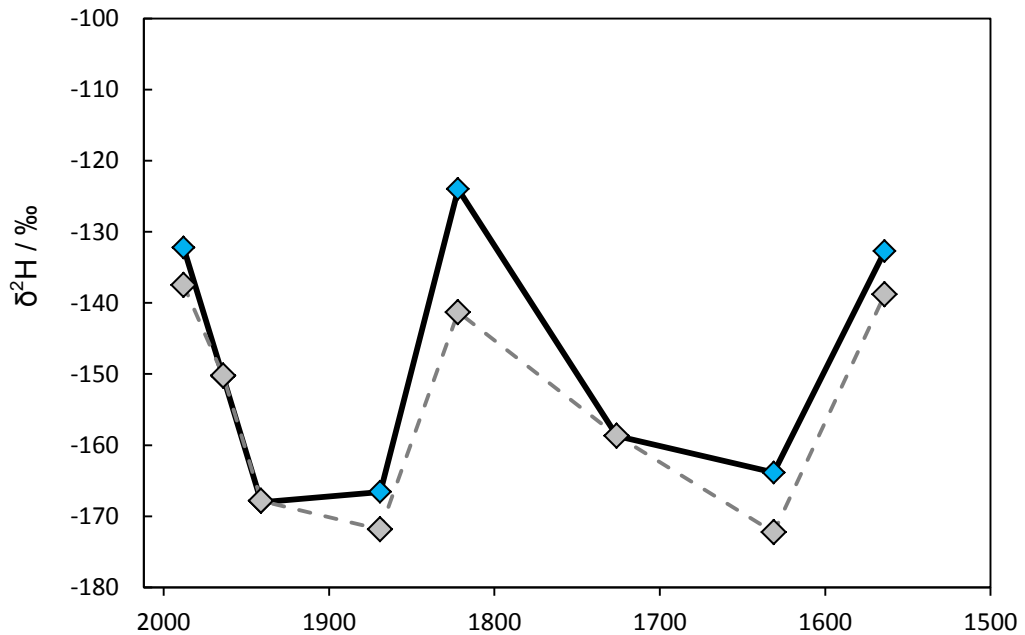


Fig. 8.18: Measured (blue) and modelled (grey) hydrogen isotope composition of the $n\text{-C}_{29}$ alkane from the Stiffkey core samples. Modelled values were computed using the Collins et al.(1997) source apportionment model. Note how the actual and modelled values track each other more closely than observed for molecular distribution or carbon isotope composition, although modelled values are depleted in ^2H relative to measured values.

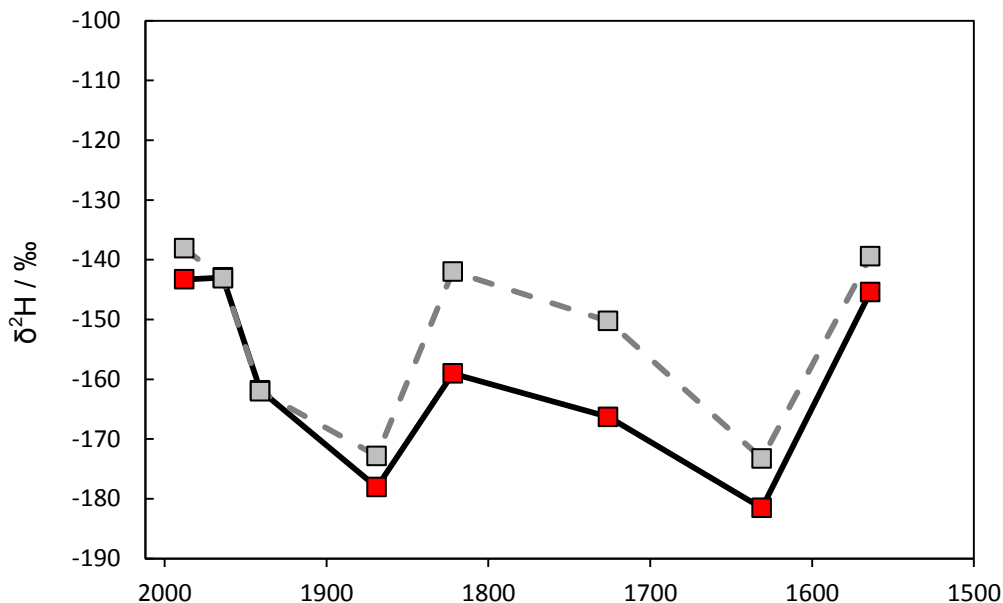


Fig. 8.19 Measured (red) and modelled (grey) hydrogen isotope composition of the $n\text{-C}_{31}$ alkane from the Stiffkey core samples. Modelled values were computed using the Collins source apportionment model. Note how the actual and modelled values track each other more closely than observed for molecular distribution or carbon isotope composition, although modelled values are enriched in ^2H relative to measured values.

These discrepancies are likely to be a result of several factors that influence the performance of the Collins model. Firstly, there are 6 potential source groups (Table 8.4), and only 6 variables provided for the model to un-mix the sediment data – the Collins model was typically designed to work with a wider range of input criteria (see for example the range of data inputs used in Collins *et al.*, 1997). Secondly, some of these variables have a degree of dependency, as they represent the carbon and hydrogen isotope compositions of the same n -alkane homologues. Nevertheless, this model is surprisingly robust in respect of the predicted values for sedimentary $\delta^2\text{H}$. This might be due to the fact that the $\delta^2\text{H}$ values are the most “extreme”, i.e. lowest, and therefore the model is seeking to fit these values first, prior to addressing the other input criteria.

8.5.3 Application of the IsoSource model to the Stiffkey core

Stable isotope data alone was used for the IsoSource model, as test runs using a mix of isotopic and molecular data resulted in the model being unable to un-mix the sediments. The isotope data for plants and sediments used can be found in Table 8.4. In fact, isotope data could only be used for either $n\text{-C}_{29}$ or $n\text{-C}_{31}$ (Table 8.4), as IsoSource could not resolve the mixtures when using $\delta^{13}\text{C}$ and $\delta^2\text{H}$ from both of these homologues at the same time. Data were analysed for those sub-samples

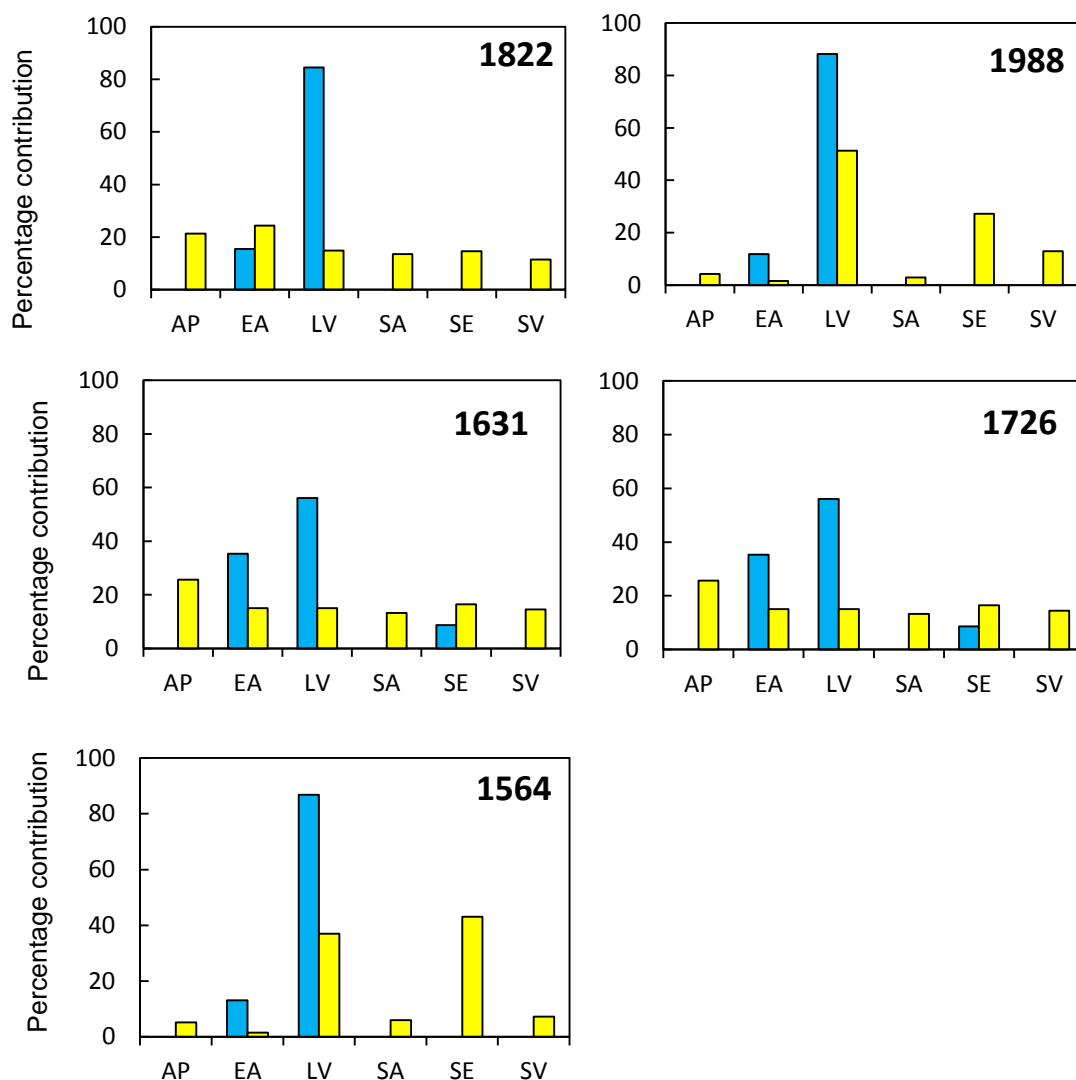


Figure 8.20: Comparison of the predicted vegetation inputs from IsoSource (yellow) with output from the Collins (1997) model (blue). Note that IsoSource generally predicts a mixture of all species, while the Collins et al. model typically suggests the signal is dominated by only two or three species. Abbreviations: AP, *Atriplex portulacoides*; EA, *Elytrigia atherica*; LV, *Limonium vulgare*; SA, *Spartina anglica*; SE, *Salicornia europaea*; SV, *Suaeda vera*.

where abrupt changes in vegetation was predicted by the Collins *et al.* (1997) model (i.e. sub-sections dating from 1988, 1822, 1726, 1631 and 1564; Fig. 8.20). Unlike the Collins model, where only two species were predicted to contribute alkanes to sediments for core sub-sections, IsoSource consistently predicts input from each of the 6 species used for modelling (Fig. 8.20). This is likely due to the Collins model attempting to “fit” the most extreme $^2\text{H}/^1\text{H}$ values before addressing other input criteria, while IsoSource seeks to average the input criteria to produce the result.

The dominant species identified also vary between the two models, with *Salicornia europaea* (1564, and 1988, Fig. 8.20) and *Atriplex portulacoides* (1726 and 1822,

Fig. 8.20) identified by IsoSource as important contributors to the core sub-samples. This is plausible from an ecological perspective, given that *Atriplex portulacoides* has been identified as an important plant species in the UM (Boorman and Ashton, 1997). The IsoSource output would therefore appear to be more in keeping with the natural environment at Stiffkey than the results obtained using Collins model discussed above. For example, the broad distribution of species identified as having contributed to the sediments (Fig. 8.20) appears closer to: (i) what was observed during sampling; and (ii) what has been previously recorded for Stiffkey marsh (Boorman and Ashton, 1997). Using the percent inputs calculated from IsoSource, weighted average hydrogen and carbon isotope compositions of $n\text{-C}_{29}$ were determined, to evaluate how closely modelled values tracked measured values. This time, the model performed well for both carbon and hydrogen, with the exception of the sub-sample dating to the early 1820's (Fig. 8.21 A and B).

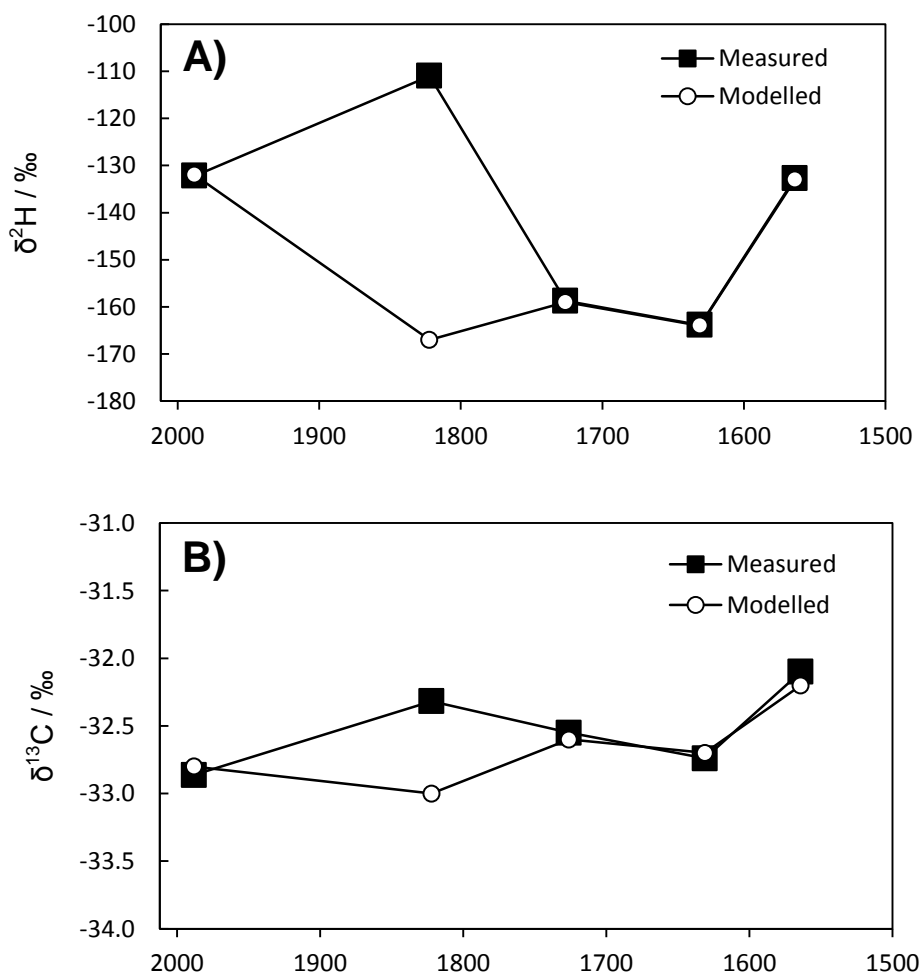


Figure 8.21: Modelled versus measured hydrogen isotope composition (A) and carbon isotope composition of $n\text{-C}_{29}$. (B). White circles show modelled values, black circles show measured values, Modelled values were calculated as weighted averages, using the percentage inputs generated by IsoSource.

8.5.4 Application of the IsoConc model to the Stiffkey core

Given the varied findings presented in Section 8.5.2 and 8.5.3 above, when models sought to identify inputs at the species level, a different approach was adopted when trialling the IsoConc model. This time, plant data from 2011 was grouped into three categories. These groups included C₃ monocots, C₄ monocots, and C₃ dictots/succulents (Table 8.5). The rationale behind these groupings rests on the biochemical distinctions theorised to be driving the broad variation in carbon and hydrogen isotope composition of leaf wax *n*-alkanes (discussed in detail in Chapters 5 and 7) between; (a) the dicots and succulents (producers of nitrogenous and carbohydrate osmoregulatory compounds) ; and (b) and the monocots (producers of primarily carbohydrate osmoregulatory compounds) (Briens and Lahrer, 1982). Naturally, the C₄ monocot *Spartina anglica* was assigned to a separate category, given that it has a carbon isotope composition that reflects its C₄ carbon fixation pathway (Chapter 5). Although *S. anglica* only became prevalent around the UK coastline in the 1870's, *S. alterniflora* was imported from the United States in the 1820's while *S. maritima* is native to the coastlines of Europe (Ainouche *et al.*, 2004). It is therefore assumed that a C₄ end member of the *Spartina* family was present at Stiffkey throughout the time interval covered by the core.

As it has been assumed in several studies that the sedimentary lipids record a seasonally averaged isotopic signal (e.g. Niedermeyer *et al.*, 2010; Leider *et al.*, 2013), the isotope values used for modelling represent averaged *n*-C₂₉ δ²H and δ¹³C data for all species from the 2011 growing season for the C₃ monocot, C₄ monocot and dicot/succulent groups (Table 8.5). Grouping data in this way is more valuable for future palaeoclimate applications, as it is unlikely that the precise plant species contributing to sedimentary OM will be known for complex depositional environments such as marine cores. Rather, it will be groupings of plant functional types that will be most useful for determining an accurate fractionation factor for interpreting sedimentary lipid ²H/¹H values. Based on the findings of Chapter 7, this study therefore makes the first assignment of plants into groups for source apportionment modelling using IsoConc based on biochemical, rather than physiological, factors.

In addition to grouping the data, the concentration values inputted into IsoConc had to be calculated for both hydrogen and carbon, as *n*-alkanes contain different amounts of these elements. To do this, the molar mass of the *n*-C₂₉ alkane was calculated (408.12 g mol⁻¹) and used to determine the molar mass of carbon (348.29

g mol⁻¹) and hydrogen (59.83 g mol⁻¹) that make up this molecule. From this calculation, it was then possible to calculate the different concentrations of carbon and hydrogen contributing to *n*-C₂₉ corresponding to the 3 functional plant groups (Table 8.6).

Table 8.5: Seasonally averaged carbon and hydrogen isotope values of *n*-C₂₉ (data from 2011) used for modelling source apportionment using IsoConc

Plant group	$\delta^{13}\text{C}$	$\delta^2\text{H}$
C ₃ monocots	-35.2 ± 2	-200 ± 14
C ₄ monocots	-25.4 ± 1	-145 ± 10
Dicots/succulents	-33.5 ± 2	-124 ± 12

Table 8.6: Calculation of the concentration of hydrogen and carbon in the *n*-C₂₉ contributed from each of the plant functional groups defined in this study

Biochemical functional group	Total concentration of <i>n</i> -C ₂₉ (μg g ⁻¹ DM)	Concentration of H (μg g ⁻¹ DM)	Concentration of C (μg g ⁻¹ DM)
C3 monocot	85	13	72
C4 monocot	71	10	61
Dicots/succulents	396	58	338

It is worth noting therefore that a fundamental assumption of this modelling work is that the entire *n*-alkane output of each plant group defined is ultimately incorporated into the marsh sediments. This is unlikely to be the case, but to date this approach represents a significant advance on existing methodologies, and therefore is a valuable starting point for future research investigating the incorporation of leaf wax biomarkers into sediments. This is an active area of current research (Sachse *et al.*, 2012) and further work is needed to fully understand the factors influencing the entrainment of leaf wax biomarkers into soils and sediments (see Fig. 8.1 for more details).

Combining the information pertaining to the carbon and hydrogen isotope composition of $n\text{-C}_{29}$ for each functional group (Table 8.5) with the total concentration of C and H (contained within $n\text{-C}_{29}$) available for incorporation into the sediments (Table 8.6) it was possible to compute the percentage inputs based upon these seasonally averaged data (Table 8.7; Fig. 8.22). The IsoConc model was able to resolve all sediment samples (Table 8.7), with results indicating that the C_3 monocot group was often responsible for up to >50% of the vegetation input. Core samples dating from the 1560's (highlighted in green, Fig. 8.22), the 1820's (highlighted in red, Fig. 8.22) and the 1980's (highlighted in pink, Fig. 8.22) were exceptions to this general trend - C_3 dicots and C_4 monocots in these sub-samples contributed more significant amounts of $n\text{-C}_{29}$ than C_3 monocots (Table 8.7). Interestingly, these three sub-samples are also those where the greatest shifts in sedimentary $n\text{-alkane}$ $^2\text{H}/^1\text{H}$ are also observed down-core (in Section 8.6), suggesting that some of that isotopic variation is indeed due to changes in surface plant assemblages and not climatic factors.

To test the output of the IsoConc model, predicted percentage contributions were once again used to determine weighted average $n\text{-C}_{29}$ carbon and hydrogen values for comparison with measured values. The seasonally averaged $n\text{-C}_{29}$ $^2\text{H}/^1\text{H}$ and $^{13}\text{C}/^{12}\text{C}$ for the species (Table 8.5) were used for this calculation. Modelled values for $n\text{-C}_{29}$ $\delta^2\text{H}$ (Fig. 8.23 B) match closely with measured values. However, although IsoConc models the carbon isotope composition of $n\text{-C}_{29}$ more successfully than the Collins or IsoSource models, there are still areas where predicted values depart significantly from measured ones. This is particularly true of the core sample that dates from the 1800s (Fig. 8.23 A), where predicted values are $\sim 3\text{‰}$ higher than measured values.

8.5.5 Summary: use of source apportionment models to track vegetation inputs

This exercise, using three different mixing models to evaluate source inputs to sediments, suggests that such approaches may be important to future studies using lipid biomarkers in soils and sediments. This approach would be supported by the fact that the three different models, using different input criteria, all identify vegetation shifts in specific sub-sections from the core (particularly the sample from the 1820's). Further development is naturally required to refine such techniques, however (in particular to build in uncertainty, as discussed in Section 8.5.1). It is suggested that future studies should focus on the definition and characterisation of

Table 8.7: Percentage inputs of each of the defined plant groups, defined by the IsoConc model (Philips and Koch, 2002)

Depth	Age	C ₃ Monocot	C ₄ Monocot	Dicot/succulent
5	1988	24	37	39
10	1964	52	29	19
15	1941	58	36	6
30	1869	59	33	7
40	1822	0	56	44
60	1726	54	34	9
80	1631	60	31	9
94	1564	16	53	31

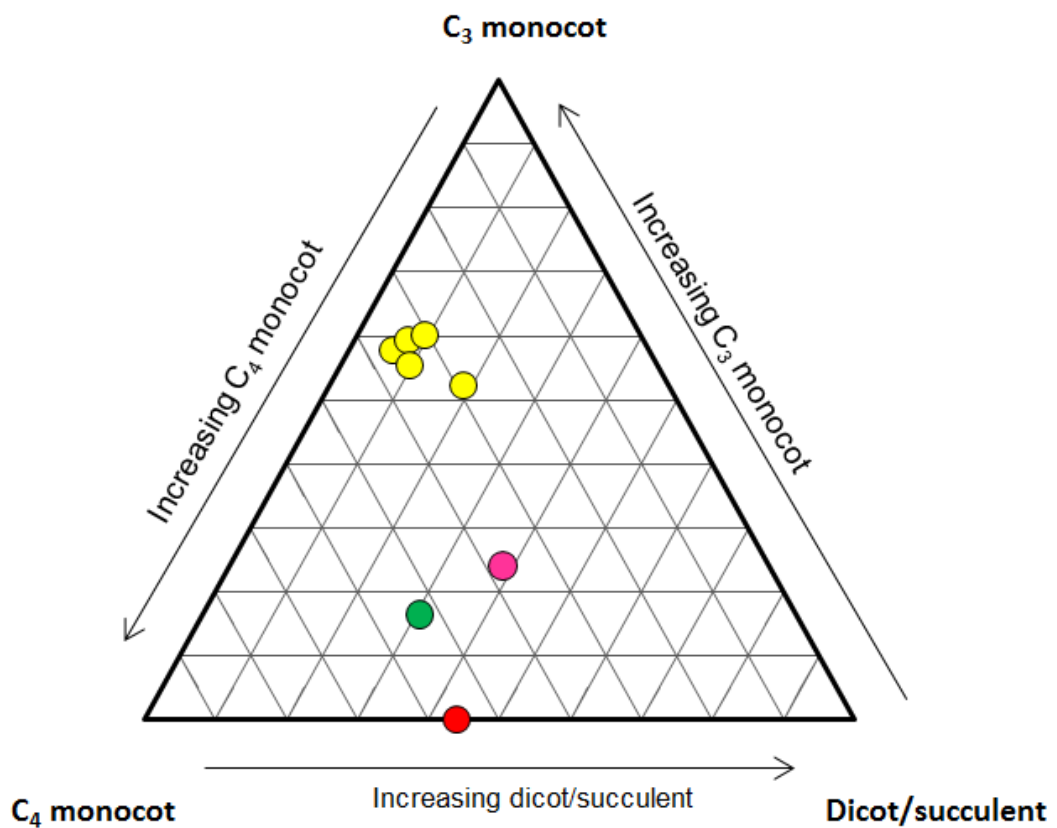


Figure 8.22: Ternary plot (produced using “Ternplot”, Marshall, 1996). Samples highlighted include those from the 1520s (green), the 1820s (red) and the 1980s (pink), for which the IsoConc model predicts different vegetation inputs than for the other core samples which cluster together (yellow).

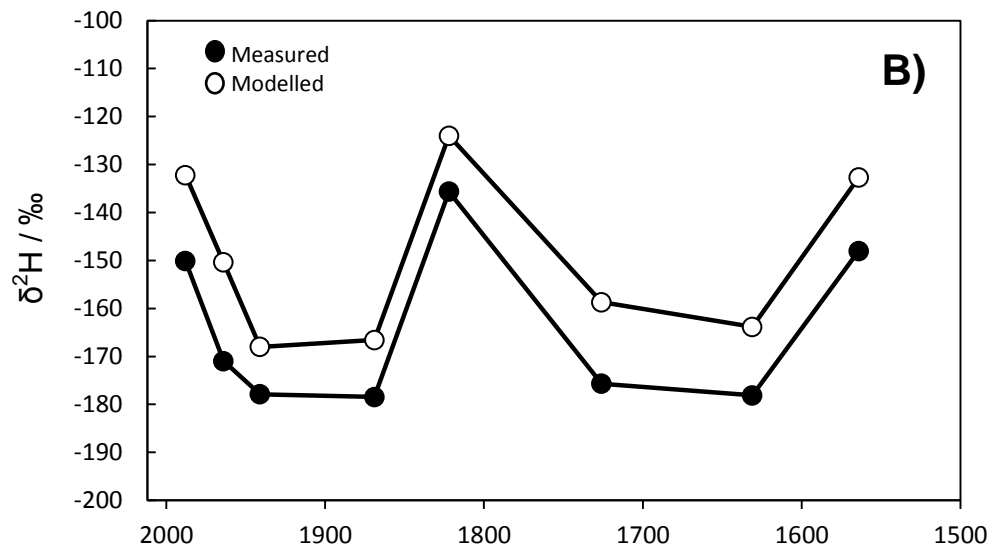
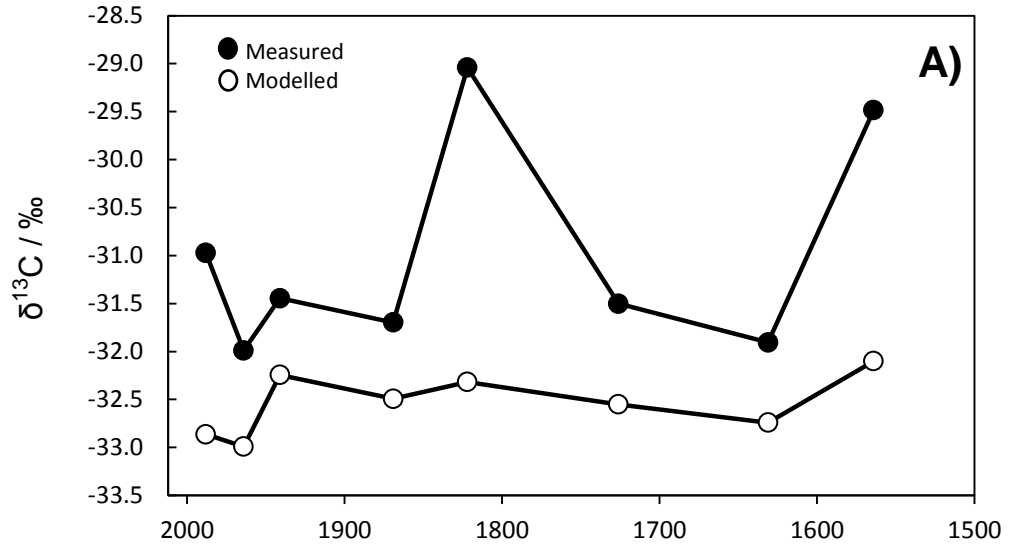


Figure 8.23: Modelled versus measured carbon isotope composition of $n\text{-C}_{29}$ (A) carbon isotope composition; and (B) hydrogen isotope composition. White circles show modelled values, black circles show measured values. Modelled values were calculated as weighted averages, using the percentage inputs generated by IsoConc and the seasonally averaged carbon and hydrogen isotope composition for each plant functional group (Table 8.7).

plant functional groups based on their biochemical adaptations to environmental conditions, as trialled here with the IsoConc model. The findings presented in Chapters 6 and 7, while in not yet conclusive, indicate that processes influencing cellular metabolism exert the greatest influence over *n*-alkane $^2\text{H}/^1\text{H}$. Therefore the development of plant functional groups based on biochemical factors (instead of the traditional characterisations based on physiological features, e.g. grasses, shrubs, trees) is likely to be of considerable importance for future palaeoclimate studies.

Another issue that also requires further study would be the fact that the Stiffkey core comes from a site that dates back only as far as the Holocene (Allen, 2000). During this period, changes in the isotopic composition of precipitation are unlikely to have reached the magnitude that has been reported for other geological epochs such as the PETM (e.g. Pagani *et al.*, 2006b). The current dataset does not allow for evaluation of how well the model would be able to disaggregate vegetation inputs in situations where the source water available for uptake was shifting as a result in changes in the isotopic composition of precipitation. Despite the importance of biochemical mechanisms in controlling leaf wax $^2\text{H}/^1\text{H}$, it remains the case that large shifts in $\delta^2\text{H}_{\text{PPT}}$ would ultimately be reflected in *n*-alkane data as fundamentally all H entering photosynthetic organisms comes from water in the first instance (Schmidt *et al.*, 2003; Wang *et al.*, 2013). Such changes could confound the setting of suitable isotope signatures of plant functional groups, which will be based on modern vegetation signals. The carbon isotope composition of atmospheric CO_2 has also changed through time, particularly as a result of human activity (e.g. Francey *et al.*, 1999; Cuntz, 2011). While it is possible to calculate $\Delta^{13}\text{C}$ values for modern plants, negating the influence of changes in source $\delta^{13}\text{C}$ values (Farquhar *et al.*, 1989), such data will not be available for a core sequence.

One approach to mitigate these issues for $^2\text{H}/^1\text{H}$ would be to collect data for plant functional groups from areas where $\delta^2\text{H}_{\text{PPT}}$ is known to vary significantly, to assess how epsilon values vary in response to changing environmental conditions. In terms of *n*-alkane $\delta^{13}\text{C}$, it may be possible to obtain estimates of the carbon isotope composition of CO_2 from other proxy records. These could then potentially be used to correct sedimentary *n*-alkane $^{13}\text{C}/^{12}\text{C}$ for the influence of source air $\delta^{13}\text{C}$ shifts. To conclude, the results of this study suggest that mixing models can identify areas where vegetation change contributes to shifts in $\delta^2\text{H}_{\text{SED}}$, but it is clear that more work is necessary to develop a method for identifying, quantifying and correcting for these changes in the geological record.

8.6 A CASE STUDY FROM THE STIFFKEY CORE

The findings presented in this chapter have considerable implications for the use of leaf wax *n*-alkanes in palaeohydrological studies. In order to investigate these issues in detail, *n*-alkane molecular distribution, carbon isotope composition and hydrogen isotope composition (Fig. 8.24) from eight sub-samples from the 1 m core was used as a case study to evaluate different approaches for reconstructing $\delta^2\text{H}_{\text{PPT}}$. The sediment record revealed a steady down-core decrease in ACL values, while the carbon isotope composition of *n*-C₂₉ and *n*-C₃₁ varied by only 1 - 3‰, respectively (Fig. 8.24). The hydrogen isotope composition of *n*-C₂₉, however, showed isotopic shifts of up to ~ 70‰, with rapid changes in ²H/¹H values from -159 to -111‰ between the 1720's and the 1820's (Fig. 8.24), and a negative shift back to -178‰ by the 1860's. *n*-C₂₉ $\delta^2\text{H}$ then rose to values of -132‰ by the late 1980's (Fig. 8.25). The hydrogen isotope composition of *n*-C₃₁ only recorded variations of up to ~ 40‰, with a positive shift observed between the early 1600's and the early 1800s, a negative shift of 20‰ between the 1820's and the 1860's, and a positive shift of 35‰ between the 1860's and the late 1980's (Fig. 8.25).

As this is a temperate site (rH does not fall below 70%, Chapter 4), the hydrogen isotope composition of the *n*-C₂₉ alkane should, following the assumptions relied upon in palaeohydrological studies, either record variation in the ²H/¹H values of precipitation (Pagani *et al.*, 2006b; Sachse *et al.*, 2012), or the differing inputs of saline and freshwater in saltmarshes (Romero and Feakins, 2011). As the overall intention of this Chapter was not to recreate the hydrogen isotope composition of palaeoprecipitation on the north Norfolk coast in detail – rather, the focus is on the fact that different methods of calculating palaeoprecipitation $\delta^2\text{H}$ can result in widely divergent reconstructed records – data are interpreted here as reflecting precipitation (i.e. following Pagani *et al.*, 2006), although it is accepted that the mixing of saline and freshwater in saltmarsh sites will be more complex in natural ecosystems.

In order to test different methods of calculating palaeoprecipitation $\delta^2\text{H}$ ($\delta^2\text{H}_{\text{PPT}}$), three different approaches were applied to these data. As the dominant inputs to the sediments at Stiffkey come from C₃ species, $\delta^2\text{H}_{\text{PPT}}$ was first calculated using the “fixed fractionation” approach used by Pagani *et al.* (2006), which assumes that $\epsilon_{\text{wax/water}}$ ranges from only -100 to -130‰ for C₃ terrestrial plants. Secondly, $\delta^2\text{H}_{\text{PPT}}$ was recreated using the IsoConc percentage inputs from C₃ monocots, C₄ monocots

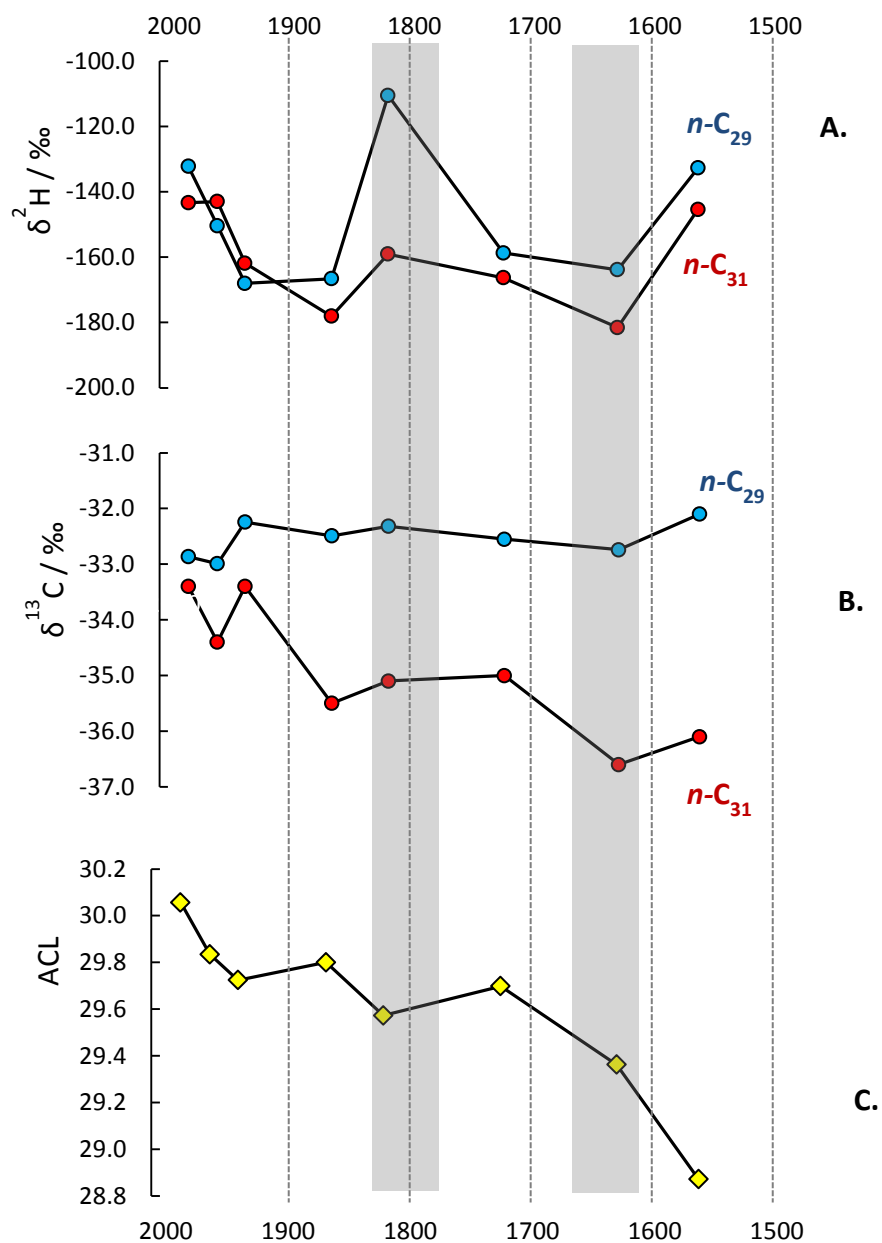


Figure 8.24: Record of the isotopic and molecular composition of *n*-alkanes from the 1 m core collected in the UM at Stiffkey. A = $\delta^2\text{H}/\text{‰}$ values, with $n\text{-C}_{29}$ shown in blue, and $n\text{-C}_{31}$ shown in red; B = $\delta^{13}\text{C}/\text{‰}$ values, with $n\text{-C}_{29}$ shown in blue and $n\text{-C}_{31}$ shown in red; and C = ACL values. Sediment ages are calculated with reference to the linear sedimentation rates published by Andrews et al. (2000). The grey shaded areas highlight the main shifts in the hydrogen isotope composition of the *n*-alkanes discussed in the main text.

and C₃ dicots/succulents, using typical fractionation factors derived for these functional types by Sachse *et al.* (2012), which are consistently more positive than those calculated for the Stiffkey species (reported in Chapter 6). Finally, $\delta^2\text{H}_{\text{PPT}}$ was recreated using the same IsoConc percentage inputs from C₃ monocots, C₄ monocots and C₃ dicots/succulents, but applying the seasonally-averaged fractionation factors calculated from the Stiffkey data for these groups (Appendix 7).

Figure 8.25 shows the results of these calculations. The fixed fractionation factor calculations from the *n*-C₂₉ alkane either produce values for $\delta^2\text{H}_{\text{PPT}}$ that range from -5 to -49‰ (using $\epsilon = -130\text{‰}$; Fig. 8.25 A), or -38 to -80‰ (using $\epsilon = -100\text{‰}$; Fig. 8.25 B). A sharp negative shift in recreated $\delta^2\text{H}_{\text{PPT}}$ occurred between the 1820's and the 1870's using this approach (Fig. 8.25 A and B). $\delta^2\text{H}_{\text{PPT}}$ calculated using the IsoConc percentage inputs for the biochemically defined groups and the typical fractionation factors of Sachse *et al.* (2012) also had shifts in $\delta^2\text{H}$ values of up to 25‰ occurring between the 1820's and the 1870's (Fig. 8.25 C), and ranged overall from -9 to -36‰. In contrast, $\delta^2\text{H}_{\text{PPT}}$ reconstructed using the IsoConc percentage inputs and the values for ϵ averaged for each plant group (Fig. 8.25 D) did not show such dramatic fluctuations, with the maximum shift of only ~20‰ taking place over more than 100 years. The range of $\delta^2\text{H}_{\text{PPT}}$ values calculated using these site-specific net fractionation values is from -17 to -41‰. In addition to these differences in the magnitude of fluctuation in $\delta^2\text{H}_{\text{PPT}}$ values, it is also interesting to note that there are very different temporal patterns in positive and negative shifts among these reconstructed values. The “fixed fractionation” and “typical fractionation” models both result in their most positive values in the early 1820s, with their lowest values occurring in the 1600's and late 1860's (Fig. 8.25 A, B and C). $\delta^2\text{H}_{\text{PPT}}$ from the Stiffkey net fractionation figures, however, does not record a positive shift in the 1820's, nor does it have the same temporal negative shifts as the other signals (Fig. 8.25 D).

As stated above, the overall aim of this Chapter is not to reconstruct $\delta^2\text{H}_{\text{PPT}}$ from the north Norfolk coast. It is however interesting to note that in all cases shown above, $\delta^2\text{H}_{\text{PPT}}$ is generally more positive than would be expected from north Norfolk, given the current OIPC estimates for modern rainfall (Chapter 6). In addition, the “fixed fractionation” and “typical fractionation” models (Fig. 8.26 a, b and c) both show a significant positive shift in rainfall $^2\text{H}/^1\text{H}$ in the early 1820's, at a time when the Northern Hemisphere was experiencing the Little Ice Age (Mann *et al.*, 2009) and the Maunder Minimum (Shindell *et al.*, 2001), which are both acknowledged to be periods of colder conditions, with temperatures potentially 1.5 °C lower than present

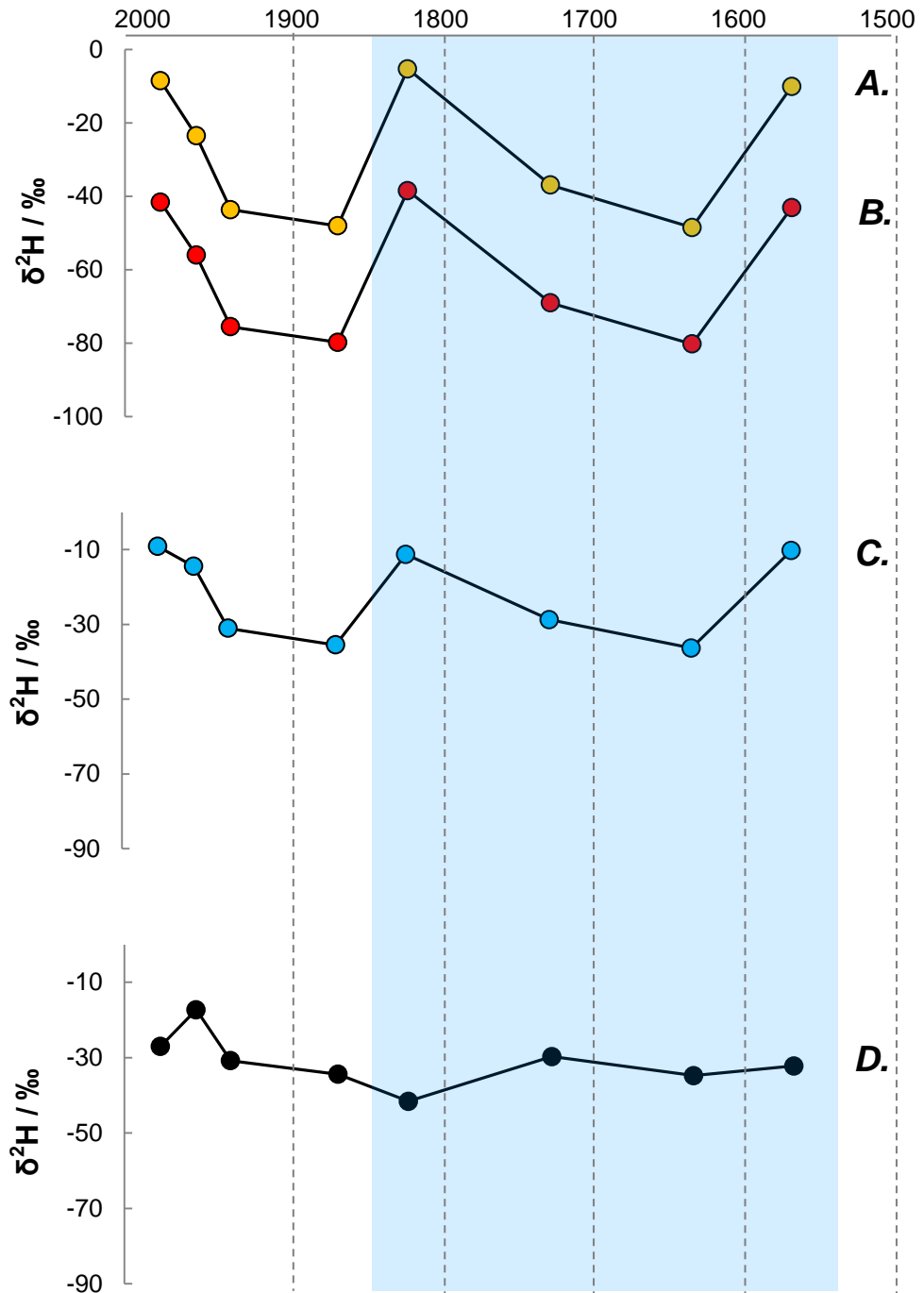


Figure 8.25: Reconstruction of the hydrogen isotope composition of palaeoprecipitation from a 1 m sediment core from Stiffkey saltmarsh. Three different methods have been used to determine $\delta^2\text{H}_{\text{PPT}}$: A) fixed values for net apparent fractionation of -100‰ (Pagani et al., 2006); B) fixed values for net apparent fractionation of -130‰ (Pagani et al., 2006); C) Weighted average value for net apparent fractionation calculated from IsoConc output and typical fractionation values for plant groups (Sachse et al., 2012); D) Weighted average value for net apparent fractionation calculated from IsoConc output and site-specific fractionation values calculated from the Stiffkey plant data. The blue shaded area shows the period during which the Little Ice Age and the Maunder Minimum occurred (Shindell et al., 2001; Mann et al., 2009).

(Shindell *et al.*, 2001). As these cooler conditions would result in lower $\delta^2\text{H}_{\text{PPT}}$ values (Dansgaard, 1964), it is unlikely that positive shifts in $\delta^2\text{H}_{\text{PPT}}$ can explain this trend. Because this sub-section from the core was identified by all mixing models as being influenced by vegetation change (Figs 8.14, 8.20 and 8.22), it is perhaps more plausible that the dramatic shift seen in the measured sedimentary $n\text{-C}_{29}$ hydrogen isotope data (Fig. 8.24), the “fixed fractionation”, and “typical fractionation” reconstructed records (Fig. 8.25 A, B and C), stems mainly from changes in the composition of plant communities, rather than significant climate shifts.

There are several hypotheses that could explain why all of the calculated $\delta^2\text{H}_{\text{PPT}}$ values are all more positive than would be expected from modern day precipitation which ranges from -70‰ to -43‰ (OIPC; Bowen and Revenaugh, 2003; Appendix 5). Firstly, it could simply be a factor of the degree of uncertainty associated with reconstructing the hydrogen isotope composition of palaeorainfall, currently estimated to be as high as ~30‰ (Polissar and d’Andrea, 2014). Equally, it could be that there are additional inputs of non-local organic material (OM) to the sediments at Stiffkey (*cf.* Section 8.4.3), which could either (a) incorporate lipids from plants that have not been sampled as part of this study, or (b) contain lipids that are far older than the date of the core. Modern sedimentary material, for example, is transported along the coast and deposited during tidal inundation could therefore contribute to the lipids present in the sediments. Sands and shingles are transported along the north Norfolk coast in a westward direction, and wave-modified ebb tidal deltas have been identified as significant sediment sinks in the region (Andrews *et al.*, 2000). As some of these deltas are eastwards of Stiffkey, it is possible that reworked sediment is eroded and transported to Stiffkey as a result of the tidal activity.

In addition, whilst no rivers discharge directly onto Stiffkey marsh, the site is bordered by agricultural land. It is possible therefore that aeolian transport of eroded soils from arable land with limited crop cover (especially the fine silt fraction), represents another source of OM arriving at the site. Again, this material would be likely to contain lipids from plant species that are not typically encountered at Stiffkey. Alkanes may also be generated *in situ* in the sediment from microbial activity (Zech *et al.*, 2011), or from root and rhizome contributions. Studies have shown that microbes can produce long-chain n -alkanes, while roots are also covered with n -alkyl lipids including long-chain alkanes (Marseille *et al.*, 1999). Different alkane distribution patterns have also been observed in the flowers and seeds of C_4 plants (Bull *et al.*, 2013) suggesting that such inputs from other plant

organs could also provide a source of compounds that were not sampled as part of this study. Future research therefore needs to address the relative importance of *n*-alkane contributions from a range of plant parts to ensure that source apportionment can be carried out successfully.

Support for the idea that there is a fraction of older OM contained in the sediments at Stiffkey is provided by the ^{137}Cs record from the site published by Andrews *et al.* (2000). Surface samples from an upper marsh core contained ~ 30 Bq/Kg ^{137}Cs (Andrews *et al.*, 2000). As ^{137}Cs is no longer deposited from the atmosphere, the presence of this radionuclide tracer is often used to evaluate erosion, reworking and redistribution of sedimentary material (He and Walling, 1996; Vandenbygaart, 2001). The presence of such concentrations therefore strongly suggests that older material is being regularly mixed with the sediments at the site. Most of this ^{137}Cs likely entered the system during the period from 1945 to the 1960s (Ritchie and McCarty, 2003), so it seems that there is a degree of reworking of sediments dating from this time interval along the coastline. Cesium is often bound strongly to the clay fraction of soils and sediments (Gerzabek *et al.*, 1992; He and Walling, 1996). Given that plant-derived *n*-alkanes bound to the clay size fraction of soils and sediments are known to be older than that found in associated sands (Cayet and Lichtfouse., 2001), it is logical that clays and silts contributing ^{137}Cs to the Stiffkey sediments could also contain older leaf wax *n*-alkane fractions.

In addition to this reworked material from the 20th century, it is also possible that more ancient organic material is also being deposited from the marine environment. This hypothesis could be tested by carrying out radiocarbon dating of the *n*-alkanes. Recent developments in ^{14}C methodologies now allowed for consideration of the age of OM at the molecular level, and a combined stable and radiogenic isotopic approach can allow for concurrent determination of both source and age of specific compounds attributable to identifiable sources in sedimentary materials (Eglinton *et al.*, 1998; Pearson *et al.*, 2000; Eglinton *et al.*, 2002). Analysis of molecular distribution, $\delta^{13}\text{C}$ and ^{14}C of marine photoautotrophic alkenes, vascular plant derived *n*-alkanes (*n*-C₂₉ and *n*-C₃₁) and shorter chain (*n*-C₂₃ – *n*-C₂₇) *n*-alkanes in off-shore sediments from the Black Sea allowed, for example, for the determination of the relative proportions and modern and fossil OM contributing to the sediment, which included the identification of a small but important contribution of fossil hydrocarbons to the shorter chain (*n*-C₂₃ – *n*-C₂₇) *n*-alkanes. A similar approach was also applied in Eglinton *et al.* (2002) to determine the provenance and age of dust inputs into northeast African coastal sediments. Unfortunately, such analyses are

Table 8.8: Data used for calculation of δ^2H_{PPT} for the Stiffkey surface sediments

Ridge (data averaged from 2012)		
Species	n -C ₂₉ contribution	$\epsilon_{C29/OIPC}$
PA	17	-153 ± 18
AP	11	-106 ± 18
SV	23	-76 ± 27
EA	48	-182 ± 24
WA net apparent fractionation value		-144 ± 22‰
Upper marsh (data averaged from 2012)		
Species	n -C ₂₉ contribution	$\epsilon_{C29/OIPC}$
SE	1	-86 ± 5
SA	27	-106 ± 21
SV	14	-76 ± 27
LV	52	-74 ± 5
AP	7	-106 ± 18
WA net apparent fractionation value		-85 ± 15‰
Sediment data (October 2011)		
Site	δ^2H_{SED}	Calculated δ^2H_{PPT}
Ridge	-178 ± 7	-40 ± 9
UM	-139 ± 1	-59 ± 1

Errors in this table show: a) standard deviation of seasonally averaged $\epsilon_{n-C29/OIPC}$ values for plant species; b) absolute difference between sample duplicates for δ^2H_{SED} ; and c) the calculated range of δ^2H_{PPT} using upper and lower ranges for δ^2H_{SED} .

outside of the scope of this thesis, but represent a valuable avenue for future studies to further constrain the importance of the contribution from ancient and/or reworked organic material to the leaf wax biomarker sediment record. Such studies could also make use of the combined inorganic and organic analytical approach discussed in Section 8.4.3.

To further explore whether surface sediments at Stiffkey contained an element of reworked material, their hydrogen isotope composition was used to calculate $\delta^2\text{H}_{\text{PPT}}$ values using the net fractionation factors derived for the Stiffkey plants growing at the upper marsh and ridge sites (Table 8.8). This time, the calculated $\delta^2\text{H}_{\text{PPT}}$ values ranged from -40 to -59‰, resulting in an average of $-50\text{‰} \pm 10\text{‰}$. These values are close to the annual mean MAP hydrogen isotope composition predicted from the OIPC model ($-57\text{‰} \pm 10\text{‰}$, Appendix 5) (Fig. 8.26).

The fact that the calculated $\delta^2\text{H}_{\text{PPT}}$ values from these surface sediments show a closer affinity with the OIPC $\delta^2\text{H}_{\text{PPT}}$ predictions than samples from the 1 m core suggests that the influence of modern plant biomass is stronger than that of any reworked material at the marsh surface. Analysis of the carbon content of the core (Appendix 7) suggests that the OM content reduces with depth, however. Therefore it is likely that the influence of reworked or ancient material may be stronger down-core, as the amount of contemporaneous plant biomass is reduced. A more detailed survey of surface sediments at the marsh, including sampling of the banks of the inlet ditches, and suspended sediment traps, would allow for a comprehensive investigation into the importance of any organic matter contribution from reworked marine sediments to the saltmarsh site. As discussed above, the addition of compound-specific ^{14}C dating would also be required to fully constrain this issue.

8.7 CONCLUSION

This study has considerable implications for palaeohydrological reconstruction based on the hydrogen isotope composition of leaf wax *n*-alkanes. Changes in sedimentary *n*-alkane $^2\text{H}/^1\text{H}$ values ranging from 16‰ (Schefuß *et al.*, 2005) to 40‰ (Tierney and deMonocal, 2013) have been interpreted as indicators of climatic shifts in the scientific literature, often in conjunction with the assumption that vegetation change has to be considerable in order to drive shifts in sedimentary lipid $\delta^2\text{H}$ signals. The modelled scenarios presented here, however, show that simple

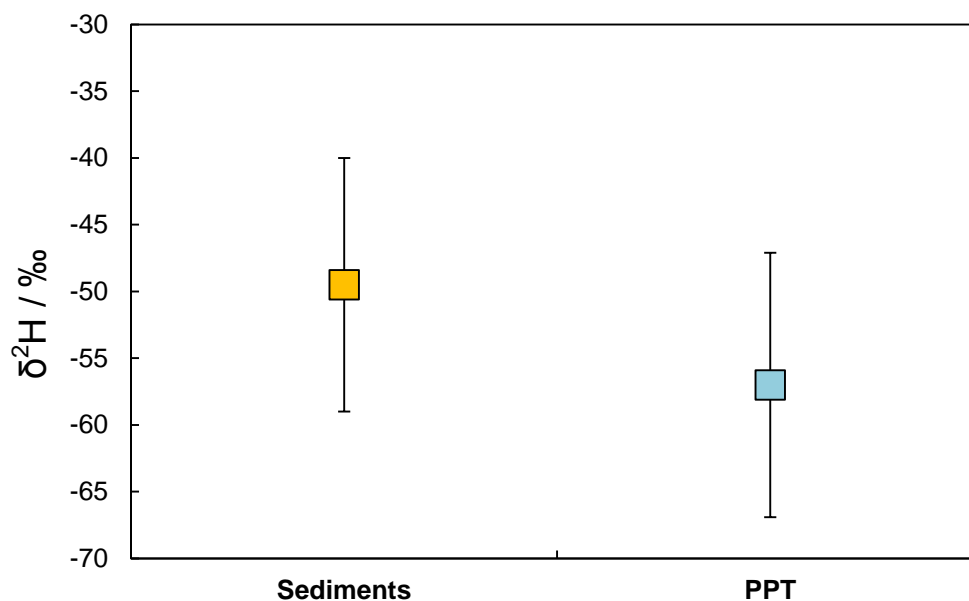


Figure 8.26: Calculated hydrogen isotope composition of precipitation from surface sediments (yellow), compared with the hydrogen isotope composition of precipitation (PPT) from the OIPC model (blue). Error bars show (a) absolute difference between measured UM and R δ^2H_{SED} , and (b) standard deviation of predicted OIPC monthly δ^2H values, respectively.

changes in vegetation assemblages can result in shifts of up to 35‰ in the $^2H/^1H$ value of the $n-C_{29}$ alkane available for incorporation into sediments. The magnitude of these vegetation-driven shifts is not surprising given: (i) the previously reported interspecies variation in leaf wax $^2H/^1H$ values of >100‰; and (ii) the substantial differences in the production of n -alkanes among the species growing at the Stiffkey site. These findings provide the first evidence that the sedimentary biomarker $^2H/^1H$ record is more sensitive to modest changes in surface vegetation than previously assumed. In order to separate climatic shifts from changes in plant communities, therefore, methods to detect (and ultimately correct for) vegetation change need further development. Despite driving significant shifts in the hydrogen isotope composition of lipids the modelled changes in plant communities at Stiffkey would only produce a maximum coeval shift of 1‰ in the carbon isotope composition of $n-C_{29}$. Such low variation in the geological record has been interpreted as being indicative of a stable plant community (e.g. Schefuß *et al.*, 2005) suggesting that in many cases subtle vegetation change will be difficult to detect using combined carbon isotope measurements. In addition, variation in molecular distribution parameters (e.g. ACL, CPI and the ratio of $n-C_{27}$ to $n-C_{31}$) down the 1 m core is limited, meaning that these parameters may also be inadequate for successfully

identifying this type of modest vegetation change. The work on plant-source mixing models, although in the early stages, represents a valuable contribution to the field, and opens new directions for future study. Such research needs to focus on identifying other, long-lived, plant compounds that may be more discriminatory among plant types, to allow for more sophisticated source apportionment modelling. While *n*-alkanes are ubiquitous in plant leaf wax (e.g. Kunst *et al.*, 2007), other compounds are not, and therefore may provide additional tools for source apportionment. Recent studies have suggested that compounds such as terpenoids, for example, can assist in constraining the relative proportion of angiosperms and conifers (Diefendorf *et al.*, 2014). The addition of other proxy data such as charcoal (Nelson *et al.*, 2013), pollen (Feakins, 2013) and plant macrofossils (Fickens *et al.*, 1998) may also be advantageous to future source apportionment modelling, although the relationship between other proxies such as pollen and *n*-alkane production needs to be evaluated to ascertain whether those species that produce the most pollen also produce the greatest amount of *n*-alkanes, and vice versa. The adoption of an integrated inorganic and organic geochemical framework, as proposed in Section 8.4.3, is also recommended.

Future research also needs to focus on detailed and systematic investigation of the net apparent fractionation ($\epsilon_{\text{wax/water}}$) between plants categorised by biochemical functional groups, to ensure that source water $^2\text{H}/^1\text{H}$ values can be recreated accurately. Reconstructed $\delta^2\text{H}_{\text{PPT}}$ from the Stiffkey core data illustrates that the selection of appropriate $\epsilon_{\text{wax/water}}$ values is critical for accurate palaeohydrological reconstructions. Particular caution is recommended as findings presented here indicate that the use of globally-averaged “typical” fractionation factors may not be appropriate for specific geographical locations.

Finally, as this study has demonstrated that the isotopic signal recorded in leaf wax biomarkers in temperate saltmarsh sediments is more sensitive to changes in surface vegetation than previously assumed, wider surveys are required to explore the effects of small-scale vegetation change to the molecular and isotopic signal of sedimentary lipids across a broad range of depositional and sedimentary environments. Such studies will be critical for the future development of leaf wax biomarkers as palaeoclimatic and palaeohydrological proxies, to ensure successful disaggregation of vegetation shifts and climatic signals when interpreting *n*-alkane data from the geological record.

8.8 SUMMARY

- Small to moderate change in surface vegetation assemblages has the potential to drive shifts in sedimentary *n*-alkane $^2\text{H}/^1\text{H}$ of up to 40‰.
- Molecular distribution ratios do not have the chemotaxonomic potential to distinguish between inputs from the Stiffkey species.
- $\delta^{13}\text{C}$ among C_3 Stiffkey species is insufficient to identify changes in surface vegetation that can cause shifts in $^2\text{H}/^1\text{H}$ of 40‰.
- Source apportionment models have the potential to identify and quantify source inputs from plant functional groups.
- Using fixed net apparent fractionation values for recreating palaeoprecipitation $^2\text{H}/^1\text{H}$ from Stiffkey sediments results in shifts of up to 70‰, which are not plausible given other records of climate shifts from the same period.
- Future research is needed to develop new methods to identify, quantify and correct for vegetation change in sedimentary sequences to ensure that the influence of plant community change can be decoupled from climate shifts when interpreting biomarker records.
- The combination of other analytical methods, such as trace element analysis, has the potential to assist identifying sources of sedimentary material in depositional environments. This could assist evaluating the relative importance of local and non-local sources of sediment and associated organic matter.

Chapter 9

Summary and conclusion

The overarching aim of this thesis was to evaluate the relative importance of environmental and biochemical mechanisms in controlling the molecular distribution and stable isotopic composition of leaf wax *n*-alkanes. A detailed understanding of the influence of these mechanisms is crucial to ensure accurate interpretation of *n*-alkanes from the sedimentary record, and provide palaeoecological and palaeohydrological reconstructions which can feed into models of past and future climate. Research focused particularly on the hydrogen isotope composition of *n*-alkanes, given the exponential advance in the use of these biomarkers in palaeohydrological reconstructions (e.g. Pagani *et al.*, 2006; Tierney *et al.*, 2008, 2010, 2011; Sachse *et al.*, 2012 and references therein).

This thesis makes several novel contributions to knowledge by carrying out a detailed investigation of leaf wax *n*-alkanes from seven species common to saltmarsh habitats. This chapter summarises the key findings of this project, with reference to the research objectives identified in the Introduction. The implications of these findings for the use of leaf wax *n*-alkanes in palaeoclimate reconstruction are also discussed relative to these objectives. Limitations in this study and new directions for future research are highlighted throughout where appropriate.

9.1. MOLECULAR DISTRIBUTION AND CONCENTRATION

Research objective: *Evaluate the extent of variability in leaf wax *n*-alkane concentration and composition among seven saltmarsh plants, both spatially across the marsh sub-environments, and temporally across a growing season.*

Significant interspecies variation was observed in the molecular distribution patterns of *n*-alkanes from the seven plants sampled at Stiffkey. These distribution patterns did not vary systematically among different PFTs (e.g. grasses, herbs, and woody shrubs). ACL among the different species showed a limited range across all sampling intervals (24 to 31; Chapter 4), with diverse PFTs having near identical ACL profiles. Individual plants from the same species growing at multiple locations

within the marsh also showed a degree of variability in the molecular distribution pattern of their *n*-alkanes. With the exception of C_{max} , however, which was consistently lower in the UM for all species, the nature of this variability was species-specific, suggesting it was not controlled by differences in saltmarsh micro-environmental conditions.

n-Alkane molecular distribution ratios, such as ACL, continue to be used to reconstruct palaeovegetation assemblages, from which environmental conditions can be qualitatively extrapolated. These applications persist despite the identification of non-systematic variation in distribution patterns among plant species and functional types (Bush *et al.*, 2012; Bush and McInerney, 2013). Results from Stiffkey (Chapter 4) show that ACL values are an unsuitable proxy for distinguishing different plant contributions to the marsh sediments, given their relatively small range. In contrast, calculated molecular distribution ratios, such as the proportion of *n*-C₃₁ to *n*-C₂₇ (e.g. Zech *et al.*, 2010), showed such variability among PFTs that they were not able to successfully distinguish between woody and non-woody species. Results from this study therefore illustrate that reliance on molecular distribution patterns to distinguish vegetation types from coastal and near-shore sedimentary lipids is not recommended. As Chapter 2 highlights, saltmarsh are the most productive biomes on Earth (Little, 2000) so these findings are valuable for studies seeking to interpret leaf wax biomarker records from coastal sites at the forefront of sea level change.

The concentration of *n*-alkanes also varied widely across the sampled species (Chapter 4). *Limonium vulgare* generally produced >200 $\mu\text{g g}^{-1}$ DM of *n*-C₂₉, which was typically at least twice the amount of any other species present at the site. Previous studies have highlighted differences in *n*-alkane concentration between angiosperms and gymnosperms (Diefendorf *et al.*, 2011), however the nature of such differences among angiosperms growing in the same geographical location, remains poorly constrained. This further complicates the evaluation of preservation bias in lipids extracted from sediments, as those species producing greater concentrations of *n*-alkanes are likely to be over-represented in the geological record. The findings of this study illustrate the importance of constraining angiosperm alkane production further, as they imply that significant preservation bias is also likely among such plants. An added complication is provided by the fact that *n*-alkane concentrations produced by the Stiffkey species were not static, and showed temporal variation throughout a growing season. It is therefore

recommended that future studies attempting to quantify *n*-alkane inputs to sediments based on modern taxa; (i) collect more empirical data to evaluate the range in *n*-alkane concentration among other groups of angiosperms in a single geographical location; and (ii) ensure to sample species across a growing season to consider the extent of this temporal variability in other biomes.

Spatial variation in concentration among those plants growing at different locations within the marsh did not appear to be dependent upon environmental conditions, local weather or the extent of site exposure. Instead, this variation is interpreted in light of previous studies identifying genetic variation among populations of species such as *Suaeda vera* and *Salicornia europaea* at Stiffkey (Davy *et al.*, 1985; Noble, 1990). Admittedly, the strength of this conclusion is somewhat limited by the fact that genetic analysis of other species sampled across the marsh sub-habitats was not carried out as part of this study. The fact that *n*-alkane concentrations (and indeed molecular distribution patterns, discussed above) show no systematic variation among all species across the sampling sites, however, point to genetic variation at the genus level being an important driver of interspecies variation in *n*-alkane production. This presents a significant problem for reconstructing palaeovegetation sequences based on *n*-alkane data, as the genetic composition of a plant species can vary through time (e.g. Ainouche *et al.*, 2004). Therefore, even if modern plant species are collected in the vicinity of a sediment core to provide information about the leaf waxes of modern vegetation growing at a site, there is no guarantee that these species have not evolved genetically during the geological past, with accompanying shifts in their leaf wax molecular distribution and concentration. Further research is required to evaluate the importance of genetic diversity on leaf wax *n*-alkane composition, to ensure accurate interpretation of sedimentary lipid biomarkers.

9.2 THE RELATIVE INFLUENCE OF ENVIRONMENTAL AND BIOCHEMICAL MECHANISMS ON *n*-ALKANE $\delta^{13}\text{C}$

Research objective: *Quantify the extent of variability in bulk and leaf wax *n*-alkane $\delta^{13}\text{C}$ signatures across a range of C_3 and C_4 species growing at a temperate coastal saltmarsh, and to identify whether they are being influenced by the same biochemical and environmental factors.*

Variation in *n*- C_{29} $\delta^{13}\text{C}$ among the C_3 species at Stiffkey ranged from 5 to 9‰ across the 2011 and 2012 growing seasons (Chapter 5). In contrast, interspecies variation

in bulk carbon isotope composition did not typically exceed 4‰ throughout the same period (Chapter 5). Bulk and *n*-alkane $\delta^{13}\text{C}$ from the same species growing in multiple sub-environments also exhibited some variability, but this was only in the order of 1 to 2‰ among individuals. Critically from the perspective of using bulk and *n*-alkane carbon isotope values interchangeably to investigate plant-environment interactions, temporal trends in bulk and *n*-alkane $\delta^{13}\text{C}$ did not co-vary for all species across the growing seasons. In general terms, the C_3 grasses and reeds had similar temporal shifts in $\delta^{13}\text{C}$ at the bulk and molecular level, while dicots and shrubs in some cases exhibited an inverse relationship between ^{13}C -enrichment and depletion. This variation in $\delta^{13}\text{C}$ trends resulted in considerable intra- and inter-species variability (ranging from -4 to -13‰) in the offset between bulk and WA *n*-alkane $\delta^{13}\text{C}$ values.

These findings go to the heart of the research objective identified in Chapter 1, and suggest that there is a degree of decoupling between the mechanisms controlling $\delta^{13}\text{C}$ at the bulk and molecular level. Comparison of the molecular distribution data (Chapter 4) with carbon isotope composition suggested that for some species, seasonal changes in the abundance of *n*-alkane homologues might be an important biochemical processes influencing *n*-alkane $\delta^{13}\text{C}$ signatures. In addition, the existence of relationships between *n*-alkane $\delta^{13}\text{C}$ and: (i) C content; (ii) N content; and (iii) foliar $\delta^{15}\text{N}$ values suggest biochemical adaptations to salinity stress may influence *n*-alkane $\delta^{13}\text{C}$. In plants adapted to salt stress, production of osmoregulatory solutes (nitrogenous compounds and/or carbohydrates) may influence the partitioning of pyruvate to fates other than acetyl-CoA, shifting the isotopic composition of lipid biomarkers (Diefendorf *et al.*, 2011). Mechanisms controlling metabolic fluxes through these biochemical processes, (e.g. the glutamate pathway which produces proline, Szabados and Savouré, 2010), may therefore exert an additional important control over the $\delta^{13}\text{C}$ signal of lipid biomarkers. As analysis of carbohydrates and amino acids were outside of the scope of this thesis, this hypothesis requires further research to fully evaluate the extent that the production of such compounds in plants subjected to environmental stress influences: (i) post-photosynthetic carbon isotope fractionation (e.g. Tcherkez *et al.*, 2011; Cernusak *et al.*, 2013); and (ii) the $\delta^{13}\text{C}$ of carbon incorporated into secondary compounds. If confirmed, however, the implications are that *n*-alkane $\delta^{13}\text{C}$ signals may contain a significant amount of information regarding stress adaptations in modern and ancient plants.

Data presented here have important implications for studies seeking to link shifts in *n*-alkane $\delta^{13}\text{C}$ (and by implication $\Delta^{13}\text{C}$) to changes in environmental conditions and physical parameters (e.g. Diefendorf *et al.*, 2010). The range in offset between bulk and *n*-alkane $\delta^{13}\text{C}$ observed among the Stiffkey C_3 species, for example, results in different patterns of carbon isotope discrimination depending upon whether bulk or compound-specific data is used for calculating $\Delta^{13}\text{C}$. Diefendorf *et al.* (2010) based the findings of their study investigating global trends in carbon isotope discrimination on the premise that $\Delta^{13}\text{C}$ in C_3 species is moderated by stomatal control of gas exchange at the leaf level, which in turn is responsive to changes in water availability. This is well established for bulk plant material, where $\Delta^{13}\text{C}$ trends are often used to draw qualitative conclusions about interspecies differences in WUE among C_3 species growing at the same geographical location (see for example Donovan and Ehleringer, 1994; Cernusak *et al.*, 2013). However the Stiffkey data show that the $\Delta^{13}\text{C}$ value of a given species is dependent upon whether bulk leaf tissue, *n*- C_{27} , *n*- C_{29} or weighted alkane $\delta^{13}\text{C}$ is used for calculating $\Delta^{13}\text{C}$. This strongly suggests that comparing bulk and *n*-alkane-derived $\Delta^{13}\text{C}$ values, (and even in some instances comparing $\Delta^{13}\text{C}$ values calculated from different alkane chain lengths), may produce conflicting results. The implicit assumption made by Diefendorf *et al.* (2010) that the influence of moisture availability on stomatally moderated gas exchange is also the dominant mechanism recorded in leaf wax biomarkers may also be invalid, as results from this study suggest that it is the metabolically-driven post photosynthetic fractionation of carbon (e.g. Tcherkez *et al.*, 2011) that is potentially the most important control on leaf wax biomarker $\delta^{13}\text{C}$ signals.

These findings open new avenues for empirical studies to further understand the metabolic processes fractionating carbon during the production of secondary compounds. In order to fully account for interspecies variation in *n*-alkane $\delta^{13}\text{C}$, such studies should consider fractionation steps occurring throughout the fixation of C and incorporation of it into leaf wax biomarkers. Such research should include, for example, gas exchange measurements, analysis of important precursors for *n*-alkane biosynthesis (e.g. FAs) and the production of other compounds (e.g. amino acids, proline) within a plant cell in response to changing environmental conditions. This kind of linked analytical approach will aid future interpretation of leaf wax *n*-alkane $\delta^{13}\text{C}$ in both modern plant ecology and palaeoecological reconstruction, by establishing the key environmental and biochemical parameters that influence carbon isotope fractionation at the molecular level.

9.3 THE RELATIVE INFLUENCE OF ENVIRONMENTAL AND BIOCHEMICAL MECHANISMS ON *n*-ALKANE $^2\text{H}/^1\text{H}$

Research objective: Investigate whether differences in the $^2\text{H}/^1\text{H}$ of leaf water (driven by mechanisms that control the movement of water molecules inside, outside and within the leaf) can account for interspecies variation in *n*-alkane $^2\text{H}/^1\text{H}$ among seven saltmarsh plants.

This thesis presents a systematic study of the relationship between the hydrogen isotope composition of soil, xylem and leaf water, and the $^2\text{H}/^1\text{H}$ of the *n*-C₂₉ alkane from a range of C₃ and C₄ saltmarsh plants growing at Stiffkey marsh (Chapter 6). Data exhibited significant interspecies variation in fractionation between leaf water and leaf wax, ranging from -79 to -229‰ across the 2012 growing season. The > 100‰ range in reported $\delta^2\text{H}_{n\text{-C}_{29}}$ data (Chapter 6), and the 150‰ range in $\epsilon_{\text{wax/lw}}$ values, extend beyond the typical values for C₃ and C₄ plants put forward in previous studies (e.g. Bi *et al.*, 2005). From these results, it is possible to conclude that reconstruction of palaeohydrological regimes based on estimates such as these may not capture the full complexity of the hydrogen isotope information recorded by these plant groups.

The magnitude of interspecies differences in *n*-alkane $\delta^2\text{H}$ could not be explained by reference to spatial or temporal shifts in the hydrogen isotope composition of soil, xylem or leaf water. A key conclusion of this study is therefore that environmental and physical mechanisms controlling leaf water isotopic composition cannot fully account for the interspecies variation in *n*-alkane hydrogen isotope data. Instead, these data indicate that biochemical mechanisms may play a more important role in controlling interspecies variation in: (i) *n*-alkane $^2\text{H}/^1\text{H}$ composition; and (ii) fractionation between source water and *n*-alkane $^2\text{H}/^1\text{H}$, than abiotic factors.

Previous research has already theorised that biochemical processes may have a role to play in determining leaf biomarker $^2\text{H}/^1\text{H}$ (e.g. Feakins and Sessions, 2010; Sachse *et al.*, 2012). However little is currently known about how this mechanism operates in terrestrial plants. This study makes a significant contribution to knowledge, therefore, by establishing that biochemical processes can be more important than environmental mechanisms in controlling *n*-alky lipid $^2\text{H}/^1\text{H}$. Findings presented here highlight that future studies should make use of an integrated analytical approach, and focus on distinguishing biochemically moderated fractionation from environmental and physical factors across a range of plant species and functional types growing in diverse habitats.

9.4 CAN METABOLIC AND BIOCHEMICAL PROCESSES INFLUENCE *n*-ALKANE $^2\text{H}/^1\text{H}$?

Research objective: Identification of potential biochemical mechanisms that may account for interspecies variation in *n*-alkane $^2\text{H}/^1\text{H}$ among the saltmarsh plants.

Findings presented in Chapter 7 provide a first order evaluation of potential biochemical mechanisms which may influence interspecies biomarker $^2\text{H}/^1\text{H}$ variation in the Stiffkey species. Data from a range of compounds, including phytol, fatty acids and starch (synthesised in the chloroplast), in comparison with *n*-alkane $^2\text{H}/^1\text{H}$ (synthesised in the cytosol) suggests that a range of mechanisms may account for interspecies $^2\text{H}/^1\text{H}$ variation across these cell compartments. For phytol (unlike *n*-alkanes), the C_4 monocot *Spartina anglica* had the most positive $\delta^2\text{H}$ values. C_4 species can generate NADPH from the decarboxylation of malate or aspartate, which can result in tissues such as cellulose being ^2H -enriched relative to C_3 species (Fogel and Cifuentes, 1993), a factor which is rarely considered when seeking to explain differences in $^2\text{H}/^1\text{H}$ among species with different carbon fixation pathways (see for example the discussion of WUE in Hou *et al.*, 2007). In addition, differences in leaf water $^2\text{H}/^1\text{H}$ could not account for the magnitude of interspecies variation in phytol $^2\text{H}/^1\text{H}$ among the C_3 species. This chapter therefore explores whether phytochemical variation could account for differences in phytol $^2\text{H}/^1\text{H}$ among the C_3 species sampled, in light of previous research identifying differences in the protein content of PSI and PSII (Zolla *et al.*, 2002; 2003). Although measurement of the concentration of PSI and PSII proteins was outside the scope of this study, the fact $^2\text{H}/^1\text{H}$ differed systematically among dicots and monocots raises the exiting prospect that differences in protein content could be recorded in biomarker $^2\text{H}/^1\text{H}$ as a result of differences in the efficiency of biophotolysis. It is however stressed that in the absence of further experimental work to explore the validity of this proposition, such arguments remains purely speculative.

Relative ^2H -enrichment and depletion in the FAME data also showed interspecies variation among the sampled plants. Interestingly, $^2\text{H}/^1\text{H}$ from palmitic and linolenic acid is strongly correlated, while linoleic acid has no relationship with either of them. Linoleic acid $^2\text{H}/^1\text{H}$, however, does have a relationship with leaf water $^2\text{H}/^1\text{H}$. While this relationship is difficult to explain without further analysis, it is possible that exchange of H with cellular water can account for the link between H_2O and linoleic acid (Baliff *et al.* 2009). In addition, the relationship between the hydrogen isotope composition of palmitic and linolenic acid may be attributable to the fact that linolenic acid can also be produced from chloroplast membrane lipids (Wasternack,

2007). These data highlight the complexities of H cycling in plant metabolic networks, and illustrate the need for an integrative approach (e.g. Van Dongen *et al.*, 2011) when seeking to understand biochemical processes that could influence secondary compound $^2\text{H}/^1\text{H}$.

The other significant finding from these data is that the way in which plants respond biochemically to environmental stress may be recorded in their leaf wax biomarker $^2\text{H}/^1\text{H}$. The production of osmoregulatory solutes, a generic stress response of plants to a range of environmental stresses including salinity, drought, temperature and UV light (Hare and Cress, 1997), would appear to have an important influence on the partitioning of pyruvate in plant cellular metabolism. As pyruvate is a key precursor for acetogenic lipid synthesis, such perturbation of metabolic networks, increasing the flux of material through, for example: (i) the glutamate pathway to produce proline; (ii) the production of enhanced levels of amino acids; or (iii) the production of mannitol from mannose (Herold and Lewis, 1988; Ashraf and Foodad, 2007; Szabados and Savouré, 2010; Wang *et al.*, 2013; Fig. 7.28 and 7.29, Chapter 7), would appear capable of altering secondary compound $^2\text{H}/^1\text{H}$.

A prominent feature of studies of modern *n*-alkane $^2\text{H}/^1\text{H}$ is the consistent ^2H -depletion of monocot *n*-alkanes relative to dicots. This cannot easily be explained by physiological mechanisms (Smith and Freeman, 2006). In addition to the discussion above relating to differences in PSI and PSII, this thesis proposes that broad differences in the nature of the dominant compounds produced in response to environmental stress by monocots (carbohydrates) and dicots (carbohydrates and/or nitrogenous compounds) (Briens and Lahrer, 1982) could potentially account for these trends. It is suggested that the enhanced production of carbohydrate compounds for osmoregulation in monocots may result in a higher percentage of H in pyruvate from NADPH, and drive the ^2H -depletion in monocot leaf wax biomarkers relative to dicots. The relative ^2H -enrichment in dicots could also be influenced by the catalysis of osmoregulatory compounds once the external stress has abated (Hare and Cress, 1997). Catalysis of (predominantly) nitrogenous compounds in dicots and the carbohydrates in monocots could give rise to a ^2H -enriched pool of recycled H within the cells of dicots, as proteins are generally ^2H -enriched relative to carbohydrates (Schmidt *et al.*, 2003). Such a result, if confirmed by future research, suggests that much of the biochemical information contained within leaf wax $^2\text{H}/^1\text{H}$ remains to be discovered. Indeed, there seems to be a very real potential for leaf wax $^2\text{H}/^1\text{H}$ to record metabolic information in a manner analogous to that reported for lipids from microorganisms (e.g. Valentine, 2009).

Such findings have wide reaching implications for the current interpretations of sedimentary *n*-alkanes commonly found in the literature. Although further work is required to fully understand the biological mechanisms and processes driving shifts leaf wax *n*-alkane $^2\text{H}/^1\text{H}$, critically, these data show that the assumption that a typical, relatively consistent fractionation factor can summarise the relationship between source water, leaf water and leaf wax biomarker, may fail to capture the complexity of H cycling in plant metabolic networks.

9.5 DISTINGUISHING SHIFTS IN PALAEOHYDROLOGY FROM CHANGES IN VEGETATION IN SEDIMENTARY SEQUENCES

Research objective: Investigate the sensitivity of the Stiffkey sedimentary record to changes in surface plant cover and evaluate approaches to identifying and quantifying vegetation change.

A common assumption either implicit or explicit in many studies recreating palaeohydrological conditions from lipid biomarkers is that vegetation change is only a problem for data interpretation if it is on a large scale (e.g. Tierney *et al.*, 2010; Feakins, 2013; Nelson *et al.*, 2013). In a stark contrast to this, data presented in Chapter 8 suggests that small/moderate vegetation change (modelled here using two plausible anthropogenic and natural scenarios) can drive shifts of up to 40‰ in weighted average *n*-C₂₉ $^2\text{H}/^1\text{H}$ available for incorporation into sediments. Further, coeval shifts in *n*-C₂₉ $\delta^{13}\text{C}$ calculated for the modelled scenarios were only $\leq 1\%$, which would be unlikely to be viewed as significant from the perspective of interpreting sedimentary $^2\text{H}/^1\text{H}$ data (e.g. Schefuß *et al.* 2005).

These findings suggest that the importance of disaggregating the influence of vegetation change from climate shifts has been significantly underestimated in current studies. The use of statistical mixing models for estimating the composition of surface vegetation appears to offer a potential method for identifying and quantifying vegetation change (especially where plants are collected into functional groups based on their biochemical differences as discussed above), but this method (like others currently proposed to identify and correct for vegetation change in the sedimentary archive) has limitations. In particular, using modern vegetation $\delta^2\text{H}$ and $\delta^{13}\text{C}$ measurements to derive source groups for un-mixing could be confounded by historical changes in the isotopic composition of precipitation and atmospheric CO₂, over long geological timescales.

The implications of these findings for palaeohydrological reconstruction are further demonstrated in Chapter 8 through the use of three different approaches for recreating the $^2\text{H}/^1\text{H}$ of palaeoprecipitation (“fixed” net apparent fractionation, Pagani *et al.*, 2006b; “typical” fractionation factors previously published for plant functional groups based on gross physiology, Sachse *et al.*, 2012; fractionation factors determined as part of this study for the Stiffkey species). Trends observed in the reconstructed record differ considerably depending upon which method is used. This research suggests that those instances where a biomarker record shows a markedly different trend from another palaeohydrological proxy (e.g. Tierney and deMonocal 2013) may, at least in part, arise from: (i) a failure to account for small-scale shifts in palaeovegetation assemblages; and (ii) the method used to calculate palaeoprecipitation $^2\text{H}/^1\text{H}$.

9.6 FINAL COMMENT

A number of important questions have been raised by this thesis concerning theoretical and practical issues relating to the use of leaf wax *n*-alkanes as palaeoclimatic and palaeohydrological proxies. In particular, the precise nature of metabolic and biochemical information recorded in *n*-alkane carbon and hydrogen isotope signals clearly requires further study. Without further understanding of the cellular metabolic processes controlling these signals, it would appear that the quantitative reconstruction of past climates remains difficult from leaf wax biomarker data. In addition, practical issues remain to be solved regarding distinguishing vegetation change from climate shifts in the sedimentary record. This study concludes, therefore, that more work is required to allow confidence in the use of biomarkers in the study of past climate. The ongoing development of palaeoclimate proxies is, however, an iterative process. Indeed, advances often result in more detailed information being obtained from the geological record than could have been previously anticipated. The data presented here show fascinating glimpses of the nature of metabolic and biochemical information that could be recorded in leaf wax *n*-alkanes. Once we fully understand the biochemical processes driving the molecular and isotopic composition of leaf wax biomarkers, it is likely that our knowledge of the relationship between plants and their environment, both in modern contexts and though the geological past, will be greatly enhanced.

References

- Adam, P. (2002). Saltmarshes in a time of change. *Environmental conservation* **29**: 39-61.
- Ainouche, M. L., Baumel, A. and Salmon, A. (2004). *Spartina anglica* CE Hubbard: a natural model system for analysing early evolutionary changes that affect allopolyploid genomes. *Biological Journal of the Linnean Society* **82**: 475-484.
- Akhani, H., Trimborn, P. and Ziegler, H. (1997). Photosynthetic pathways in Chenopodiaceae from Africa, Asia and Europe with their ecological, phytogeographical and taxonomical importance. *Plant Systematics and Evolution* **206**: 187-221.
- Allègre, C. J. (2008). *Isotope Geology*, Cambridge University Press.
- Allen, J. (2000). Morphodynamics of Holocene salt marshes: a review sketch from the Atlantic and Southern North Sea coasts of Europe. *Quaternary Science Reviews* **19**: 1155-1231.
- Allison, S. (1992) The influence of rainfall variability on the species composition of a northern California salt marsh plant assemblage. *Plant Ecology*. **101**:145-160.
- Anarat-Cappillino, G. and Sattely, E. S. (2014). The chemical logic of plant natural product biosynthesis. *Current Opinion in Plant Biology* **19**: 51-58.
- Andersen, K. K., Azuma, N., Barnola, J.-M., Bigler, M., Biscaye, P., Caillon, N., Chappellaz, J., Clausen, H. B., Dahl-Jensen, D. and Fischer, H. (2004). High-resolution record of Northern Hemisphere climate extending into the last interglacial period. *Nature* **431**: 147-151.
- Anderson, N. J., Bugmann, H., Dearing, J. A. and Gaillard, M.-J. (2006). Linking palaeoenvironmental data and models to understand the past and to predict the future. *Trends in Ecology & Evolution* **21**: 696-704.
- Andrews, J., Boomer, I., Bailiff, I., Balson, P., Bristow, C., Chroston, P., Funnell, B., Harwood, G., Jones, R. and Maher, B. (2000). Sedimentary evolution of the north Norfolk barrier coastline in the context of Holocene sea-level change. *Geological Society, London, Special Publications* **166**: 219-251.
- Araújo, W. L., Tohge, T., Ishizaki, K., Leaver, C. J. and Fernie, A. R. (2011). Protein degradation—an alternative respiratory substrate for stressed plants. *Trends in Plant Science* **16**: 489-498.
- Arens, N. C., Jahren, A. H. and Amundson, R. (2000). Can C₃ plants faithfully record the carbon isotopic composition of atmospheric carbon dioxide? *Paleobiology* **26**: 137-164.
- Ashraf, M. and Foolad, M. R. (2007). Roles of glycine betaine and proline in improving plant abiotic stress resistance. *Environmental and Experimental Botany* **59**: 206-216.
- Baas, M., Pancost, R., van Geel, B. and Sinninghe Damsté, J. S. (2000). A comparative study of lipids in *Sphagnum* species. *Organic Geochemistry* **31**: 535-541.
- Bai, Y., Fang, X., Nie, J., Wang, Y. and Wu, F. (2009). A preliminary reconstruction of the paleoecological and paleoclimatic history of the Chinese Loess Plateau from the application of biomarkers. *Palaeogeography, Palaeoclimatology, Palaeoecology* **271**: 161-169.
- Baillif, V., Robins, R. J., Le Feunteun, S., Lesot, P. and Billault, I. (2009). Investigation of fatty acid elongation and desaturation steps in *Fusarium lateritium* by quantitative two-dimensional deuterium NMR spectroscopy in chiral oriented media. *Journal of Biological Chemistry* **284**: 10783-10792.
- Baker, E. A. (1982). Chemistry and morphology of plant epicuticular waxes. In: D. F. Cutler, Alvin, K. L., Price, C. E (Eds) *The Plant Cuticle*. New York, Academic Press: 139 - 165.

- Bakker, J. (1978). Changes in a salt-marsh vegetation as a result of grazing and mowing—A five-year study of permanent plots. *Vegetatio* **38**: 77-87.
- Barbour, M. M., Schurr, U., Henry, B. K., Wong, S. C., Farquhar, G. D. (2000) Variation in the oxygen isotope ratio of phloem sap sucrose from castor bean. Evidence in support of the Péclet effect. *Plant Physiol.* **123**, 671-680.
- Barbour, M., Roden, J., Farquhar, G., Ehleringer, J. (2004) Expressing leaf water and cellulose oxygen isotope ratios as enrichment above source water reveals evidence of a Péclet effect. *Oecologia* **138**, 426-435.
- Bar-Matthews, M., Ayalon, A. and Kaufman, A. (1997). Late Quaternary paleoclimate in the eastern Mediterranean region from stable isotope analysis of speleothems at Soreq Cave, Israel. *Quaternary Research* **47**: 155-168.
- Bauwe, H. (2011). *Photorespiration: the bridge to C₄ photosynthesis. C₄ photosynthesis and related CO₂ concentrating mechanisms*, Springer: 81-108.
- Beerling, D. J., Hewitt, C. N., Pyle, J. A. and Raven, J. A. (2007). Critical issues in trace gas biogeochemistry and global change. *Philosophical Transactions of the Royal Society A: Mathematical, Physical and Engineering Sciences* **365**: 1629-1642.
- Beisel, K., Janke, S., Hoffman, D., Koppchen, S., Schurr, U., Matsubara, S. (2010) "Continuous Turnover of Carotenes and Chlorophyll *a* in Mature Leaves of *Arabidopsis* Revealed by ¹⁴CO₂ Pulse-Chase Labeling". *Plant Physiology*, **152**: 2188-2199.
- Bellasio, C. and Griffiths, H. (2014). Acclimation to low light by C₄ maize: implications for bundle sheath leakiness. *Plant, Cell & Environment* **37**: 1046-1058.
- Benner, R., Fogel, M., Sprague, E. and Hodson, R. (1987). Depletion of C in lignin and its implications for stable carbon isotope studies. *Nature* **329**: 708-710.
- Bernard, A. and Joubès, J. (2013). *Arabidopsis* cuticular waxes: advances in synthesis, export and regulation. *Progress in Lipid Research* **52**: 110-129.
- Bert, D., Leavitt, S. W. and Dupouey, J. L. (1997). Variations of wood δ¹³C and water-use efficiency of *Abies alba* during the last century. *Ecology* **78**: 1588-1596.
- Bertness, M. D. and Ewanchuk, P. J. (2002). Latitudinal and climate-driven variation in the strength and nature of biological interactions in New England salt marshes. *Oecologia* **132**: 392-401.
- Bi, X., Sheng, G., Liu, X., Li, C., Fu, J. (2005) Molecular and carbon and hydrogen isotopic composition of *n*-alkanes of plant leaf waxes. *Organic Geochemistry*. **36**, 1405-1417.
- Bianchi, A. and Bianchi, G. (1990). Surface lipid composition of C₃ and C₄ plants." *Biochemical Systematics and Ecology* **18**: 533-537.
- Billault, I., Guiet, S., Mabon, F. and Robins, R. (2001). Natural Deuterium Distribution in Long-Chain Fatty Acids Is Nonstatistical: A Site-Specific Study by Quantitative ²H NMR Spectroscopy. *ChemBioChem* **2**: 425-431.
- Bohnert, H., Jensen, R. (1996) Strategies for engineering water-stress tolerance in plants. *T.I.B. Tech.*, **14**, 89 – 97.
- Boom, A., Carr, A.S., Chase, B.M., Grimes, H.L., Meadows, M.E., Leaf wax *n*-alkanes and δ¹³C values of CAM plants from arid southwest Africa, *Organic Geochemistry* **67**: 99 – 102.
- Boomer, I. and Horton, B. P. (2006). Holocene relative sea-level movements along the North Norfolk Coast, UK. *Palaeogeography, Palaeoclimatology, Palaeoecology* **230**: 32-51.
- Boomer, I. and Woodcock, L. (1999). The nature and origin of Stiffkey Meals, North Norfolk coast. *Bulletin of the Geological Society of Norfolk* **49**: 3-13.
- Boorman, L. (1967) *Limonium vulgare* Mill. and *L. humile* Mill. *Journal of Ecology*. **55**, 221-

232.

Boorman, L. A. and Ashton, C. (1997). The productivity of salt marsh vegetation at Tollesbury, Essex, and Stiffkey, Norfolk, England. *Mangroves and Salt Marshes* **1**: 113-126.

Bos, D., Bakker, J. P., Vries, Y. and Lieshout, S. (2002). Long-term vegetation changes in experimentally grazed and ungrazed back-barrier marshes in the Wadden Sea. *Applied Vegetation Science* **5**: 45-54.

Bowen G. J., Wassenaar L. I., Hobson K. A. (2005) Global application of stable hydrogen and oxygen isotopes to wildlife forensics. *Oecologia* **143**, 337-348.

Bowen, G. J. and Revenaugh, J. (2003). Interpolating the isotopic composition of modern meteoric precipitation. *Water Resources Research* **39**: 1299. DOI: 10.129/2003WR002086.

Bowsher, C., Steer, M., Tobin, A. (2008). *Plant Biochemistry*. New York, NY, USA, Garland Science.

Braconnot, P., Harrison, S. P., Kageyama, M., Bartlein, P. J., Masson-Delmotte, V., Abe-Ouchi, A., Otto-Bliesner, B. and Zhao, Y. (2012). Evaluation of climate models using palaeoclimatic data. *Nature Climate Change* **2**: 417-424.

Brader, A. V., van Winden, J. F., Bohncke, S. J., Beets, C. J., Reichart, G.-J. and de Leeuw, J. W. (2010). Fractionation of hydrogen, oxygen and carbon isotopes in *n*-alkanes and cellulose of three *Sphagnum* species. *Organic Geochemistry* **41**: 1277-1284.

Briens, M. and Larher, F. (1982). Osmoregulation in halophytic higher plants: a comparative study of soluble carbohydrates, polyols, betaines and free proline. *Plant, Cell & Environment* **5**: 287-292.

Britton, K., Müldner, G. and Bell, M. (2008). "Stable isotope evidence for salt-marsh grazing in the Bronze Age Severn Estuary, UK: implications for palaeodietary analysis at coastal sites." *Journal of Archaeological Science* **35**: 2111-2118.

Broström, A., Nielsen, A. B., Gaillard, M.-J., Hjelle, K., Mazier, F., Binney, H., Bunting, J., Fyfe, R., Meltsov, V. and Poska, A. (2008). "Pollen productivity estimates of key European plant taxa for quantitative reconstruction of past vegetation: a review." *Vegetation History and Archaeobotany* **17**: 461-478.

Broström, A., Sugita, S. and Gaillard, M.-J. (2004). "Pollen productivity estimates for the reconstruction of past vegetation cover in the cultural landscape of southern Sweden." *The Holocene* **14**: 368-381.

Brown, C., Pezeshki, S. and DeLaune, R. (2006). "The effects of salinity and soil drying on nutrient uptake and growth of *Spartina alterniflora* in a simulated tidal system." *Environmental and Experimental Botany* **58**: 140-148.

Brugnoli, E., Hubick, K. T., von Caemmerer, S., Wong, S. C. and Farquhar, G. D. (1988). "Correlation between the carbon isotope discrimination in leaf starch and sugars of C₃ plants and the ratio of intercellular and atmospheric partial pressures of carbon dioxide." *Plant Physiology* **88**: 1418-1424.

Buchmann, N., Brooks, J., Rapp, K. and Ehleringer, J. (1996). "Carbon isotope composition of C₄ grasses is influenced by light and water supply." *Plant Cell and Environment*, **19**: 392-402.

Buggle, B., Wiesenberg, G. L. B. and Glaser, B. (2010). "Is there a possibility to correct fossil *n*-alkane data for postsedimentary alteration effects?" *Applied Geochemistry* **25**: 947-957.

Bull, I. D., van Bergen, P. F., Bol, R., Brown, S., Gledhill, A. R., Gray, A. J., Harkness, D. D., Woodbury, S. E. and Evershed, R. P. (1999). "Estimating the contribution of *Spartina anglica* biomass to salt-marsh sediments using compound specific stable carbon isotope measurements." *Organic Geochemistry* **30**: 477-483.

- Bull, I., D., Cryer, D., Zhang, A. and Eglinton, G. (2013) Molecular distributions and $\delta^{13}\text{C}$ values of n-alkanes as palaeovegetational biomarkers. British Organic Geochemistry Society Annual Meeting, Plymouth
- Bunting, M. J., Armitage, R., Binney, H. A. and Waller, M. (2005). "Estimates of 'relative pollen productivity' and 'relevant source area of pollen' for major tree taxa in two Norfolk (UK) woodlands." *The Holocene* **15**: 459-465.
- Burke, D., Weis, J., Weis, P. (2000) Release of Metals by the Leaves of the Salt Marsh Grasses *Spartina alterniflora* and *Phragmites australis*. *Estuarine and Coastal Shelf Science*. **51**, 153-159.
- Bush, R. T. and McInerney, F. A. (2013). "Leaf wax n-alkane distributions in and across modern plants: Implications for paleoecology and chemotaxonomy." *Geochimica et Cosmochimica Acta* **117**: 161-179.
- Bush, R. T., McInerney, F. A., Chen, D. (2012). Do plant n-alkane distributions record climate more than plant type? Geological Society of America. Charlotte, USA.
- Callaway, J. C., Delaune, R. D. and Patrick Jr, W. H. (1998). "Heavy metal chronologies in selected coastal wetlands from Northern Europe." *Marine Pollution Bulletin* **36**: 82-96.
- Callaway, J. C., DeLaune, R. D. and Patrick, W. H., Jr. (1996). "Chernobyl ^{137}Cs Used to Determine Sediment Accretion Rates at Selected Northern European Coastal Wetlands." *Limnology and Oceanography* **41**: 444-450.
- Callaway, J., Delaune, R., Patrick JR, W. (1996) Chernobyl ^{137}Cs used to determine sediment accretion rates at selected northern European coastal wetlands. *Limnology and Oceanography*. **41**, 444-450.
- Canuel, E. A., Freeman, K. H. and Wakeham, S. G. (1997). "Isotopic compositions of lipid biomarker compounds in estuarine plants and surface sediments." *Limnology and Oceanography* **42**: 1570-1583.
- Castañeda, I. S. and Schouten, S. (2011). "A review of molecular organic proxies for examining modern and ancient lacustrine environments." *Quaternary Science Reviews* **30**: 2851-2891.
- Castañeda, I. S., Mulitza, S., Schefuß, E., Lopes dos Santos, R. A., Sinninghe Damsté, J. S. and Schouten, S. (2009). "Wet phases in the Sahara/Sahel region and human migration patterns in North Africa." *Proceedings of the National Academy of Sciences* **106**: 20159-20163.
- Cayet, C. and Lichtfouse, E. (2001). " $\delta^{13}\text{C}$ of plant-derived n-alkanes in soil particle-size fractions." *Organic Geochemistry* **32**: 253-258
- Cerling, T. E. and Quade, J. (1993). "Stable carbon and oxygen isotopes in soil carbonates." *Geophysical Monograph Series* **78**: 217-231.
- Cerling, T. E. and Sharp, Z. D. (1996). "Stable carbon and oxygen isotope analysis of fossil tooth enamel using laser ablation." *Palaeogeography, Palaeoclimatology, Palaeoecology* **126**: 173-186.
- Cerling, T. E., Harris, J. M., MacFadden, B. J., Leakey, M. G., Quade, J., Eisenmann, V. and Ehleringer, J. R. (1997). "Global vegetation change through the Miocene/Pliocene boundary." *Nature* **389**: 153-158.
- Cerling, T., Quade, J., Wang, Y. and Bowman, J. (1989). "Carbon isotopes in soils and palaeosols as ecology and palaeoecology indicators." *Nature* **341**: 138-139.
- Cernusak, L. A., Mejia-Chang, M., Winter, K. and Griffiths, H. (2008). "Oxygen isotope composition of CAM and C_3 *Clusia* species: non-steady-state dynamics control leaf water ^{18}O enrichment in succulent leaves." *Plant, Cell & Environment* **31**: 1644-1662.

- Cernusak, L. A. and Kahmen, A. (2013). "The multifaceted relationship between leaf water ^{18}O enrichment and transpiration rate." *Plant, Cell & Environment* **36**: 1239-1241.
- Cernusak, L. A., Ubierna, N., Winter, K., Holtum, J. A., Marshall, J. D. and Farquhar, G. D. (2013). "Environmental and physiological determinants of carbon isotope discrimination in terrestrial plants." *New Phytologist* **200**: 950-965.
- Chen, Y.-E., Zhao, Z.-Y., Zhang, H.-Y., Zeng, X.-Y. and Yuan, S. (2013). "The significance of CP29 reversible phosphorylation in thylakoids of higher plants under environmental stresses." *Journal of Experimental Botany* **64**: 1167-1178
- Chikaraishi, Y. and Naraoka, H. (2003). "Compound-specific δD - $\delta^{13}\text{C}$ analyses of *n*-alkanes extracted from terrestrial and aquatic plants." *Phytochemistry* **63**: 361-371.
- Chikaraishi, Y., Naraoka, H. and Poulson, S. (2004). "Carbon and hydrogen isotopic fractionation during lipid biosynthesis in a higher plant (*Cryptomeria japonica*)." *Phytochemistry* **65**: 323-330.
- Chikaraishi, Y., Naraoka, H. and Poulson, S. (2004). "Hydrogen and carbon isotopic fractionations of lipid biosynthesis among terrestrial (C_3 , C_4 and CAM) and aquatic plants." *Phytochemistry* **65**: 1369-1381.
- Chikaraishi, Y., Matsumoto, K., Ogawa, N. O., Suga, H., Kitazato, H. and Ohkouchi, N. (2005). "Hydrogen, carbon and nitrogen isotopic fractionations during chlorophyll biosynthesis in C_3 higher plants." *Phytochemistry* **66**: 911-920
- Chikaraishi, Y. and Naraoka, H. (2007). " $\delta^{13}\text{C}$ and δD relationships among three *n*-alkyl compound classes (*n*-alkanoic acid, *n*-alkane and *n*-alkanol) of terrestrial higher plants." *Organic Geochemistry* **38**: 198-215.
- Chikaraishi, Y., Tanaka, R., Tanaka, A. and Ohkouchi, N. (2009). "Fractionation of hydrogen isotopes during phytol biosynthesis." *Organic Geochemistry* **40**: 569-573.
- Clarke, J. and Richards, R. (1988). "The effects of glaucousness, epicuticular wax, leaf age, plant height, and growth environment on water loss rates of excised wheat leaves." *Canadian Journal of Plant Science* **68**: 975-982.
- Cohen, E., Cvitaš, T., Frey, J., Homström, B., Kuchitsu, K., Marquardt, R. Mills, I., Pavese, F., Quack, M., Stohner, J., Strauss, H., Takami, M., Thor, A. (Eds) (2007) *Quantities, Units and Symbols in Physical Chemistry*. R. Soc. Chem. Publ. 265 pp. 3rd ed.
- Collins, A. L., Walling, D. E. and Leeks, G. J. L. (1997). "Source type ascription for fluvial suspended sediment based on a quantitative composite fingerprinting technique." *CATENA* **29**: 1-27.
- Collister, J., Rieley, G., Stern, B., Eglinton, G. and Fry, B. (1994). "Compound-specific $\delta^{13}\text{C}$ analyses of leaf lipids from plants with differing carbon dioxide metabolisms." *Organic Geochemistry* **21**: 619-627.
- Conte, M. H. and Weber, J. C. (2002). "Plant biomarkers in aerosols record isotopic discrimination of terrestrial photosynthesis." *Nature* **417**: 639-641.
- Conte, M. H., Weber, J. C., Carlson, P. J. and Flanagan, L. B. (2003). "Molecular and carbon isotopic composition of leaf wax in vegetation and aerosols in a northern prairie ecosystem." *Oecologia* **135**: 67-77.
- Craig, H. and Gordon, L. I. (1965). "Deuterium and oxygen 18 variations in the ocean and the marine atmosphere." In: E Tongiorgi, ed, *Proceedings of a Conference on Stable Isotopes in Oceanographic and paleotemperatures*, Spoleto, Italy, pp 9–130
- Cranwell, P. (1973) Chain-length distribution of *n*-alkanes from lake sediments in relation to post-glacial environmental change. *Freshwater Biology* **3**: 259-265.
- Cuntz, M. (2011). "Carbon cycle: a dent in carbon's gold standard." *Nature* **477**: 547-548.

- Da Ines, O., Graf, W., Franck, K., Albert, A., Winkler, J., Scherb, H., Stichler, W. and Schäffner, A. (2010). "Kinetic analyses of plant water relocation using deuterium as tracer—reduced water flux of *Arabidopsis* pip2 aquaporin knockout mutants." *Plant Biology* **12**: 129-139.
- Dansgaard, W. (1964). "Stable isotopes in precipitation." *Tellus* **16**: 436-468.
- das Neves, J. P. C., Ferreira, L. F. P., Vaz, M. M. and Gazarini, L. C. (2008). "Gas exchange in the salt marsh species *Atriplex portulacoides* L. and *Limoniastrum monopetalum* L. in Southern Portugal." *Acta Physiologiae Plantarum* **30**: 91-97.
- Davy, A. (2009) "Life on the edge: saltmarshes ancient and modern". *Trans. Norfolk Norwich Nat. Soc.* 2009 42(1): 1-11.
- Davy, A. and Smith, H. (1985). "Population differentiation in the life-history characteristics of salt-marsh annuals." *Vegetatio* **61**: 117-125
- Davy, A. J., Brown, M. J., Mossman, H. L. and Grant, A. (2011). "Colonization of a newly developing salt marsh: disentangling independent effects of elevation and redox potential on halophytes." *Journal of Ecology* **99**: 1350-1357.
- Davy, A., Bishop, G. (1991) *Triglochin maritima* L. *Journal of Ecology*. **72**, 531-555.
- Dawson, L., Towers, W., Mayes, R., Craig, J., Vaisanen, R. and Waterhouse, E. (2004). "The use of plant hydrocarbon signatures in characterizing soil organic matter." *Geological Society London Special Publications* **232**: 269.
- Dawson, T. E., Mambelli, S., Plamboeck, A. H., Templer, P. H. and Tu, K. P. (2002). "Stable isotopes in plant ecology." *Annual Review of Ecology and Systematics*: 507-559.
- Del Castillo, J. B., Brooks, C., Cambie, R., Eglinton, G., Hamilton, R. and Pellitt, P. (1967). "The taxonomic distribution of some hydrocarbons in gymnosperms." *Phytochemistry* **6**: 391-398.
- Dickens, G. R., O'Neil, J. R., Rea, D. K. and Owen, R. M. (1995). "Dissociation of oceanic methane hydrate as a cause of the carbon isotope excursion at the end of the Paleocene." *Paleoceanography* **10**: 965-971.
- Diefendorf, A. F., Freeman, K. H., Wing, S. L. and Graham, H. V. (2011). "Production of *n*-alkyl lipids in living plants and implications for the geologic past." *Geochimica et Cosmochimica Acta*. **75**: 7472 – 7485.
- Diefendorf, A. F., Mueller, K. E., Wing, S. L., Koch, P. L. and Freeman, K. H. (2010). "Global patterns in leaf ¹³C discrimination and implications for studies of past and future climate." *Proceedings of the National Academy of Sciences* **107**: 5738.
- Dirghangi, S. S. and Pagani, M. (2013). "Hydrogen isotope fractionation during lipid biosynthesis by *Haloarcula marismortui*". *Geochimica et Cosmochimica Acta* **119**: 381-390
- Dirghangi, S. S. and Pagani, M. (2013). "Hydrogen isotope fractionation during lipid biosynthesis by *Tetrahymena thermophile*." *Organic Geochemistry* **64**: 105-111.
- Dodd, R. S. and Poveda, M. M. (2003). "Environmental gradients and population divergence contribute to variation in cuticular wax composition in *Juniperus communis*." *Biochemical Systematics and Ecology* **31**: 1257-1270.
- Dodd, R. S., Afzal Rafii, Z. and Bousquet-Melou, A. (2000). "Evolutionary divergence in the pan-Atlantic mangrove *Avicennia germinans*." *New Phytologist* **145**: 115-125.
- Dodd, R. S., Blasco, F., Rafii, Z. A. and Torquebiau, E. (1999). "Mangroves of the United Arab Emirates: ecotypic diversity in cuticular waxes at the bioclimatic extreme." *Aquatic Botany* **63**: 291-304.

- Dombrowski, J. E. (2003). "Salt stress activation of wound-related genes in tomato plants." *Plant Physiology* **132**: 2098-2107.
- Dongmann G, Nürnberg HW, Förstel H, Wagener K. 1974. On the enrichment of H² 18O in the leaves of transpiring plants. *Radiation and Environmental Biophysics*, **11**: 41–52.
- Donovan, L. A. and Ehleringer, J. R. (1991). "Ecophysiological differences among juvenile and reproductive plants of several woody species." *Oecologia* **86**: 594-597.
- Donovan, L. A. and Ehleringer, J. R. (1994). "Carbon isotope discrimination, water-use efficiency, growth, and mortality in a natural shrub population." *Oecologia* **100**: 347-354.
- Douglas, P. M. J., Pagani, M., Brenner, M., Hodell, D. A. and Curtis, J. H. (2012). "Aridity and vegetation composition are important determinants of leaf-wax δ D values in southeastern Mexico and Central America." *Geochimica et Cosmochimica Acta* **97**: 24-45.
- Drake, B. G. (1989). "Photosynthesis of salt marsh species." *Aquatic botany* **34**: 167-180.
- Duan, J. R., Billault, I., Mabon, F. and Robins, R. (2002). "Natural Deuterium Distribution in Fatty Acids Isolated from Peanut Seed Oil: A Site-Specific Study by Quantitative ²H NMR Spectroscopy." *ChemBioChem* **3**: 752-759.
- Duarte, B., Santos, D., Marques, J. and Caçador, I. (2014). "Biophysical probing of *Spartina maritime* photo-system II changes during prolonged tidal submersion periods." *Plant Physiology and Biochemistry* **77**: 122-132.
- Duarte, C. M., Losada, I. J., Hendriks, I. E., Mazarrasa, I. and Marbà, N. (2013). "The role of coastal plant communities for climate change mitigation and adaptation." *Nature Climate Change* **3**: 961-968
- Duarte, C. M., Middelburg, J. J. and Caraco, N. (2005). "Major role of marine vegetation on the oceanic carbon cycle." *Biogeosciences* **2**: 1-8.
- Dungait, J. A. J., Docherty, G., Straker, V. and Evershed, R. P. (2010). "Seasonal variations in bulk tissue, fatty acid and monosaccharide δ^{13} C values of leaves from mesotrophic grassland plant communities under different grazing managements." *Phytochemistry* **71**: 415-428.
- Dungait, J. A., Docherty, G., Straker, V. and Evershed, R. P. (2008). "Interspecific variation in bulk tissue, fatty acid and monosaccharide δ^{13} C values of leaves from a mesotrophic grassland plant community." *Phytochemistry* **69**: 2041-2051.
- Dungait, J. A., Docherty, G., Straker, V. and Evershed, R. P. (2011). "Variation in bulk tissue, fatty acid and monosaccharide δ^{13} C values between autotrophic and heterotrophic plant organs." *Phytochemistry* **72**: 2130-2138.
- Duquesnay, A., Breda, N., Stievenard, M. and Dupouey, J. (1998). "Changes of tree-ring δ^{13} C and water-use efficiency of beech (*Fagus sylvatica* L.) in north-eastern France during the past century." *Plant, Cell & Environment* **21**: 565-572.
- Eglinton, G., Gonzalez, A., Hamilton, R. and Raphael, R. (1962). "Hydrocarbon constituents of the wax coatings of plant leaves: a taxonomic survey." *Phytochemistry* **1**: 89-102.
- Eglinton, G. and Hamilton, R. J. (1967). "Leaf epicuticular waxes." *Science* **156**: 1322-1335.
- Eglinton, T. I., Aluwihare, L. I., Bauer, J. E., Druffel, E. R. and McNichol, A. P. (1996). "Gas chromatographic isolation of individual compounds from complex matrices for radiocarbon dating." *Analytical Chemistry* **68**: 904-912.
- Eglinton, T., Eglinton, G., Dupont, L., Sholkovitz, E., Montluçon, D. and Reddy, C. (2002). "Composition, age, and provenance of organic matter in NW African dust over the Atlantic Ocean." *Geochemistry, Geophysics, Geosystems* **3**: 1-27.
- Eglinton, T. I. and Eglinton, G. (2008). "Molecular proxies for paleoclimatology." *Earth and*

Planetary Science Letters **275**: 1-16.

Ehleringer, J. R., Sage, R. F., Flanagan, L. B. and Pearcy, R. W. (1991). "Climate change and the evolution of C4 photosynthesis." *Trends in Ecology & Evolution* **6**: 95-99.

Ehleringer, J., Phillips, S. and Comstock, J. (1992). "Seasonal variation in the carbon isotopic composition of desert plants." *Functional Ecology* **6**: 396-404.

Eley Y., Pedentchouk, N., Dawson, L. (2012) Tracing higher plant inputs to coastal sediments: an integrated isotopic and molecular approach for forensic investigation. In: Morrison, R., O'Sullivan, G, eds. (2012) Environmental Forensics: Proceedings of the 2011 INEF Conference, Royal Society of Chemistry. pp 218 – 232.

Eley, Y., Dawson, L., Black, S., Andrews, J. and Pedentchouk, N. (2014). "Understanding $^2\text{H}/^1\text{H}$ systematics of leaf wax *n*-alkanes in coastal plants at Stiffkey saltmarsh, Norfolk, UK." *Geochimica et Cosmochimica Acta* **128**: 13-28.

Ellison, A. (1987) Effects of competition, disturbance and herbivory on *Salicornia europaea*. *Ecology* **68**, 576-586.

Ellsworth, P. Z., Williams, D. G. (2007) Hydrogen isotope fractionation during water uptake by woody xerophytes. *Plant Soil* **291**, 93-107.

Enders, S. K., Pagani, M., Pantoja, S., Baron, J. S., Wolfe, A. P., Pedentchouk, N. and Nunez, L. (2008). "Compound-specific stable isotopes of organic compounds from lake sediments track recent environmental changes in an alpine ecosystem, Rocky Mountain National Park, Colorado." *Limnology and Oceanography* **53**: 1468

Evans, J. R. (1989). "Photosynthesis and nitrogen relationships in leaves of C₃ plants." *Oecologia* **78**: 9-19.

Evans, J. R. and Von Caemmerer, S. (2013). "Temperature response of carbon isotope discrimination and mesophyll conductance in tobacco." *Plant, Cell & Environment* **36**: 745-756.

Faboya, O. and Goddard, O. D. (1980). "Leaf wax *n*-alkane constituents of the genus *Khaya*." *Phytochemistry* **19**: 2462-2463.

Farquhar, G. D., O'Leary, M. and Berry, J. (1982). "On the relationship between carbon isotope discrimination and the intercellular carbon dioxide concentration in leaves." *Functional Plant Biology* **9**: 121-137.

Farquhar, G. D. (1983). "On the nature of carbon isotope discrimination in C4 species." *Functional Plant Biology* **10**: 205-226.

Farquhar, G. and Richards, R. (1984). "Isotopic composition of plant carbon correlates with water-use efficiency of wheat genotypes." *Functional Plant Biology* **11**: 539-552.

Farquhar, G. D., Ehleringer, J. R. and Hubick, K. T. (1989). "Carbon isotope discrimination and photosynthesis." *Annual Review of Plant Biology* **40**: 503-537.

Farquhar G. D. and Lloyd J. (1993) Carbon and oxygen isotope effects in the exchange of carbon dioxide between terrestrial plants and the atmosphere. In: *Stable Isotopes and Plant Carbon Water Relations*. pp. 47-70, J. R. Ehleringer, A. E. Hall and G. D. Farquhar (Eds). Academic Press.

Farquhar, G. and Gan, K. S. (2003). "On the progressive enrichment of the oxygen isotopic composition of water along a leaf." *Plant, Cell & Environment* **26**: 1579-1597.

Farquhar, G., Cernusak, L. (2005) On the isotopic composition of leaf water in the non-steady state. *Functional Plant Biology*. **32**, 293-303.

Farquhar, J., Johnston, D. T., Wing, B. A., Habicht, K. S., Canfield, D. E., Airieau, S. and Thieme, M. H. (2003). "Multiple sulphur isotopic interpretations of biosynthetic pathways:

- implications for biological signatures in the sulphur isotope record." *Geobiology* **1**: 27-36.
- Feakins, S. J. (2013). "Pollen-corrected leaf wax D/H reconstructions of northeast African hydrological changes during the late Miocene." *Palaeogeography, Palaeoclimatology, Palaeoecology* **374**: 62-71.
- Feakins, S. J. and Eglinton, T. I. (2005). "Biomarker records of late Neogene changes in northeast African vegetation." *Geology* **33**: 977-980.
- Feakins, S. J. and Sessions, A. L. (2010). "Controls on the D/H ratios of plant leaf waxes in an arid ecosystem." *Geochimica et Cosmochimica Acta* **74**: 2128-2141.
- Feakins, S. J. and Sessions, A. L. (2010). "Crassulacean acid metabolism influences D/H ratio of leaf wax in succulent plants." *Organic Geochemistry* **41**: 1269-1276.
- Feakins, S. J., Warny, S. and Lee, J.-E. (2012). "Hydrologic cycling over Antarctica during the middle Miocene warming." *Nature Geoscience* **5**: 557-560.
- Febrero, A., Fernández, S., Molina-Cano, J. L. and Araus, J. L. (1998). "Yield, carbon isotope discrimination, canopy reflectance and cuticular conductance of barley isolines of differing glaucousness." *Journal of Experimental Botany* **49**: 1575-1581.
- Feng, X. (1999). "Trends in intrinsic water-use efficiency of natural trees for the past 100-200 years: A response to atmospheric CO₂ concentration." *Geochimica et Cosmochimica Acta* **63**: 1891-1903.
- Ficken, K. J., Wooller, M. J., Swain, D. L., Street-Perrott, F. A. and Eglinton, G. (2002). "Reconstruction of a subalpine grass-dominated ecosystem, Lake Rutundu, Mount Kenya: a novel multi-proxy approach." *Palaeogeography, Palaeoclimatology, Palaeoecology* **177**: 137-149.
- Flanagan, L. B. and Ehleringer, J. R. (1991). "Stable Isotope Composition of Stem and Leaf Water: Applications to the Study of Plant Water Use." *Functional Ecology* **5**: 270-277.
- Flanagan, L. B., Comstock, J. P. and Ehleringer, J. R. (1991). "Comparison of Modeled and Observed Environmental Influences on the Stable Oxygen and Hydrogen Isotope Composition of Leaf Water in *Phaseolus vulgaris* L." *Plant Physiology* **96**: 588-596.
- Flexas, J., Ribas-Carbó, M., Hanson, D. T., Bota, J., Otto, B., Cifre, J., McDowell, N., Medrano, H. and Kaldenhoff, R. (2006). "Tobacco aquaporin NtAQP1 is involved in mesophyll conductance to CO₂ in vivo." *The Plant Journal* **48**: 427-439.
- Flexas, J., Diaz-Esperajo, A., GalmES, J., Kaldenhoff, R., Medrano, H. and Ribas-Carbo, M. (2007). "Rapid variations of mesophyll conductance in response to changes in CO₂ concentration around leaves." *Plant, Cell & Environment* **30**: 1284-1298.
- Flexas, J., Barbour, M. M., Brendel, O., Cabrera, H. M., Carriquí, M., Díaz-Espejo, A., Douthe, C., Dreyer, E., Ferrio, J. P. and Gago, J. (2012). "Mesophyll diffusion conductance to CO₂: An unappreciated central player in photosynthesis." *Plant Science* **193**: 70-84.
- Fischer, C. R., Bowen, B. P., Pan, C., Northen, T. R. and Banfield, J. F. (2013). "Stable-Isotope Probing Reveals That Hydrogen Isotope Fractionation in Proteins and Lipids in a Microbial Community Are Different and Species-Specific." *ACS Chemical Biology* **8**: 1755-1763.
- Fogel, M. L. and Cifuentes, L. A. (1993). *Isotope fractionation during primary production. Organic Geochemistry*, Springer: 73-98.
- Francey, R., Allison, C., Etheridge, D., Trudinger, C., Enting, I., Leuenberger, M., Langenfelds, R., Michel, E. and Steele, L. (1999). "A 1000-year high precision record of $\delta^{13}\text{C}$ in atmospheric CO₂." *Tellus B* **51**: 170-193.
- Franke, R. and Schreiber, L. (2007). "Suberin—a biopolyester forming apoplastic plant

- interfaces." *Current Opinion in Plant Biology* **10**: 252-259.
- Freeman, K. H. and Colarusso, L. A. (2001). "Molecular and isotopic records of C₄ grassland expansion in the late miocene." *Geochimica et Cosmochimica Acta* **65**: 1439-1454.
- Funnell, B. M., Boomer, I. and Jones, R. (2000). "Holocene evolution of the Blakeney Spit area of the North Norfolk coastline." *Proceedings of the Geologists' Association* **111**: 205-217.
- Furbank, R. T. and Taylor, W. C. (1995). "Regulation of photosynthesis in C₃ and C₄ plants: a molecular approach." *The Plant Cell* **7**: 797.
- Gao., L., Burnier, A., Huang, Y. (2012) Quantifying instantaneous regeneration rates of plant leaf waxes using stable hydrogen isotope labelling. *Rapid Communications in Mass Spectrometry*, **26**, 115–122
- Garcés, R. and Mancha, M. (1993). "One-step lipid extraction and fatty acid methyl esters preparation from fresh plant tissues." *Analytical biochemistry* **211**: 139-143.
- Garcin, Y., Schwab, V. F., Gleixner, G., Kahmen, A., Todou, B., Sene, O., Onana, J. M., Achoundong, G., Sachse, D. (2012) Hydrogen isotope ratios of lacustrine sedimentary n-alkanes as proxies of tropical African hydrology: insights from a calibration transect across Cameroon. *Geochimica et Cosmochimica Acta*, **79**, 106-126.
- Gehrels, W. R., Belknap, D. F. and Kelley, J. T. (1996). "Integrated high-precision analyses of Holocene relative sea-level changes: lessons from the coast of Maine." *Geological Society of America Bulletin* **108**: 1073-1088.
- Gerzabek, M. H., Mohamad, S. A. and Muck, K. (1992). "Cesium-137 in soil texture fractions and its impact on cesium-137 soil-to-plant transfer." *Communications in Soil Science & Plant Analysis* **23**: 321-330.
- Glenn, E. P., Nelson, S. G., Ambrose, B., Martinez, R., Soliz, D., Pabendinskas, V. and Hultine, K. (2012). "Comparison of salinity tolerance of three *Atriplex* spp. in well-watered and drying soils." *Environmental and Experimental Botany* **83**: 62-72.
- Good, A. G. and Zaplachinski, S. T. (1994). "The effects of drought stress on free amino acid accumulation and protein synthesis in *Brassica napus*." *Physiologia Plantarum* **90**: 9-14.
- Gosling, W. D., Mayle, F. E., Tate, N. J. and Killeen, T. J. (2009). "Differentiation between Neotropical rainforest, dry forest, and savannah ecosystems by their modern pollen spectra and implications for the fossil pollen record." *Review of Palaeobotany and Palynology* **153**: 70-85.
- Griffiths, H. and Helliker, B. R. (2013). "Mesophyll conductance: internal insights of leaf carbon exchange." *Plant, Cell & Environment* **36**: 733-735.
- Griffiths, H., Weller, G., Toy, L. F. and Dennis, R. J. (2013). "You're so vein: bundle sheath physiology, phylogeny and evolution in C₃ and C₄ plants." *Plant, Cell & Environment* **3**: 249-261.
- Grossi, V. and Raphael, D. (2003). "Long-chain (C₁₉–C₂₉) 1-chloro- *n*-alkanes in leaf waxes of halophytes of the Chenopodiaceae." *Phytochemistry* **63**: 693-698.
- Guy, R. D. and Wample, R. L. (1984). "Stable carbon isotope ratios of flooded and nonflooded sunflowers (*Helianthus annuus*)." *Canadian Journal of Botany* : 1770-1774.
- Guy, R. D., Reid, D. M. and Krouse, H. R. (1986). "Factors affecting ¹³C/¹²C ratios of inland halophytes. I: Controlled studies on growth and isotopic composition of *Puccinellia nuttalliana*." *Canadian Journal of Botany* **64**: 2693-2699.
- Haddadchi, A., Nosrati, K. and Ahmadi, F. (2014). "Differences between the source contribution of bed material and suspended sediments in a mountainous agricultural

- catchment of western Iran." *CATENA* **116**: 105-113.
- Handley, L. and Raven, J. A. (1992). "The use of natural abundance of nitrogen isotopes in plant physiology and ecology." *Plant, Cell & Environment* **15**: 965-985.
- Handley, L., Austin, A., Stewart, G., Robinson, D., Scrimgeour, C., Raven, J. and Schmidt, S. (1999). "The ^{15}N natural abundance ($\delta^{15}\text{N}$) of ecosystem samples reflects measures of water availability." *Functional Plant Biology* **26**: 185-199.
- Handley, L., Pearson, P. N., McMillan, I. K. and Pancost, R. D. (2008). "Large terrestrial and marine carbon and hydrogen isotope excursions in a new Paleocene/Eocene boundary section from Tanzania." *Earth and Planetary Science Letters* **275**: 17-25.
- Hare, P. and Cress, W. (1997). "Metabolic implications of stress-induced proline accumulation in plants." *Plant Growth Regulation* **21**: 79-102
- Hare, P., Cress, W. and Van Staden, J. (1998). "Dissecting the roles of osmolyte accumulation during stress." *Plant, Cell & Environment* **21**: 535-553.
- Harwood, J. L. (1988). "Fatty acid metabolism." *Annual Review of Plant Physiology and Plant Molecular Biology* **39**: 101-138.
- Harwood, J. L. (1998). *Plant Lipid Biosynthesis: Fundamentals and Agricultural Applications*, Cambridge University Press.
- Hatch, M. D. (1992). "C4 photosynthesis: an unlikely process full of surprises." *Plant and Cell Physiology* **33**: 333-342.
- Hayes, J. M. (2001). "Fractionation of carbon and hydrogen isotopes in biosynthetic processes." *Reviews in mineralogy and geochemistry* **43**: 225-277.
- Hayes, J., Freeman, K. H., Popp, B. N. and Hoham, C. H. (1990). "Compound-specific isotopic analyses: A novel tool for reconstruction of ancient biogeochemical processes." *Organic Geochemistry* **16**: 1115-1128.
- He, Q. and Walling, D. (1996). "Interpreting particle size effects in the adsorption of ^{137}Cs and unsupported ^{210}Pb by mineral soils and sediments." *Journal of Environmental Radioactivity* **30**: 117-137.
- He, Q. and Walling, D. (1997). "The distribution of fallout ^{137}Cs and ^{210}Pb in undisturbed and cultivated soils." *Applied Radiation and Isotopes* **48**: 677-690.
- Helliker, B., Ehleringer, J. (2002). Differential ^{18}O enrichment of leaf cellulose in C3 versus C4 grasses. *Functional Plant Biology* **29**, 435-442.
- Hellings, S. E. and Gallagher, J. L. (1992). "The Effects of Salinity and Flooding on *Phragmites australis*." *Journal of Applied Ecology* **29**: 41-49.
- Herold, A. and Lewis, D. H. (1977). "Mannose and Green Plants: Occurrence, Physiology and Metabolism, and Use as a Tool to Study the Role of Orthophosphate." *New Phytologist* **79**: 1-40.
- Hilkert, A., Douthitt, C., Schluter, H., Brand, W. 1999. Isotope ratio monitoring gas chromatography/mass spectrometry of D/H by high temperature conversion isotope ratio mass spectrometry. *Rapid Communications in Mass Spectrometry* **13**, 1226-1230.
- Hill, M, Mountford, J. , Roy, D., Bunce, R. 1999 ECOFACT 2a Technical Annex 490 - Ellenberg's indicator values for British Plants. DETR.
- Hill, M. O., Roy, D. B., Mountford, J. O. and Bunce, R. G. H. (2000). "Extending Ellenberg's indicator values to a new area: an algorithmic approach." *Journal of Applied Ecology* **37**: 3-15.
- Hobbie, E., Werner, R.(2004). "Intramolecular, compound specific, and bulk carbon isotope patterns in C3 and C4 plants: a review and synthesis." *New Phytologist* **161**: 371-385.

- Holloway, P. J. (1982). Structure and histochemistry of plant cuticular membranes: an overview. *The Plant Cuticle*. D. F. Cutler, Alvin, K. L., Price, C. E. New York, Academic Press: 1 - 32.
- Holst, I., Moreno, J. E. and Piperno, D. R. (2007). "Identification of teosinte, maize, and *Tripsacum* in Mesoamerica by using pollen, starch grains, and phytoliths." *Proceedings of the National Academy of Sciences* **104**: 17608-176
- Hoover, R. (2001) "Composition, molecular structure, and physicochemical properties of tuber and root starches: a review". *Carbohydrate Polymers*, **45**: 253-267.
- Hostettler, C., Kölling, K., Santelia, D., Streb, S., Kötting, O. and Zeeman, S. C. (2011). Analysis of starch metabolism in chloroplasts. *Chloroplast Research in Arabidopsis*, Springer: 387-410.
- Hou, J., D'Andrea, W. J. and Huang, Y. (2008). "Can sedimentary leaf waxes record D/H ratios of continental precipitation? Field, model, and experimental assessments." *Geochimica et Cosmochimica Acta* **72**: 3503-3517.
- Hou, J., D'Andrea, W. J., MacDonald, D. and Huang, Y. (2007). "Hydrogen isotopic variability in leaf waxes among terrestrial and aquatic plants around Blood Pond, Massachusetts (USA)." *Organic Geochemistry* **38**: 977-984.
- Hren, M. T., Pagani, M., Erwin, D. M. and Brandon, M. (2010). "Biomarker reconstruction of the early Eocene paleotopography and paleoclimate of the northern Sierra Nevada." *Geology* **38**: 7-10.
- Huang, Y. a., Street-Perrott, F. A., Metcalfe, S. E., Brenner, M., Moreland, M. and Freeman, K. (2001). "Climate change as the dominant control on glacial-interglacial variations in C3 and C4 plant abundance." *Science* **293**: 1647-1651.
- Huang, Y., Dupont, L., Sarnthein, M., Hayes, J. M. and Eglinton, G. (2000). "Mapping of C4 plant input from North West Africa into North East Atlantic sediments." *Geochimica et Cosmochimica Acta* **64**: 3505-3513.
- Huang, Y., Shuman, B., Wang, Y. and Webb, T. (2002). "Hydrogen isotope ratios of palmitic acid in lacustrine sediments record late Quaternary climate variations." *Geology* **30**: 1103.
- Huang, Y., Street-Perrott, F. A., Perrott, R. A., Metzger, P. and Eglinton, G. (1999). "Glacial-interglacial environmental changes inferred from molecular and compound-specific $\delta^{13}\text{C}$ analyses of sediments from Sacred Lake, Mt. Kenya." *Geochimica et Cosmochimica Acta* **63**: 1383-1404.
- Huber, C. G., Timperio, A.-M. and Zolla, L. (2001). "Isoforms of photosystem II antenna proteins in different plant species revealed by liquid chromatography-electrospray ionization mass spectrometry." *Journal of Biological Chemistry* **276**: 45755-45761.
- Jacob, J., Huang, Y., Disnar, J., Sifeddine, A., Boussafir, M., Albuquerque, A., Turcq, B. (2007) "Paleohydrological changes during the last deglaciation in Northern Brazil". *Quaternary Science Reviews*, **26**: 1004-1015.
- Jackson, A. L., Inger, R., Bearhop, S. and Parnell, A. (2009). "Erroneous behaviour of MixSIR, a recently published Bayesian isotope mixing model: a discussion of Moore & Semmens (2008)." *Ecology Letters* **12**(3): E1-E5.
- Jefferies, R. (1977). "Growth responses of coastal halophytes to inorganic nitrogen." *The Journal of Ecology*. **65** 847-865.
- Jefferies, R. and Perkins, N. (1977). "The effects on the vegetation of the additions of inorganic nutrients to salt marsh soils at Stiffkey, Norfolk." *The Journal of Ecology*. **65** 867-882.

- Jeffree, C. E. (2006). The fine structure of the plant cuticle. *Biology of the plant cuticle*. M. Riederer, Müller, C. Oxford, Blackwell Publishing: 11 - 144.
- Jeffries, R. (1977) Growth responses of coastal halophytes to inorganic nitrogen. *The Journal of Ecology*. **65**, 847-865.
- Jeffries, R., Perkins, N. (1977) The effects on the vegetation of the additions of inorganic nutrients to salt marsh soils at Stiffkey, Norfolk. *Journal of Ecology*. **65**, 867-882.
- Jensen, A. (1985). "The effect of cattle and sheep grazing on salt-marsh vegetation at Skallingen, Denmark." *Vegetatio* **60**: 37-48.
- Jetter, R. and Schäffer, S. (2001). "Chemical composition of the *Prunus laurocerasus* leaf surface. Dynamic changes of the epicuticular wax film during leaf development." *Plant Physiology* **126**: 1725-1737.
- Jetter, R., Schäffer, S. and Riederer, M. (2000). "Leaf cuticular waxes are arranged in chemically and mechanically distinct layers: evidence from *Prunus laurocerasus* L." *Plant, Cell & Environment* **23**: 619-628.
- Jetter, R., Schäffer, S. (2006) Chemical composition of the *Prunus laurocerasus* leaf surface. Dynamic changes of the epicuticular wax film during leaf development. *Plant Physiology*, **126**: 1725 – 1737.
- Johnson, D. A., Richards, R. A. and Turner, N. C. (1983). "Yield, water relations, gas exchange, and surface reflectances of near-isogenic wheat lines differing in glaucousness." *Crop Science* **23**: 318-325.
- Johnston, D. T., Farquhar, J., Wing, B. A., Kaufman, A. J., Canfield, D. E. and Habicht, K. S. (2005). "Multiple sulfur isotope fractionations in biological systems: a case study with sulfate reducers and sulfur disproportionators." *American Journal of Science* **305**: 645-660.
- Jones, P., Osborn, T. and Briffa, K. (2001). "The evolution of climate over the last millennium." *Science* **292**: 662-667.
- Kahmen, A., Simonin, K., Tu, K., Merchant, A., Callister, A., Siegwolf, R., Dawson, T., Arndt, S. (2008) Effects of environmental parameters, leaf physiological properties and leaf water relations on leaf water ¹⁸O enrichment in different *Eucalyptus* species, *Plant Cell Environment*. **31**, 738-751.
- Kahmen, A., Simonin, K., Tu, K., Goldschmidt, G., Dawson, T. (2009) The influence of species and growing conditions on the ¹⁸-O enrichment of leaf water and its impact on 'effective path length'. *New Phytologist*, **184**, 619-630.
- Kahmen, A., Hoffmann, B., Schefuß, E., Arndt, S. K., Cernusak, L. A., West, J. B. and Sachse, D. (2013). "Leaf water deuterium enrichment shapes leaf wax *n*-alkane δD values of angiosperm plants II: Observational evidence and global implications." *Geochimica et Cosmochimica Acta* **111**: 50-63.
- Kahmen, A., Schefuß, E. and Sachse, D. (2013). "Leaf water deuterium enrichment shapes leaf wax *n*-alkane δD values of angiosperm plants I: Experimental evidence and mechanistic insights." *Geochimica et Cosmochimica Acta* **111**: 39-49.
- Kawamura, K., Ishimura, Y. and Yamazaki, K. (2003). "Four years' observations of terrestrial lipid class compounds in marine aerosols from the western North Pacific." *Global Biogeochemical Cycles* **17**: 1003.
- Kiehl, K., Eischeid, I., Gettner, S. and Walter, J. (1996). "Impact of different sheep grazing intensities on salt marsh vegetation in northern Germany." *Journal of Vegetation Science* **7**: 99-106.
- Kirkels, F. M., Jansen, B. and Kalbitz, K. (2013). "Consistency of plant-specific *n*-alkane patterns in plaggens ecosystems: A review." *The Holocene* **23**: 1355-1368.
- Kishor, P., Sangam, S., Amrutha, R., Laxmi, P., Naidu, K., Rao, K., Rao, S., Reddy, K.,

- Theriappan, P., Sreenivasulu, N. (2005) "Regulation of proline biosynthesis, degradation, uptake and transport in higher plants: Its implications in plant growth and abiotic stress tolerance". *Current Science*, **88**: 424-438.
- Kohn, M. J. (2010). "Carbon isotope compositions of terrestrial C3 plants as indicators of (paleo) ecology and (paleo) climate." *Proceedings of the National Academy of Sciences* **107**: 19691-19695.
- Kolattukudy, P. (1970). "Biosynthesis of cuticular lipids." *Annual Review of Plant Physiology* **21**: 163-192.
- Kolattukudy, P. E. and Liu, T.-Y. J. (1970). "Direct evidence for biosynthetic relationships among hydrocarbons, secondary alcohols and ketones in Brassica oleracea." *Biochemical and Biophysical Research Communications* **41**: 1369-1374.
- Kolattukudy, P. E., Buckner, J. S. and Liu, T.-Y. J. (1973). "Biosynthesis of secondary alcohols and ketones from alkanes." *Archives of Biochemistry and Biophysics* **156**: 613-620.
- Kriwoken, L. K., Hedge, P. (2000) Exotic species and estuaries: managing *Spartina anglica* in Tasmania, Australia. *Ocean Coast. Management* **43**, 573-584.
- Kromdijk, J., Ubierna, N., Cousins, A. B. and Griffiths, H. (2014). "Bundle-sheath leakiness in C4 photosynthesis: a careful balancing act between CO₂ concentration and assimilation." *Journal of Experimental Botany*. doi: 10.1093/jxb/eru157
- Kruger, N. J. and von Schaewen, A. (2003). "The oxidative pentose phosphate pathway: structure and organisation." *Current Opinion in Plant Biology* **6**: 236-246.
- Kunst, L. and Samuels, A. L. (2003). "Biosynthesis and secretion of plant cuticular wax." *Progress in Lipid Research* **42**: 51-80.
- Kunst, L. and Samuels, L. (2009). "Plant cuticles shine: advances in wax biosynthesis and export." *Current Opinion in Plant Biology* **12**: 721-727.
- Kuypers, M. M., Pancost, R. D. and Damste, J. S. S. (1999). "A large and abrupt fall in atmospheric CO₂ concentration during Cretaceous times." *Nature* **399**: 342-345.
- Ladd, S. and Sachs, J. P. (2012). "Inverse relationship between salinity and *n*-alkane δD values in the mangrove *Avicennia marina*." *Organic Geochemistry* **48**: 25-36.
- Ladd, S. N. and Sachs, J. P. (2013). "Positive correlation between salinity and *n*-alkane δ¹³C values in the mangrove *Avicennia marina*." *Organic Geochemistry* **64**: 1-8.
- Lalli, C., Parsons, T. (1997) *Biological Oceanography: an Introduction*. Butterworth Heinman, 320 pages
- Lamont, B., Groom, P., Cowling, R. (2002) High leaf mass per area of related species assemblages may reflect low rainfall and carbon isotope discrimination rather than low phosphorus and nitrogen concentrations. *Functional Ecology* **16**: 403-412.
- Layman, C. A., Araujo, M. S., Boucek, R., Hammerschlag-Peyer, C. M., Harrison, E., Jud, Z. R., Matich, P., Rosenblatt, A. E., Vaudo, J. J. and Yeager, L. A. (2012). "Applying stable isotopes to examine food-web structure: an overview of analytical tools." *Biological Reviews* **87**: 545-562.
- Leaney, F., Osmond, C., Allison, G. and Ziegler, H. (1985). "Hydrogen-isotope composition of leaf water in C3 and C4 plants: its relationship to the hydrogen-isotope composition of dry matter." *Planta* **164**: 215-220.
- Leider, A., Hinrichs, K.-U., Schefuß, E. and Versteegh, G. J. (2013). "Distribution and stable isotopes of plant wax derived *n*-alkanes in lacustrine, fluvial and marine surface sediments along an Eastern Italian transect and their potential to reconstruct the hydrological cycle." *Geochimica et Cosmochimica Acta* **117**: 16-32.

- Lichtenthaler, H. K. (1999). "The 1-deoxy-D-xylulose-5-phosphate pathway of isoprenoid biosynthesis in plants." *Annual review of plant biology* **50**: 47-65.
- Lichtfouse, E., Elbisser, B., Balesdent, J., Mariotti, A. and Bardoux, G. (1994). "Isotope and molecular evidence for direct input of maize leaf wax n-alkanes into crop soils." *Organic Geochemistry* **22**: 349-351.
- Lissner, J. and Schierup, H.-H. (1997). "Effects of salinity on the growth of *Phragmites australis*." *Aquatic botany* **55**: 247-260.
- Little, C. (2000) *The Biology of Soft Shores and Estuaries*. Oxford University Press, 264 pages
- Liu, W. and Huang, Y. (2005). "Compound specific D/H ratios and molecular distributions of higher plant leaf waxes as novel paleoenvironmental indicators in the Chinese Loess Plateau." *Organic Geochemistry* **36**: 851-860.
- Liu, W. and Yang, H. (2008). "Multiple controls for the variability of hydrogen isotopic compositions in higher plant n-alkanes from modern ecosystems." *Global Change Biology* **14**: 2166-2177.
- Liu, W., Yang, H., Li, L. (2006) Hydrogen isotopic compositions of n-alkanes from terrestrial plants correlate with their ecological life forms. *Oecologia* **150**, 330-338.
- Lockheart, M. J., Van Bergen, P. F. and Evershed, R. P. (1997). "Variations in the stable carbon isotope compositions of individual lipids from the leaves of modern angiosperms: implications for the study of higher land plant-derived sedimentary organic matter." *Organic Geochemistry* **26**: 137-153.
- Loescher, W. (1987) "Physiology and metabolism of sugar alcohols in higher plants". *Physiol. Plantarum*, **70**: 553-557.
- Luo, Y. H., Steinberg, L., Suda, S., Kumazawa, S. and Mitsui, A. (1991). "Extremely low D/H ratios of photoproduced hydrogen by cyanobacteria." *Plant and cell physiology* **32**: 897.
- Macko, S. A., Estep, M. L. F., Engel, M. H. and Hare, P. (1986). "Kinetic fractionation of stable nitrogen isotopes during amino acid transamination." *Geochimica et Cosmochimica Acta* **50**: 2143-2146.
- Macko, S. A., Fogel, M. L., Hare, P. and Hoering, T. (1987). "Isotopic fractionation of nitrogen and carbon in the synthesis of amino acids by microorganisms." *Chemical Geology: Isotope Geoscience section* **65**: 79-92.
- Maffei, M. (1994). "Discriminant analysis of leaf wax alkanes in the Lamiaceae and four other plant families." *Biochemical systematics and ecology* **22**: 711-728.
- Maffei, M. (1996). "Chemotaxonomic significance of leaf wax alkanes in the Gramineae." *Biochemical systematics and ecology* **24**: 53-64
- Maffei, M., Badino, S. and Bossi, S. (2004). "Chemotaxonomic significance of leaf wax n-alkanes in the Pinales (Coniferales)." *Journal of Biological Research* **1**: 3-19.
- Maffei, M., Meregalli, M. and Scannerini, S. (1997). "Chemotaxonomic significance of surface wax n-alkanes in the Cactaceae." *Biochemical systematics and ecology* **25**: 241-253.
- Magill, C. R., Ashley, G. M. and Freeman, K. H. (2013). "Water, plants, and early human habitats in eastern Africa." *Proceedings of the National Academy of Sciences* **110**: 1175-1180.
- Malamud-Roam, F. and Lynn Ingram, B. (2004). "Late Holocene $\delta^{13}\text{C}$ and pollen records of paleosalinity from tidal marshes in the San Francisco Bay estuary, California." *Quaternary Research* **62**: 134-145.
- Mann, M. E., Zhang, Z., Rutherford, S., Bradley, R. S., Hughes, M. K., Shindell, D.,

- Ammann, C., Faluvegi, G. and Ni, F. (2009). "Global signatures and dynamical origins of the Little Ice Age and Medieval Climate Anomaly." *Science* **326**: 1256-1260.
- Mansour, M. (2000) "Nitrogen containing compounds and adaptation of plants to salinity stress". *Biologica Plantarum*, **43**: 491-500.
- Maricle, B. R., Cobos, D. R. and Campbell, C. S. (2007). "Biophysical and morphological leaf adaptations to drought and salinity in salt marsh grasses." *Environmental and Experimental Botany* **60**: 458-467.
- Marseille, F., Disnar, J., Guillet, B. and Noack, Y. (1999). "*n*-Alkanes and free fatty acids in humus and A1 horizons of soils under beech, spruce and grass in the Massif-Central (Mont-Lozère), France." *European Journal of Soil Science* **50**: 433-441.
- Marténez, J. P., Lutts, S., Schanck, A., Bajji, M. and Kinet, J. M. (2004). "Is osmotic adjustment required for water stress resistance in the Mediterranean shrub *Atriplex halimus* L?" *Journal of Plant Physiology* **161**: 1041-1051.
- Mattey, D., Lowry, D., Duffet, J., Fisher, R., Hodge, E. and Frisia, S. (2008). "A 53 year seasonally resolved oxygen and carbon isotope record from a modern Gibraltar speleothem: reconstructed drip water and relationship to local precipitation." *Earth and Planetary Science Letters* **269**: 80-95.
- Mauchamp, A., Mesléard, F. (2001) Salt tolerance in *Phragmites australis* populations from coastal Mediterranean marshes. *Aquatic Botany*, **70**, 39 – 52.
- McCarroll, D. and Loader, N. J. (2004). "Stable isotopes in tree rings." *Quaternary Science Reviews* **23**: 771-801.
- McDermott, F. (2004). "Palaeo-climate reconstruction from stable isotope variations in speleothems: a review." *Quaternary Science Reviews* **23**: 901-918.
- McEvoy, J. P. and Brudvig, G. W. (2006). "Water-splitting chemistry of photosystem II." *Chemical Reviews* **106**: 4455-4483.
- McInerney, F. A., Helliker, B. R. and Freeman, K. H. (2011). "Hydrogen isotope ratios of leaf wax *n*-alkanes in grasses are insensitive to transpiration." *Geochimica et Cosmochimica Acta* **75**: 541-554.
- Meier-Augenstein, W. (1999). "Applied gas chromatography coupled to isotope ratio mass spectrometry." *Journal of Chromatography A* **842**: 351-371.
- Merah, O., Deléens, E., Souyris, I. and Monneveux, P. (2000). "Effect of Glaucousness on Carbon Isotope Discrimination and Grain Yield in Durum Wheat. *Agronomy and Crop Sciences* **185**: 259 - 265
- Meyers, P. A. (1997). "Organic geochemical proxies of paleoceanographic, paleolimnologic, and paleoclimatic processes." *Organic Geochemistry* **27**: 213-250.
- Meyers, P. A. (2003). "Applications of organic geochemistry to paleolimnological reconstructions: a summary of examples from the Laurentian Great Lakes." *Organic Geochemistry* **34**: 261-289.
- Mills, D., Zhang, G. and Benzioni, A. (2001). "Effect of different salts and of ABA on growth and mineral uptake in Jojoba shoots grown *in vitro*" *Journal of Plant Physiology* **158**: 1031-1039.
- Minden, V., Andratschke, S., Spalke, J., Timmermann, H. and Kleyer, M. (2012). "Plant trait–environment relationships in salt marshes: Deviations from predictions by ecological concepts." *Perspectives in Plant Ecology, Evolution and Systematics*. **14**: 183 – 192.
- Mitsch, W., Gosselink, J. (2000) *Wetlands* (3rd Ed), John Wiley and Sons.
- Miyazaki, T. (2006). *Water Flow in Soils*, Taylor and Francis, 440 pages.

- Moeller, I., Spencert, T. and French, J. (1996). "Wind wave attenuation over saltmarsh surfaces: preliminary results from Norfolk, England." *Journal of Coastal Research*, **12**: 1009-1016.
- Moore, J. W. and Semmens, B. X. (2008). "Incorporating uncertainty and prior information into stable isotope mixing models." *Ecology Letters* **11**: 470-480.
- Mulholland, S. C. (1989). "Phytolith shape frequencies in North Dakota grasses: a comparison to general patterns." *Journal of Archaeological Science* **16**: 489-511.
- Napier, J. A., Haslam, R. P., Beaudoin, F. and Cahoon, E. B. (2014). "Understanding and manipulating plant lipid composition: Metabolic engineering leads the way." *Current Opinion in Plant Biology* **19**: 68-75.
- Naraoka, H., Uehara, T., Hanada, S. and Kakegawa, T. (2010). $\delta^{13}\text{C}$ - δD distribution of lipid biomarkers in a bacterial mat from a hot spring in Miyagi Prefecture, NE Japan." *Organic Geochemistry* **41**: 398-403.
- Nawrath, C. (2006). "Unraveling the complex network of cuticular structure and function." *Current Opinion in Plant Biology* **9**: 281-287.
- Nelson, N. and Yocum, C. F. (2006). "Structure and function of photosystems I and II." *Annual Review of Plant Biology* **57**: 521-565.
- Nichols, J. E., Booth, R. K., Jackson, S. T., Pendall, E. G. and Huang, Y. (2006). "Paleohydrologic reconstruction based on *n*-alkane distributions in ombrotrophic peat." *Organic Geochemistry* **37**: 1505-1513.
- Nichols, J., Booth, R. K., Jackson, S. T., Pendall, E. G. and Huang, Y. (2010). "Differential hydrogen isotopic ratios of Sphagnum and vascular plant biomarkers in ombrotrophic peatlands as a quantitative proxy for precipitation—evaporation balance." *Geochimica et Cosmochimica Acta* **74**: 1407-1416.
- Niedermeyer, E. M., Schefuß, E., Sessions, A. L., Mulitza, S., Mollenhauer, G., Schulz, M. and Wefer, G. (2010). "Orbital-and millennial-scale changes in the hydrologic cycle and vegetation in the western African Sahel: insights from individual plant wax δD and $\delta^{13}\text{C}$." *Quaternary Science Reviews* **29**: 2996-3005.
- Noble, S. (1990) *Molecular variation between populations of annual halophytes*. Thesis (Ph.D.), University of East Anglia, School of Biological Sciences, 1990
- Nosrati, K., Govers, G., Semmens, B. X. and Ward, E. J. (2014). "A mixing model to incorporate uncertainty in sediment fingerprinting." *Geoderma* **217**: 173-180.
- Nott, C. J., Xie, S., Avsejs, L. A., Maddy, D., Chambers, F. M. and Evershed, R. P. (2000). "*n*-Alkane distributions in ombrotrophic mires as indicators of vegetation change related to climatic variation." *Organic Geochemistry* **31**: 231-235.
- Ogren, W. L. (1984). "Photorespiration: pathways, regulation, and modification." *Annual Review of Plant Physiology* **35**: 415-442.
- O'Leary, M. H. (1988). "Carbon isotopes in photosynthesis." *BioScience* **38**: 328-336.
- Pagani, M., Caldeira, K., Archer, D. and Zachos, J. C. (2006a). "An ancient carbon mystery." *Science* **314**: 1556.
- Pagani, M., Pedentchouk, N., Huber, M., Sluijs, A., Schouten, S., Brinkhuis, H., Damste, J. S. S., Dickens, G. R. and the IODP Expedition 302 Expedition Scientists (2006b) Arctic hydrology during global warming at the Palaeocene/Eocene thermal maximum. *Nature* **442**, 671-675.
- Pancost, R. D. and Boot, C. S. (2004). "The palaeoclimatic utility of terrestrial biomarkers in marine sediments." *Marine Chemistry* **92**: 239-261.
- Pancost, R. D., Baas, M., van Geel, B. and Sinninghe Damsté, J. S. (2002). "Biomarkers as

- proxies for plant inputs to peats: an example from a sub-boreal ombrotrophic bog." *Organic Geochemistry* **33**: 675-690.
- Pardo, L. H. and Nadelhoffer, K. J. (2010). Using nitrogen isotope ratios to assess terrestrial ecosystems at regional and global scales. *Isoscapes*, Springer: 221-249.
- Parducci, L., Matetovici, I., Fontana, S. L., Bennett, K. D., Suyama, Y., Haile, J., Kjær, K. H., Larsen, N. K., Drouzas, A. D. and Willerslev, E. (2013). "Molecular-and pollen-based vegetation analysis in lake sediments from central Scandinavia." *Molecular Ecology* **22**: 3511-3524.
- Parida, A. K. and Das, A. B. (2005). "Salt tolerance and salinity effects on plants: a review." *Ecotoxicology and Environmental Safety* **60**: 324-349.
- Park, R. and Epstein, S. (1960). "Carbon isotope fractionation during photosynthesis." *Geochimica et Cosmochimica Acta* **21**: 110-126.
- Parnell, A., Inger, R., Bearhop, S. and Jackson, A. (2008). "SIAR: stable isotope analysis in R." The Comprehensive R Archive Network) Available at <http://cran.r-project.org/web/packages/siar/index.html> [Verified 15 July 2012].
- Parnell, A. C., Phillips, D. L., Bearhop, S., Semmens, B. X., Ward, E. J., Moore, J. W., Jackson, A. L., Grey, J., Kelly, D. J. and Inger, R. (2013). "Bayesian stable isotope mixing models." *Environmetrics* **24**: 387-399.
- Passioura, J., Ball, M. and Knight, J. (1992). "Mangroves may salinize the soil and in so doing limit their transpiration rate." *Functional Ecology*. **476**-481.
- Pearson, A. and Eglinton, T. I. (2000). "The origin of *n*-alkanes in Santa Monica Basin surface sediment: a model based on compound-specific $\Delta^{14}\text{C}$ and $\delta^{13}\text{C}$ data." *Organic Geochemistry* **31**: 1103-1116.
- Pearson, A., McNichol, A. P., Benitez-Nelson, B. C., Hayes, J. M. and Eglinton, T. I. (2001). "Origins of lipid biomarkers in Santa Monica Basin surface sediment: a case study using compound-specific $\Delta^{14}\text{C}$ analysis." *Geochimica et Cosmochimica Acta* **65**: 3123-3137.
- Pedentchouk, N., Sumner, W., Tipple, B. and Pagani, M. (2008). " $\delta^{13}\text{C}$ and δD compositions of *n*-alkanes from modern angiosperms and conifers: An experimental set up in central Washington State, USA." *Organic Geochemistry* **39**: 1066-1071.
- Phillips, D. L. and Gregg, J. W. (2001). "Uncertainty in source partitioning using stable isotopes." *Oecologia* **127**: 171-179.
- Phillips, D. L. and Gregg, J. W. (2003). "Source partitioning using stable isotopes: coping with too many sources." *Oecologia* **136**: 261-269.
- Phillips, D. L. and Koch, P. L. (2002). "Incorporating concentration dependence in stable isotope mixing models." *Oecologia* **130**: 114-125.
- Piasentier, E., Bovolenta, S. and Malossini, F. (2000). "The *n*-alkane concentrations in buds and leaves of browsed broadleaf trees." *The Journal of Agricultural Science* **135**: 311-320.
- Piperno, D. R. (1985). "Phytolith analysis and tropical paleo-ecology: Production and taxonomic significance of siliceous forms in New World plant domesticates and wild species." *Review of Palaeobotany and Palynology* **45**: 185-228.
- Piperno, D. R. (1991). "The status of phytolith analysis in the American tropics." *Journal of World Prehistory* **5**: 155-191
- Plaster, E. (2009) *Soil Science and Management*(5th Ed). Delmar Cengage Learning, pp. 142 – 165.
- Polissar, P. J. and Freeman, K. H. (2010). "Effects of aridity and vegetation on plant-wax δD in modern lake sediments." *Geochimica et Cosmochimica Acta* **74**: 5785-5797.

- Pollard, M., Beisson, F., Li, Y. and Ohlrogge, J. B. (2008). "Building lipid barriers: biosynthesis of cutin and suberin." *Trends in Plant Science* **13**: 236-246
- Post-Beittenmiller, D. (1996). "Biochemistry and molecular biology of wax production in plants." *Annual review of Plant Biology* **47**: 405-430.
- Pyankov, V. I., Ziegler, H., Akhiani, H., Deigele, C. and Lüttge, U. (2010). "European plants with C4 photosynthesis: geographical and taxonomic distribution and relations to climate parameters." *Botanical Journal of the Linnean Society* **163**: 283-304.
- Pye, K. (1992) Saltmarshes on the barrier coastline of north Norfolk, eastern England. In: Allen, J. R. L & Pye, K. (Eds.) Saltmarshes: Morphodynamics, Conservation and Engineering Significance, pp. 148-179, Cambridge University Press.
- Quade, J., Cerlinga, T. E., Barry, J. C., Morgan, M. E., Pilbeam, D. R., Chivas, A. R., Lee-Thorp, J. A. and van der Merwe, N. J. (1992). "A 16-Ma record of paleodiet using carbon and oxygen isotopes in fossil teeth from Pakistan." *Chemical Geology: Isotope Geoscience section* **94**: 183-192.
- Quemerais, B., Mabon, F., Naullet, N. and Martin, G. (1995). "Site-specific isotope fractionation of hydrogen in the biosynthesis of plant fatty acids." *Plant, Cell & Environment* **18**(9): 989-998.
- Rao, Z., Zhu, Z., Jia, G., Henderson, A. C. G., Xue, Q. and Wang, S. (2009). "Compound specific δD values of long chain n-alkanes derived from terrestrial higher plants are indicative of the $[\delta]D$ of meteoric waters: Evidence from surface soils in eastern China." *Organic Geochemistry* **40**: 922-930.
- Ratnayake, N. P., Suzuki, N., Okada, M. and Takagi, M. (2006). "The variations of stable carbon isotope ratio of land plant-derived n-alkanes in deep-sea sediments from the Bering Sea and the North Pacific Ocean during the last 250,000 years." *Chemical Geology* **228**: 197-208.
- Reina-Pinto, J. J. and Yephremov, A. (2009). "Surface lipids and plant defenses." *Plant Physiology and Biochemistry* **47**: 540-549.
- Reynard, L. and Hedges, R. (2008). "Stable hydrogen isotopes of bone collagen in palaeodietary and palaeoenvironmental reconstruction." *Journal of Archaeological Science* **35**: 1934-1942.
- Rhodes, D., Handa, S. and Bressan, R. A. (1986). "Metabolic changes associated with adaptation of plant cells to water stress." *Plant Physiology* **82**: 890-903.
- Rhodes, D., Nadolska-Orczyk, A. and Rich, P. (2002). Salinity, osmolytes and compatible solutes. In: Lauchli, A., Luttge, U. (Eds) Salinity: Environment-plants-molecules. Kluwer Academic Publishers. pp 181-204.
- Richards, R., Rawson, H. and Johnson, D. (1986). "Glaucousness in Wheat: Its Development and Effect on Water-use Efficiency, Gas Exchange and Photosynthetic Tissue Temperatures*." *Functional Plant Biology* **13**: 465-473.
- Richardson, C. J. (2000) Freshwater wetlands. In: Barbour, M., Billings, W. (Eds) (2000) North American Wetlands. Cambridge University Press, pp. 449 – 501.
- Riederer, M. and Schneider, G. (1990). "The effect of the environment on the permeability and composition of Citrus leaf cuticles." *Planta* **180**: 154-165.
- Riederer, M. and Schreiber, L. (2001). "Protecting against water loss: analysis of the barrier properties of plant cuticles." *Journal of Experimental Botany* **52**: 2023-2032.
- Ripullone, F., Matsuo, N., Stuart-Williams, H., Wong, S. C., Borghetti, M., Tani, M. and Farquhar, G. (2008). "Environmental effects on oxygen isotope enrichment of leaf water in cotton leaves." *Plant Physiology* **146**: 729-736.

- Ritchie, J. C. and McCarty, G. W. (2003). "137Cesium and soil carbon in a small agricultural watershed." *Soil and Tillage Research* **69**(1): 45-51.
- Roderick M. L. and Cochrane M. J. (2002) On the conservative nature of the leaf mass–area relationship. *Annals of Botany*. **89**, 537– 542.
- Roeske, C. A. and O'Leary, M. H. (1984). "Carbon isotope effects on enzyme-catalyzed carboxylation of ribulose bisphosphate." *Biochemistry* **23**(25): 6275-6284.
- Romero, I., C., Feakins, S. J. (2011) Spatial gradients in plant leaf wax D/H across a coastal salt marsh in southern California. *Organic Geochem.* **42**, 618-629.
- Rommerskirchen, F., Plader, A., Eglinton, G., Chikaraishi, Y. and Rullkötter, J. (2006). "Chemotaxonomic significance of distribution and stable carbon isotopic composition of long-chain alkanes and alkan-1-ols in C4 grass waxes." *Organic Geochemistry* **37**: 1303-1332.
- Rowell, D. (1994) *Soil Science: Methods and Applications*. Routledge, 360 pages.
- Royles, J., Ogée, J., Wingate, L., Hodgson, D. A., Convey, P. and Griffiths, H. (2012). "Carbon isotope evidence for recent climate-related enhancement of CO₂ assimilation and peat accumulation rates in Antarctica." *Global Change Biology* **18**: 3112-3124.
- Sachse, D., Billault, I., Bowen, G., Chikaraishi, Y., Dawson, T., Feakins, S., Freeman, K., Magill, C., McInerney, F., van der Meer, M., Polissar, P., Robins, R., Sachs, J., Schmidt, H., Sessions, A., White, J., West, J., Kahmen, A. (2012) Molecular paleohydrology: interpreting the hydrogen-isotopic composition of lipid biomarkers from photosynthesising organisms. *Annual Review Earth Planetary Science* **40**, 221-249.
- Sachse, D., Gleixner, G., Wilkes, H., Kahmen, A. (2010) Leaf wax n-alkane δ D values of field-grown barley reflect leaf water δ D values at the time of leaf formation. *Geochim. Cosmochim. Acta* **74**, 6741-6750.
- Sachse, D., Radke, J. and Gleixner, G. (2004). "Hydrogen isotope ratios of recent lacustrine sedimentary n-alkanes record modern climate variability." *Geochimica et Cosmochimica Acta* **68**: 4877-4889.
- Sachse, D., Radke, J. and Gleixner, G. (2006). " δ D values of individual n-alkanes from terrestrial plants along a climatic gradient - Implications for the sedimentary biomarker record." *Organic Geochemistry* **37**: 469-483.
- Samuels, L., Kunst, L. and Jetter, R. (2008). "Sealing plant surfaces: cuticular wax formation by epidermal cells." *Plant Biology* **59**: 683.
- Šantrůček, J., Květoň, J., Šetlík, J. and Bulíčková, L. (2007). "Spatial variation of deuterium enrichment in bulk water of snowgum leaves." *Plant Physiology* **143**: 88-97.
- Sarker, D., Halder, A. (2005) *Physical and Chemical Methods in Soil Analysis*. New Age International Publishers, 192 pages.
- Sauer, P. E., Eglinton, T. I., Hayes, J. M., Schimmelmann, A. and Sessions, A. L. (2001). "Compound-specific D/H ratios of lipid biomarkers from sediments as a proxy for environmental and climatic conditions." *Geochimica et Cosmochimica Acta* **65**: 213-222.
- Saurer, M., Siegwolf, R. T. W. and Schweingruber, F. H. (2004). "Carbon isotope discrimination indicates improving water-use efficiency of trees in northern Eurasia over the last 100 years." *Global Change Biology* **10**: 2109-2120.
- Schatz, A.-K., Zech, M., Buggle, B., Gulyás, S., Hambach, U., Marković, S. B., Sümegi, P. and Scholten, T. (2011). "The late Quaternary loess record of Tokaj, Hungary: Reconstructing palaeoenvironment, vegetation and climate using stable C and N isotopes and biomarkers." *Quaternary International* **240**: 52-61.

- Schefuß, E., Ratmeyer, V., Stuu, J.-B. W., Jansen, J. and Sinninghe Damsté, J. S. (2003). "Carbon isotope analyses of *n*-alkanes in dust from the lower atmosphere over the central eastern Atlantic." *Geochimica et Cosmochimica Acta* **67**: 1757-1767.
- Schefuß, E., Schouten, S. and Schneider, R. R. (2005). "Climatic controls on central African hydrology during the past 20,000 years." *Nature* **437**: 1003-1006.
- Schefuß, E., Kuhlmann, H., Mollenhauer, G., Prange, M. and Pätzold, J. (2011). "Forcing of wet phases in southeast Africa over the past 17,000 years." *Nature* **480**: 509-512.
- Schirmer, A., Rude, M. A., Li, X., Popova, E. and del Cardayre, S. B. (2010). "Microbial Biosynthesis of Alkanes." *Science* **329**: 559-562.
- Schirmer, U., Breckle, S. (1982) The role of bladders for salt removal in some Chenopodiaceae (mainly *Atriplex* species). In: Sen, D., Rajpurohit, K. (Eds.) (1982) *Tasks for vegetation science 2: Contributions to the ecology of halophytes*, Dr W Junk Publishers, pp 215-231.
- Schmidt, G. A. (2010). "Enhancing the relevance of palaeoclimate model/data comparisons for assessments of future climate change." *Journal of Quaternary Science* **25**: 79-87.
- Schmidt, H. L., Werner, R. A. and Eisenreich, W. (2003). "Systematics of ²H patterns in natural compounds and its importance for the elucidation of biosynthetic pathways." *Phytochemistry Reviews* **2**: 61-85.
- Schmittner, A., Urban, N. M., Shakun, J. D., Mahowald, N. M., Clark, P. U., Bartlein, P. J., Mix, A. C. and Rosell-Mele, A. (2011). "Climate sensitivity estimated from temperature reconstructions of the Last Glacial Maximum." *Science* **334**: 1385-1388.
- Schröder, H. K., Kiehl, K. and Stock, M. (2002). "Directional and non-directional vegetation changes in a temperate salt marsh in relation to biotic and abiotic factors." *Applied Vegetation Science* **5**: 33-44.
- Schwender, J., Ohlrogge, J. and Shachar-Hill, Y. (2004). "Understanding flux in plant metabolic networks." *Current Opinion in Plant Biology* **7**: 309-317.
- Seibt, U., Rajabi, A., Griffiths, H. and Berry, J. A. (2008). "Carbon isotopes and water use efficiency: sense and sensitivity." *Oecologia* **155**: 441-454.
- Seki, O., Meyers, P. A., Kawamura, K., Zheng, Y. and Zhou, W. (2009). "Hydrogen isotopic ratios of plant wax *n*-alkanes in a peat bog deposited in northeast China during the last 16kyr." *Organic Geochemistry* **40**: 671-677.
- Sessions, A. L. (2006). "Seasonal changes in D/H fractionation accompanying lipid biosynthesis in *Spartina alterniflora*." *Geochimica et Cosmochimica Acta* **70**: 2153-2162.
- Sessions, A., Burgoyne, T., Schimmelfmann, A. and Hayes, J. (1999). "Fractionation of hydrogen isotopes in lipid biosynthesis." *Organic Geochemistry* **30**: 1193-1200.
- Shani, U. and Dudley, L. (2001). "Field studies of crop response to water and salt stress." *Soil Science Society of America Journal* **65**: 1522-1528.
- Sharkey, T. D. (2012). "Mesophyll conductance: constraint on carbon acquisition by C3 plants." *Plant, Cell & Environment* **35**: 1881-1883.
- Sharkey, T. D., Kobza, J., Seemann, J. R. and Brown, R. H. (1988). "Reduced cytosolic fructose-1, 6-bisphosphatase activity leads to loss of O₂ sensitivity in a *Flaveria linearis* mutant." *Plant Physiology* **86**: 667-671.
- Shepherd, T. and Wynne Griffiths, D. (2006). "The effects of stress on plant cuticular waxes." *New Phytologist* **171**: 469-499.
- Shepherd, T., Robertson, G., Griffiths, D., Birch, A. and Duncan, G. (1995). "Effects of environment on the composition of epicuticular wax from kale and swede." *Phytochemistry* **40**: 407-417.

- Shindell, D. T., Schmidt, G. A., Mann, M. E., Rind, D. and Waple, A. (2001). "Solar forcing of regional climate change during the Maunder Minimum." *Science* **294**: 2149-2152.
- Shu, Y., Feng, X., Posmentier, E. S., Sonder, L. J., Faiia, A. M., Yakir, D. (2008) Isotopic studies of leaf water. Part 1: A physically based two-dimensional model for pine needles. *Geochimica et Cosmochimica Acta* **72**, 5175-5188.
- Shuman, B., Huang, Y., Newby, P. and Wang, Y. (2006). "Compound-specific isotopic analyses track changes in seasonal precipitation regimes in the Northeastern United States at ca 8200calyrBP." *Quaternary Science Reviews* **25**: 2992-3002.
- Silva, K. M. M. d., Agra, M. d. F., Santos, D. Y. A. C. d. and Oliveira, A. F. M. d. (2012). "Leaf cuticular alkanes of *Solanum* subg. *Leptostemonum* Dunal (Bitter) of some northeast Brazilian species: Composition and taxonomic significance." *Biochemical Systematics and Ecology* **44**: 48-52.
- Simoneit, B. R., Sheng, G., Chen, X., Fu, J., Zhang, J. and Xu, Y. (1991). "Molecular marker study of extractable organic matter in aerosols from urban areas of China." *Atmospheric Environment*. **25**: 2111-2129.
- Sinninghe Damsté, J. S., Verschuren, D., Ossebaar, J., Blokker, J., van Houten, R., van der Meer, M. T. J., Plessen, B. and Schouten, S. (2011). "A 25,000-year record of climate-induced changes in lowland vegetation of eastern equatorial Africa revealed by the stable carbon-isotopic composition of fossil plant leaf waxes." *Earth and Planetary Science Letters* **302**: 236-246.
- Sluijs, A., Schouten, S., Pagani, M., Woltering, M., Brinkhuis, H., Damsté, J. S. S., Dickens, G. R., Huber, M., Reichert, G.-J., Stein, R., Matthiessen, J., Lourens, L. J., Pedentchouk, N., Backman, J., Moran, K. and the Expedition, S. (2006). "Subtropical Arctic Ocean temperatures during the Palaeocene/Eocene thermal maximum." *Nature* **441**: 610-613.
- Smith, D., Mayes, R. and Raats, J. (2001). "Effect of species, plant part, and season of harvest on n-alkane concentrations in the cuticular wax of common rangeland grasses from southern Africa." *Crop and Pasture Science* **52**: 875-882.
- Smith, F. A. and Freeman, K. H. (2006). "Influence of physiology and climate on δD of leaf wax n-alkanes from C3 and C4 grasses." *Geochimica et Cosmochimica Acta* **70**: 1172-1187.
- Smith, F. A., Wing, S. L. and Freeman, K. H. (2007). "Magnitude of the carbon isotope excursion at the Paleocene–Eocene thermal maximum: The role of plant community change." *Earth and Planetary Science Letters* **262**: 50-65.
- Soepboer, W., Sugita, S., Lotter, A. F., van Leeuwen, J. F. and van der Knaap, W. O. (2007). "Pollen productivity estimates for quantitative reconstruction of vegetation cover on the Swiss Plateau." *The Holocene* **17**: 65-77.
- Song, J., Shi, G., Xing, S., Yin, C., Fan, H. and Wang, B. (2009). "Ecophysiological responses of the euhalophyte *Suaeda salsa* to the interactive effects of salinity and nitrate availability." *Aquatic botany* **91**: 311-317.
- Song, X., Barbour, M. M., Farquhar, G. D., Vann, D. R. and Helliker, B. R. (2013). "Transpiration rate relates to within-and across-species variations in effective path length in a leaf water model of oxygen isotope enrichment." *Plant, Cell & Environment* **36**: 1338-1351.
- Sønstebø, J., Gielly, L., Brysting, A., Elven, R., Edwards, M., Haile, J., Willerslev, E., Coissac, E., Rioux, D. and Sannier, J. (2010). "Using next-generation sequencing for molecular reconstruction of past Arctic vegetation and climate." *Molecular Ecology Resources* **10**: 1009-1018.
- Sternberg, L. and Deniro, M. J. (1983). "Isotopic composition of cellulose from C3, C4, and CAM plants growing near one another." *Science* **220**: 947-949.

- Sternberg, L. D. S., Deniro, M. J. and Johnson, H. B. (1986). "Oxygen and hydrogen isotope ratios of water from photosynthetic tissues of CAM and C3 plants." *Plant Physiology* **82**: 428-431.
- Sternberg, L. O. R., Deniro, M. J. and Ting, I. P. (1984). "Carbon, hydrogen, and oxygen isotope ratios of cellulose from plants having intermediary photosynthetic modes." *Plant Physiology* **74**: 104.
- Stobart, A., Henry, G. (1984) "The turnover of chlorophyll in greening wheat leaves". *Phytochemistry*, **23**: 27-30.
- Suh, M. C., Samuels, A. L., Jetter, R., Kunst, L., Pollard, M., Ohlrogge, J. and Beisson, F. (2005). "Cuticular lipid composition, surface structure, and gene expression in Arabidopsis stem epidermis." *Plant Physiology* **139**: 1649-1665.
- Szabados, L. and Savouré, A. (2010). "Proline: a multifunctional amino acid." *Trends in Plant Science* **15**: 89-97.
- Taiz, L., Ziegler, E. (2010). *Plant Physiology*, Sinauer Associates, Inc.
- Tan, W. B., Wang, G. A., Han, J. M., Liu, M., Zhou, L. P., Luo, T., Cao, Z. Y. and Cheng, S. Z. (2009). " $\delta^{13}\text{C}$ and water-use efficiency indicated by $\delta^{13}\text{C}$ of different plant functional groups on Changbai Mountains, Northeast China." *Chinese Science Bulletin* **54**: 1759-1764.
- Tanner, B. R., Uhle, M. E., Kelley, J. T. and Mora, C. I. (2007). " C_3/C_4 variations in salt-marsh sediments: An application of compound specific isotopic analysis of lipid biomarkers to late Holocene paleoenvironmental research." *Organic Geochemistry* **38** 474-484.
- Tanner, B. R., Uhle, M. E., Mora, C. I., Kelley, J. T., Schuneman, P. J., Lane, C. S. and Allen, E. S. (2010). "Comparison of bulk and compound-specific $\delta^{13}\text{C}$ analyses and determination of carbon sources to salt marsh sediments using n-alkane distributions (Maine, USA)." *Estuarine, Coastal and Shelf Science* **86**: 283-291.
- Tazoe, Y., Von Caemmerer, S., Estavillo, G. M. and Evans, J. R. (2011). "Using tunable diode laser spectroscopy to measure carbon isotope discrimination and mesophyll conductance to CO_2 diffusion dynamically at different CO_2 concentrations." *Plant, Cell & Environment* **34**: 580-591.
- Tcherkez, G. and Farquhar, G. D. (2005). "Viewpoint: Carbon isotope effect predictions for enzymes involved in the primary carbon metabolism of plant leaves." *Functional Plant Biology* **32**: 277-291.
- Tcherkez, G., Mahé, A. and Hodges, M. (2011). " $^{12}\text{C}/^{13}\text{C}$ fractionations in plant primary metabolism." *Trends in Plant Science* **16**(9): 499-506.
- Tester, R., Karkalas, J., Qi, X. (2004) "Starch – composition, fine structure and architecture". *Journal of Cereal Science*, **39**: 151-165.
- Terwilliger, V. J., Eshetu, Z., Disnar, J.-R., Jacob, J., Paul Adderley, W., Huang, Y., Alexandre, M. and Fogel, M. L. (2013). "Environmental changes and the rise and fall of civilizations in the northern Horn of Africa: An approach combining δD analyses of land-plant derived fatty acids with multiple proxies in soil." *Geochimica et Cosmochimica Acta* **111**: 140-161.
- Thevs, N., Zerbe, S., Gahlert, F., Midjit, M., Succow, M. (2007) Productivity of reed (*Phragmites australis* Trin. ex Steud.) in continental-arid NW China in relation to soil, groundwater, and land-use. *J. App. Bot. Food Sci.* **81**, 62-68.
- Tholen, D., Ethier, G., Genty, B., Pepin, S. and ZHU, X. G. (2012). "Variable mesophyll conductance revisited: theoretical background and experimental implications." *Plant, Cell & Environment* **35**: 2087-2103.
- Thompson, L. G., Mosley-Thompson, E., Davis, M. E., Lin, P.-N., Henderson, K. and

- Mashiotta, T. A. (2003). Tropical glacier and ice core evidence of climate change on annual to millennial time scales. *Climate Variability and Change in High Elevation Regions: Past, Present & Future*, Springer: 137-155.
- Tierney, J. E., Russell, J. M., Huang, Y., Damsté, J. S. S., Hopmans, E. C. and Cohen, A. S. (2008). "Northern hemisphere controls on tropical Southeast African climate during the past 60,000 years." *Science* **322**: 252.
- Tierney, J. E., Oppo, D. W., Rosenthal, Y., Russell, J. M. and Linsley, B. K. (2010). "Coordinated hydrological regimes in the Indo-Pacific region during the past two millennia." *Paleoceanography* **25** (1).
- Tierney, J., Russell, J., Huang Y. (2010) A molecular perspective on Late Quaternary climate and vegetation change in the Lake Tanganyika basin, East Africa. *Quaternary Science Reviews*, **29**, 787 – 800
- Tierney, J. E., Lewis, S. C., Cook, B. I., LeGrande, A. N. and Schmidt, G. A. (2011). "Model, proxy and isotopic perspectives on the East African Humid Period." *Earth and Planetary Science Letters* **307**: 103-112.
- Tierney, J. E., Russell, J. M., Sinninghe Damsté, J. S., Huang, Y. and Verschuren, D. (2011). "Late Quaternary behavior of the East African monsoon and the importance of the Congo Air Boundary." *Quaternary Science Reviews* **30**: 798-807.
- Tierney, J. E., DeMenoacal, P. B. (2013). "Abrupt Shifts in Horn of Africa Hydroclimate Since the Last Glacial Maximum." *Science* **342**: 843-846.
- Tipple, B. J. and Pagani, M. (2007). "The early origins of terrestrial C4 photosynthesis." *Annu. Rev. Earth Planet. Sci.* **35**: 435-461.
- Tipple, B. J., Meyers, S. R. and Pagani, M. (2010). "Carbon isotope ratio of Cenozoic CO₂: A comparative evaluation of available geochemical proxies." *Paleoceanography* **25**(3).
- Tipple, B. J., Pagani, M., Krishnan, S., Dirghangi, S. S., Galeotti, S., Agnini, C., Giusberti, L. and Rio, D. (2011). "Coupled high-resolution marine and terrestrial records of carbon and hydrologic cycles variations during the Paleocene–Eocene Thermal Maximum (PETM)." *Earth and Planetary Science Letters* **311**: 82-92.
- Tipple, B., Berke, M., Doman, C., Khachatryan, S., Ehleringer, J. (2013). Leaf-wax *n*-alkanes record the plant-water environment at leaf flush. *Proceedings of the National Academy of Sciences* **110**, 2659-2664.
- Tipple, B., Pagani, M. (2013) Environmental control on eastern broadleaf forest species' leaf wax distributions and D/H ratios. *Geochimica et Cosmochimica Acta*, **111**, 64-77.
- Tischler, C. and Burson, B. (1995). "Evaluating different bahiagrass cytotypes for heat tolerance and leaf epicuticular wax content." *Euphytica* **84**: 229-235.
- Ubierna, N., Farquhar, G. (2014) "Advances in measurements and models of photosynthetic carbon isotope discrimination in C₃ plants". *Plant, Cell and Environment*, **37**: 1494 – 1498.
- UK Meteorological Office. Met Office Integrated Data Archive System (MIDAS) Land and Marine Surface Stations Data (1853-current), NCAS British Atmospheric Data Centre, 2012, 10th March 2013; Available from http://badc.nerc.ac.uk/view/badc.nerc.ac.uk_ATOM_dataent_ukmo-midas
- Ullrich, W. R. (2002). Salinity and nitrogen nutrition. *Salinity: Environment - Plants - Molecules*. A. Lauchli, Luttge, U. Dordrecht, Boston, London, , Kluwer Academic Publishers. pp. 229-248. .
- Ungar, I. A. and Woodell, S. R. J. (1996). "Similarity of Seed Banks to Aboveground Vegetation in Grazed and Ungrazed Salt Marsh Communities on the Gower Peninsula, South Wales." *International Journal of Plant Sciences* **157**: 746-749.
- Vadez, V., Kholova, J., Medina, S., Kakkera, A. and Anderberg, H. (2014). "Transpiration

efficiency: new insights into an old story." *Journal of Experimental Botany*. doi: 0.1093/jxb/eru040

Valentine, D. L. (2009). "Isotopic remembrance of metabolism past." *Proceedings of the National Academy of Sciences* **106**: 12565-12566.

Van Dongen, J. T., Gupta, K. J., Ramírez-Aguilar, S. J., Araújo, W. L., Nunes-Nesi, A. and Fernie, A. R. (2011). "Regulation of respiration in plants: a role for alternative metabolic pathways." *Journal of Plant Physiology* **168**: 1434-1443.

Van Rampelbergh, M., Fleitmann, D., Verheyden, S., Cheng, H., Edwards, L., De Geest, P., De Vleeschouwer, D., Burns, S. J., Matter, A. and Claeys, P. (2013). "Mid-to late Holocene Indian Ocean Monsoon variability recorded in four speleothems from Socotra Island, Yemen." *Quaternary Science Reviews* **65**: 129-142.

van Soelen, E., Wagner-Cremer, F., Sinninghe-Damsté., J., Reichart, G. (2013) Reconstructing tropical cyclone frequency using hydrogen isotope ratios of sedimentary n-alkanes in northern Queensland, Australia. *Palaeogeography, Palaeoclimatology, Palaeoecology*, **376**, 66 – 72.

VandenBygaart, A. (2001). "Erosion and deposition history derived by depth-stratigraphy of ¹³⁷Cs and soil organic carbon." *Soil and Tillage Research* **61**: 187-192.

Veeneklaas, R. M., Dijkema, K. S., Hecker, N. and Bakker, J. P. (2013). "Spatio-temporal dynamics of the invasive plant species *Elytrigia atherica* on natural salt marshes." *Applied Vegetation Science* **16**: 205-216.

Veneklaas, R., Bockelmann, A., Reusch, T. B. and Bakker, J. (2011). "Effect of grazing and mowing on the clonal structure of *Elytrigia atherica*: a long-term study of abandoned and managed sites." *Preslia* **83**: 455-470.

Vimeux, F., Ginot, P., Schwikowski, M., Vuille, M., Hoffmann, G., Thompson, L. G. and Schotterer, U. (2009). "Climate variability during the last 1000 years inferred from Andean ice cores: A review of methodology and recent results." *Palaeogeography, Palaeoclimatology, Palaeoecology* **281**: 229-241

Vince, S. W., Snow, A. A. (1984) Plant zonation in an Alaskan salt marsh: I. Distribution, abundance and environmental factors. *Journal of Ecology*. **72**, 651-667.

Vogel, J. (2008). "Unique aspects of the grass cell wall." *Current Opinion in Plant Biology* **11**: 301-307.

Vogts, A., Moossen, H., Rommerskirchen, F. and Rullkötter, J. (2009). "Distribution patterns and stable carbon isotopic composition of alkanes and alkan-1-ols from plant waxes of African rain forest and savanna C3 species." *Organic Geochemistry* **40**: 1037-1054.

Volkmar, K., Hu, Y. and Steppuhn, H. (1998). "Physiological responses of plants to salinity: a review." *Canadian Journal of Plant Science* **78**: 19-27.

Von Caemmerer, S. v. and Farquhar, G. (1981). "Some relationships between the biochemistry of photosynthesis and the gas exchange of leaves." *Planta* **153**: 376-387.

von Wettstein-Knowles, Penny (July 2012) Plant Waxes. In: eLS. John Wiley & Sons, Ltd: Chichester. DOI: 10.1002/9780470015902.a0001919.pub2

Voznesenskaya, E. V., Franceschi, V. R., Chuong, S. D. X. and Edwards, G. E. (2006). "Functional characterization of phosphoenolpyruvate carboxykinase-type C4 leaf anatomy: immuno-, cytochemical and ultrastructural analyses." *Annals of Botany* **98**: 77-91.

Waisel, Y. 1972. Biology of halophytes, Academic Press, California.

Wang, N., Zong, Y., Brodie, C. R. and Zheng, Z. (2014). "An examination of the fidelity of n-alkanes as a palaeoclimate proxy from sediments of Palaeolake Tianyang, South China." *Quaternary International* **333**: 100-109.

Wang, X. C., Chen, R. F. and Berry, A. (2003). "Sources and preservation of organic matter in Plum Island salt marsh sediments (MA, USA): long-chain *n*-alkanes and stable carbon isotope compositions." *Estuarine, Coastal and Shelf Science* **58**: 917-928.

Wang, Y., Griffin, P., Jin, K., Fogel, M. L., Steele, A. and Cody, G. D. (2013). "Tracing H isotope effects in the dynamic metabolic network using multi-nuclear (^1H / ^2H and ^{13}C) solid state NMR and GC-MS." *Organic Geochemistry* **57**: 84-94.

Wasternack, C. (2007). "Jasmonates: an update on biosynthesis, signal transduction and action in plant stress response, growth and development." *Annals of Botany* **100**(4): 681-697.

Watanabe, N. (1994). "Near-isogenic lines of durum wheat: their development and plant characteristics." *Euphytica* **72**: 143-147.

Werner, R. A., Buchmann, N., Siegwolf, R. T., Kornexl, B. E. and Gessler, A. (2011). "Metabolic fluxes, carbon isotope fractionation and respiration—lessons to be learned from plant biochemistry." *New Phytologist* **191**: 10-15.

West, A. G., Patrickson, S. J., Ehleringer, J. R. (2006) Water extraction times for plant and soil materials used in stable isotope analysis. *Rapid Commun. Mass. Sp.* **20**, 1317-1321.

White JWC (1988) Stable hydrogen isotope ratios in plants: A review of current theory and some potential applications. In: PW Rundel, JR Ehleringer, KA Nagy, eds, *Stable Isotopes in Ecological Research*. Springer-Verlag, Berlin, pp 142-162

Willerslev, E., Davison, J., Moora, M., Zobel, M., Coissac, E., Edwards, M. E., Lorenzen, E. D., Vestergård, M., Gussarova, G. and Haile, J. (2014). "Fifty thousand years of Arctic vegetation and megafaunal diet." *Nature* **506**: 47-51.

Williamson, J. D., Jennings, D. B., Guo, W.-W., Pharr, D. M. and Ehrenshaft, M. (2002). "Sugar Alcohols, Salt Stress, and Fungal Resistance: Polyols—Multifunctional Plant Protection?" *Journal of the American Society for Horticultural Science* **127**: 467-473.

Wong, S. C., Cowan, I. R. and Farquhar, G. D. (1985). "Leaf conductance in relation to rate of CO₂ assimilation: III. Influences of water stress and photoinhibition." *Plant Physiology* **78**: 830.

Yakir, D. (1992). "Variations in the natural abundance of oxygen-18 and deuterium in plant carbohydrates." *Plant, Cell & Environment* **15**: 1005-1020.

Yakir D (1998) Oxygen-18 of leaf water: a crossroad for plant-associated isotopic signals. In H Griffiths, ed, *Stable Isotopes: Integration of Biological and Geochemical Processes*. BIOS Scientific Publishers, Oxford, pp 147–168

Yamada, K. and Ishiwatari, R. (1999). "Carbon isotopic compositions of long-chain *n*-alkanes in the Japan Sea sediments: implications for paleoenvironmental changes over the past 85 kyr." *Organic Geochemistry* **30**: 367-377.

Yamamoto, S., Hasegawa, T., Tada, R., Goto, K., Rojas-Consuegra, R., Díaz-Otero, C., García-Delgado, D. E., Yamamoto, S., Sakuma, H. and Matsui, T. (2010). "Environmental and vegetational changes recorded in sedimentary leaf wax *n*-alkanes across the Cretaceous-Paleogene boundary at Loma Capiro, Central Cuba." *Palaeogeography, Palaeoclimatology, Palaeoecology* **295**: 31-41.

Yang, H. and Huang, Y. (2003). "Preservation of lipid hydrogen isotope ratios in Miocene lacustrine sediments and plant fossils at Clarkia, northern Idaho, USA." *Organic Geochemistry* **34**: 413-423.

Zachos, J. C., Röhl, U., Schellenberg, S. A., Sluijs, A., Hodell, D. A., Kelly, D. C., Thomas, E., Nicolo, M., Raffi, I. and Lourens, L. J. (2005). "Rapid acidification of the ocean during the Paleocene-Eocene thermal maximum." *Science* **308**: 1611-1615.

Zech, M., Andreev, A., Zech, R., MÜLLER, S., Hambach, U., Frechen, M. and Zech, W.

- (2010). "Quaternary vegetation changes derived from a loess-like permafrost palaeosol sequence in northeast Siberia using alkane biomarker and pollen analyses." *Boreas* **39**: 540-550.
- Zech, M., Pedentchouk, N., Buggle, B., Leiber, K., Kalbitz, K., Marković, S. B. and Glaser, B. (2011). "Effect of leaf litter degradation and seasonality on D/H isotope ratios of *n*-alkane biomarkers." *Geochimica et Cosmochimica Acta* **75**: 4917-4928.
- Zhang, B. L., Quemerais, B., Martin, M. L., Martin, G. J. and Williams, J. M. (1994). "Determination of the natural deuterium distribution in glucose from plants having different photosynthetic pathways." *Phytochemical Analysis* **5**: 105-110.
- Zhang, X., Gillespie, A. L. and Sessions, A. L. (2009). "Large D/H variations in bacterial lipids reflect central metabolic pathways." *Proceedings of the National Academy of Sciences* **106**: 12580-12586.
- Zhang, Z. and Sachs, J. P. (2007). "Hydrogen isotope fractionation in freshwater algae: I. Variations among lipids and species." *Organic Geochemistry* **38**: 582-608.
- Zhang, Z., Zhao, M., Eglinton, G., Lu, H. and Huang, C. (2006). "Leaf wax lipids as paleovegetational and paleoenvironmental proxies for the Chinese Loess Plateau over the last 170 kyr." *Quaternary Science Reviews* **25**: 575-594.
- Zhou, W., Xie, S., Meyers, P. and Zheng, Y. (2005). "Reconstruction of late glacial and Holocene climate evolution in southern China from geolipids and pollen in the Dingnan peat sequence." *Organic Geochemistry* **36**: 1272-1284.
- Zhou, W., Xie, S., Meyers, P. and Zheng, Y. (2005). "Reconstruction of late glacial and Holocene climate evolution in southern China from geolipids and pollen in the Dingnan peat sequence." *Organic Geochemistry* **36**: 1272-1284.
- Zhou, W., Zheng, Y., Meyers, P. A., Jull, A. and Xie, S. (2010). "Postglacial climate-change record in biomarker lipid compositions of the Hani peat sequence, Northeastern China." *Earth and Planetary Science Letters* **294**: 37-46
- Zhou, Y., Grice, K., Stuart-Williams, H., Farquhar, G. D., Hocart, C. H., Lu, H. and Liu, W. (2010). "Biosynthetic origin of the saw-toothed profile in $\delta^{13}\text{C}$ and $\delta^2\text{H}$ of *n*-alkanes and systematic isotopic differences between *n*-, iso- and anteiso-alkanes in leaf waxes of land plants." *Phytochemistry* **71**: 388-403.
- Zhu, J.-K. (2001). "Plant salt tolerance." *Trends in Plant Science* **6**: 66-71.
- Zhu, J.-K. (2002). "Salt and drought stress signal transduction in plants." *Annual review of Plant Biology* **53**: 247.
- Zolla, L., Rinalducci, S., Timperio, A. M. and Huber, C. G. (2002). "Proteomics of light-harvesting proteins in different plant species. Analysis and comparison by liquid chromatography-electrospray ionization mass spectrometry. Photosystem I." *Plant Physiology* **130**: 1938-1950.
- Zolla, L., Timperio, A.-M., Walcher, W. and Huber, C. G. (2003). "Proteomics of light-harvesting proteins in different plant species. Analysis and comparison by liquid chromatography-electrospray ionization mass spectrometry. Photosystem II." *Plant Physiology* **131**: 198-214.
- Zygadlo, J. A., Maestri, D. M. and Grosso, N. R. (1994). "Alkane distribution in epicuticular wax of some Solanaceae species." *Biochemical Systematics and Ecology* **22**: 203-209.

APPENDIX 1

CONFERENCE ABSTRACTS ARISING FROM THIS THESIS

In Chronological order from 2011

European Geosciences Union, Vienna, 2011

Geophysical Research Abstracts
Vol. 13, EGU2011-361-2, 2011
EGU General Assembly 2011
© Author(s) 2011

Molecular and isotopic composition of organic compounds from higher plants: a useful tool for forensic provenancing? (Poster presentation)

Yvette Eley (1,2), Nikolai Pedentchouk (1), Jurian Hoogewerff (2), Lorna Dawson (3), and Alexandra Guedes (4)

(1) School of Environmental Sciences, University of East Anglia, Norwich, United Kingdom, (2) School of Chemistry, University of East Anglia, Norwich, United Kingdom, (3) The Macaulay Land Use Research Institute, Craigiebuckler, Aberdeen, United Kingdom, (4) Centro de Geologia e Departamento de Geociências, Ambiente e Ordenamento do Território, Faculdade de Ciências, Universidade do Porto, Porto, Portugal

Soil is a common trace evidential material recovered during forensic casework, and is therefore a vital source of investigative information. Previous research has shown that relative distributions of well-preserved long-chain n- alkanes in soils, originating from the epicuticular waxes of higher plants, can be related to overlying vegetation (Lichtfouse et al., 1994) and thus may provide a method for linking a soil sample to a location of interest (Dawson et al., 2004): In addition, wax marker profiles can be useful for the identification of vegetation fragments on questioned items. However, such molecular distribution patterns have limited discriminatory potential between individual plant species, as most distributions of n-alkanes show a considerable degree of overlap in the range of n-C25 to C33(Buggle et al., 2010).

Despite the potential for organic compounds to assist in the discrimination of soils, compound specific isotopic analysis of biomarkers remains unexploited. D/H ratios of plant n-alkanes are related regional environmental water via leaf water from which they are biosynthesised (Sachse et al., 2010). This relationship allows for allocation of geographical locations through the use of predictable isotopic ratios of global precipitation (Bowen et al., 2007). Examination of ¹³C/¹²C signatures reflects factors such as soil moisture availability (Pedentchouk et al., 2008) and photosynthetic pathway. In conjunction, these isotopic signatures display a degree of species-specific discrimination (Pedentchouk et al., 2008).

This project combines analysis of molecular structure with ¹³C/¹²C and D/H signatures of *Triticum* spp (wheat), *Sorghum bicolor* (Sorghum), *Zea mays* (maize) and *Oryza sativa* (rice) and their host soils at a range of specific locations. These grass species have been selected on the basis of their environmental importance as a natural groundcover and their widespread global use in agriculture. To ensure that study sites cover a wide range of climatic zones, soils sampled from Europe as part of the TRACE project (<http://www.trace.eu.org>), supplemented by study sites in Scotland (in association with the Macaulay Institute) and Portugal(in association with the University of Porto), will be analysed. Differential preservation rates of n-alkanes among soil particle-size fractions (Cayet and Lichtfouse, 2001), and the influence of soil types and climate on n-alkane soil profiles will also be evaluated. The results of isotopic analysis of n-alkanes in combination with their molecular distributions will provide crucial information for determining the discriminatory potential of these biomarkers in soil for forensic applications.

International Network of Environmental Forensics (INEF), Cambridge, July 2011

Tracing plant inputs to sediments: a combined isotopic and molecular forensic approach

(Oral presentation; Joint First Prize for best student oral presentation)

Yvette Eley (1,2), Nikolai Pedentchouk (1), Lorna Dawson (2).

(1) School of Environmental Sciences, University of East Anglia, Norwich, United Kingdom, (2) The James Hutton Research Institute, Craigiebuckler, Aberdeen, United Kingdom

The relationship between surface vegetation and organic material contained within soils and sediments can represent an important source of information when attempting to link a questioned soil sample, taken as part of a forensic investigation to a location of interest. Previous research has shown that molecular parameters of well-preserved, long-chain *n*-alkanes from epicuticular waxes of higher plants are well preserved in soils and represent an opportunity to reconstruct a surface vegetation profile which may assist in sourcing sample origin. However, molecular distribution data alone often fails to provide species-specific information, as patterns of *n*-alkanes can overlap among different plant types.

Compound-specific stable isotopic analysis of plant and soil long-chain *n*-alkanes has been shown to provide greater resolution when seeking to discriminate between plant species, although studies seeking to characterise the molecular and isotopic *n*-alkane profile of vegetation and sediments in a particular location to ascertain the power of this multi-method approach are limited. Here we present *n*-alkane molecular, $\delta^{13}\text{C}$ and δD data from plant and sediment samples taken from four locations ranging from sand flat to high marsh, at a salt marsh near Stiffkey on the north Norfolk coast. This site contains both C_3 and C_4 grasses (*Spartina anglica* and *Elytrigia atherica*), along with succulent species (*Suaeda vera*), and angiosperms (such as *Limonium vulgare* and *Atriplex portulacoides*). We observed differences of $>10\text{‰}$ among species with respect to *n*-alkane $\delta^{13}\text{C}$, and up to 20‰ when considering *n*-alkane δD .

Statistical analysis of sediment samples taken from different locations within Stiffkey salt marsh demonstrates that they reflect the isotopic and molecular distributions of the dominant higher plant species in that location. These characteristics could potentially be mapped to create a predictive model for plant biomarkers in marsh sediments at the site. Our study shows that a combined analytical approach to *n*-alkane analysis in a forensic context could enhance the resolution of surface vegetation reconstruction and thus improve the ability to provenance soils. Because the dominant species identified at Stiffkey are common at coastal sites around the UK and in Europe, a thorough understanding of their molecular and stable isotopic composition would prove valuable on a national and international scale.



Development of Isotopic Proxies for Palaeoenvironmental Interpretation: A Carbon Perspective (DIPPI-C), Durham, 2012

Compound-specific carbon isotope variation among plant functional types at Stiffkey saltmarsh, the north Norfolk coast: Implications for plant ecology and palaeoclimatology (Poster presentation)

Yvette Eley (1), Nikolai Pedentchouk (1), Julian Andrews (1)

1 School of Environmental Sciences, University of East Anglia,

Palaeoclimate studies of fossil plant material employing $\delta^{13}\text{C}$ measurements traditionally focus either on the variation in the ^{13}C content of organic material as a record of the $^{13}\text{C}/^{12}\text{C}$ composition of atmospheric CO_2 , or the distribution of C_3 vs. C_4 vegetation to infer broad-scale climatic shifts. The development of compound-specific isotope techniques has allowed for increased resolution of information available from plant $\delta^{13}\text{C}$ data. However, studies that investigate the influence of biotic and abiotic factors on terrestrial plant biomarkers across a range of plant functional types (PFTs) are still limited.

We present leaf-wax n-alkyl lipid $\delta^{13}\text{C}$ data from an ongoing project studying the most dominant higher plant species (C_3 and C_4 grasses; succulents; evergreens) at Stiffkey saltmarsh. We observe large intraseasonal variations in n-alkane $\delta^{13}\text{C}$ values, which range from 0.6 to 6‰. The pattern of carbon isotope fractionation at specific micro-environmental zones within the marsh is related to PFT. This study will evaluate the extent to which the varied responses of PFTs to edaphic factors across the study site influence the carbon isotope signatures of leaf wax biomarkers used in palaeoclimate studies. Additionally, these data will further our understanding of plant potential responses to ecological and environmental changes in the future.

23rd Meeting of the British Organic Geochemical Society,
Leeds, 2012

δD values of leaf waters and n -alkanes from C_3 and C_4 plants at Stiffkey salt marsh, Norfolk, UK: Implications for understanding the factors that control D/H composition of leaf wax lipids

(Oral presentation; First Prize for best student oral presentation)

Eley, Y.¹, Pedentchouk, N.¹, Andrews, J.¹

¹ University of East Anglia, School of Environmental Sciences, Norwich Research Park, Norwich, Norfolk, NR4 7TJ, UK.

y.eley@uea.ac.uk

Interest in n -alkyl lipids as biomarkers of palaeoclimatological and palaeohydrological regimes has intensified as a result of advances in compound-specific hydrogen stable isotope analysis. Whilst previous studies have demonstrated a link between plant wax δD and the isotopic composition of source water, mechanisms responsible for the variation in n -alkyl lipid δD values observed among plant species at individual locations remain poorly understood.

To evaluate the role of various environmental, physiological and biochemical factors on the D/H composition of n -alkyl lipids, we analysed a range of C_3 and C_4 plants from 3 locations within a salt marsh in the UK. The D/H composition of leaf water did not vary by more than $\sim 30\text{‰}$, while that of individual n -alkanes differed by as much as $\sim 100\text{‰}$ among various plant species, resulting in an interspecies range in the $\epsilon_{\text{wax/lw}}$ values of -140 to -220‰ . (Fig.1).

Because mechanisms leading to variation in environmental water, plant water uptake, and leaf water isotopic composition could not explain the range of n -alkane δD values, we propose that additional biochemical

mechanisms, including variation in the D/H composition of substrates used for lipid biosynthesis represents an additional source of species-specific hydrogen isotope variation. Results of this study suggest that an integrated physical and biochemical approach is required to account for the patterns observed in the D/H composition of modern plants and plant biomarkers in modern and ancient sediments.

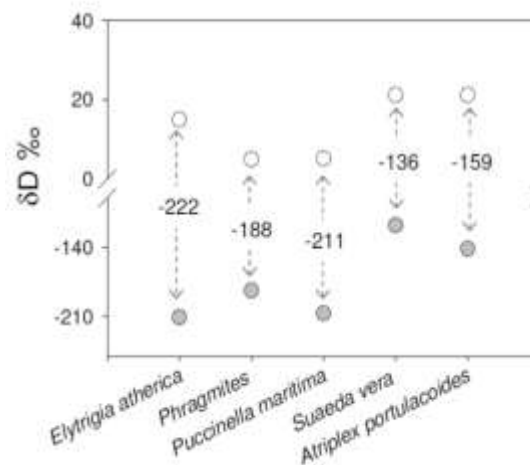


Figure 1: Measured δD_{lw} (white circles) and $\delta D_{n\text{-C}_{29}}$ (grey circles) for a range of saltmarsh plants, showing calculated D/H fractionation values ($\epsilon_{\text{wax/lw}}$ ‰) for each species. Standard error was $< 1\text{‰}$ for leaf water and $< 5\text{‰}$ for n -alkane analyses.

24th Meeting of the British Organic Geochemical Society, Plymouth, 2013

Hydrogen isotope systematics of *n*-alkanes from Stiffkey saltmarsh (Oral presentation)

Eley, Y., Pedentchouk, N.

¹ University of East Anglia, School of Environmental Sciences, Norwich Research Park,
Norwich, Norfolk, NR4 7TJ, UK.

Interpretation of sedimentary *n*-alkyl lipid $\delta^2\text{H}$ data is complicated by a limited understanding of factors controlling interspecies variation in biomarker $^2\text{H}/^1\text{H}$ composition. Previous research has sought to explain any differences in $\delta^2\text{H}$ values among plant species by reference to the physical processes that control the movement of water molecules inside/outside and within the leaf. However, the relative importance of biochemical differences on the $^2\text{H}/^1\text{H}$ ratio of leaf wax lipids extracted from morphologically distinct plant species growing at the same location remains largely unexplored. To distinguish between the effects of interrelated environmental, physical and biochemical controls on the hydrogen isotope composition of *n*-alkyl lipids, we conducted $\delta^2\text{H}$ analysis of soil, xylem, and leaf waters and *n*-alkanes from a range of C_3 and C_4 plants growing at a UK saltmarsh (i) across multiple sampling sites, (ii) throughout the 2012 growth season, and (iii) at different times of the day.

Our results show that soil water $^2\text{H}/^1\text{H}$ varied by up to 35‰ with marsh sub-environment, and exhibited site-specific seasonal shifts up to a maximum of 31‰. Maximum interspecies variation in xylem water was 38‰, while leaf waters differed seasonally by a maximum of 29‰. Leaf wax *n*-alkane $^2\text{H}/^1\text{H}$, however, consistently varied by over 100‰ throughout the 2012 growth season, resulting in an interspecies range in the $\epsilon_{\text{wax/lw}}$ values of -79 to -227‰. From the discrepancy in the magnitude of these isotopic differences, we conclude that mechanisms driving variation in the $^2\text{H}/^1\text{H}$ composition of leaf water, including (i) spatial changes in soil water $^2\text{H}/^1\text{H}$, (ii) temporal changes in soil water $^2\text{H}/^1\text{H}$, (iii) differences in xylem water $^2\text{H}/^1\text{H}$ (reflecting any fractionation occurring during root uptake), and (iv) differences in leaf water evaporative ^2H -enrichment due to varied plant life forms, cannot explain the range of *n*-alkane $\delta^2\text{H}$ values we observed.

Our on-going work seeks to identify key biochemical processes that may account for interspecies variation in leaf lipid $^2\text{H}/^1\text{H}$. Analysis of chloroplast-bound phytol will allow us to investigate whether the potential existence of different NADPH pools influences the $\delta^2\text{H}$ of compounds synthesized in different plant compartments. Examination of starch $^2\text{H}/^1\text{H}$ will help us determine whether variation in carbohydrate recycling may explain the range of lipid $\delta^2\text{H}$ in key species at our site. Finally, we will examine whether seasonal changes in leaf wax composition, including the nature and amount of precursor compounds, affect the *n*-alkyl $^2\text{H}/^1\text{H}$ signal. This research will allow us to further explore the role of $^2\text{H}/^1\text{H}$ fractionation during biosynthesis of leaf lipids and to assess the importance of this fractionation when explaining the variation in *n*-alkane $^2\text{H}/^1\text{H}$ composition among different plant species.

American Geophysical Union, San Francisco, December 2013

Hydrogen isotope systematics in C₃ and C₄ saltmarsh plants: the importance of biochemical processes in controlling interspecies variation in *n*-alkane ²H/¹H composition (Oral presentation)

Eley, Y., Pedentchouk, N.

University of East Anglia, School of Environmental Sciences, Norwich, NR7 4TJ, UK
y.eley@uea.ac.uk

Palaeohydrological studies have increasingly utilised the ²H/¹H composition of leaf wax *n*-alkyl lipids to extract information from the geological record. Interpretation of the sedimentary biomarker δ²H signal, however, requires detailed understanding of the mechanisms controlling hydrogen isotope fractionation between source water and *n*-alkyl lipids (ε/w). The existence of large ranges in published *n*-alkyl δ²H and ε/w among modern plant species growing at a single location suggests that the lipid signal incorporated into the sedimentary record could be sensitive to relatively small-scale changes in vegetation assemblages. The mechanisms responsible for these interspecies differences are currently poorly constrained. Previous research has had limited success explaining *n*-alkyl δ²H by reference to physical processes controlling the movement of water inside/outside and within the leaf, while the relative importance of biochemical processes remains largely unexplored.

This project aims to identify the mechanisms controlling interspecies variation in *n*-alkane ²H/¹H among a range of C₃ and C₄ plants from a Norfolk saltmarsh in the UK. To distinguish between environmental, physical and biochemical controls, we conducted ²H/¹H analysis of soil, xylem, and leaf waters and *n*-alkanes (i) across multiple sampling sites within the marsh, (ii) throughout the 2012 growth season, and (iii) at different times of the day. We also measured the ²H/¹H of chloroplast phytol in 7 samples collected at the end of 2012. Leaf wax *n*-alkane δ²H varied among the sampled species by over 100‰ throughout the 2012 growth season. Environmental processes that could influence control source water ²H/¹H did not fully account for this interspecies variation - soil water ²H/¹H varied by only 35‰ with marsh sub-environment and exhibited site-specific seasonal shifts by no more than 31‰. Maximum interspecies variation in xylem water was 38‰, while leaf waters differed by only 29‰. We therefore concluded that mechanisms driving variation in the ²H/¹H composition of leaf water are not sufficient to explain the range of *n*-alkane δ²H values we observed in north Norfolk saltmarsh.

Comparison of the relationship between the δ²H of chloroplast phytol and leaf water reveals a strong relationship ($R^2 = 0.7$), while that between the δ²H of *n*-alkanes vs. leaf water ($R^2 = 0.4$) and the δ²H of *n*-alkanes vs. phytol ($R^2 = 0.1$) does not. This implies that the δ²H values of leaf wax *n*-alkanes in some of the plants we have investigated are largely decoupled from the ²H/¹H composition of leaf water and biosynthates in the chloroplast and, instead, are strongly influenced by biochemical process that control NADPH and/or other secondary compounds synthesised in the cytosol. Our data highlight the fact that further research is needed (i) to identify the biochemical mechanisms influencing the δ²H signal of leaf wax *n*-alkyl lipids across a broad range of modern plants, and (ii) to constrain the relationship between these mechanisms and source water ²H/¹H. Only then can the hydrogen isotope information recorded in ancient sediments be fully understood.



Different response of bulk and *n*-alkane $\delta^{13}\text{C}$ signatures to seasonal shifts in environmental conditions in a temperate coastal ecosystem
(Oral presentation)

Yvette Eley (1), Nikolai Pedentchouk (1), and Lorna Dawson (2)

(1) School of Environmental Sciences, University of East Anglia, Norwich NR4 7TJ, UK
(y.eley@uea.ac.uk),

(2) The James Hutton Institute, Craigiebuckler, Aberdeen, AB15 8QH, UK

The carbon isotope signal recorded in land plants represents an important reservoir of information for reconstructing climatically driven shifts in plant ecophysiology and biochemistry. Analytical advances have led to widespread usage of compound-specific (CS) carbon isotope analysis of leaf wax biomarkers, such as *n*-alkanes, in addition to traditional bulk isotope methods, to identify shifts in the relative percentage of C_3 and C_4 vegetation contributing to the sedimentary record. Recent studies, however, have extended the application of leaf wax biomarkers, using bulk and *n*-alkane $\delta^{13}\text{C}$ values interchangeably to derive information about plant-environment relations, both in modern ecosystems and throughout the geological past. Even though previous work on C_3 plants has confirmed that a relationship exists between the biochemistry of photosynthetic activity and environmental conditions (resulting from changes to the balance between photosynthetic demand and stomatal conductance) at the bulk level, further research is needed to establish whether the $^{13}\text{C}/^{12}\text{C}$ composition of leaf wax biomarkers responds to climatic drivers in the same way.

To address this question, we collected bulk and *n*-alkane $\delta^{13}\text{C}$ data from plants growing at Stiffkey marsh on the north Norfolk coast, UK over a period of 15 months. Maximum interspecies variation in weighted average (WA) *n*-alkane $\delta^{13}\text{C}$ among C_3 species was typically 2-3‰ greater than bulk. We observed a close correlation in the bulk and WA *n*-alkane $\delta^{13}\text{C}$ seasonal trends from C_3 grasses and reeds ($R^2=0.9$, $P < 0.05$). However, for other species (including C_3 and C_4 plants), no statistically significant relationship was observed between their respective bulk and WA *n*-alkane carbon isotope values. This variation in $\delta^{13}\text{C}$ trends resulted in considerable intra- and inter-species variability (ranging from -4 to -13‰) in the offset between bulk and WA *n*-alkane $\delta^{13}\text{C}$ values. In addition, we identified a positive correlation ($R^2=0.7$, $P < 0.05$), for all species (with the exception of from *Suaeda vera*) between the relative abundance of the *n*- C_{25} and *n*- C_{27} *n*-alkane homologues and *n*- C_{29} alkane $\delta^{13}\text{C}$ values.

We explain the discrepancy between bulk and *n*-alkane $\delta^{13}\text{C}$ signatures by referring to possible interspecies variation in post-photosynthetic carbon isotope fractionation. Our data imply that for some species, seasonal changes in the abundance of *n*-alkane homologues might be an important biochemical processes influencing *n*-alkane $\delta^{13}\text{C}$ signatures. We further theorise that interspecies variation in *n*-alkane $\delta^{13}\text{C}$ values may arise from biochemical differences in salinity adaptation - in plants adapted to salt stress, the production of osmoregulatory solutes (amino acids and/or carbohydrates) may influence the partitioning of pyruvate to fates other than acetyl-CoA, shifting the isotopic composition of lipid biomarkers. Mechanisms controlling metabolic fluxes through these biochemical processes may therefore potentially exert an additional important control over the $\delta^{13}\text{C}$ signal of lipid biomarkers. We therefore conclude that it may not be valid to use bulk and *n*-alkane $\delta^{13}\text{C}$ data interchangeably to examine plant-environment interactions. These findings open new avenues for empirical studies to further understand the metabolic processes fractionating carbon during the synthesis of leaf wax lipid biomarkers, enhancing interpretation of the biomarker signal from the geological record.

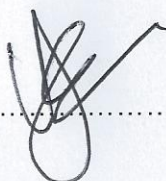
PAPERS ARISING FROM THIS THESIS

Eley, Y., Dawson, L., Black, S., Andrews, J., Pedentchouk, N. (2014) Understanding of $^2\text{H}/^1\text{H}$ systematic of leaf wax *n*-alkanes in coastal plants at Stiffkey saltmarsh, Norfolk, UK. *Geochimica et Cosmochimica Acta*, 128, 13 – 28.

Thesis pages 360 - 375

Statement regarding the ownership of the work presented in this paper:

Yvette Eley carried out all the measurements for this study, interpreted the data, and wrote the paper. The co-authors contributed comments and feedback on the various drafts.



A handwritten signature in black ink, consisting of several overlapping loops and a long horizontal stroke extending to the right, positioned above a dotted line.

Yvette Eley



Understanding $^2\text{H}/^1\text{H}$ systematics of leaf wax *n*-alkanes in coastal plants at Stiffkey saltmarsh, Norfolk, UK

Yvette Eley^{a,*}, Lorna Dawson^b, Stuart Black^c, Julian Andrews^a,
Nikolai Pedentchouk^a

^a School of Environmental Sciences, University of East Anglia, Norwich NR4 7TJ, UK

^b The James Hutton Institute, Craigiebuckler, Aberdeen AB15 8QH, UK

^c Department of Archaeology, School of Archaeology, Geography and Environmental Science, University of Reading, Whiteknights, Shinfield Road, Reading, Berkshire RG6 6AB, UK

Received 23 February 2012; accepted in revised form 26 November 2013; Available online 15 December 2013

Abstract

Interpretation of sedimentary *n*-alkyl lipid $\delta^2\text{H}$ data is complicated by a limited understanding of factors controlling interspecies variation in biomarker $^2\text{H}/^1\text{H}$ composition. To distinguish between the effects of interrelated environmental, physical and biochemical controls on the hydrogen isotope composition of *n*-alkyl lipids, we conducted linked $\delta^2\text{H}$ analyses of soil water, xylem water, leaf water and *n*-alkanes from a range of C_3 and C_4 plants growing at a UK saltmarsh (i) across multiple sampling sites, (ii) throughout the 2012 growing season, and (iii) at different times of the day. Soil waters varied isotopically by up to 35‰ depending on marsh sub-environment, and exhibited site-specific seasonal shifts in $\delta^2\text{H}$ up to a maximum of 31‰. Maximum interspecies variation in xylem water was 38‰, while leaf waters differed seasonally by a maximum of 29‰. Leaf wax *n*-alkane $^2\text{H}/^1\text{H}$, however, consistently varied by over 100‰ throughout the 2012 growing season, resulting in an interspecies range in the $\epsilon_{\text{wax}/\text{leaf water}}$ values of -79‰ to -227‰ . From the discrepancy in the magnitude of these isotopic differences, we conclude that mechanisms driving variation in the $^2\text{H}/^1\text{H}$ composition of leaf water, including (i) spatial changes in soil water $^2\text{H}/^1\text{H}$, (ii) temporal changes in soil water $^2\text{H}/^1\text{H}$, (iii) differences in xylem water $^2\text{H}/^1\text{H}$, and (iv) differences in leaf water evaporative ^2H -enrichment due to varied plant life forms, cannot explain the range of *n*-alkane $\delta^2\text{H}$ values we observed. Results from this study suggests that accurate reconstructions of palaeoclimate regimes from sedimentary *n*-alkane $\delta^2\text{H}$ require further research to constrain those biological mechanisms influencing species-specific differences in $^2\text{H}/^1\text{H}$ fractionation during lipid biosynthesis, in particular where plants have developed biochemical adaptations to water-stressed conditions. Understanding how these mechanisms interact with environmental conditions will be crucial to ensure accurate interpretation of hydrogen isotope signals from the geological record.

© 2013 Elsevier Ltd. All rights reserved.

1. INTRODUCTION

The use of *n*-alkyl lipids to investigate palaeoclimatological and palaeohydrological regimes has received considerable attention in the last decade as a result of initial analytical advances in compound-specific stable

hydrogen isotope methodology (e.g. Hilkert et al., 1999; Meier-Augenstein, 1999). Of particular importance for the utility of these compounds as palaeoclimate proxies is the relationship between their $^2\text{H}/^1\text{H}$ composition and that of environmental water. Previous studies have demonstrated a link between the $\delta^2\text{H}$ values of *n*-alkyl lipids from modern plants and source water across geographically and climatically diverse transects (Huang et al., 2002; Sachse et al., 2004, 2006; Garcin et al., 2012; Tipple and Pagani, 2013; Kahmen et al., 2013b). However, when leaf wax biomarkers

* Corresponding author. Tel.: +44 (0)1603 593990; fax: +44 (0)1603 591327.

E-mail address: y.eley@uea.ac.uk (Y. Eley).

from a range of plant species from the same biosynthetic group at individual locations are considered, significant variation in the $\delta^2\text{H}$ values of *n*-alkyl lipids – of up to 80‰ – have been observed (Sachse et al., 2006; Hou et al., 2007; Pedentchouk et al., 2008; Feakins and Sessions, 2010).

Palaeoclimatic reconstructions of source water isotopic composition (Pagani et al., 2006; Tierney et al., 2008) and moisture availability and aridity (Schefuß et al., 2005; Leider et al., 2013) have often implicitly and/or explicitly relied on the assumption that the biosynthetic $^2\text{H}/^1\text{H}$ fractionation that takes place between the intracellular water and lipids within the plant is relatively invariant within C_3 and C_4 plant groups. The magnitude of variability in the $\delta^2\text{H}$ values of *n*-alkyl lipids among plant species growing at the same geographical location suggests, however, that this assumption may not necessarily be valid. Interpretation of sedimentary *n*-alkyl $\delta^2\text{H}$ data is further complicated by limited understanding of the reasons for this large interspecies variability. Sachse et al. (2012) provided a comprehensive review of the current state of knowledge regarding the factors that control hydrogen isotope composition of lipid biomarkers in photosynthetic organisms. This review highlighted the importance of both physical (mainly through influencing intracellular water $^2\text{H}/^1\text{H}$) and biochemical mechanisms in controlling $^2\text{H}/^1\text{H}$ composition of photosynthates. However, the relative importance of these separate but interrelated controls remains largely unexplored, particularly when morphologically and biochemically distinct plant species growing in a natural environment are considered.

Previous research has mainly focused on using empirical and modelling studies to investigate various physical processes that control source and intracellular water. First, there were studies (e.g. Hou et al., 2007; Pedentchouk et al., 2008) in which a range of plants were considered, but coupled leaf water and *n*-alkane $^2\text{H}/^1\text{H}$ measurements were not conducted. Instead, these studies relied on isotopic measurements of environmental water and leaf wax *n*-alkyl compounds, and any differences in $^2\text{H}/^1\text{H}$ fractionation were explained by reference to the physical processes that controlled the movement of water molecules inside, outside and within the leaf according to leaf-water models (Farquhar and Lloyd, 1993; Barbour et al., 2000, 2004). The implicit assumption of these models (initially developed for understanding oxygen isotope systematics of plant water) is that they can fully describe hydrogen isotope systematics of leaf water, and thus also account for the differences in the $\delta^2\text{H}$ values of leaf wax lipids among different species. The lack of actual measurements of leaf water isotopic composition, however, prevents such studies from evaluating the relative importance of physical and biochemical factors that control leaf water and biosynthate $^2\text{H}/^1\text{H}$ signatures.

Other studies have focused on the analysis of modelled and/or empirical leaf water and *n*-alkyl lipid $^2\text{H}/^1\text{H}$ compositions to avoid the limitations inherent in the above approach. McInerney et al. (2011) examined the impact of relative humidity on leaf wax $\delta^2\text{H}$ by analysing *n*-alkanes from grasses grown both in controlled environmental chambers and across a range of climatically different field

sites. Modelled leaf water $\delta^2\text{H}$ values, however, were more positive than would have been expected from empirical *n*-alkane $\delta^2\text{H}$ data. McInerney et al. (2011) suggested that ^2H -enriched leaf waters were not the biosynthetic precursor for leaf wax synthesis, as the best correlation between source water and lipid $\delta^2\text{H}$ values was obtained though using 100% xylem water. The potential for biochemical mechanisms to explain differences in fractionation between C_3 and C_4 plants was mentioned, but the design of the study did not allow for assessment of its relative importance. Sachse et al. (2010) also focused on monocot species, analysing field-grown barley (*Hordeum vulgare*) across one growing season. This study found a correlation between midday leaf water and *n*- C_{31} alkane $\delta^2\text{H}$ values. However, their model, which assumed a 1:1 relationship between leaf water (source) and leaf wax (product), overestimated ^2H -enrichment of the *n*- C_{31} alkane. The authors proposed that this discrepancy could be due to a ^2H -depleted pool of water used during biosynthesis, which may have originated from spatial inhomogeneity in ^2H -enrichment along the length of a leaf. This study did not address the question of whether biochemical mechanisms might explain the lack of a 1:1 relationship between source water and *n*-alkane $^2\text{H}/^1\text{H}$.

The potential for biochemical processes to influence leaf wax $^2\text{H}/^1\text{H}$ has been considered previously in limited circumstances. Kahmen et al. (2013a) investigated whether evaporative ^2H -enrichment in leaf water was recorded in the leaf waxes of five angiosperm species grown under controlled growth chamber conditions. The results of this study suggested that the influence of evaporative ^2H -enrichment was species-specific; with 18–68% of the leaf water ^2H -enrichment reflected in *n*-alkanes. However, interspecies variation of up to 65‰ was observed in $^2\text{H}/^1\text{H}$ fractionation between xylem water and *n*-alkanes. This range in fractionation could not be attributed to differences in measured leaf water evaporative ^2H -enrichment among the studied species. The authors, therefore, theorised that species-specific variation in NADPH sources used for lipid biosynthesis could have been the reason for this variation. Sessions (2006) studied seasonal shifts in the C_4 saltmarsh grass *Spartina alterniflora*, growing in seawater, which were assumed to have the same isotopic composition throughout the sampling period. The relative ^2H -depletion in lipid $^2\text{H}/^1\text{H}$ observed during the summer months – contrary to the anticipated ^2H -enrichment in summer – was interpreted as a change in the organic substrate used for lipid biosynthesis, i.e. current photosynthate in summer, versus stored carbohydrates during the winter. Feakins and Sessions (2010) considered whether changes in the source of biosynthates influenced species-specific variation in $^2\text{H}/^1\text{H}$ among CAM plants. Hydrogen isotope fractionation between source water and *n*-alkanes differed by 92‰ among species. However, the authors had not measured xylem or leaf water $\delta^2\text{H}$ as part of this study, but theorised that these differences may have arisen from metabolic moderation of fractionation between leaf water and leaf wax by using a percentage of NADPH generated from heterotrophic pathways for lipid biosynthesis.

Remarkably, the inadequacy of relying solely on physical mechanisms to explain leaf water empirical $\delta^2\text{H}$ data was shown by [Shu et al. \(2008\)](#), who modelled leaf water oxygen and hydrogen isotope compositions along the length of a pine needle. Even though their model could describe along-leaf variation in empirical $\delta^{18}\text{O}$ data, it could not do it for $\delta^2\text{H}$ data. The authors proposed that this discrepancy was due to the fact that “certain unknown biological processes may not have been incorporated into our 2D model . . . it calls for a re-evaluation of all the other models for hydrogen isotopic simulations of leaf water since they too lack these processes”. The results of this study implied that interpretation of both leaf water and *n*-alkyl lipid $\delta^2\text{H}$ values required a new approach that integrated $^2\text{H}/^1\text{H}$ fractionation during physical processes that control water movement in, out and within the leaf with that which takes place at various stages of photosynthesis.

As a result of all the previous research we can therefore hypothesise that if interspecies differences in the $^2\text{H}/^1\text{H}$ composition of leaf wax lipids are driven primarily by differences in the isotopic composition of leaf water, there are several theoretical scenarios that may account for the observed variability among plant species growing at the same site. These include: (i) differences in the isotopic composition of soil water among site sub-environments; (ii) differences in the isotopic composition of soil water throughout the growing season; (iii) interspecies differences in xylem water reflecting root uptake of soil water and transport to the site of evaporation in the leaf, and (iv) interspecies differences in the isotopic composition of leaf water among plant life forms due to differences in leaf structure. The focus of this paper is to test all of these scenarios and to evaluate whether they provide a comprehensive explanation for differences in the $^2\text{H}/^1\text{H}$ composition of lipids from a range of C_3 and C_4 plant species (grasses, succulents, evergreens and perennial herbs) sampled at Stiffkey salt marsh, Norfolk, UK across the entire growing season from March to September in 2012. The broad range of plant life forms was specifically chosen due to (a) their gross variation in leaf morphology, and (b) their well-studied differences in biochemical adaptations to their environment, which provided an ideal platform to test the relative importance of physical and biochemical mechanisms in explaining interspecies variation in the $\delta^2\text{H}$ values of leaf wax *n*-alkanes in terrestrial plant species growing in a geographically restricted natural environment.

In this study, we focus on a saltmarsh environment at the land/sea divide. These ecosystems contribute significant amounts of organic material to the marine environment ([Mitsch and Gosselink, 2000](#)). Indeed, globally saltmarshes are known to have higher levels of primary production than other coastal biomes such as mangroves, and greatly exceed the productivity of grasslands, cultivated plant communities and forest ecosystems ([Mitsch and Gosselink, 2000](#); [Richardson, 2000](#)), with $\sim 50\%$ of organic carbon in ocean sediments being derived from vegetated sedimentary environments ([Duarte et al., 2005](#)). Findings from this study will therefore have important implications for palaeoclimate reconstructions based on the $\delta^2\text{H}$ profiles of leaf wax lipids from coastal and marine sediments. In addition,

biochemical adaptations employed by the selected species at Stiffkey to ameliorate water stress are not unique to saltmarsh settings – other xeromorphic plant species growing in a variety of other water stressed habitats such as arid regions, are also known to make use of similar biochemical responses to maintain their osmotic potential ([Bohnert and Jensen, 1996](#)), and thus the conclusions can be translated to such other environments. Understanding the relative importance of biochemistry in controlling the hydrogen isotope composition of leaf wax biomarkers in plant biochemical mechanisms is therefore important for helping in the reconstruction of past climates across a range of different biomes. The data presented here thus allows us to make far-reaching inferences regarding the interaction between physical and biochemical mechanisms across a wide variety of plant life forms.

2. STUDY LOCATIONS AND SAMPLING METHODS

2.1. Study location

Stiffkey marsh is typical of an open coast back-barrier saltmarsh ([Moeller et al., 1996](#); [Allen, 2000](#)) ([Fig. 1](#)). The site can be divided into ecologically distinct zones. The low marsh (LM) and upper marsh (UM), defined by [Jeffries \(1977\)](#), are separated by a well-drained gravel and sand ridge (R, [Fig. 1](#)) formed by onshore emplacement of offshore barrier sediments ([Boomer and Woodcock, 1999](#)). Seawater inundation onto the upper marsh is by tidal flow through a dendritic channel network across the marsh and also by spring tidal inundation. Neap tides range from 2 to 3 m, although they can be as low as 0.2 m ([Pye, 1992](#); [Callaway et al., 1996](#)). Spring tides can be in excess of 5 m and storm surges from the North Sea can occur ([Callaway et al., 1998](#); [Andrews et al., 2000](#)). There are no rivers or streams draining onto the marsh, therefore rainwater accounts for all near-surface fresh water inputs to the site.

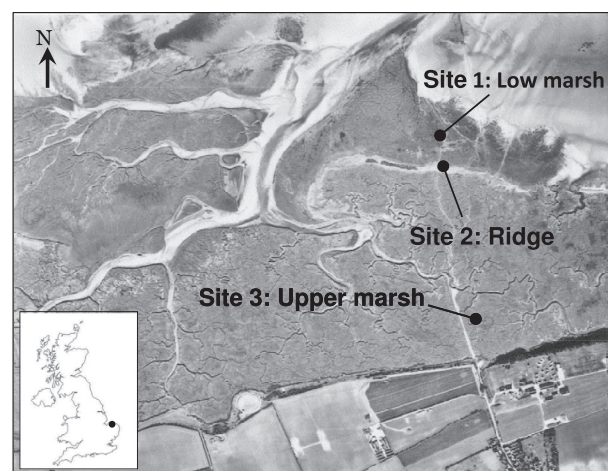


Fig. 1. Aerial photograph (scale *c.* 2.0×1.8 km) of Stiffkey marsh, North Norfolk, UK showing the location of the three study sites. Note the presence of an intricate network of inlet channels delivering seawater to low-lying areas adjacent to Site 3 in the upper marsh. (Copyright: Cambridge University Collection of Air Photographs).

2.2. Surface vegetation

Stiffkey vegetation cover can be zoned according to topography and degree of tidal inundation (Jeffries, 1977; Jeffries and Perkins, 1977; Davy et al., 2011). Plant types include grasses (*Spartina anglica*, *Elytrigia atherica*, *Phragmites australis*, *Puccinella maritima*), succulents (*Suaeda vera*, *Salicornia europaea*) and dicots (*Limonium vulgare*, *Atriplex portulacoides*). The low marsh at Stiffkey, which receives regular tidal inundation, is colonised by C₄ grass *S. anglica*, C₃ annuals *S. europaea* and *Limonium vulgare*, and occasionally the C₃ shrub *A. portulacoides*. The gravel ridge supports a range of C₃ grasses such as *E. atherica*, with stands of the reed *P. australis* found on the seaward side. *S. vera* and *A. portulacoides* also grow in ≤1 m high bushes on the ridge. *L. vulgare*, *A. portulacoides* and *S. vera* are particularly abundant in the upper marsh, however, *S. anglica* and *S. europaea* proliferate around lower-lying brackish pools and water-logged ground surrounding old drainage channels.

The distribution of coastal plants at Stiffkey can be explained by considering ‘Ellenberg’ values for salinity tolerance produced as part of the 1999 ‘Ecofact’ project (Hill et al., 1999). An Ellenberg rating of 0 indicates a species with no salt tolerance, whilst 9 is applied to species known to favour extremely saline conditions in which hypersalinity and salt precipitation are common. Under this classification scheme, *S. anglica* (7) is identified as a species of the lower salt marsh; *Salicornia europea* (9) is a species found in extremely saline and hypersaline conditions; *A. portulacoides* and *L. vulgare* (6) are most common in mid-level salt marshes; *S. vera* (5) is found typically on the upper edges of marshes where tidal inundation does not often reach; *E. atherica* (4) is most suited to salt meadows and upper marsh environments; and *P. australis* (2) is a species that can live in both saline and non-saline habitats but is more predominant in non-saline environments. Species present at the site are adapted for survival in continually damp/wet soils, with the exception of *E. atherica*, which can tolerate only moderately damp conditions (Hill et al., 1999). The selected species at Stiffkey vary in terms of the compatible solutes they use for osmoregulation and amelioration of the harsh saltmarsh conditions. The main compounds synthesised for these purposes include proteins, amino-acids and sugars/carbohydrates (Bohnert and Jensen, 1996). These biological mechanisms are important since their existence is not limited to saltmarsh plants; indeed they are also widely found in other drought tolerant species (Bohnert and Jensen, 1996).

2.3. Sampling strategy

Plant samples were collected for a pilot study in June 2011, and then also in March, May August and September during the 2012 growing season. Sampling of all species collected on each occasion took place between 12:00 and 14:00 from three sites at Stiffkey (Fig. 1). This two-hour sampling window was unavoidable as a result of high tides. In June 2011, plant species were sampled (i) by plant type (grass,

succulent, perennial etc.) and (ii) where possible from multiple locations within the marsh (LM, R, UM), to evaluate the relative importance of marsh sub-environment on leaf lipid ²H/¹H (Supplementary information Table 1). Our sampling strategy for the period from March to September 2012 was based upon the key findings from the initial results obtained in June 2011. The 2012 sampling focused on gross interspecies differences in hydrogen isotope fractionation between leaf wax, leaf water and environmental water across the growing season. Seven species were selected for study during the 2012 period across the three sampling sites (Supplementary information Table 2).

In June 2011 samples were collected for paired leaf wax and leaf water analysis. During 2012, however, sampling also included soil water samples for the entire growing season. In September 2012, we sampled xylem water as well as leaves from all species between 12:00 and 14:00. In addition we collected soil, leaf and xylem water from *E. atherica*, *S. vera*, and *A. portulacoides* at the ridge between 7:30 and 8:00 to allow for investigation of the potential influence of diurnal shifts in xylem and leaf water on *n*-alkane ²H/¹H compositions. These three species were chosen because of their close proximity to each other and because they showed the maximum range in *n*-alkane δ²H values among species at one sampling site.

In order to ensure that samples collected were statistically representative of each species at a given location, samples for *n*-alkane or leaf water extraction were collected in triplicate. Further, each individual analysed sample represents a composite of at least five leaves (dependant on plant leaf morphology) taken from at least three different plants at a particular sampling site. The exception to this was the succulent *S. europea*: this species has no distinct leaves but instead has green photosynthetically active jointed stems (Ellison, 1987). Samples comprising at least five green stems were collected during 2012 for both *n*-alkane and leaf water analysis from this succulent species. Samples for soil water extraction were collected in triplicate in March, May and September 2012 from the top ~10 cm of soil in each location. Stem samples were collected in triplicate for each species in September 2012; each sample represents a minimum of three stem samples of greater than 5 cm in length. Leaf, stem and soil water samples were placed directly into exetainers, capped, taped with PTFE tape in the field, and then frozen in the laboratory until water extraction. Samples for *n*-alkane analysis were dried at 40 °C for 72 h, and then stored at room temperature in the dark prior to lipid extraction.

3. ANALYTICAL METHODS

3.1. Leaf, xylem and soil water extraction

Leaf, xylem and soil water extractions were carried out using cryogenic vacuum distillation based upon the design and operating procedure presented by West et al. (2006). Duplicates of each sample were extracted to enable consideration of (a) reproducibility of the extraction method, and (b) inherent intraspecies variability in leaf/xylem/soil water

isotopic composition. Samples were heated to 80 °C within an evacuated glass line and water was distilled and trapped in an adjacent collection vial submerged in liquid nitrogen. Each station on the extraction line was coupled to a pressure gauge, allowing for accurate determination of completion and monitoring of line stability during sample collection. At the commencement of each series of extractions, line vacuum pressures at all stations were consistently ≤ 5 mTorr, which exceeds the 60 mTorr recommended by West et al. (2006). All leaf, xylem and soil samples were extracted for at least 2 h to avoid $^2\text{H}/^1\text{H}$ fractionation during distillation.

3.2. Water isotopic analysis

Hydrogen isotope signatures of extracted waters were measured using a Delta XP ThermoFisher isotope-ratio mass spectrometer interfaced with a pyrolysis TC/EA equipped with a liquid autosampler. The $\delta^2\text{H}$ values reported here are based on ten analytical replicates of each sample. The first five replicates of each sample were discarded to prevent distortion by memory effects associated with the use of liquid autosampler. The $\delta^2\text{H}$ values are expressed relative to the VSMOW scale based upon analysis of a suite of international and in-house standards analysed in the same sequence with the water samples. Additional standards (GISP, in-house tap water) were treated as unknowns to evaluate instrument accuracy. Root mean square (RMS) errors for $^2\text{H}/^1\text{H}$ measurements of international and in-house standards were 1.0‰ ($n = 108$). During all sample and standard measurements, three reference gas pulses were passed through the mass spectrometer. Reproducibility of H_2 reference gas $\delta^2\text{H}$ values after H_3^+ correction was typically $\pm 0.5\%$. Typical standard error among analytical replicates of the same sample was 4‰, while comparison of mean values for leaf and xylem sample duplicates showed that the absolute difference between them was in all cases also less than 4‰. Soil sample duplicates could not be successfully processed for all sampling intervals due to difficulties in extracting sufficient amounts of water from them for reliable stable isotope measurements (Supplementary information Table 4). However when they were possible, mean values did not vary by more than 4‰ among sample replicates. We adopted a conservative approach and assumed that level of variability for all singular soil water samples presented here.

3.3. *n*-Alkane extraction and identification

Leaf wax lipids were extracted from whole leaves by sonication with HPLC grade hexane to obtain the total lipid fraction. The number of leaves used varied among species, from ~ 3 for *P. australis* to > 50 for *S. vera*. Samples were extracted by sonication and the extract was concentrated to 1 mL under nitrogen gas using a turbovap prior to chromatographic separation. Duplicates of each sample were extracted, to ensure reproducibility of the extraction process, and to evaluate intraspecies variability in the leaf wax signal. The hydrocarbon fraction was eluted with HPLC grade hexane during column chromatography, using activated silica

gel (70–230 mesh, Merck KGaA). Analysis of the molecular distribution of *n*-alkanes for each species was carried out by injection into an Agilent 7820A gas chromatograph equipped with a flame ionisation detector and an Agilent DB-5 capillary column (30 m \times 0.32 mm \times 0.25 μm) (Agilent Technologies Inc., Santa Clara, USA). The oven temperature was raised from 50 °C to 150 °C at 20 °C min^{-1} , and then at 8 °C min^{-1} to 320 °C (10 min). *n*-Alkanes were identified by comparison of their elution times with *n*- C_{16} to *n*- C_{30} alkane standard (A. Schimmelmann, Indiana University). Average chain length (ACL) and carbon preference index (CPI; Supplementary information Tables 1 and 2) values were calculated following the approach of Zhang et al. (2006).

3.4. *n*-Alkane hydrogen isotope analysis

The $^2\text{H}/^1\text{H}$ composition of *n*-alkanes was determined using a Delta V Advantage ThermoFisher isotope-ratio mass spectrometer interfaced with GC-Isolink Trace GC Combustion and High temperature conversion (HTC) system operating at 1420 °C. The initial GC oven temperature was set at 50 °C, which was then raised at a rate of 30 °C min^{-1} to 220 °C. A second temperature ramp to a final temperature of 320 °C at a rate of 6 °C min^{-1} followed. The final temperature was held for 5 min. The $\delta^2\text{H}$ values are based on duplicate analyses of well-resolved peaks and reported on the VSMOW scale, based on in-house reference gases (H_2 , $> 99.995\%$ purity, BOC) adjusted at the beginning and at the end of each sequence using a standard mixture of the *n*- C_{16} to *n*- C_{30} alkane standard. Root mean square (RMS) errors for $^2\text{H}/^1\text{H}$ measurements of this standard were 4.0‰ ($n = 780$). During all sample and standard measurements, six reference gas pulses were passed through the mass spectrometer. Reproducibility of H_2 reference gas $\delta^2\text{H}$ values after H_3^+ correction was $\pm 6\%$. Typical absolute differences in *n*- C_{29} measurements between analytical replicates of the same sample did not exceed 6‰, while absolute differences in mean values among sample replicates of the same species (an indicator of intraspecies variability) was on average 4‰, with a maximum of 10–14‰ for *A. portulacoides* (August 2012), *P. australis* (September 2012) and *S. vera* (September 2012) (Supplementary information Table 4).

4. RESULTS

4.1. Soil water $^2\text{H}/^1\text{H}$ composition

Soil water from the sandflat was most ^2H -depleted in March (-27%) and most ^2H -enriched in May ($+2\%$) (SI Table 4). Between May and September 2012, soil water from the sandflat remained constant within analytical error, varying by only 3‰. Upper marsh soil water samples were not successfully stored for March, however, similar seasonal consistency to that observed in the sandflat was revealed when comparing the May ($+2\%$) and September (-2%) soil water samples taken from this location. The greatest seasonal shift in soil water at the site was found at the ridge, where values ranged from -36% in March

to -5‰ in September (Supplementary information Table 4). Soil waters collected before 8:00 in September 2012 had a mean value of -21‰ , indicating they were 16‰ ^2H -depleted compared with samples collected between 12:00 and 14:00 (Supplementary information Table 5).

4.2. Xylem water $^2\text{H}/^1\text{H}$ composition

Xylem waters from the September 2012 sampling interval showed that stem waters were more negative than the soil waters across all sampling sites (Fig. 2). *E. atherica* had the most negative xylem water of all species sampled (-43‰), while *L. vulgare* had the most positive (-4‰). Total interspecies variation in xylem water $\delta^2\text{H}$ was 39‰ (Supplementary information Table 4). Xylem samples collected from *E. atherica*, *A. portulacoides* and *S. vera* at the ridge site in September 2012 (a) between 7:30 and 8:00, and (b) between 12:00 and 14:00, varied by no more than $2\text{--}3\text{‰}$. This was lower than both analytical reproducibility (4‰) and intraspecies variability in $^2\text{H}/^1\text{H}$ isotopic composition (4‰). The range of xylem water values among the species sampled in the early morning was 20‰ , which was slightly higher than that observed among xylem water samples collected between 12:00 and 14:00 (13‰) (Supplementary information Table 5).

4.3. Leaf water $^2\text{H}/^1\text{H}$ composition

Leaf waters extracted from all species collected at Stiffkey in June 2011 varied by no more than 29‰ . For those species sampled from multiple locations, upper marsh leaf water samples were generally more ^2H -enriched than those sampled from other locations, but the range of variation was low compared to gross interspecies differences: $\delta^2\text{H}_{\text{LW}}$ from *A. portulacoides* varied by 13‰ across the marsh, with the most ^2H -depleted leaf water found at the ridge site and the most ^2H -enriched in the upper marsh; $\delta^2\text{H}_{\text{LW}}$ from *Triglochin maritima* varied by 10‰ between

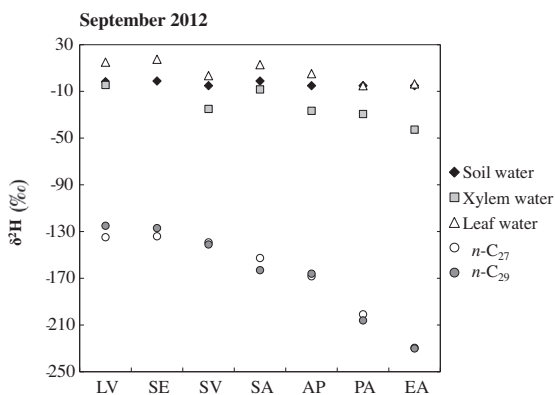


Fig. 2. Measured soil water $\delta^2\text{H}$ (black diamonds), xylem water $\delta^2\text{H}$ (grey squares), leaf water $\delta^2\text{H}$ (white triangles), and n -alkane $\delta^2\text{H}$ (circles) values from all species sampled in September 2012. LV = *Limonium vulgare*, SE = *Salicornia europaea*, SV = *Suaeda vera*, SA = *Spartina anglica*, AP = *Atriplex portulacoides*, PA = *Phragmites australis*, EA = *Elytrigia atherica*. The standard error did not exceed 2‰ for soil, xylem, leaf waters and 9‰ for n -alkane measurements.

the lower and upper marsh. Small shifts of 6‰ were observed in the evergreen succulent *S. vera*, and the perennial herb *L. vulgare*, with the most ^2H -enriched value occurring in the upper marsh for *Suaeda* and the lower marsh for *Limonium* (Fig. 4; Supplementary information Table 3).

Leaf water samples collected during 2012 showed a total range among all species sampled of 46‰ between the most ^2H -depleted values (-26‰ , *L. vulgare*, March) and the most ^2H -enriched ($+20\text{‰}$, *S. europaea*, September). Species-specific variation in leaf water $\delta^2\text{H}$ was most limited in March (6‰) and greatest in August (29‰). Leaf waters from all species were generally most ^2H -depleted in March, and ^2H -enriched in September. *E. atherica* and *P. australis* were generally the most ^2H -depleted in terms of leaf water $\delta^2\text{H}$, whilst *S. anglica*, *L. vulgare* and *S. europaea* were typically among the most ^2H -enriched. The exception to this overall pattern among species occurred in March, when all species were characterised by $\delta^2\text{H}$ values between -26‰ and -20‰ (Fig. 5; Supplementary information Table 4). These extremely negative leaf water $\delta^2\text{H}$ profiles were significantly different (Minitab v.16, 2013, Student's t -test, $P > 0.05$, $n = 10$ individuals per sampling interval comparing those species growing from March to September 2012) to those observed for the same species in all other sampling intervals during 2012.

Leaf water samples collected at 7:30–8:00 and 12:00–14:00 from *E. atherica*, *A. portulacoides* and *S. vera* at the ridge site allowed us to investigate diurnal shifts in leaf water isotopic composition. The C_3 grass *E. atherica* showed the greatest shift in the $\delta^2\text{H}$ of leaf water: it was 19‰ more positive at 12:00–14:00 than at 7:30–8:00. Leaf waters from two other plants showed a ^2H -enrichment of only $5\text{--}6\text{‰}$ (Fig. 6; Supplementary information Table 5).

Statistical analysis (Minitab v.16, 2013) of interspecies variation in leaf water isotopic composition at each sampling interval indicated that leaf water $^2\text{H}/^1\text{H}$ was not significantly different (Mann–Whitney U test, $P > 0.05$, $n = 8$ for comparison of species growing from March to September 2012; $n = 6$ for comparison of species growing from May to September 2012) among the Stiffkey species. However, *P. australis*, the species that generally had the most ^2H -depleted leaf water isotopic signatures, was an exception. Leaf water from *Phragmites* was significantly different

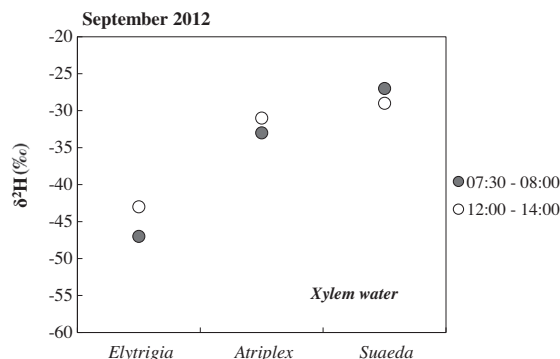


Fig. 3. Measured xylem water $\delta^2\text{H}$ values for three species sampled at the ridge site between 7:30 and 8:00 and again between 12:00 and 14:00 on 7th September, 2012. The maximum standard error associated with these measurements was 2‰ .

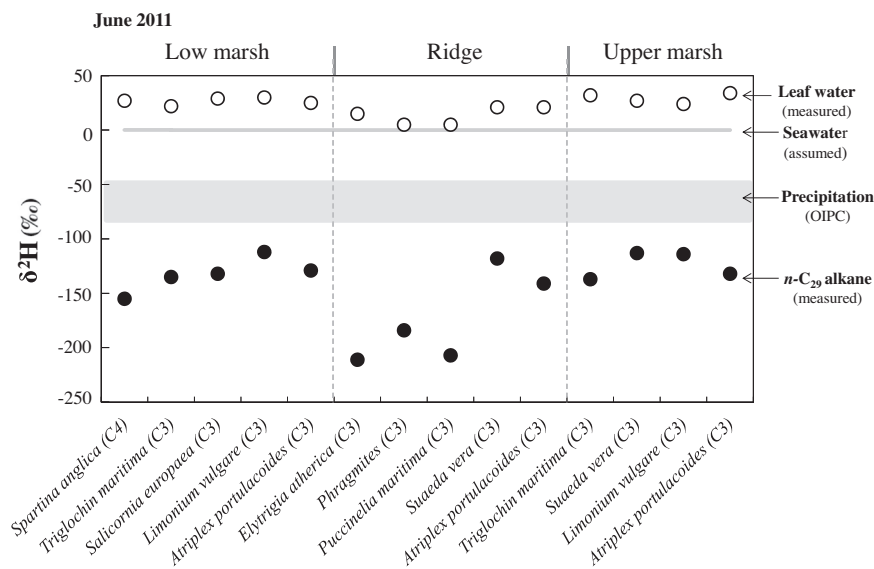


Fig. 4. Measured $n\text{-C}_{29}$ alkane $\delta^2\text{H}$ (black circles) and leaf water $\delta^2\text{H}$ (white circles) values for all plants sampled across the Stiffkey marsh in June 2011 (“C3” and “C4” refer to plant biochemical pathways). Predicted $\delta^2\text{H}$ values of seawater (grey line) and precipitation (grey shading) are also shown. Plants are grouped by sampling site (Low marsh, Ridge, Upper marsh). Each data point represents a collection of five or more leaves, from a minimum of three separate plants. Maximum standard error associated with these measurements was 5‰ for $n\text{-alkane}$ values and 1‰ for leaf waters. The isotopic composition of sea water (0‰) is highlighted by the straight grey line, whilst the grey shaded area illustrates the maximum seasonal range in precipitation $^2\text{H}/^1\text{H}$ composition estimated using the Online Isotopes in Precipitation Calculator (Bowen et al., 2005).

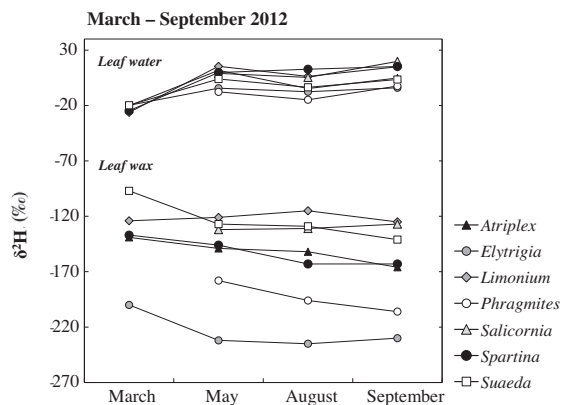


Fig. 5. Seasonal variation in $n\text{-C}_{29}$ alkane $\delta^2\text{H}$ and leaf water $\delta^2\text{H}$ values for all plants sampled during the 2012 growing season. Each data point represents a collection of five or more leaves, from a minimum of three separate plants. The maximum standard error associated with these measurements was 8‰ for $n\text{-C}_{29}$ alkane and 2‰ for leaf water.

from the C_4 grass *S. anglica*, and the C_3 species *S. europaea*, *L. vulgare*, and *A. portulacoides* (Student’s t -test, $P < 0.05$, $n = 6$ individuals per species), but could not be distinguished statistically from leaf water from the other C_3 monocot *E. atherica*.

4.4. $n\text{-Alkane } ^2\text{H}/^1\text{H}$ composition

Analysis of molecular distributions of $n\text{-alkanes}$ from the sampled species (Supplementary information Tables 1 and 2) showed that $n\text{-C}_{27}$ and $n\text{-C}_{29}$ alkanes were the most

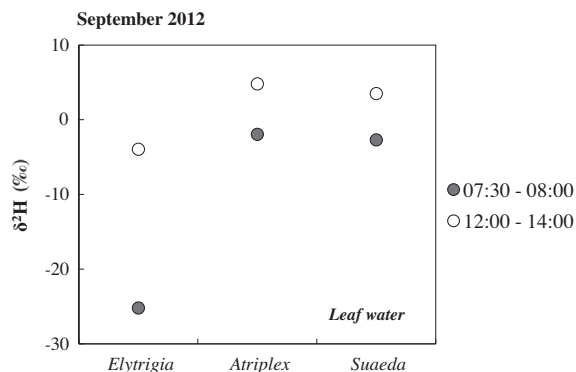


Fig. 6. Measured leaf water $\delta^2\text{H}$ values for three species sampled at the ridge site between 7:30 and 8:00 and again between 12:00 and 14:00 on 7th September, 2012. The maximum standard error associated with these measurements was 2‰.

abundant across all species. Because $n\text{-C}_{27}$ and $n\text{-C}_{29}$ alkane $\delta^2\text{H}$ values were strongly correlated across the growing season (Fig. 2 in the Supplementary information), we focused only on $n\text{-C}_{29}$ $\delta^2\text{H}$ values in all subsequent data analysis. The mean $n\text{-C}_{29}$ $\delta^2\text{H}$ values from June 2011 showed a total interspecies variation of 98‰, with the C_3 grass *E. atherica* having the most ^2H -depleted $n\text{-C}_{29}$ value and *S. vera* the most ^2H -enriched. Species collected from multiple sampling sites showed very limited micro-habitat dependent variation ranging from 1‰ (i.e. below the observed maximum intraspecies variability of 6‰ in $n\text{-C}_{29}$ $^2\text{H}/^1\text{H}$) (*S. vera*) to 9‰ (*A. portulacoides*). The greatest interspecies range in $\delta^2\text{H}_{n\text{-C}_{29}}$ was observed at the ridge site (93‰), while the

lowest occurred in the upper marsh (24‰). *n*-C₂₉ from C₃ grasses was on average 45‰ more ²H-depleted than that from the C₄ *S. anglica*. Overall, we observed the following pattern for *n*-C₂₉ alkane δ²H values: succulents > perennial herbs > evergreen shrubs > C₄ grass > C₃ monocots (Fig. 4; Supplementary information Table 3).

The mean δ²H values of *n*-C₂₉ alkane from the 2012 growing season were remarkably consistent for each individual species across all the sampling intervals (Fig. 5; Supplementary information Table 4). Seasonal variation from March – September was the highest in the evergreen succulent *S. vera* (44‰), and the lowest in the annual succulent *S. europaea* (5‰). For all other species, seasonal variation in their leaf wax ²H/¹H composition fell within the range of 10–35‰. Statistical analysis (Minitab v.16, 2013) confirmed that these differences are not significant (Mann–Whitney *U* test, *P* > 0.05, *n* = 10 for March 2012; *n* = 14 for May, August and September 2012).

The greatest interspecies variation in *n*-C₂₉ occurred in August (120‰), however variability among species exceeded 100‰ for all 2012 study intervals. *E. atherica* and *P. australis* consistently recorded the most negative δ²H values. However, unlike in the leaf water – where *Phragmites* was generally more negative than *Elytrigia* – the *n*-C₂₉ alkane δ²H values of *Elytrigia* were between 23‰ and 54‰ more negative than those of *Phragmites* across the entire growing season. In addition, the most ²H-enriched *n*-C₂₉ values were observed in *S. vera*, *L. vulgare* and *S. europaea*, with *S. anglica* – a species with one of the more positive leaf water δ²H values – having intermediate *n*-C₂₉ alkane δ²H values across all sampling intervals (Fig. 5). Cross-plotting the *n*-C₂₉ alkane δ²H data and ACL values (Fig. 1 in the Supplementary information) for September 2012 did not show any correlation between these two parameters (Fig. 3 in the Supplementary information).

Statistical analysis of interspecies variation in leaf wax hydrogen isotope compositions among all sampled species across the study period (Minitab v.16, 2013) revealed that the ²H/¹H values of waxes were significantly different among most species (Mann–Whitney *U* test, *P* < 0.05, *n* = 8 for species growing from March to September 2012; *n* = 6 for species growing from May to September 2012). Notable exceptions include (a) *S. vera*, and *L. vulgare*, and (b) the two succulents *S. vera* and *S. europaea*.

4.5. ²H/¹H fractionation between soil, xylem and leaf water and *n*-C₂₉ alkane

Halophyte species are exceptions to the rule that plants do not fractionate environmental water during root uptake (Waisel, 1972; Ellsworth and Williams, 2007). ²H-discrimination occurring during water uptake among the Stiffkey halophytic species was calculated using the approach of Ellsworth and Williams (2007): Δ²H = δ²H_{soil water} – δ²H_{xylem water}.

Δ²H was the highest in the evergreen species *A. portulacoides* and *S. vera* for all halophyte species at Stiffkey (28‰) and the lowest in *L. vulgare* (4‰). The C₄ grass *S. anglica* had a Δ²H value of 13‰. The values reported here exceed

those of Ellsworth and Williams (2007), who only reported data from woody xerophytes.

Epsilon values were calculated to approximate ²H/¹H fractionation between mean *n*-C₂₉ δ²H values and soil water (ε_{wax/sw}), xylem water (ε_{wax/xw}), and leaf water (ε_{wax/lw}) using the following equation:

$$\varepsilon_{\text{wax/water}} = \frac{(^2\text{H}/^1\text{H})_{\text{wax}}}{(^2\text{H}/^1\text{H})_{\text{water}}} - 1 = \frac{(\delta^2\text{H})_{\text{wax}} + 1}{(\delta^2\text{H})_{\text{water}} + 1} - 1$$

where δ²H_{water} represents the hydrogen isotope composition of the leaf water or soil water as appropriate. Epsilon and delta values are reported in per mil (‰), and therefore this equation implies multiplication by 1000 (Cohen et al., 2007).

In June 2011, the total variation in ε between *n*-C₂₉ and leaf water exceeded 100‰ (Fig. 7a and b). Similar differences were identified throughout the 2012 growing season when the total variation in ε_{wax/lw} exceeded 86‰ for all sampling intervals (Fig. 8). The greatest range in ε_{wax/lw} during the growing season was observed in August (109‰), and the lowest in September (86‰). The C₃ grass *E. atherica* consistently had the lowest ε_{wax/lw} value (–184‰ to –229‰), whilst *S. vera* and *L. vulgare* recorded the highest (–79‰ to –144‰). Across all species, there was a general trend for ε_{wax/lw} to become lower as the growing season progresses (Fig. 8; Supplementary information Table 4). The variation in fractionation factors calculated for the plant species at Stiffkey is the largest range in ε_{wax/lw} reported to date for saltmarsh environments (c.f. Romero and Feakins, 2011). ε_{wax/sw} values for species growing at the three sites in 2012 ranged from –64‰ for *Salicornia* in March to –228‰ for *E. atherica* in September. ε_{wax/sw} variability among the different plant species exceeded 89‰ throughout the growing season (Supplementary information Table 4).

The C₄ grass, *S. anglica*, has ε_{wax/lw} values that are higher (by up to 74‰) than those observed for the C₃ grass *E. atherica*. When the *Spartina* data are compared with other C₃ species collected in March and May 2012, ε_{wax/lw} for *Spartina* is only 5–6‰ higher than in *Atriplex*, although it is 15–36‰ lower than the apparent fractionation observed in *Suaeda* and *Limonium*. As the growing season progresses, the difference in ε_{wax/lw} among these species increases: in August, where the maximum variation is observed, the ²H/¹H fractionation between leaf water and leaf wax *n*-C₂₉ in *Spartina* is between 25‰ and 53‰ lower than these other C₃ shrubs and herbs (Supplementary information Table 2).

5. DISCUSSION

Many previous studies have sought to explain variation in *n*-alkane ²H/¹H composition among different plant species by reference to the physical processes that control the movement of water molecules inside, outside and within the leaf. If we therefore, assume that interspecies variation in our leaf wax lipid δ²H is primarily driven by differences in the isotopic composition of leaf water, it follows that the >100‰ range in *n*-alkane ²H/¹H compositions observed should be accounted for by a series of scenarios which affect

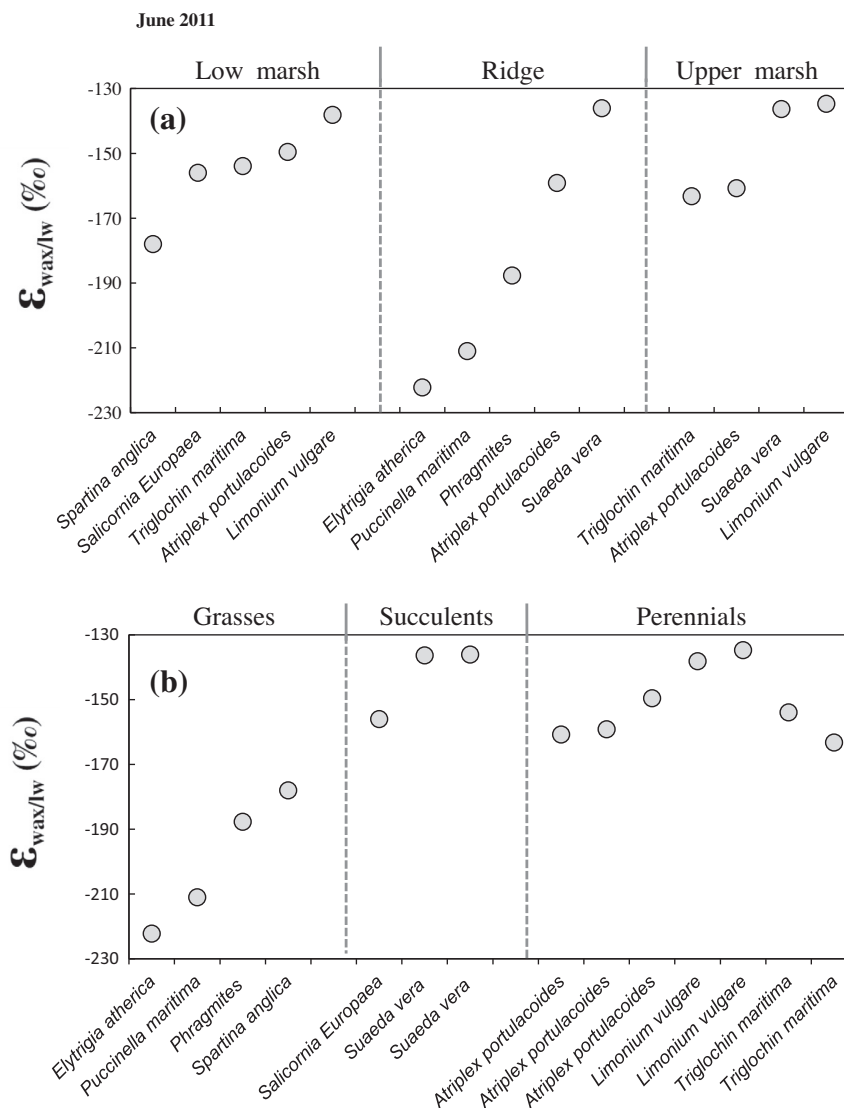


Fig. 7. Calculated fractionation ($\epsilon_{\text{wax/lw}} \text{‰}$) between $n\text{-C}_{29}$ alkane $\delta^2\text{H}$ and leaf water $\delta^2\text{H}$ from samples collected in June 2011 at Stiffkey saltmarsh. Plants are grouped according to (a) sampling locations and (b) the plant types.

leaf water $\delta^2\text{H}$. These mechanisms include: (i) differences in the isotopic composition of soil water among the three marsh sub-environments; (ii) differences in the isotopic composition of soil water throughout the growing season; (iii) interspecies differences in the isotopic composition of xylem water, reflecting root uptake of soil water and transport to the leaf, and; (iv) interspecies differences in the isotopic composition of leaf water among plant life forms due to differences in leaf structure, affecting the transpiration of water within the leaf. Each of these scenarios will be considered below, to assess whether they can account for the variation observed in $\delta^2\text{H}_{n\text{-C}_{29}}$ among the Stiffkey plants.

5.1. The significance of spatial differences in soil water

Salt marshes are of great significance in lowland coastal regions (Allen, 2000) and represent important depositional environments because they are divisible into discrete micro-

environmental zones based on topography and tidal inundation (Vince and Snow, 1984). This characteristic makes salt marshes ideal for studying plant/environment interactions (Vince and Snow, 1984; Romero and Feakins, 2011). Soils and sediments at Stiffkey receive water inputs from two sources: Sea water, which inundates the lower marsh and low-lying areas of the upper marsh daily, and meteoric precipitation, which is especially important on the ridge where no tidal inundation occurs.

Previous studies (Romero and Feakins, 2011) show that environmental water varies in isotopic composition across salt marsh sites. Our data from 2012 demonstrates this (Supplementary information Table 4), showing that the LM and UM (both sites that regularly receive inputs of saline water) have relatively similar isotopic compositions of source water (-2‰ to $+2\text{‰}$ between May and September 2012). Soil water from the ridge at Stiffkey is up to 35% more ^2H -depleted than the other two sampling sites.

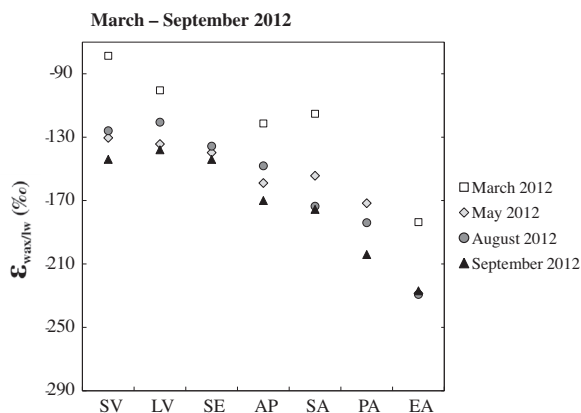


Fig. 8. Calculated fractionation ($\epsilon_{\text{wax/lw}}$ ‰) between $n\text{-C}_{29}$ alkane $\delta^2\text{H}$ and leaf water $\delta^2\text{H}$ from samples collected across the 2012 growing season at Stiffkey saltmarsh. SV = *Suaeda vera*, LV = *Limonium vulgare*, SE = *Salicornia europaea*, AP = *Atriplex portulacoides*, SA = *Spartina anglica*, PA = *Phragmites australis*, EA = *Elytrigia atherica*.

Despite these spatial changes in the isotopic composition of environmental water, large variations in the $\epsilon_{\text{wax/lw}}$ values observed within each sub-environment at Stiffkey (LM, R, UM) in June 2011 (Fig. 7a) suggest that source water isotopic composition is not a major factor controlling the hydrogen isotope signals preserved in the $n\text{-C}_{29}$ alkane. This is supported by the limited variation observed in leaf water and n -alkane samples from selected plant species sampled in June 2011. Although no soil waters were collected in June, sampling of species growing in more than one location at Stiffkey allows for evaluation of the impact of marsh sub-environment on the $^2\text{H}/^1\text{H}$ composition of leaf waters and leaf wax lipids. In theory, if spatial variation in environmental water across these sub-environments is significant, we would expect samples of the same individual species from multiple sites to have different $\delta^2\text{H}$ leaf water and n -alkane compositions. Minor discrepancies in leaf water are observed in each species depending upon the particular sub-environment, for example 13‰ between *A. portulacoides* at the R and UM sites and 10‰ between *T. maritima* at the LM and UM sites (Fig. 4). However, the magnitude of this spatial variability is insignificant when compared with the range of interspecies $\delta^2\text{H}_{\text{lw}}$ values observed across the marsh as a whole (29‰). Differences in mean $\delta^2\text{H}_{n\text{-C}_{29}}$ values for these species also show insignificant variation depending on sampling site – *Limonium*, *Triglochin* and *Suaeda* all vary by less than 5‰ between the LM and UM, while *Atriplex* shifts isotopically by 12‰ (Fig. 4; SI Table 3). Again, the magnitude of these site-specific isotopic differences in individual species is negligible when compared with the $\sim 100\%$ interspecies variation in $\delta^2\text{H}_{n\text{-C}_{29}}$ among all sampled plants. In addition, $\epsilon_{\text{wax/lw}}$ values from *Suaeda*, and *Limonium* show remarkable consistency across multiple sampling sites, with the maximum site-specific variation in one species (10‰ in *Triglochin*; 11‰ in *Atriplex*) an order of magnitude less than the total range in $\epsilon_{\text{wax/lw}}$ observed in the data set as a whole (Fig. 7a and b). We conclude, therefore, that

differences in the isotopic composition of soil water among site sub-environments cannot explain interspecies variation in leaf water or n -alkane $^2\text{H}/^1\text{H}$ composition.

5.2. The significance of temporal differences in soil water

In order to examine the influence of environmental water fully, it is important to consider whether differences in plant growth strategy expose them to seasonal variation in the source water $\delta^2\text{H}$ signal. There is conflict in previous research over whether the n -alkane $^2\text{H}/^1\text{H}$ is “locked in” at the beginning of the growing season or continually shifts in response to environmental or biological stimuli. Sachse et al. (2010) concluded that the n -alkane $\delta^2\text{H}$ values for field-grown barley were fixed early during the growing season and did not show seasonal shifts as the plants matured. A similar conclusion was reached by Tipple et al. (2013), who analysed the $^2\text{H}/^1\text{H}$ composition of n -alkanes, stem water, and leaf water from the riparian angiosperm *Populus angustifolia* throughout a growing season. Leaf water values showed considerable seasonal variation of 55‰, however, n -alkane $\delta^2\text{H}$ values remained relatively consistent in the mature leaf. This was interpreted to reflect the fixing of the n -alkane $\delta^2\text{H}$ signal during the bud break period, where new waxes are produced from water and stored sugars, suggesting that the n -alkane $^2\text{H}/^1\text{H}$ composition reflected these mixed biosynthetic sources rather than providing an integrated signal of the growing season as a whole. In contrast, other studies propose that leaf waxes turnover continuously. Jetter and Schäffer (2006) considered that wax production was dynamic, with turnover and recycling of dominant compound classes during leaf development, whilst Gao et al. (2012) quantified regeneration rates of leaf wax compounds by the application of labelled irrigation water and concluded that $n\text{-C}_{27}$ – $n\text{-C}_{31}$ n -alkanes are replaced over a timescale of 71–128 days.

Plant species growing at our study site are regularly exposed to strong winds from the North Sea, in combination with rain, and tidal inundation. These environmental factors are likely to abrade waxes from the surface of leaves, which means plants have to produce further wax to maintain their protective coating (Shepherd and Griffiths, 2006; Kahmen et al., 2013a). Given their exposed coastal location, it is likely that plants growing at Stiffkey were regularly required to replenish their leaf waxes throughout the growing season. On that basis, we hypothesise that if plants at Stiffkey were synthesising their leaf waxes at different times of year, they may be utilising soil water with different $^2\text{H}/^1\text{H}$ compositions. We therefore, tested whether any temporal variation in soil water isotopic composition (-36% in March, $+2\%$ in May 2012) could adequately account for the interspecies variation in leaf wax $\delta^2\text{H}$ we observed in our data.

Plants at Stiffkey are known to have varied growth strategies. *S. vera*, for example, is an evergreen succulent (Schirmer and Breckle, 1982), *A. portulacoides* is an evergreen shrub (Correrria das Neves et al., 2008), whilst *L. vulgare* (Boorman, 1967), *S. anglica* and *P. australis* (Burke et al., 2000) are all perennials (the latter two species are grasses, while the former is a flowering perennial). In addition to

our soil water data, mean monthly interpolated $\delta^2\text{H}$ profiles of meteoric water at Stiffkey, obtained using the Online Isotopes in Precipitation Calculator (OIPC), version 2.2 (Bowen et al., 2005), were also used for consideration of this temporal parameter (Supplementary information Table 6).

In order to evaluate the importance of temporal changes in soil water isotope composition, it is first necessary to consider sources of water inputs at the marsh. At the LM and UM sites, seawater is the main source and is assumed to have an invariant isotopic value throughout the year (see for example Sessions, 2006). At Site 3 seawater ingress is through a dendritic network of tidal channels (Fig. 1), and the proliferation of *T. maritima* and *S. europaea*, species known to require saline water, attest to the importance of sea-water inputs to the upper marsh (Davy and Bishop, 1991; Allison, 1992). However, early in the growing season, March soil water $\delta^2\text{H}$ from the lower marsh shows a considerably more ^2H -depleted value than for other sampling intervals. Examination of local weather station monitoring data (MIDAS, UK Meteorological Office) shows that on the day of sampling rainfall occurred at the site before sampling and after the last high tide. The estimated value for $\delta^2\text{H}$ of precipitation in North Norfolk in March is c. -62‰ (OIPC), and assuming a seawater $\delta^2\text{H}$ value of 0‰ , we calculate that rainfall contributed $\sim 40\%$ of the $^2\text{H}/^1\text{H}$ soil water signal in this sample. It is likely, however, that with the next high tide, the importance of this meteoric water input would be negated. The $\delta^2\text{H}$ data from May and September 2012 support this, as they have a ‘near-seawater’ isotopic signature, ranging from -2‰ to $+2\text{‰}$ (SI Table 4). Therefore, regardless of the season during which LM and UM plant species synthesised leaf waxes, temporal isotopic shifts in soil water cannot explain interspecies variation in the $n\text{-C}_{29}$ alkane $\delta^2\text{H}$ values observed in these two locations.

In contrast, the ridge is only rarely inundated by tides and is dominated by meteoric precipitation, which explains why our most ^2H -depleted soil water is found at this site (Supplementary information Table 4). Examination of mean monthly interpolated $\delta^2\text{H}$ values of meteoric water at the Stiffkey site (OIPC; Supplementary information Table 6) for our sampling periods show, however, modelled precipitation $^2\text{H}/^1\text{H}$ ranges from -62‰ (March) to -48‰ (September). Soil waters from the ridge are consistently more ^2H -enriched than these meteoric precipitation $\delta^2\text{H}$ profiles, which we attribute to two likely causes. Firstly, as daytime temperatures rise during the growing season, soil evaporation will increase, particularly from the near-surface depths sampled, resulting in increasing ^2H -enrichment in the remaining pore water. Secondly, as the water table at the site is relatively high, an upwards movement of water through soil capillaries (“capillary rise”, Plaster, 2009), particularly during warmer summer months, may carry ^2H -enriched sea-water towards the soil surface (Plaster, 2009). When we consider these temporal shifts in environmental water $^2\text{H}/^1\text{H}$ composition in the context of the interspecies variability in leaf wax n -alkane hydrogen isotope compositions observed at this particular sampling site, it is clear that temporal variation in the isotopic composition of soil water and precipitation cannot explain the $\delta^2\text{H}_{n\text{-C}_{29}}$ range among the ridge

species. In our study, soil water $\delta^2\text{H}$ varied by 31‰ at the ridge across the 2012 growing season, while the average interspecies range in $\delta^2\text{H}_{n\text{-C}_{29}}$ consistently exceeded 100‰ .

In addition to consideration of seasonal shifts in the isotopic composition of environmental water, soil samples collected from the ridge between 7:30 and 8:00 on the 7th of September 2012 allowed us to investigate diurnal changes in soil water $\delta^2\text{H}$. Sachse et al. (2010) suggested that one reason a direct 1:1 relationship was not observed between the $\delta^2\text{H}$ of midday leaf water and $\delta^2\text{H}_{n\text{-C}_{29}}$ in barley was that plants were synthesising these compounds from water that had not been subjected to diurnal ^2H -enrichment. In our study, the hydrogen isotope signature of soil water from the ridge between 7:30 and 8:00 was 16‰ lower compared with soil samples collected between 12.00 and 14.00 (SI Table 5), while leaf waxes from species sampled at the ridge in September varied by $\sim 90\text{‰}$. Therefore, diurnal variation in environmental water also cannot explain the range in interspecies $\delta^2\text{H}_{n\text{-C}_{29}}$ observed in the coastal plants at Stiffkey.

5.3. The significance of soil water uptake by halophytes and non-halophytes

Sachse et al. (2010) considered the possibility of a ^2H -depleted pool of water occurring in plants as a source of hydrogen for lipid synthesis, whereas McInerney et al. (2011) suggested that xylem water could be used by the plant in preference to leaf waters for lipid biosynthesis. Xerophytes and halophytes are exceptions to the general rule that isotopic fractionation does not occur during water uptake by plants (Ellsworth and Williams, 2007). In these drought and salinity tolerant plants, the mechanism of water uptake by roots is via the symplastic pathway, requiring transport from cell to cell. This transport from cytoplasm of one cell to cytoplasm of the next cell requires energy, and hence leads to diffusional $^2\text{H}/^1\text{H}$ fractionation of water molecules, with xylem waters becoming ^2H -depleted relative to environmental water (Ellsworth and Williams, 2007).

Xylem waters collected between 12:00 and 14:00 at Stiffkey on the 7th of September 2012 allow us to consider whether interspecies variation in fractionation occurring during water uptake ($\Delta^2\text{H}$) can explain the variation in $\delta^2\text{H}_{n\text{-C}_{29}}$ in our data set. $\Delta^2\text{H}$ values for the Stiffkey halophytes (those species with an Ellenberg value in excess of 4) show a much greater range than that published by Ellsworth and Williams (2007); however the maximum fractionation observed for *Atriplex* is still only 28‰ , compared with a minimum fractionation of 4‰ in *L. vulgare*. This variation in fractionation during water uptake does not explain the 41‰ difference between their $\delta^2\text{H}_{n\text{-C}_{29}}$ values. Equally, *Atriplex* and *Suaeda* growing on the ridge have the same $\Delta^2\text{H}$ values (28‰), but their $\delta^2\text{H}_{n\text{-C}_{29}}$ values differ by 25‰ .

Some species at Stiffkey are merely salt tolerant and not classified as true halophytes. These include the common reed *P. australis* (Hill et al., 1999; Mauchamp and Mesléard, 2001) and *E. atherica* (Hill et al., 1999). Interestingly, these species also show xylem water values more negative than the soil water at their sampling location at the ridge site

(Fig. 2). Because these plants are not true halophytes, it is unlikely that this is due to their utilisation of the symplastic pathway. Rather, we suggest this phenomenon arises from these species having rooting depths below that sampled for soil water, i.e. deeper than c. 10 cm. This would allow them to take up water that has not been subjected to evaporative ^2H -enrichment. *P. australis* in particular has been known to develop roots as deep as 3 m (Thevs et al., 2007), which would allow it to exploit groundwater below the sampling range of this study.

5.4. The significance of leaf water

Physical differences among plants with different life forms, leading to various patterns of utilisation of environmental water, have been used to explain variation in $\delta^2\text{H}$ *n*-alkane values observed between both woody plants and grass (Liu et al., 2006). For instance, morphological characteristics have been identified as factors exerting a strong influence upon leaf water isotopic ^{18}O -enrichment (Helliiker and Ehleringer, 2002; Barbour et al., 2004). Kahmen et al. (2008) suggested that leaf water isotopic ^{18}O -enrichment can differ even among species that are closely related because of differences in the “effective path length” (the distance that water is required to flow from source to evaporation site) in their leaves, which would influence the flow of isotopically enriched water back from the substomatal cavity. Similar factors could potentially influence hydrogen isotopic composition of leaf water as well.

Studies seeking to apply factors relating to leaf water ^2H -enrichment to *n*-alkane data have attempted to explain observed variation in *n*-alkane $^2\text{H}/^1\text{H}$ in terms of differences in plant life form on the basis that these physical differences could have influenced evapotranspiration of the source water used by the plant during biosynthesis (Liu et al., 2006). At Stiffkey, plants display very different life forms ranging from succulents, grasses and shrubs. However, leaf waters extracted from morphologically distinct species at the same site in June 2011 (Fig. 4) show very little variation in their $\delta^2\text{H}$ values. For example, the ridge contains a range of plant species that differ significantly with respect to their leaf morphology. The reed *P. australis* has large, elongated leaves up to 30 cm long and 2 cm wide, while the leaf succulent *S. vera* has leaves that are only 3 mm in length and approximately 1.5 mm in diameter. However, the $\delta^2\text{H}_{\text{lw}}$ values range from +5‰ to +21‰ whilst $\delta^2\text{H}_{n\text{-C}_{29}}$ values differ by over 65‰ between these species. Similar patterns can be found in the seasonal data from 2012, where statistical analysis (Mann–Whitney *U* test, $P > 0.05$, $n = 8$ for comparison of species growing from March to September 2012; $n = 6$ for comparison of species growing from May to September 2012) confirms that interspecies variation in leaf water hydrogen isotope composition is generally not significant. Even if we compare species with extreme variation in leaf morphology such as *P. australis* and *S. vera* – where a statistically significant difference in leaf water does exist – leaf water $^2\text{H}/^1\text{H}$ between these two plants only ranges from 6‰ to 12‰ between May and September 2012. Leaf wax *n*- C_{29} $^2\text{H}/^1\text{H}$ values, however, differ consistently by over 50‰ during the same period (Fig. 5).

When all the species sampled at Stiffkey are considered, variability in leaf water $\delta^2\text{H}$ composition is three times lower than that observed in $\delta^2\text{H}_{n\text{-C}_{29}}$ in June 2011, and consistently 4–5 times lower throughout the seasonal time series from 2012. $^2\text{H}/^1\text{H}$ composition of *n*-alkanes ($\delta^2\text{H}_{n\text{-C}_{29}}$) varies across all seasonal sampling periods at Stiffkey by over 100‰, with the greatest variability observed in August (120‰). In contrast, leaf waters across the same period ($\delta^2\text{H}_{\text{lw}}$) show a total variation of only 29‰ (Supplementary information Table 4). This contrast between a large variability of *n*-alkane $\delta^2\text{H}$ and a small range of leaf water $\delta^2\text{H}$ values is particularly striking at the beginning and mid stages of the growing season. In March 2012, the mean values of *n*- C_{29} alkane show 103‰ variation among sampled species, with only 6‰ shifts in leaf water, whilst in August 2012 the *n*- C_{29} range exceeds 120‰ and leaf waters vary by only 29‰. *P. australis* generally has the most negative leaf water $^2\text{H}/^1\text{H}$ profile, whilst *L. vulgare*, *S. anglica* and *Salicornia* have leaf waters that are all generally ^2H -enriched compared with other species. Statistical analysis (Student's *t*-test, $P > 0.05$, $n = 10$ individuals per sampling interval comparing those species growing from March to September 2012) of seasonal shifts in leaf water $^2\text{H}/^1\text{H}$ among each species shows that March 2012 is significantly different from all other months. The range in leaf water $\delta^2\text{H}$ in March 2012 is quite limited compared with all other sampling periods. Even if the *n*-alkane $^2\text{H}/^1\text{H}$ profiles of our sampled species are in fact fixed at the time of leaf expansion, e.g. as suggested by Tipple et al. (2013), the range in $\delta^2\text{H}_{n\text{-C}_{29}}$ alkanes observed in March 2012 (103‰) have therefore to be attributed to something other than leaf water isotopic composition.

In addition, our data also show that ^2H -depletion and ^2H -enrichment in leaf water and *n*- C_{29} alkane values do not co-vary, i.e. any similarity in leaf water $^2\text{H}/^1\text{H}$ composition does not necessarily lead to a similarity in *n*-alkane $\delta^2\text{H}$ values. Fig. 2 presents data from the September 2012 sampling period, and shows that for species with very similar leaf water $^2\text{H}/^1\text{H}$ compositions, *n*-alkane values can vary considerably. For example, whilst *L. vulgare* and *Salicornia* have the most ^2H -enriched leaf water and *n*-alkane values, *A. portulacoides*, *S. vera* and *E. atherica* have leaf water values within 8‰ of each other whereas their *n*-alkane values vary by up to 89‰. In addition, the difference between $\delta^2\text{H}_{\text{lw}}$ of *Limonium* and *Elytrigia* is 19‰, while the range in *n*- C_{29} between these species $\delta^2\text{H}$ reaches 105‰.

Similar discrepancies between the magnitude of differences in the hydrogen isotope composition of leaf waters and the hydrogen isotope composition of the *n*- C_{29} alkane are found throughout all the sampling periods. For example, data collected in June 2011 (Fig. 4; Supplementary information Table 2) *T. maritima* from the low marsh has the most ^2H -depleted leaf water value (+22‰) of plants found in this sub-environment, but this does not result in *T. maritima* having the most ^2H -depleted *n*- C_{29} alkane value. Similarly, the C_4 grass *S. anglica* has the most ^2H -depleted *n*- C_{29} alkane (−156‰) value in the low marsh, but one of the more ^2H -enriched leaf waters (+27‰). This lack of correlation between leaf water and leaf wax $\delta^2\text{H}$ at the plant species level is also apparent in the June 2011 dataset

when species having very similar leaf water values – *L. vulgare* and *S. europaea* differ by only 1‰ in the low marsh – synthesised *n*-C₂₉ alkanes that differ by as much as 20‰ (Fig. 4).

At the ridge, where the greatest range in $\varepsilon_{\text{wax/lw}}$ values is observed in June 2011, this lack of correlation between leaf water and *n*-C₂₉ alkane ²H/¹H composition is also present (Fig. 4). Here, it is the C₃ reed, *P. australis* that has the most ²H-depleted leaf water (+5‰), but the *n*-C₂₉ *n*-alkane $\delta^2\text{H}$ value for this species does not follow this trend (Fig. 4). The most ²H-depleted *n*-C₂₉ alkane value on the ridge is in fact found in another C₃ grass, *E. atherica*, which has a leaf water $\delta^2\text{H}$ value of +15‰. As observed in the low marsh, similar leaf water δD values do not result in similar *n*-C₂₉ alkane $\delta^2\text{H}$ values: *A. portulacoides*, and *S. vera* and *E. atherica* all record leaf water ²H/¹H values ranging from +15‰ to +21‰, but differ by 93‰ in terms of their *n*-C₂₉ alkane $\delta^2\text{H}$ values. Even in the upper marsh, where the $\delta^2\text{H}$ values display the smallest overall range among plant species, *T. maritima* and *A. portulacoides* record the highest leaf water $\delta^2\text{H}$ values but in contrast have lowest *n*-C₂₉ alkane $\delta^2\text{H}$ values (Fig. 4). Statistical analysis of interspecies variation in *n*-C₂₉ hydrogen isotope composition supports our finding that leaf water ²H/¹H is of limited relative importance in controlling leaf wax $\delta^2\text{H}$ values. Variation in midday leaf water $\delta^2\text{H}$ among the sampled species was not found to be statistically significant, while in contrast interspecies variation in *n*-C₂₉ $\delta^2\text{H}$ was, suggesting some other mechanism was responsible for the >100‰ range in *n*-C₂₉ we report.

Previous research has suggested that some plants may utilise pre-dawn leaf water that has not been subject to diurnal evaporative enrichment when synthesising leaf wax *n*-alkanes (Sachse et al., 2010). Leaf water samples collected between 7:30 and 8:00 from three species capturing the full range of *n*-C₂₉ alkane $\delta^2\text{H}$ values at the ridge site (*E. atherica*, *A. portulacoides* and *S. vera*) show a maximum variation of 25‰ (Fig. 6). However, it is insufficient to explain the 89‰ range in the *n*-C₂₉ alkane $\delta^2\text{H}$ values from these species. Taken in consideration with the xylem water discussed above, it becomes apparent that even in the case of the most extreme theoretical scenario whereby *E. atherica* – the species with the lowest ²H/¹H *n*-C₂₉ value – made use of early morning xylem water (–47‰) for lipid synthesis, while *S. vera* (the species with the highest ²H/¹H *n*-C₂₉ value) instead used evaporatively ²H-enriched midday leaf water (+4‰), the maximum range in the pools of water for lipid synthesis would be 51‰ which still does not satisfactorily explain the 89‰ difference in $\delta^2\text{H}_{n\text{-C}_{29}}$ between them.

5.5. Comparison of ²H/¹H fractionation among C₃ and C₄ plants at Stiffkey with previously published research

Earlier work has suggested that C₃ vs. C₄ plants have relatively invariant fractionation factors between *n*-alkanes and leaf/source water. Examples include the generalised apparent fractionation factors between leaf water and *n*-alkyl lipids calculated for C₃ (–117 ± 27‰) and C₄ (–132 ± 12‰) plants (Chikaraishi and Naraoka, 2003; Chikaraishi et al.,

2004), which continue to be applied to modern vegetation studies (Tipple et al., 2013) and palaeoclimate reconstructions (van Soelen et al., 2013; Lieder et al., 2013). Our data suggest these predicted values may not reflect the true extent of plant lipid ²H/¹H diversity – if, for example, fractionation is calculated between leaf water and the *n*-C₂₉ alkane for September 2012, only half of the C₃ plants sampled have $\varepsilon_{\text{wax/lw}}$ values that fall within the range predicted by Chikaraishi and Naraoka (2003) and Chikaraishi et al. (2004) (Supplementary information Table 4). The remaining C₃ species, which include *E. atherica*, *P. australis* and *A. portulacoides*, have $\varepsilon_{\text{wax/water}}$ values that are 26–83‰ lower than the predicted values. This lack of agreement with estimated values is found throughout our dataset – in June 2011, only two C₃ species conform to the predicted values (Fig. 7b), while between March and August 2012, only *L. vulgare*, *S. vera* and *S. europaea* have $\varepsilon_{\text{wax/lw}}$ values that regularly fall within the predicted –90‰ to –144‰ range for C₃ species (Chikaraishi and Naraoka, 2003; Chikaraishi et al., 2004). With regards to the C₄-plant group, our calculated $\varepsilon_{\text{wax/lw}}$ values for the C₄ grass *S. anglica* for both June 2011 (–178‰) and the 2012 growing season (–115‰ to –176‰ between March and September) exceed the range of –120‰ to –144‰ for C₄ species published by Chikaraishi and Naraoka (2003) and Chikaraishi et al. (2004) (Fig. 7b; Fig. 8).

A consistent difference in apparent fractionation among C₃ and C₄ species has also been identified in some studies. For example, Chikaraishi and Naraoka (2003) presented data suggesting that C₄ species had higher apparent fractionation factors compared with C₃ angiosperms and gymnosperms. However, plant functional types were not distinguished in this study, and large standard deviations for the mean $\varepsilon_{\text{wax/w}}$ values (C₃ = –116 ± 25‰, C₄ = –133 ± 12‰) give rise to a degree of overlap in the range of these values. Bi et al. (2005) published data suggesting that in fact C₄ species are typified by *n*-alkane ²H/¹H compositions of –150.4 ± 42.6‰, while *n*-alkane $\delta^2\text{H}$ signatures in C₃ species average –175.7 ± 29.5‰. Smith and Freeman (2006) limited their study to C₃ and C₄ grasses, and found that ε values were ~20‰ more negative in C₃ grasses relative to C₄ grasses, resulting in more negative *n*-alkane ²H/¹H compositions in C₃ grasses. Their result for C₃ and C₄ monocots cannot be explained by gross anatomical differences in leaves and, therefore, it has been hypothesised that differences in the interveinal distance among C₃ and C₄ grasses – alongside difference in the extent of the backflow of enriched water from around the stomata – are responsible for the variation (Smith and Freeman, 2006; Tierney et al., 2010).

One implication of such studies is that the considerable scatter in *n*-alkane $\delta^2\text{H}$ among plants at a specific site is primarily a function of the very negative apparent fractionation between water and leaf wax lipids inherent in C₃ grasses. Our data show that the C₃ grass *E. atherica* consistently has the largest $\varepsilon_{\text{wax/lw}}$ value (up to –227‰), followed by the C₃ monocot reed *P. australis* (up to –204‰), while the average value for the C₄ *S. anglica* in 2012 is –154 ± 29‰. However, the maximum seasonal variability among Stiffkey species, when excluding both C₃ monocots, is still as high as 97‰, while for each sampling interval this

variability ranges from 30‰ to 50‰ (Supplementary information, Table 4). Similarly, if the C₃ monocots are excluded from consideration in our June 2011 dataset (SI Table 3), the maximum variability excluding *Elytrigia*, *Phragmites* and *Puccinellia maritima* is still 44‰. Our data imply that interspecies variation in apparent fractionation in the species at our study site is not explained by differences in C₃ versus C₄ photosynthetic pathways, or indeed in plant life form. The magnitude of variability when C₃ monocots are excluded from consideration also demonstrates that it may not always be accurate to assume that one plant functional type dictates the magnitude of interspecies variation in *n*-alkane ²H/¹H at any given location.

6. CONCLUSION

We have carried out a systematic study of the relationship between the hydrogen isotope composition of soil, xylem and leaf water and the ²H/¹H of the *n*-C₂₉ alkane within a range of halophytic and non-halophytic C₃ and C₄ plants growing at Stiffkey marsh in Norfolk, UK. Our data display significant interspecies variation in fractionation between leaf water and leaf wax, ranging from –79‰ to –229‰ across the 2012 growing season. The >100‰ range of our δ²H_{*n*-C₂₉} data, and the 150‰ range in ε_{wax/lw} values, extend beyond the typical values for C₃ and C₄ plants put forward in previous studies. We thus infer that reconstruction of palaeohydrological regimes based on estimates such as these may not capture the full complexity of the hydrogen isotope information recorded by these plant groups. The range in our *n*-alkane δ²H cannot be explained by reference to spatial or temporal shifts in the hydrogen isotope composition of soil, xylem or leaf water. We therefore conclude that environmental and physical mechanisms controlling leaf water isotopic composition cannot fully account for the interspecies variation in our *n*-alkane hydrogen isotope data. Instead, our data show that biochemical mechanisms may play a more important role in controlling interspecies variation in (i) *n*-alkane ²H/¹H composition, and (ii) fractionation between source water and *n*-alkane ²H/¹H, than abiotic factors.

Previous research has already identified that biochemical processes may have an important role to play in determining leaf biomarker ²H/¹H. However little is currently known about how this mechanism operates in terrestrial plants. We suggest that future studies should make use of an integrated approach and focus on distinguishing biochemically moderated fractionation from environmental and physical factors. The 100‰ range in *n*-alkane δ²H compositions recorded at Stiffkey highlights the fact that any attempt to reconstruct palaeohydrological information from sedimentary leaf-wax lipids needs to fully account for any shifts in ²H/¹H composition arising from changes in higher plant assemblages. Further research is necessary to improve our understanding of the relative importance of biosynthetic processes responsible for interspecies variation in leaf-wax lipid ²H/¹H, because this will determine the nature of the information – environmental signals versus differences in plant biochemistry – recorded in these biomarkers.

Only then can the use of *n*-alkane ²H/¹H analysis for palaeoclimate reconstructions be fully evaluated.

ACKNOWLEDGEMENTS

The authors gratefully acknowledge the assistance of Annette Eley, Louise Jones and Joseph Dillon during sample collection, Liz Rix for technical and analytical support during data generation and Professor Anthony Davy who provided valuable insights regarding halophyte plant adaptations in salt marshes. The authors also wish to thank Franz Street and Mike Andrews (University of Reading, UK) for technical and analytical support during the extraction of leaf, soil and stem waters. Professor John Allen (University of Reading, UK), is thanked for the useful discussions regarding salt marsh formation and geomorphology on the north Norfolk coast. We also thank A. Kahmen, S. Feakins, our Associate Editor P. Hernes and 3 anonymous reviewers for their helpful and constructive comments. This research was funded in part by the University of East Anglia.

APPENDIX A. SUPPLEMENTARY DATA

Supplementary data associated with this article can be found, in the online version, at <http://dx.doi.org/10.1016/j.gca.2013.11.045>.

REFERENCES

- Allen J. (2000) Morphodynamics of Holocene salt marshes: a review sketch from the Atlantic and Southern North Sea coasts of Europe. *Quatern. Sci. Rev.* **19**, 1155–1231.
- Allison S. (1992) The influence of rainfall variability on the species composition of a northern California salt marsh plant assemblage. *Plant Ecol.* **101**, 145–160.
- Andrews J., Boomer I., Bailiff I., Balson P., Bristow C., Chronston P., Funnell B., Harwood G., Jones R. and Maher B. (2000) Sedimentary evolution of the north Norfolk barrier coastline in the context of Holocene sea-level change. *Geol. Soc. Spec. Publ.* **166**, 219–251.
- Barbour M. M., Schurr U., Henry B. K., Wong S. C. and Farquhar G. D. (2000) Variation in the oxygen isotope ratio of phloem sap sucrose from castor bean. Evidence in support of the Péclet effect. *Plant Physiol.* **123**, 671–680.
- Barbour M., Roden J., Farquhar G. and Ehleringer J. (2004) Expressing leaf water and cellulose oxygen isotope ratios as enrichment above source water reveals evidence of a Péclet effect. *Oecologia* **138**, 426–435.
- Bi X., Sheng G., Liu X., Li C. and Fu J. (2005) Molecular and carbon and hydrogen isotopic composition of *n*-alkanes of plant leaf waxes. *Org. Geochem.* **36**, 1405–1417.
- Bohnert H. and Jensen R. (1996) Strategies for engineering water-stress tolerance in plants. *Trends Biotechnol.* **14**, 89–97.
- Boomer I. and Woodcock L. (1999) The nature and origin of Stiffkey Meals, North Norfolk coast. *Bull. Geol. Soc. Norfolk* **49**, 3–13.
- Boorman L. (1967) *Limonium vulgare* Mill. and *L. humile* Mill. *J. Ecol.* **55**, 221–232.
- Bowen G. J., Wassenaar L. I. and Hobson K. A. (2005) Global application of stable hydrogen and oxygen isotopes to wildlife forensics. *Oecologia* **143**, 337–348.
- Burke D., Weis J. and Weis P. (2000) Release of metals by the leaves of the salt marsh grasses *Spartina alterniflora* and *Phragmites australis*. *Estuar. Coast. Shelf Sci.* **51**, 153–159.

- Callaway J. C., Delaune R. D. and Patrick W. H. (1998) Heavy metal chronologies in selected coastal wetlands from Northern Europe. *Mar. Pollut. Bull.* **36**, 82–96.
- Callaway J., Delaune R. and Patrick, JR, W. (1996) Chernobyl ^{137}Cs used to determine sediment accretion rates at selected northern European coastal wetlands. *Limnol. Oceanogr.* **41**, 444–450.
- Chikaraishi Y. and Naraoka H. (2003) Compound-specific δD and $\delta^{13}\text{C}$ analyses of *n*-alkanes extracted from terrestrial and aquatic plants. *Phytochemistry* **63**, 361–371.
- Chikaraishi Y., Naraoka H. and Poulson S. (2004) Hydrogen and carbon isotopic fractionations of lipid biosynthesis among terrestrial (C_3 , C_4 and CAM) and aquatic plants. *Phytochemistry* **65**, 1369–1381.
- Cohen, E., Cvitaš, T., Frey, J., Homström, B., Kuchitsu, K., Marquardt, R., Mills, I., Pavese, F., Quack, M., Stohner, J., Strauss, H., Takami, M. and Thor, A. (eds.) (2007) *Quantities, Units and Symbols in Physical Chemistry*, 3rd ed. R. Soc. Chem. Publ., 265 pp.
- Corerria das Neves J., Ferrerria L., Vaz M. and Gazarini L. (2008) Gas exchange in the salt marsh species *Atriplex portulacoides* L. and *Limoniastrum monopetalum* L. in Southern Portugal. *Acta Physiol. Plant.* **30**, 91–97.
- Davy A. and Bishop G. (1991) *Triglochin maritima* L.. *J. Ecol.* **72**, 531–555.
- Davy A., Brown M., Mossman H. and Grant A. (2011) Colonisation of a newly developing salt marsh: disentangling independent effects of elevation and redox potential on halophytes. *J. Ecol.* **99**, 1350–1357.
- Duarte C. M., Middelburg J. and Caraco N. (2005) Major role of marine vegetation on the oceanic carbon cycle. *Biogeosciences* **2**, 1–8.
- Ellison A. (1987) Effects of competition, disturbance and herbivory on *Salicornia europaea*. *Ecology* **68**, 576–586.
- Ellsworth P. Z. and Williams D. G. (2007) Hydrogen isotope fractionation during water uptake by woody xerophytes. *Plant Soil* **291**, 93–107.
- Farquhar G. D. and Lloyd J. (1993) Carbon and oxygen isotope effects in the exchange of carbon dioxide between terrestrial plants and the atmosphere. In *Stable Isotopes and Plant Carbon Water Relations* (eds. J. R. Ehleringer, A. E. Hall and G. D. Farquhar). Academic Press, pp. 47–70.
- Feakins S. J. and Sessions A. L. (2010) Crassulacean acid metabolism influences D/H ratio of leaf wax in succulent plants. *Org. Geochem.* **41**, 1269–1276.
- Gao L., Burnier A. and Huang Y. (2012) Quantifying instantaneous regeneration rates of plant leaf waxes using stable hydrogen isotope labelling. *Rapid Commun. Mass Spectrom.* **26**, 115–122.
- Garcin Y., Schwab V. F., Gleixner G., Kahmen A., Todou B., Sene O., Onana J. M., Achoundong G. and Sachse D. (2012) Hydrogen isotope ratios of lacustrine sedimentary *n*-alkanes as proxies of tropical African hydrology: insights from a calibration transect across Cameroon. *Geochim. Cosmochim. Acta* **79**, 106–126.
- Helliker B. and Ehleringer J. (2002) Differential ^{18}O enrichment of leaf cellulose in C_3 versus C_4 grasses. *Funct. Plant Biol.* **29**, 435–442.
- Hilkert A., Douthitt C., Schluter H. and Brand W. (1999) Isotope ratio monitoring gas chromatography/mass spectrometry of D/H by high temperature conversion isotope ratio mass spectrometry. *Rapid Commun. Mass Spectrom.* **13**, 1226–1230.
- Hill, M., Mountford, J., Roy, D., Bunce, R. (1999) *ECOFAC 2a Technical Annex 490 - Ellenberg's indicator values for British Plants*. DETR.
- Hou J., D'Andrea W. J., Macdonald D. and Huang Y. (2007) Hydrogen isotopic variability in leaf waxes among terrestrial and aquatic plants around Blood Pond, Massachusetts (USA). *Org. Geochem.* **38**, 977–984.
- Huang Y., Shuman B., Wang Y. and Webb T. (2002) Hydrogen isotope ratios of palmitic acid in lacustrine sediments record late Quaternary climate variations. *Geology* **30**, 1103–1106.
- Jeffries R. (1977) Growth responses of coastal halophytes to inorganic nitrogen. *J. Ecol.* **65**, 847–865.
- Jeffries R. and Perkins N. (1977) The effects on the vegetation of the additions of inorganic nutrients to salt marsh soils at Stiffkey, Norfolk. *J. Ecol.* **65**, 867–882.
- Jetter R. and Schäffer S. (2006) Chemical composition of the *Prunus laurocerasus* leaf surface. Dynamic changes of the epicuticular wax film during leaf development. *Plant Physiol.* **126**, 1725–1737.
- Kahmen A., Simonin K., Tu K., Merchant A., Callister A., Siegwolf R., Dawson T. and Arndt S. (2008) Effects of environmental parameters, leaf physiological properties and leaf water relations on leaf water ^{18}O enrichment in different Eucalyptus species. *Plant Cell Environ.* **31**, 738–751.
- Kahmen A., Schefuss E. and Sachse D. (2013a) Leaf water deuterium enrichment shapes leaf wax *n*-alkane δD values of angiosperm plants I: Experimental evidence and mechanistic insights. *Geochim. Cosmochim. Acta* **111**, 39–49.
- Kahmen A., Hoffman B., Schefuss E., Arndt S., Cernusak L., West J. and Sachse D. (2013b) Leaf water deuterium enrichment shapes leaf wax *n*-alkane δD values of angiosperm plants II: Observational evidence and global implications. *Geochim. Cosmochim. Acta* **111**, 50–63.
- Leider A., Hinrichs K-U., Schefuß E. and Versteegh G. (2013) Distribution and stable isotopes of plant wax derived *n*-alkanes in lacustrine, fluvial and marine sediments along an Eastern Italian transect and their potential to reconstruct the hydrological cycle. *Geochim. Cosmochim. Acta*.
- Liu W., Yang H. and Li L. (2006) Hydrogen isotopic compositions of *n*-alkanes from terrestrial plants correlate with their ecological life forms. *Oecologia* **150**, 330–338.
- Mauchamp A. and Mesléard F. (2001) Salt tolerance in *Phragmites australis* populations from coastal Mediterranean marshes. *Aquat. Bot.* **70**, 39–52.
- McInerney F. A., Helliker B. R. and Freeman K. H. (2011) Hydrogen isotope ratios of leaf wax *n*-alkanes in grasses are insensitive to transpiration. *Geochim. Cosmochim. Acta* **75**, 541–554.
- Meier-Augenstein W. (1999) Applied gas chromatography coupled to isotope ratio mass spectrometry. *J. Chromatogr. A* **842**, 351–371.
- Mitsch W. and Gosselink J. (2000) *Wetlands*, 3rd ed. John Wiley and Sons.
- Moeller I., Spencer T. and French J. (1996) Wind wave attenuation over saltmarsh surfaces: preliminary results from Norfolk, England. *J. Coastal Res.* **12**, 1009–1016.
- Pagani M., Pedentchouk N., Huber M., Sluijs A., Schouten S., Brinkhuis H., Damste J. S. S., Dickens G. R. and The IODP Expedition 302 Expedition Scientists, (2006) Arctic hydrology during global warming at the Palaeocene/Eocene thermal maximum. *Nature* **442**, 671–675.
- Pedentchouk N., Sumner W., Tipple B. and Pagani M. (2008) $\Delta^{13}\text{C}$ and δD compositions of *n*-alkanes from modern angiosperms and conifers: an experimental set up in central Washington State, USA. *Org. Geochem.* **39**, 1066–1071.
- Plaster, E. (2009) *Soil Science and Management*, 5th ed. Delmar Cengage Learning. pp. 142–165.
- Pye K. (1992) Saltmarshes on the barrier coastline of north Norfolk, eastern England. In: Allen, J. R. L & Pye, K. (Eds.) *Saltmarshes: Morphodynamics, Conservation and Engineering Significance*, pp. 148–179, Cambridge University Press.

- Richardson, C. J. (2000) Freshwater wetlands. In: Barbour, M., Billings, W. (Eds) (2000) *North American Wetlands*. Cambridge University Press, pp. 449–501.
- Romero I. C. and Feakins S. J. (2011) Spatial gradients in plant leaf wax D/H across a coastal salt marsh in southern California. *Org. Geochem* **42**, 618–629.
- Sachse D., Gleixner G., Wilkes H. and Kahmen A. (2010) Leaf wax *n*-alkane δD values of field-grown barley reflect leaf water δD values at the time of leaf formation. *Geochim. Cosmochim. Acta* **74**, 6741–6750.
- Sachse D., Radke J. and Gleixner G. (2004) Hydrogen isotope ratios of recent lacustrine sedimentary *n*-alkanes record modern climate variability. *Geochim. Cosmochim. Acta* **68**, 4877–4889.
- Sachse D., Radke J. and Gleixner G. (2006) ΔD values of individual *n*-alkanes from terrestrial plants along a climatic gradient-implications for the sedimentary biomarker record. *Org. Geochem* **37**, 469–483.
- Sachse D., Billault I., Bowen G., Chikaraishi Y., Dawson T., Feakins S., Freeman K., Magill C., McInerney F., van der Meer M., Polissar P., Robins R., Sachs J., Schmidt H., Sessions A., White J., West J. and Kahmen A. (2012) Molecular paleohydrology: interpreting the hydrogen-isotopic composition of lipid biomarkers from photosynthesising organisms. *Annu. Rev. Earth Planet. Sci.* **40**, 221–249.
- Schefuß E., Schouten S. and Schneider R. R. (2005) Climatic controls on central African hydrology during the past 20,000 years. *Nature* **437**, 1003–1006.
- Schirmer U., Breckle S. (1982) The role of bladders for salt removal in some Chenopodiaceae (mainly *Atriplex* species). In: *Tasks for vegetation science 2: Contributions to the ecology of halophytes* (eds. D. Sen, K. Rajpurohit). Dr W Junk Publishers. pp. 215–231.
- Sessions A. L. (2006) Seasonal changes in D/H fractionation accompanying lipid biosynthesis in *Spartina alterniflora*. *Geochim. Cosmochim. Acta* **70**, 2153–2162.
- Shepherd T. and Griffiths D. (2006) The effects of stress on plant cuticular waxes. *New Phytol.* **171**, 469–499.
- Shu Y., Feng X., Posmentier E. S., Sonder L. J., Faiia A. M. and Yakir D. (2008) Isotopic studies of leaf water. Part 1: A physically based two-dimensional model for pine needles. *Geochim. Cosmochim. Acta* **72**, 5175–5188.
- Smith, F., Freeman, K. (2006) Influence of physiology and climate on δD of leaf wax *n*-alkanes from C3 and C4 grasses. *Geochim. Cosmochim. Acta* **70**, 1172–1187.
- Thevs N., Zerbe S., Gahlert F., Midjit M. and Succow M. (2007) Productivity of reed (*Phragmites australis* Trin. ex Steud.) in continental-arid NW China in relation to soil, groundwater, and land-use. *J. Appl. Bot. Food Qual.* **81**, 62–68.
- Tierney J., Russell J., Huang Y., Sinninghe Damsté J., Hopmans E. and Cohen A. (2008) Northern Hemisphere controls on tropical southeast African climate during the past 60,000 years. *Science* **322**, 252–255.
- Tierney J., Russell J. and Huang Y. (2010) A molecular perspective on Late Quaternary climate and vegetation change in the Lake Tanganyika basin, East Africa. *Quatern. Sci. Rev.* **29**, 787–800.
- Tipple B., Berke M., Doman C., Khachatryan S. and Ehleringer J. (2013) Leaf-wax *n*-alkanes record the plant-water environment at leaf flush. *Proc. Natl. Acad. Sci. USA* **110**, 2659–2664.
- Tipple B. and Pagani M. (2013) Environmental control on eastern broadleaf forest species' leaf wax distributions and D/H ratios. *Geochim. Cosmochim. Acta* **111**, 64–77.
- UK Meteorological Office. Met Office Integrated Data Archive System (MIDAS) Land and Marine Surface Stations Data (1853-current), NCAS British Atmospheric Data Centre, 2012, 10th March 2013. Available from: http://badc.nerc.ac.uk/view/badc.nerc.ac.uk__ATOM__dataent_ukmo-midas.
- van Soelen E., Wagner-Cremer F., Sinninghe-Damsté J., Reichert G. (2013) Reconstructing tropical cyclone frequency using hydrogen isotope ratios of sedimentary *n*-alkanes in northern Queensland, Australia. *Palaeogeogr. Palaeoclimatol. Palaeoecol.* **376**, 66–72.
- Vince S. W. and Snow A. A. (1984) Plant zonation in an Alaskan salt marsh: I. Distribution, abundance and environmental factors. *J. Ecol.* **72**, 651–667.
- Waisel Y. (1972) *Biology of Halophytes*. Academic Press, California.
- West A. G., Patrickson S. J. and Ehleringer J. R. (2006) Water extraction times for plant and soil materials used in stable isotope analysis. *Rapid Commun. Mass. Spectrom.* **20**, 1317–1321.
- Zhang Z., Zhao M., Eglington G., Lu H. and Huang C. (2006) Leaf wax lipids as paleovegetational and paleoenvironmental proxies for the Chinese Loess Plateau over the last 170 kyr. *Quatern. Sci. Rev.* **25**, 575–594.

Associate editor: Peter Hernes

Appendix 3:
Additional data pertaining to
Chapter 4

Appendix 3

JUNE 2011 Species	Concentration in $\mu\text{g g DM}^{-1}$														
	C21	C22	C23	C24	C25	C26	C27	C28	C29	C30	C31	C32	C33	C34	C35
<i>Atriplex portulacoides</i>	0.4	16.5	3.0	1.8	34.0	2.8	52.3	5.0	44.4	0.7	6.1	0.2	0.3	16.5	0.0
<i>Atriplex portulacoides</i>	0.4	19.3	3.4	1.9	42.7	3.0	59.5	2.1	47.7	0.9	7.4	0.3	0.4	19.1	0.0
Average	0.4	17.9	3.2	1.8	38.4	2.9	55.9	3.5	46.0	0.8	6.7	0.2	0.4	17.8	0.0
Absolute difference	0.0	1.8	0.3	0.1	5.6	0.2	4.6	1.4	2.1	0.1	0.8	0.1	0.1	1.7	0.0
<i>Elytrigia atherica</i>	0.4	13.2	3.0	0.8	4.3	2.0	13.6	2.8	99.8	1.9	75.7	0.5	7.3	14.1	0.0
<i>Elytrigia atherica</i>	0.3	9.4	3.8	1.7	7.6	4.5	27.5	4.6	176.0	2.5	96.4	0.6	11.0	10.4	0.3
Average	0.4	11.3	3.4	1.2	6.0	3.2	20.5	3.7	137.9	2.2	86.1	0.5	9.2	12.2	0.2
Absolute difference	0.1	1.9	0.5	0.6	2.1	1.6	8.9	1.2	48.8	0.4	13.3	0.1	2.4	1.9	0.2
<i>Limonium vulgare</i>	0.0	10.0	1.9	1.6	65.1	18.1	715.9	70.3	811.4	30.7	440.8	14.5	70.0	12.0	9.3
<i>Limonium vulgare</i>	0.0	10.8	2.0	1.1	51.0	13.2	635.8	61.2	843.3	44.8	635.0	31.1	169.7	14.9	31.3
Average	0.0	10.4	1.9	1.4	58.1	15.7	675.9	65.7	827.4	37.8	537.9	22.8	119.8	13.5	20.3
Absolute difference	0.0	0.5	0.0	0.2	7.0	2.5	40.1	4.5	20.5	9.0	124.0	10.6	63.8	1.9	14.1
<i>Phragmites australis</i>	0.3	26.5	2.7	1.4	12.1	2.0	32.2	6.3	56.1	0.6	4.5	0.0	0.0	28.0	0.0
<i>Phragmites australis</i>	0.4	23.5	3.2	1.3	10.3	2.0	23.3	5.1	30.1	0.5	2.3	0.0	0.0	25.5	0.0
Average	0.3	25.0	3.0	1.4	11.2	2.0	27.8	5.7	43.1	0.5	3.4	0.0	0.0	26.7	0.0
Absolute difference	0.1	1.5	0.3	0.0	0.9	0.0	4.5	0.6	13.0	0.0	1.1	0.0	0.0	1.2	0.0
<i>Puccinellia maritima</i>	0.7	9.4	3.4	1.1	7.9	2.7	13.3	3.7	93.4	2.2	73.4	0.6	13.2	10.1	0.4
<i>Puccinellia maritima</i>	0.2	9.7	2.5	1.2	9.1	3.8	14.2	4.6	103.7	2.5	86.4	0.8	15.0	10.6	0.5
Average	0.5	9.5	2.9	1.1	8.5	3.3	13.8	4.2	98.5	2.4	79.9	0.7	14.1	10.4	0.4
Absolute difference	0.2	0.2	0.4	0.1	0.7	0.7	0.6	0.6	6.5	0.2	8.3	0.1	1.1	0.3	0.0
<i>Spartina anglica</i>	1.8	11.0	2.6	0.5	6.2	2.1	40.1	7.7	125.4	3.8	25.2	0.3	0.5	9.5	0.0
<i>Spartina anglica</i>	1.8	11.5	3.2	0.7	5.1	1.9	27.2	6.3	110.6	4.4	37.0	0.7	0.9	10.9	0.0
Average	1.8	11.2	2.9	0.6	5.6	2.0	33.7	7.0	118.0	4.1	31.1	0.5	0.7	10.2	0.0
Absolute difference	0.0	0.3	0.4	0.1	0.5	0.1	6.4	0.7	7.4	0.4	7.5	0.2	0.3	0.9	0.0

JUNE 2011		Concentration in $\mu\text{g g DM}^{-1}$														
Species		C21	C22	C23	C24	C25	C26	C27	C28	C29	C30	C31	C32	C33	C34	C35
<i>Salicornia europaea</i>		0.2	12.7	1.8	0.5	3.6	1.1	3.0	1.2	3.8	1.1	2.5	0.9	0.8	14.3	0.2
<i>Salicornia europaea</i>		0.2	23.4	2.0	0.9	5.0	1.1	5.7	1.0	7.8	0.7	4.9	0.5	1.2	25.6	0.3
Average		0.2	18.1	1.9	0.7	4.3	1.1	4.4	1.1	5.8	0.9	3.7	0.7	1.0	20.0	0.2
Absolute difference		0.0	6.8	0.1	0.2	0.9	0.0	1.8	0.1	2.6	0.2	1.6	0.2	0.3	7.2	0.0
<i>Suaeda vera</i>		0.5	16.5	12.8	1.3	30.5	1.8	24.9	2.3	48.9	2.1	34.4	0.6	0.6	16.9	0.0
<i>Suaeda vera</i>		0.4	14.0	9.0	1.6	31.3	3.9	73.1	10.3	137.5	6.7	53.6	1.6	1.4	14.0	0.0
Average		0.4	15.2	10.9	1.5	30.9	2.8	49.0	6.3	93.2	4.4	44.0	1.1	1.0	15.5	0.0
Absolute difference		0.1	1.3	1.9	0.2	0.6	1.3	30.9	5.1	56.8	2.9	12.3	0.7	0.5	1.5	0.0
<i>Triglochin maritima</i>		0.3	8.3	2.3	0.7	3.2	1.1	9.9	2.9	35.8	8.1	43.5	4.1	7.0	8.3	0.4
<i>Triglochin maritima</i>		0.6	11.3	4.6	1.0	6.0	1.5	18.1	3.6	41.6	7.1	37.2	2.8	5.1	10.6	0.3
Average		0.5	9.8	3.5	0.8	4.6	1.3	14.0	3.2	38.7	7.6	40.4	3.4	6.0	9.4	0.3
Absolute difference		0.2	1.9	1.5	0.2	1.8	0.3	5.2	0.5	3.7	0.5	3.2	0.7	0.9	1.5	0.1

AUGUST 2011		Concentration in $\mu\text{g g DM}^{-1}$														
Species	Site	C21	C22	C23	C24	C25	C26	C27	C28	C29	C30	C31	C32	C33	C34	C35
<i>Spartina anglica</i>	UM	0.1	0.0	0.4	0.3	2.0	1.6	13.9	5.3	70.0	2.8	16.5	0.2	0.4	0.0	0.0
<i>Spartina anglica</i>	UM	0.4	0.0	1.0	0.5	3.4	2.7	30.0	10.3	145.9	6.4	32.7	0.5	0.7	0.0	0.0
Average		0.3	0.0	0.7	0.4	2.7	2.1	22.0	7.8	107.9	4.6	24.6	0.4	0.6		
Absolute difference		-0.1	0.0	0.3	0.1	0.7	0.5	8.0	2.5	37.9	1.8	8.1	0.1	0.1		
<i>Suaeda vera</i>	UM	0.2	0.2	7.0	0.9	17.8	1.1	33.8	1.5	37.0	1.0	16.3	0.3	0.3	0.0	0.0
<i>Suaeda vera</i>	UM	0.0	0.0	2.0	0.4	6.5	0.7	18.0	0.7	18.3	0.4	7.8	0.1	0.1	0.0	0.0
Average				4.5	0.7	12.1	0.9	25.9	1.1	27.7	0.7	12.0	0.2	0.2		
Absolute difference				2.5	0.3	5.7	0.2	7.9	0.4	9.3	0.3	4.2	0.1	0.1		
<i>Atriplex portulacoides</i>	UM	0.4	0.8	3.9	4.4	30.4	7.5	76.4	4.4	57.3	0.7	11.9	0.8	0.7	0.0	0.0
<i>Atriplex portulacoides</i>	UM	0.4	1.0	4.6	5.1	45.8	8.2	77.4	3.6	50.9	0.3	9.0	0.5	0.5	0.0	0.0
Average		0.4	0.9	4.2	4.7	38.1	7.9	76.9	4.0	54.1	0.5	10.5	0.7	0.6		
Absolute difference		0.0	-0.1	-0.3	-0.4	-7.7	-0.3	-0.5	0.4	3.2	0.2	1.5	0.2	0.1		
<i>Salicornia europaea</i>	UM	0.1	0.1	1.6	0.2	1.6	0.2	1.2	0.2	1.1	0.1	0.9	0.1	0.2	0.0	0.0
<i>Salicornia europaea</i>	UM	0.9	0.9	14.5	2.3	15.2	3.0	12.2	4.6	13.8	5.1	12.1	4.7	5.1	2.4	1.3
Average		0.5	0.5	8.0	1.3	8.4	1.6	6.7	2.4	7.4	2.6	6.5	2.4	2.7		
Absolute difference		-0.4	-0.4	-6.4	-1.0	-6.8	-1.4	-5.5	-2.2	-6.3	-2.5	-5.6	-2.3	-2.5		
<i>Limonium vulgare</i>	UM	0.0	0.0	0.0	0.0	1.4	1.1	47.3	13.8	159.5	17.2	199.8	14.4	57.4	2.2	17.5
<i>Limonium vulgare</i>	UM	0.0	0.0	0.0	0.0	1.9	1.2	61.6	18.4	220.2	20.7	238.5	16.6	67.4	2.3	18.4
Average						1.7	1.1	54.5	16.1	189.8	18.9	219.1	15.5	62.4	2.3	17.9
Absolute difference						-0.2	-0.1	7.1	2.3	30.4	1.8	19.3	1.1	5.0	0.1	0.4

Appendix 3

AUGUST 2011		Concentration in $\mu\text{g g DM}^{-1}$														
Species	Site	C21	C22	C23	C24	C25	C26	C27	C28	C29	C30	C31	C32	C33	C34	C35
<i>Spartina anglica</i>	LM	0.6	0.0	0.8	0.4	3.0	2.2	17.0	7.9	114.1	7.0	44.9	0.7	1.1	0.0	0.0
<i>Spartina anglica</i>	LM	0.5	0.0	0.8	0.5	3.6	2.4	20.0	7.7	104.3	5.6	31.9	0.6	1.4	0.0	0.0
Average		0.5	0.0	0.8	0.4	3.3	2.3	18.5	7.8	109.2	6.3	38.4	0.7	1.3	0.0	0.0
Absolute difference		0.0	0.0	0.0	0.1	0.4	0.2	1.8	0.1	4.9	0.7	6.5	0.1	0.2	0.0	0.0
<i>Salicornia europaea</i>	LM	0.2	0.1	1.6	0.2	1.5	0.1	1.0	0.1	0.9	0.1	0.6	0.0	0.1	0.0	0.0
<i>Salicornia europaea</i>	LM	0.3	0.2	1.9	0.2	1.5	0.1	0.9	0.1	0.8	0.1	0.6	0.0	0.1	0.0	0.0
Average		0.3	0.1	1.8	0.2	1.5	0.1	1.0	0.1	0.8	0.1	0.6	0.0	0.1	0.0	0.0
Absolute difference		0.0	0.0	-0.1	0.0	0.0	0.0	0.1	0.0	0.0	0.0	0.0	0.0	0.0	0.0	0.0
<i>Atriplex portulacoides</i>	LM	0.4	1.0	3.9	3.3	41.6	4.8	69.4	2.8	50.0	1.3	15.5	0.0	0.0	0.0	0.0
<i>Atriplex portulacoides</i>	LM	0.5	1.0	5.1	5.6	54.6	9.9	112.5	9.8	79.7	1.2	16.8	0.0	0.0	0.0	0.0
Average		0.5	1.0	4.5	4.5	48.1	7.4	90.9	6.3	64.8	1.3	16.2	0.0	0.0	0.0	0.0
Absolute difference		0.0	0.0	-0.6	-1.1	-6.5	-2.5	-21.5	-3.5	-14.8	0.1	-0.6	0.0	0.0	0.0	0.0
<i>Suaeda vera</i>	R	0.0	0.5	8.6	1.7	24.2	3.9	76.4	6.6	57.8	2.9	23.7	1.7	1.5	0.0	0.0
<i>Suaeda vera</i>	R	0.2	0.3	6.2	1.2	18.1	2.5	55.3	4.5	48.6	1.8	21.2	0.8	0.8	0.0	0.0
Average			0.4	7.4	1.4	21.1	3.2	65.9	5.5	53.2	2.4	22.5	1.2	1.2	0.0	0.0
Absolute difference			0.1	1.2	0.3	3.1	0.7	10.5	1.1	4.6	0.5	1.3	0.4	0.4	0.0	0.0
<i>Atriplex portulacoides</i>	R	0.0	0.5	2.3	3.1	21.3	5.7	47.1	6.3	39.7	0.6	5.4	0.0	0.0	0.0	0.0
<i>Atriplex portulacoides</i>	R	0.1	0.4	1.6	2.2	17.4	3.7	35.0	2.5	34.8	0.6	5.7	0.0	0.1	0.0	0.0
Average			0.4	2.0	2.7	19.4	4.7	41.0	4.4	37.3	0.6	5.6	0.0		0.0	0.0
Absolute difference			0.1	0.3	0.4	1.9	1.0	6.0	1.9	2.4	0.0	-0.2	0.0		0.0	0.0
<i>Elytrigia atherica</i>	R	0.0	0.0	0.5	0.4	1.3	2.0	4.0	2.8	22.2	0.8	15.5	0.2	1.6	0.0	0.0
<i>Elytrigia atherica</i>	R	0.0	0.0	0.7	0.6	1.9	2.4	6.1	3.5	27.4	1.5	29.6	0.3	2.6	0.0	0.0
Average				0.6	0.5	1.6	2.2	5.1	3.2	24.8	1.2	22.5	0.3	2.1		
Absolute difference				0.2	0.1	0.4	0.3	1.5	0.5	3.7	0.5	10.0	0.1	0.7		
<i>Phragmites australis</i>	R	0.0	0.0	2.9	3.1	17.1	5.4	30.4	11.1	42.8	0.9	1.3	0.0	0.0	0.0	0.0
<i>Phragmites australis</i>	R	0.0	0.0	2.0	1.9	11.5	3.5	21.0	7.8	31.3	0.6	1.0	0.0	0.0	0.0	0.0
Average				2.4	2.5	14.3	4.4	25.7	9.4	37.1	0.7	1.2				
Absolute difference				0.5	0.6	2.8	0.9	4.7	1.7	5.7	0.1	0.2				

Appendix 3

OCTOBER 2011		Concentration in $\mu\text{g g DM}^{-1}$													
Species	C21	C22	C23	C24	C25	C26	C27	C28	C29	C30	C31	C32	C33	C34	C35
<i>Atriplex portulacoides</i>	3.2	5.3	3.2	3.3	17.2	6.6	45.9	3.7	38.4	0.5	5.8	0.0	0.4	0.0	0.0
<i>Atriplex portulacoides</i>	0.0	0.0	0.9	0.7	4.7	1.3	12.8	0.9	14.1	0.0	3.1	0.0	0.0	0.0	0.0
Average	1.6	2.7	2.1	2.0	11.0	4.0	29.3	2.3	26.2	0.2	4.5	0.0	0.2	0.0	0.0
Absolute difference	1.6	2.7	1.2	1.3	6.3	2.7	16.5	1.4	12.2	0.2	1.3	0.0	0.2	0.0	0.0
<i>Elytrigia atherica</i>	0.0	1.9	1.5	1.8	5.1	8.1	19.1	11.9	82.8	4.7	68.6	0.8	8.1	0.0	0.0
<i>Elytrigia atherica</i>	1.8	3.8	3.0	3.2	8.9	14.4	32.8	20.7	138.4	8.5	112.8	1.0	12.3	0.0	0.0
Average	0.9	2.9	2.2	2.5	7.0	11.2	26.0	16.3	110.6	6.6	90.7	0.9	10.2	0.0	0.0
Absolute difference	0.9	0.9	0.7	0.7	1.9	3.2	6.9	4.4	27.8	1.9	22.1	0.1	2.1	0.0	0.0
<i>Limonium vulgare</i>	0.0	0.0	0.0	0.0	2.2	2.3	101.6	32.2	266.8	17.8	159.4	8.3	35.6	1.2	9.3
<i>Limonium vulgare</i>	0.0	0.0	0.0	0.0	0.8	1.2	54.3	17.6	144.7	12.2	113.6	6.0	25.4	0.8	7.0
Average	0.0	0.0	0.0	0.0	1.5	1.7	78.0	24.9	205.8	15.0	136.5	7.1	30.5	1.0	8.1
Absolute difference	0.0	0.0	0.0	0.0	0.7	0.6	23.7	7.3	61.0	2.8	22.9	1.2	5.1	0.2	1.1
<i>Phragmites australis</i>	0.0	3.6	2.0	3.2	22.4	7.0	42.7	15.9	58.2	1.3	3.3	0.0	0.4	0.0	0.0
<i>Phragmites australis</i>	0.0	0.0	0.9	1.5	10.1	3.0	17.5	6.2	22.5	0.4	0.8	0.0	0.0	0.0	0.0
Average	0.0	1.8	1.5	2.4	16.2	5.0	30.1	11.1	40.4	0.9	2.1	0.0	0.2	0.0	0.0
Absolute difference	0.0	1.8	0.6	0.9	6.2	2.0	12.6	4.8	17.9	0.4	1.2	0.0	0.2	0.0	0.0
<i>Spartina anglica</i>	0.0	0.0	0.4	0.4	3.1	1.5	17.4	6.7	91.0	4.7	25.0	0.4	0.8	0.0	0.0
<i>Spartina anglica</i>	0.0	0.0	0.7	0.7	4.8	2.1	23.3	9.2	118.0	6.3	34.1	0.5	1.2	0.0	0.0
Average	0.0	0.0	0.6	0.5	4.0	1.8	20.4	8.0	104.5	5.5	29.5	0.4	1.0	0.0	0.0
Absolute difference	0.0	0.0	0.2	0.2	1.1	0.4	3.8	1.6	17.1	1.0	5.7	0.1	0.2	0.0	0.0
<i>Salicornia europaea</i>	3.9	2.1	3.2	0.5	4.3	0.7	12.0	0.6	6.3	0.3	2.2	0.0	0.0	0.0	0.0
<i>Salicornia europaea</i>	3.0	0.0	2.3	0.4	3.0	0.5	7.4	0.4	3.8	0.0	1.3	0.0	0.0	0.0	0.0
Average	3.5	1.0	2.8	0.4	3.6	0.6	9.7	0.5	5.1	0.2	1.8	0.0	0.0	0.0	0.0
Absolute difference	0.4	1.0	0.4	0.1	0.7	0.1	2.3	0.1	1.3	0.2	0.5	0.0	0.0	0.0	0.0
<i>Suaeda vera</i>	0.0	0.0	1.7	0.5	7.9	2.1	66.1	4.7	60.5	1.2	12.2	0.0	0.0	0.0	0.0
<i>Suaeda vera</i>	0.0	0.0	2.3	0.7	10.6	2.0	73.6	4.4	47.8	0.9	9.0	0.0	0.0	0.0	0.0
Average	0.0	0.0	2.0	0.6	9.2	2.0	69.9	4.5	54.2	1.0	10.6	0.0	0.0	0.0	0.0
Absolute difference	0.0	0.0	-0.3	-0.1	-1.4	0.0	-3.7	0.1	6.4	0.2	1.6	0.0	0.0	0.0	0.0

Appendix 3

MARCH 2012		Concentration in $\mu\text{g g DM}^{-1}$													
Species	C21	C22	C23	C24	C25	C26	C27	C28	C29	C30	C31	C32	C33	C34	C35
<i>Limonium vulgare</i>	0.0	0.0	0.0	0.0	14.5	6.7	211.5	61.0	454.6	42.7	420.8	33.7	134.6	6.8	58.5
<i>Limonium vulgare</i>	0.0	0.0	0.0	0.0	13.4	5.4	167.6	44.1	316.7	29.7	285.9	21.7	79.0	3.7	32.9
Average	0.0	0.0	0.0	0.0	13.9	6.0	189.6	52.6	385.7	36.2	353.3	27.7	106.8	5.2	45.7
Absolute difference	0.0	0.0	0.0	0.0	0.5	0.6	22.0	8.5	69.0	6.5	67.5	6.0	27.8	1.6	12.8
<i>Elytrigia atherica</i>	0.6	0.0	5.1	1.6	19.3	4.3	92.9	13.0	551.8	10.0	359.9	3.0	67.1	0.0	2.0
<i>Elytrigia atherica</i>	0.6	0.0	5.6	2.6	22.3	6.4	121.7	16.9	646.9	12.4	386.8	3.5	74.0	0.0	2.8
Average	0.6	0.0	5.4	2.1	20.8	5.4	107.3	15.0	599.4	11.2	373.3	3.2	70.6	0.0	2.4
Absolute difference	0.0	0.0	0.3	0.5	1.5	1.1	14.4	2.0	47.6	1.2	13.4	0.2	3.4	0.0	0.4
<i>Suaeda vera</i>	0.0	0.0	12.8	2.0	47.3	6.1	160.0	8.2	236.8	7.9	132.4	0.0	0.0	0.0	0.0
<i>Suaeda vera</i>	0.0	0.0	7.3	1.0	24.1	5.2	124.5	7.8	164.7	5.5	72.7	0.0	1.5	0.0	0.0
Average	0.0	0.0	10.1	1.5	35.7	5.6	142.2	8.0	200.8	6.7	102.5	0.0	0.7	0.0	0.0
Absolute difference	0.0	0.0	2.8	0.5	11.6	0.4	17.7	0.2	36.1	1.2	29.9	0.0	-0.7	0.0	0.0
<i>Spartina anglica</i>	0.0	0.0	0.9	0.8	4.3	1.8	17.2	7.5	74.5	5.6	23.6	1.0	0.8	0.0	0.0
<i>Spartina anglica</i>	1.2	1.2	1.4	0.9	5.0	1.6	22.2	7.4	78.4	5.8	25.0	0.9	1.0	0.8	0.8
Average	0.6	0.6	1.1	0.8	4.7	1.7	19.7	7.4	76.4	5.7	24.3	1.0	0.9	0.4	0.4
Absolute difference	0.6	0.6	2.0	0.0	0.4	0.1	2.5	0.0	2.0	0.1	0.7	0.0	0.1	0.4	4.0
<i>Atriplex portulacoides</i>	2.5	1.8	9.0	6.0	85.6	14.9	183.2	10.9	175.3	3.1	41.6	0.4	1.1	0.0	0.0
<i>Atriplex portulacoides</i>	0.0	2.9	5.7	3.5	35.0	6.9	69.9	6.5	61.5	0.0	13.5	0.0	0.0	0.0	0.0
Average	1.2	2.3	7.3	4.8	60.3	10.9	126.6	8.7	118.4	1.6	27.6	0.2	0.5	0.0	0.0
Absolute difference	1.2	-0.6	1.6	1.2	25.3	4.0	56.7	2.2	56.9	1.6	14.0	0.2	0.5	0.0	0.0

Appendix 3

MAY 2012		Concentration in $\mu\text{g g DM}^{-1}$													
Species	C21	C22	C23	C24	C25	C26	C27	C28	C29	C30	C31	C32	C33	C34	C35
<i>Atriplex portulacoides</i>	1.4	1.2	4.8	3.7	48.0	7.8	69.0	6.3	53.6	1.0	10.0	0.0	0.0	0.0	0.0
<i>Atriplex portulacoides</i>	1.6	1.2	5.1	3.5	55.0	7.2	65.5	16.5	50.1	1.0	6.6	0.0	0.0	0.0	0.0
Average	1.5	1.2	5.0	3.6	51.5	7.5	67.2	11.4	51.8	1.0	8.3	0.0	0.0	0.0	0.0
Absolute difference	0.1	0.0	0.2	0.1	4.6	0.3	1.7	6.6	1.7	0.0	1.7	0.0	0.0	0.0	0.0
<i>Elytrigia atherica</i>	0.6	0.0	1.3	0.5	3.5	1.1	5.6	1.6	40.3	1.2	39.6	0.4	7.0	0.0	0.4
<i>Elytrigia atherica</i>	0.7	0.0	2.4	1.0	0.6	1.8	26.8	3.0	153.1	2.3	101.8	1.1	27.5	0.0	0.7
Average	0.6	0.0	1.8	0.7	2.1	1.4	16.2	2.3	96.7	1.7	70.7	0.8	17.3	0.0	0.5
Absolute difference	0.1	0.0	0.7	0.3	0.0	0.4	0.4	0.0	73.2	0.0	40.4	0.1	13.3	0.0	0.2
<i>Limonium vulgare</i>	0.5	0.0	4.2	0.6	20.9	3.0	175.7	19.2	331.6	14.4	243.5	8.3	49.4	1.2	11.5
<i>Limonium vulgare</i>	0.0	0.0	7.2	0.0	34.6	4.9	280.1	26.6	449.9	17.9	346.9	12.2	79.5	1.5	15.6
Average	0.2	0.0	5.7	0.3	27.8	4.0	227.9	22.9	390.8	16.2	295.2	10.2	64.4	1.3	13.5
Absolute difference	0.2	0.0	1.9	0.3	8.9	1.2	67.8	4.8	9.3	1.7	19.5	0.8	1.8	0.2	2.7
<i>Phragmites australis</i>	0.0	0.0	1.7	0.0	2.1	0.0	5.3	0.0	4.9	0.0	0.0	0.0	0.0	0.0	0.0
<i>Phragmites australis</i>	0.5	0.3	0.9	0.4	1.9	0.2	6.3	0.5	6.6	0.0	0.2	0.0	0.0	0.0	0.0
Average	0.2	0.1	1.3	0.2	2.0	0.1	5.8	0.3	5.7	0.0	0.1	0.0	0.0	0.0	0.0
Absolute difference	0.0	0.0	0.2	0.2	0.1	0.2	0.7	0.3	1.1	0.0	0.1	0.0	0.0	0.0	0.0
<i>Salicornia europaea</i>	0.5	0.2	0.7	0.0	0.7	0.2	1.0	0.2	2.0	0.2	1.3	0.0	0.3	0.0	0.0
<i>Salicornia europaea</i>	0.6	0.0	1.2	0.0	0.9	0.0	0.8	0.0	1.0	0.0	0.7	0.0	0.0	0.0	0.0
Average	0.5	0.1	0.9	0.0	0.8	0.1	0.9	0.1	1.5	0.1	1.0	0.0	0.1	0.0	0.0
Absolute difference	0.1	0.1	0.3	0.0	0.2	0.1	0.1	0.1	0.5	0.1	0.3	0.0	0.1	0.0	0.0
<i>Spartina anglica</i>	3.5	0.0	3.7	0.5	4.3	1.0	19.2	2.7	32.4	1.5	8.6	0.0	0.0	0.0	0.0
<i>Spartina anglica</i>	1.8	0.0	2.2	0.7	6.5	2.1	36.3	6.4	64.9	3.2	12.1	0.0	0.0	0.0	0.0
Average	2.6	0.0	3.0	0.6	5.4	1.6	27.8	4.5	48.6	2.3	10.3	0.0	0.0	0.0	0.0
Absolute difference	0.1	0.0	0.4	0.1	0.5	0.1	1.0	0.3	2.1	0.1	0.1	0.0	0.0	0.0	0.0
<i>Suaeda vera</i>	0.5	0.5	6.8	0.7	17.1	2.4	47.6	1.8	54.1	1.3	34.3	0.0	0.3	0.0	0.0
<i>Suaeda vera</i>	0.5	0.0	5.4	0.6	13.6	1.3	38.5	1.8	43.4	1.2	28.1	0.0	0.5	0.0	0.0
Average	0.5	0.5	6.1	0.6	15.4	1.8	43.1	1.8	48.7	1.2	31.2	0.0	0.4	0.0	0.0
Absolute difference	0.0		0.7	0.1	1.7	0.5	4.5	0.0	5.3	0.1	3.1	0.0	0.1	0.0	0.0

Appendix 3

AUGUST 2012		Concentration in $\mu\text{g g DM}^{-1}$													
Species	C21	C22	C23	C24	C25	C26	C27	C28	C29	C30	C31	C32	C33	C34	C35
<i>Atriplex portulacoides</i>	0.7	0.8	4.0	3.5	27.6	7.0	63.9	5.6	53.9	0.9	8.7	0.0	0.0	0.0	0.0
<i>Atriplex portulacoides</i>	0.5	0.6	3.4	2.3	31.6	4.2	47.4	1.7	32.5	0.4	5.6	0.0	0.0	0.0	0.0
Average	0.6	0.7	3.7	2.9	29.6	5.6	55.6	3.7	43.2	0.7	7.2	0.0	0.0	0.0	0.0
Absolute difference	0.1	0.1	0.3	0.6	2.0	1.4	8.3	2.0	10.7	0.2	1.6	0.0	0.0	0.0	0.0
<i>Elytrigia atherica</i>	0.0	0.0	1.7	1.2	3.1	4.3	13.2	2.7	94.3	2.1	50.2	0.6	3.4	0.0	0.0
<i>Elytrigia atherica</i>	0.0	0.0	1.7	1.2	3.1	3.4	13.7	2.8	91.1	2.1	47.9	0.7	3.3	0.0	0.0
Average	0.0	0.0	1.7	1.2	3.1	3.8	13.5	2.7	92.7	2.1	49.1	0.6	3.4	0.0	0.0
Absolute difference	0.0	0.0	0.0	0.0	0.0	0.4	0.4	0.0	1.6	0.0	1.2	0.1	0.1	0.0	0.0
<i>Limonium vulgare</i>	0.0	0.0	0.0	0.0	11.8	3.4	154.0	18.9	214.5	14.0	207.0	11.2	56.9	0.0	16.0
<i>Limonium vulgare</i>	0.0	0.0	0.0	0.0	7.1	2.4	114.1	18.7	228.8	16.6	237.1	12.5	59.7	0.0	14.3
Average	0.0	0.0	0.0	0.0	9.4	2.9	134.0	18.8	221.6	15.3	222.1	11.9	58.3	0.0	15.1
Absolute difference	0.0	0.0	0.0	0.0	2.4	0.5	19.9	0.1	9.3	1.7	19.5	0.8	1.8	0.0	0.8
<i>Phragmites australis</i>	0.4	0.7	2.4	1.5	13.0	1.9	16.9	6.0	20.1	0.3	1.4	0.0	0.0	0.0	0.0
<i>Phragmites australis</i>	0.4	0.7	2.7	1.4	13.0	1.5	13.9	5.2	13.5	0.0	0.6	0.0	0.0	0.0	0.0
Average	0.4	0.7	2.5	1.4	13.0	1.7	15.4	5.6	16.8	0.2	1.0	0.0	0.0	0.0	0.0
Absolute difference	0.0	0.0	0.2	0.0	0.0	0.2	1.5	0.4	3.3	0.2	0.4	0.0	0.0	0.0	0.0
<i>Salicornia europaea</i>	0.9	0.2	3.8	0.2	1.6	0.2	1.2	0.1	1.4	0.1	1.0	0.0	0.2	0.0	0.0
<i>Salicornia europaea</i>	0.9	0.2	3.5	0.2	1.5	0.2	1.0	0.1	1.1	0.1	0.7	0.0	0.2	0.0	0.0
Average	0.9	0.2	3.6	0.2	1.6	0.2	1.1	0.1	1.3	0.1	0.9	0.0	0.2	0.0	0.0
Absolute difference	0.0	0.0	0.2	0.0	0.1	0.0	0.1	0.0	0.1	0.0	0.1	0.0	0.0	0.0	0.0
<i>Spartina anglica</i>	0.6	0.0	1.1	0.0	1.5	0.4	4.3	1.7	20.9	1.0	5.0	0.0	0.0	0.0	0.0
<i>Spartina anglica</i>	0.8	0.0	1.6	0.0	2.3	0.6	5.8	2.2	24.2	1.2	5.2	0.0	0.0	0.0	0.0
Average	0.7	0.0	1.4	0.0	1.9	0.5	5.1	2.0	22.5	1.1	5.1	0.0	0.0	0.0	0.0
Absolute difference	0.1	0.0	0.4	0.0	0.5	0.1	1.0	0.3	2.1	0.1	0.1	0.0	0.0	0.0	0.0
<i>Suaeda vera</i>	0.0	0.3	5.9	0.9	21.5	2.3	74.9	6.0	76.8	2.6	25.8	0.6	0.5	0.0	0.0
<i>Suaeda vera</i>	0.0	0.0	4.3	0.6	14.6	1.3	61.6	2.4	47.4	1.1	17.4	0.0	0.0	0.0	0.0
Average	0.0	0.3	5.1	0.8	18.1	1.8	68.3	4.2	62.1	1.8	21.6	0.3	0.5	0.0	0.0
Absolute difference	0.0		0.8	0.2	3.4	0.5	6.7	1.8	14.7	0.8	4.2	0.3		0.0	0.0

Appendix 3

SEPTEMBER 2012		Concentration in $\mu\text{g g DM}^{-1}$													
Species	C21	C22	C23	C24	C25	C26	C27	C28	C29	C30	C31	C32	C33	C34	C35
<i>Atriplex portulacoides</i>	0.8	0.8	36.3	3.8	28.9	7.0	66.1	12.3	63.5	1.6	13.1	0.0	0.0	0.0	0.0
<i>Atriplex portulacoides</i>	0.3	0.3	1.1	0.9	5.4	1.3	11.6	2.2	10.6	0.2	2.1	0.0	0.0	0.0	0.0
Average	0.6	0.5	18.7	2.4	17.1	4.1	38.9	7.3	37.1	0.9	7.6	0.0	0.0	0.0	0.0
Absolute difference	0.2	0.3	17.6	1.4	11.7	2.8	27.2	5.0	26.5	0.7	5.5	0.0	0.0	0.0	0.0
<i>Elytrigia atherica</i>	0.2	0.3	2.1	1.7	5.1	7.5	18.0	10.0	57.9	3.9	46.7	0.7	4.9	0.0	0.3
<i>Elytrigia atherica</i>	0.2	0.2	1.8	1.4	4.4	6.7	16.5	9.7	55.7	3.9	49.0	0.7	5.0	0.0	0.1
Average	0.2	0.2	2.0	1.5	4.8	7.1	17.3	9.9	56.8	3.9	47.9	0.7	4.9	0.0	0.2
Absolute difference	0.0	0.0	0.1	0.1	0.0	0.4	0.4	0.0	1.1	0.0	1.4	0.1	0.1	0.0	0.1
<i>Limonium vulgare</i>	0.0	0.0	0.0	0.8	4.4	2.3	100.5	24.2	275.0	21.8	246.7	15.7	72.5	3.1	24.1
<i>Limonium vulgare</i>	0.0	1.1	1.2	1.1	11.0	6.6	220.2	53.6	347.3	40.8	341.6	28.0	112.3	3.6	27.2
Average	0.0	1.1	1.2	1.0	7.7	4.5	160.4	38.9	311.2	31.3	294.2	21.8	92.4	3.3	25.6
Absolute difference	0.0			0.2	4.2	2.8	77.7	19.1	9.3	1.7	19.5	0.8	1.8	0.3	2.0
<i>Phragmites australis</i>	0.4	0.8	2.8	2.6	20.6	3.6	25.9	9.7	30.5	0.9	2.6	0.0	0.0	0.0	0.0
<i>Phragmites australis</i>	0.3	0.7	2.5	2.3	18.5	3.3	22.6	8.5	26.1	0.7	1.6	0.0	0.0	0.0	0.0
Average	0.3	0.7	2.6	2.5	19.6	3.4	24.2	9.1	28.3	0.8	2.1	0.0	0.0	0.0	0.0
Absolute difference	0.0	0.0	0.2	0.2	1.1	0.2	1.7	0.6	2.2	0.1	0.5	0.0	0.0	0.0	0.0
<i>Salicornia europaea</i>	0.0	0.4	3.8	1.0	5.5	1.7	6.6	1.2	4.8	0.7	3.0	0.6	0.4	0.0	0.0
<i>Salicornia europaea</i>	0.0	0.0	1.1	0.0	1.3	0.3	2.4	0.6	2.6	0.4	1.7	0.0	0.4	0.0	0.0
Average	0.0	0.4	2.5	1.0	3.4	1.0	4.5	0.9	3.7	0.6	2.3	0.3	0.4	0.0	0.0
Absolute difference	0.0		1.4		2.1	0.7	2.1	0.3	1.1	0.2	0.6	0.3	0.0	0.0	0.0
<i>Spartina anglica</i>	0.4	0.3	0.6	0.5	2.0	1.7	8.3	3.4	30.7	1.6	5.7	0.0	0.0	0.0	0.0
<i>Spartina anglica</i>	0.6	0.0	1.2	1.2	5.3	3.4	20.5	10.2	110.8	7.6	38.0	0.0	0.0	0.0	0.0
Average	0.5	0.1	0.9	0.8	3.7	2.6	14.4	6.8	70.7	4.6	21.9	0.0	0.0	0.0	0.0
Absolute difference	0.1	0.1	0.4	0.4	0.5	0.1	1.0	0.3	2.1	0.1	0.1	0.0	0.0	0.0	0.0
<i>Suaeda vera</i>	0.0	0.0	1.9	0.3	5.5	0.9	29.8	2.1	18.9	0.4	4.5	0.0	0.0	0.0	0.0
<i>Suaeda vera</i>	0.0	0.0	5.9	1.1	20.8	3.0	101.9	7.0	68.8	1.7	17.5	0.0	0.0	0.0	0.0
Average	0.0	0.0	3.9	0.7	13.2	1.9	65.9	4.5	43.9	1.1	11.0	0.0	0.0	0.0	0.0
Absolute difference	0.0		2.6	0.3	10.0	1.4	46.8	3.2	32.5	0.8	8.5	0.0		0.0	0.0

Appendix 3

JUNE 2011 species	% distribution (normalised Σ odd- chain C21 to C35 alkanes)							
	C21	C23	C25	C27	C29	C31	C33	C35
<i>Atriplex portulacoides</i>	0.3	2.0	22.5	34.7	29.4	4.1	0.2	0.0
<i>Atriplex portulacoides</i>	0.3	2.0	25.2	35.1	28.1	4.3	0.2	0.0
Average	0.3	2.0	23.9	34.9	28.8	4.2	0.2	0.0
Absolute difference	0.0	0.0	1.3	0.2	0.7	0.1	0.0	0.0
<i>Elytrigia etherica</i>	0.2	1.4	2.0	6.4	47.0	35.7	3.5	0.0
<i>Elytrigia etherica</i>	0.1	1.1	2.3	8.2	52.3	28.6	3.3	0.1
Average	0.1	1.3	2.1	7.3	49.7	32.2	3.4	0.0
Absolute difference	0.1	0.2	0.1	0.9	2.6	3.5	0.1	0.0
<i>Limonium vulgare</i>	0.0	0.1	2.9	31.8	36.1	19.6	3.1	0.4
<i>Limonium vulgare</i>	0.0	0.1	2.0	25.2	33.5	25.2	6.7	1.2
Average	0.0	0.1	2.5	28.5	34.8	22.4	4.9	0.8
Absolute difference	0.0	0.0	0.4	3.3	1.3	2.8	1.8	0.4
<i>Phragmites australis</i>	0.2	2.3	10.2	27.3	47.5	3.8	0.0	0.0
<i>Phragmites australis</i>	0.5	4.1	13.1	29.6	38.4	2.9	0.0	0.0
Average	0.4	3.2	11.6	28.5	42.9	3.4	0.0	0.0
Absolute difference	0.1	0.9	1.4	1.2	4.6	0.4	0.0	0.0
<i>Puccinellia maritima</i>	0.3	1.6	3.7	6.1	43.3	34.0	6.1	0.2
<i>Puccinellia maritima</i>	0.1	1.0	3.7	5.8	42.4	35.3	6.1	0.2
Average	0.2	1.3	3.7	6.0	42.8	34.7	6.1	0.2
Absolute difference	0.1	0.3	0.0	0.2	0.4	0.7	0.0	0.0
<i>Spartina anglica</i>	0.8	1.2	2.9	18.6	58.0	11.7	0.2	0.0
<i>Spartina anglica</i>	0.9	1.6	2.5	13.6	55.4	18.5	0.5	0.0
Average	0.9	1.4	2.7	16.1	56.7	15.1	0.3	0.0
Absolute difference	0.0	0.2	0.2	2.5	1.3	3.4	0.1	0.0
<i>Salicornia europaea</i>	1.0	9.0	17.2	14.4	18.3	11.9	3.7	1.1
<i>Salicornia europaea</i>	0.6	6.3	16.2	18.5	25.1	15.7	3.7	0.8
Average	0.8	7.6	16.7	16.4	21.7	13.8	3.7	1.0
Absolute difference	0.2	1.3	0.5	2.0	3.4	1.9	0.0	0.1
<i>Suaeda vera</i>	0.3	7.9	19.0	15.5	30.4	21.4	0.4	0.0
<i>Suaeda vera</i>	0.1	2.7	9.5	22.1	41.6	16.2	0.4	0.0
Average	0.2	5.3	14.2	18.8	36.0	18.8	0.4	0.0
Absolute difference	0.1	2.6	4.7	3.3	5.6	2.6	0.0	0.0
<i>Triglochin maritima</i>	0.3	1.9	2.7	8.3	30.0	36.5	5.8	0.3
<i>Triglochin maritima</i>	0.5	3.6	4.7	14.0	32.1	28.7	4.0	0.2
Average	0.4	2.7	3.7	11.1	31.1	32.6	4.9	0.3
Absolute difference	0.1	0.8	1.0	2.8	1.1	3.9	0.9	0.1

Appendix 3

August 2011		% distribution (normalised Σ odd-chain C21 to C35 alkanes)							
Species	Site	C21	C23	C25	C27	C29	C31	C33	C35
<i>Spartina anglica</i>	LM	0.3	0.4	1.5	8.5	57.2	22.5	0.6	0.0
<i>Spartina anglica</i>	LM	0.3	0.4	2.0	11.1	58.2	17.8	0.8	0.0
Average		0.3	0.4	1.7	9.8	57.7	20.1	0.7	0.0
Absolute difference		0.0	0.0	0.2	1.3	0.5	2.3	0.1	0.0
<i>Salicornia europaea</i>	LM	3.7	24.3	22.8	15.5	12.8	9.5	1.7	0.0
<i>Salicornia europaea</i>	LM	4.1	27.5	22.4	13.4	11.3	8.2	1.7	0.0
Average		3.9	25.9	22.6	14.4	12.0	8.9	1.7	0.0
Absolute difference		0.2	1.6	0.2	1.1	0.8	0.6	0.0	0.0
<i>Atriplex portulacoides</i>	LM	0.2	2.0	21.4	35.8	25.7	8.0	0.0	0.0
<i>Atriplex portulacoides</i>	LM	0.2	1.7	18.4	37.9	26.9	5.7	0.0	0.0
Average		0.2	1.9	19.9	36.8	26.3	6.8	0.0	0.0
Absolute difference		0.0	0.2	1.5	1.1	0.6	1.2	0.0	0.0
<i>Suaeda vera</i>	R	0.0	4.1	11.5	36.5	27.6	11.3	0.7	0.0
<i>Suaeda vera</i>	R	0.1	3.8	11.2	34.3	30.1	13.1	0.5	0.0
Average		0.0	4.0	11.4	35.4	28.8	12.2	0.6	0.0
Absolute difference		0.0	0.1	0.2	1.1	1.3	0.9	0.1	0.0
<i>Atriplex portulacoides</i>	R	0.0	1.8	16.2	35.7	30.1	4.1	0.0	0.0
<i>Atriplex portulacoides</i>	R	0.1	1.6	16.7	33.6	33.4	5.5	0.1	0.0
Average		0.1	1.7	16.4	34.6	31.8	4.8	0.1	0.0
Absolute difference		0.1	0.1	0.3	1.1	1.7	0.7	0.1	0.0
<i>Elytrigia atherica</i>	R	0.0	0.9	2.6	7.9	43.3	30.2	3.1	0.0
<i>Elytrigia atherica</i>	R	0.0	1.0	2.5	8.0	35.7	38.6	3.4	0.0
Average		0.0	0.9	2.5	7.9	39.5	34.4	3.2	0.0
Absolute difference		0.0	0.0	0.0	0.1	3.8	4.2	0.1	0.0
<i>Phragmites australis</i>	R	0.0	2.6	14.8	26.5	37.2	1.2	0.0	0.0
<i>Phragmites australis</i>	R	0.0	2.4	14.3	26.0	38.9	1.2	0.0	0.0
Average		0.0	2.5	14.6	26.3	38.1	1.2	0.0	0.0
Absolute difference		0.0	0.1	0.3	0.2	0.9	0.0	0.0	0.0
<i>Spartina anglica</i>	UM	0.1	0.4	1.7	12.3	61.6	14.5	0.4	0.0
<i>Spartina anglica</i>	UM	0.2	0.4	1.5	12.8	62.2	14.0	0.3	0.0
Average		0.1	0.4	1.6	12.5	61.9	14.2	0.3	0.0
Absolute difference		0.0	0.0	0.1	0.3	0.3	0.3	0.1	0.0
<i>Suaeda vera</i>	UM	0.1	5.9	15.2	28.8	31.5	13.9	0.2	0.0
<i>Suaeda vera</i>	UM	0.0	3.7	11.8	32.7	33.3	14.1	0.2	0.0
Average		0.1	4.8	13.5	30.8	32.4	14.0	0.2	0.0
Absolute difference		0.1	1.1	1.7	2.0	0.9	0.1	0.0	0.0
<i>Atriplex portulacoides</i>	UM	0.2	1.9	15.2	38.3	28.7	6.0	0.3	0.0
<i>Atriplex portulacoides</i>	UM	0.2	2.2	22.1	37.3	24.6	4.4	0.3	0.0
Average		0.2	2.1	18.7	37.8	26.6	5.2	0.3	0.0
Absolute difference		0.0	0.1	3.4	0.5	2.1	0.8	0.0	0.0
<i>Salicornia europaea</i>	UM	1.9	21.0	20.4	15.9	14.2	11.9	2.8	0.0
<i>Salicornia europaea</i>	UM	1.0	14.8	15.5	12.5	14.0	12.3	5.2	1.3
Average		1.4	17.9	18.0	14.2	14.1	12.1	4.0	0.7
Absolute difference		0.5	3.1	2.5	1.7	0.1	0.2	1.2	-0.7
<i>Limonium vulgare</i>	UM	0.0	0.0	0.3	8.9	30.0	37.6	10.8	3.3
<i>Limonium vulgare</i>	UM	0.0	0.0	0.3	9.2	33.0	35.7	10.1	2.8
Average		0.0	0.0	0.3	9.1	31.5	36.7	10.5	3.0
Absolute difference		0.0	0.0	0.0	0.2	1.5	0.9	0.3	0.3

Appendix 3

OCTOBER 2011		% distribution (normalised Σ odd- chain C21 to C35 alkanes)							
species	Site	C21	C23	C25	C27	C29	C31	C33	C35
<i>Spartina anglica</i>	LM	0.0	0.3	2.3	12.6	66.1	18.2	0.6	0.0
<i>Spartina anglica</i>	LM	0.0	0.4	2.6	12.8	64.8	18.7	0.6	0.0
Average		0.0	0.3	2.4	12.7	65.4	18.4	0.6	0.0
Absolute difference		0.0	0.0	1.0	0.1	0.6	0.3	0.0	0.0
<i>Salicornia europaea</i>	LM	2.0	11.1	15.0	42.0	22.1	7.8	0.0	0.0
<i>Salicornia europaea</i>	LM	2.4	12.8	16.3	40.3	20.9	7.3	0.0	0.0
Average		2.2	12.0	15.7	41.1	21.5	7.5	0.0	0.0
Absolute difference		0.2	0.8	0.6	1.0	3.0	0.3	0.0	0.0
<i>Atriplex portulacoides</i>		0.0	9.8	45.4	35.5	6.7	0.0	0.0	0.0
<i>Atriplex portulacoides</i>	LM	0.0	10.7	47.4	38.1	6.4	0.0	0.0	0.0
Average	LM	0.0	10.3	46.4	36.8	6.5	0.0	0.0	0.0
Absolute difference		0.0	0.4	1.0	1.0	2.0	1.0	0.0	0.0
<i>Limonium vulgare</i>	LM	0.0	0.0	2.8	26.0	42.6	26.1	2.3	0.2
<i>Limonium vulgare</i>	LM	0.0	0.0	1.6	28.1	44.9	23.2	2.1	0.2
Average		0.0	0.0	2.2	27.1	43.7	24.6	2.2	0.2
Absolute difference		0.0	0.0	0.6	1.0	2.0	1.0	0.1	0.0
<i>Suaeda vera</i>	R	0.0	1.2	5.3	44.5	40.8	8.2	0.0	0.0
<i>Suaeda vera</i>	R	0.0	1.6	7.4	51.3	33.3	6.3	0.0	0.0
Average		0.0	1.4	6.3	47.9	37.1	7.3	0.0	0.0
Absolute difference		0.0	0.2	1.1	3.4	3.7	3.0	2.0	0.0
<i>Atriplex portulacoides</i>	R	0.4	2.9	15.5	41.2	34.5	5.2	0.3	0.0
<i>Atriplex portulacoides</i>	R	0.0	2.5	13.3	36.0	39.5	8.8	0.0	0.0
Average		0.2	2.7	14.4	38.6	37.0	7.0	0.2	0.0
Absolute difference		0.2	1.0	2.0	2.0	2.5	1.8	0.2	0.0
<i>Elytrigia atherica</i>	R	0.0	0.8	2.8	10.3	44.7	37.0	4.4	0.0
<i>Elytrigia atherica</i>	R	0.1	1.0	2.9	10.6	44.9	36.6	4.0	0.0
Average		0.0	0.9	2.8	10.5	44.8	36.8	4.2	0.0
Absolute difference		0.0	0.1	0.1	0.2	0.1	1.0	0.2	0.0
<i>Phragmites australis</i>	R	0.0	1.6	17.4	33.1	45.1	2.5	0.3	0.0
<i>Phragmites australis</i>	R	0.0	1.8	19.4	33.7	43.4	1.6	0.0	0.0
Average		0.0	1.7	18.4	33.4	44.3	2.1	0.2	0.0
Absolute difference		0.0	0.1	1.0	0.3	0.8	0.5	0.2	0.0
<i>Limonium vulgare</i>	UM	0.0	0.0	0.4	17.7	46.4	27.7	6.2	1.6
<i>Limonium vulgare</i>	UM	0.0	0.0	0.2	15.7	41.9	32.9	7.3	2.0
Average		0.0	0.0	0.3	16.7	44.1	30.3	6.8	1.8
Absolute difference		0.0	0.0	0.1	1.0	2.0	1.0	0.6	0.2
<i>Salicornia europaea</i>	UM	15.7	41.0	22.9	10.8	9.6	0.0	0.0	0.0
<i>Salicornia europaea</i>	UM	14.5	39.2	24.1	12.0	10.2	0.0	0.0	0.0
Average		15.1	40.1	23.5	11.4	9.9	0.0	0.0	0.0
Absolute difference		0.6	0.9	0.6	1.0	2.0	1.0	0.0	0.0
<i>Suaeda vera</i>	UM	0.0	6.6	24.6	48.1	19.1	1.6	0.0	0.0
<i>Suaeda vera</i>	UM	0.0	8.2	27.0	44.9	16.3	3.5	0.0	0.0
Average		0.0	7.4	25.8	46.5	17.7	2.6	0.0	0.0
Absolute difference		0.0	0.8	1.2	1.0	2.0	1.0	0.0	0.0
<i>Atriplex portulacoides</i>	UM	0.0	17.9	51.4	23.9	6.8	0.0	0.0	0.0
<i>Atriplex portulacoides</i>	UM	0.0	17.9	44.6	30.6	6.9	0.0	0.0	0.0
Average		0.0	17.9	48.0	27.2	6.9	0.0	0.0	0.0
Absolute difference		0.0	0.0	3.4	1.0	2.0	1.0	0.0	0.0

Appendix 3

March 2012		% distribution (normalised Σ odd- chain C21 to C35 alkanes)						
species	C21	C23	C25	C27	C29	C31	C33	C35
<i>Spartina anglica</i>	0.0	0.7	3.1	12.6	54.3	17.2	0.7	0.0
<i>Spartina anglica</i>	0.0	0.0	3.5	15.3	53.9	17.2	0.0	0.0
Average		0.3	3.3	13.9	54.1	17.2	0.4	
Absolute difference		0.3	0.2	1.3	0.2	0.0	0.4	
<i>Suaeda vera</i>	0.0	1.8	5.8	30.1	39.7	17.5	0.0	0.0
<i>Suaeda vera</i>	0.0	2.1	7.7	26.0	38.4	21.5	0.0	0.0
Average		1.9	6.7	28.0	39.1	19.5		
Absolute difference		0.2	0.9	2.1	0.7	2.0		
<i>Atriplex portulacoides</i>	0.0	2.8	17.1	34.0	29.9	6.6	0.0	0.0
<i>Atriplex portulacoides</i>	1.1	2.3	14.9	34.9	33.2	7.1	0.0	0.0
Average	1.1	2.5	16.0	34.4	31.6	6.9		
Absolute difference		0.3	1.1	-0.4	1.6	0.3		
<i>Elytrigia atherica</i>	0.0	0.4	1.7	9.3	49.7	29.7	5.7	0.2
<i>Elytrigia atherica</i>	0.0	0.5	1.7	8.2	48.8	31.8	5.9	0.2
Average		0.4	1.7	8.8	49.3	30.8	5.8	0.2
Absolute difference		0.0	0.0	0.6	0.4	1.1	0.1	0.0
<i>Limonium vulgare</i>	0.0	0.4	1.3	16.7	31.5	28.5	7.9	3.4
<i>Limonium vulgare</i>	0.0	0.2	1.0	14.6	31.4	29.0	9.3	4.0
Average		0.3	1.2	15.6	31.5	28.8	8.6	3.7
Absolute difference		0.1	0.2	1.0	0.1	0.3	0.7	0.3

May 2012		% distribution (normalised Σ odd- chain C21 to C35 alkanes)						
species	C21	C23	C25	C27	C29	C31	C33	C35
<i>Atriplex portulacoides</i>	0.7	2.3	23.2	33.4	25.9	4.8	0.0	0.0
<i>Atriplex portulacoides</i>	0.8	2.4	25.8	30.7	23.5	3.1	0.0	0.0
Average	0.7	2.4	24.5	32.0	24.7	4.0	0.0	0.0
Absolute difference	0.0	0.0	1.3	1.3	1.2	0.9	0.0	0.0
<i>Elytrigia atherica</i>	0.5	1.3	3.4	5.5	39.1	38.3	6.8	0.4
<i>Elytrigia atherica</i>	0.2	0.7	0.2	8.3	47.4	31.6	8.5	0.2
Average	0.4	1.0	1.8	6.9	43.2	34.9	7.7	0.3
Absolute difference	0.2	0.3	1.6	1.4	4.2	3.4	0.9	0.1
<i>Limonium vulgare</i>	0.1	0.5	2.4	19.9	37.5	27.5	5.6	1.3
<i>Limonium vulgare</i>	0.0	0.6	2.7	21.9	35.2	27.2	6.2	1.2
Average	0.0	0.5	2.5	20.9	36.4	27.4	5.9	1.3
Absolute difference	0.0	0.0	0.2	1.0	1.1	0.2	0.3	0.0
<i>Phragmites australis</i>	0.0	12.0	14.7	38.1	35.2	0.0	0.0	0.0
<i>Phragmites australis</i>	2.7	4.8	10.9	35.8	37.0	0.9	0.0	0.0
Average	1.3	8.4	12.8	36.9	36.1	0.5	0.0	0.0
Absolute difference	1.3	3.6	1.9	1.2	0.9	0.5	0.0	0.0
<i>Salicornia europaea</i>	6.5	9.5	9.8	13.4	27.1	17.3	4.0	0.0
<i>Salicornia europaea</i>	11.2	22.3	18.3	15.9	19.3	13.0	0.0	0.0
Average	8.9	15.9	14.1	14.6	23.2	15.1	2.0	0.0
Absolute difference	2.3	6.4	4.3	1.3	3.9	2.2	2.0	0.0
<i>Spartina anglica</i>	4.5	4.8	5.6	24.9	41.8	11.1	0.0	0.0
<i>Spartina anglica</i>	1.4	1.6	4.8	26.6	47.7	8.9	0.0	0.0
Average	2.9	3.2	5.2	25.8	44.7	10.0	0.0	0.0
Absolute difference	1.6	1.6	0.4	0.9	2.9	1.1	0.0	0.0
<i>Suaeda vera</i>	0.3	4.1	10.2	28.4	32.3	20.5	0.2	0.0
<i>Suaeda vera</i>	0.4	4.0	10.1	28.6	32.2	20.9	0.4	0.0
Average	0.3	4.0	10.2	28.5	32.3	20.7	0.3	0.0
Absolute difference	0.0	0.1	0.1	0.1	0.1	0.2	0.1	0.0

Appendix 3

AUGUST 2012 species	% distribution (normalised Σ odd- chain C21 to C35 alkanes)							
	C21	C23	C25	C27	C29	C31	C33	C35
<i>Atriplex portulacoides</i>	0.4	2.3	15.6	36.1	30.5	4.9	0.0	0.0
<i>Atriplex portulacoides</i>	0.4	2.6	24.3	36.4	25.0	4.3	0.0	0.0
Average	0.4	2.4	19.9	36.3	27.7	4.6	0.0	0.0
Absolute difference	0.0	0.2	4.3	0.1	2.8	0.3	0.0	0.0
<i>Elytrigia atherica</i>	0.0	0.9	1.7	7.5	53.3	28.4	1.9	0.0
<i>Elytrigia atherica</i>	0.0	1.0	1.8	8.0	53.3	28.0	1.9	0.0
Average	0.0	1.0	1.8	7.7	53.3	28.2	1.9	0.0
Absolute difference	0.0	0.0	0.0	0.3	0.0	0.2	0.0	0.0
<i>Limonium vulgare</i>	0.0	0.0	1.7	21.8	30.3	29.3	8.0	2.3
<i>Limonium vulgare</i>	0.0	0.0	1.0	16.0	32.2	33.3	8.4	2.0
Average	0.0	0.0	1.3	18.9	31.2	31.3	8.2	2.1
Absolute difference	0.0	0.0	0.3	2.9	0.9	2.0	0.2	0.1
<i>Phragmites australis</i>	0.6	3.7	20.2	26.2	31.2	2.1	0.0	0.0
<i>Phragmites australis</i>	0.8	5.1	24.5	26.2	25.5	1.2	0.0	0.0
Average	0.7	4.4	22.3	26.2	28.3	1.7	0.0	0.0
Absolute difference	0.1	0.7	2.2	0.0	2.8	0.4	0.0	0.0
<i>Salicornia europaea</i>	8.4	34.8	14.9	10.7	12.7	9.0	2.0	0.0
<i>Salicornia europaea</i>	9.0	36.1	15.5	10.2	11.6	7.8	1.7	0.0
Average	8.7	35.5	15.2	10.5	12.2	8.4	1.8	0.0
Absolute difference	0.3	0.6	0.3	0.2	0.6	0.6	0.2	0.0
<i>Spartina anglica</i>	1.6	2.9	4.0	11.8	57.2	13.7	0.0	0.0
<i>Spartina anglica</i>	1.7	3.8	5.2	13.3	55.0	11.9	0.0	0.0
Average	1.7	3.3	4.6	12.6	56.1	12.8	0.0	0.0
Absolute difference	0.1	0.4	0.6	0.8	1.1	0.9	0.0	0.0
<i>Suaeda vera</i>	0.0	2.7	9.8	34.3	35.2	11.8	0.2	0.0
<i>Suaeda vera</i>	0.0	2.9	9.7	40.9	31.4	11.6	0.0	0.0
Average	0.0	2.8	9.8	37.6	33.3	11.7	0.1	0.0
Absolute difference	0.0	0.1	0.1	3.3	1.9	0.1	0.1	0.0

Appendix 3

SEPTEMBER 2012		% distribution (normalised Σ odd- chain C21 to C35 alkanes)						
species	C21	C23	C25	C27	C29	C31	C33	C35
<i>Atriplex portulacoides</i>	0.3	15.5	12.3	28.2	27.1	5.6	0.0	0.0
<i>Atriplex portulacoides</i>	0.9	3.0	15.0	32.4	29.4	5.9	0.0	0.0
Average	0.6	9.2	13.7	30.3	28.2	5.7	0.0	0.0
Absolute difference	0.3	6.3	1.3	2.1	1.1	0.1	0.0	0.0
<i>Elytrigia atherica</i>	0.1	1.3	3.2	11.3	36.3	29.3	3.1	0.2
<i>Elytrigia atherica</i>	0.1	1.2	2.8	10.6	35.9	31.5	3.2	0.1
Average	0.1	1.2	3.0	11.0	36.1	30.4	3.1	0.2
Absolute difference	0.0	0.1	0.2	0.4	0.2	1.1	0.1	0.1
<i>Limonium vulgare</i>	0.0	0.0	0.6	12.7	34.7	31.2	9.2	3.0
<i>Limonium vulgare</i>	0.0	0.1	0.9	18.4	29.1	28.6	9.4	2.3
Average	0.0	0.1	0.7	15.6	31.9	29.9	9.3	2.7
Absolute difference	0.0	0.1	0.2	2.9	2.8	1.3	0.1	0.4
<i>Phragmites australis</i>	0.4	2.8	20.6	25.8	30.4	2.6	0.0	0.0
<i>Phragmites australis</i>	0.4	2.8	21.3	25.9	30.1	1.8	0.0	0.0
Average	0.4	2.8	20.9	25.9	30.2	2.2	0.0	0.0
Absolute difference	0.0	0.0	0.4	0.0	0.2	0.4	0.0	0.0
<i>Salicornia europaea</i>	2.3	12.4	17.7	21.2	15.7	9.6	1.3	0.0
<i>Salicornia europaea</i>	3.0	10.0	11.5	21.5	23.3	15.5	3.2	0.0
Average	2.6	11.2	14.6	21.4	19.5	12.5	2.3	0.0
Absolute difference	0.4	1.2	3.1	0.1	3.0	2.9	1.0	0.0
<i>Spartina anglica</i>	0.7	1.1	3.7	15.0	55.6	10.4	0.0	0.0
<i>Spartina anglica</i>	0.3	0.6	2.7	10.3	55.7	19.1	0.0	0.0
Average	0.5	0.8	3.2	12.7	55.7	14.7	0.0	0.0
Absolute difference	0.2	0.3	0.5	2.4	0.0	4.4	0.0	0.0
<i>Suaeda vera</i>	0.0	2.9	8.5	46.4	29.4	7.0	0.0	0.0
<i>Suaeda vera</i>	0.0	2.6	9.2	44.7	30.2	7.7	0.0	0.0
Average	0.0	2.8	8.8	45.6	29.8	7.3	0.0	0.0
Absolute difference	0.0	0.2	0.3	0.8	0.4	0.4	0.0	0.0

Appendix 4:
Additional data pertaining to
Chapter 5

APPENDIX 4

Standards for CHN analysis

Instrument ML	Peak area N	Peak area C	mg N	mg C
LOD	1698	37831	0.0001	0.0007
ML	16980	378310	0.0009	0.0075

amount (mg)=m*area+C

N cal	$y = 0.0000000571x - 0.0087041149$	
C cal	$y = 0.0000000196x - 0.0007346701$	
	m	c
N	0.0000000571	-0.0087041149
C	0.0000000196	-0.0007346701

	Tin capsule blank N	Tin capsule blank C
	2736	65515
	3597	68170
	2466	73869
mean	2933	69185
stdev	591	4268

Post blank correction

Standard check	% N	% C
Sulphanilamide	16.66%	41.68%
	16.71%	41.74%
	16.74%	41.81%
	16.78%	41.90%
	16.76%	42.03%
	16.62%	41.58%
	16.68%	41.85%
	16.77%	41.95%
	16.75%	41.95%
	16.75%	42.00%
mean	16.72%	41.85%
sd	0.05%	0.15%
Actual values	16.27%	41.85%

APPENDIX 4

Standard check	% N	% C
acetanilide	9.90%	71.05%
	9.72%	71.06%
	9.75%	71.10%
	9.78%	71.35%
	9.83%	71.59%
	9.65%	70.80%
	9.78%	71.09%
	9.90%	71.32%
	9.71%	71.45%
	9.58%	71.35%
mean	9.76%	71.22%
sd	0.10%	0.23%
Actual values	10.36%	71.09%

Standards for bulk $\delta^{13}\text{C}$ and $\delta^{15}\text{N}$

	$\delta^{15}\text{N}$	$\delta^{13}\text{C}$
	6.15‰	-17.98
	Collagen	Collagen
	5.95	-17.81
	6.03	-17.86
	5.95	-18.05
	6.03	-17.96
	5.91	-18.19
	5.97	-17.52
	6.07	-17.87
	5.98	-17.86
	6.07	-17.93
	6.16	-17.91
	6.05	-17.97
	5.81	-17.96
	5.98	-18.04
	6.05	-18.06
	6.06	-18.00
	6.21	-18.09
	5.89	-17.91
	5.98	-17.59
	6.08	-17.92
	6.14	-18.11
	5.87	-17.90
	6.03	-17.96
	5.95	-17.647
	6.00	-16.977
	6.01	-17.325
	5.97	-17.31
	5.96	-17.65
	5.97	-17.86
Mean	6.00	-17.83
SD	0.09	0.27

n-alkane replicate data, June 2011

Sample Site	Sample rep	Species	C23	C25	C27	C29	C31	C33	C35
1	1	<i>Spartina anglica</i>		-23.5	-25.4	-25.5	-25.1		
1	1	<i>Spartina anglica</i>		-23.1	-25.3	-25.2	-24.6		
1	2	<i>Spartina anglica</i>		-23.1	-25.2	-26.0	-25.1		
1	2	<i>Spartina anglica</i>		-22.9	-24.4	-25.5	-24.6		
1	1	<i>Salicornia europaea</i>	-32.9	-32.9	-33.2	-33.3	-33.5		
1	1	<i>Salicornia europaea</i>	-32.8	-32.7	-33.2	-33.1	-33.9		
1	2	<i>Salicornia europaea</i>	-32.1	-32.3	-30.2	-28.4	-29.7		
1	2	<i>Salicornia europaea</i>	-32.4	-32.8	-30.9	-29.0	-30.0		
2	1	<i>Atriplex portulacoides</i>		-30.0	-29.4	-29.9	-31.0		
2	1	<i>Atriplex portulacoides</i>		-30.0	-29.3	-29.9	-31.3		
2	2	<i>Atriplex portulacoides</i>		-32.0	-31.6	-32.8	-34.1		
2	2	<i>Atriplex portulacoides</i>		-31.9	-31.6	-32.7	-33.8		
2	1	<i>Elytrigia atherica</i>	-35.3	-36.4	-37.6	-37.8	-37.1		
2	1	<i>Elytrigia atherica</i>	-34.9	-35.9	-36.6	-37.1	-36.3		
2	2	<i>Elytrigia atherica</i>	-34.6	-35.6	-36.0	-36.7	-35.7		
2	2	<i>Elytrigia atherica</i>	-34.6	-35.6	-36.0	-36.7	-35.5		
2	1	<i>Suaeda vera</i>	-35.5	-35.3	-36.4	-35.4	-35.4		
2	1	<i>Suaeda vera</i>	-35.7	-35.4	-36.5	-35.4	-35.4		
2	2	<i>Suaeda vera</i>	-35.4	-35.4	-36.1	-35.0	-35.3		
2	2	<i>Suaeda vera</i>	-35.7	-35.9	-37.6	-35.4			
2	1	<i>Phragmites australis</i>	-32.6	-32.9	-32.6	-32.5			
2	1	<i>Phragmites australis</i>	-32.6	-33.0	-32.8	-32.5			
2	2	<i>Phragmites australis</i>		-33.1	-33.0	-33.1			
2	2	<i>Phragmites australis</i>		-33.2	-33.1	-33.3			
3	1	<i>Limonium vulgare</i>		-33.5	-33.2	-32.4	-31.9	-32.5	
3	1	<i>Limonium vulgare</i>		-33.5	-33.3	-32.4	-31.9	-32.2	
3	2	<i>Limonium vulgare</i>		-33.6	-33.8	-33.0	-32.6	-33.4	
3	2	<i>Limonium vulgare</i>		-34.0	-33.8	-33.0	-32.6	-32.5	

n-alkane replicate data, August 2011

Sampling site	Sample rep	Species	C23	C25	C27	C29	C31	C33	C35
1	1	<i>Spartina anglica</i>			-24.3	-24.9	-24.8		
1	1	<i>Spartina anglica</i>			-23.4	-24.3	-24.3		
1	2	<i>Spartina anglica</i>			-24.2	-24.6	-25.0		
1	2	<i>Spartina anglica</i>			-24.1	-24.8	-24.9		
1	1	<i>Salicornia europaea</i>	-32.9	-32.8	-33.1	-32.9	-33.4		
1	1	<i>Salicornia europaea</i>	-32.8	-32.7	-32.8	-33.3	-33.0		
1	2	<i>Salicornia europaea</i>	-32.4	-32.4	-32.3	-32.6			
1	2	<i>Salicornia europaea</i>	-32.2	-32.8	-32.6	-32.7			
2	1	<i>Suaeda vera</i>	-34.6	-34.6	-36.8	-35.5	-34.4		
2	1	<i>Suaeda vera</i>	-35.1	-34.9	-37.4	-36.1	-34.6		
2	2	<i>Suaeda vera</i>	-34.1	-34.5	-35.5	-34.4	-33.7		
2	2	<i>Suaeda vera</i>	-35.1	-35.3	-36.5	-35.8	-33.3		
2	1	<i>Atriplex portulacoides</i>		-30.1	-29.5	-31.0	-34.0		
2	1	<i>Atriplex portulacoides</i>		-30.2	-29.7	-31.1	-32.5		
2	2	<i>Atriplex portulacoides</i>		-30.2	-29.8	-31.3	-31.7		
2	2	<i>Atriplex portulacoides</i>		-30.3	-30.0	-31.3	-31.9		
2	1	<i>Elytrigia atherica</i>		-32.5	-34.4	-35.5	-33.7	-33.1	
2	1	<i>Elytrigia atherica</i>		-32.7	-34.0	-35.2	-33.9	-33.8	
2	2	<i>Elytrigia atherica</i>		-32.7	-34.2	-35.0	-32.8	-32.0	
2	2	<i>Elytrigia atherica</i>		-32.6	-34.5	-35.2	-33.0	-33.0	
2	1	<i>Phragmites australis</i>	-31.5	-33.5	-33.2	-33.1			
2	1	<i>Phragmites australis</i>	-31.6	-33.3	-33.2	-33.2			
2	2	<i>Phragmites australis</i>	-31.4	-33.4	-33.3	-33.2			
2	2	<i>Phragmites australis</i>	-31.2	-33.4	-33.4	-33.5			
3	1	<i>Limonium vulgare</i>			-34.4	-35.2	-34.9	-34.0	
3	1	<i>Limonium vulgare</i>			-34.5	-35.1	-34.7	-34.1	
3	2	<i>Limonium vulgare</i>			-34.2	-34.9	-34.3	-34.1	
3	2	<i>Limonium vulgare</i>			-34.0	-34.7	-34.3	-34.2	

n-alkane replicate data, October 2011

APPENDIX 4

Sampling site	Sample rep	Species	C23	C25	C27	C29	C31	C33	C35
1	1	<i>Spartina anglica</i>			-24.5	-25.7	-27.8		
1	1	<i>Spartina anglica</i>			-24.4	-25.2	-27.8		
1	2	<i>Spartina anglica</i>			-24.2	-25.1	-25.2	-26.5	
1	2	<i>Spartina anglica</i>			-24.2	-25.2	-25.0		
1	1	<i>Salicornia europaea</i>	-32.6	-33.2	-31.7	-31.8	-32.5		
1	1	<i>Salicornia europaea</i>		-32.9	-31.6	-31.1	-31.8		
1	2	<i>Salicornia europaea</i>		-30.7	-32.2	-33.0	-32.5	-33.2	
1	2	<i>Salicornia europaea</i>		-31.6	-33.0	-33.8	-33.4	-33.4	
2	1	<i>Suaeda vera</i>		-35.3	-38.1	-37.3			
2	1	<i>Suaeda vera</i>		-35.1	-38.3	-37.5			
2	2	<i>Suaeda vera</i>		-35.3	-38.5	-37.7	-35.3		
2	2	<i>Suaeda vera</i>		-35.2	-37.8	-36.8			
2	1	<i>Atriplex portulacoides</i>		-30.3	-30.0	-30.7			
2	1	<i>Atriplex portulacoides</i>		-31.0	-30.6	-31.3			
2	2	<i>Atriplex portulacoides</i>	-29.8	-31.0	-30.6	-31.1	-32.2		
2	2	<i>Atriplex portulacoides</i>		-30.6	-30.5	-31.1	-32.5		
2	1	<i>Elytrigia atherica</i>			-35.0	-35.4	-34.2		
2	1	<i>Elytrigia atherica</i>		-34.6	-35.9	-35.9	-34.7		
2	2	<i>Elytrigia atherica</i>		-33.9	-34.8	-34.9	-33.9	-33.9	
2	2	<i>Elytrigia atherica</i>		-34.0	-34.9	-35.1	-33.9	-34.2	
2	1	<i>Phragmites australis</i>		-33.1	-33.3	-33.3			
2	1	<i>Phragmites australis</i>		-33.4	-33.3	-33.2			
2	2	<i>Phragmites australis</i>		-32.9	-33.0	-33.2			
2	2	<i>Phragmites australis</i>		-33.7	-33.4	-33.5			
3	1	<i>Limonium vulgare</i>			-34.6	-34.2	-33.2		
3	1	<i>Limonium vulgare</i>			-33.9	-33.6	-32.5		
3	2	<i>Limonium vulgare</i>			-34.4	-35.2	-33.8		
3	2	<i>Limonium vulgare</i>			-34.4	-33.9	-32.9		
1	1	<i>Limonium vulgare</i>			-33.8	-33.6	-32.3	-30.7	
1	1	<i>Limonium vulgare</i>			-33.6	-33.4	-32.2	-30.4	
1	2	<i>Limonium vulgare</i>			-35.4	-34.7	-33.5		
1	2	<i>Limonium vulgare</i>			-35.2	-34.6	-33.4		
1	1	<i>Atriplex portulacoides</i>		-31.9	-32.2	-32.9	-34.1		
1	1	<i>Atriplex portulacoides</i>		-34.0	-31.2	-32.1			
1	2	<i>Atriplex portulacoides</i>		-30.8	-30.9	-31.7			
1	2	<i>Atriplex portulacoides</i>		-30.1	-30.0	-30.9			
3	1	<i>Atriplex portulacoides</i>	-29.2	-29.8	-29.5	-30.0			
3	1	<i>Atriplex portulacoides</i>	-29.1	-30.0	-29.3	-30.0	-31.4		
3	2	<i>Atriplex portulacoides</i>	-29.5	-30.6	-30.1	-31.3	-32.6		
3	2	<i>Atriplex portulacoides</i>	-29.2	-30.2	-29.8	-31.0	-31.9		
3	1	<i>Suaeda vera</i>		-34.2	-36.2	-35.2	-34.0		
3	1	<i>Suaeda vera</i>		-33.5	-35.5	-35.2	-34.2		
3	2	<i>Suaeda vera</i>		-33.9	-35.8	-35.0	-34.0		
3	2	<i>Suaeda vera</i>		-34.2	-35.7	-34.8	-33.9		
3	1	<i>Salicornia europaea</i>	-31.8	-31.5	-31.7	-31.4			
3	1	<i>Salicornia europaea</i>	-31.4	-31.6	-31.5	-31.8			
3	2	<i>Salicornia europaea</i>	-31.7	-31.4	-30.6	-31.3			
3	2	<i>Salicornia europaea</i>	-31.5	-31.1	-30.6	-31.8			

APPENDIX 4

n-alkane replicate data, March 2012

Sampling site	Sample rep	Species	C23	C25	C27	C29	C31	C33	C35
1	1	<i>Spartina anglica</i>		-21.5	-23.9	-24.7	-24.8		
1	1	<i>Spartina anglica</i>		-21.4	-23.9	-24.5	-24.7		
1	2	<i>Spartina anglica</i>		-23.1	-24.5	-25.6	-25.3		
1	2	<i>Spartina anglica</i>		-22.8	-24.3	-25.1	-25.0		
2	1	<i>Suaeda vera</i>	-36.5		-40.0	-39.1	-38.3		
2	1	<i>Suaeda vera</i>	-36.9	-38.1	-39.8	-39.0	-38.5		
2	2	<i>Suaeda vera</i>	-35.9	-37.0	-39.2	-38.1	-37.4		
2	2	<i>Suaeda vera</i>	-36.2	-36.9	-39.1	-37.8	-37.4		
2	1	<i>Atriplex portulacoides</i>		-32.3	-31.7	-33.0			
2	1	<i>Atriplex portulacoides</i>		-32.1	-31.4	-31.1			
2	2	<i>Atriplex portulacoides</i>		-32.3	-32.3	-31.5			
2	2	<i>Atriplex portulacoides</i>		-32.2	-32.2	-31.9			
2	1	<i>Elytrigia atherica</i>		-35.9	-37.8	-36.6	-36.7		
2	1	<i>Elytrigia atherica</i>		-35.8	-37.4	-36.5	-36.7		
2	2	<i>Elytrigia atherica</i>		-35.5	-37.4	-36.4	-36.6		
2	2	<i>Elytrigia atherica</i>		-35.5	-37.3	-36.3	-36.5		
3	1	<i>Limonium vulgare</i>			-36.3	-36.5	-35.2		
3	1	<i>Limonium vulgare</i>			-36.0	-36.6	-35.3		
3	2	<i>Limonium vulgare</i>			-36.3	-36.3	-34.7		
3	2	<i>Limonium vulgare</i>			-36.0	-36.1	-34.7		

n-alkane replicate data, May 2012

Sampling site	Sample rep	Species	C21	C23	C25	C27	C29	C31	C33	C35
2	1	<i>Suaeda vera</i>			-36.8	-39.8	-37.6	-36.0		
2	1	<i>Suaeda vera</i>			-37.0	-39.4	-37.3	-36.0		
2	2	<i>Suaeda vera</i>		-36.7	-37.5	-39.8	-37.8	-36.3		
2	2	<i>Suaeda vera</i>		-36.7	-37.6	-40.0	-38.1	-36.3		
1	1	<i>Spartina anglica</i>			-23.9	-26.3	-26.7			
1	1	<i>Spartina anglica</i>			-24.0	-26.0	-26.3			
1	2	<i>Spartina anglica</i>				-25.5	-26.1			
1	2	<i>Spartina anglica</i>				-25.9	-26.5			
1	1	<i>Salicornia europaea</i>	-31.3	-33.2	-33.4	-33.6	-31.1	-33.1		
1	1	<i>Salicornia europaea</i>	-31.1	-32.3	-32.7	-32.8	-31.4	-32.6		
1	2	<i>Salicornia europaea</i>				-32.3	-30.7	-31.9		
1	2	<i>Salicornia europaea</i>				-31.4	-30.6	-31.7		
2	1	<i>Phragmites australis</i>	-29.8	-31.2	-32.3	-32.7	-33.3			
2	1	<i>Phragmites australis</i>	-30.1	-31.4	-32.4	-32.7	-35.1			
2	2	<i>Phragmites australis</i>	-26.4	-30.9	-32.6	-32.8	-33.7			
2	2	<i>Phragmites australis</i>	-26.6	-31.2	-33.0	-33.1	-33.9			
3	1	<i>Limonium vulgare</i>			-32.2	-32.1	-31.9	-31.4		
3	1	<i>Limonium vulgare</i>			-32.2	-31.9	-31.8	-31.5		
3	2	<i>Limonium vulgare</i>			-31.6	-30.8	-30.4	-30.0		
3	2	<i>Limonium vulgare</i>			-31.6	-30.7	-30.4	-30.6		
2	1	<i>Elytrigia atherica</i>			-37.5	-38.3	-39.7	-38.9		
2	1	<i>Elytrigia atherica</i>			-37.3	-38.2	-39.8	-39.3	-39.2	
2	2	<i>Elytrigia atherica</i>			-38.4	-39.2	-39.5	-39.5	-39.7	
2	2	<i>Elytrigia atherica</i>			-38.0	-39.2	-39.4	-39.5	-39.5	
2	1	<i>Atriplex portulacoides</i>			-33.5	-29.9	-31.9	-31.8		
2	1	<i>Atriplex portulacoides</i>			-33.4	-32.1	-31.6			
2	2	<i>Atriplex portulacoides</i>			-32.4	-28.7	-30.8	-30.2		

APPENDIX 4

n-alkane replicate data, August 2012

Sampling site	Sample rep	Species	C21	C23	C25	C27	C29	C31	C33	C35
2	1	<i>Atriplex portulacoides</i>			-32.4	-32.3	-33.0			
2	1	<i>Atriplex portulacoides</i>			-32.4	-32.2	-32.9			
2	2	<i>Atriplex portulacoides</i>			-31.6	-31.4	-31.7			
2	2	<i>Atriplex portulacoides</i>			-31.4	-31.4	-31.8			
2	1	<i>Elytrigia atherica</i>				-36.6	-38.0	-36.5		
2	1	<i>Elytrigia atherica</i>				-36.6	-37.5	-36.3		
2	2	<i>Elytrigia atherica</i>				-36.7	-37.8	-36.8		
2	2	<i>Elytrigia atherica</i>				-36.8	-37.8	-36.7		
3	1	<i>Limonium vulgare</i>			-31.6	-32.4	-32.0	-32.0	-31.7	
3	1	<i>Limonium vulgare</i>			-31.1	-32.4	-32.2	-32.0	-31.8	
3	2	<i>Limonium vulgare</i>			-32.1	-32.9	-32.6	-31.8	-31.5	
3	2	<i>Limonium vulgare</i>				-32.0	-32.9	-32.6	-31.8	-31.7
2	1	<i>Phragmites australis</i>			-32.2	-32.4	-32.7			
2	1	<i>Phragmites australis</i>			-32.2	-32.2	-32.7			
2	2	<i>Phragmites australis</i>			-32.7	-32.8	-32.9			
2	2	<i>Phragmites australis</i>			-32.7	-32.8	-33.2			
1	1	<i>Salicornia europaea</i>	-33.0	-32.4	-32.7	-32.6	-33.2	-33.3		
1	1	<i>Salicornia europaea</i>	-33.3	-32.5	-32.8	-32.7	-33.3	-33.4		
1	2	<i>Salicornia europaea</i>	-33.6	-32.8	-33.0	-32.8	-33.4	-33.7		
1	2	<i>Salicornia europaea</i>	-33.6	-32.8	-33.3	-33.1	-33.5	-33.5		
1	1	<i>Spartina anglica</i>				-24.1	-24.7			
1	1	<i>Spartina anglica</i>				-24.1	-24.7			
1	2	<i>Spartina anglica</i>				-23.9	-24.7			
1	2	<i>Spartina anglica</i>				-24.0	-24.6			
2	1	<i>Suaeda vera</i>			-35.6	-37.6	-36.5	-34.8		
2	1	<i>Suaeda vera</i>			-35.5	-37.6	-36.4	-35.3		
2	2	<i>Suaeda vera</i>			-34.6	-36.4	-35.3	-33.8		
2	2	<i>Suaeda vera</i>			-34.5	-36.3	-35.3	-33.8		

n-alkane replicate data, September 2012

Sample Site	Sample rep	Species	C21	C23	C25	C27	C29	C31	C33	C35
2	1	<i>Suaeda vera</i>			-35.7	-38.0	-36.7			
2	1	<i>Suaeda vera</i>			-35.8	-38.0	-36.6			
2	2	<i>Suaeda vera</i>			-35.4	-37.5	-36.2			
2	2	<i>Suaeda vera</i>			-35.5	-37.4	-36.2			
1	1	<i>Spartina anglica</i>			-23.4	-25.6	-26.1	-25.4		
1	1	<i>Spartina anglica</i>			-23.8	-25.7	-26.0	-25.3		
1	2	<i>Spartina anglica</i>			-21.6	-23.4	-25.3	-25.4		
1	2	<i>Spartina anglica</i>			-21.4	-23.2	-24.8	-25.0		
1	1	<i>Salicornia europaea</i>	-32.3	-33.0	-33.0	-33.0	-31.8	-32.5		
1	1	<i>Salicornia europaea</i>	-32.6	-33.3	-33.2	-33.2	-32.0	-32.6		
1	2	<i>Salicornia europaea</i>	-31.6	-31.7	-32.2	-32.2	-31.3	-31.4		
1	2	<i>Salicornia europaea</i>	-31.8	-31.9	-32.2	-32.2	-31.3	-31.8		
2	1	<i>Phragmites australis</i>	-31.9	-32.7	-32.9	-32.9	-32.9			
2	1	<i>Phragmites australis</i>	-31.7	-32.7	-32.8	-32.8	-32.7			
2	2	<i>Phragmites australis</i>			-32.2	-32.4	-32.5			
2	2	<i>Phragmites australis</i>			-32.2	-32.3	-32.6			
3	1	<i>Limonium vulgare</i>			-31.3	-32.5	-32.5	-32.0	-31.6	
3	1	<i>Limonium vulgare</i>			-31.4	-32.3	-32.4	-31.7	-31.4	
3	2	<i>Limonium vulgare</i>				-33.1	-33.3	-32.7		
3	2	<i>Limonium vulgare</i>				-33.1	-33.3	-32.6		
2	1	<i>Elytrigia atherica</i>			-35.2	-36.6	-37.0	-35.3		
2	1	<i>Elytrigia atherica</i>			-34.9	-36.5	-36.9	-35.2		
2	2	<i>Elytrigia atherica</i>			-35.6	-36.9	-37.0	-35.3		
2	2	<i>Elytrigia atherica</i>			-35.5	-36.7	-37.0	-35.2		
2	1	<i>Atriplex portulacoides</i>	-31.1	-32.0	-31.9	-31.9	-32.3	-32.3		
2	1	<i>Atriplex portulacoides</i>	-31.0	-32.1	-31.9	-31.9	-32.3	-32.5		
2	2	<i>Atriplex portulacoides</i>			-31.8	-31.5	-31.6	-32.0		
2	2	<i>Atriplex portulacoides</i>			-31.8	-31.4	-31.6			

APPENDIX 4

Bulk carbon and nitrogen isotope composition , 2011 sampling interval

Sample month	Species	$\delta^{15}\text{N}$	$\delta^{13}\text{C}$
Jun-11	<i>Atriplex portulacoides</i>	6.7	-25.7
Jun-11	<i>Atriplex portulacoides</i>	6.6	-25.8
Jun-11	<i>Elytrigia atherica</i>	5.1	-28.5
Jun-11	<i>Elytrigia atherica</i>	4.9	-28.7
Jun-11	<i>Limonium vulgare</i>	4.8	-25.8
Jun-11	<i>Limonium vulgare</i>	4.8	-25.7
Jun-11	<i>Phragmites australis</i>	6.4	-25.5
Jun-11	<i>Phragmites australis</i>	6.7	-25.5
Jun-11	<i>Salicornia europaea</i>	8.9	-28.1
Jun-11	<i>Salicornia europaea</i>	8.8	-28.1
Jun-11	<i>Spartina anglica</i>	7.5	-14.1
Jun-11	<i>Spartina anglica</i>	7.4	-13.8
Jun-11	<i>Suaeda vera</i>	7.0	-29.8
Jun-11	<i>Suaeda vera</i>	7.2	-29.8
Aug-11	<i>Atriplex portulacoides</i>	8.3	-25.2
Aug-11	<i>Atriplex portulacoides</i>	7.8	-25.3
Aug-11	<i>Elytrigia atherica</i>	3.0	-25.5
Aug-11	<i>Elytrigia atherica</i>	3.1	-25.6
Aug-11	<i>Limonium vulgare</i>	5.5	-26.8
Aug-11	<i>Limonium vulgare</i>	5.3	-26.9
Aug-11	<i>Phragmites australis</i>	7.6	-26.0
Aug-11	<i>Phragmites australis</i>	7.8	-26.0
Aug-11	<i>Salicornia europaea</i>	10.0	-25.7
Aug-11	<i>Salicornia europaea</i>	10.1	-25.9
Aug-11	<i>Spartina anglica</i>	8.4	-14.2
Aug-11	<i>Spartina anglica</i>	8.4	-14.3
Aug-11	<i>Suaeda vera</i>	9.6	-29.4
Aug-11	<i>Suaeda vera</i>	9.1	-29.4
Oct-11	<i>Atriplex portulacoides</i>	9.7	-25.0
Oct-11	<i>Atriplex portulacoides</i>	8.4	-24.8
Oct-11	<i>Elytrigia atherica</i>	4.1	-26.1
Oct-11	<i>Elytrigia atherica</i>	2.8	-25.7
Oct-11	<i>Limonium vulgare</i>	3.1	-25.4
Oct-11	<i>Limonium vulgare</i>	3.4	-25.2
Oct-11	<i>Phragmites australis</i>	5.0	-25.7
Oct-11	<i>Phragmites australis</i>	5.9	-25.9
Oct-11	<i>Salicornia europaea</i>	8.0	-26.4
Oct-11	<i>Salicornia europaea</i>	7.5	-25.3
Oct-11	<i>Spartina anglica</i>	7.4	-14.7
Oct-11	<i>Spartina anglica</i>	7.6	-13.8
Oct-11	<i>Suaeda vera</i>	9.5	-28.5
Oct-11	<i>Suaeda vera</i>	12.3	-28.1

APPENDIX 4

Bulk carbon and nitrogen isotope composition, 2012 sampling interval

Sample month	Species	%N	%C
Mar-12	<i>Atriplex portulacoides</i>	10.0	-27.4
Mar-12	<i>Atriplex portulacoides</i>	9.1	-28.4
Mar-12	<i>Elytrigia atherica</i>	3.9	-28.6
Mar-12	<i>Elytrigia atherica</i>	3.7	-28.6
Mar-12	<i>Limonium vulgare</i>	3.7	-27.7
Mar-12	<i>Limonium vulgare</i>	2.9	-26.5
Mar-12	<i>Spartina anglica</i>	6.2	-13.7
Mar-12	<i>Spartina anglica</i>	7.2	-13.6
Mar-12	<i>Suaaeda vera</i>	9.6	-31.3
Mar-12	<i>Suaaeda vera</i>	9.4	-31.6
May-12	<i>Atriplex portulacoides</i>	9.2	-27.4
May-12	<i>Atriplex portulacoides</i>	9.1	-27.5
May-12	<i>Elytrigia atherica</i>	2.7	-30.7
May-12	<i>Elytrigia atherica</i>	2.7	-30.7
May-12	<i>Limonium vulgare</i>	4.5	-24.9
May-12	<i>Limonium vulgare</i>	4.8	-25.1
May-12	<i>Phragmites australis</i>	5.1	-25.9
May-12	<i>Phragmites australis</i>	5.0	-26.0
May-12	<i>Salicornia europaea</i>	8.9	-27.5
May-12	<i>Salicornia europaea</i>	8.9	-27.6
May-12	<i>Spartina anglica</i>	7.3	-13.5
May-12	<i>Spartina anglica</i>	7.4	-13.5
Jun-12	<i>Suaaeda vera</i>	7.7	-30.3
May-12	<i>Suaaeda vera</i>	8.2	-30.5
Aug-12	<i>Atriplex portulacoides</i>	7.3	-26.0
Aug-12	<i>Atriplex portulacoides</i>	7.3	-26.0
Aug-12	<i>Elytrigia atherica</i>	3.1	-27.8
Aug-12	<i>Elytrigia atherica</i>	3.3	-27.7
Aug-12	<i>Limonium vulgare</i>	4.7	-25.2
Aug-12	<i>Limonium vulgare</i>	4.7	-25.2
Aug-12	<i>Phragmites australis</i>	6.3	-25.2
Aug-12	<i>Phragmites australis</i>	6.6	-25.2
Aug-12	<i>Salicornia europaea</i>	6.7	-27.4
Aug-12	<i>Salicornia europaea</i>	7.1	-27.5
Aug-12	<i>Spartina anglica</i>	8.9	-13.0
Aug-12	<i>Spartina anglica</i>	8.3	-13.0
Aug-12	<i>Suaaeda vera</i>	5.9	-29.1
Aug-12	<i>Suaaeda vera</i>	6.1	-29.2
Sep-12	<i>Atriplex portulacoides</i>	9.5	-26.6
Sep-12	<i>Atriplex portulacoides</i>	9.4	-26.5
Sep-12	<i>Elytrigia atherica</i>	2.6	-27.5
Sep-12	<i>Elytrigia atherica</i>	2.9	-27.6
Sep-12	<i>Limonium vulgare</i>	6.6	-25.5
Sep-12	<i>Limonium vulgare</i>	6.5	-25.4
Sep-12	<i>Phragmites australis</i>	7.1	-25.1
Sep-12	<i>Phragmites australis</i>	7.0	-25.1
Sep-12	<i>Salicornia europaea</i>	6.3	-26.5
Sep-12	<i>Salicornia europaea</i>	6.4	-26.4
Sep-12	<i>Spartina anglica</i>	9.2	-13.4
Sep-12	<i>Spartina anglica</i>	8.7	-13.4
Sep-12	<i>Suaaeda vera</i>	10.2	-28.9
Sep-12	<i>Suaaeda vera</i>	9.8	-29.1

APPENDIX 4

Percentage composition of C and N, 2011 sampling interval

Sample month	Species	Sample mass (mg)	%N	%C
Jun-11	<i>Atriplex portulacoides</i>	1.948	2.06%	36.16%
Jun-11	<i>Atriplex portulacoides</i>	1.921	2.04%	36.15%
Jun-11	<i>Elytrigia atherica</i>	1.937	1.24%	44.16%
Jun-11	<i>Elytrigia atherica</i>	2.015	1.23%	44.17%
Jun-11	<i>Limonium vulgare</i>	2.058	2.51%	37.84%
Jun-11	<i>Limonium vulgare</i>	2.023	2.52%	37.99%
Jun-11	<i>Phragmites australis</i>	2.134	2.34%	42.52%
Jun-11	<i>Phragmites australis</i>	2.169	2.49%	44.48%
Jun-11	<i>Salicornia europaea</i>	1.989	2.00%	26.92%
Jun-11	<i>Salicornia europaea</i>	1.970	2.00%	27.00%
Jun-11	<i>Spartina anglica</i>	2.013	1.95%	39.42%
Jun-11	<i>Spartina anglica</i>	2.042	1.95%	39.37%
Jun-11	<i>Suaeda vera</i>	2.072	3.09%	36.30%
Jun-11	<i>Suaeda vera</i>	2.111	3.08%	36.13%
Aug-11	<i>Suaeda vera</i>	2.027	1.18%	35.84%
Aug-11	<i>Suaeda vera</i>	2.093	1.29%	36.56%
Aug-11	<i>Spartina anglica</i>	2.091	2.08%	41.31%
Aug-11	<i>Spartina anglica</i>	2.118	2.08%	41.36%
Aug-11	<i>Salicornia europaea</i>	2.083	1.16%	23.95%
Aug-11	<i>Salicornia europaea</i>	2.121	1.13%	22.06%
Aug-11	<i>Phragmites australis</i>	1.981	1.84%	44.87%
Aug-11	<i>Phragmites australis</i>	2.037	1.91%	45.51%
Aug-11	<i>Limonium vulgare</i>	1.914	2.25%	37.18%
Aug-11	<i>Limonium vulgare</i>	2.051	2.23%	37.19%
Aug-11	<i>Atriplex portulacoides</i>	2.032	1.30%	32.11%
Aug-11	<i>Atriplex portulacoides</i>	2.071	1.25%	31.84%
Aug-11	<i>Elytrigia atherica</i>	2.088	0.70%	44.86%
Aug-11	<i>Elytrigia atherica</i>	2.112	0.74%	44.92%
Oct-11	<i>Atriplex portulacoides</i>	1.8620	1.98%	33.04%
Oct-11	<i>Atriplex portulacoides</i>	2.2200	1.91%	32.79%
Oct-11	<i>Elytrigia atherica</i>	2.0610	1.91%	45.01%
Oct-11	<i>Elytrigia atherica</i>	1.8960	1.78%	44.57%
Oct-11	<i>Limonium vulgare</i>	1.9330	2.01%	36.26%
Oct-11	<i>Limonium vulgare</i>	1.8280	1.79%	35.16%
Oct-11	<i>Phragmites australis</i>	2.2110	2.52%	45.11%
Oct-11	<i>Phragmites australis</i>	1.842	2.39%	44.75%
Oct-11	<i>Salicornia europaea</i>	2.0740	1.94%	27.91%
Oct-11	<i>Salicornia europaea</i>	1.9590	2.27%	29.19%
Oct-11	<i>Spartina anglica</i>	2.0730	2.38%	40.55%
Oct-11	<i>Spartina anglica</i>	2.1650	2.79%	39.93%
Oct-11	<i>Suaeda vera</i>	2.194	2.59%	34.37%
Oct-11	<i>Suaeda vera</i>	2.241	2.60%	34.90%

APPENDIX 4

Percentage composition of C and N, 2012 sampling interval

Sample month	Species	Sample mass (mg)	%N	%C
Mar-12	<i>Suaaeda vera</i>	1.926	3.29%	34.81%
Mar-12	<i>Suaaeda vera</i>	1.942	3.38%	35.32%
Mar-12	<i>Limonium vulgare</i>	2.069	0.98%	33.97%
Mar-12	<i>Limonium vulgare</i>	2.186	0.98%	33.89%
Mar-12	<i>Elytrigia atherica</i>	2.022	1.24%	43.25%
Mar-12	<i>Elytrigia atherica</i>	2.110	1.33%	44.54%
Mar-12	<i>Spartina anglica</i>	2.055	1.07%	36.83%
Mar-12	<i>Spartina anglica</i>	2.112	1.00%	34.76%
Mar-12	<i>Atriplex portulacoides</i>	1.918	1.56%	34.43%
Mar-12	<i>Atriplex portulacoides</i>	2.106	1.65%	35.01%
May-12	<i>Atriplex portulacoides</i>	2.172	1.48%	37.36%
May-12	<i>Atriplex portulacoides</i>	2.103	1.46%	37.31%
May-12	<i>Elytrigia atherica</i>	2.061	1.37%	44.22%
May-12	<i>Elytrigia atherica</i>	1.981	1.38%	44.57%
May-12	<i>Limonium vulgare</i>	2.208	3.87%	40.20%
May-12	<i>Limonium vulgare</i>	2.112	3.93%	40.71%
May-12	<i>Suaaeda vera</i>	2.000	3.72%	40.79%
May-12	<i>Suaaeda vera</i>	2.030	3.74%	40.81%
May-12	<i>Phragmites australis</i>	2.065	3.09%	45.05%
May-12	<i>Phragmites australis</i>	2.104	3.00%	44.96%
May-12	<i>Salicornia europaea</i>	2.105	1.23%	21.57%
May-12	<i>Salicornia europaea</i>	2.193	1.21%	21.60%
May-12	<i>Spartina anglica</i>	2.143	2.93%	39.29%
May-12	<i>Spartina anglica</i>	1.958	2.92%	39.40%
Aug-12	<i>Suaaeda vera</i>	2.027	2.38%	35.93%
Aug-12	<i>Suaaeda vera</i>	2.224	2.45%	36.21%
Aug-12	<i>Atriplex portulacoides</i>	2.032	1.09%	31.25%
Aug-12	<i>Atriplex portulacoides</i>	2.142	1.03%	31.34%
Aug-12	<i>Elytrigia atherica</i>	1.905	0.47%	44.98%
Aug-12	<i>Elytrigia atherica</i>	2.035	0.54%	44.41%
Aug-12	<i>Limonium vulgare</i>	2.044	1.77%	38.13%
Aug-12	<i>Limonium vulgare</i>	1.958	1.74%	38.25%
Aug-12	<i>Phragmites australis</i>	1.934	2.25%	44.98%
Aug-12	<i>Phragmites australis</i>	1.995	2.31%	45.15%
Aug-12	<i>Salicornia europaea</i>	2.083	0.54%	24.66%
Aug-12	<i>Salicornia europaea</i>	2.082	0.47%	23.45%
Aug-12	<i>Spartina anglica</i>	2.081	1.24%	41.42%
Aug-12	<i>Spartina anglica</i>	2.050	1.23%	40.68%
Sep-12	<i>Salicornia europaea</i>	1.959	1.02%	29.47%
Sep-12	<i>Salicornia europaea</i>	2.171	1.08%	29.55%
Sep-12	<i>Spartina anglica</i>	1.959	1.33%	41.04%
Sep-12	<i>Spartina anglica</i>	2.089	1.38%	41.04%
Sep-12	<i>Suaaeda vera</i>	2.172	2.99%	35.78%
Sep-12	<i>Suaaeda vera</i>	1.960	3.08%	36.52%
Sep-12	<i>Phragmites australis</i>	2.082	2.22%	45.46%
Sep-12	<i>Phragmites australis</i>	1.921	2.20%	45.55%
Sep-12	<i>Elytrigia atherica</i>	1.932	0.60%	44.17%
Sep-12	<i>Elytrigia atherica</i>	1.998	0.63%	44.21%
Sep-12	<i>Atriplex portulacoides</i>	2.131	1.08%	34.63%
Sep-12	<i>Atriplex portulacoides</i>	2.032	0.96%	34.30%
Sep-12	<i>Limonium vulgare</i>	2.173	3.04%	40.60%
Sep-12	<i>Limonium vulgare</i>	1.938	3.03%	40.61%

Appendix 5:
Additional data pertaining to
Chapter 6

Appendix 5

Table showing all replicates of *n*-alkane and leaf water ²H/¹H measurements from June 2011

Location	Plant Species	Plant type	$\delta^2\text{H } n\text{-C}_{27}$	AD*	$\delta^2\text{H } n\text{-C}_{29}$	AD*	$\delta^2\text{H } n\text{-C}_{31}$	AD*	$\delta^2\text{H}_{\text{Leaf water}}$	SE _{leaf water}	$\epsilon_{\text{wax/leaf water}} (\text{‰})$
Site 1	<i>Spartina anglica</i>	C ₄ grass	-147		-160	2	-166	1			
	<i>Spartina anglica</i>		-141		-154		-162				
			-144	3	-157	3	-164	2	27	1	-179
Site 1	<i>Triglochin maritima</i>	C ₃ perennial herb	-124		-133		-135				
	<i>Triglochin maritima</i>		-125		-133		-133				
			-124	1	-133	0	-134	1	22	0	-152
Site 1	<i>Salicornia Europaea</i>	C ₃ perennial succulent	-137		-132		-129				
	<i>Salicornia Europaea</i>		-125		-132		-125				
			-131	6	-132	0	-127	2	29	0	-156
Site 1	<i>Limonium vulgare</i>	C ₃ perennial herb	-109		-107		-109				
	<i>Limonium vulgare</i>		-124		-119		-121				
			-116	7	-113	6	-115	6	30	0	-139
Site 1	<i>Atriplex portulacoides</i>	C ₃ evergreen shrub	-130		-126		-117				
	<i>Atriplex portulacoides</i>		-132		-129		-117				
			-131	1	-127	1	-117	0	25	0	-148
Site 2	<i>Elytrigia atherica</i>	C ₃ grass	-202		-212		-218				
	<i>Elytrigia atherica</i>		-193		-209		-222				
			-197	4	-211	1	-220	2	15	0	-223

Appendix 5

Table showing all replicates of *n*-alkane and leaf water ²H/¹H measurements from all sampling intervals in 2012

Month	Plant species	δ ² H C ₂₇	AD [*]	δ ² H C ₂₉	AD	δ ² H C ₃₁	AD	δ ² HSW	AD ^{**}	δ ² H _{XW}	AD	δ ² H _{LW}	AD	ε ² H _{C29/sw}	ε ² H _{C29/XW}	ε ² H _{C29/LW}
March	<i>Atriplex portulacoides</i>	-142		-140		-124		-36				-22				
	<i>Atriplex portulacoides</i>	-142		-138		-132		-				-18				
		-142	0	-139	1	-128	4	-36	4	-	-	-20	2	-107	-	-121
	<i>Elytrigia atherica</i>	-196		-204		-197		-36				-21				
	<i>Elytrigia atherica</i>	-192		-197		-197		-				-19				
		-194	2	-201	4	-197	0	-36	4	-	-	-20	1	-171	-	-184
	<i>Limonium vulgare</i>	-134		-124		-125		-				-25			-	
	<i>Limonium vulgare</i>	-133		-123		-125		-				-28				
		-134	1	-124	1	-125	0	-	-	-	-	-26	1		-	-100
	<i>Spartina anglica</i>	-127		-135		-133		-23				-26				
	<i>Spartina anglica</i>	-132		-138		-139		-28				-24				
		-130	3	-137	2	-136	3	-26	3	-	-	-25	1	-114	-	-115
<i>Suaeda vera</i>	-110		-101		-103		-36				-18					
<i>Suaeda vera</i>	-105		-94		-94		-				-22					
	-108	3	-98	4	-99	5	-36	4	-	-	-20	2	-64	-	-79	
May	<i>Atriplex portulacoides</i>	-147		-148		-131		-33				9				
	<i>Atriplex portulacoides</i>	-157		-151		-139		-				15				
		-152	4	-150	2	-135	4	-33	4	-	-	12	3	-120	-	-160
	<i>Elytrigia atherica</i>	-219		-229		-225		-33				-7				
	<i>Elytrigia atherica</i>	-234		-234		-240		-				-2				
		-227	7	-232	3	-233	8	-33	4	-	-	-5	2	-205	-	-228
	<i>Limonium vulgare</i>	-132		-118		-124		2				15				
	<i>Limonium vulgare</i>	-141		-125		-122		-				16				
		-137	4	-122	4	-123	1	2	4	-	-	15	1	-123	-	-135
	<i>Phragmites</i>	-163		-175		-	-	-33				-12				
	<i>Phragmites</i>	-165		-180		-	-	-				-4				
		-164	2	-178	2	-	-	-33	4	-	-	-8	4	-149	-	-171

Appendix 5

Table showing all replicates of *n*-alkane and leaf water ²H/¹H measurements from all sampling intervals in 2012

Month	Plant species	δ ² H _{C₂₇}	AD*	δ ² H _{C₂₉}	AD	δ ² H _{C₃₁}	AD	δ ² H _{SW}	AD**	δ ² H _{XW}	AD	δ ² H _{LW}	AD	ε ₂ H _{C₂₉/sw}	ε ₂ H _{C₂₉/XW}	ε ₂ H _{C₂₉/LW}
May	<i>Salicornia Europaea</i>	-137		-135		-136		2				9				
	<i>Salicornia Europaea</i>	-146		-128		-132		1				10				
		-142	5	-132	4	-134	2	2	0	-	-	10	0	-133	-	-140
	<i>Spartina anglica</i>	-140		-142		-138		2				11				
	<i>Spartina anglica</i>	-151		-149		-144		1				10				
		-146	6	-146	3	-141	3	2	0	-	-	10	0	-147	-	-154
Aug	<i>Suaeda vera</i>	-130		-125		-124		-33				5				
	<i>Suaeda vera</i>	-130		-128		-122		-				3				
		-130	0	-127	2	-123	1	-33	4	-	-	4	1	-97	-	-130
	<i>Atriplex portulacoides</i>	-168		-163		-141						-2				
	<i>Atriplex portulacoides</i>	-150		-142		-129						-1				
		-159	9	-153	10	-135	6	-	-	-	-	-1	1	-	-	-151
	<i>Elytrigia atherica</i>	-230		-235		-235						-6				
	<i>Elytrigia atherica</i>	-228		-234		-234						-10				
		-229	1	-235	0	-235	1	-	-	-	-	-8	2	-	-	-229
	<i>Limonium vulgare</i>	-133		-118		-128						8				
	<i>Limonium vulgare</i>	-132		-111		-123						6				
		-133	1	-115	4	-126	3	-	-	-	-	7	1	-	-	-120
	<i>Phragmites</i>	-181		-191	3	-	-					-15				
	<i>Phragmites</i>	-189		-201		-	-					-16				
		-185	4	-196	5	-	-	-	-	-	-	-16	1	-	-	-183
<i>Salicornia Europaea</i>	-132		-131		-137						4					
<i>Salicornia Europaea</i>	-132		-131		-134						5					
	-132	0	-131	0	-136	2	-	-	-	-	5	1	-	-	-135	
<i>Spartina anglica</i>	-153		-161		-157						14					
<i>Spartina anglica</i>	-162		-165		-165						11					
	-158	5	-163	2	-161	4	-	-	-	-	13	1	-	-	-173	
<i>Suaeda vera</i>	-132		-132		-127						2					
<i>Suaeda vera</i>	-128		-126		-116						10					
	-130	2	-129	3	-122	5	-	-	-	-	6	4	-	-	-134	

Appendix 5

Table showing all replicates of *n*-alkane and leaf water ²H/¹H measurements from all sampling intervals in 2012

Month	Plant species	δ ² H _{C₂₇}	AD*	δ ² H _{C₂₉}	AD	δ ² H _{C₃₁}	AD	δ ² H _{SW}	AD**	δ ² H _{XW}	AD	δ ² H _{LW}	AD	ε ² H _{C₂₉/sw}	ε ² H _{C₂₉/XW}	ε ² H _{C₂₉/LW}
Sep	<i>Atriplex portulacoides</i>	-163		-162		-149		-3		-30		6				
	<i>Atriplex portulacoides</i>	-173		-169		-		-		-31		4				
		-168	5	-166	4	-	-	-3	4	-31	1	5	1	-163	-139	-170
	<i>Elytrigia atherica</i>	-232		-230		-233		3		-41		-10				
	<i>Elytrigia atherica</i>	-227		-230		-230		-		-45		-5				
		-230	2	-230	0	-232	1	-3	4	-43	2	-7	2	-228	-196	-224
	<i>Limonium vulgare</i>	-133		-118		-120		0		-4		13				
	<i>Limonium vulgare</i>	-137		-132		-131		-		-4		17				
		-135	2	-125	7	-126	5	0	4	-4	0	15	2	-125	-122	-138
	<i>Phragmites</i>	-216		-220		-		-3		-29		-2				
	<i>Phragmites</i>	-186		-192		-		-		-29		-3				
		-201	15	-206	14	-	-	-3	4	-29	0	-2	1	-204	-182	-204
	<i>Salicornia Europaea</i>	-129		-121		-123		-1		-	-	22				
	<i>Salicornia Europaea</i>	-139		-133		-123		-		-	-	18				
		-134	5	-127	6	-123	0	-1	4	-	-	20	2	-126		-144
	<i>Spartina anglica</i>	-145		-169		-144		-1		-10		17				
	<i>Spartina anglica</i>	-160		-157		-150		-		-8		14				
		-153	7	-163	6	-147	3	-1	4	-9	1	15	2	-162	-155	-176
<i>Suaeda vera</i>	-131		-131		-123		-3		-30		4					
<i>Suaeda vera</i>	-148		-151		-128		-		-31		3					
	-140	8	-141	10	-126	3	-3	4	-30	0	4	0	-138	-114	-144	

Appendix 5

Table showing diurnal differences in xylem water, soil water and leaf water from plants at the Ridge site, Sept. 2012

Location	Plant species	$\delta^2\text{H}_{\text{xylem water}}$	SE _{xylem water}	$\delta^2\text{H}_{\text{soil water}}$	SE _{soil water}	$\delta^2\text{H}_{\text{leaf water}}$	SE _{leaf water}
Site 2	<i>Atriplex portulacoides</i>	-35		-25		1.7	
	<i>Atriplex portulacoides</i>	-31		-19		-2.3	
		-33	2	-22	3	-0.3	2
Site 2	<i>Elytrigia atherica</i>	-49		-25		-25	
	<i>Elytrigia atherica</i>	-46		-19		-26	
		-48	2	-22	3	-25	0
Site 2	<i>Suaeda vera</i>	-29		-25		-2	
	<i>Suaeda vera</i>	-25		-19		-4	
		-27	2	-22	3	-3	1

Table 5b: Hydrogen isotopic composition of leaf water, soil water and xylem water sampled between 12:00 and 14:00; September 2012

Location	Plant species	$\delta^2\text{H}_{\text{xylem water}}$	SE _{xylem water}	$\delta^2\text{H}_{\text{soil water}}$	SE _{soil water}	$\delta^2\text{H}_{\text{leaf water}}$	SE _{leaf water}
Site 2	<i>Atriplex portulacoides</i>	-30		-3		6	
	<i>Atriplex portulacoides</i>	-31		-		4	
		-31	1	-3	4	5	1
Site 2	<i>Elytrigia atherica</i>	-41		-3		-10	
	<i>Elytrigia atherica</i>	-45		-		-5	
		-43	2	-3	4	-7	2
Site 2	<i>Suaeda vera</i>	-30		-3		4	
	<i>Suaeda vera</i>	-31		-		3	
		-30	0	-3	4	4	0

Appendix 5

Table 6: Modelled precipitation isotope data for Stiffkey marsh using OIPC (Bowen et. al., 2005)

Estimates for latitude 52.9585°, longitude 0.92355°, altitude 1 m:

	Jan	Feb	Mar	Apr	May	Jun	Jul	Aug	Sept	Oct	Nov	Dec
$\delta^2\text{H}$ (‰, V-SMOW)	-70	-65	-62	-62	-52	-49	-44	-43	-48	-56	-67	-70
$\delta^{18}\text{O}$ (‰, V-SMOW)	-10	-9	-9	-9	-8	-7	-6	-6	-7	-9	-10	-10

(OPIC version 2.2)

Appendix 5

Leaf water standard data

	USGS 67400 (1.2‰)	NTW (-47‰)		
	0.015	-47.60	-46.65	-48.86
	1.367	-46.68	-46.86	-45.98
	0.521	-47.07	-46.77	-47.24
	0.139	-46.55	-46.90	-47.15
	0.383	-47.20	-46.91	-49.44
	1.078	-46.22	-47.04	-49.05
	1.002	-47.55	-46.98	-49.36
	-0.33	-47.41	-47.07	-48.53
	-0.058	-48.85	-46.95	-46.68
	1.247	-46.58	-47.09	-46.58
	1.005	-47.93	-48.70	-46.98
	0.782	-48.86	-49.41	-48.06
	2.45	-47.66	-49.84	-47.20
	1.271	-47.06	-50.71	-48.76
	1.583	-48.18	-49.86	-47.55
	1.78	-46.40	-49.18	-49.00
	0.168	-46.46	-49.61	-46.02
	0.237	-46.48	-46.35	-47.27
	0.168	-46.39	-47.52	-48.02
	0.237	-46.42	-47.33	-46.22
	0.735	-46.46	-55.67	-47.36
	0.048	-46.47	-47.11	-48.82
	0.46	-46.58	-49.11	-46.63
	1.367	-46.67	-46.49	-46.98
	1.509	-45.89	-46.69	-47.77
	1.662		-46.71	-46.99
	0.699			
	1.737			
Mean	0.83	-47.58		
SD	0.70	1.45		

Appendix 6:
Additional data pertaining to
Chapter 7

Appendix 6

Hydrogen isotope analysis of acetylated phthalic acid

Derivatisation	Peak intensity (mV)	Retention time	$\delta^2\text{H}$
Acetylated phthalic acid	2601	541.9	-142.1
Acetylated phthalic acid	2468	542.4	-148.6
Acetylated phthalic acid	2831	543.4	-143.9
Acetylated phthalic acid	2723	543.8	-146.5
Acetylated phthalic acid	2816	544	-142.5
Acetylated phthalic acid	2919	544.4	-140.4
Acetylated phthalic acid	2941	544.4	-141.1
Acetylated phthalic acid	3097	545.9	-147.1
Acetylated phthalic acid	3146	546.1	-148.8
Mean	-145‰ ± 3‰		

Hydrogen isotope analysis of methylated phthalic acid

Derivatisation	Peak intensity (mV)	Retention time	$\delta^2\text{H}$
Methylated phthalic acid	6828	1097.7	-114.6
Methylated phthalic acid	6688	1097.7	-114.7
Methylated phthalic acid	6667	1097.7	-115.0
Methylated phthalic acid	6859	1098.1	-114.8
Methylated phthalic acid	6842	1098.1	-115.1
Methylated phthalic acid	10974	1100	-116.1
Methylated phthalic acid	11018	1100	-115.1
Methylated phthalic acid	10918	1100	-114.9
Methylated phthalic acid	10950	1100	-115.8
Methylated phthalic acid	11182	1100.2	-115.5
Methylated phthalic acid	11041	1100.2	-115.0
Mean	-115‰ ± 0.5‰		

Hydrogen isotope analysis of starch post equilibration experiment

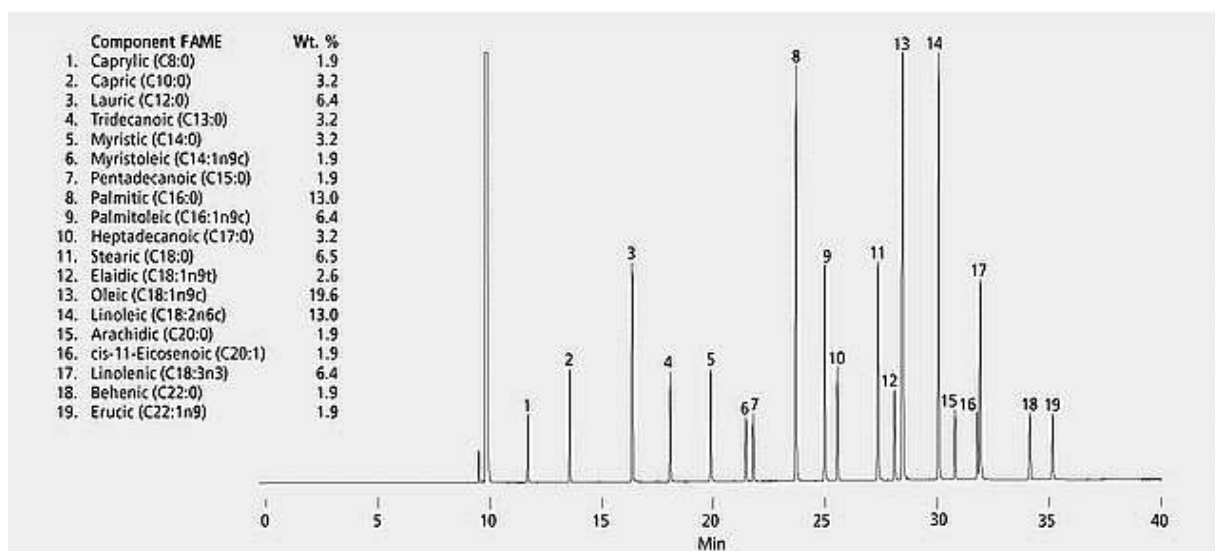
Species	Evian		Norwich Tap	
	Rep.1	Rep.2	Rep.1	Rep.2
<i>Atriplex portulacoides</i>	-135.3	-139.5	-127.3	-134.8
<i>Suaeda vera</i>	-121.9		-113.2	
<i>Barley</i>	-43.8	-44.2	-40.8	-37.6
<i>Wild wheat</i>	-32.1	-31.9	-25.1	-30.9
<i>Quinoa</i>	-92.1	-94.7	-95.8	-89.8
<i>Potato</i>	-63.8	-61.8	-58.9	-50.5

Appendix 6

Bulk hydrogen isotope analysis of plant tissue

Month	Bulk $\delta^2\text{H}$	
	Rep. 1	Rep. 2
March		
<i>Atriplex portulacoides</i>	-93.3	-86.3
<i>Elytrigia atherica</i>	-100.5	-96.2
<i>Limonium vulgare</i>	-61.3	-62.8
<i>Spartina anglica</i>	-60.8	-59.8
<i>Suaeda vera</i>	-87.5	-84.3
May		
<i>Atriplex portulacoides</i>	-102.7	-97.5
<i>Elytrigia atherica</i>	-127.9	-123.2
<i>Limonium vulgare</i>	-85.3	-85.6
<i>Phragmites australis</i>	-84.6	-86.2
<i>Salicornia europaea</i>	-95.5	-91.3
<i>Spartina anglica</i>	-65.4	-72.7
<i>Suaeda veera</i>	-92.2	-90.2
August		
<i>Atriplex portulacoides</i>	-104.2	-105.6
<i>Elytrigia atherica</i>	-128.1	-135.5
<i>Limonium vulgare</i>	-92.4	-90.6
<i>Phragmites australis</i>	-92.7	-101.9
<i>Salicornia europaea</i>	-88.0	-96.1
<i>Spartina anglica</i>	-87.2	-100.0
<i>Suaeda veera</i>	-90.5	-90.5
September		
<i>Atriplex portulacoides</i>	-115.8	-115.3
<i>Elytrigia atherica</i>	-132.8	-132.4
<i>Limonium vulgare</i>	-90.0	-89.8
<i>Phragmites australis</i>	-105.5	-104.1
<i>Salicornia europaea</i>	-91.3	-89.7
<i>Spartina anglica</i>	-82.1	-82.0
<i>Suaeda veera</i>	-105.6	-101.2

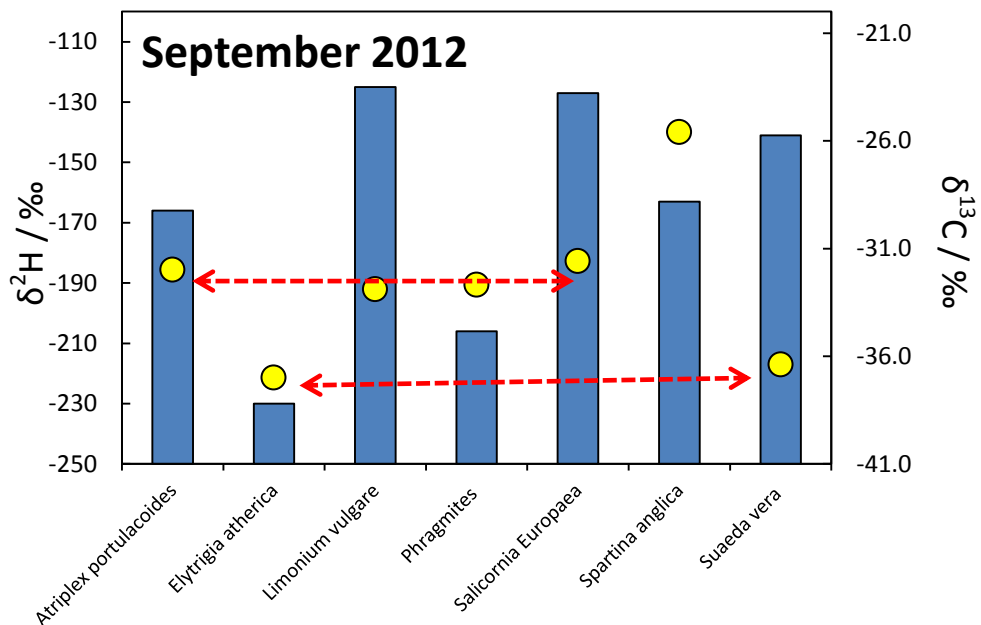
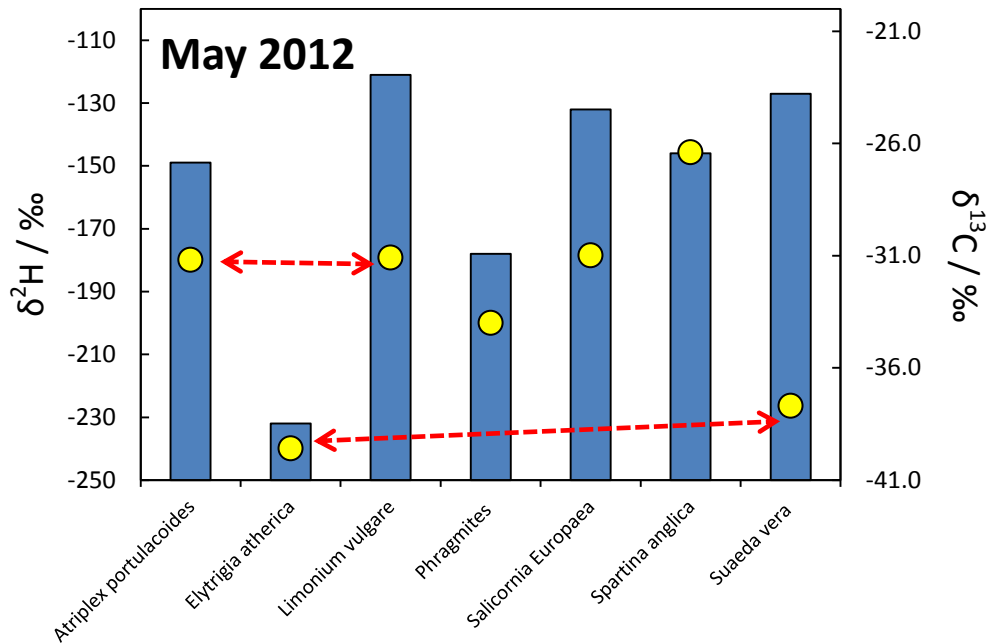
Supelco grain FAME chromatogram (Sigma Aldrich)



Appendix 7:
Additional data pertaining to
Chapter 8

Appendix 7

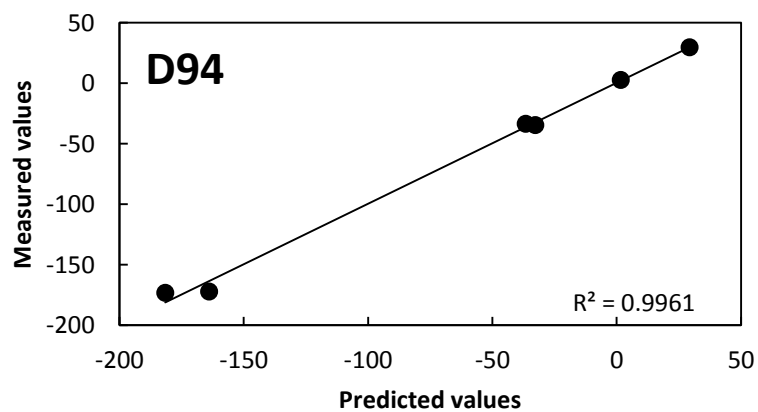
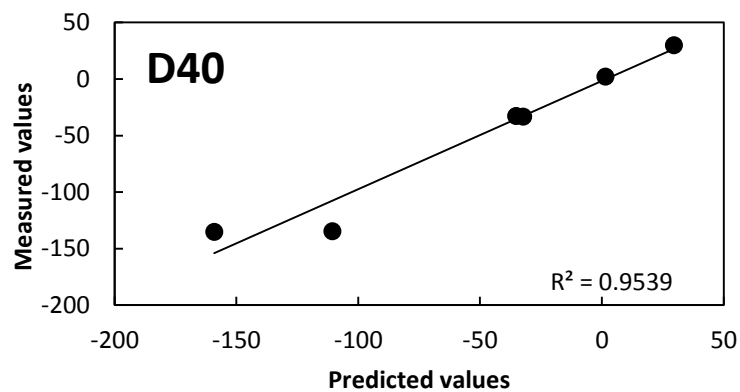
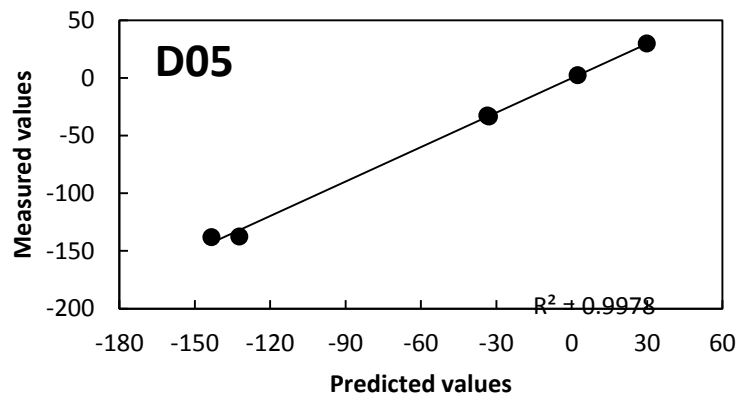
Comparison of carbon and hydrogen isotope composition of $n\text{-C}_{29}$ from two additional sampling intervals in 2012 at Stiffkey



Figures show $^2\text{H}/^1\text{H}$ (blue bars) and $^{13}\text{C}/^{12}\text{C}$ (yellow circles). Red arrows highlight where it is difficult to separate species with very different $^2\text{H}/^1\text{H}$ using carbon isotope composition.

Appendix 7

Collins model comparison: actual and predicted input criteria



Comparison of measured input values and values predicted by the Collins (1997) model for three depths from the 1m core at Stiffkey. The R^2 values for all such comparisons exceed 0.9. These figures show how it is the $^2\text{H}/^1\text{H}$ values (ringed in red) that are of most significance for this model, and highlights how it does not always cope well with these very negative values.

Appendix 7

Example of the excel spreadsheet used for the Collins (1997) mixing model (40cm depth)

Tracer Properties	$\delta^{13}C_{29}$	δD_{C29}	$\delta^{13}C_{C31}$	δD_{C31}	ACL	MD Ratio
	-32.7	-164	-34.0	-182	29.4	1.65

Source Groups	$\delta^{13}C_{29}$	δD_{C29}	$\delta^{13}C_{C31}$	δD_{C31}	ACL	MD Ratio	Changing cells	Check cell	Unit cells
AP	-32.0	-166	-32.2	-149	26.9	0.932246175	0		1
EA	-37.0	-230	-35.3	-232	29.4	3.293043643	0.091733801	1.00	0
LV	-32.9	-125	-32.3	-126	29.8	2.041926005	0.908266226		
SA	-25.6	-163	-32.1	-147	28.9	0.902157007	0		
SE	-31.6	-127	-25.3	-123	27.1	4.377089114	0		
SV	-36.4	-141	-35.0	-125	27.7	0.654101585	0		

	$X^{n-C29} (d^{13}C)$	$X^{n-C29} (dD)$	$X^{n-C31} (d^{13}C)$	$X^{n-C31} (dD)$	X^{ACL}	$X^{D} Ratio$
Predicted	-34.74454146	-172.238257	-33.64966449	-173.2556284	29.63250253	2.604789019
Mean	X_1	X_2	X_3	X_4	X_9	X_10
	-32.58	-158.67	-32.03	-150.27	28.31	2.03
Summary						
$(X^i - X_i)^2$	4.016182187	70.41319391	8.704479648	68.7966006	0.072946678	0.907475541
$(X_i - X_j)^2$	0.024701361	26.83585344	20.85444444	978.6469444	1.103224141	0.145354111
Num/Denom	Target cell					
1.480281467E-01	8.51972E-01					

Example of the excel spreadsheet that runs the Collins model (Collins *et al.*, 1997). The blue-shaded boxes are data from the sample to be unmixed, while the data in the yellow boxes relates to the plants (i.e. the source groups). The spreadsheet is set up using Excel “Solver” with the changing cells (that show the relative percentage inputs) set that they must be ≤ 1 , and ≥ 0 (values set in the “Unit cells”). The “check cell” shows the sum of the changing cells, to ensure they add up to 1. The red-shaded “Predicted” values are the model predictions for each input criteria. The mean values are simply the mean the data for each input criteria. The summary boxes $((X^i - X_i)^2)$ and $((X_i - X_j)^2)$ are the squares of the differences between the mean and original input values, and the predicted and original input values. The “Num/Denom” box is the sum of $(X^i - X_i)^2 / (X_i - X_j)^2$. The “Target cell” checks that $1 - \text{Num/denom}$ is as close to 1 as possible (i.e. this is a check of the quality of the model predictions).

Appendix 7

Table showing the calculation of the mean $\epsilon^{2}\text{H}_{\text{wax/OIPC}}$ values for each plant functional group used for calculating $\delta^{2}\text{H}_{\text{PPT}}$ from sediment samples

PFT	Plant species	$\epsilon\text{D}_{\text{wax/OIPC}}$ (‰)	Mean values	
C3 monocot	<i>Elytrigia atherica</i>	-147		
C3 monocot	<i>Elytrigia atherica</i>	-190		
C3 monocot	<i>Phragmites</i>	-133		
C3 monocot	<i>Elytrigia atherica</i>	-201	C3 monocots:	
C3 monocot	<i>Phragmites</i>	-160	Mean	-170
C3 monocot	<i>Elytrigia atherica</i>	-191	SD	25
C3 monocot	<i>Phragmites</i>	-166		
C4 monocot	<i>Spartina anglica</i>	-80		
C4 monocot	<i>Spartina anglica</i>	-99	C4 monocots:	
C4 monocot	<i>Spartina anglica</i>	-125	Mean	-106
C4 monocot	<i>Spartina anglica</i>	-121	SD	21
Dicot/succulent	<i>Atriplex portulacoides</i>	-82		
Dicot/succulent	<i>Limonium vulgare</i>	-66		
Dicot/succulent	<i>Suaeda vera</i>	-37		
Dicot/succulent	<i>Atriplex portulacoides</i>	-102		
Dicot/succulent	<i>Limonium vulgare</i>	-73		
Dicot/succulent	<i>Salicornia Europaea</i>	-84		
Dicot/succulent	<i>Suaeda vera</i>	-79		
Dicot/succulent	<i>Atriplex portulacoides</i>	-114		
Dicot/succulent	<i>Limonium vulgare</i>	-75		
Dicot/succulent	<i>Salicornia Europaea</i>	-92		
Dicot/succulent	<i>Suaeda vera</i>	-90		
Dicot/succulent	<i>Atriplex portulacoides</i>	-124	Dicots/succulents:	
Dicot/succulent	<i>Limonium vulgare</i>	-81	Mean	-85
Dicot/succulent	<i>Salicornia Europaea</i>	-83	SD	20
Dicot/succulent	<i>Suaeda vera</i>	-98		

Appendix 7

Molecular distribution of *n*-alkanes extracted from the Stiffkey core. Data is presented as the percentage abundance of each alkane homologue, normalised to the total peak height of all measured alkanes

Depth (cm)	C ₂₁	C ₂₂	C ₂₃	C ₂₄	C ₂₅	C ₂₆	C ₂₇	C ₂₈	C ₂₉	C ₃₀	C ₃₁	C ₃₂	C ₃₃	C ₃₄	C ₃₅	ACL	CPI
5	1.65	1.37	2.20	1.37	2.47	1.37	9.07	3.85	22.80	3.57	32.14	3.30	11.54	0.55	2.75	30.06	10.92
10	1.90	1.59	1.90	1.27	2.22	1.59	12.70	4.76	25.08	2.54	30.48	1.90	10.16	0.32	1.59	29.83	11.52
15	2.50	2.25	2.75	2.25	3.25	2.25	11.75	4.50	23.25	2.75	28.75	2.00	9.25	0.50	2.00	29.76	10.07
30	4.08	3.27	4.49	3.27	5.31	3.27	11.43	4.08	18.78	2.45	23.27	1.63	12.24	0.82	1.63	29.72	8.19
40	5.76	5.19	6.34	5.19	6.34	4.03	10.09	4.61	15.56	2.88	18.44	1.73	10.95	1.15	1.73	29.57	5.74
60	6.32	5.75	6.32	4.60	6.32	4.02	8.62	3.45	14.37	2.87	20.69	1.72	10.92	1.72	2.30	29.70	6.33
80	8.30	6.79	7.55	6.04	7.55	5.28	8.68	3.77	14.34	2.26	17.36	1.51	8.30	0.75	1.51	29.36	5.35
94	9.04	7.23	9.64	7.23	8.43	6.63	9.64	4.82	11.45	3.61	11.45	1.81	6.02	1.20	1.81	28.87	3.24

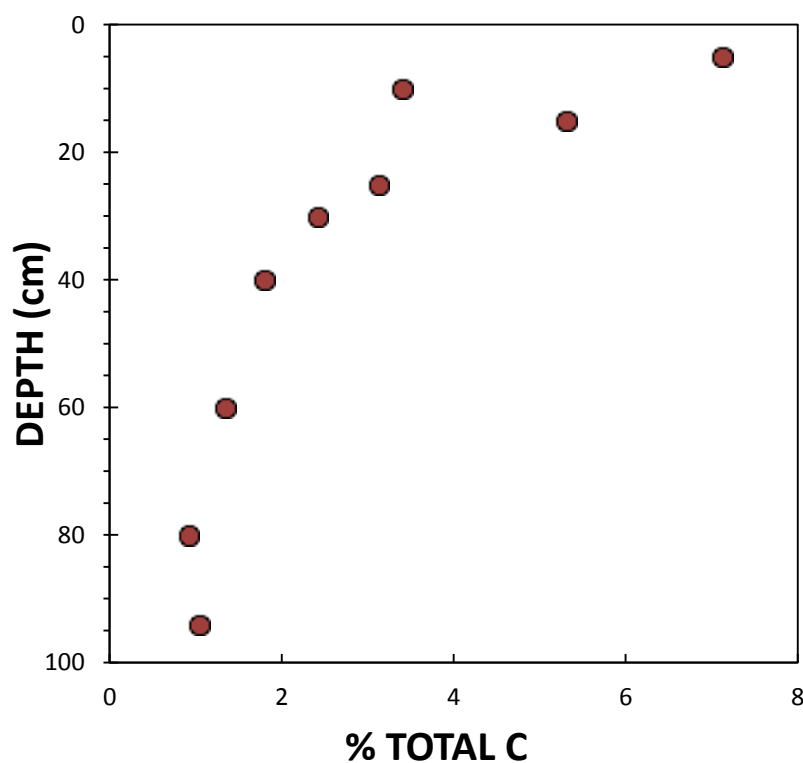
Appendix 7

Carbon and hydrogen isotope composition of *n*-alkanes extracted from the Stiffkey sediment core

Depth (cm)	$\delta^{13}\text{C}$				$\delta^2\text{H}$	
	C ₂₉		C ₃₁		C ₂₉	C ₃₁
5	-32.6	-33.1	-32.3	-33.4	-132.2	-143.3
10	-33.5	-32.5	-33.6	-34.4	-150.4	-143.0
15	-32.4	-32.1	-33.0	-33.6	-168.0	-161.9
30	-32.5	-32.5	-33.3	-33.5	-166.6	-178.1
40	-32.5	-32.5	-32.9	-35.1	-122.0	-159.1
60	-32.2	-32.4	-30.4	-30.6	-158.7	-166.3
80	-32.6	-	-33.7	-36.6	-163.9	-181.6
94	-32.6	-32.7	-32.5	-36.1	-132.7	-145.4

**Duplicate analysis of the same sample for carbon isotope composition was consistently better than 1‰ for $\delta^{13}\text{C}_{n\text{-C}_{29}}$ and 2‰ for $\delta^{13}\text{C}_{n\text{-C}_{31}}$. Duplicates were not analysed for $\delta^2\text{H}$ due to insufficient material remaining. A conservative approach has therefore been adopted, based upon the maximum variability observed for other sediment $^2\text{H}/^1\text{H}$ measurements, and RMS errors of 7‰ for all sediment $^2\text{H}/^1\text{H}$ values.*

Plot of total organic carbon in the Stiffkey core sediments



Appendix 7

Hydrogen Isotope analysis of Stiffkey surface sediments

Ridge			
	Replicate 1	Replicate 2	Replicate 3
Sample 1	-187	-181	-186
Sample 2	-173	-170	-170
Upper marsh			
Sample 1	-142	-139	-139
Sample 2	-141	-138	-134

** Analytical reproducibility of triplicate $^2\text{H}/^1\text{H}$ measurements of the same sample did not exceed $\pm 7\text{‰}$*